Immunogenicity of vaccines for malaria-exposed populations

Georgina Sophie Amundsen Bowyer

St Cross College

University of Oxford

A thesis submitted for the degree of
Doctor of Philosophy

Trinity Term 2018

Word count: ≈ 50,000 (excluding tables, figure legends, references and appendix)

Immunogenicity of vaccines for malaria-exposed populations

Georgina Sophie Amundsen Bowyer, St Cross College, University of Oxford

Thesis submitted for the degree of Doctor of Philosophy, Trinity Term 2018

Abstract

An efficacious malaria vaccine will be a necessary tool for malaria eradication, however current vaccine candidates have only demonstrated a moderate level of short-term efficacy. Additionally, these vaccines often display reduced immunogenicity and efficacy in the malaria-exposed target populations compared with the malaria-naïve populations in which they are initially tested. Reduced vaccine immunogenicity in malaria-exposed populations may affect vaccines for diseases other than malaria. The 2014-2016 Ebola outbreak in West Africa highlighted the need to produce effective vaccines against emerging infectious diseases. Many of the outbreak pathogens for which such vaccines are being developed have geographical distributions that overlap with areas of malaria transmission. Therefore being able to effectively vaccinate malaria-exposed individuals is a key requirement for this new generation of vaccines. This thesis aims to characterise the immunogenicity of candidate malaria and Ebola vaccines in detail and explores potential mechanisms of reduced immunogenicity in malaria-exposed populations. Experiments demonstrated that concomitant administration of viral vectored and VLP-based malaria vaccines caused a Th1-skewed cytokine response that was associated with reduced antibody titres and efficacy, similar to the immunosuppressive effect of acute malaria infection. Humoral, but not cellular, responses to malaria and Ebola vaccines were reduced in malaria-exposed adults and children but not in infants. Although this reduction was associated with malaria exposure in some cases, it was clear that other factors were involved. Further experiments revealed a role for cytomegalovirus infection in the reduction of vaccine immunogenicity in both malaria-naïve and malaria-exposed young adults. Overall this thesis highlights the importance of understanding what impacts immunogenicity in order to optimise vaccines for the target populations.

Acknowledgements

Firstly, I would like to thank my supervisors Professor Adrian Hill and Associate Professor Katie Ewer for the opportunity to conduct this research and for your support and guidance throughout the DPhil. I am very grateful to have had the independence and freedom to explore my research questions. Thanks also to Associate Professor Tess Lambe and Dr. Alex Spencer for their advice and guidance. A special thank you to Dr. Pete Crompton, Dr. Nyamekye Obeng-Adjei and Dr. Silvia Portugal for welcoming me into their lab. I found their work truly inspiring and the experience I had at the NIH provided an excellent foundation for my DPhil project. I would also like to thank Dr. Julia Bollrath and Professor Fiona Powrie for giving me my first experience of research and inspiring me to pursue a career in science. Thanks must also go to Tim Waterboer and his lab for generously agreeing to run the samples on their multiplex assay at no cost.

This research would not have been possible without the dedication and hard work of the clinical trials teams and the participation of the volunteers in Oxford, Southampton, Surrey, The Gambia, Burkina Faso, Kenya and Senegal. I would like to thank in particular, the lab team in Kilifi, Kenya for giving me such a warm welcome when I visited. The hard work of the clinical trials lab team has also been invaluable to this study: Carly Bliss, Danny Wright, Jonathan Powlson, Richard Morter, Duncan Bellamy, Catherine Mair and Amy Flaxman. I am lucky to have worked with such a committed and enthusiastic team. I have had the pleasure of supervising some excellent medical students during my time at the Jenner Institute: Thanks to Claudia Snudden, Erika Lam, Amy Grobbelaar, Alex Munster and Sophie Roche for keeping me on my toes and to Hannah Sharpe for CMV discussions and help with the CMV project.

Importantly, a thank you to Wolfson College Boat Club and to my amazing crew mates in particular, who have been there for me throughout. Finally, a huge thank you to my wonderful family, for their unwavering support and belief. I am where I am today because of you. A special thank you also to my best friend and partner Matt for always being there for me.

Table of Contents

List of Figures

List of Tables

List of Abbreviations

ACT	Artemisinin-based combination therapy
Ad	Adenovirus
AF	Alexa-Fluor
AIAD	antigen-independent antibody deposition
AIM	activation-induced markers
AMA1	apical membrane antigen 1
AMP	antimicrobial peptide
APC	antigen presenting cell
APC	allophycocyanin
ASC	antibody-secreting cell
ATP	adenosine triphosphate
BCG	bacille Calmette–Guérin
BCIP/NBT	5-Bromo-4-chloro-3-indolyl phosphate/nitroblue tetrazolium
Bcl-6	B cell lymphoma 6 protein
BCR	B cell receptor
BDBV	*Bundibugyo ebolavirus*
BKV	BK virus
BSA	bovine serum albumin
BV	Brilliant Violet
C-1	one day prior to CHMI
CCVTM	Centre for Clinical Vaccinology and Tropical Medicine
CD	cluster of differentiation
CDC	Center for Disease Control
CDR	complementarity determining region
CGD	chronic granulomatous disease
ChAd	chimpanzee adenovirus
CHMI	controlled human malaria infection
CM	central memory
CMV	cytomegalovirus
CRF	clinical research facility
CRP	C-reactive protein
CSP	circumsporozoite protein
CTLA-3	cytotoxic T lymphoctye-associated protein 3
cTfh	circulating T follicular helper cells
CTL	cytotoxic T lymphoctye
CTLA-4	cytotoxic T lymphoctye-associated protein 4
CXCL	CXC chemokine ligand
CXCR	CXC-chemokine receptor
Cy	cyanine
DAMP	danger-associated molecular pattern
DAPI	4',6-diamidino-2-phenylindole
DC	dendritic cell

DLN	draining lymph node
DMSO	dimethyl-sulfoxide
DNA	deoxyribonucleic acid
DPBS	Dulbecco's PBS
DRC	Democratic Republic of Congo
DTP	diphtheria, tetanus and pertussis
EBOV	*Zaire ebolavirus*
EBV	Epstein-Barr virus
ELISA	enzyme-linked immunosorbant assay
ELISpot	enzyme-linked immunospot assay
EM	effector memory
EPI	Expanded Program on Immunization
ETU	Ebola treatment unit
EU	ELISA units
EVD	Ebola virus disease
Fab	fragment antigen-binding
FACS	fluorescence-activated cell sorting
FasL	Fas ligand
Fc	fragment crystallisable
FcR	Fc receptor
FcRL	FcR ligand
FCS	foetal calf serum
FITC	fluorescein isothiocyanate
FOXP3	forkhead box p3
FSC	forward scatter
GAP	genetically attenuated parasites
GC	germinal centre
GCP	good clinical practice
GFP	green fluorescent protein
GMP	good manufacturing practice
GP	glycoprotein
GSK	GlaxoSmithKline
HBcAg	hepatitis B core antigen
HBeAg	hepatitis B antigen e
HBsAg	hepatitis B surface antigen
HBV	hepatitis B virus
HCV	hepatitis C virus
HCW	healthcare worker
HHV-6	human herpes virus type 6
HHV-7	human herpes virus type 7
HI	heat-inactivated
HIV	human immunodeficiency virus
HLA	human leukocyte antigen
HSP	heat shock protein
HSV	herpes simplex virus

HSV-1	herpes simplex virus type 1
HSV-2	herpes simplex virus type 2
HTLV-1	human T-lymphotrophic virus 1
HZ	haemozoin
ICAM-1	intercellular adhesion molecule 1
ICOS	inducible T cell costimulator
ICS	intracellular cytokine staining
IFA	immunofluorescence assay
IFN	interferon
IFNγ	interferon gamma
Ig	immunoglobulin
IL	interleukin
IM	intramuscular
IQR	interquartile range
ISI	inhibition of sporozoite invasion
ITN	insecticide-treated net
IV	intravenous
J&J	Johnson and Johnson
JCV	John Cunningham virus
KEMRI	Kenya Medical Research Institute
KLRG1	killer cell lectin-like receptor G1
KSHV	Kaposi's sarcoma-associated virus
LBP	LPS binding protein
LLOD	lower limit of detection
LLPC	long-lived plasma cell
LPS	lipopolysaccharide
LSA1	liver-stage antigen 1
LSHTM	London School of Hygiene and Tropical Medicine
LTBI	latent TB infection
MAC	membrane attack complex
MBC	memory B cell
MCV	Merkel cell polyoma virus
ME	multiple epitope string
MHC	major histocompatability complex
MIF	macrophage inhibitory factor
MM	Matrix-M
MPEC	memory precursor effector cell
MSP	merozoite surface protein
MVA	modified vaccinia virus Ankara
NAI	naturally acquired immunity
NaSCN	sodium thiocyanate
NHP	non-human primate
NHS	normal human serum
NIH	National Institutes of Health
NIHR	National Institute for Health Research

NK	natural killer
NO	nitric oxide
NP	nucleoprotein
NRS	normal rabbit serum
OD	optical density
PAMP	pathogen-associated molecular pattern
PBMC	peripheral blood mononucleocyte
PBS	phosphate buffered saline
PBS/T	phosphate buffered saline with 0.05%Tween 20
PCR	polymerase chain reaction
PD1	programmed cell death protein 1
PDL1	programmed death-ligand 1
PE	pre-erythrocytic
PE	R-phycoerythrin
PerCP	peridinin chlorophyll protein
PFA	paraformaldehyde
PfEMP-1	*Plasmodium falciparum* erythrocyte membrane protein 1
PfSPZ	cryopreserved *P. falciparum* sporozoite vaccine
pfu	plaque forming units
PHA	phytohaemagglutinin-L
pNPP	para-nitrophenylphosphate
PRR	pattern recognition receptor
QC	quality control
RAS	radiation attenuated sporozoites
RBC	red blood cell
RESTV	*Reston ebolavirus*
RH5	reticulocyte-binding homologue 5
RORγt	RAR-related orphan receptor gamma 2
ROS	reactive oxygen species
RT	room temperature
RUNMC	Radboud University Nijmegen Medical Centre
rVSV-ZEBOV	recombinant VSV vaccine expressing Zaire Ebola GP
SD	standard deviation
SEB	staphylococcal enterotoxin B
SFC/10^6 PBMC	spot-forming cells per million PBMC
SLEC	short-lived effector cell
SLO	secondary lymphoid organ
Spz	sporozoites
SSC	side scatter
SUDV	*Sudan ebolavirus*
TAFV	*Taï Forest ebolavirus*
TB	tuberculosis
T-bet	T-box expressed in T cells
TBS	Tris buffered saline

T_{CM}	central memory T cell
TCR	T cell receptor
T_{EM}	effector memory T cell
T_{EMRA}	effector memory RA T cell
Tfh	T follicular helper cell
Th	T helper cell
Th1	T helper 1
Th2	T helper 2
TLR	Toll-like receptor
TMB	tetramethylbenzidine
TNF	tumour necrosis factor
TRAP	thrombospondin-related adhesion protein
Treg	regulatory T cells
T_{RM}	resident memory T cell
U.S. FDA	U.S. Food and Drug Administration
USMMVP	U.S. Military Malaria Vaccine Program
VLP	virus-like particle
VP	viral protein
vp	viral particles
VSA	variant surface antigen
VSV	vesicular stomatitis virus
VZV	varicella zoster virus
WHO	World Health Organization
WRAIR	Walter Reed Army Institute of Research
WTCRF	Wellcome Trust clinical research facility

Papers published from these studies

The following papers include work presented in this thesis:

Bowyer G, Grobbelaar A, Rampling T, Venkatraman N, Morelle D, Ballou RW, Hill AVS, Ewer KJ: **CXCR3+ T Follicular Helper Cells Induced by Co-Administration of RTS,S/AS01B and Viral-Vectored Vaccines Are Associated With Reduced Immunogenicity and Efficacy Against Malaria.** Front Immunol. 2018 Jul 25;9:1660. doi: 10.3389/fimmu.2018.01660.

Bowyer G, Rampling T, Powlson J, Morter R, Wright D, Hill AVS, Ewer KJ: **Activation-induced Markers Detect Vaccine-Specific $CD4^+$ T Cell Responses Not Measured by Assays Conventionally Used in Clinical Trials.** Vaccines (Basel). 2018 Jul 31;6(3). pii: E50. doi: 10.3390/vaccines6030050.

Statement of Authorship

This thesis has been composed by Georgina Bowyer and all work presented is that of Georgina Bowyer, unless stated otherwise. Design of immunological work, running of cellular and antibody assays and statistical analyses were conducted by Georgina Bowyer. Clinical trial blood processing, ELISpots and intracellular cytokine staining were conducted by Georgina Bowyer and the clinical trials research assistants. All other assays were conducted by Georgina Bowyer. Clinical trials were designed by A.V.S. Hill and the clinical trials clinicians. Clinical trials regulatory and ethics applications, and clinical care were conducted by the clinical trials team, clinicians and research nurses.

1

Introduction

1.1. Vaccine Immunology

Several of the earliest successful vaccines were developed empirically using whole killed pathogen, live-attenuated pathogen or a related species (e.g. *Mycobacterium bovis* bacille Calmette–Guérin [BCG] against tuberculosis [TB], vaccinia virus against smallpox). However, many of the diseases that we do not yet have efficacious vaccines for are more complex and require a more rational approach in order to design an effective vaccine [1]. A key aspect of rational vaccine design is a thorough understanding of the human immune system, how target pathogens interact with the immune system and how vaccines work to induce protective responses.

The human immune system has traditionally been divided into two branches: innate and adaptive. There is extensive overlap and interplay between these systems and their integrated function is essential for effective responses against many of the pathogens humans encounter.

1.1.1. Innate immunity

The innate immune system plays a central role in the control of many infectious and inflammatory processes. Innate immunity is characterised by fast-acting responses that serve to clear infection and activate an adaptive immune response. The innate immune system consists of both cellular (macrophages, dendritic cells [DCs], mast cells, eosinophils, natural killer [NK]

cells, neutrophils and NK T cells) and humoral components (the complement system, LPS binding protein [LBP], C-reactive protein [CRP], antimicrobial peptides [AMP]).

1.1.1.1. Sensing infection

A central feature of innate immunity is the ability to mount a rapid response using a limited number of invariant germline-encoded receptors to target conserved microbial components. There are three main recognition strategies used by the innate immune system to sense infection. The first is the sensing of microbial non-self by pattern-recognition receptors (PRRs) that detect common microbial sequences known as pathogen-associated molecular patterns (PAMPs) [2]. PRRs such as Toll-like receptors (TLRs) are families of receptors that each recognise distinct repertoires of conserved microbial molecules. (reviewed in [3]). This allows the innate immune system to discriminate between groups of pathogens and induce an appropriate cascade of effector responses. The TLR family consists of 10 members (TLR1–TLR10) in humans and 12 (TLR1–TLR9, TLR11–TLR13) in mice. TLR1, 2, 4, 5, 6 and 10 are expressed on the cell surface, while TLR3, 7, 8, 9, 11, 12 and 13 are expressed in the endosomal compartment [4]. Intracellular TLRs recognise nucleic acids derived from bacteria and viruses, in addition to self-nucleic acids in autoimmune conditions and molecules from intracellular bacteria and parasites. In particular Plasmodium-derived GPI anchors are detected by TLR2/MyD88, triggering production of proinflammatory cytokines IL-1 and TNFα. TLR4 and TLR9 have also been implicated in the recognition of Plasmodium [5]. However, most of this knowledge is derived from *in vitro* experiments and mouse models of *P. berghei* infection.

The importance of this system is illustrated by the immunodeficiency phenotypes caused by genetic defects which result in recurrent invasive infections caused by a narrow spectrum of pathogens. For example, deficiency of the signal transduction adaptor MYD88 results in recurrent infections with pyogenic gram positive bacteria including *Streptococcus pneumoniae* [6]. Polymorphisms in these receptors or components in their signalling pathways are also associated with differential susceptibility for particular infections. For example, polymorphisms in the adaptor molecule MAL/TIRAP (which mediates signalling through TLR1, 2, 4 and 6) have been associated with susceptibility to TB, malaria and pneumococcal disease [7]. Signalling through PRRs ultimately results in the production of active interleukin 1β (IL-1β) and IL-18, which mediate downstream inflammatory responses.

The second recognition strategy is the detection of endogenous danger signals or danger-associated molecular patterns (DAMPs) [8-11]. DAMPs are cell-derived molecules such as heat shock proteins (HSPs), uric acid and adenosine triphosphate (ATP). The presence of these molecules signal cell damage, either in the presence or absence of inflammation, and triggers an immune response. Detection of DAMPs by their receptors (which include TLRs) activates signalling pathways that induce effector functions. Depending on the pathway stimulated, DAMPs may induce the production of proinflammatory cytokines that exacerbate inflammation or induce cell survival signals and inhibit apoptosis. This system is highly regulated and inhibitory receptors such as CD24 and Siglec-10 limit DAMP-mediated inflammation [12].

The final recognition strategy is the detection of “missing self” through inhibitory receptors that signal when their ligands are downregulated on cells as a consequence of infection. This is most clearly demonstrated by NK cells, which express an array of activating and inhibitory receptors. Infected cells are able to process pathogen-derived proteins and present peptides on MHC class I molecules on the cell surface. Peptide-MHC complexes can then be recognised and killed by $CD8^+$ T cells in the adaptive immune response [13]. For this reason, many viruses have evolved

immune evasion mechanisms that enable them to downregulate MHC class I from the cell surface and evade detection by $CD8^+$ T cells [14]. To counteract this, NK cells are able to recognise "missing self", attacking cells that do not express sufficient levels of MHC class I molecules [15,16]. In humans this is achieved by two classes of MHC-specific inhibitory receptors: the KIR Ig-like receptors [17-20] and the CD94/NKG2A lectin-like inhibitory receptor [21,22]. It is likely that a combination of missing inhibitory signals and the presence of activating signals triggers NK cell effector functions [23].

1.1.1.2. Innate effector mechanisms

When a pathogen has been detected by the mechanisms discussed above, a cascade of events occurs and innate effector mechanisms are activated to clear or control infection until a robust adaptive immune response has developed.

Macrophages circulating the body are able to recognise extracellular pathogens through cell surface receptors as described above. Upon pathogen recognition macrophages are activated to produce cytokines and chemokines which initiate local inflammation and attract other leukocytes from the circulation to the inflammation site. Local inflammation can also be triggered by activation of the complement system, which consists of around 25 proteins circulating in inactive forms. Activation of complement can occur independently of the adaptive immune system by the alternative and lectin activation pathways when complement components bind directly to the pathogen surface and multimerise to form a membrane attack complex (MAC) [24]. The MAC forms a pore in the pathogen membrane causing lysis and cell death. Binding of complement components to the pathogen surface also opsonizes the pathogen, increasing susceptibility to phagocytosis. Phagocytosis is the engulfment of microorganisms, foreign particles and cell debris by phagocytes such as macrophages and neutrophils. Phagocytosed objects are then killed and digested by enzymes within phagolysosomes. Reactive oxygen species (ROS) and nitric oxide (NO) are also produced in

phagolysosomes as part of the "respiratory burst" [25]. The importance of the respiratory burst is illustrated by chronic granulomatous disease (CGD), which occurs as a result of defects in this system and causes susceptibility to recurrent bacterial and fungal infections [26]. NK cells are another important effector within innate immunity, playing key roles in defence against viral infections and tumour surveillance in particular [27,28]. As discussed briefly above, NK cells express an array of activating and inhibitory receptors. NK cells become activated through a combination of recognition of viral antigens by activating receptors and downregulation of inhibitory receptor ligands (such as MHC class I). Once activated, NK cells are capable of contact-dependent killing of target cells through the use of cytotoxic proteins (perforin, granzymes), Fas ligand and membrane-bound or secreted cytokines [29-31]. NK cells also produce cytokines such as IFNγ that further induce or regulate immune effector mechanisms [32]. The important role of NK cells within the immune system is best illustrated by patients with NK cell deficiencies, who suffer from a particular susceptibility to herpesvirus infections (particularly varicella zoster virus [VZV], cytomegalovirus [CMV], Epstein-Barr virus [EBV] and herpes simplex virus [HSV]) as well as other viral infections [33].

1.1.1.3. Integration with the adaptive immune system

A further crucial role for the innate immune system is to initiate an adaptive immune response. Inflammatory cytokines induced as part of the innate immune response can potentiate an adaptive immune response. Chemokines aid migration of leukocytes, including antigen presenting cells (APCs) to the site of inflammation. Professional APCs such as DCs are a key bridge between innate and adaptive immunity, stimulating T cells to respond to antigen [34]. DCs are able to load antigenic peptides onto either MHC class I or II molecules, allowing presentation to both $CD4^+$ and $CD8^+$ T cells [35].

Immature DCs in the periphery efficiently take up antigen. Exposure to PAMPs or DAMPs, as discussed above, results in DC activation and upregulation of costimulatory ligands on the DC

surface. T cell receptor recognition of peptide-MHC complexes on the DC surface provides the first signal for T cell activation. The second signal or co-stimulation (e.g. through CD28 on T cells and CD80 or CD86 on DCs), is necessary for T cell activation. In absence of this signal or in the presence of a co-inhibitory second signal (e.g. through CTLA-4 on T cells and CD80 or CD86 on DCs) T cells become unresponsive. The third signal (cytokines produced by the DC) determines the type of $CD4^+$ T cell that will develop – for example Th1, Th2 or Treg. Different PAMP and DAMPs appear to polarise DCs to produce different cytokines and thereby instruct the type of adaptive response that will develop [36]. Additionally, different DC subsets recognise and respond to different stimulants in different ways [37]. Two major subsets of DCs exist in the blood: myeloid DCs (mDCs) and plasmacytoid (pDCs). Plasmacytoid DCs express high levels of TLR7 and TLR9, which transduce signals from viral nucleic acids. This subset has a variable ability to polarise $CD4^+$ T cells towards Th1 or Th2 depending on the context. Myeloid DCs include $CD1c^+$ and $CD141^+$ subsets. $CD141^+$ mDCs recognise viral nucleic acids through TLR3 and 8, resulting in the production of TNFα, CXCL10 and IFNλ. This subset also has an enhanced ability to cross-present antigen to $CD8^+$ T cells. $CD1c^+$ DCs express a wide range of TLRs and respond to stimulants such as LPS, flagellin and poly(IC), resulting in production of TNFα, IL-8 and IL-10. This subset can also produce IL-12 and IL-23, implying that they may be involved in both Th1 and Th17 sensitisation.

Antigen presentation is mediated by MHC class I molecules on most cell types and MHC class II molecules found on a subset of cells, including professional APCs. MHC class I molecules present endogenously derived peptides that are typically 8-10 amino acids long to $CD8^+$ T cells. MHC class II molecules present exogenously derived peptides of 11-30 amino acids long to $CD4^+$ T cells [38]. Exogenously derived peptides can also be presented on MHC class I through cross-presentation and endogenously derived peptides can be presented on MHC class II through autophagy and non-autophagic pathways.

1.1.2. Adaptive immunity

Although the innate immune system is effective at clearing many pathogens, it is restricted by the limited range of germline-encoded receptors. As these receptors recognise molecular patterns that have been conserved over the course of evolution, many pathogens have evolved to either conceal or change these molecules and evade recognition. The adaptive immune system, characterised by an enormous selection of somatically-recombined receptors, is able to specifically detect each unique antigen and is therefore equipped to respond to diverse and evolving threats. The hallmark feature of the adaptive immune system is the generation of immunological memory, enabling more rapid and robust responses on secondary encounter.

1.1.2.1. Cell-mediated immunity

Cell-mediated immunity is an important defence against intracellular pathogens and cancers in particular. The key effectors in this arm of the adaptive immune system are $CD8^+$ cytotoxic T lymphoctyes (CTLs). Naïve CTLs are activated in secondary lymphoid organs (SLOs) by APCs, which present antigens on MHC class I molecules either through direct infection or cross-presentation [39].

The T cell receptor (TCR) is a member of the Ig superfamily and consists of a heterodimer formed of α and β chains (predominantly) or γ and δ chains (around 5% of human T cells). Each of these chains contains a variable and a constant region. The variable region of each chain contains three complementarity-determining regions (CDRs) which are responsible for antigen recognition. TCR diversity is generated by somatic recombination of V(D)J gene segments [40].

After antigen recognition, CTLs undergo multiple rounds of replication, resulting in huge numbers of antigen-specific CTLs [41,42]. Antigen-induced $CD8^+$ T cell responses are heterogeneous and consist of short-lived effector cells (SLECs) and memory precursor effector cells (MPECs) [43,44]. IL-2 signalling delivered shortly after infection determines the fate of $CD8^+$ T cells: IL-2 promotes SLEC development whilst if IL-2 is reduced or absent $CD8^+$ T cells have

reduced effector functions and preferentially develop into MPECs [45]. Activated CTLs upregulate inflammatory chemokine receptor CXCR3, aiding their migration into inflamed peripheral tissues [46]. $CD8^+$ T cells continue to interact with APCs and $CD4^+$ Th cells at the site of inflammation. Recognition of a target cell (infected cells displaying cognate peptide-MHCI combinations) initiates CTL-mediated cell killing. CTL killing mechanisms include perforin, which forms a pore in the target cell membrane, granzyme, which degrades cellular proteins causing apoptosis, and Fas ligand, which initiates Fas-mediated apoptosis in cells expressing Fas [47]. Each of these mechanisms enables CTLs to kill infected cells and contain infection.

Another key role for $CD8^+$ T cells is cytokine production, predominantly IFNγ, which has multiple functions. IFNγ upregulates components of the MHCI and MHCII antigen presentation pathway, increasing the quantity and diversity of peptides presented for $CD8^+$ and $CD4^+$ T cell recognition respectively. Additionally, IFNγ upregulates chemokines such as CXCL10 that attract more leukocytes to the inflamed tissue and further skews immune responses towards a Th1 phenotype [48].

Formation of memory is crucial aspect of cell-mediated immunity. Memory T cells can be broadly divided into central (T_{CM}, $CD45RA^-CCR7^+$) or effector (T_{EM}, $CD45RA^-CCR7^-$) memory subsets, which have different tissue homing, proliferation capacity and effector functions [49]. T_{EM} are able to immediately exert effector functions upon reactivation whilst T_{CM} mediate reactive memory, proliferating and differentiating into effector cells in response to antigen stimulation. More recently, the role of tissue-resident subsets (T_{RM}) in responses to vaccination and infection has begun to be elucidated [50,51].

An experimental model conceived by Sallusto and Lanzavecchia explained how different memory populations could result from the selective survival of effector cells and intermediates generated in the primary response [52]. This model proposes that the differentiation state of a T cell clone is determined by the duration of antigen and cytokine stimulation a T cell, which is

partly determined by the TCR affinity. T cell clones with high affinity TCRs will outcompete those with lower affinity TCRs for limited resources such as cytokines, antigen and DC help, and therefore receive stimulation for a longer duration. Additionally, polarisation of the T helper response towards Th1 is determined by the availability of IL-12 produced by recently stimulated DCs [52]. Pathogens and adjuvants differ in their ability to induce IL-12 production by DCs. Conditions that elicit high concentrations of IL=12 result in a Th1-polarised response, while those that do not induce IL-12 or induce IL-4 result in a Th2-polarised response.

1.1.2.2. Humoral immunity

The clonally diverse B cell receptor (BCR) is formed by combinatorial gene rearrangements in the Ig loci. V, D and J gene segments are rearranged in the heavy (H) chain locus whist V and J gene segments are rearranged in the light (L) chain locus [53]. The BCR is composed of two Ig H chains and two Ig L chains forming two antigen binding sites unique to that B cell clone. BCRs serve the critical roles of signal transduction and internalization of antigen for processing and presentation to Th cells. Antibodies are the secreted form of the BCR and consist of a fragment antigen-binding (Fab) region containing two antigen binding sites and a fragment crystallisable (Fc) region involved in effector functions through binding of Fc receptors (FcRs, Figure 1.1). In humans there are five different isotypes defined by the type of H chain used: IgD, IgM, IgG, IgA and IgE. Each of these isotypes has different effector functions determined by which FcRs they bind. Human IgG can be one of four isotypes (IgG1, IgG2, IgG3 and IgG4), and IgA can be IgA1 or IgA2. Each of these subclasses also have different properties and effector functions (Table 1.1).

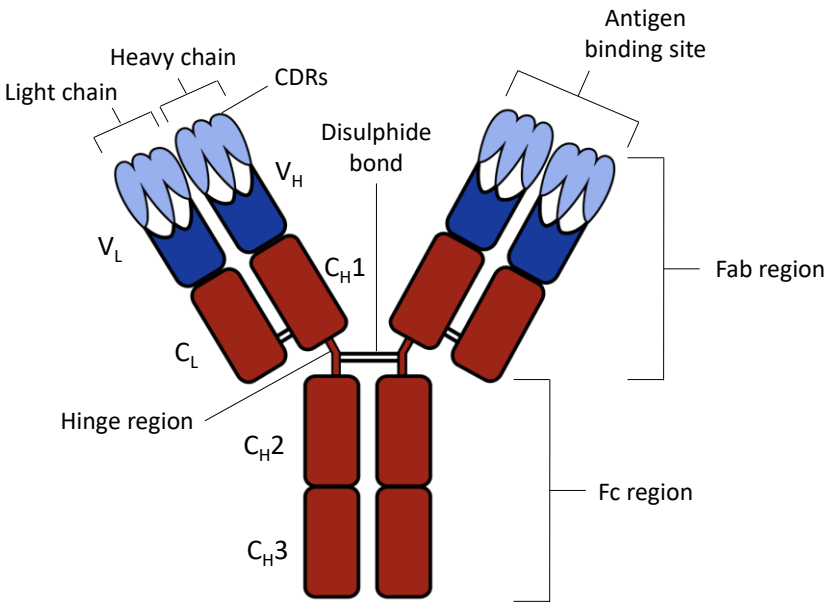

Figure 1.1. Antibody structure

Antibody structure consisting of two identical heavy chains and two identical light chains linked by disulphide bonds. The class of antibody is determined by the heavy chain used: μ (IgM), γ (IgG), α (IgA), ε (IgE) or δ (IgD), whilst light chains may be λ or κ. Additionally there are four subtypes of IgG (IgG1,2, 3 and 4) depending on the γ chain used. The light chains consist of a variable domain (V_L) and a constant domain (C_L), while heavy chains are formed from a variable domain (V_H) and three (IgD, IgG, IgA) or four (IgM and IgE) constant domains (C_H). The variable domains of both the heavy and light chains form the antigen binding sites whilst effector functions are mediated through the Fc region. The flexible hinge region is present in IgG, IgD and IgA but not in IgM or IgE.

Image own work, modified from Anypodetos https://commons.wikimedia.org/wiki/File:Antibody_with_CDRs.svg, CC BY.

Table 1.1. Antibody classes and effector functions

Immunoglobulin type	IgM	IgD	IgG1	IgG2	IgG3	IgG4	IgA	IgE
Physical properties								
Heavy chain	μ	δ	γ	γ	γ	γ	α	ε
Molecular weight (kDa)	970	184	146	146	165	146	160	188
Serum concentration (mg/mL)	1.5	0.03	9	3	1	0.5	2	$5x10^{-5}$
Half-life in serum (days)	10	3	21	20	7	21	6	2
Anatomic Distribution								
Transport across epithelium	+	-	-	-	-	-	+++	-
Transport across placenta	-	-	+++	+	++	+	-	-
Diffusion into extravascular sites	+	-	+++	+++	+++	+++	++	+
Functional activity								
Neutralisation	+	-	++	++	++	++	++	-
Opsonisation	-	-	+++	*	++	+	+	-
Sensitisation for killing by NK cells	-	-	++	-	++	-	-	-
Sensitisation of mast cells	-	-	+	-	+	-	-	+++
Complement activation	+++	-	++	+	+++	-	+	-

Table adapted from [54] Figures 2-28 and 2-29. IgG2 acts as an opsonin in the presence of one genetic variant of the phagocyte FcR which occurs in around 50% of Caucasions. The propoerties of IgA1 and IgA2 are similar and included under IgA.*

B cells develop in the bone marrow and undergo further maturation and activation within SLOs. B cell activation begins when cognate antigen binds to the BCR. B cell activation by foreign proteins is primarily a T cell-dependent process, although B cells can be activated in a T cell-independent manner. Antigen binding to the BCR initiates BCR signalling and endocytosis of the antigen-BCR complex. Antigen is processed and presented as peptides on MHC class II molecules to $CD4^+$ Th cells that were activated by the same antigen. After TCR-peptide/MHCII binding, Th (often T follicular helper cells [Tfh]) provide essential help to B cells for this process in the form of cytokine production (IL-4, IL-21) and the expression of costimulatory molecules (CD40L, ICOS) [55].

There are several distinct phenotypes of Th cells based on the expression of particular transcription factors and the cytokines produced. Th2 cells, defined by the expression of

transcription factor GATA3 and production of IL-4, IL-5 and IL-6, effectively help B cells, promoting secretion of IgG, IgM and IgA. In contrast, Th1 cells, driven by the transcription factor T-bet, predominantly produce IL-2 and IFNγ and provide less effective help to B cells for antibody production but were involved in killing bacteria within macrophages in mouse models [56]. Th17 cells express RORγt, produce IL-17 and induce neutrophils to clear *Candida* spp., helminths and some bacterial species [57]. The regulatory subset, Treg, express FOXP3 and play a crucial role in regulating inflammation and inhibiting self-reactive Th cells [58]. The most recent additions include Th9 and Th22 cells which produce IL-9 and IL-22 respectively and have multiple roles that are still being elucidated [59,60]. The development of these different subsets of Th cells is directed by the tissue microenvironment. The precise composition of cytokines present during a response is likely the result of a number of factors including the type of infecting microorganism, host genetics, previous immune history, dose of antigen and route of immunisation, all of which may therefore shape the type of Th that develops. In turn, the type of Th cell that a B cell interacts with can determine the isotype of antibody produced [61].

B cells proliferate and may undergo Ig class-switching, differentiating into plasmablasts that produce IgM in extrafollicular responses. However, activated B cells may also enter a lymphoid follicle and form a germinal centre (GC) response. Durable, high-affinity IgG is generated in these GC reactions, during which B cells undergo class-switching, somatic hypermutation, and differentiation into memory B cells and long-lived plasma cells. Tfh expressing CD4, CXCR5, ICOS and the transcription factor Bcl-6 provide help to GC B cells during this process and are key to the selection of high affinity clones that drive affinity maturation [62]. GC Tfh can leave the GC and develop into resting memory Tfh. Memory Tfh exist mainly within the SLOs and bone marrow but can recirculate in the blood [63,64]. These circulating $PD1^{+}CXCR5^{+}CD45RA^{-}$ $CD4^{+}$ T cells appear to be a peripheral counterpart of conventional lymphoid resident Tfh, potentially representing GC responses, and are a useful tool for human studies, in which lymphoid tissue is rarely available for analysis [63,65,66]. Circulating T follicular helper cells (cTfh) are also

heterogeneous and may be further defined by expression of chemokine receptors CXCR3 and CCR6: Th17-like (cTfh17) $CXCR3^{-}CCR6^{+}$, double-positive $CXCR3^{+}CCR6^{+}$, Th1-like (cTfh1) $CXCR3^{+}CCR6^{-}$, and Th2-like (cTfh2) $CXCR3^{-}CCR6^{-}$. These subsets have been associated with varying degrees of helper activity in different contexts [67]. In particular, $CXCR3^{-}$ Tfh have been associated with the production of broadly neutralizing antibodies against HIV [68] and Tfh17 induced by rVSV-ZEBOV vaccination were associated with antibody responses against Ebola [69]. Therefore, the type of cTfh induced by vaccination may be an indicator of the quality of the GC reaction and subsequently produced antibodies. Additionally, it has been proposed that these memory Tfh may retain their phenotype on reactivation [62]. If this is the case, then the context in which an antigen is originally seen (e.g. the cytokine microenvironment) could shape the efficiency and effector functions of secondary responses. This has broad implications for vaccine development and particularly for malaria vaccines, as the infant immune system may be repeatedly exposed to an antigen in the context of natural infection prior to vaccination with the same antigen.

Long-lived responses are critical for the success of most vaccines in order to achieve long-term herd immunity and durable individual protection. A longitudinal study conducted over 26 years demonstrated that antibody responses against viral antigens from live infections were extremely stable with estimated half-lives of 50 years for VZV and greater than 200 years for other viruses such as measles and mumps [70]. Responses to protein antigens from non-replicating sources, such as diphtheria and tetanus, were shorter-lived but still had estimated half-lives of 11-19 years. Long-lived plasma cells (LLPCs) in the bone marrow are predominantly responsible for the durable production of these antibody responses [71]. Persistent antigen may play a role in the generation of humoral immunity in chronic immune reactions, maintaining memory B cells (MBC) and inducing differentiation into short-lived plasmablasts [72]. However, this is not required for the long-term maintenance of humoral memory [73,74]. Pre-existing antibodies secreted by LLPCs, or “constitutive humoral memory”, is an important first line of defence

against reinfection but MBC enable an anamnestic response on antigen re-encounter that forms a "reactive humoral memory" [75,76]. MBC persist after an initial antigen challenge and may persist for decades in the absence of antigen [70,77]. On antigen re-encounter these cells are able to rapidly proliferate and may either differentiate into plasmablasts to produce antibody or re-enter a GC reaction and undergo further rounds of affinity maturation, supported by memory Tfh.

There are different phenotypes of MBC; IgG+ MBC preferentially differentiate into plasmablasts, whilst IgM+ MBC proliferate more and enter GC reactions [78]. However, MBC expressing each different Ig subclass and isotype may also have different roles [79]. Additionally, in a similar way to Th phenotypes, distinct B cell phenotypes may be induced depending on the antigen, infection or immunisation route, dose or adjuvant used [80]. Classical MBC express the co-stimulatory molecules CD21 and CD27. However $CD21^{-/lo}CD27^{-}$ exhausted or atypical MBCs have been described in a number of chronic infections such as HIV [81] and hepatitis C [82], as well as in malaria-exposed individuals [83-85]. These MBC have been shown to have a reduced ability to proliferate and differentiate into antibody-secreting cells and may contribute to the slow generation of humoral immunity to malaria [86] and poor humoral immunity against HIV [81].

1.2. Malaria

1.2.1. Global health impact: the need for a vaccine

In 2016 there were 216 million cases and 446,000 deaths from malaria. Around 90% of cases and deaths occur in sub-Saharan Africa, predominantly in children under 5 years old. Malaria is a global burden reported in 91 countries and affecting nearly half the world's population (Figure 1.2 [87]). However, of the 91 countries reporting malaria transmission, 15 (all in sub-Saharan Africa except India) carried 80% of the global malaria burden [87]. In addition to the huge toll on

lives and health within Africa, malaria also has major impacts on the economic productivity of endemic areas [88].

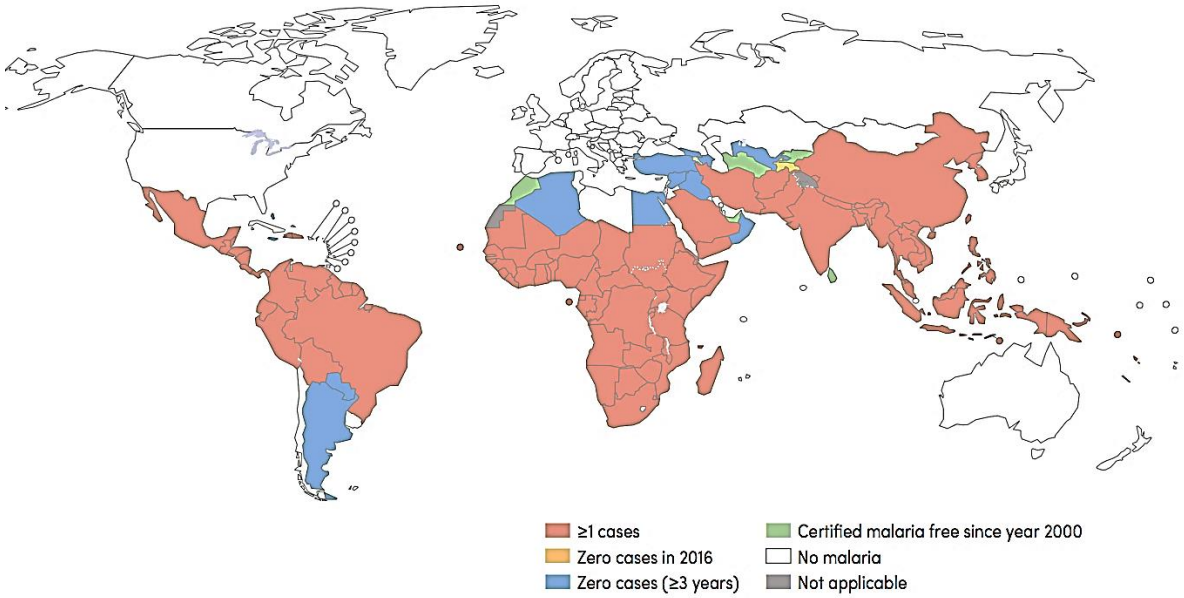

Figure 1.2. Populations at risk from malaria
Countries with indigenous cases of malaria cases in 2000 and their status by 2016. Countries in red are those which had indigenous malaria cases in 2016. Countries in blue have not reported an indigenous malaria case for at least three years and can apply to the WHO for certification of malaria-free status.

Image source: WHO world malaria report 2017 [87].

Malaria is a vector-borne tropical disease caused by protozoan parasites of the genus *Plasmodium* transmitted by female *Anopheles* spp. mosquitoes. Five species are known to regularly cause disease in humans: *P. falciparum*, *P. vivax*, *P. ovale*, *P. malariae*, and occasionally *P. knowlsei*. However, the majority of infections are caused by *P. falciparum* and *P. vivax*, both of which can cause severe disease. *P. falciparum* can cause severe disease in the form of cerebral malaria, severe anaemia, and pregnancy associated malaria. *P. vivax* can lay dormant as hypnozoites in the liver and cause recurrent bouts of malaria. The vast majority of cases in sub-Saharan Africa are caused by *P. falciparum* (99% in 2016). *P. vivax* incidence in sub-Saharan Africa is low because the majority of the population are negative for Duffy antigen, inhibiting *P. vivax* entry into red blood cells (RBC). It was previously thought that Duffy negative individuals could not be infected with *P. vivax*. However, more recently *P. vivax* infections have been

identified in Duffy negative individuals, although these are generally low-level asymptomatic parasitaemias (reviewed in [89]). However, outside of Africa, *P. vivax* is the predominant cause of malaria.

Over the last couple of decades there have been significant reductions in malaria incidence and mortality – there were 262 million cases in 2000 and nearly one million deaths [90].This was largely due to vector control efforts, (particularly the use of insecticide-treated bed nets), seasonal chemoprophylaxis and artemisinin-based combination therapy (ACT) for effective treatment [91]. However, most recently progress towards malaria elimination has stalled and the latest WHO malaria report indicated that malaria incidence increased by 5 million cases from 2015 and the number of deaths remained constant. Changes in malaria incidence in different countries are shown in Figure 1.3. It should be noted that despite this recent stagnation, the majority of these countries still have significantly lower malaria incidences than in the year 2000.

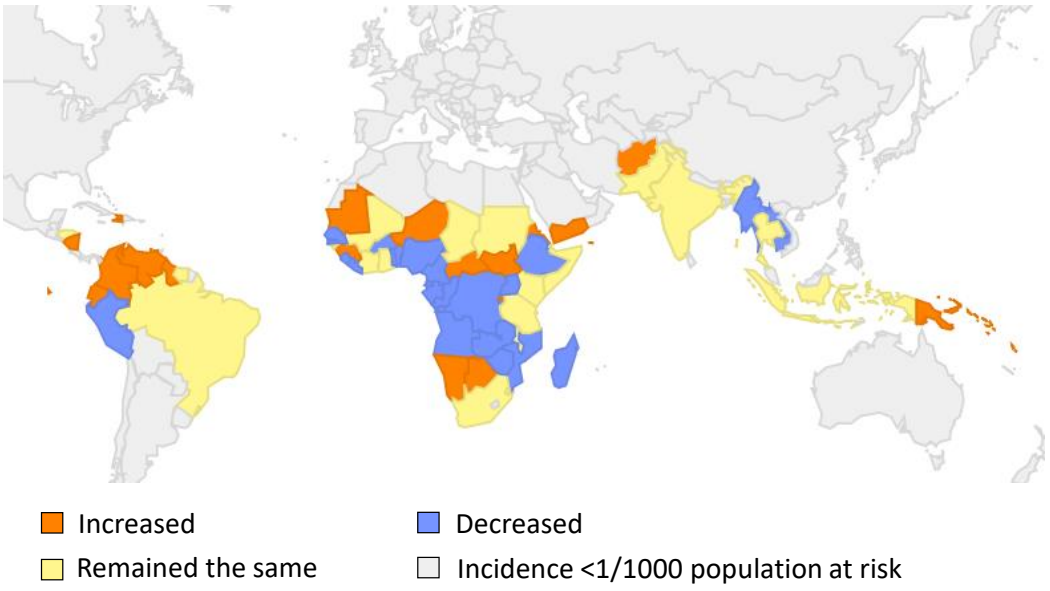

Figure 1.3. Global changes in malaria incidence

Changes in malaria incidence (confirmed cases) between 2015 and 2016. Map includes data for countries with indigenous malaria cases in 2000. Countries in grey had less than 1 case/1000 population at risk in 2016. “Increased”: increase in incidence greater than >1/1000 population at risk (living in areas with malaria transmission). “Decreased”: decrease in incidence > 1/1000 population at risk. “Remained the same”: change in incidence was <1/1000 but >-1/1000 population at risk.

Image own work, data sourced from WHO world malaria report 2017 [87] and Global Health Observatory data repository [92]

This stall in the reduction of malaria is thought to have occurred partly due to a reduction in the per capita funding in 34 out of 41 high-burden countries [87]. Other factors challenging the continued success of malaria elimination programmes include the spread of antimicrobial resistance (and particularly the danger of artemisinin resistance spreading out from the Greater Mekong subregion [93]), insecticide resistance (resistance to pyrethroids used in ITNs is present in 81% of malaria endemic countries [87]) and climate change causing unpredictable changes in transmission patterns [94]. With all of these challenges, an effective malaria vaccine is an essential part of achieving malaria elimination goals [95].

1.2.2. Lifecycle

The complexity of *Plasmodium* spp. lifecycles is one reason why after over 30 years of research and development, there is still no licensed malaria vaccine. This thesis focuses on humoral immunity to vaccines against *P. falciparum* and vaccine immunogenicity in malaria-exposed African countries. Therefore, the stages of the malaria lifecycle are outlined below with particular reference to *P. falciparum* (summarised in Figure 1.4).

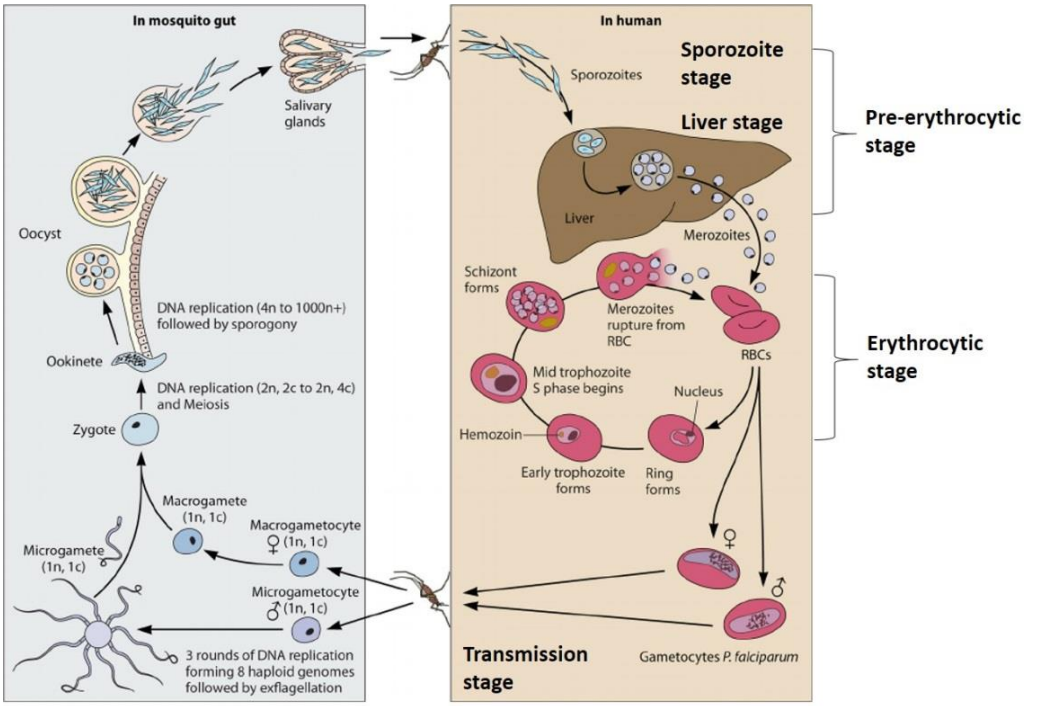

Figure 1.4. *Plasmodium* Lifecycle

Plasmodium spp. parasites are transmitted via a female Anopheles mosquito host (left) to a human host (right) during a blood meal. Some sporozoites remain in the dermis, others end up in the draining lymph node, whilst the rest travel in the bloodstream to the liver. Sporozoites invade liver cells, where they develop and replicate to form merozoites. After around seven days merozoites exit liver cells and enter the bloodstream, where they invade red blood cells (RBC) and begin the asexual reproductive stage. The replication cycle of the merozoites within RBCs lasts 36–72 hours (dependent on the *Plasmodium* species). Merozoites released from RBCs can invade other RBCs and continue to replicate, or may differentiate into gametocytes. Gametocytes concentrate in skin capillaries and can be taken up by a mosquito during a blood meal. Sexual reproductive stages occur within the mosquito midgut, resulting in formation of a motile ookinete, which embeds in the midgut epithelium forming an oocyst. Oocysts undergo cycles of replication to form sporozoites, which migrate to the salivary glands, ready to initiate a new infection at the next blood meal. Figure and legend adapted from [96].

1.2.2.1. Pre-erythrocytic stage

Sporozoites are injected into the host dermis along with the anticoagulants and the anaesthetic that mosquitoes inject prior to taking a blood meal. Infected mosquitoes have been shown to carry around 800-1000 sporozoites [97]. However, this varies widely and mosquitoes have been observed to carry as many as 40,000 sporozoites [97]. Tens to hundreds of sporozoites may be transferred per infectious bite, although these studies were mostly conducted using *P. berghei* infections of mice [98-101]. Recent work has demonstrated that sporozoites remain within the

dermis for between one and three hours after inoculation [102,103]. Sporozoites are highly motile and able to move by gliding motility and cell traversal. A proportion of these sporozoites will leave the dermis through a blood vessel [99,103], whilst others remain in the skin and around 20% end up in the draining lymph nodes, where they initiate an adaptive immune response [104]. Sporozoites in the bloodstream are rapidly carried to the liver, where they traverse the sinusoidal endothelial cells to access the liver parenchyma. Sporozoites traverse through multiple hepatocytes before arresting in one and entering the next stage of development within a parasitophorous vacuole [105,106]. Further development and multiple rounds of asexual replication result in the formation of thousands of merozoites, which are released into the circulation within merosomes between 7-10 days after infection [107].

1.2.2.2. Erythrocytic stage

Once free in the circulation merozoites invade RBC in a dynamic process that only takes two minutes [108]. Merozoites undergo multiple rounds of schizogeny within the RBC to form 10-30 new merozoites [109]. Merozoite egress occurs when the schizont ruptures the RBC and each new merozoite can then go on to infect a new RBC. This cycle of invasion, shizogeny and rupture occurs every 48 hours in *P. falciparum* infection and is responsible for the cyclical fevers and anaemia associated with the clinical presentation of malaria.

1.2.2.3. Sexual stage

Merozoites may also undergo sexual differentiation into gametocytes within RBC, which are transmitted to the mosquito host during a blood meal. The signals inducing this developmental pathway are still unclear but gametocyte production is increased by factors that negatively impact asexual multiplication such as drug treatment [110,111] or high parasitaemia [112]. Additionally, parasite-derived extracellular vesicles from infected RBC may be a mechanism of quorum sensing and can trigger gametocytogenesis [113]. Final maturation of the gametocytes and sexual reproduction occurs within the mosquito midgut, forming a zygote. The zygote

develops into a motile ookinete, which embeds into the midgut epithelium, where it forms an oocyst. Sporozoites develop within the oocyst and upon rupture, migrate to the salivary glands, where they are able to continue the lifecycle when the mosquito takes its next blood meal.

1.2.3. Pathogenesis

The pre-erythrocytic stage of infection is clinically silent. Clinical symptoms occur in synchrony with rupture of infected RBCs and release of parasite debris such as the malaria pigment haemozoin (HZ). Common malaria symptoms are mostly non-specific and include fever, chills, rigors, headache, fatigue, muscle aches and nausea. Severe malaria is complex and affects many different tissues. Some of the more severe manifestations of malaria, thought to be primarily due to low oxygen delivery are: severe respiratory distress, metabolic acidosis, cerebral malaria, hypoglycaemia, renal failure and pulmonary oedema [114]. Additionally *P. falciparum* infection during pregnancy (particularly in primigravidae) can cause preterm birth, foetal growth restriction, low birth weight and congenital malaria [115]. Oxygen restriction is mainly caused by the sequestration of infected RBC, which express adhesion molecules such as PfEMP1, which binds ICAM-1 and CD36 expressed on endothelial cells. This interaction between the parasite and host results in sequestration of infected RBC in the microvasculature of organs and an obstruction of blood flow [116]. The mechanisms causing these severe clinical manifestations are complex and not fully elucidated. However, it is thought that much of the pathology is caused by the immune response to infection [117].

1.2.4. Immunopathology

Severe malaria is characterised by high circulating levels of inflammatory cytokines, including TNFα, IL-1 and IL-6, and low levels of anti-inflammatory cytokines such as IL-10 [118-120]. TNFα, IL-1 and IL-6 are endogenous pyrogens and induce an inflammatory cascade [121]. IFNγ also plays a clear role in pathogenesis as mice deficient in IFNγ receptor do not develop cerebral malaria [122]. Equally in humans higher IFNγ levels have been correlated with increased disease

severity [123,124]. Cerebral malaria is uncommon in very young children with little malaria exposure but occurs after a number of infections [125]. It has been suggested that this may be due to priming of malaria-specific T cells in early life, leading to excessive IFNγ production on reinfection [126]. However, there is a clear role for proinflammatory cytokines and NO in the clearance of parasitaemia [127]. Similarly, IFNγ also plays an essential role in the clearance of infection and PBMC from Gabonese children with mild malaria were more efficient IFNγ producers in response to parasite-derived peptides than PBMC from children with severe malaria [128]. Naturally acquired clinical immunity may be dependent on a fine balance between the production of proinflammatory cytokines for parasite clearance and immunoregulation to avoid tissue pathology [117].

1.2.5. Naturally acquired immunity

In stably endemic regions the risk of severe disease and death from malaria is highest in young children and declines rapidly such that severe malaria is rare in adults [129]. However, susceptibility to clinical malaria episodes falls at a much slower rate and although febrile episodes are less common in adulthood, risk of infection continues throughout life. Asymptomatic parasitaemia appears to be a common occurrence and there is no evidence for the development of sterile immunity [130]. The decline in disease severity occurs in parallel with the development of a broad antibody repertoire against an array of *P. falciparum* antigens [131].

The precise immunological mechanisms that provide naturally acquired immunity (NAI) are still unclear [132]. However, there is a large body of evidence supporting a role for antibody against antigens expressed in the erythrocytic stages. For example, naturally infected children were observed to control parasitaemia after passive transfer of antibody from semi-immune adults [133-135]. Antibody may help clear parasitaemia through multiple mechanisms including inhibition of RBC invasion, inhibition of cytoadherence by infected RBC and antibody-dependent cytotoxicity [136-139]. In addition to IgG, which is most often focused on, IgM may play a role in

protection against infection. IgM-specific for galactose-alpha-1,3-galactose (α-gal), probably raised against commensal bacteria, cross-reacts with an epitope also found on *Plasmodium* spp. sporozoites (most likely acquired from mosquito derived proteins) [140]. Levels of α-gal-specific IgM have been correlated with protection from malaria infection in humans [141]. This is part of a developing understanding of the role of the microbiota in protection from malaria [142].

It is likely that the slow nature of NAI development is partly due to the antigenic diversity of *P. falciparum* [143]. The parasite-encoded variant surface antigens (VSA) presented on the infected RBC surface are thought to be key antibody targets but are highly variable [144]. The most well-characterised, PfEMP1, is encoded by around 60 *var* genes which undergo frequent non-homologous recombination and can therefore change even within the course of an infection [145]. The presence of strain-specific differences and clonally variable surface antigens means that a diverse repertoire of antibodies may be required to effectively clear an infection, which could explain why clinical immunity is only gradually acquired after multiple infections. The importance of antibodies against these antigens has been demonstrated in a number of studies in which antibodies against different groups of *var* gene products have been differentially associated with susceptibility to severe malaria [146,147].

Cellular defences also play a role in defence against malaria: IFNγ produced by NK and T cells activates macrophages to produce NO and can also inhibit intrahepatocyte growth [148]. $CD8^+$ T cells can recognise infected hepatocytes through parasite-derived peptides presented on MHC class I molecules at the cell surface and mediate direct cell killing through release of granzymes and perforin or via FasL [149]. Low level antibody and T cell responses against pre-erythrocytic antigens such as circumsporozoite protein (CSP) and thrombospondin-related adhesion protein (TRAP) have been observed in naturally exposed individuals [150]. It has been suggested that CSP-specific MBCs induced by natural exposure may play a role in NAI [151]. Additionally, cytokine responses against liver-stage antigen 1 (LSA-1) have been associated with parasite

clearance and protection from clinical malaria [152]. IFNγ, $CD8^+$ T cells and antibodies against sporozoites have all been shown to be protective [153]. A recent study observed that IFNγ responses to blood-stage antigens were common and associated with recent malaria exposure but not protection from subsequent infection [154]. In contrast, although responses to pre-erythrocytic antigens were uncommon, they were not associated with exposure and were associated with protection from subsequent infection. However, other studies suggest that responses against the pre-erythrocytic stages have little involvement with the development of NAI [155,156] and may instead be an indicator of exposure level [157].

The development of malaria immunity is balanced against immunopathology and immune regulation [117]. In this model, primary malaria infections in infants induce low levels of IFNγ and TNFα, which clear infection with minimal symptoms. However, malaria-specific T cells primed during the initial infection produce much higher amounts of IFNγ and TNFα in subsequent infections, increasing the risk of severe malaria. Further infections induce anti-parasite responses that effectively reduce the parasite load, reducing pathology and allowing the development of effective antibody responses. Additionally, a switch in the predominant T cell phenotype from IFNγ-producing Th1 cells to IL-10/TGFβ-producing regulatory T cells (Treg), allows a reduction in parasite load without excessive production of inflammatory mediators.

1.2.6. Malaria-related immunosuppression

Although polymorphism and antigenic variation are a likely cause for the slow acquisition of NAI, there is considerable evidence that malaria infection suppresses the host immune response in favour of parasite survival [158-163]. Immunosuppression in individuals repeatedly infected with malaria may be advantageous to the host (by limiting tissue damage caused by excessive immune responses) in addition to being a parasite mechanism of immune evasion.

There is a body of evidence demonstrating that blood-stage infection inhibits the formation of efficient memory responses against pre-erythrocytic infection. In one study proliferative T cell

responses to malaria antigens were reduced in all malaria patients regardless of disease severity or parasite density [164]. This immune unresponsiveness persisted for four weeks after treatment in nearly 40% of the patients. Suppression of responses to non-malaria antigens was also observed, but only in patients with moderately severe or cerebral malaria. The observed reduction in antigen responsiveness was associated with a loss of both Th and Treg cells from circulation [164]. In another study, *P. falciparum*-specific T cell responses were reduced in patients acutely infected with *P. falciparum* compared with uninfected semi-immune controls and these responses were short-lived [165]. During longer infections, there was no evidence of *P. falciparum*-specific T cells responses. In these cases, there was also a change in the composition of the T cells in circulation, with a decreased CD4:CD8 ratio. However, in acute infections, this was caused by a reduction in $CD4^+$ T cells, whilst in chronic infections this was caused by an increase in circulating $CD8^+$ T cells. These findings suggest that patients acutely or recently infected with malaria may respond differently to vaccination than malaria-naïve individuals and should be a factor considered in the design of Phase II and Phase III clinical vaccine trials.

1.2.6.1. Association between malaria infection and increased susceptibility to bacterial infection

Malaria-related immunosuppression may have broader consequences as several studies have suggested that humoral responses to unrelated antigens may also be suppressed by malaria infection [158-160]. Reduced antibody responses to tetanus vaccination were observed in malaria-exposed children in The Gambia compared with those that received malaria chemoprophylaxis [158]. This was followed up by later work which demonstrated reduced humoral immune responses to *Salmonella typhi* and tetanus vaccines in children with concurrent malaria [159]. Children with acute malaria infections also had reduced responses to meningococcal vaccine and these responses remained impaired even when vaccination occurred one month after resolution of infection [160]. The finding that suppression may remain after resolution of infection and can impact not only the development of immunity against malaria

but also responses to heterologous antigens highlights the potential clinical impact of malaria-associated immunosuppression.

The broader impact of malaria infection on the immune system has also been illustrated by the association between malaria infection and a higher incidence of other infectious diseases. A higher incidence of intercurrent bacterial infections was reported in children with repeat malaria infections in the 1970's [159]. However, more recent work has provided evidence of a direct causal relationship between malaria infection and increased susceptibility to bacterial disease [166]. In the first part of this study bacteraemia was observed less frequently in patients with sickle cell trait (HbAS), which is protective for malaria. In the second part of this study, a longitudinal analysis showed that bacteraemia incidence decreased in parallel with decreasing malaria incidence in coastal Kenya. This association is also apparent in regions where malaria has been eliminated or substantially reduced (e.g. Sri Lanka and Bioko Island, Equatorial Guinea). In these regions malaria elimination or reduction led to much greater reductions in mortality than predicted from estimates of malaria-related deaths [167,168]. This relationship has also been demonstrated by the use of insecticide treated nets (ITNs), which had a greater than expected impact on child mortality [169]. The precise mechanisms linking malaria and bacterial infection are unclear and are likely multifactorial. However, there is a growing body of evidence describing mechanisms by which malaria infection modulates the immune response in ways that are detrimental to the development of protective immune responses.

1.2.6.2. Disruption of T and B cell responses to pre-erythrocytic (PE) malaria

Malaria infection can be a highly inflammatory process and T cells that are chronically activated during chronic or repeated bouts of infection can become anergic [170] or functionally exhausted [171]. *Plasmodium* may directly exert an effect on CD4 and CD8 T cells through the activation of checkpoint inhibitors PDL1, LAG2 and CTLA3 [172]. Several other studies have also indicated a direct role for blood-stage infection on inhibiting the immune response against liver-

stage parasites [161,163]. In addition to cell-mediated killing of infected hepatocytes, antibodies against PE antigens can block hepatocyte infection *in vitro* and *in vivo* and could be a useful defence against malaria [173-175]. However, PE antigen-specific antibodies are slow to develop and found at low levels in malaria-endemic settings [176]. This may be explained by the ability of blood-stage infection to directly impair responses against the PE stage and could benefit the parasite by leaving the host susceptible to the next infection. Within a highly malaria-exposed population, this benefits the parasite by increasing the likelihood of establishing infection within the next human host. However, in addition to impeding ongoing responses, *Plasmodium* has also been shown to alter previously established responses [163]. Keitany *et al* demonstrated that blood-stage infection altered the quality of CSP-specific MBCs in mice, directly impairing responses to secondary infection. The CSP-specific B cell responses underwent premature contraction and the formation of splenic LLPCs was disrupted. The aberrant GC response that occurred in mice infected with wild-type *Plasmodium yoelii* but not in those infected with the attenuated form, resulted in the formation of CSP-specific MBCs with significantly lower CD73 and CD80 (markers of T cell interaction) expression and these cells primarily expressed unswitched BCRs [163]. Similarly, blood-stage infection in mice has also been shown to deplete pre-established heterologous LLPCs and MBCs, resulting in the loss of antibody responses and increased susceptibility to infections other than malaria too [177-179].

1.2.6.3. Impaired DC function

Another mechanism by which *Plasmodium* can either directly or indirectly modulate host immune responses is through modulation of DC function. DCs serve as a critical bridge between innate and adaptive responses, presenting antigens to T cells and producing cytokines that influence the type of response that develops [36]. Depending on the type of interaction and the signals received, T cells can either be primed or tolerised by interacting with DCs. DC-T cell interactions require multiple signals, with the first being presentation of antigen on MCHII (signal 1) and the second being co-stimulatory signals (signal 2).

There is evidence that malaria-related immunosuppression is directly associated with impaired DC-T interactions. During malaria infection signal 1 is intact, whilst signal 2 may be compromised [180]. Presentation of antigen in the absence of signal 2 can result in tolerance as a mechanism of preventing autoimmunity and inappropriate inflammatory responses. However, it appears that *Plasmodium* is able to co-opt this function to prevent effective anti-*Plasmodium* immune responses and enhance its survival. There is also evidence that *P. falciparum* infection inhibits DC maturation, resulting in a shift from IL-12 towards IL-10 production [161]. Parasitised RBCs have been shown to directly bind immature DCs (through interaction between PfEMP-1 on the iRBC and CD36 or CD51 on DCs). This interaction inhibits DC maturation and is associated with the reduced IL-12, increased IL-10 and inability to prime effective T cell responses [181].

Other work in mice and humans has suggested that DCs are activated by malaria infection [182,183]. However, these activated DCs have an unusual phenotype characterised by the upregulation of costimulatory molecules and production of chemokines and cytokines that are not usually produced during inflammatory responses [183]. *P. falciparum*-activated DCs prime antigen-specific $CD4^+$ T cells to become Th1 effectors that although involved in targeting intracellular pathogens are not optimal for antibody responses [183]. Direct modulation of DCs by parasite products has also been demonstrated. A *Plasmodium*-encoded cytokine directly suppresses T cell immunity [184]. This *Plasmodium* orthologue of macrophage inhibitory factor (MIF) enhances inflammatory cytokine production and induces antigen-experienced $CD4^+$ T cells to develop into SLECs rather than memory precursors. These SLEC $CD4^+$ T cells were more susceptible to apoptosis. *Plasmodium* MIF (PMIF) binds the host MIF receptor (CD74) on APCs and enhances TNFα and IL-12 production. Although this enhances APC activation, it results in Th1-skewed $CD4^+$ T cells producing IFNγ. High levels of both IL-12 and IFNγ can interfere with memory T cell formation by preferentially inducing SLEC responses [185]. In a study of the most advanced malaria vaccine candidate, RTS,S, protected individuals had more IL-2-producing CSP-specific $CD4^+$ T cells [186]. In mice, the presence of PMIF results in a reduction in the frequency

of IL-2-producing $CD4^+$ T cells [184]. In contrast, there was an increase in the frequency of IFNγ- and TNFα-producing $CD4^+$ T cells, which also expressed the Th1 transcription factor T-bet. The study by Sun *et al* also demonstrated a direct effect on protective immunity: T cells activated in the presence of PMIF conferred a lower degree of protection to mice challenged with *P. berghei*. Direct interaction between this parasite-derived cytokine orthologue and host DCs is able to skew T cell responses towards a Th1 phenotype and preferentially elicit SLECs at the expense of the formation of long-lived protective memory T cells. Additionally, *P. falciparum*-activated DCs have been shown to have similar transcriptional profiles to DCs activated by several viral vaccines [183]. This is interesting because it may have implications for the design of multi-stage targeting regimens utilising T cell-inducing viral-vectored vaccines and antibody inducing virus-like particles (VLPs).

1.2.6.4. Haemozoin

Haemozoin (HZ) is a haeme polymer produced by intraerythrocytic *Plasmodium* as a non-toxic form for storing toxic host haeme after haemoglobin catabolism [187]. HZ accumulates in macrophages, other leukocytes and a wide range of tissues throughout the body [188]. HZ may be able to activate immune responses through binding to TLR9 [189] possibly in combination with other *Plasmodium* DNA [190]. DCs exposed to HZ rapidly accumulate pigment, rendering them functionally impaired with reduced LPS-responsiveness and a failure to induce efficient T cell responses [180]. This process is sufficient to cause this effect (in absence of anti-inflammatory cytokines and other mechanisms) as transfer of antigen-pulsed HZ loaded DCs into naïve, uninfected recipient mice resulted in a similar failure of DCs to interact efficiently with T cells. Additionally, HZ-treated DCs fail to upregulate costimulatory molecules in response to TLR stimulation and CD40 ligation [180]. Additionally, deposition of HZ within the bone marrow may have long-term consequences on both bone structure and immune responses (described in more detail in Chapter 1.2.6.9).

1.2.6.5. Atypical MBCs

Hyporesponsive MBCs were first described in chronic HIV infections [81]. HIV-associated atypical MBCs were $CD27^{-}CD21^{lo}$, expressed FcRL4 and failed to proliferate in response to BCR cross-linking, therefore they were described as "exhausted". Other chronic infections, including hepatitis C and TB also drive the expansion of atypical MBCs and this may play a role in the inability to clear infection [191,192]. These cells are characterised by low expression of co-stimulatory receptors CD21 and CD27 (expressed by classical MBCs) and expression of markers not usually associated with MBCs such as T-bet and inhibitory FcRLs. An expansion of a similar subset is observed in malaria-exposed individuals [83]. Although one study suggested that these cells may be functional, producing neutralising *P. falciparum*-specific antibodies [193], this study did not directly detect antibody secretion from atypical MBC and more recent studies suggest these cells are poor antibody producers [86,194]. However, this may also reflect heterogeneity within the subset and atypical MBCs from individuals living in different malaria transmission settings may have different functional capacities [195]. This subset, which only represented 3-5% of peripheral B cells in malaria-naïve adults in the USA, expanded to 50% of circulating B cells within individuals chronically exposed to malaria [86]. These cells were hyporesponsive to BCR stimulation exhibiting reduced proliferation, diminished cytokine secretion and impaired ability to produce antibodies [195]. Atypical MBCs from malaria-exposed individuals have a distinct transcriptional profile to classical or activated MBCs [86] and an overlap in gene expression pattern with the exhausted MBCs observed in HIV [194]. However, in the case of chronic malaria exposure, these cells expressed FcRL5 rather than FcRL4 indicating the heterogeneity of these cells in different disease processes. Heterogeneity of atypical MBCs was also apparent within individuals, with some expressing FcRL5 and others not. Atypical MBCs that were $FcRL5^{+}$ were significantly more deficient in the ability to secrete antibody in response to BCR crosslinking than $FcRL5^{-}$ atypical MBCs. A longitudinal analysis in Malian children showed a correlation

between the incidence of febrile malaria and the expansion of T-bet^{hi} CXCR3^{+} atypical MBCs [196]. The level of T-bet expression was inversely correlated with BCR signalling and was driven by the Th1 cytokine environment. The lifespan of these cell types and possibility for long-term skewed immunity in individuals with chronic malaria exposure is unclear. However, atypical MBCs in HIV can persist for months after clearance of viraemia by anti-retroviral treatment and full normalisation of the MBC compartment can take years [81].

1.2.6.6. CXCR3^{+} cTfh

Circulating Tfh are also skewed towards a Th1 phenotype (express T-bet and CXCR3, produce IFNγ) by malaria [197]. Co-culture studies demonstrated that these cells provided less help for B cell isotype switching, proliferation and differentiation into antibody secreting cells than CXCR3^{-} cTfh (which most closely resemble bona fide GC Tfh [68]) [197]. They also provided less help to MBCs for differentiation into plasmablasts and were not associated with malaria-specific antibody responses. This less efficient Tfh phenotype is driven by malaria-induced Th1 inflammatory cytokines [197,198]. The chemokine ligands for CXCR3 (CXCL9, CXCL10, CXCL11) are induced by IFNγ and produced by neutrophils and inflammatory monocytes in the periphery [199]. During infection of CXCL10 knockout mice with *P. berghei*, CXCR3^{+} Th and Tfh accumulate in the spleen and enhance responses to infection [200]. Therefore the inefficient development of *Plasmodium*-specific antibody responses may also be driven by a temporal and spatial effect of the Th/Tfh cells induced in infection being drawn away from GC reactions in the SLOs towards peripheral sites of inflammation. In addition, malaria infection has been shown to cause GC disfunction and disrupt splenic architecture, which will also impair efficient T-B interactions and result in suboptimal antibody responses [162,163,198].

1.2.6.7. Tregs

Tregs utilise two key mechanisms to control immune responses: IL-10-mediated inhibition and CTLA-4-mediated repression of co-stimulation by APCs. An increased ratio of Treg:Th has been

observed in some studies [165] but not in others [164]. The role of Tregs in malaria is also unclear as some studies have indicated a role in suppressing protective responses [201,202] whilst others have shown Tregs to enhance protection [203]. Treg expansion during malaria infection has been associated with higher parasite densities and was shown to interfere with normal Tfh-B cell interactions [201]. The reason for the discrepancies between these studies may due to the temporally different roles of Tregs during malaria infection. Early in infection Tregs may play a protective role but later on disrupt the formation of protective humoral immune responses [202].

1.2.6.8. Effect of asymptomatic parasitaemia

Although NAI develops eventually after many years of repeat infections, semi-immune adults still often carry a large burden of "asymptomatic" parasitaemia. Using data taken from a number of cross-sectional studies of parasitaemia in malaria-endemic regions, around 5% of individuals in low-transmission areas had asymptomatic parasitaemia, whereas this could be over 50% in high transmission areas [204]. Asymptomatic infections have been observed to persist in the absence of new infections after 13 months [205] and in a malaria-endemic region, untreated asymptomatic infections had a mean duration of 194 days [206]. In areas of low transmission, this persistence of asymptomatic parasitaemia over the dry season aids the parasite by providing a reservoir to reseed transmission when mosquito populations rise again in the following rainy season [207]. Asymptomatic infections may also provide a tool for gametocyte transmission as asymptomatic infections are more likely to have gametocytes and gametocyte carriers were found to be more attractive to mosquitoes, increasing the likelihood of transmission in these individuals [208]. However, although these infections have vastly reduced inflammation compared with infection in children and malaria-naïve adults, there is emerging evidence that these infections are not truly asymptomatic and likely have a significant impact on the host, including chronic anaemia, increased incidence of bacterial coinfection and cognitive impairment [209].

1.2.6.9. Chronic impacts of malaria

One recent study demonstrated that HZ deposition in the bone results in chronic bone loss and is a significant cause of long-term "hidden" pathologies caused by repeated malaria infections [210]. Engulfment of HZ and other malaria products by osteoclasts in the bone marrow elicits a strong proinflammatory response (IL-6, IL-1α, IL-1β, TNFα). Prolonged inflammation in the bone marrow can cause inflammatory osteoporosis by increasing osteoclast activity. Persistence of HZ in these niches can result in sustained inflammation that causes chronic bone loss and growth retardation [211]. Additionally, prolonged immune activation driven by chronic immune activation may increase the risk of lymphoma formation [212] and enhanced telomere degradation has been described in birds chronically infected with *Plasmodium spp*. [213]. This suggests that malaria has many previously unappreciated impacts on chronically exposed individuals that include both immune modulation and changes in tissue homeostasis.

There is a growing body of evidence demonstrating how blood-stage infection is able to inhibit effective adaptive immune responses and memory formation. The potential clinical impacts of this phenomenon are beginning to be understood. As blood-stage infection can impair the development of immune responses against pre-erythrocytic antigens, this has a clear impact for the immunogenicity of malaria vaccines in malaria-exposed populations. However, it is also clear that malaria infection can impact heterogeneous responses and therefore may impact the immunogenicity of other vaccines in these populations. The impact of malaria exposure on the immunogenicity of both malaria and Ebola vaccination is the central focus of this thesis.

1.2.7. Vaccines for malaria

Despite control measures such as ITNs, seasonal chemoprophylaxis and ACT, which have had a significant impact on malaria incidence, an efficacious vaccine is likely a necessary tool for malaria elimination; it has been estimated that only in areas with the lowest levels of

transmission (fewer than three infective bites per person per year) could malaria be eliminated through a combination of current control methods [214].

As protective responses induced naturally take many years of repeated infection to develop, it is likely that an effective vaccine response will differ from NAI. Additionally, NAI only provides protection against clinical disease and semi-immune individuals often carry a high burden of parasitaemia asymptomatically [204]. Although these infections are clinically silent, there is emerging evidence that they may have a higher impact than previously appreciated [209]. For these reasons, development of candidate malaria vaccines has not solely focused on the erythrocytic stage. Vaccines are being developed against sporozoites, liver-stage, blood-stage and sexual stages of the parasite and a combination approach may be required to achieve high-level efficacy [215,216]. Therefore a successful vaccine or vaccine regimen against malaria will likely need to induce both $CD8^+$ T cell responses against the intracellular hepatocyte infection as well as $CD4^+$ and B cell responses against the erythrocytic and sporozoite forms [217].

Since the first attempt to vaccinate humans against malaria using formalin-inactivated *P. vivax*-infected RBC in 1946 [218], there have been over 200 clinical trials and many more pre-clinical trials of vaccines against *P. vivax* or *P. falciparum* (listed by clinicaltrials.gov [219]). Despite this significant effort, there is still no licensed malaria vaccine. The updated Malaria Vaccine Technology Roadmap [220] provides a goal of the development of a vaccine which achieves 75% efficacy over a two year period. However the original goal targeted for 2015 of a vaccine that provides over 50% efficacy lasting more than one year has still not been achieved. Current vaccination strategies, key antigen targets at each stage of the parasite lifecycle and clinical progress of key vaccine candidates are summarised below.

1.2.7.1. Whole sporozoite vaccines

Whole sporozoite vaccines use sporozoites that are modified in some way or given with drug cover to prevent development of blood-stage infection. Therefore, vaccinees experience only

the clinically silent stage of infection whilst raising an immune response against sporozoites that protects against wild-type sporozoite challenge. Radiation attenuated sporozoites (RAS) was one of the first malaria vaccine methods to be tested and was able to provide >90% protection in humans [221,222]. A major drawback of this method was the requirement for over 1000 mosquito bites to achieve protection [222].

A key advancement was the aseptic isolation of RAS which could then be cryopreserved and delivered by intravenous (IV) injection (PfSPZ vaccine) [174]. In non-human primate (NHP) models protection induced by PfSPZ vaccination was mediated by liver-resident $CD8^+$ T cells against CSP [223]. This vaccination strategy has provided a high level of sterile protection against homologous CHMI in malaria-naïve adults. Sterile protection was observed in 64% (9/14) of individuals given three doses of $9.0x10^5$ sporozoites at eight-week intervals and challenged with the same strain 19 weeks later [224]. Additionally 83% (5/6) of individuals were sterilely protected from a repeat challenge with a heterologous strain 33 weeks after the last PfSPZ dose. Heterologous protection was also demonstrated by an initial challenge at 3 weeks after the last PfSPZ dose but was not durable, with only 10% (1/10) of individuals protected against heterologous CHMI 24 weeks after the last dose [225]. PfSPZ has been shown to be deliverable and safe in Malian adults and there was evidence of significant protection with only 66% (27/41) of vaccinees developing malaria in the following malaria season compared with 93% (37/40) of unvaccinated controls [226].

However, it appears that malaria-exposed adults may be hyporesponsive to this vaccination strategy as anti-CSP IgG titres were significantly lower in Mali and Equatorial Guinea compared with the US [226,227]. Unfortunately comparison of immunogenicity and efficacy of this strategy with alternative vaccines is difficult due to the different doses, regimens, efficacy endpoints and statistical analyses used. Difficulties with this vaccination strategy include the requirement for a

liquid nitrogen cold chain, difficulties with IV delivery in young infants, particularly in resource-poor settings and the need for aseptic mosquito dissection in specialised insectaries.

An alternative whole sporozoite strategy is the delivery of wild-type sporozoites by mosquito bites under chloroquine cover, allowing full liver-stage development but killing the parasites upon entry into the circulation and preventing the development of blood-stage infection. The first human study of this method in 2009 used administration of chloroquine for 13 weeks, during which volunteers received three "doses" of 12-15 infectious mosquito bites at one-month intervals. This regimen provided 100% (10/10) sterile protection against homologous CHMI eight weeks later [228]. This regimen also provides durable protection, with 67% (4/6 volunteers sterilely protected against homologous CHMI after two years [229]. However, this requires mass drug administration which may be difficult to implement and could effectively be achieved by seasonal chemoprophylaxis alone. Additionally, concurrent infections in vaccinees within endemic areas could interfere with administered mosquito bites and there is a possibility of breakthrough infection. As with PfSPZ, protection against heterologous CHMI was limited [230]. A third strategy is the use of genetically attenuated parasites (GAP) which also arrest development in the liver-stage [231]. Again, breakthrough infections are a potential problem with this method [232]. However, recent evaluation of GAP with three mutations did not cause breakthrough infections, was safe and immunogenic [233]. Phase II trials to assess efficacy of these vaccines are ongoing.

1.2.7.2. Subparticle sporozoite vaccines

Whilst briefly in the skin and bloodstream, sporozoites are a target for humoral immunity. Antibodies against the main sporozoite surface protein, CSP may provide protection by inhibiting gliding motility, cell traversal and hepatocyte invasion [234,235]. However, due to the short window of opportunity, very high levels of circulating anti-CSP-specific IgG may be needed to induce sterilising immunity. The most developed subparticle sporozoite vaccine is RTS,S/AS01.

RTS,S is a VLP formed of the 18 copies of the NANP repeat region and a portion of the C-terminal domain of PfCSP fused to the hepatitis B surface antigen (HBsAg) in a 1:4 ratio [236]. This is formulated with GlaxoSmithKline's (GSK's) proprietary liposomal-based AS01 adjuvant system. This vaccine has demonstrated significant efficacy in a Phase III study of infants but this protection was short-lived and will likely require a yearly booster dose to maintain protection [237]. In infants aged 5-17 months, a 0-1-2 month schedule had an efficacy of 43.6% over the initial year but this was reduced to 16.8% over four years [238]. This vaccine has received a positive opinion from the European regulatory authorities and WHO have recommended large-scale pilot implementations of the three dose regimen with a fourth booster dose at month 20 [239]. High antibody titres against the NANP repeats from CSP are associated with protection [240] but $CD4^+$ T cells may also have a role [241]. However, a full mechanism explaining protection remains to be elucidated. Clinical testing has also begun on a similar VLP vaccine, R21, which consists of a single subunit without the excess HBsAg [242]. It is hoped that the increased ratio of PfCSP to HBsAg may lead to improved anti-NANP IgG titres compared with RTS,S. Clinical trials are being conducted to test R21 formulated with Matrix-M or AS01B adjuvants. In mice, adjuvanted R21 induced high titres of NANP-specific IgG, even at low doses [242]. High levels of sterile protection against *P. berghei* challenge were observed and efficacy could be increased by co-administration with viral-vectored vaccines [242].

1.2.7.3. Liver-stage vaccines

Liver-stage vaccines aim to induce potent $CD8^+$ T cell responses against parasite antigens expressed on the surface of infected hepatocytes. Viral vector and DNA vaccines both work by delivering a gene sequence to the host cell, which is then transcribed and translated into a protein product and can be processed and presented to immune cells on MHC molecules. DNA vaccines initially showed promise in mice [243] but had much lower immunogenicity in humans [244]. Boosting a DNA prime with a viral vectored vaccine enhanced immunogenicity and provided partial protection against CHMI in malaria-naïve adults [245-247]. However, more

recent work has focused on heterologous prime-boost with adenovirus and poxvirus vectors. These regimens have been tested against a wide range of diseases including Ebola [248], hepatitis C [249], TB [250], influenza [251], and malaria [252] and have good safety profiles. The use of chimpanzee adenoviruses (ChAd) instead of human adenoviruses avoids the problem that many people have pre-existing neutralising titres against human adenoviruses [253]. Although in sub-Saharan Africa, pre-existing antibody titres against ChAd serotypes can also be high, no association with vaccine responses or reactogenicity has been observed [254]. For malaria vaccination, the leading candidate viral vector regimen uses ChAd serotype 63 (ChAd63) prime and modified vaccinia virus Ankara (MVA) boost eight weeks later [252]. Both vectors express the gene for *P. falciparum* thrombospondin related adhesion protein (TRAP) (a protein essential for sporozoite motility and hepatocyte invasion [255]) fused to a multi-epitope (ME) string. The ME string contains predominantly $CD8^+$ T cell epitopes from several malaria antigens including LSA1, CSP and TRAP, in addition to some $CD4^+$ T cell and B cell epitopes [256]. This regimen is safe and induces potent T cell and antibody responses [252]. Sterile protection was achieved by this regimen in 21% (3/14) of individuals undergoing heterologous CHMI, with a further 36% demonstrating a delay to parasitaemia [252]. Immunogenicity translated well into Kenyan adults [257] and protection in Kenyans was high, with a 67% reduction in infection over eight weeks [258]. However, no efficacy was observed in Senegal [259]. The UK and Kenyan efficacy trials indicated a T cell correlate of protection, although anti-TRAP IgG may also contribute [260]. This regimen was also safe and immunogenic in infants in Burkina Faso and The Gambia [261,262]. Efficacy results from a Phase IIb study in infants in Burkina Faso are awaited. Work is also ongoing to identify new liver-stage antigens that may confer higher levels of protection [263].

1.2.7.4. Blood-stage vaccines

Protection against blood-stage malaria is thought to be primarily mediated by antibodies that target infected RBC or inhibit invasion into RBC [264]. Efforts have been focused on a few merozoite antigens and this field has struggled to produce an efficacious vaccine. Induction of

strain specific antibody and redundant invasion pathways have been particular problems [216]. Additionally *in vitro* studies have indicated that antibodies have less than one minute to block invasion by merozoites [265] and therefore it is likely that exceptionally high circulating titres of high affinity antibody would be required to successfully block invasion. Perhaps the most promising candidate antigen to date is *P. falciparum* reticulocyte-binding homologue 5 (RH5). Interaction between RH5 and basigin (CD147) is essential for RBC invasion [266]. RH5 is highly conserved and antibody against it has been shown to inhibit *in vitro* all *P. falciparum* strains tested so far [267,268]. Pre-clinical trials of protein RH5 vaccines have been successful in mice and NHPs, in which protection was mediated by high titres of anti-RH5 antibody with growth inhibitory activity [268,269]. Human vaccination against RH5 can induce high titres of neutralising antibody [270] but there are currently no human efficacy data for an RH5-based vaccine. Various different platforms based on RH5, including viral vectored administration, protein-in-adjuvant and VLPs are now being tested in humans.

1.2.7.5. Transmission blocking vaccines

Transmission blocking vaccines aim to block the sexual stage of malaria, which occurs within the mosquito midgut. Vaccines against this stage induce antibodies in the human host, which kill gametocytes or prevent their fusion to form ookinetes within the mosquito vector [271]. Although this does not protect the vaccinee from infection or clinical symptoms, in endemic populations with high levels of asymptomatic carriers, transmission reduction could provide protection through herd immunity [271]. A number of candidate antigens have been identified from the gametocyte (Pfs48/45, Pfs230) and ookinete (Pfs25) surface and have performed well in pre-clinical studies [272]. In initial clinical trials a high concentration of anti-Pfs25 antibody was required for a 50% reduction in oocyst intensity [273] and the level required to impact transmission in the field is still unclear [274,275].

These initial efficacy results provide the malaria vaccine field with a platform on which to build. No vaccine has yet demonstrated efficacy in the field that meets the goals initially outlined by WHO for 2015. Vaccines that elicit significant levels of protection in the malaria-naïve populations they are first tested in are often found to have reduced immunogenicity and efficacy in malaria-exposed populations. A better understanding of the immune responses elicited by these vaccines, particularly within malaria-exposed individuals will likely be required for further advances.

1.3. Ebola

The need to effectively vaccinate adults in malaria-exposed populations was dramatically highlighted by the Ebola outbreak that occurred in West Africa in 2014-2016. In addition to examining the impact of malaria exposure on the response to malaria vaccines, I have investigated the impact on responses to non-malaria antigens. In late 2014 clinical testing of Ebola vaccine candidates begun at the Jenner Institute. Candidate regimens were tested in nine different clinical trials involving five different vaccines. In this thesis, with the focus on examining what impacts vaccine immunogenicity in malaria-exposed populations, I report the immunogenicity of a candidate Ebola vaccine regimen testing ChAd3-EBO-Z boosted one week later with MVA-EBO-Z. The testing of this regimen almost simultaneously in the UK and Senegal enabled a direct comparison of vaccine immunogenicity in UK and African populations and an investigation into the effect of malaria exposure.

1.3.1. Ebola virus disease

Ebola virus disease (EVD) is a severe and often fatal disease caused by Filoviruses of the genus *Ebolavirus*. Of the five officially identified species, *Zaire ebolavirus* (EBOV), *Sudan ebolavirus* (SUDV) and *Bundibugyo ebolavirus* (BDBV) have caused EVD in humans [276]. The other species are *Reston ebolavirus* (RESTV), which infects NHPs and pigs but has not caused symptomatic human infection [277], and *Taï Forest ebolavirus* (TAFV) which has caused only one, moderately

severe human infection [278]. Additionally, a sixth *Ebolavirus* species *Bombali ebolavirus* was recently isolated from bats in Sierra Leone [279]. However, there is currently no direct evidence that this has infected humans.

EVD causes an acute illness with initial symptoms that include fever, headache, sore throat, weakness, abdominal pain and nausea. This is followed by diarrhoea, vomiting, symptoms of impaired kidney and liver function, and in around 18-36% of cases, a haemorrhagic fever [276]. The average case fatality rate, which is highest for EBOV, is around 50% but has been as high as 80-90% past outbreaks [280,281]. The first documented cases occurred during simultaneous outbreaks in Yambuku, Democratic Republic of Congo (DRC, then Zaire) [282] and Nzara, South Sudan (then part of Sudan) in 1976 [283]. Since then, there have been over 20 EVD epidemics, mostly caused by EBOV or SUDV. Evidence points to bats as a reservoir species [284,285], with symptomatic infections identified in chimpanzees and duikers [286,287]. Transmission to humans is thought to occur through contact with infected animals and can then occur from person to person through contact with infectious body fluids [288].

1.3.2. 2014-2016 epidemic

Prior to December 2013, there had been a total of 2344 cases and 1546 deaths from EVD across DRC, Republic of Congo, Sudan, Gabon and Uganda [289]. These were mostly sporadic incidences occurring in remote locations and transmission occurred between infected individuals and their carers, family members and healthcare workers. The majority of these outbreaks involved less than 100 cases with the largest occurring in Uganda in 2000-2001 (SUDV) and involving 425 cases and 224 deaths [289]. However an epidemic of unprecedented proportions occurred in West Africa in 2014-2016 which saw 28,646 cases and 11,323 fatalities [290]. The index case is now thought to have been an 18-month-old boy in Meliandou, Guinea at the end of December 2013, however it took until late March 2014 until the first cases were officially recognised. There had never been a case of EVD in West Africa before and Guinea is 1700 miles from Gabon, the

closest country to have previously reported EVD. The occurrence of the outbreak close to the border between two other countries, Liberia and Sierra Leone, resulted in the spread of infection to these countries in the first incidence of an EVD outbreak occurring across multiple countries. Although the epidemic centred around Guinea, Sierra Leone and Liberia, cases were also reported in Nigeria, Senegal and Mali. Outside of Africa, cases occurred in Europe and the USA where healthcare workers were repatriated or infected travellers were incubating the virus. In Spain and USA onward transmission to healthcare workers caring for infected patients also occurred.

Aside from the international impact this outbreak was unique for a number of other reasons: crucially, it was the first to spread from isolated rural areas to urban areas including the capital cities of all three of the hardest-hit countries. Here, densely populated areas with poor sanitation contributed to the spread and strain on already over-stretched healthcare resources. The outbreak also took an enormous toll on healthcare workers (HCWs), with an incidence 100-fold higher than the general population in the early stages of the outbreak. Overall, HCWs accounted for 12% of cases, with a higher fatality rate – 58.2% compared with 39.5% in the general population [290,291]. In regions where there were only one or two doctors per 100,000 people, every loss of a doctor or nurse considerably added to the strain on healthcare resources. Finally, in August 2014 the outbreak was declared by WHO as a "public health emergency of international concern". This initiated an international response with deployment of HCWs, staff from non-governmental organisations, laboratory staff and military personnel on a scale never seen before. For example, the Center for Disease Control (CDC) deployed four times as many staff during the outbreak than during the smallpox eradication campaign [290]. The international reach of the outbreak also sparked an increased level of funding and effort into the research of therapeutics and vaccines in a race against time to find something that could help end the outbreak.

1.3.3. Ebola therapeutics

Part of the reason for the high fatality rate of EVD is a lack of targeted treatments. Management of fluid loss and rehydration is about all that could be done for patients in many of the Ebola treatment units (ETUs). For patients treated in the USA and Europe, one-third received mechanical ventilation and one-fifth received renal support [292]. The availability of resources to provide this level of support for patients is likely the primary reason for the better clinical outcomes observed (a mortality rate of 18.5%) [292]. A number of experimental therapies were tested during the outbreak, initially on a compassionate basis and then in more organised clinical trials. One of the most advanced at the time of the outbreak was a cocktail of anti-Ebola monoclonal antibodies named ZMapp, which had previously performed well in NHPs [293]. ZMapp was tested in a clinical trial against the standard of care but only 72 patients out of the 200 planned could be recruited and although mortality was reduced with ZMapp (22% versus 37% in controls), this was not statistically significant [294]. Convalescent plasma from Ebola survivors was also a possible strategy but showed no benefit in a trial in Guinea [295]. A number of anti-viral agents such as Favipiravir were also tested. However, in the outbreak setting it was not often possible for ethical and practical reasons to test therapeutics in randomised studies to determine efficacy and therefore it is unclear how well these really worked [296,297].

1.3.4. Ebola vaccines

The Ebola virus has seven genes encoding several proteins: nucleoprotein (NP), viral protein 40 (VP40) polymerase cofactor VP35, transcription activator VP30, VP24, an RNA-dependent RNA-polymerase and a glycoprotein (GP) [298]. GP is the single protein expressed on the surface of the Ebola virion and plays an essential role in attachment, fusion and entry into host cells [299]. Therefore, GP is a key antigenic target for vaccines and has been the focus of most vaccine research. A number of pre-clinical trials of different vaccines had taken place during the 1990s

and early 2000's. However, only four phase I clinical trials had been completed prior to the 2014-2016 outbreak [300]. The first Ebola vaccine trial in humans in 2003 was of a three-plasmid DNA vaccine consisting of the genes for a transmembrane-mutated GP from EBOV and SUDV and the EBOV NP [301]. Later trials attempted to enhance immune responses using a recombinant adenovirus serotype 5 (rAd5) vector encoding the GP gene with a point mutation [302]. However, immunity was decreased by pre-existing anti-Ad5 immunity. This sparked a move towards development of viral vectored vaccines using less frequent human serotypes (Ad26, Ad35) and chimpanzee adenoviruses (ChAd3, ChAd63). ChAd3 expressing either EBOV GP alone (monovalent) or EBOV and SUDV GP (bivalent) demonstrated 100% efficacy against lethal Ebola challenge in NHPs [303]. Additionally, durable protection was observed 10 months after vaccination if ChAd3 was boosted with bivalent MVA [303]. At the time of the outbreak, the ChAd3 vaccine was one of the most advanced candidates. A recombinant replication-competent vesicular stomatitis virus (rVSV)-based vaccine with EBOV GP replacing the VSV GP had also progressed through pre-clinical testing and showed good efficacy in NHPs [304,305].

During the outbreak the enhanced funding and the acceleration of regulatory and ethical reviews of trial protocols expedited clinical development of Ebola vaccine candidates. The two leading vaccine candidates that entered Phase I clinical trials were the ChAd3-vectored vaccines and the rVSV vaccine [300]. Monovalent and bivalent ChAd3 vaccines were tested in the US, UK and other European countries [248,306,307] and later in Mali [308]. ChAd3 was also trialled in combinations with Ad26- and MVA-vectored vaccines [248,309]. The MVA-vectored vaccine initially tested (MVA-BN-Filo) was a quadrivalent vaccine encoding GPs from EBOV, SUDV and Marburg virus, with NP from TAFV. A monovalent MVA-EBO-Z carrying just the EBOV GP insert has since been developed and tested in clinical trials (clinical trials.gov: NCT02451891, NCT02485912). A number of other novel Ebola vaccine candidates have also been developed since the outbreak, including a new rAd5-based vaccine and a VLP-based vaccine [300,310].

The WHO chose two vaccine candidates (ChAd3-EBO-Z and rVSVΔG-ZEBOV-GP) to be tested sequentially in a phase III ring vaccination study in Guinea. The rVSV vaccine was chosen to be assessed first and by the time this was complete there were too few incidents remaining to assess efficacy of a second candidate. Therefore, the only human efficacy of an Ebola vaccine candidate to date is for rVSVΔG-ZEBOV-GP. The rVSV vaccine demonstrated 100% short-term protective efficacy in an open-label, cluster-randomised ring vaccination trial in Sierra Leone and Guinea [311,312]. Although not yet licensed, rVSVΔG-ZEBOV-GP has been granted Breakthrough Therapy designation by the U.S. FDA and Priority Medicines status from the European Medicines agency and is currently being used to support outbreak control in the DRC [313]. This vaccine has now been tested in eight phase I and four phase II/III clinical trials involving around 17,000 subjects. In these studies it was moderately reactogenic but safe, immunogenic and provided at least short-term efficacy [314].

Multiple trials have indicated that rVSVΔG-ZEBOV-GP effectively induces Ebola GP-specific antibodies [315-317] but T cell responses may be limited [318]. ChAd3 induced comparable antibody titres, with neutralising activity, and these could be boosted by a dose of MVA, even if given with a very short interval of just one week [248]. This vaccine regimen additionally induces high levels of Ebola-specific T cells [248]. Immune correlates of protection have been difficult to define and it is likely that both GP-specific antibodies and $CD8^+$ T cells play a role in protection [319]. There is evidence for protection being mediated by vaccine-induced humoral immunity from NHP studies [303,304]. Additionally in humans early and increasing IgG titres against Ebola are associated with better survival rates [320,321].However, passive transfer of antibody in NHP studies and human infection has not always had a protective effect suggesting other components may also be involved [295,322]. Durable protection in particular has been associated with $CD8^+$ T cells producing TNFα and IFNγ [303]. Additionally $CD8^+$ T cell depletion studies in macaques vaccinated with a rAd5 vaccine also demonstrated a clear role for $CD8^+$ T cells [323]. Transcriptomic analysis of survivors from the recent outbreak revealed $CD8^+$ T cell memory

signature compared with those with fatal outcomes [324]. Although it appears likely that both T cells and antibody play a role in protection more work is needed to better define immunological correlates of protection in humans. It is also possible that correlates of protection are different for different vaccines and that protection mediated by vaccine-induced immunity may well differ from protective responses observed in survivors.

Although the outbreak was largely contained through community engagement, infection control measures and effective contact tracing [289], the outbreak sparked an advance in vaccine research and preparedness for outbreaks. However, the importance that these vaccines work well in the populations that need them should not be forgotten. For Ebola and other emerging infectious diseases such as Chikungunya and Zika, this means effectively vaccinating malaria-exposed adults. One of the focuses of this thesis is the impact of malaria on vaccine responses and the Ebola vaccine trials conducted in the UK and West Africa were an important opportunity to gain insight into this.

1.4. CMV

During my research into the factors associated with reduced vaccine responses in African cohorts compared with UK cohorts I discovered an association between cytomegalovirus (CMV) serostatus and reduced immunogenicity of viral vectored vaccines in both UK and African cohorts. Therefore, I provide here an overview of CMV and a summary of the literature surrounding the impact of CMV on the immune system and associations with vaccine responses.

1.4.1. CMV epidemiology and pathogenesis

Human CMV is a betaherpesvirus which causes what is most often a mild or asymptomatic acute infection followed by the establishment of life-long latency. The exact site of latency is unclear but appears to be in cells of myeloid lineage [325]. It is thought that CMV can replicate productively in a number of cell types and genomic viral DNA has been detected in

monocytes/macrophages, lymphocytes, $CD34^+$ bone marrow cells, immature DCs and endothelial cells [326]. Reactivation is usually asymptomatic in immunocompetent hosts but can cause significant morbidity and mortality in immunocompromised hosts (e.g. AIDS and transplant patients) in which it can cause retinitis, hepatitis, encepahilitis and pneumonitis [327]. Transplacental transmission can result in congenital disorders including neuronal impairments, growth retardation, jaundice [328].

CMV is transmitted in body fluids including breast milk, saliva and blood or transplacentally and seroconversion often occurs in childhood [329]. CMV is highly prevalent: around 30-50% of young adults in developed countries are seropositive and this increases with age to over 90% in elderly adults [329]. In less developed countries CMV seroconversion occurs early in life and almost all young adults are seropositive [330].

1.4.2. Immune responses to CMV

CMV is the largest of the human herpesviruses, containing a 235kb genome encoding around 165 genes [331]. A large portion of these genes are devoted to evading the human immune system. A major immune evasion mechanism is the downregulation of MHC I to reduce antigen presentation to $CD8^+$ T cells [332]. CMV achieves this through multiple mechanisms, including proteins that block the generation or export of MHC I-peptide complexes [333-335]. CMV is also able to hinder peptide presentation on MHC II through a protein that targets MHC class II DR-α and DR-β to the proteasome for degradation [336]. The downregulation of these molecules should make these cells a target for NK cell-mediated lysis through the recognition of "missing self". However, CMV also encodes factors to impede NK cell recognition, including the expression of virus-encoded MHC class I homologues [337]. Additionally CMV encodes a protein homologous to a host signal peptide that stabilises expression of the non-classical MHC I molecule HLA-E on the cell surface [338]. Peptide-HLA-E is recognised by the inhibitory NK cell receptor CD94/NKG2A and prevents NK-cell mediated lysis of infected cells [338]. CMV also

encodes a number of other homologues that subvert the host immune system including homologues of chemokines, chemokine receptors, FcRs, the immunosuppressive cytokine IL10 and anti-apoptotic proteins [339,340].

CMV's extensive immune evasion arsenal aids the establishment of latency. However CMV infection is not immunologically silent and significant CMV-specific antibody and T cell responses are mounted [341]. While the immune response to CMV does not clear infection, it is clear that a robust immune response is required to control infection [341]. CMV stimulates TLRs activating signalling pathways in DCs and macrophages that result in the production of type 1 IFNs and the subsequent activation of NK cells [342]. NK cells play a key role in the response to CMV. In mice, NK cells are involved in the clearance of experimental murine CMV (MCMV) infection [343] and there is also evidence that NK cells play a role in control of human CMV infection [344].

There are stark differences in NK cell phenotypes between CMV+ and CMV- individuals. CMV has a wide tissue and cell tropism which includes bone marrow stromal cells. As this is a tissue important for the generation and maintenance of NK cells, it is possible that latent CMV in the bone marrow could modulate NK cell maturation and education [345]. CMV infection results in the expansion of terminally differentiated NK cells and the increase in $CD56^{dim}CD16^{-}NKG2C^{+}$ NK cells has been well characterised [346-349]. NKG2C is an activating receptor for the non-classical MHC class I HLA-E, which is stabilised at the surface of CMV-infected cells by a CMV-derived signal peptide [350]. Therefore expansion of $NKG2C^{+}$ NK cells may be a host protective response allowing NK cells to recognise and become activated by CMV-infected cells. These cells are long-lived and have stable epigenetic imprints that resemble those in memory T cells [351]. $NKG2C^{+}$ cells have a reduced cytokine responsiveness but those that are $CD57^{-}$ can be strongly boosted by vaccination compared with those that are $CD57^{+}$ [352]. The mechanisms driving the expansion of these cell subsets in CMV infection are still unclear. However, if CMV+ individuals have high frequencies of these highly differentiated NK cells that are hyporesponsive to cytokines, this

may mean that CMV+ individuals respond less well to vaccines relying on cytokine-driven pathways.

There is a role for antibody in the effective response against CMV, mainly in restricting viral dissemination and limiting disease severity [353]. However, T cells are thought to have the predominant role in control of CMV infection [354]. In MCMV models depletion of $CD8^+$ T cells resulted in the reactivation and dissemination of disease [355]. In humans $CD8^+$ T cells are also important for control and this is clear from both bone marrow and solid organ transplant patients, in which development of CMV-specific CTL responses is associated with control of CMV viraemia and recovery from infection [356,357]. A huge proportion of the T cell repertoire is committed to CMV: 10% of the circulating peripheral $CD8^+$ T cells may be CMV-specific in healthy carriers and this increases with age with frequencies of around 40% observed in some elderly individuals [358-360]. Frequencies as high as 70% of $CD8^+$ T cells have been reported against just a single CMV epitope [361].

This dramatic inflation of CMV-specific T cells over time has been termed “memory inflation” [362]. It is unclear exactly what drives CMV-associated memory inflation but antigen persistence and chronic or repeated stimulation of CMV-specific T cells are thought to play a role [362]. However, recent studies have shown that the CMV-specific T cell pool undergoes continuous expansions and contractions in the absence of detectable CMV [358,363]. These studies suggested that the fluctuations in CMV-specific T cells may be due to a “bystander effect” of infection, with immune activation providing heterologous stimulation. It is unclear why this may occur uniquely to CMV-specific (and possibly EBV-specific) T cells. These inflated populations of T cells display a terminally differentiated memory and possibly senescent phenotype characterised by expression of CD57, killer cell lectin-like receptor G1 (KLRG1), re-expression of CD45RA and downregulation of CD27 and CD28 [364]. Memory inflation also occurs within the $CD4^+$ T cell pool [365], which are also integral to the control of CMV infection [366,367]. Similar to

the $CD8^+$ T cell responses, a large proportion of the $CD4^+$ T cell pool in CMV-infected individuals is CMV-specific. Around 9% of the $CD4^+$ T cell pool may be CMV-specific [360] and frequencies up as high as 40% have been reported [368]. Traditionally $CD4^+$ T cells were thought to have indirect involvement in control of latent viruses through providing help for $CD8^+$ T cells killing and for antibody production. However, studies have shown that $CD4^+$ T cells may gain a cytolytic phenotype and directly kill CMV-infected cells [369,370].

1.4.3. CMV-associated reduction in vaccine responses

It has been suggested that the large expansion in CMV-specific T cells with age is a contributing factor to immune senescence - the functional changes and dysregulation of the immune system that occur with age and are associated with increased susceptibility to infection and poor vaccine responses [371]. Immune senescence is characterised by a reduction in naïve cells, accumulation of memory T cells and a decline in immune responsiveness [372]. CMV seropositivity has been included as part of an "immune risk phenotype" which predicted an increased mortality rate in octogenarians [373-375]. Other parameters in the immune risk phenotype included an inverted $CD4^+$:$CD8^+$ T cell ratio and increased proportion of highly differentiated $CD28^-CD8^+$ T cells, all of which may be driven by CMV [362]. Evidence suggests that CMV and healthy ageing have distinct impacts on the immune system, particularly within the $CD4^+$ T cell compartment [376].

This long-lasting imprint that CMV makes on the immune system may impact vaccine responsiveness in CMV+ individuals. Most research in this area to date has focused on the impaired responses to influenza vaccination in elderly individuals. However, this is a growing field of research and there has been evidence of both negative and positive associations between CMV and vaccine responses in different age groups and contexts. An inverse correlation between CMV IgG titres and antibody responses to seasonal influenza vaccine was reported in elderly individuals (>69 years) [377]. Individuals with higher CMV IgG titres in this

study had significantly higher levels of NK cells, lower B cell frequencies, lower $CD4^+$ T cells, increased $CD8^+$ T cells and a decreased CD4:CD8 ratio. Additionally, these individuals had impaired T cell function with lower anti-CD3 responses measured by IFNγ ELISpot but robust CMV-specific T cell responses. This study provides evidence for an association between the decline in vaccine responses in the elderly, the aging of the immune system and the intensity of responses towards CMV. Latent CMV infection was also associated with poor memory CD4 responses to influenza A in another elderly cohort [378] and another study has indicated a faster decline in antibody responses to diphtheria booster vaccination in CMV+ elderly individuals [376]. However other studies have demonstrated no difference in vaccine responses between CMV+ and CMV- elderly individuals [379,380].

The impact of CMV on vaccine responses in young adults and children is even less clear. Several studies have indicated a negative impact of CMV on humoral responses to influenza vaccine in young adults [381-383], while others have indicated a negligible or even positive impact [384,385]. It has been suggested that these conflicting results could be due to differences in the duration of CMV infection. In mouse models, early in infection there was a MCMV-induced enhancement of anti-viral immunity whilst immunosenescence and hyporesponsiveness were observed in chronic infection [384]. In young (Gambian) children CMV may be beneficial for vaccine responses: CMV infection alone had no impact on responses but co-infection with CMV and Epstein-Barr virus (EBV) enhanced antibody responses to meningococcal polysaccharide vaccine and measles vaccine, countering the reduction that was observed in single EBV infection [386]. In support of this, recent data from a Swedish birth cohort showed EBV but not CMV carriage was associated with accelerated decay of antibody responses to measles vaccination over the first 10 years of life [387]. Mechanisms driving these differences in vaccine responses in CMV- and CMV+ individuals are also unclear. However, where potent cytokine-driven responses are important for vaccine immunogenicity the impact of CMV may be clearer. *In vitro* NK cell cytokine responses to previously encountered vaccine antigens including influenza and whole

cell pertussis were impaired in CMV+ individuals [388,389]. Impaired NK cell IFNγ responses to exogenous cytokines in CMV+ individuals are well documented[388,390,391]. This may partly be due to the reduced frequencies of less-differentiated $CD56^{bright}$ and $CD56^{dim}CD57^{-}$ NK cells in CMV+ individuals as these are more responsive to cytokines than the expanded $CD57^{+}$ NK cells [388,389]. Similarly, within the T cell subset, the expansion of terminally differentiated effectors and reduction in less-differentiated $CD27^{+}CD28^{+}$ T cell subsets may partly explain the reduction in vaccine responses in some contexts. Additionally, inflationary memory $CD4^{+}$ T cells have been shown to be IFNγ-producing Th1 cells, which might explain the poor antibody-mediated immune responses seen CMV+ individuals with high frequencies of these cells [392-394]

It is clear that CMV is associated with profound phenotypic differences in T cell and NK cell populations, with a shift towards a terminally differentiated phenotype. Numerous studies support a role of these cells, which may be hyporesponsive to antigenic stimulation and functionally impaired, in immunosenescence. It is less clear what impact CMV carriage and the expansion of these cell subsets might have on vaccine responses, particularly in young adults and children. The impact of CMV on vaccine immunogenicity may well be context-specific: different vaccines, adjuvants, age groups, genetic backgrounds and co-infections among other factors may well determine whether CMV carriage has an impact and whether it is beneficial or impeding. This may be a particularly important question when comparing vaccine immunogenicity in cohorts from different populations with differing rates of CMV seroprevalence, as is the case between the UK and most African countries [330,395].

1.5. Thesis Aims and Outline

1.5.1. Aims

1. Evaluate the immunogenicity of a novel malaria vaccine strategy combining two different vaccine platforms in humans: viral vectored vaccines ChAd63 and MVA with the virus like particle vaccine RTS,S.

2. Optimise assays to measure antibody responses to vaccination in malaria-exposed cohorts.

3. Investigate the reduction in vaccine immunogenicity in malaria-exposed cohorts.

4. Develop an assay based on activation-induced markers to detect antigen-specific T cell responses to vaccination and assess the assay for use in clinical trials.

5. Use this assay to investigate the quantity and quality of the T cell response to viral-vectored Ebola vaccines in malaria-naïve and malaria-exposed populations. Additionally, use this assay to investigate the association between CMV and reduced vaccine responses.

1.5.2. Outline

Chapter 2 describes the materials and methods used in these studies.

Chapter 3 investigates the reduction in humoral immunity and efficacy when ChAd63-ME-TRAP and MVA-ME-TRAP are concomitantly administered with RTS,S/AS01B.

Chapter 4 describes the effect of antigen-independent antibody deposition in samples from highly malaria-exposed individuals on ELISA results and optimises the assay to reduce false positives caused by this phenomenon.

Chapter 5 assesses responses to vaccination in malaria-exposed populations and examines the relationship between malaria exposure and reduced humoral responses to vaccination.

Chapter 6 Investigates the use of an assay based around activation-induced markers to detect antigen-specific T cells in clinical trials.

Chapter 7 details the association between CMV seropositivity, T cell phenotypes and the response to the Ebola vaccine candidates ChAd3-EBO-Z and MVA-EBO-Z in UK and Senegalese cohorts.

Chapter 8 summarises the findings of this work and discusses implications and future directions.

2

Materials and Methods

2.1. Materials

2.1.1. Reagents

Table 2.1 details all of the commercially available reagents used in this study, except from antibodies used for flow cytometry, which are listed in individual tables for each panel.

Table 2.1. Commercially available reagents used in this study

Reagent/ Material	Supplier	Catalogue Number
15mL falcons	Sarstedt	554502
175cm^2 cell culture flask	Corning	431086
25cm^2 cell culture flask	Corning	430639
4-nitro-phenyl-phosphate	Sigma-Aldrich	N2765-100TAB
50mL falcons	Sarstedt	547254
5mL polypropylene FACS tubes	Becton Dickinson	352063
5mL polystyrene FACS tubes with cell strainer cap	Becton Dickinson	352235
75cm^2 cell culture flask	Corning	430641
96-well cell culture plate	Corning	3595
96-well U-bottom plates	Becton Dickinson	353077
96-well V-bottom plates	Thermo Scientific	611V96
Anti-CD28	eBioscience	16-0289-81
Anti-CD49d	eBioscience	16-0499-85
Anti-human IgG-AlexaFluor488	Invitrogen	A11013
Anti-human IgG-Alkaline Phosphatase (AP)	Sigma-Aldrich	A3187.5ML
Anti-human IgM-AlexaFluor594	Invitrogen	A21216

Reagent/ Material	Supplier	Catalogue Number
AQUA Live/Dead stain	Invitrogen	L34957
ARC beads	Invitrogen	A10346
BCIP/NBT development buffer	Europa Bioproducts	MO711A
BD Cytofix/cytoperm kit	BD Biosciences	554714
Benzonase	Millipore	70664
Blocker Casein in PBS	Thermo Scientific	37528
Bovine Serum Albumin (BSA)	Sigma-Aldrich	A7906-100G
Brefeldin-A	Invitrogen	00-4506-51
Brilliant stain buffer	BD Biosciences	563794
Carbonate-bicarbonate tablets	Sigma-Aldrich	C3041-100CAP
Casyton	OLS OMNI Life Science	5651808
Chambered microscope slides	Thermo Scientific	C24779
ChonBlock™ blocking/sample dilution ELISA buffer	Chondrex	9068
ChonBlock™ detection antibody dilution buffer	Chondrex	90681
CoolCell™	BioCision	BCS-170
Cryovials	Star lab	E3110-6112
DAPI stain	Sigma-Aldrich	D9542-5MG
DEA buffer	Thermo Scientific	34064
Dimethyl-sulfoxide (DMSO)	Sigma-Aldrich	D2650
Dulbecco's PBS (DPBS)	Sigma-Aldrich	D8537-500ML
Foetal Calf Serum (FCS)	Gibco	10500-064
Fluoroshield mounting medium with DAPI	Abcam	ab104139
Goat anti-human IgA-AP	Sigma-Aldrich	A9669-1ML
Goat anti-human IgG-HRP	ADI	10120
Goat anti-human IgM biotin	Sigma-Aldrich	B1265-2ML
Human cytomegalovirus IgG ELISA kit	Abcam	ab108724
IFNγ SA-ALP antibody kits	Mabtech	3420-25A
LEGENDplex Th cytokine assay	Biolegend	740722
Leucosep tubes	Fisher Scientific	15805547
L-Glutamine	Sigma-Aldrich	G7513-100ML
Lymphoprep	STEMCELL Technologies	07851

Reagent/ Material	Supplier	Catalogue Number
Monensin	Invitrogen	00-4505-51
Mouse anti-human IgG1 Fc biotin	Invitrogen	MH1515
Mouse anti-human IgG2 biotin	Invitrogen	05-3540
Mouse anti-human IgG3 biotin	Invitrogen	MH1031
Mouse anti-human IgG4 Fc biotin	Invitrogen	MH1542
Multiscreen IP ELISpot plates	Millipore	MAIPS4510
Nunc-Immuno MaxiSorp plates	Thermo Scientific	442404
One-Comp beads	eBioscience	01-1111-41
Paraformaldehyde (PFA)	Alfa Aesar	43368
Penicillin-Streptomycin	Sigma-Aldrich	P0781-100ML
PHA	InvivoGen	inh-phap
Phosphate buffered saline (PBS) powder	Sigma-Aldrich	P2194
Phosphate buffered saline (PBS) tablets	Sigma-Aldrich	P4417-100TAB
Red blood cell lysis solution	Qiagen	158904
RPMI-1640 medium	Sigma-Aldrich	R0883-500ML
Sodium azide (NaN_3)	Sigma-Aldrich	S2002
Sodium thiocyanate	Sigma-Aldrich	251410-500G
Staphylococcal enterotoxin B (SEB)	Sigma-Aldrich	S4881
Stop solution	ADI	80100
TMB substrate	ADI	80091
Trypan blue	Gibco	15250061
Trypsin	Gibco	12604-013
Tween-20	Sigma-Aldrich	P7949-500ML

2.1.2. Solutions

R0 medium: RPMI (Sigma) containing 1% sterile filtered Penicillin-Streptomycin (Sigma), 1% L-Glutamine (Sigma).

R10 medium: RPMI (Sigma) containing 1% sterile filtered Penicillin-Streptomycin, 1% L-Glutamine and 10% heat-inactivated, sterile-filtered foetal calf serum, previously screened for low reactivity (Labtech International)

FACS buffer: PBS containing 0.1% BSA and 0.01% sodium azide

ELISpot/ELISA coating buffer: Carbonate-bicarbonate tablets (Sigma, C3041) dissolved in PBS (15mM Na_2CO_3, 35mM $NaHCO_3$, pH 9.3)

PBS/Tween (PBS/T): PBS (Sigma, P2194) with 0.5% Tween-20

2.1.3. Vaccines and adjuvants

2.1.3.1. RTS,S/AS01B

RTS,S/AS01B was developed and manufactured by GSK Vaccines. RTS,S consists of two proteins RTS and S expressed in *Saccharomyces cerevisiae*. RTS is a polypeptide formed from a portion of the CSP antigen from the *P. falciparum* strain NF54 fused to the amino terminal end of the hepatitis B virus surface antigen (HBsAg). The other polypeptide is the HBsAg expressed alone. RTS and S spontaneously assemble into mixed polymeric particulate structures, forming hepatitis B viral-like particles. A ratio of RTS to S of 1:4 was required for particles to form.

AS01B is an adjuvant system containing two immunostimulants formulated with liposomes: monophosphoryl lipid A (MPL, 50µg, produced by GSK) and *Quillaja saponaria* Molina, fraction 21 (QS-21, 50µg, licensed by GSK from Antigenics Inc).

2.1.3.2. R21/MM

The R21 vaccine is biosimilar to RTS,S, except that it is formed from a single CSP-HBsAg fusion protein expressed in *Pichia pastoris*, which allowed particles to form in the absence of excess HBsAg [242].

Matrix-M is a saponin-based adjuvant developed by Novavax. It consists of two populations of matrix particles formed by purified saponin from *Q. saponaria* Molina formulated with cholesterol and phospholipid.

2.1.3.3. ChAd63-ME-TRAP

Chimpanzee adenovirus strain 63 (ChAd63) was isolated from a captivity-born chimpanzee at the New Iberia research facility (NIRC, University of Louisiana at Lafayette, New Iberia, LA). Deletion of the E1 region of the viral genome rendered the virus replication deficient. Further deletions of the viral genome were made in the E3 and E4 regions and Ad5E4orf6 was inserted [396]. ChAd63-ME-TRAP was manufactured using HEK293 cells under good manufacturing practice (GMP) conditions by the Oxford University Clinical Biomanufacturing Facility (CBF), Churchill Hospital, Oxford.

The viral vector encodes for the insert ME-TRAP, which is a multiple epitope string (ME) fused to the full sequence of the *P. falciparum* T9/96 pre-erythrocytic antigen thrombospondin-related adhesion protein (TRAP). ME consists of cytotoxic T lymphocyte (CTL) epitopes from a variety of potentially protective antigens and is included to ensure an immune response to the vaccine in the majority of vaccinated individuals. These epitopes include 14 $CD8^+$ T cell epitopes and three $CD4^+$ epitopes from tetanus toxoid, bacille Calmette-Guérin (BCG) and *P. falciparum* CSP, (PfCSP), two B cell epitopes, (NANP) from PfCSP and the adhesion motif of TRAP (TRAP-AM). The string also includes the H-2Kd pb9 epitope facilitating pre-clinical evaluation in BALB/c mice. The ME-TRAP hybrid is a 2398 base-pair insert which encodes for a single polypeptide of 789 amino acids [246].

2.1.3.4. MVA-ME-TRAP

Modified vaccinia virus Ankara (MVA) is a highly attenuated, replication-deficient strain of vaccinia virus. This was produced by over 500 passages through chicken embryo fibroblast (CEF) cells. The viral vector expresses the same ME-TRAP construct as described above for ChAd63-

ME-TRAP. Clinical grade MVA-ME-TRAP was produced under GMP conditions by Impfstoffwerk Dessau-Tornau GmbH, Rosslau, Germany.

2.1.3.5. ChAd3-EBO-Z

The ChAd serotype 3 (ChAd3) vectored vaccine is a replication-deficient ChAd expressing the wild-type (WT) glycoprotein from the Mayinga strain of Ebola Zaire virus (EBO-Z). The drug substance was manufactured at Advent (GSK), and the drug product was manufactured under good manufacturing practice (GMP) conditions at the Vaccine Research Center Vaccine Pilot Plant, under contract with the Vaccine Clinical Materials Program, Leidos Biomedical Research.

2.1.3.6. MVA-EBO-Z

The MVA-EBO-Z vaccine consists of a replication-deficient MVA expressing EBO-Z. The drug substance was manufactured in the immortal avian cell line AGE1.CR.Pix. under GMP conditions by Emergent BioSolutions, Gaithersburg, MD, USA.

2.1.3.7. MVA-BN® Filo

The MVA-BN® Filo vaccine was manufactured at IDT Biologika in Germany under contract FBS-0044-009 with NIAID and Fisher BioServices. The vaccine is a multivalent recombinant MVA (Modified Vaccinia virus Ankara, strain Bavarian Nordic [MVA-BN®]) encoding four filovirus antigens: the surface glycoproteins of Marburg virus, Ebola virus and Sudan virus as well as the nucleoprotein of Tai Forest Ebolavirus. MVA-BN® Filo was grown in primary chicken embryo fibroblast cells under serum free conditions and formulated in trisbuffered saline at 4.4 x 108 TCID50 per 0.5 mL dose in single-dose vials.

2.2. Methods – Clinical studies

2.2.1. Summary of clinical trials

The studies in this thesis use PBMC and serum samples from Jenner Institute clinical vaccine trials conducted in the UK and at trial sites across Africa. These are summarised in Table 2.2.

Table 2.2. Summary of clinical trials
vp: viral particles, pfu: plaque forming unit

Study Code	Clinical phase	Population	Age group (number enrolled)	Vaccines	Doses	Regimen	Thesis chapter	Publication
VAC40	Phase Ib	Kenyan adult males	18-50 years (30)	ChAd63-ME-TRAP and MVA-ME-TRAP	ChAd: $1x10^{10}$ or $5x10^{10}$ vp, MVA: $2x10^{8}$ pfu	8 week prime-boost interval	4, 5	[397,398]
VAC41	Phase Ib	Gambian adults and children	18-50 years (16), 2-6 years (36)	ChAd63-ME-TRAP and MVA-ME-TRAP	ChAd: $1x10^{10}$ or $5x10^{10}$ vp, MVA: $1x10^{8}$ or $2x10^{8}$ pfu	8 week prime-boost interval	4, 5	Adults: [397,398] Children: [262]
VAC42	Phase Ib	Gambian infants	5-12 months (36), 10 weeks (36)	ChAd63-ME-TRAP and MVA-ME-TRAP	ChAd: $1x10^{10}$ or $5x10^{10}$ vp, MVA: $1x10^{8}$ pfu	8 week prime-boost interval	4, 5	[262]
VAC43	Phase Ia	UK adults	18-50 years (42)	ChAd63-ME-TRAP and MVA-ME-TRAP	ChAd: $5x10^{10}$ vp, MVA: $2x10^{8}$ pfu	Various regimens with 4 and 8 week intervals	3	[399]
VAC45	Phase I/IIa	UK adults	18-45 years (36)	ChAd63-ME-TRAP and MVA-ME-TRAP, ChAd63-CSP and MVA-CSP	ChAds: $5x10^{10}$ vp, MVAs: $2x10^{8}$ pfu	8 week prime-boost interval	3, 4, 5	[260]
VAC46	Phase IIb	Kenyan adult males	18-50 years (121)	ChAd63-ME-TRAP and MVA-ME-TRAP	ChAd: $5x10^{10}$ vp, MVA: $2x10^{8}$ pfu	8 week prime-boost interval	4, 5	[400]
VAC50	Phase I/IIb	Burkinabe infants	5-17 months (30 in Phase I lead-in, 700 in Phase IIb)	ChAd63-ME-TRAP and MVA-ME-TRAP	ChAd: $5x10^{10}$ vp, MVA: $1x10^{8}$ pfu	8 week prime-boost interval	4, 5	Phase I: [262] Phase II: manuscript in preparation
VAC53	Phase I/IIa	UK adults	18-50 years (31)	R21 /Matrix-M	2, 10 or 50µg R21 with or without 50µg Matrix-M	3 doses at 4 week intervals	5	Manuscript in preparation

Study Code	Clinical phase	Population	Age group (number enrolled)	Vaccines	Doses	Regimen	Thesis chapter	Publication
VAC55	Phase I/IIa	UK adults	18-50 years (48)	RTS,S/AS01B, ChAd63-ME-TRAP and MVA-ME-TRAP	50µg RTS,S/AS01B, ChAd: $5x10^{10}$ vp, MVA: $2x10^{8}$ pfu	3 doses of RTS,S/AS01B at 4 week intervals alone or in with ChAd63-ME-TRAP at week 2 and MVA-ME-TRAP at week 10	3	[401]
VAC59	Phase I/IIa	UK adults	18-45 years (45)	RTS,S/AS01B, ChAd63-ME-TRAP and MVA-ME-TRAP	50µg RTS,S/AS01B, ChAd: $5x10^{10}$ vp, MVA: $2x10^{8}$ pfu	3 doses of RTS,S/AS01B at 4 week intervals either alone or co-administered with ChAd63-ME-TRAP at week 0 and MVA-ME-TRAP at week 4 and week 8	3	Manuscript accepted at NPJ Vaccines
VAC60	Phase Ib	Burkinabe adults	18-45 years (13)	R21 /Matrix-M	10µg R21 with 50µg Matrix-M	3 doses at 4 week intervals	4, 5	Manuscript in preparation
EBL01	Phase Ia	UK adults	UK adults (60)	ChAd3-EBO-Z and MVA-BN-Filo	ChAd: 1, 2.5 or $5x10^{10}$ vp, MVA: $1x10^{8}$ or $1.5x10^{8}$ pfu	3-10 week prime-boost interval	4	[248]
EBL04	Phase Ia	UK adults	18-50 years (40)	ChAd3-EBO-Z and MVA-EBO-Z	ChAd: $3.6x10^{10}$ vp, MVA: $1x10^{8}$ or $1.5x10^{8}$ pfu	Single dose of MVA or ChAd3-EBO-Z and MVA-EBO-Z at a 1 or 4 week interval	4, 5, 6, 7	Manuscript in preparation
EBL06	Phase Ib	Senegalese adults	18-50 years (40)	ChAd3-EBO-Z and MVA-EBO-Z	ChAd: $3.6x10^{10}$ vp, MVA: $1x10^{8}$ pfu	1 week prime-boost interval	4, 5, 7	Manuscript in preparation

2.2.2. Vaccination

Volunteers for all UK studies were recruited and vaccinated at the CCVTM, Oxford, the NIHR WTCRF, Southampton, the Surrey Clinical Research Centre, Guildford or the NIHR/Wellcome Trust Imperial CRF in Hammersmith, London. All adult volunteers in the studies discussed in this thesis received vaccinations via intramuscular (IM) injection into the deltoid muscle of arm. Infant participants (under two years) received IM vaccinations in the anterolateral thigh.

2.2.3. Ethics and regulatory approval

All studies included in this thesis were conducted in accordance with International Council for Harmonisation of Technical Requirements for Pharmaceuticals for Human Use guidelines, good clinical practice (GCP) and the Declaration of Helsinki (2008). UK studies were also performed in accordance with the UK Genetically Modified Organisms Regulations (2000). Written informed consent was provided by all volunteers or a responsible parent. Each study was approved by the appropriate regulatory authorities and registered with ClinicalTrials.gov. Details are provided in Table 2.3. For each study the Local Safety Committee provided oversight and GCP compliance was independently monitored by the Clinical Trials and Research Governance Team of the University of Oxford.

Table 2.3. Clinical trial regulatory approvals

Study code	UK ethical committee	Local regulatory board (where trial is outside of the UK)	ClinicalTrials.gov
VAC40	OXTREC 12-10	Kenya Medical Research Institute National Ethics Committee	NCT01379430
VAC41	OXTREC 64-09	Medicines Board of The Gambia	NCT01373879
VAC42	OXTREC 26-11	Medicines Board of The Gambia	NCT01450293
VAC43	NRES Committee South Central - Oxford A 10/H0604/96	N/A	NCT01364883
VAC45	NRES Committee South Central - Oxford A 12/SC/0037	N/A	NCT01623557
VAC46	OXTREC 59-11	Kenya Medical Research Institute National Ethics Committee	NCT01666925
VAC50	OXTREC 41-12	Ethics Committee for Health Research in Burkina Faso –CERS 2012-6-37	NCT01635647
VAC53	NRES Committee South Central - Oxford A 15/SC/0386	N/A	NCT02572388
VAC55	NRES Committee South Central - Oxford A 13/SC/0208	N/A	NCT01883609
VAC59	NRES Committee South Central - Oxford A 14/SC/0227	N/A	NCT02252640
VAC60	OXTREC 36-15	Ethics Committee for Health Research in Burkina Faso –CERS 2014-10-118	NCT02925403
EBL01	OXREC A - 14/SC/1256	N/A	NCT02240875
EBL04	NRES Committee South Central - Oxford A 15/SC/0108	N/A	NCT02451891
EBL06	OXTREC 27-15	Senegal national research ethics committee: C.N.E.R.S. Comité National d'Ethique pour la Recherche en Santé. SEN15/19.	NCT02485912

Ethical approval for the seroprevalence study included in this thesis was provided by the institutional review board of the Centre National de Recherche et de Formation sur le Paludisme (Burkina Faso ChAd neutralising antibody seroprevalence study) [254].

2.3. Methods – Controlled human malaria infection (CHMI)

CHMI studies were designed according to a consensus document produced by investigators from the USMMVP, Sanaria, University of Maryland, University of Oxford, RUNMC, The Seattle Biomedical Research Institute and the KEMRI-Wellcome Kilifi Research Programme for the standardisation of design and conduct of *P. falciparum* sporozoite challenge trials. CHMI was administered by mosquito bite according to an established standard operating procedure. Mosquitoes from the Walter Reed Army Institute of Research (WRAIR), Maryland, USA, are infected via a membrane feeder containing parasite material (fully sensitive 3D7 *P. falciparum*), RBC and AB human serum. The blood products came from volunteers who were recruited through WRAIR and were screened according to US Red Cross guidelines (*Trypanosoma cruzi*, HIV 1 and 2, HBV, HCV, HTLV, West Nile Virus and syphilis). Infected mosquitoes were supplied directly from a WRAIR representative and transferred to the CL3 insectary in the Sir Alexander Fleming Building, Imperial College London. Challenges were performed within the insectary. Each volunteer was exposed to the bites of five infectious mosquitoes (by placing their forearms over a net-covered pot containing mosquitoes for 5-10 minutes). Fed mosquitoes (as indicated by the presence of a blood meal in the abdomen) were individually dissected and assessed for sporozoite load (graded 0 to +4; a gland rating of +2 or more, representing 10 or more observed sporozoites, qualifies as infectious). The bite-challenge procedure continues until the subject has been bitten by five infectious mosquitoes.

From seven days post-CHMI volunteers underwent daily follow-up at the CCVTM, Oxford. Diagnosis of clinical malaria was based on development of symptoms and detection of blood-stage parasitaemia by thick blood smear and/or qPCR. Volunteers were treated at the earliest detection of blood-stage infection by microscopy and vaccine efficacy was determined by measurements of time to diagnosis (primary efficacy endpoint), or measurements of parasitaemia by qPCR (secondary efficacy endpoint). For each CHMI study time to diagnosis for

vaccinated individuals was compared with that for malaria-naïve unvaccinated control volunteers that underwent challenge at the same time.

2.4. Methods – Immunology

2.4.1. Blood collection

Blood was drawn from enrolled volunteers by trial physicians or research nurses at pre-specified time points for each study. Blood was collected in heparin-treated vacutainers for PBMC separation and plasma collection, untreated vacutainers for serum collection and EDTA-treated vacutainers for *P. falciparum* qPCR after CHMI. All blood samples were processed with 6 hours of blood draw to ensure sample quality. Untreated vacutainers were centrifuged at 1800rpm (764G) for 5 minutes at room temperature (RT). Serum was aseptically transferred into labelled cryovials for each volunteer and stored at -80°C.

2.4.2. Peripheral blood mononuclear cell (PBMC) separation

All processing was completed under sterile conditions. Up to 30mL of heparinized blood was poured into each Leucosep tube containing 15mL of Lymphoprep below the porous filter disc. These tubes were centrifuged at 1000g for 13 minutes at room temperature to separate PBMC from RBC. At this stage 2-4mL plasma was pipetted off into labelled cryovials for each volunteer for serological analyses. Samples were frozen at -80°C until use. The fraction containing PBMC was poured off into labelled 50mL falcon tubes for each volunteer. Tubes were topped up to 50mL with R0 and spun at 1800rpm (764G) for 5 minutes at RT. After washing, the supernatant was poured off and the cell pellet was resuspended in 30mL R0. At this stage, if there were multiple tubes for each volunteer they were combined into a single tube per volunteer. Cells were spun (1800rpm [764G], 5 minutes, RT) then resuspended in 10mL of R10 for counting. Cells were rested for a minimum of 30 minutes at 37°C and 5% CO_2 before counting and further processing.

2.4.3. Counting PBMC

Cells were counted using a CASY counter (Roche Applied Science) set up to count human PBMC. Two independent counts were measured for each sample and the average count per mL calculated. Cells were then resuspended in R10 to the appropriate concentration for the assays being conducted.

2.4.4. IFNγ ELISpot

Ex vivo (18 hour stimulation) ELISpot assays were performed using Multiscreen IP ELISpot plates, human IFNγ SA-ALP antibody kits and BCIP NBT-plus chromogenic substrate. Plates were coated with 50µL per well of anti-IFNγ at 10µg/mL in coating buffer under sterile conditions. Plates were left for 3-8 hours at room temperature or up to 48 hours at 4°C before use. After coating incubation plates were washed three times with PBS then blocked with 100µL R10 per well for 1-8 hours before plating cells. Plates were kept sterile at all times. Cells were cultured in R10 and antigens were tested in triplicate. For ME-TRAP and CSP ELISpots 50µL of each peptide pool at 20µg/mL (ME-TRAP) or 5µg/mL (CSP) was added to the ELISpot plate from the previously prepared peptide plates. For each well 250,000 PBMC added in 50µL of R10, resulting in a final peptide concentration of 10µg/mL (ME-TRAP) or 2.5µg/mL (CSP). For GP ELISpots 50µL of each peptide pool at 7.5µg/mL was added to the ELISpot plate in addition to 200,000 PBMC in 100µL of R10, resulting in a final peptide concentration of 2.5µg/mL. A mixture of staphylococcal enterotoxin B (SEB, 0.02µg/mL) and phytohaemmagglutinin-L (PHA, 10µg/mL) was used as a positive control in all ELISpot assays. Wells with R10 only and no peptide were included in all assays as a negative control. For CSP ELISpots, a CTL pool (10µg/mL final concentration) was included as an additional positive control. This is a well-defined pool of 23 $CD8^+$ epitopes from Influenza A, EBV and CMV. Details are given in Table A1. After 18-20 hours incubation at 37°C and 5% CO_2, cells were removed into disinfectant and plates were washed six times with PBS/T. Detector antibody (biotinylated anti-IFNγ) was added at 1µg/mL in PBS, 50µL per well and

incubated at RT for 2-4 hours. Plates were washed again as before and incubated with 50µL/well 1:1000 streptavidin-alkaline phosphatase (S-AP) for 1-2 hours at RT. Plates were washed again and 50µL/well development buffer was added for 3-5 minutes until clearly defined spots began to appear. Development buffer was washed off thoroughly with tap water and plates were left to dry before counting.

Plates were counted using an automated ELISpot counter (AID Diagnostika GmbH, algorithm C) using identical settings for all plates and counts were adjusted only to remove artefacts. For ME-TRAP and CSP ELISpots the total spot-forming cells per million PBMC (SFC/10^6 PBMC) for each pool was calculated using the average of each triplicate multiplied by four. For GP ELISpots only 200,000 cells were used per well so the average was multiplied by five. Responses in unstimulated (negative control) wells were subtracted and then responses in individual pools were summed for each strain of the TRAP antigen, CSP or GP. Responses greater than the median + 2 standard deviations (SD) of the negative control wells and greater than the lower limit of detection (LLOD) were considered positive. The LLOD for this assay was defined as the lowest number of spots that was precisely distinguishable from the unstimulated control well and was calculated as the median + 2SD of all unstimulated control wells run for each study. The LLOD values for the assays in this thesis are 50 SFC/10^6 PBMC for the Ebola GP ELISpot, 28 SFC/10^6 PBMC for the ME-TRAP ELISpot and 12 SFC/10^6 PBMC for the CSP ELISpot. All responses below the LLOD were adjusted to the LLOD. ELISpot plate layouts are shown in Figure A1.

As assays were conducted using fresh PBMC in real time over the course of the trial, samples were tested in batches according to the date of the volunteer visit. Representative examples of the unstimulated and positive control results across different assay dates are shown in Figure A2.

2.4.5. Peptides

Peptides were custom synthesised at a minimum purity of 70% with a free amine and a free acid at the N and C terminus respectively. We received HPLC chromatograms and mass spectral analysis from the manufacturer to confirm purity and identity respectively. Peptides were dissolved in DMSO to a storage concentration of between 50 and 200mg/mL and then pooled at working concentrations of 20µg/mL (ME-TRAP), 5µg/ml (CSP) or 7.5µg/mL (GP) per peptide according to standard operating procedures for peptide pool preparation.

2.4.5.1. ME-TRAP

TRAP peptides were designed to cover the length of the TRAP antigen. Peptides were 20 amino acids long, overlapping by 10 amino acids (Neopeptide). Pools were included for both the vaccine strain, T9/96 (TT), and the challenge strain, 3D7 (TD). For each of these antigens there were six pools of 7-10 peptides at 20µg/mL. The sequences of the peptides in pool 6 are identical between the two strains, therefore there is no 3D7 pool 6 but the T9/96 pool 6 response was added to the summed 3D7 response. Megapools containing all of the peptides for each strain were also included. Peptide sequences are shown in Table A2.

ME responses were assayed using a single pool containing 20 peptides of varying lengths as described in [246]. Sequences and pool configurations are shown in Table A3.

2.4.5.2. CSP

CSP peptides spanned the length of the antigen and were 15 amino acids in length, overlapping by 11 amino acids. Peptides were combined into three pools of 8-12 peptides at 5µg/mL. Peptide sequences and pool configurations are shown in Table A4.

2.4.5.3. Ebola Glycoprotein (GP)

Peptides used covered the length of the Ebola Zaire Mayinga GP. Peptides were mainly 15 amino acids in length, overlapping by 11 amino acids. The sequences were provided by NIH and are the

same as those used in a previous study [303]. There were seven pools consisting of peptides from the GP chain 1 (GP1, amino acids 33-501) and two pools containing peptides from the GP chain 2 (GP2, amino acids 504-676). No Zaire Ebola GP megapools were included. However, two megapools were included for Sudan Gulu Ebola GP – MP1 (peptides 1-84) and MP2 (peptides 85-167) at the peak time point to test cross-strain reactivity. All peptide pools for this assay were made up to a working concentration of 7.5µg/mL. Peptide sequences and pool configurations are shown in Table A5 and Table A6.

2.4.6. Intracellular cytokine staining (ICS)

In parallel with the ELISpot, stimulations were set up using fresh PBMC to enable analysis of vaccine-induced responses to T9/96 TRAP, 3D7 TRAP, CSP or GP using flow cytometry. A single megapool was used to assess responses to each antigen. Sequences are detailed in Tables A2, A4 and A5. Megapools were tested at final concentrations of 2µg/mL for T9/96 TRAP, 3D7 TRAP or CSP and 2.5µg/mL for GP. An unstimulated condition and a positive control stimulated with 1µg/mL SEB were run for each sample. Each stimulation was set up in a 5mL polystyrene FACS tube containing $2x10^6$ PBMC in 1mL of R10. Anti-CD28 and anti-CD49d at final concentrations of 1µg/mL and 2µL of anti-CD107a-PE-Cy5 were added to each tube. Samples were stimulated for 18 hours at 37°C and 5% CO_2. Brefeldin A and Monensin, both at 1µg/mL, were added for the last 16 hours.

After overnight stimulation, samples were stained and acquired the same day on an LSRII flow cytometer (BD Biosciences, San Jose, CA, USA). Responses were assessed by a nine-colour staining panel. Cells were incubated with a dead cell discrimination dye (5µL of AQUA diluted 1:40 in dH_2O) for 20 minutes at RT. PBMC were permeabilised and then stained intracellularly at RT for 30 minutes with the antibodies detailed in Table 2.4, except for anti-CD107a, which was included in the stimulation. Cells were then washed and fixed in 1% paraformaldehyde (PFA).

Compensation was performed using single-stained One-Comp beads for monoclonal antibodies and ARC beads for AQUA.

Acquisition was performed on the day of staining on a BD LSRII and FACSDiva v6.2 (BD Biosciences, Franklin Lakes, New Jersey). Data was prepared and analysis performed using FlowJo v9.6.2 or v10.1 (Treestar Inc). Cells were gated on lymphocytes, singlets, live $CD3^+$, $CD8^-$ $CD4^+$ or $CD4^-CD8^+$ and then IFNγ, IL-2, TNFα and CD107a. Dead cells ($AQUA^+$), monocytes ($CD14^+$) and B cells ($CD19^+$) were excluded from the analysis (gating strategy shown in Figure A3). Responses to peptide were determined after subtraction of the response in the unstimulated control for each sample, and considered positive if the count was >20 and frequency higher than the autologous unstimulated control and the LLOD (the reciprocal of the lowest $CD4^+$ and $CD8^+$ counts for each trial). For ICS data used in this study: VAC59 LLOD $CD4^+$=0.002, LLOD $CD8^+$=0.002. For EBL04 and EBL06 LLOD $CD4^+$=0.0046 and $CD8^+$=0.0046). Assays were conducted using fresh PBMC, therefore samples were tested in batches on the date of the volunteer visit. Representative examples of the unstimulated and positive control results across different assay dates are shown in Figure A2. In most experiments, the yield of viable cells from cryopreserved specimens was around 6×10^6, with a viability of at least 90%. A reduction of recovery from 8-$10x10^6$ to 6×10^6 cells might be expected due to cell loss during the freeze-thawing and subsequent washing processes. In a representative experiment the median yield was $6.3x10^6$ IQR ($5.7x10^6$ - $8.7x10^6$) with a median viability of 94.4% (93.5-96.3%).

Table 2.4. Clinical trials intracellular cytokine staining panel

Antibody / Reagent	Fluorochrome	Clone	Supplier	Cat no	Titre	Volume per test (µL) - in 1mL
CD3	AF700	UCHT1	eBioscience	56-0038-82	1:1000	1
CD4	APC	RPA-T4	eBioscience	17-0049-42	1:500	2
CD8	APC-AF780	RPA-T8	eBioscience	47-0088-42	1:200	5
CD14	eF450	61D3	eBioscience	48-0149-42	1:1000	1
CD19	eF450	HIB19	eBioscience	48-0199-42	1:1000	1
IFNγ	FITC	4S.B3	eBioscience	11-7319-82	1:2000	0.5
IL-2	PE	MQ1-17H12	eBioscience	12-7029-82	1:1000	1
TNFα	PE-Cy7	MAb11	eBioscience	25-7349-82	1:10,000	0.1
CD107a	PE-Cy5	eBioH4A3	eBioscience	15-1079-42	1:500	2µL added to stimulation
LIVE/DEAD marker	AQUA	n/a	Invitrogen	L34955	1:1600	5µL of 1:40 stained before ICS

2.4.7. Freezing PBMC

PBMC remaining after ELISpot and ICS set up were frozen at 6-10 million cells/mL/vial. Cells were chilled at 4°C in FCS (0.5mL of FCS per vial to be frozen). After 30 minutes an equal volume of ice-cold FCS with 20% DMSO was added and mixed. Cells were aliquoted into cryovials and incubated at -80°C overnight in CoolCell^{TM} cell freezing containers (Sigma, CLS432006) before transfer to liquid nitrogen.

2.4.8. Thawing PBMC

Cryopreserved cells were removed from storage in liquid nitrogen and thawed in a 37°C water bath. Once cells were almost fully thawed, they were transferred to labelled 15mL falcon tubes containing 10mL pre-warmed R10. Cells were centrifuged at 1800rpm (764G) for 5 minutes at RT before resuspension in 2mL R10 with 5µL benzonase nuclease (25U/10^6 PBMC). Cells were rested at 37°C and 5% CO_2 for 2 hours before washing and resuspension in R10 as required for the assay being conducted.

2.4.9. Cell phenotyping by flow cytometry – circulating Tfh (cTfh), memory T cell and B cell phenotyping

Cell phenotyping was conducted using cryopreserved cells. Cells were thawed according to the protocol described in 2.4.8. After counting as described in 2.4.3, cells were resuspended to approximately $10x10^6$ cells per mL in R10. Staining and acquisition was conducted on the day that cells were thawed. For each sample $1\text{-}2x10^6$ cells were aliquoted into a well in a 96-well V-bottom plate. Cells were centrifuged at 1800rpm (764G), RT for 5 minutes, then resuspended in 200µL FACS buffer and centrifuged again. Cells were incubated with a dead cell discrimination dye (AQUA 1:500) for 20 minutes at RT, washed again as before, then stained with 50µL of antibody staining cocktail at RT for 30 minutes. Details of the cTfh, memory T cell and B cell panels are shown in Table 2.5, 2.6 and 2.7, respectively. Cells were washed a final time, resuspended in 1% PFA and acquired the same day on a BD LSRII and FACSDiva v6.2. Compensation was performed using single-stained One-Comp beads for monoclonal antibodies and ARC beads for AQUA. Analyses were conducted according to the gating strategies shown in Figures A4, A5 and A6.

Table 2.5. cTfh phenotyping panel

Antibody / Reagent	Fluorochrome	Clone	Supplier	Cat no	Titre	Volume per test (µL) - in 50µL
CD3	AF700	UCHT1	eBioscience	56-0038-82	1:33	1.5
CD4	APC-eF780	RPA-T4	eBioscience	47-0049-42	1:50	1
CD45RA	eF450	HI101	Biolegend	304123	1:50	1
CXCR5	PerCP-eF710	J252D4	Biolegend	356910	1:25	2
CXCR3	APC	1C6/CXCR3	Biolegend	353708	1:17	3
CCR6	PE	G034E3	Biolegend	353410	1:25	2
PD-1	BV650	EH12.2H7	Biolegend	329950	1:100	0.5
LIVE/DEAD marker	AQUA	n/a	Invitrogen	L34955	1:500	0.1µL stained before ICS

Table 2.6. B cell phenotyping panel

Antibody / Reagent	Fluorochrome	Clone	Supplier	Cat no	Titre	volume per test (µL) - in 50µL
CD19	AF700	HIB19	eBioscience	56-0199-42	1:17	3
CD20	Ev655	2H7	eBioscience	86-0209-42	1:167	0.3
CD21	APC	HB5	eBioscience	17-0219-42	1:33	1.5
CD27	BV711	O323	Biolegend	302834	1:17	3
IgD	APC/Cy7	IA6-2	Biolegend	348218	1:100	0.5
IgG	BV421	G18-145	BD Biosciences	562581	1:33	1.5
IgM	PE-CF594	G20-127	BD Biosciences	562539	1:67	0.75
LIVE/DEAD marker	AQUA	n/a	Invitrogen	L34955	1:500	0.1µL stained before ICS

Table 2.7. T cell memory phenotyping panel

Antibody / Reagent	Fluorochrome	Clone	Supplier	Cat no	Titre	volume per test (µL) - in 50µL
CD14	eF506	61D3	eBioscience	69-0149-42	1:50	1
CD19	eF506	HIB19	eBioscience	69-0199-42	1:50	1
CD45RA	eV605	HI100	eBioscience	83-0458-42	1:50	1
CD27	BV711	O323	Biolegend	302834	1:17	3
CD28	BV421	CD28.2	Biolegend	302929	1:50	1
CD4	APC	RPA-T4	eBioscience	47-0049-42	1:50	1
CD3	AF700	UCHT1	eBioscience	56-0038-42	1:50	1
CD8	APC-AF780	RPA-T8	eBioscience	47-0088-42	1:17	3
CCR7	FITC	G043H7	Biolegend	353215	1:50	1
CD57	PerCP-Cy5.5	HNK-1	Biolegend	359621	1:33	1.5
KLRG1	PE	14C2A07	Biolegend	368610	1:17	3
LIVE/DEAD marker	AQUA	n/a	Invitrogen	L34955	1:500	0.1µL stained before ICS

2.4.10. Activation-induced markers (AIM) assay

The activation-induced markers assay was conducted in a similar way to previously published work [402-404]. AIM assays were conducted using cryopreserved cells. Cells were thawed according to the protocol described in 2.4.8. After counting as described in 2.4.3, cells were resuspended to approximately $10x10^6$ cells per mL in R10. PBMC ($1\text{-}2x10^6$ cells per well in a 96-well U-bottom plate) were stimulated overnight (20 hours at 37°C and 5% CO_2). Cells were either

stimulated with 0.5µg/mL of a pool of CMV pp65 peptides (PM-PP65-1, Cambridge Bioscience) or 2µg/mL of Zaire Ebola GP peptides (Neoscientific, MA, USA). An unstimulated well and a positive control well stimulated with 1µg/mL SEB were included for each sample. Anti-CD107a-PE-Cy5 was included in the stimulation at 0.1µL/well. After overnight stimulation cells were washed twice in FACS buffer, resuspended in 100µL FACS buffer then stained for 20 minutes at RT by addition of 100µL per well of the antibody staining mix described in Table 2.8, except for anti-CD107a, which was included in the stimulation. Cells were washed twice as before, fixed with 4% PFA for 10 minutes at 4°C, washed twice again, resuspended in 100µL FACS buffer and acquired immediately on a BD LSRII and FACSDiva v6.2. Data analysis was conducted in FlowJo version 10.1 (Treestar Inc) according to the gating strategy shown in Figure A7.

Table 2.8. Activation-induced markers panel

Antibody / Reagent	Fluorochrome	Clone	Supplier	Cat no	Titre	volume per test (µL) - in 200µL
CD14	eF506	61D3	eBioscience	69-0149-42	1:200	1
CD19	eF506	HIB19	eBioscience	69-0199-42	1:200	1
CD45RA	v605	HI100	eBioscience	83-0458-42	1:200	1
CD3	AF700	UCHT1	eBioscience	56-0038-42	1:133	1.5
CD4	APC-eF780	RPA-T4	eBioscience	47-0049-42	1:133	1.5
CD8	BV711	RPA-T8	Biolegend	301043	1:400	0.5
CD57	PE	HNK-1	Biolegend	359611	1:200	1
KLRG1	BV421	14C2A07	Biolegend	368604	1:66	3
OX40	PE-Cy7	Ber-ACT35	Biolegend	350012	1:100	2
CD25	FITC	M-A251	Biolegend	356106	1:100	2
PDL1	APC	B7-H1	Biolegend	329708	1:133	1.5
LIVE/DEAD marker	AQUA	n/a	Invitrogen	L34955	1:2000	0.1µL
CD107a	PE-Cy5	eBioH4A3	eBioscience	15-1079-42	1:2000	0.1µL added to stimulation

2.4.11. LEGENDplex assay

Cytokine concentrations were measured in the supernatants from the PBMC stimulations in 2.4.10 (CSP or GP) in addition to supernatant from 1-2x10^6 PBMC stimulated with 10^6 pfu of modified vaccinia Ankara (MVA). Supernatants were taken after the 20 hour PBMC stimulation and stored at -20°C in 96-well U-bottom polypropylene plates until use. Cytokine concentrations were measured using the LEGENDplex human Th cytokine panel 13-plex assay (Biolegend, San Diego, California) according to the manufacturer's instructions. Concentrations of IL-2, IL-4, IL-5, IL-6, IL-9, IL-10, IL-13, IL-17A, IL-17F, IL-21, IL-22, IFNγ, and TNFα were analysed. The samples were read on the same day on a BD LSR II using FACSDiva v6.2 (BD Biosciences, Franklin Lakes, New Jersey) with 5000 beads acquired per sample. Data analysis was conducted using the LEGENDplex data analysis software.

2.4.12. Immunofluorescence assay (IFA)

Chambered microscope slides coated with *P. falciparum* sporozoites were stored at -80°C until use. Slides were brought to RT and then fixed for 15 minutes in 4% paraformaldehyde. After washing twice in PBS for 5 minutes, slides were blocked for 1 hour in casein. Slides were washed as before and 10µL of serum sample diluted 1:100 in casein was added to each well. Slides were incubated for 30 minutes at RT in a humidity chamber then wells were individually washed with PBS three times for 5 minutes. Secondary antibody (anti-IgG-AlexaFluor488) was diluted 1:800 in casein and 15µL was added to each well. Slides were incubated for 30-45 minutes in a humidity chamber at RT protected from the light. After a final wash, slides were rinsed in distilled water and left to dry before mounting with DAPI-containing media. Slides were set overnight at 4°C before being examined under a Leica DMI3000 B microscope. Images were captured in QCapturePro (Surrey, BC, Canada) software using brightfield illumination, GFP and DAPI filters at set exposure levels. ImageJ software was used to measure the median fluorescence intensity for five sporozoites in each well and an average was taken.

2.4.13. Inhibition of sporozoite invasion assay (ISI)

The inhibition of sporozoite invasion assay was carried out as previously described [405,406]. For the experiments included in this thesis human hepatoma cells (HC04 or Huh7) cultured in R10 were added to 96-well culture plates at 30,000 cells/well and left to settle overnight at 37°C, 5% CO_2. Viable GFP-labelled *P. berghei* sporozoites expressing *P. falciparum* CSP at the *P. berghei* CSP locus (*P. berghei* PfCSP@CSP) were obtained by dissecting infected *Anopheles stephensi* mosquitoes. Salivary glands were pooled into RPMI 1640 medium and homogenised. Sporozoites were counted and diluted to 100,000/mL in RPMI 1640. Culture medium was aspirated from the hepatoma cells then 100µL of serum diluted 1:5 in R10 and 100µL of sporozoite dilution (10,000 sporozoites, 10% final serum concentration) were added to each well. Samples were tested in duplicate, "hepatoma only" wells and positive control wells containing hepatoma cells and sporozoites but no serum were included. Baseline (pre-vaccination) and post-vaccination samples were run for each volunteer tested. After incubation for 20-26h at 37°C media was aspirated and plates were washed with 90µL/well DPBS. Cells were trypsinized, re-suspended in 65µL DPBS with 1% bovine serum albumin (BSA) and acquired immediately using a BD LSRII and FACSDiva v6.2. DAPI stain was added to each sample just before acquisition. Data was analysed in FlowJo software v10.6 (TreeStar Inc., Ashland, Oregon) using the gating strategy in Figure A8.

2.4.14. Standardised enzyme-linked immunosorbent assays (ELISA)

2.4.14.1. TRAP

Nunc MaxiSorp 96-well plates were coated with 0.5µg/mL of TRAP antigen (details in [260]) in carbonate-bicarbonate coating buffer and left overnight at 4°C. Plates were washed 6x with PBS/T, then blocked with 1% BSA in PBS/T for 1 hour at RT. Serum was diluted in PBS/T containing 0.2% BSA at concentrations of 1:100, 1:500, 1:1000, 1:5000 or 1:10,000 depending on antibody concentration and added to the plate in triplicate. Plates were incubated at RT for 2

hours then washed as before. A secondary antibody (goat anti-human whole IgG conjugated to AP) was added at a dilution of 1:1000 in PBS/T 0.2% BSA for 1 hour at RT. After a final wash, plates were developed by adding 4-nitrophenyl phosphate in diethanolamine buffer. Four blank wells with no sample were included to gauge assay background. A positive reference standard (made from pooled TRAP-positive serum) was used on each plate to give a standard curve. The standard pool was added in duplicate at an initial dilution of 1:100 (in PBS/T 0.2% BSA) and diluted 2-fold 10 times. The top of the standard curve was given an arbitrary value of 20 ELISA Units (EU). Optical density (OD) was read at 405nm (OD405) using an ELx800 microplate reader (BioTek, Winooski, VT, USA). The OD values read from the plate during development were fitted to a four-parameter standard curve using SOFTmax PRO software (Molecular Devices, San Jose, CA, USA). EU values for test sera were calculated from their OD values using the standard curve. An internal development control was included on every plate in triplicate made up from a 1:800 dilution (in PBS/T 0.2% BSA) of the positive standard. A seropositive cut-off value was determined from the mean + 3SD of 148 malaria-naïve adult samples run on this assay (65 ELISA Units).

2.4.14.2. NANP (CSP)

Standardised ELISAs to measure antibodies against the NANP repeat region of CSP were conducted using a synthetically produced peptide consisting of six NANP repeats and a cysteine residue $(NANP)_6C$ (thinkpeptides, ProImmune, Oxford, UK). Assays were conducted as for the TRAP ELISA, except that plates were coated with 0.2µg/mL $(NANP)_6C$, in DPBS overnight at 4°C. The blocking and dilution buffer used for this assay was casein in PBS (Sigma C7594). The standard curve and internal control were produced from sera containing high levels of anti-CSP antibodies induced by RTS,S/AS01B vaccination in a clinical study previously run at the Jenner Institute (VAC55, NCT01883609). A seropositive cut-off value was not determined for this assay as the majority of malaria-naïve individuals have results of 1 EU or less.

2.4.14.3. Ebola GP

Standardised ELISAs to measure antibodies against Ebola Zaire GP were conducted as for the CSP and TRAP ELISAs. Plates were coated with recombinant trimerised Zaire Ebola GP at 1µg/mL in DPBS at 4°C overnight (details of recombinant Ebola GP are available in [248]). Blocking and dilutions were conducted using casein in PBS as for the CSP ELISA. The positive control was formed of a pool of sera from individuals vaccinated with the ChAd3-MVA-EBO-Z vaccines in a clinical study previously run at the Jenner Institute (EBL01, NCT02240875). A seropositive cut-off value was determined from the mean + 3SD of 59 Ebola-naïve adult samples run on this assay (166 ELISA Units).

2.4.14.4. AMA-1 and MSP-1

Standardised ELISAs to measure antibodies against AMA-1 were conducted as for the ELISAs above. Plates were coated with 2µg/mL recombinant AMA-1 (3D7 strain) or MSP-1_{19} in DPBS overnight at 4°C. Blocking and dilutions were conducted using casein in PBS. For the assays presented in this thesis, seropositive cut-off values were determined from the mean + 3SD of 14 malaria-naïve adult samples run on each assay (AMA-1: 14 EUs, MSP-1: 11 EUs).

2.4.15. Isotype ELISAs

Isotype ELISAs were conducted using the conditions described in 2.4.14 for each of the antigens, except that all serum samples were diluted to 1:100 and added to the plate in duplicate wells on each of six plates. One of six secondary antibodies against IgG1, IgG2, IgG3, IgG4, IgM or IgA was added to each plate at 1:1000 in casein (for NANP and GP ELISAs) or PBS/T 0.2% BSA (for TRAP ELISAs). Plates were washed again and Extravadin-AP diluted 1:1000 in casein (GP, NANP) or PBS/T 0.2% BSA (TRAP) was added (50µL/well, 30 minutes, RT) to all plates except for IgA. The anti-IgA secondary antibody used was conjugated to AP and therefore the Extravidin-AP incubation step was not required. Plates were washed a final time before developing as for the standardised ELISA protocol above. Blank wells and internal development controls were

included on each plate. Raw OD values were recorded. A "seropositive cut-off" value was calculated for each isotype or subclass using the mean + 3 SD of 33 UK malaria- and Ebola-naïve serum samples.

2.4.16. Avidity ELISAs

IgG antibody avidity was assessed by sodium thiocyanate (NaSCN)-displacement ELISA. The assays were conducted as for total IgG ELISAs except that sera were individually diluted in casein to a level calculated to reach an OD405 of 1.0 (using total IgG EU results for each sample), and plated at 50µL/well in 16 wells of a 96 well plate. Plates were incubated for 2 hours at RT before chaotropic agent NaSCN was added in duplicate at increasing concentrations down the plate (0 to 7 Molar [M]). Plates were incubated for 15 minutes at RT before washing with PBS/T, then incubated with secondary antibody and developed with the same conditions as for the ELISAs described in 2.4.14. The concentration of NaSCN required to reduce the OD405 to 50% of that in wells where no NaSCN (IC50) was used as a measure of avidity.

2.4.17. Anti-schizont ELISA

Anti-schizont ELISAs were conducted as previously described [407]**.** Nunc MaxiSorp 96-well plates were coated with *P. falciparum* schizont extract from the same batch and diluted to 1 µg/mL of protein in DPBS (A4 and 3D7 parasite strains [408]). Plates were incubated overnight at RT, before washing six times with PBS/T and blocking for 1 hour at RT with casein in PBS. Following this, wells were washed again and incubated for 2 hours at RT with 100µL of test sera (1:100 dilution in casein buffer). Plates were then washed six times in PBS/T and secondary antibody (goat anti-human whole IgG conjugated to AP) was added at a dilution of 1:1000 in casein buffer for 1 hour at RT. Plates were developed as for ELISA assays described in 2.4.14 and OD405 was measured. A positive cut-off value of 0.250 OD405 was calculated based on the mean + 3SD of 30 UK malaria-naïve samples. The same positive controls (hyper-immune sera) were run in duplicate on each plate to allow for standardisation of plate-to-plate variation.

Negative controls (naïve sera) and blank wells (no serum added) were also included on each plate. All samples were run in parallel on lysate from uninfected RBC (1µg/mL total protein concentration) as an additional negative control.

2.4.18. CMV ELISA kit

Total IgG titres against CMV were assessed using a commercially available ELISA kit (Abcam: ab108724) according to the manufacturer's instructions. Plates were pre-coated and pre-blocked. Samples were diluted to 1:100 in the sample dilution buffer provided with the kit. 100µL of diluted sample, positive control, negative control or cut-off IgG were added to individual wells on the pre-coated plate. Samples were incubated for 1 hour at 37° before washing three times with 300µL per well of washing buffer (provided in the kit). Pre-diluted secondary antibody (anti-IgG conjugated to horse-radish peroxidase) was added at 100µL per well and plates were incubated for 30 minutes at RT in the dark. After washing again as before, 100µL of TMB substrate was added per well and plates were left to develop for 15 minutes at RT protected from light. An equal volume of stop solution was added per well and the absorbance was read immediately at 450nm using a BioTek ELx800 microplate reader. Arbitrary units and cut-off values were determined as per the manufacturer's instructions.

2.4.19. MVA-specific IgG ELISA

Anti-MVA ELISAs were conducted using pre-coated and pre-blocked 96-well ELISA plates that were kindly donated by Dr. Huw Davies, University of California, Irvine. Plates were coated with MVA protein WR113/D8L, blocked with casein in Tris buffered saline (TBS), dried and stored at 4°C until use. Serum samples were diluted 1:200 in blocking buffer (1% Casein in TBS supplemented with 10% E. coli lysate) and incubated at RT for 30 minutes to block anti-E. coli reactivity. Samples were then added to the plate in duplicate, 50µL/well. Plates were incubated for 45 minutes at RT before washing six times with PBS. Secondary antibody (goat anti-human IgG conjugated to Horseradish Peroxidase, ADI, H-HuG.211) was added 100µL/well at 1:100 in

PBS and plates were incubated at RT for 45 minutes. Plates were washed six times in PBS before adding 100µL of TMB substrate per well and covering plates to protect from light. After 10 minutes, the reaction was stopped by adding 100µL/well of stop solution. OD450 was read on an ELx800 microplate reader (BioTek) with Gen5 software v2.07(BioTek).

2.4.20. Multiplex serology

Multiplex serology was conducted by Tim Waterboer's lab in the Infection and Cancer Epidemiology Program, German Cancer Research Center (DKFZ), Heidelberg, Germany, as previously described [409]. Proteins were expressed as glutathione S-transferase fusion proteins and affinity-purified by incubation of glutathione-displaying beads in bacterial lysate. Spectrally distinct bead sets, each carrying one particular antigen, were mixed, incubated with serum, and differentiated in a flow cytometer-like analyser (xMAP; Luminex Corp). Antibodies bound to the antigens were detected via fluorescent secondary reagents. Antigens included in the assay are detailed in Table 2.9.

Table 2.9. Antigens included in multiplex serology

Pathogen	Antigens tested
BK virus (BKV)	VP1
Chlamydia trachomatis (*C. trachomatis*)	mompD, mompA, tarpDF1, PorB, pGP3
Cytomegalovirus (CMV)	pp150N, pp52, pp28
Epstein-Barr virus (EBV)	VCAp18, EBNA1, ZEBRA, EAD
Helicobacter pylori (H. pylori)	CagA, VacA, OMP, GroEL, Catalase, Urea
Hepatitis B virus (HBV)	HBcAg, HBeAg
Hepatitis C virus (HCV)	Core, NS3
Herpes simplex virus type 1 (HSV-1)	1gG
Herpes simplex virus type 2 (HSV-2)	2mgG
Human herpes virus type 6 (HHV-6)	IE1B, IE1A, p101k
Human herpes virus type 7 (HHV-7)	U14
Human immunodeficiency virus (HIV)	gag, env
Human T-lymphotrophic virus 1 (HTLV-1)	gag, env
John Cunningham virus (JCV)	VP1
Kaposi's sarcoma-associated herpes virus (KSHV)	LANA, K81
Merkel cell polyomavirus (MCV)	VP1
Toxoplasma gondii (*T. gondii*)	p22, sag1
Varicella zoster virus (VZV)	gEgI

Pathogen-specific serostatus was determined according to previous validation work. For EBV and CMV, seropositivity was determined by seropositivity against at least 2 antigens. For HHV-6, seropositivity was determined by seropositivity against any of the 3 tested HHV-6 antigens. For KSHV serostatus was determined by being seropositive against LANA and/or K8.1. For HBV serostatus was determined by being seropositive against HBcAg and HBeAg. For HCV serostatus was determined by being seropositive against Core and NS3. For *T. gondii* serostatus was determined by being seropositive against sag1 and/or p22. For HTLV-1 serostatus was determined by being seropositive against HTLV-1 gag and/or HTLV-1 env. For HIV-1 serostatus was determined by being seropositive against HIV-1 gag and HIV-1 env. *H. pylori* serostatus was determined by being seropositive against at least 2 out of 6 antigens. For *C. trachomatis* serostatus was determined by being seropositive against pGP3.

2.5. Statistics

Data were tested for normal distribution by D'Agostina-Pearson omnibus normality test, and parametric or non-parametric tests used as appropriate. Most data were analysed using a non-parametric method due to small sample size in human studies. For these samples medians with inter-quartile ranges (IQR) are presented. Differences between two groups were tested using Mann-Whitney analysis and differences between multiple groups were tested using Kruskal-Wallis with Dunn's multiple comparisons post-test. Wilcoxon matched-pairs analysis was used to compare responses at two time points within a group and Friedman's test was used to compare data across multiple time points within a group. Spearman's rank was calculated for correlations. For all statistical analyses $P<0.05$ was considered significant and all P values are two-tailed. Analyses were performed in GraphPad Prism, version 7**.** Binomial logistic regression analysis was used to model the effect of multiple variables on protection from CHMI in Chapter 3. This was conducted in R v3.5.0. Multiple linear regression analysis was used to determine whether anti-schizont and CMV serostatus or immune markers were independently associated

with vaccine-specific T cell and antibody responses in Chapter 7. These analyses were conducted in Prism 8.0.1.

3

Developing a multi-stage malaria vaccine program: Impact of co-administration of RTS,S/AS01B and viral vectored vaccines on immunogenicity and efficacy against malaria

3.1. Introduction

The most advanced vaccine candidate, RTS,S, has shown significant efficacy against clinical malaria in a Phase III trial [237,410-413]. In the first year after vaccination, efficacy was 55.8% in children aged 5 - 17 months and 31.3% in infants aged 6 – 12 weeks [410,411,413]. However, this efficacy waned quickly, dropping to almost nothing in year three [237] and a fourth dose at 18 months may be necessary [238,412]. To improve efficacy, it may be necessary to develop a vaccine regimen targeting multiple stages of the parasite lifecycle [217]. Besides RTS,S, which targets the pre-liver stage, other vaccines are being developed to target liver- and blood-stage parasites, or block transmission and these could be combined into a multistage malaria vaccine regimen [217,258,272,414]. It is likely that for a multistage regimen to provide high level efficacy, it will need to induce both T cell and antibody responses [217].

RTS,S appears to provide protection primarily by inducing antibody responses against the NANP repeat region of the circumsporozoite protein (CSP) on the sporozoite surface [240,415-417]. In contrast, viral vectored vaccines ChAd63-ME-TRAP and MVA-ME-TRAP provide protection through $CD8^+$ T cell responses against infected hepatocytes [252]. We hypothesised that by

vaccinating individuals with both RTS,S and viral vectors we could mobilise both arms of the immune system and enhance efficacy by targeting the parasite through multiple lines of attack.

We first tested RTS,S/AS01B and viral vectored vaccines in a staggered regimen to determine the safety, immunogenicity and efficacy of the combination [401]. Efficacy against controlled human malaria infection (CHMI) was higher for volunteers receiving the combination of vaccines (14/17 subjects protected; vaccine efficacy (VE) 82% [95% CI 64-100]) than for those receiving RTS,S/AS01B alone (12/16 subjects protected; VE 75% [95% CI 54-96]). This suggested that TRAP-specific T cell responses could add to the protective effect of RTS,S-induced antibody responses. However, this regimen required five separate clinic visits over a period of 10 weeks. For this to be an economically and logistically feasible option for deployment in malaria-endemic regions, it was necessary to reduce the number of clinic visits required. Therefore, a further Phase I/IIa trial was conducted to assess concomitant administration of RTS,S/AS01B with viral vectored vaccines [418]. On the basis of high efficacy in two previous trials, additional groups were included to test a reduced third dose of RTS,S/AS01B ($1/5^{th}$, 10μg)[419,420]. Co-administration of these two vaccine platforms resulted in a significant reduction in humoral immunogenicity and efficacy with only 11/19 volunteers protected (VE 58% 95% CI [33-76]), compared with 14/17 (82%, 95% CI [55-94]) in the groups receiving RTS,S/AS01B alone.

To investigate the mechanisms underlying this reduction in humoral immunogenicity, I conducted a thorough analysis of the differences in antibody quality and cTfh responses in volunteers receiving RTS,S/AS01B alone (R), RTS,S/AS01B given with viral vectors in a staggered regimen (R2V) or co-administered (R+V). Details of each trial are summarised in Table 3.1. Vaccination and bleed schedules for each of these trials are illustrated in Figure 3.1.

Table 3.1. Trial summaries

R: 50µg RTS,S/AS01B, r: 10µg RTS,S/AS01B, A: $5x10^{10}$ viral particles (vp) ChAd63-ME-TRAP, M: $2x10^{8}$ plaque forming units (pfu) MVA-ME-TRAP, CHMI: controlled human malaria infection.

	Co-administration study (VAC59)					Staggered study (VAC55)		
	RTS,S/AS01B (R)		**RTS,S/AS01B co-administered with viral vectors (R+V)**			**RTS,S/ AS01B and viral vectors staggered (R2V)**	**RTS,S/ AS01B (R)**	
Group	**G1 R-R-R**	**G2 R-R-r**	**G3 RA-RM-RM**	**G4 RA-RM-rM**	**controls**	**R-A-R-R-M**	**R-R-R**	**controls**
No. volunteers enrolled	10	10	10	11	4	20	17	6
No. volunteers at C-1	9	10	10	9	4	17	16	6
No. volunteers challenged	8	9	10	9	4	17	16	6
Week 0	R	R	RA	RA		R	R	
Week 2						A		
Week 4	R	R	RM	RM		R	R	
Week 8	R	r	RM	rM		R	R	
Week 10						M		
Week 11	CHMI	CHMI	CHMI	CHMI	CHMI			
Week 12						CHMI	CHMI	CHMI
Efficacy: sterilely protected volunteers	6/8 (75%)	8/9 (89%)	6/10 (60%)	5/9 (56%)	0/4	(14/17) 82%	(12/16) 75%	0/6

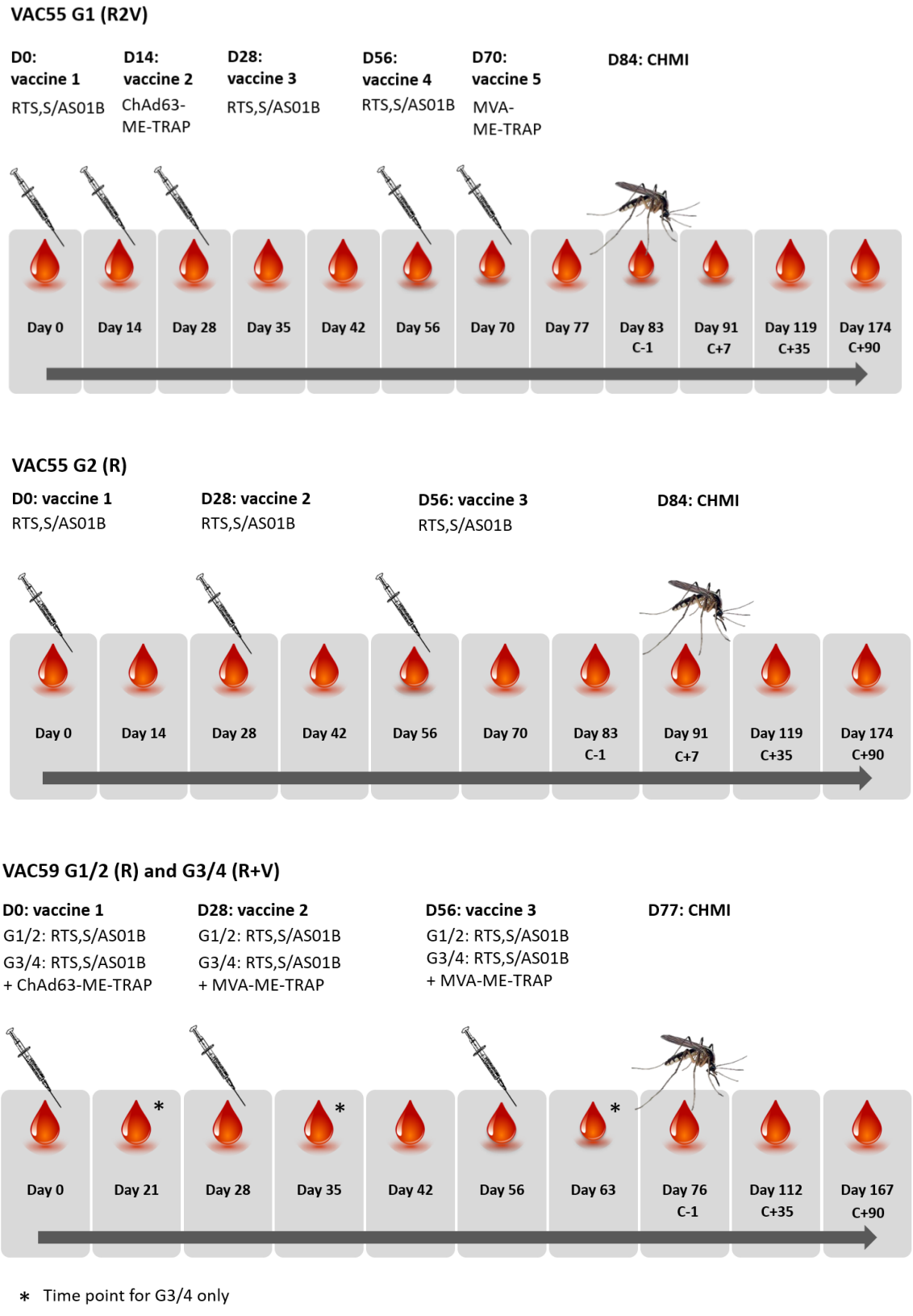

Figure 3.1. Vaccination schedules
Vaccination and bleed schedules for VAC55 and VAC59 trials. CHMI: controlled human malaria infection. D21, D35, D63, D77 time points for T cell assays only.

Total IgG, IgG subclass and isotype responses against the NANP repeat region of CSP were measured using an indirect enzyme-linked immunosorbent assay (ELISA). Antibody binding to fixed whole sporozoites was also measured by immunofluorescence assay (IFA). To further assess the quality of vaccine-induced antibody an *in vitro* assay was used to measure the ability of antibody to block sporozoite invasion into hepatocytes. The proportions of cTfh subsets and their associations with antibody responses were then investigated by flow cytometry. Additionally a cytometric bead array assay was used to measure cytokine responses to CSP and MVA.

At the time of completion this was the first study to assess the impact of vaccine co-administration on the cTfh response in humans. It also defines a functional antibody quality that may explain the improved efficacy observed in RTS,S regimens with a reduced third dose.

3.2. Study-specific methods

3.2.1. Samples and study details

Full details of these studies are available in the clinical trial reports [401,418]. Healthy adult volunteers were recruited and vaccinated at four UK sites, in Oxford, Southampton, London and Surrey. The CHMI procedure was performed as described in Chapter 2.3. Each trial used a single batch of infected mosquitoes, supplied by the Department of Entomology, WRAIR, Washington DC, USA. All vaccinations were administered intramuscularly into the deltoid region of the arm. For participants who received concomitant vaccinations, RTS,S/AS01B was administered first followed by the viral vectored vaccine in the same site no longer than five minutes later. For the staggered administration trial all doses of RTS,S were given in the left arm and each dose of viral vectored vaccine was given in the contralateral (right) arm.

3.2.2. Safety of RTS,S/AS01B and viral vectored TRAP vaccines in combination regimens

The safety profiles of RTS,S/AS01B given with ChAd63-ME-TRAP and MVA-ME-TRAP in staggered or co-administered regimens were comparable to regimens in which RTS,S/AS01B or viral vectors were administered alone. The majority of adverse events following vaccinations in all groups were mild in severity and self-limiting. Detailed safety profiles have been described elsewhere [401,418].

3.3. Results

3.3.1. RTS,S/AS01B and viral vectored TRAP vaccines in a staggered regimen are highly immunogenic and provide high levels of protection against CHMI

High levels of sterile protection against CHMI were achieved when RTS,S/AS01B was administered alone (R) or in a staggered regimen with viral vectors ChAd63-ME-TRAP and MVA-ME-TRAP (R2V) (R: 12/16 protected, 75%, 95% CI[54-96)], R2V: 13/17 protected, 82%, 95%CI[64-100]).

NANP-specific IgG titres induced by RTS,S/AS01B administered alone (VAC55 G2, R) or in a staggered regimen with viral vectored vaccines (VAC55 G1, R2V) were comparable at all time points (Figures 3.2A, 3.2B). Titres peaked for most individuals the day before CHMI (C-1, D83). Median titres at this time point were 1185 EU (IQR: 113 - 1589) in the RTS,S/AS01B only regimen (R) compared with 1240 EU (IQR: 321 - 1714) in the RTS,S/AS01B and viral vectored vaccine regimen (R2V). NANP-specific IgG titres at this time point were low in some individuals who were not sterilely protected against CHMI but were also low in a number of individuals who were sterilely protected (Figure 3.1B). Median NANP IgG titres at C-1 were lower in non-protected individuals (1347 EUs IQR[593 – 2481]) compared with protected individuals (2226

EUs IQR[1244 – 2900]), although this did not reach the significance threshold set for this study(Mann-Whitney P=0.053).

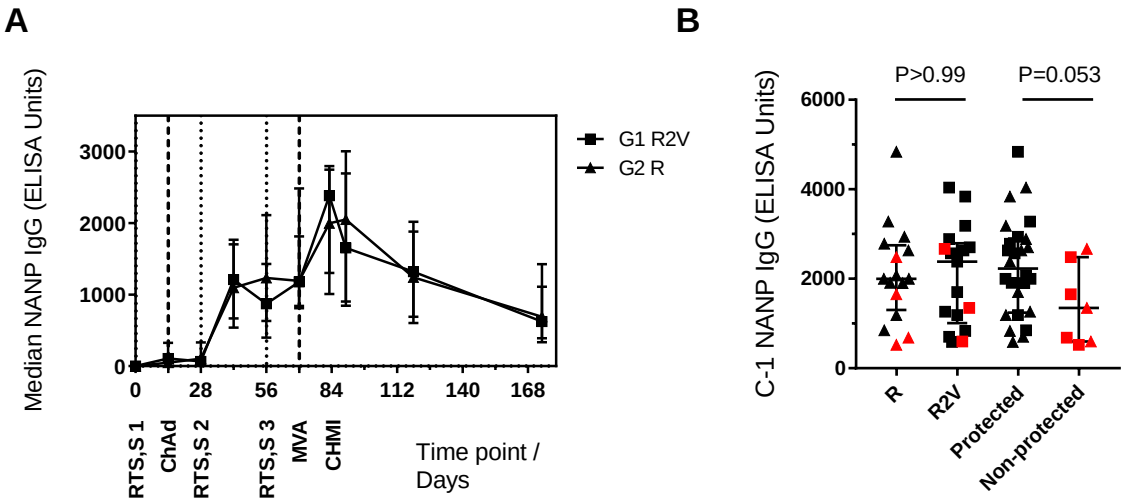

Figure 3.2. Humoral responses to RTS,S/AS01B in a staggered regimen with viral-vectored vaccines

A) Median NANP IgG time courses. RTS,S vaccinations 1, 2 and 3 are marked with dotted lines, ChAd63-ME-TRAP and MVA-ME-TRAP vaccinations (R2V group only) are marked with dashed lines. **B**) Peak (C-1) NANP IgG titres in each group. Mann-Whitney P>0.99. R2V: G1, RTS,S and viral vectored vaccines staggered, marked by squares R: G2, RTS,S/AS01B only, marked by triangles. Protected vs non-protected individuals across both groups Mann-Whitney P=0.053. Medians and inter-quartile ranges shown. Non-protected volunteers highlighted in red.

T cell responses against CSP induced by RTS,S were low (median CSP IFNγ ELISpot response at peak across all volunteers: 29 SFC/10^6 PBMC, IQR[12 – 99]). Responses were comparable in both regimens at all time points before MVA vaccination (Figure 3.3A). However, at C-1, two weeks after MVA, there were more CSP-specific T cell responses above the LLOD in the group that received viral vectored vaccines compared with those receiving RTS,S/AS01B alone, although there was no significant difference (Figure 3.3B, Mann-Whitney P=0.067). Viral vectored vaccines induced high TRAP-specific T cells after prime (median 535 SFC/10^6 PBMC IQR[220 – 1911]) and boost (2510 [835 – 4543]). These responses were comparable to those in a previously tested regimen in which viral vectors were administered alone (Figure 3.3C, VAC45 G2). Peak T cell responses against TRAP were significantly associated with peak T cell responses

against CSP (Figure 3.3D, Spearman r:0.65, P=0.010). There was no association between the size of the TRAP T cell response and the antibody response against NANP (Figure 3.2E, Spearman r:0.089, P=0.75).

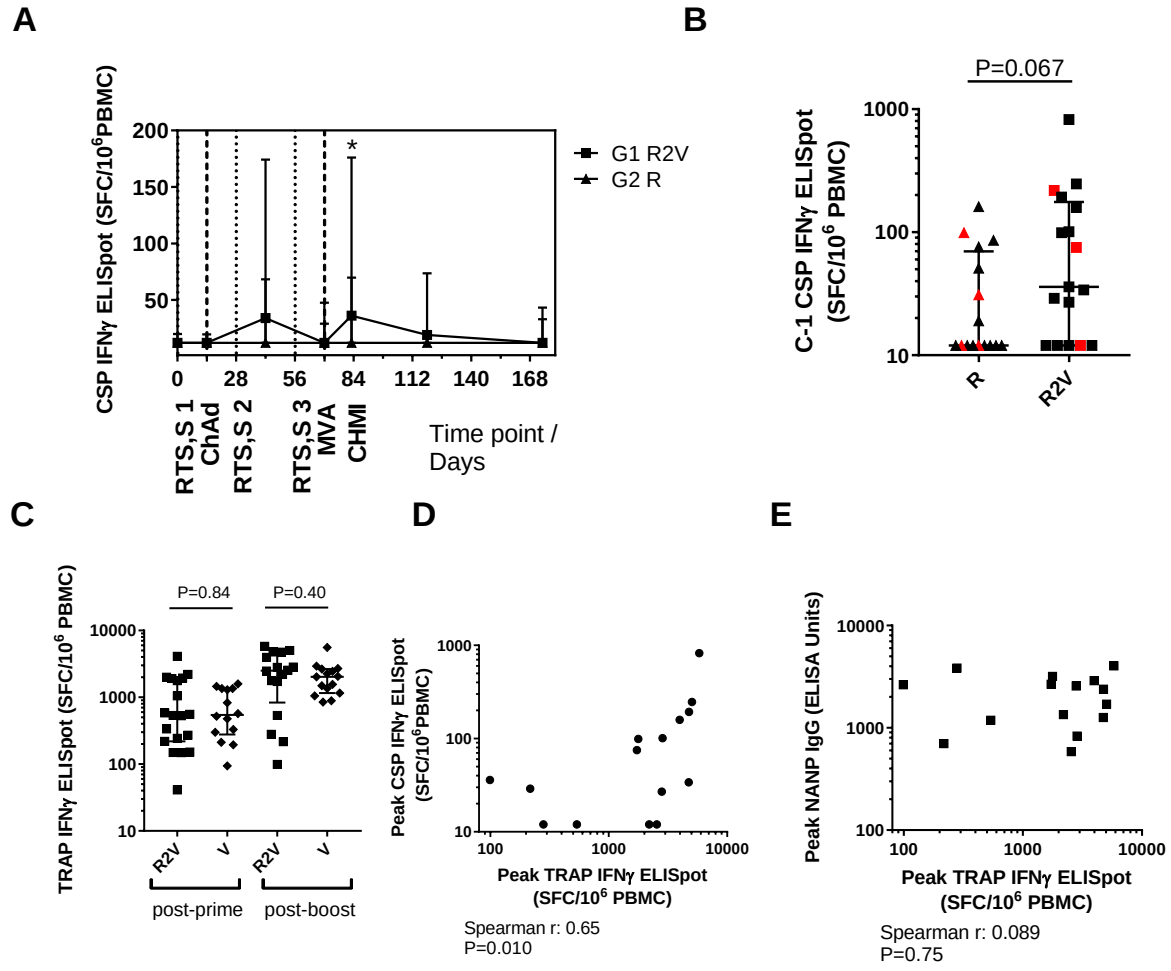

Figure 3.3. T cell responses to RTS,S and viral vectored vaccines in a staggered regimen
A) Median IFNγ ELISpot time courses – summed pools of CSP peptides. RTS, S vaccinations 1, 2 and 3 are marked with dotted lines, ChAd63-ME-TRAP and MVA-ME-TRAP vaccinations (R2V group only) are marked with dashed lines. **B**) Peak (C-1) IFNγ ELISpot responses. Non-protected volunteers are highlighted in red. Mann-Whitney P=0.067. **C**) IFNγ ELISpot responses (summed ME + T996 TRAP pools) at peak post prime (14 days after ChAd63-ME-TRAP) and peak post boost (seven days after MVA-ME-TRAP) in the staggered regimen with RTS,S/AS01B compared with a previous trial of ChAd63-ME-TRAP and MVA-ME-TRAP in a single administration regimen (VAC45). Relationship between peak TRAP IFNγ ELISpot response (one week post-boost) and **D**) peak (C-1) CSP IFNγ ELISpot response and E) peak (C-1) NANP IgG titres.

3.3.2. Co-administration of RTS,S/AS01B and viral vectored vaccines induces high T cell responses

Co-administration of RTS,S/AS01B with viral vectored vaccines resulted in a significantly higher TRAP-specific T cell response one week after the first MVA boost when compared with viral vectors administered alone (Figure 3.4A, VAC43 G5 and G6, ChAd63-ME-TRAP with MVA-ME-TRAP four weeks later, Mann-Whitney P=0.026). However, the T cell responses peaked after the initial MVA and no boost was observed after the second MVA dose administered with the third RTS,S/AS01B dose. The TRAP-specific T cell responses at this time point (D63) were not significantly different to those in a similar regimen tested previously (VAC43 G3: ChAd63-ME-TRAP with two MVA-ME-TRAP boosts, each at four week intervals). There were no significant differences in the T cell response to CSP when the two vaccine platforms were co-administered compared with RTS,S/AS01B alone (Figure 3.4B).

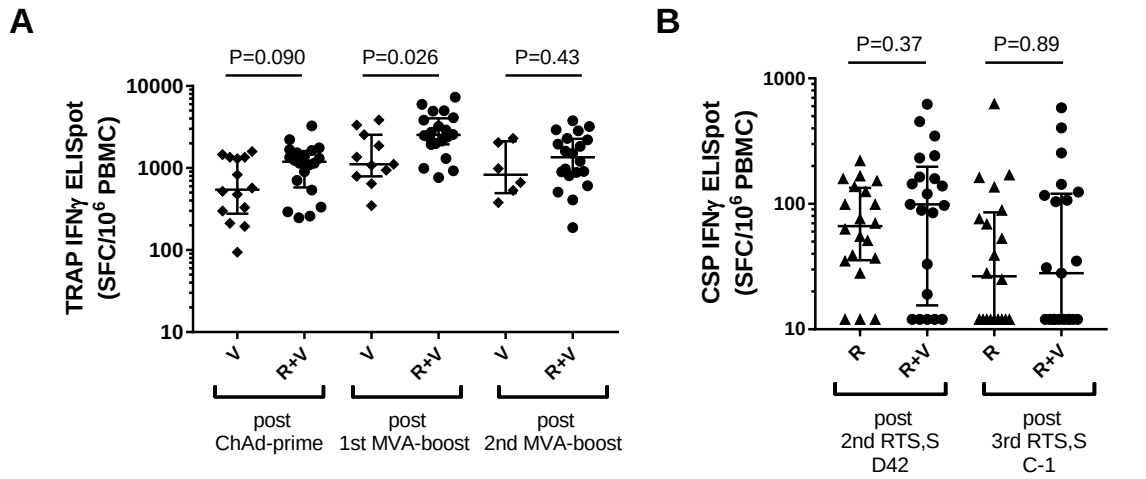

Figure 3.4. T cell responses to RTS,S and viral vectored vaccines in the co-administration regimen

A) TRAP IFNγ ELISpot after vaccination with viral vectored vaccines alone or co-administered with RTS,S/AS01B. Peak post ChAd63-ME-TRAP prime (VAC45 G2 D14 vs VAC59 G3/4 D21), peak at 1 week post first MVA boost, 4 weeks after prime (VAC43 G5/6 D35 vs VAC59 G3/4 D35) and peak post second MVA boost, 4 weeks after the initial MVA (VAC43 G3 D91 vs VAC59 G3/4 D63). Mann-Whitney t-tests. NB VAC43 G3 also had an additional Ad prime (A-A-M-M) but this is the most comparable group available). **B**) CSP IFNγ ELISpot after second and third doses of RTS,S/AS01B alone or co-administered with viral vectored vaccines. Mann-Whitney analyses. T cell responses were not measured after the first RTS,S/AS01B dose in this trial as they were so low in the previous trial (VAC55). No significant difference (NSD) between groups given reduced and standard third doses of RTS,S/AS01B, therefore they are combined for these analyses.

To determine whether the TRAP T cell responses to the second MVA dose were inhibited by anti-vector antibodies, MVA-specific IgG was measured in volunteers from the co-administration groups at baseline, post first MVA (D42) and post second MVA (C-1). Vaccination with MVA-ME-TRAP induced significant anti-MVA IgG titres, which were boosted by a second dose of MVA (Figure 3.5A). However titres of anti-MVA IgG were not significantly associated with a reduction in TRAP-specific T cells at C-1 (Figure 3.5B).

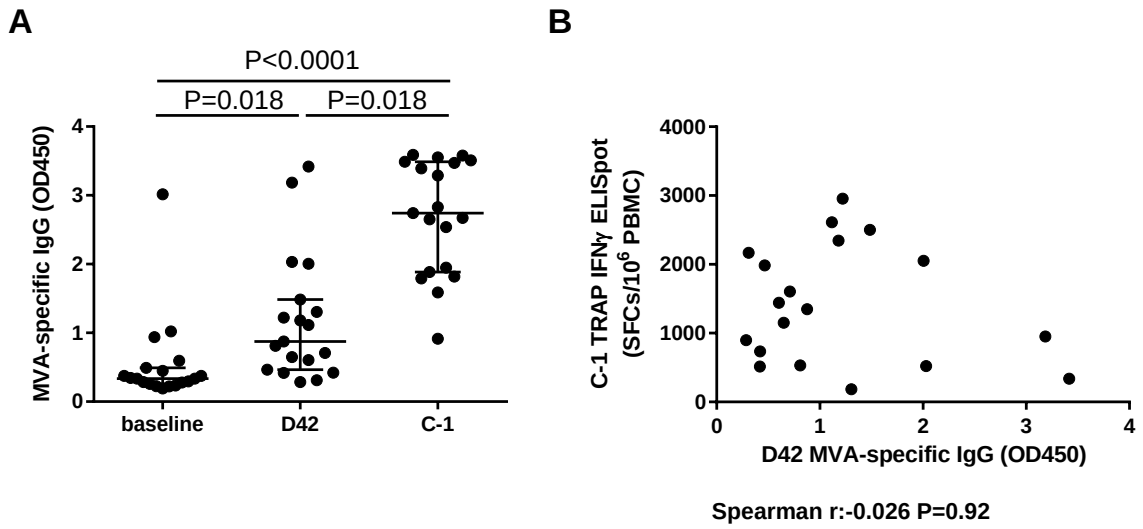

Figure 3.5. T cell responses to RTS,S and viral vectored vaccines in the co-administration regimen

A) Anti-MVA IgG titres in VAC59 G3/4 (R+V) measured by ELISA. Friedman test with Dunn's multiple comparisons post-test. **B**) Relationship between MVA-specific IgG at D42 and TRAP-specific T cell responses measured by IFNγ ELISpot at C-1.

3.3.3. Co-administration of RTS,S/AS01B and viral vectored vaccines significantly reduced the quality and quantity of antibody responses

Antibody responses against NANP were measured by ELISA at day 0 (D0), D28, D42, D56, D76 (the day before CHMI, C-1, in the co-administration trial) and 35 and 90 days after CHMI (C+35, C+90). CHMI was one week later (D84) in the staggered regimen trial (VAC55) presented in 3.3.1 to accommodate the additional vaccinations. Here, the main focus is the comparison of RTS,S/AS01B administered alone or co-administered with viral vectors, therefore antibody

responses in the co-administered regimen (VAC59) are compared with the RTS,S/AS01B groups from the same trial (as samples from directly comparable time points were available, Figure 3.6A). The staggered regimen (VAC55 G1) has been included as an additional comparison but it should be noted that the bleed schedule differed slightly (see Figure 3.1). Titres were comparable in all regimens after the first two vaccinations but failed to re-boost after the third vaccination in the co-administration regimen, leading to significantly lower titres in these groups at C-1 (Figure 3.6B, median ELISA Units, R: 1102 IQR [757-2035], R+V: 533 IQR [394-790], R2V: 1969 IQR [983 – 2724] Kruskal-Wallis P<0.0001). There were no significant differences in NANP IgG titres between groups receiving a full or reduced third dose of RTS,S/AS01B either alone or co-administered with viral vectored vaccines. The highest titres were observed in the staggered regimen at D83 (four weeks after the third dose of RTS,S/AS01B) although there was no comparable time point in the co-administration study.

Isotype and subclass responses were measured by ELISA against the NANP repeat region at C-1 in both trials (Figure 3.6C). Titres were measured for IgG1-4, IgM and IgA. No NANP-specific IgG4 was detected in any volunteers. Over 80% of volunteers given RTS,S/AS01B alone were seropositive for NANP-specific IgG2, IgG3, IgM and IgA. There were significant reductions in seroconversion for these isotypes/subclasses in groups that received concomitant viral vectored vaccinations, but this reduction was not seen in the staggered regimen. All volunteers were positive for NANP IgG1 and titres were comparable in the RTS,S/AS01B only groups (R) and the staggered administration group (R2V), but were significantly reduced in the co-administration regimen (R+V) (Figure 3.6D, median OD, R: 0.617 IQR [0.488 – 0.835], R+V: 0.415 [0.343 – 0.514], R2V: 0.570 [0.438 – 0.935] Kruskal-Wallis P=0.0062). There were no differences in IgG1 titres between groups receiving full or reduced third doses of RTS,S/AS01B (G1 R-R-R vs G2 R-R-r and G3 RA-RM-RM vs G4 RA-RM-rM, data not shown).

Antibody binding to fixed whole sporozoites was measured for all volunteers at C-1 using an indirect immunofluorescence assay (IFA). Sporozoite-binding IgG was significantly lower in the co-administration regimen but the staggered regimen was comparable to RTS,S/AS01B alone (Figure 3.6E, median fluorescence intensity, R: 238 IQR [213 – 245] R+V: 151 [98 – 175], R2V: 228 [215 – 245] Kruskal-Wallis P<0.0001). There were no differences between groups receiving full or reduced third doses of RTS,S/AS01B. Sporozoite binding was significantly associated with NANP IgG titre in the co-administration groups (Figure 3.6F, Spearman r:0.58, P=0.0094). This association was not present in the RTS,S/AS01B alone or staggered regimens (Spearman r:-0.012, P=0.96 and r:0.058, P=0.83, respectively), in which sporozoite binding was higher for a given NANP IgG titre compared to the co-administration regimen.

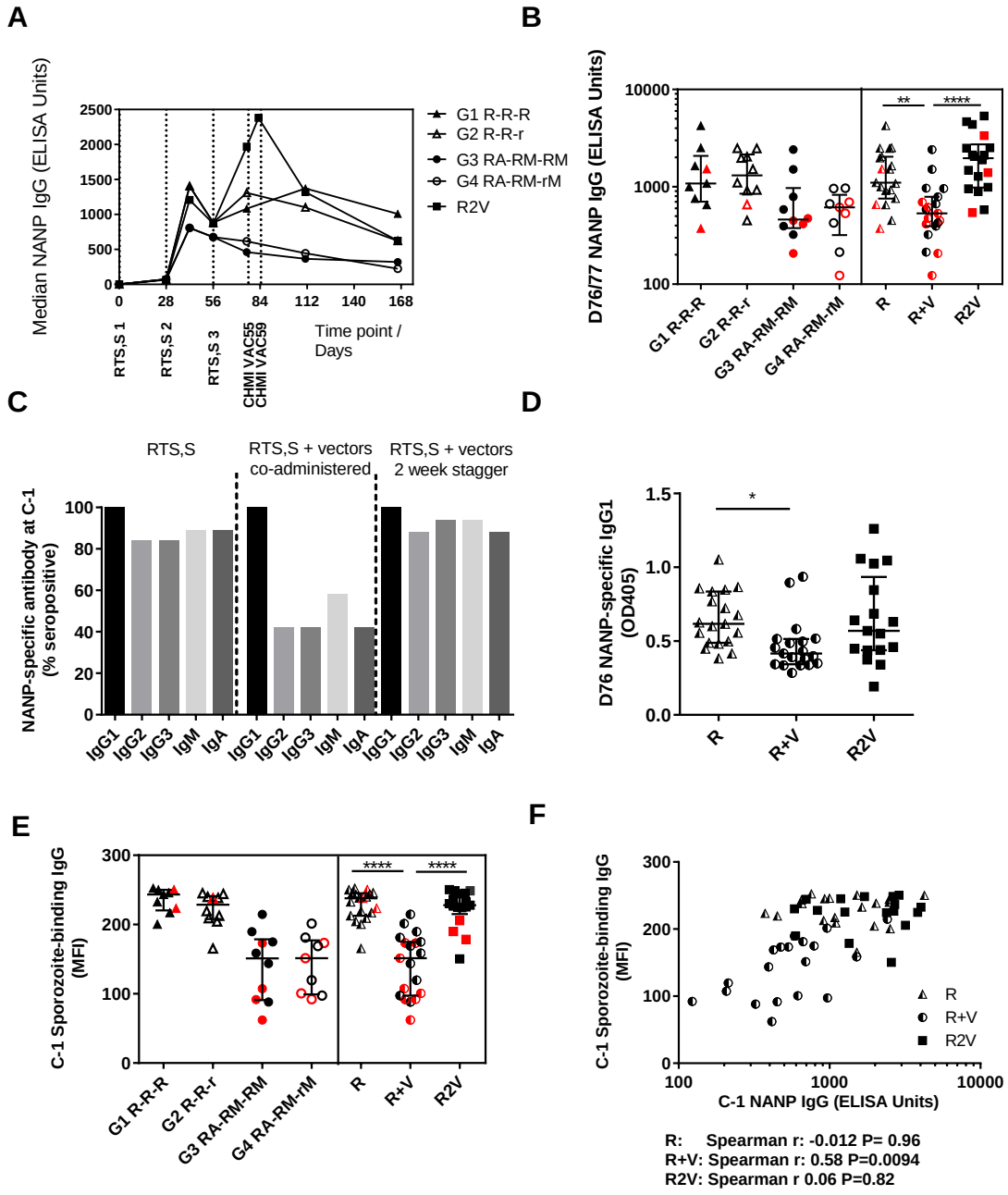

Figure 3.6. Antibody quantity and quality

A) Median NANP IgG time courses. **B**) Total IgG titres against the CSP repeat region NANP in each group at D76/77 (three weeks after 3rd dose of RTS,S/AS01B), in G1/2 combined (R) and G3/4 combined (R+V) or in the staggered regimen (R2V), Kruskal-Wallis with Dunn's post-test P<0.0001. **C**) Isotype and NANP-specific IgG subclass responses at C-1. **D**) NANP-specific IgG1 at C-1, Kruskal-Wallis P=0.0062. **E**) Median fluorescence intensity (MFI) of sporozoite-binding IgG at C-1 measured by immunofluorescence assay (IFA), Kruskal-Wallis P<0.0001. **F**) Relationship between NANP IgG titre and level of sporozoite-binding at C-1. Volunteers receiving RTS,S/AS01B alone (G1/2, R) Spearman r:-0.012, P=0.96, RTS,S/AS01B co-administered with vectors (G3/4, R+V) Spearman r:0.58, P=0.0094 or RTS,S/AS01B and viral vectors given in a staggered regimen Spearman r:0.06, P=0.82. Medians + IQRs shown and non-protected volunteers highlighted in red for all column graphs. In these studies the RTS,S/AS01B group from VAC59 was compared against the co-administration group from VAC59 and the staggered regimen from VAC55 as samples were taken at D76/77 in all of these groups but not in the RTS,S/AS01B only group from VAC55.

3.3.4. Inhibition of sporozoite invasion is associated with protection from CHMI

The functional quality of vaccine-induced antibodies was assessed using an *in vitro* assay measuring the ability of serum to block sporozoite infection of hepatoma cells[405](Gating strategy shown in Figure A8). The percentage of infection blocked by vaccine-induced antibody was significantly lower in the co-administration regimen compared with RTS,S/AS01B alone (Figure 3.7A, median percentage infection blocked R, 90% IQR [76 – 98], R+V 80% [52 - 89], Mann-Whitney P=0.016). However, blocking ability was significantly enhanced in groups receiving a reduced third dose of RTS,S/AS01B compared with those receiving three standard doses, even when this dose was co-administered with viral vectored vaccines (Figure 3.7A, medians + IQRs G1 R-R-R: 80% [71.5 – 91.5], G2 R-R-r: 96% [89.3 – 98], G3 RA-RM-RM: 55% [50 – 73.5], G4 RA-RM-rM: 89% [85 – 95], Mann-Whitney analyses R-R-R vs R-R-r P=0.014, RA-RM-RM vs RA-RM-rM P<0.0001, R-R-R and RA-RM-RM vs R-R-r and RA-RM-rM P<0.0001). Inhibition of sporozoite invasion was significantly associated with C-1 NANP IgG titre for groups receiving three standard doses of RTS,S/AS01B (Figure 3.7B, R-R-R and RA-RM-RM Spearman r:0.78 P<0.0001) but not in groups receiving a reduced third dose, in which blocking ability was higher even at lower NANP IgG titres (R-R-r and RA-RM-rM Spearman r:0.44 P=0.061). Blocking ability was associated with protection from malaria after CHMI, with significantly higher percentages of infection blocked in protected compared with non-protected volunteers (Figure 3.7C, medians + IQRs protected: 88% [75 – 97], non-protected: 71% [52 – 87.5] Mann-Whitney P=0.019). Volunteers in the co-administration groups that were protected despite having low levels of sporozoite-blocking antibody had high TRAP-specific T cell responses (Figure 3.7D).

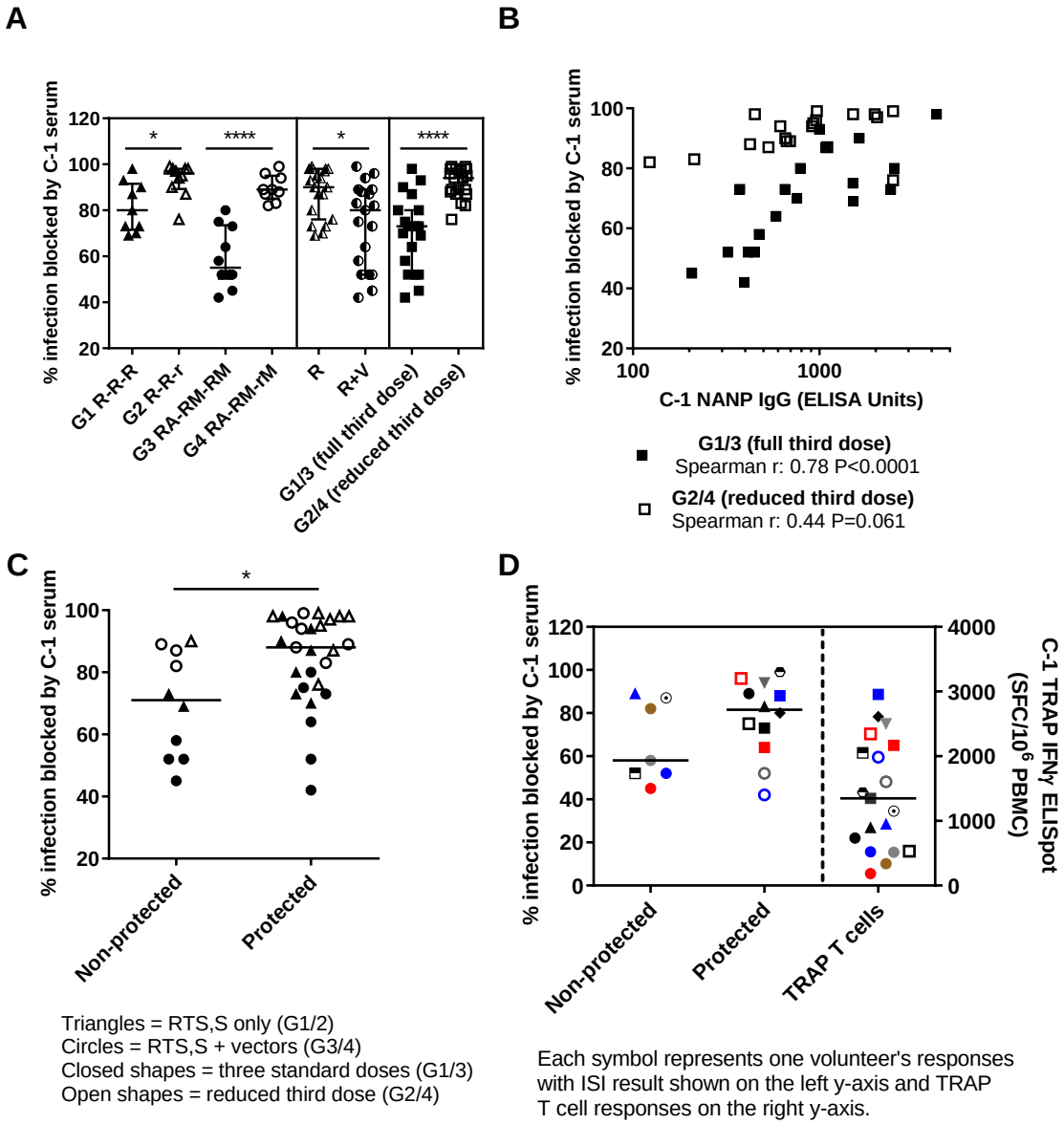

Figure 3.7. Inhibition of sporozoite invasion

A) Percentage of sporozoite invasion into hepatoma cells that was blocked by serum at C-1. Comparison of groups given three standard doses of RTS,S/AS01B or a reduced (1/5th) third dose of RTS,S/AS01B. Mann-Whitney analyses G1 R-R-R vs G2 R-R-r P=0.014, G3 RA-RM-RM vs G4 RA-RM-rM P<0.0001, G1/2 (R) vs G3/4 (R+V) P=0.016, G1/3 (full third dose of RTS,S/AS01B) vs G2/4 (reduced third dose of RTS,S/AS01B) P<0.0001, medians + IQRs. **B**) Relationship between C-1 NANP IgG titres and sporozoite blocking ability in individuals that received three full doses of RTS,S/AS01B with, or without vectored vaccines (G1 and G3, closed squares, Spearman r:0.78, P<0.0001) or a reduced third dose of RTS,S/AS01B with, or without vectored vaccines (G2 and G4, open squares, Spearman r:0.44, P=0.061). **C**) Percentage of sporozoite invasion blocked by C-1 serum from individuals protected and non-protected individuals, Mann-Whitney P=0.017. Closed triangles: G1, open triangles: G2, closed circles: G3, open circles: G4. **D**) Percentage of sporozoite invasion blocked by C-1 serum from protected and non-protected volunteers in G3/4, R+V (left Y-axis) and corresponding C-1 TRAP T cell responses (right Y-axis) for each volunteer. Lines at medians.

The relationship between blocking ability and the NANP-specific isotype/subclass titres was also assessed (Figure 3.8). Relationships between all subclasses and isotypes tested and blocking ability demonstrated a similar pattern to total IgG, with a positive correlation in G1/3 and high blocking regardless of titre in G2/4. However, IgG1 was the only isotype that showed an association with blocking ability in the data set as a whole (G1-4, Spearman r:0.42 P=0.009).

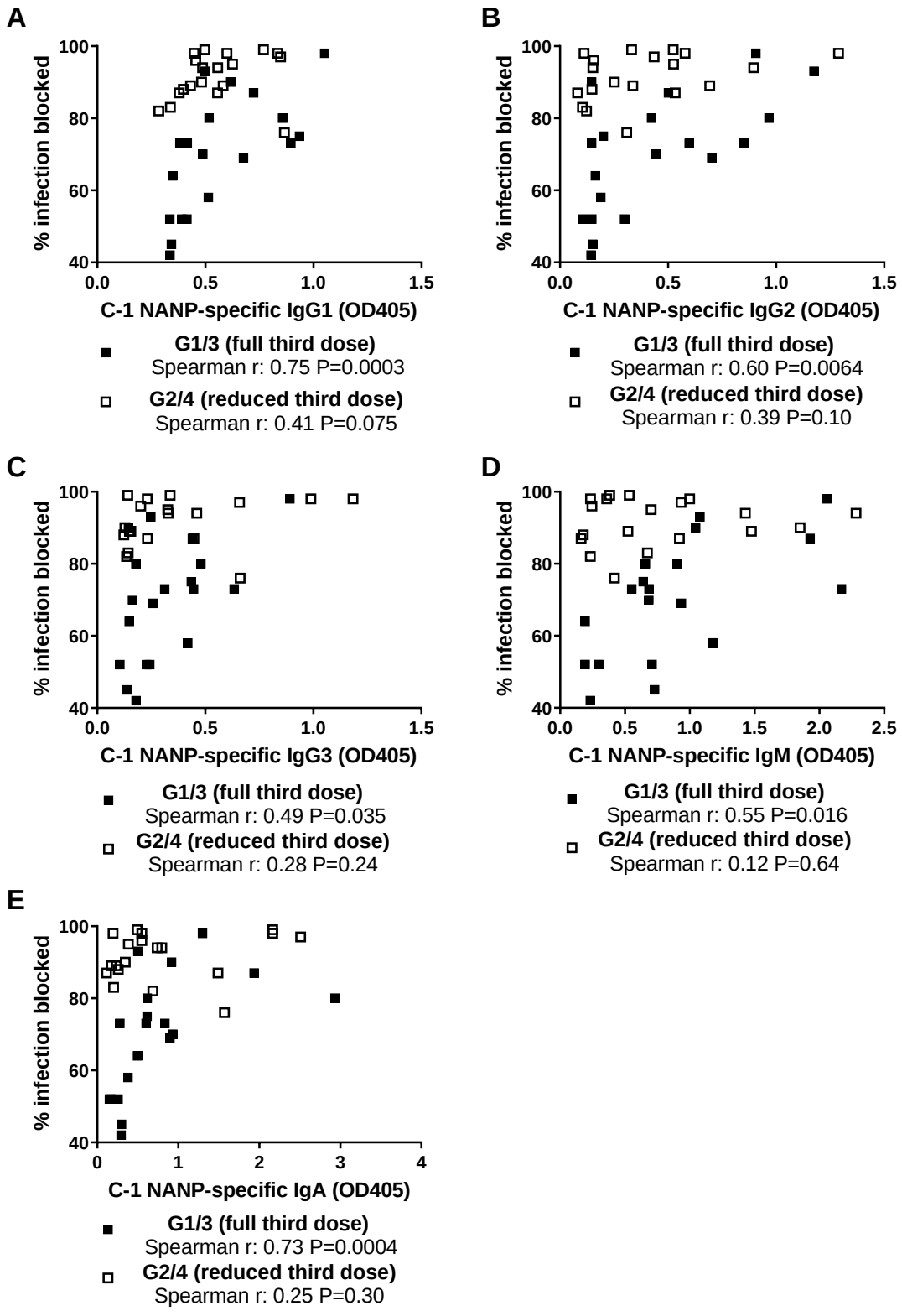

Figure 3.8. Relationship between NANP-specific isotypes/subclasses and inhibition of sporozoite invasion

Associations between NANP-specific isotypes and subclass titres at C-1 and inhibition of sporozoite invasion **A**) IgG1, **B**) IgG2, **C**) IgG3, **D**) IgM, **E**) IgA.

3.3.5. The proportion of CXCR3$^+$ cTfh increases when RTS,S/AS01B is co-administered with viral vectored vaccines and negatively correlates with antibody responses

To determine whether cellular differences associated with the reduction in antibody responses in the co-administration regimen could be detected in the blood, cTfh were phenotyped at C-1 by surface staining and flow cytometry using a defined gating strategy (Figure A4). Total cTfh were analysed for all volunteers in the co-administration study (except one volunteer in G4 for which there were no cryopreserved cells remaining) and 10 volunteers in the staggered administration study with enough cryopreserved cells remaining for the experiment (Figure 3.9A). The proportion of cTfh (PD1$^+$CXCR5$^+$) within memory CD4$^+$ T cells ranged from 0.1% - 4.8%, was comparable across groups and did not correlate with CSP- or TRAP-specific antibody responses. Subsets within cTfh were identified using CXCR3 and CCR6: cTfh17 (CXCR3$^-$CCR6$^+$), CXCR3$^+$ (including double positive (CXCR3$^+$CCR6$^+$) and cTfh1 (CXCR3$^+$CCR6$^-$)), and cTfh2 (CXCR3$^-$CCR6$^-$). Volunteers that received RTS,S/AS01B co-administered with viral vectored vaccines had significantly higher frequencies of CXCR3$^+$ cTfh and significantly lower frequencies of cTfh2 than those that received RTS,S/AS01B alone. The staggered administration group had an intermediate phenotype which was not significantly different to either of the other regimens (Figure 3.9B). There were no significant differences in the frequencies of any population between G1 R-R-R and G2 R-R-r or G3 RA-RM-RM and G4 RA-RM-rM (data not shown). In the co-administration regimen, the percentage of CXCR3$^+$ cTfh negatively correlated with antibody responses to both vaccines (Figure 3.9C, NANP Spearman r:-0.78, P=0.0001, TRAP Spearman r:-0.50, P=0.036). For groups that received RTS,S/AS01B alone, the frequency of CXCR3$^+$ cTfh was lower and there was no association with antibody responses (Figure 3.9D, Spearman r:0.32 P=0.18). Although in the staggered regimen the proportion of CXCR3$^+$ cTfh was comparable to that in the co-administration regimen, there was no association with antibody responses in that regimen

(Spearman r:0.26 P=0.47). The proportion of CXCR3$^+$ in CXCR5$^-$ memory CD4$^+$ T cells was not associated with antibody responses in any regimen (data not shown).

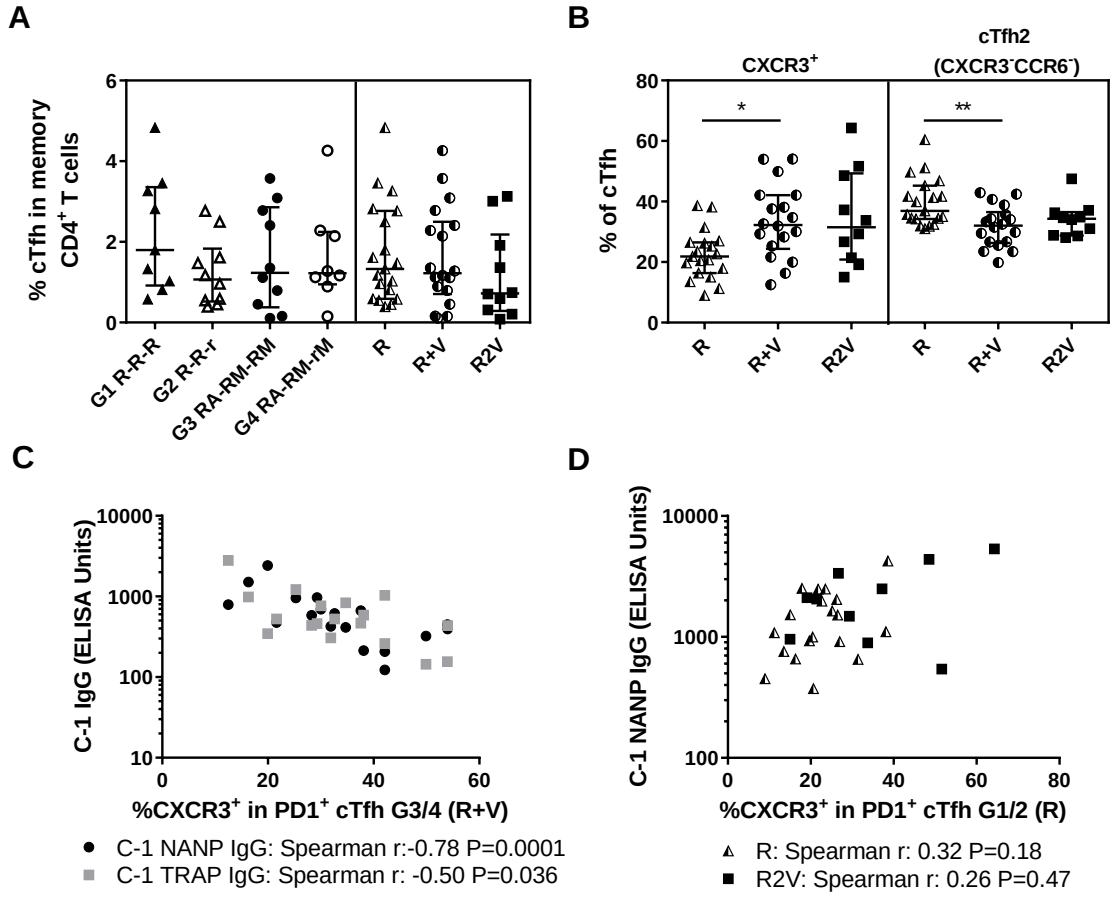

Figure 3.9. Total circulating T follicular helper cells

A) Percentage of cTfh (PD1$^+$CXCR5$^+$) within memory CD4 T cells (CD45RA$^-$) at C-1. **B**) Subsets within cTfh (at C-1) defined by chemokine receptor expression: cTfh2 (CXCR3$^-$CCR6$^-$), or CXCR3$^+$; including double positive, dp (CXCR3$^+$CCR6$^+$) and cTfh1 (CXCR3$^+$CCR6$^-$). Kruskal-Wallis analyses; CXCR3$^+$ P=0.012, cTfh2 P=0.0090. **C**). Relationship between percentage of CXCR3$^+$ cTfh and antibody responses at C-1 in individuals who received RTS,S/AS01B co-administered with viral-vectored vaccines (G3/4). NANP IgG (Spearman r:-0.78, P=0.0001), TRAP IgG (Spearman r:-0.50, P=0.036). **D**). Relationship between percentage of CXCR3$^+$ cTfh and C-1 NANP IgG in individuals vaccinated with RTS,S/AS01B alone (R, G1/2, Spearman r:0.32, P=0.18) or RTS,S/AS01B and viral vectored vaccines in a staggered regimen (R2V, Spearman r:0.26, P=0.47). R G1/2: RTS,S/AS01B vaccinated, R+V G3/4: RTS,S/AS01B and viral vectored vaccines co-administered, R2V: RTS,S/AS01B and viral vectored vaccines at a two week stagger, A: ChAd63-ME-TRAP, M: MVA-ME-TRAP, R: 50µg RTS,S/AS01B, r: 10µg RTS,S/AS01B, CHMI: controlled human malaria infection, C-1: day before CHMI.

3.3.6. Th1-biased cytokine responses driven by viral vectors are associated with the increase in CXCR3^{+} cTfh and reduction in antibody responses to RTS,S

Concentrations of T-helper cytokines in the supernatant of C-1 PBMC from the co-administration study were measured using a cytometric bead array (LEGENDplex, Biolegend). PBMC were stimulated with CSP (all groups) or MVA (G3 and G4) and concentrations of IL-5, IL-13, IL-2, IL-6, IL-9, IL-10, IFNγ, TNFα, IL-17A, IL-17F, IL-4, IL-21 and IL-22 were measured (Figure 3.10A). High concentrations of IL-2, IFNγ, TNFα, IL-6 and IL-22 were detected. The concentration of IFNγ was particularly high in the supernatant from MVA-stimulated PBMC, where all samples produced >3000 pg/mL. In comparison, IFNγ responses were significantly lower after CSP-stimulation, with no detectable IFNγ in 9/34 samples and less than 1000 pg/mL in most where responses were detected. However, PBMC from volunteers in the co-administration groups produced more IFNγ in response to CSP stimulation than those from volunteers that received RTS,S/AS01B alone (Figure 3.10B, median pg/mL + IQR, R CSP: 114 [1 – 348], R+V CSP: 311 [96-610], R+V MVA: 16,796 [11,409 – 20,462], Kruskal-Wallis P<0.0001). Additionally, IFNγ was a greater proportion of the CSP cytokine response in non-protected G3/4 (R+V) volunteers than protected G3/4 volunteers (Figure 3.10C).

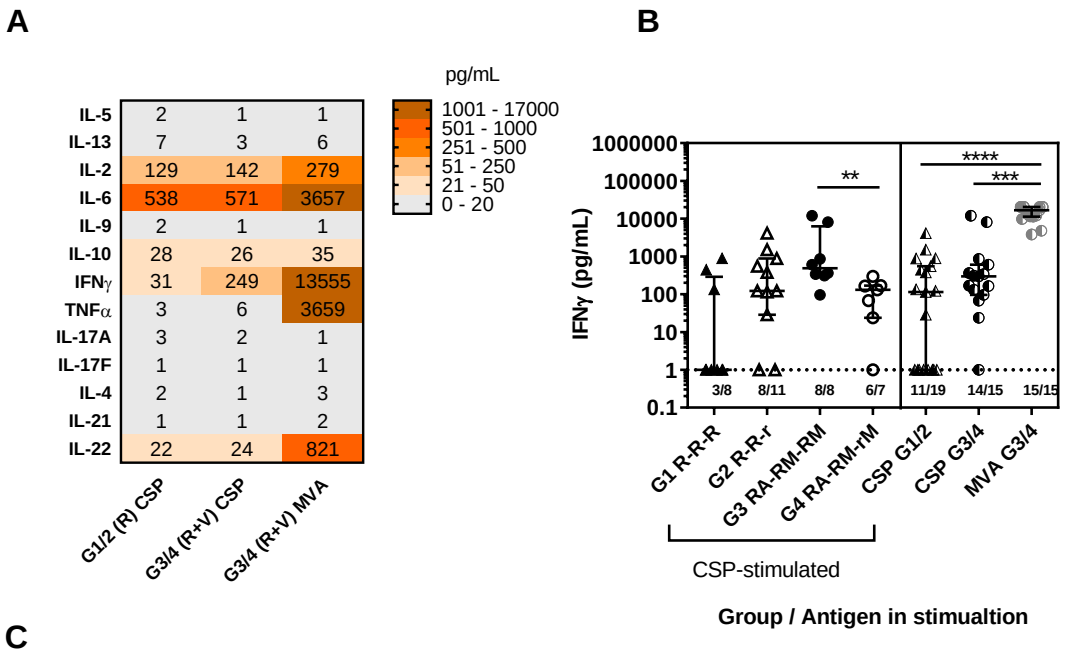

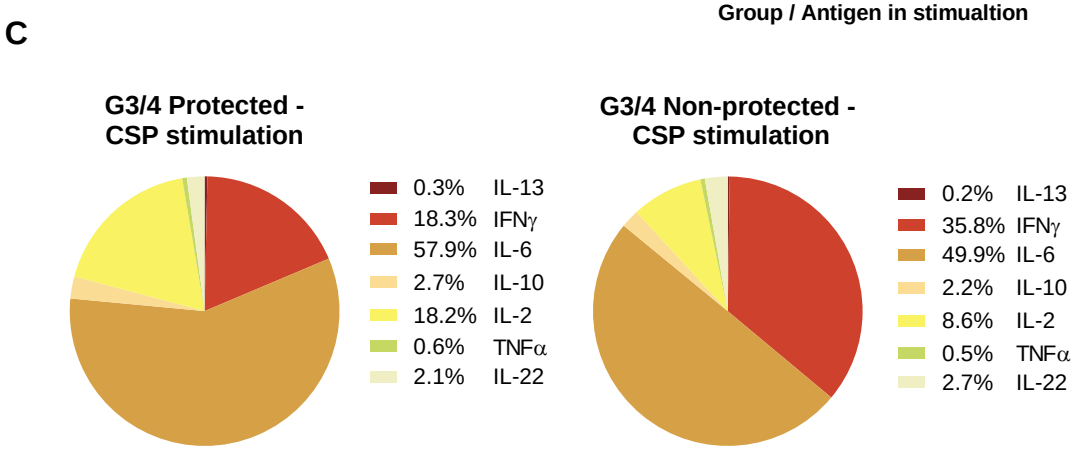

Figure 3.10. Cytokine responses to CSP and MVA

Cytokine responses measured in supernatant after stimulation of 1-2x10^6 PBMC at C-1 with CSP or MVA. Responses were measured for 19 G1/2 samples stimulated with CSP and 15 G3/4 samples for which there were enough cells to run both CSP and MVA stimulations. **A**) Geomean cytokine concentrations in supernatant of G1/2 PBMC stimulated with CSP compared with G3/4 PBMC stimulated with CSP or MVA. **B**) Concentration of IFNγ in supernatant of PBMC stimulated with CSP or MVA, Kruskal-Wallis with Dunn's multiple comparisons P<0.0001. Mann-Whitney analysis between G3 RA-RM-RM and G4 RA-RM-rM P=0.0037. Lower limit of detection (LLOD) for all cytokines in this assay was 1pg/mL. **C**) Proportions of cytokines produced in response to CSP stimulation (geomeans) in G3/4 (R+V) volunteers that were protected compared with non-protected. The level of each cytokine produced is shown as a percentage of the total cytokine response to CSP in each group.

The concentration of IFNγ in the supernatant of PBMC stimulated with CSP was positively associated with the proportion of CXCR3$^+$ cTfh (Figure 3.11A, Spearman r:0.41, P=0.01) and negatively with the proportion of cTfh17 (Figure 3.11B, Spearman r:-0.63, P<0.0001). Additionally there was a negative association between the concentration of IFNγ in the CSP-stimulated PBMC supernatant and the ability of antibody to block sporozoite entry into hepatocytes (Figure 3.11C, Spearman r:-0.79, P=0.0001). Assessment by ICS showed that only low frequencies of CSP-stimulated cTfh produced IFNγ (Figure 3.11D, less than 2% in G1/2 [R] and less than 3% in G3/4 [R+V]).

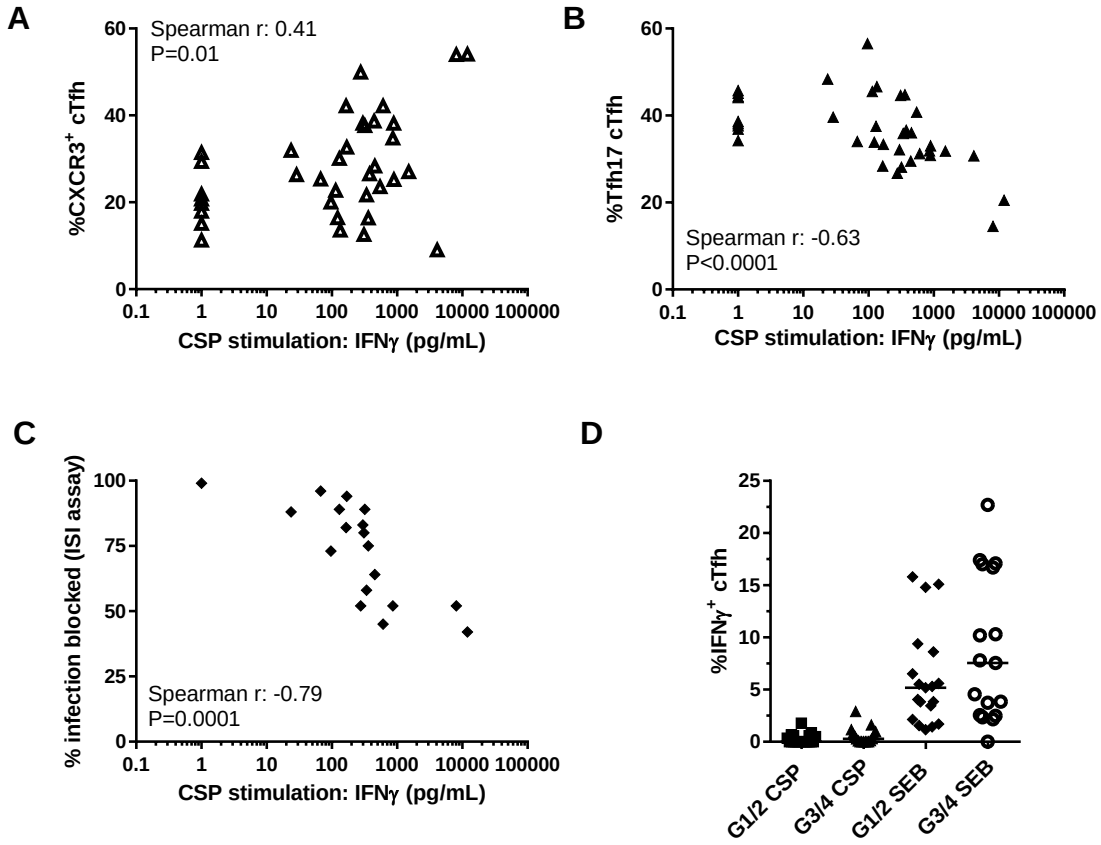

Figure 3.11. Association between Th1-biased cytokine responses and suppressed humoral immunity

Relationship between concentration of IFNγ in supernatant of PBMCs stimulated with CSP in the co-administration trial (G1-4, R and R+V combined) and: **A**) proportion of CXCR3$^+$ within cTfh (Spearman r:0.41 P=0.01), **B**) Proportion of cTfh17 (CXCR3$^+$CCR6$^-$) within cTfh (Spearman r: -0.63 P<0.0001), **C**) Percentage of infection blocked in the ISI assay (Spearman r:-0.79 P=0.0001). **D**) Proportion of IFNγ$^+$ cTfh after stimulation with CSP or SEB, Mann-Whitney analyses between G1/2 (R) and G3/4 (R+V) P=0.14 and P=0.26 for CSP and SEB stimulations respectively.

Binomial logistic regression was used to calculate the theoretical likelihood of sterile protection after malaria challenge based on different immunological measures of the response to vaccination. Independent variables were chosen based on those that showed differences in protected and non-protected volunteers or have previously been associated with protection induced by RTS,S. Immune measures included were: NANP IgG at C-1, ISI, IFA, % of $CXCR3^+$ pTfh and IFNγ produced by C-1 PBMC after CSP stimulation. This analysis was conducted for 35 volunteers in VAC59, which had results for each of these variables. The model did not predict that any of these variables was significantly associated with protection from CHMI (details in Table 3.2).

Table 3.2. Multiregression analysis
Results from a binomial logistic regression analysis modelling the role of different markers of immunogenicity in sterile protection from CHMI in VAC59 (coadministration study). Dependent variable: protection status.

Variable	B	SE	|Z|	P value
(Intercept)	-9.6	5.57	-1.7	0.084
Group	0.45	0.74	0.61	0.54
C-1 NANP Ab	0.0019	0.0012	1.6	0.12
ISI	0.033	0.038	0.86	0.39
IFA	0.02	0.016	1.2	0.22
$CXCR3^+$ Tfh	0.061	0.063	0.96	0.34
CSP-stimulated IFNγ	0.0001	0.0002	0.53	0.60

3.4. Discussion

A vaccine regimen targeting multiple stages of the *P. falciparum* life cycle is one strategy for improving on the efficacy of current malaria vaccine candidates. To achieve this, it is likely that multiple vaccine platforms will need to be combined or co-administered. I examined the immune responses induced by RTS,S/AS01B and viral vectored vaccines in single administrations, a staggered regimen including both platforms or co-administered to assess the extent of the immunological interaction.

RTS,S/AS01B administered alone or in a staggered regimen with viral vectored vaccines induces high antibody titres and a high level of efficacy against CHMI. In the first trial individuals with the highest levels of NANP IgG at C-1 (>2670 EU) were all sterilely protected. However, NANP IgG titres weren't significantly associated with protection and 71% (17/24) of individuals with titres under 2670 EU were also sterilely protected. The lowest titre in a protected individual was 585 EU whilst the highest titre in a non-protected individual was 2669 EU. This large overlap in titres between protected and non-protected individuals suggests that additional mechanisms contribute to protection induced by these vaccines.

In addition to antibodies, CSP-specific $CD4^+$ T cells have been associated with protection induced by RTS,S [417,421]. In these studies CSP-specific $CD4^+$ T cells were measured by flow cytometry and characterised as those expressing two or more of IL-2, IFNγ or TNFα after overnight stimulation with CSP peptides. In this study CSP-specific ELISpot responses ($CD4^+$ and $CD8^+$ T cells expressing IFNγ) were significantly higher in the staggered regimen after an MVA boost compared with RTS,S/AS01B alone. As identified by ICS, the majority of CSP-specific T cells (T cells producing more than one cytokine in response to CSP stimulation) were $CD4^+$ as has been reported previously for RTS,S [417,422,423]. However there were no associations between CSP-specific T cells measured by ELISpot or ICS and protection in the trials presented here. These results were reported in detail in the primary clinical trial manuscripts [401,418].

MVA has previously been shown to adjuvant both antibody and T cell responses in mice and humans [424-426]. The higher CSP-specific T cell responses observed when MVA-ME-TRAP vaccination is delivered two weeks after RTS,S/AS01B suggests that MVA may enhance the ongoing T cell responses induced by RTS,S. The correlation between the TRAP-specific T cell responses and the CSP-specific T cell response at C-1, may be evidence for a relationship between the response to viral vectored vaccines and enhanced T cell responses to RTS,S. An alternative explanation is that the enhanced responses were induced against an epitope within

the ME string. The ME string contains a CD4 epitope DPNANPN, which is also present in the N-terminal of CSP and pool 1 in the ELISpot assay. Enhanced responses to CSP in the R2V group may be due to induction of responses against the epitope DPNANPN by ChAd63-MVA-ME-TRAP, as this epitope is not present in RTS,S. This was investigated by assessing ELISpot responses to individual peptide pools. Responses to peptide pool 1 were significantly higher in the R2V group than the R group (Mann-Whitney P=0.038).

However, it is also possible that MVA-ME-TRAP vaccination could boost ongoing T cell responses in an antigen-independent manner. MVA could achieve this adjuvant effect by enhancing expression of co-stimulatory molecules on DCs or stimulating the upregulation of chemotactic molecules such as CCL3, CCL4, CXCL9, CXCL10, on tissues around the immunization site and in the draining lymph nodes (DLNs). Upregulation of these molecules attracts $CD8^+$ T cells to the sites where $CD4^+$ T cells and antigen-presenting cells interact, thereby enhancing the generation of $CD8^+$ T cell responses [425]. Upregulation of chemotactic molecules and secretion of cytokines would have an antigen-independent effect and could enhance ongoing T cell responses against CSP. However, RTS,S predominantly induced $CD4^+$ T cell responses against CSP in our trials, as has been observed previously [421,423,427]. This suggests that the increased CSP-specific ELISpot responses were more likely caused by an induction of responses against the CSP epitope in the ME string, rather than a general adjuvant effect of MVA. Although $CD4^+$ T cell responses induced by RTS,S have previously been associated with protection [428], we did not see an association in our studies. However, in these studies, we observed a higher level of protective efficacy than previously seen with RTS,S/AS01B in malaria-naïve adults – 75% in the RTS,S/AS01B group in the initial study and 82.4% in the combined RTS,S/AS01B only groups in the co-administration study compared with the 50% previously reported by Kester and colleagues [428]. This left us with only a small number of non-protected individuals in these groups and low power to detect small differences between protected and non-protected individuals.

TRAP-specific T cell responses were equally high when RTS,S/AS01B and viral vectored vaccines were co-administered compared with viral vectors alone. However, direct comparison of the T cell responses in this regimen with those in the staggered regimen and previously tested regimens with viral vectors alone was difficult due to the study design. In this study an additional MVA vaccination was administered with the second RTS,S dose at D28 to simplify the immunization protocol. This resulted in TRAP-specific T cell responses at D35 that were significantly higher than in a previously tested regimen with viral vectors alone and the same prime-boost interval. T cell responses to TRAP peaked at this time point and were not further boosted by the second dose of MVA-ME-TRAP given with the third RTS,S dose at D56. This lack of boosting by subsequent vaccinations has been observed before and it was speculated that this could be caused by an induction of anti-vector antibody responses after the first MVA dose[429]. However, in that study there was actually a weak positive correlation between the anti-vector antibody response and the TRAP-specific T cell response after one dose of MVA. I conducted a similar analysis here to determine whether anti-vector antibody responses were associated with the failure of the second MVA to further boost T cell responses. Both doses of MVA significantly enhanced anti-MVA antibody responses. However, there were was no association between the anti-MVA IgG titre after the first dose and the T cell response to TRAP after the second dose. We do not currently have an assay set up to measure neutralising antibody against MVA, however it is possible that neutralising titres (rather than total MVA-specific IgG) could be associated with lack of boost after the second dose. This would be something to consider more carefully if we were to take forward a regimen which includes multiple doses of the same viral vectored vaccine.

The reduced TRAP T cell responses at C-1 due to the additional MVA at D35 may have contributed to the reduced efficacy in the co-administration regimen compared with the staggered regimen. However, the co-administration regimen also induced a significantly lower quantity and quality of antibody compared with RTS,S/AS10B alone. A third dose of RTS,S/AS01B

failed to boost NANP IgG titres when co-administered with viral vectors and titres were significantly reduced in these groups compared to those receiving RTS,S alone and in the previously tested staggered regimen. In the first trial, all individuals with titres greater than 2670 EU were sterilely protected. In the second trial, even in the RTS,S only groups, very few individuals had titres this high by C-1 (D76), which was one week earlier than C-1 in the staggered regimen. Despite this, efficacy in the group receiving three standard doses of RTS,S/AS01B was the same in both trials (75%) and high titres of NANP IgG were clearly not essential for protection. However, the functional capacity of the antibody response was also significantly reduced when RTS,S and viral vectors were co-administered. Serum from individuals in these groups was significantly less able to block sporozoite invasion into hepatoma cells, which was a measure associated with protection.

Additionally, there were qualitative differences in RTS,S-induced antibody responses when a reduced (1/5th, 10µg) dose was given compared with three standard doses (50µg). Although NANP IgG titres were comparable, administration of a reduced third dose of RTS,S/AS01B induced antibodies that were capable of blocking a significantly higher level of sporozoite infection *in vitro*. A reduced third dose of RTS,S/AS01B has been shown to induce antibody with increased somatic hypermutation and higher avidity, and has demonstrated higher efficacy than three standard doses [416,420]. However, it was unclear whether this effect was due to the delayed boost (0, 1, 7 month regimen) or the fractional third dose. The study I conducted here is the first to demonstrate a functional difference in the antibodies induced by the reduced third dose regimen that is associated with protection. It is not known whether the quality of the antibody response is enhanced by a reduced third dose in particular or whether this could be achieved with a reduction of all three doses, which would also have economical and practical advantages. Lower vaccine doses decrease the availability of antigen and therefore could result in greater affinity maturation through increased competition between B cells for T cell help. This would lead to the preferential expansion of B cell clones with the highest affinity B cell receptors

[430,431]. Lower doses of antigen at priming also preferentially drive the induction of memory, while higher antigen doses drive differentiation of plasma cells [432]. The preferential induction of memory by reducing the priming dose could enhance responses to the subsequent vaccinations and potentially generate more durable protection. Equally, reduction of the adjuvant AS01B dose should also be tested to determine if this could enhance antibody responses.

Previous studies have demonstrated that cTfh may be useful biomarkers for GC responses in the absence of lymphoid tissue [433]. However, cTfh are a heterogeneous population composed of a number of different subsets, some of which appear to more closely resemble bona fide GC Tfh than others [65,434]. The proportions of these subsets have been associated with different diseases: Increases in cTfh2/cTfh17 subsets are associated with the production of autoantibodies and disease severity in various autoimmune diseases [65,435,436], the development of allergy [437,438] and the production of broadly neutralizing antibody in HIV^+ individuals [68,439]. In contrast, increases in $CXCR3^+$ cTfh have been implicated in the poor development of humoral immunity against malaria [162,197] and are proportionally increased in patients with primary immunodeficiency [440]. A study that observed $CXCR3^+$ cTfh to positively correlate with antibody after influenza vaccination also showed that $CXCR3^+$ Tfh that were localised to tonsillar GCs expressed Fas-L, secreted IFNγ, lacked CD154 expression and suppressed the activity of GC B cells. Therefore, although this subset was correlated with antibody responses, they were not optimal for their induction [441]. In our study co-administration of RTS,S/AS01B with viral vectored vaccines led to an increased frequency of $CXCR3^+$ cTfh compared with RTS,S/AS01B administered alone, and this phenotype was associated with the observed reduction in antibody quantity and quality. Although the observed association was for total cTfh, it would be useful to profile the antigen-specificity of these cells to determine if the increase in $CXCR3^+$ cTfh was due to the induction of cTfh specific for the vector or whether this was a change in the phenotype of the CSP-specific cTfh. There are several

methods used to look at antigen-specific cTfh, including cytokine production or CD154 expression after overnight antigen stimulation or the use of activation-induced markers (AIM) [69,403,404,441,442].

Circulating Tfh have been shown to produce cytokines, with $CXCR3^+$ cTfh in particular producing IFNγ[443]. However, the association we saw between IFNγ in the supernatant and $CXCR3^+$ cTfh was not likely due to production of IFNγ by the $CXCR3^+$ cTfh themselves as only very low percentages of cTfh were observed to produce IFNγ after CSP stimulation. This suggests that exogenous sources of IFNγ are associated with the polarization of cTfh towards a $CXCR3^+$ phenotype, although vector-specific $CXCR3^+$ cTfh could be a source IFNγ in G3/4 volunteers. MVA has previously been shown to drive a strong IFNγ response, particularly in $CD8^+$ T cells [252,444] and IFNγ enhances CXCR3 expression on T cells through STAT1 signalling [445]. It is perhaps therefore unsurprising that MVA induced a CXCR3-skewed cTfh response. However the impact of this skew on the antibody responses was less predictable, given that $CXCR3^+$ cTfh have in some contexts been positively associated with antibody responses [441,446], while in other studies they have been associated with suboptimal GC responses and poor humoral immunity [163,197]. In the study presented here, when the two different vaccine platforms were co-administered, the IFNγ-dominated cytokine responses driven by viral vectored vaccines were associated with an increase in $CXCR3^+$ cTfh and a reduction in humoral immunity and protective efficacy. However, if given two weeks after RTS,S/AS01B, the proportion of $CXCR3^+$ cTfh was no longer associated with a reduction in humoral immunogenicity.

IFNγ induces the production of chemokines CXCL9 (MIG, monokine induced by gamma-interferon), CXCL10 (IP-10, interferon-induced protein of 10kDa) and CXCL11 (I-TAC, interferon inducible T cell alpha chemoattractant), which all bind CXCR3. This chemokine system mediates the migration of Th1 $CD4^+$ T cells and CTLs to sites of Th1 inflammation in the periphery [447]. Additionally, MVA has been shown to induce high systemic levels of CXCL10 [448]. Induction of

CXCR3 ligands systemically or at the vaccination site, in combination with the $CXCR3^+$ cTfh polarization, may result in the reduction of antibody responses by causing an egress of these cTfh from the draining lymph node. This would decrease the level of help available to B cells in the GC response. A staggered regimen may reduce this effect by allowing time for the RTS,S/AS01B-induced GC response to occur before MVA-induced inflammation begins. An alternative strategy to reduce or avoid immune interference without increasing the number of clinic visits would be to reduce the MVA dose or exclude the additional MVA vaccination at week four. This additional dose was included for practical reasons to simplify the vaccination protocol and is not required to induce potent T cell responses [252,401].

3.5. Conclusions

This study demonstrates the potential of a multi-antigen targeting vaccine to increase efficacy. Even one infected hepatocyte is enough to produce thousands of merozoites and establish a blood-stage infection. The use of a combination regimen targeting two different antigens provides some redundancy to the system; RTS,S induces antibodies targeting sporozoites to inhibit entry into hepatocytes and viral vectors induce TRAP-specific T cells that target any cells that sporozoites have invaded. However, in this study co-administration of viral vectored vaccines with RTS,S/AS01B led to a reduction in humoral immunity. This was associated with the strong Th1-biased cytokine response induced by MVA and a polarization of cTfh towards a $CXCR3^+$ phenotype. This observation suggests that designing a multistage-targeting vaccine will require careful optimisation to avoid immunological interference.

4

Antigen-Independent Antibody Deposition (AIAD) in malaria-exposed populations

4.1. Introduction

During the initial clinical trials of Ebola vaccine candidates I developed a standardised Ebola GP ELISA to test antibody responses as an economical and high-throughput alternative to the only commercial kit available at the time (Zaire Ebola Glycoprotein ELISA kit, ADI). The standardised ELISA uses a positive pool to form a standard curve from which the concentration of samples is interpolated.

During assay development I tested sera from a number of clinical trials as negative controls on the assay. Individuals from Burkina Faso had significantly increased levels of antibody binding to Ebola GP-coated and uncoated ELISA plates compared with malaria-naïve individuals. This uncoated plate binding, or antigen-independent antibody deposition (AIAD) may lead to false positive ELISA results in these populations. It is essential that we are able to accurately measure humoral responses to vaccination in malaria-exposed populations (which are the target populations for the majority of vaccine programs currently being run at the Jenner Institute). Therefore, the aim of this study was to determine what impact AIAD was having on the ELISA results and then to test ways to eliminate this effect and improve ELISA accuracy.

4.2. Study-specific methods

4.2.1. Uncoated plate ELISAs

ELISAs to measure antibody binding against uncoated ELISA plates were conducted in the same way as the ELISAs detailed in the general methods (Chapter 2.4.14), except that the plate was not coated with antigen. Instead, uncoated plates were directly blocked with blocking buffer (casein, casein + 1% Tween20, casein + 10% FCS, casein + 10% normal human serum or ChonBlock™) for 1 hour at RT. After washing the plate six times with PBS/T, samples diluted at 1:100 in the blocking buffer were added to the plate in triplicate for 2 hours at RT. After washing plates as before, secondary antibody (as described in Chapter 2.4.14.1, except when the assay was blocked with ChonBlock™, for which the secondary antibody was diluted in Chondrex antibody dilution buffer) was added to the plates for 1 hour at RT. Plates were developed as described in the general methods and were read at 20 minutes (the time taken for the Ebola GP ELISA to develop) or 1 hour (to observe the impact of prolonged development times on background levels).

For comparison of EUs from uncoated and coated plates, each sample was run in triplicate on the half of the plate coated with Ebola GP and in triplicate on the uncoated half of the plate. The ELISA was conducted in the same way for the entire plate. The assay was developed using the standard curve on the coated half of the plate and the OD was read for the uncoated half at the same time. These OD values were then used to calculate EUs for each sample in the coated and uncoated halves. A cut-off value of two times the average of the blank wells (blocking buffer and secondary antibody but no sample added) at 20 minutes was chosen (OD405=0.200) and samples with OD values above this were considered positive for plate-binding antibody.

4.2.2. Samples and study details

Study details for the samples used in this chapter are summarised in Table 4.1. Full sample and study details, as well as ethics statements for the samples used in this chapter can be found in Chapter 2.2.3.

Table 4.1. Summary of clinical trials used to compare immunogenicity in malaria-exposed and malaria-naïve populations
ChAd63: Chimpanzee adenovirus serotype 63, ME: multi-epitope string, TRAP: Thrombospondin related adhesion protein, MVA: modified vaccinia virus Ankara, D0: day 0, D28: day 28, D56: day 56, MM: matrix-M vp: viral particles, pfu: plaque forming units. n=total number of volunteers enrolled in those groups.

Trial code	Country	Vaccines	Age Group	Group/s included in these studies	Doses	Regimen
N/A	Burkina Faso	N/A– ChAd IgG seroprevalence study	adults	N/A (n=100)	N/A	N/A
VAC40	Kenya	ChAd63-ME-TRAP, MVA-ME-TRAP	adults	Group 2 (n=20)	$5x10^{10}$vp ChAd, $2x10^{8}$ pfu MVA	D0: ChAd, D56: MVA
VAC41	The Gambia	ChAd63-ME-TRAP, MVA-ME-TRAP	adults	Group 1B (n=10)	$5x10^{10}$vp ChAd, $2x10^{8}$ pfu MVA	D0: ChAd, D56: MVA
			2-6 years	Group 3B (n=6)	$5x10^{10}$vp ChAd, $1x10^{8}$ pfu MVA	D0: ChAd, D56: MVA
VAC42	The Gambia	ChAd63-ME-TRAP, MVA-ME-TRAP	5-12 months	Group 1B (n=12)	$5x10^{10}$vp ChAd, $1x10^{8}$ pfu MVA	D0: ChAd, D56: MVA
			10 weeks	Group 2B (n=12)	$5x10^{10}$vp ChAd, $1x10^{8}$ pfu MVA	D0: ChAd, D56: MVA
VAC45	UK	ChAd63-ME-TRAP, MVA-ME-TRAP	adults	Group 2 (n=15)	$5x10^{10}$vp ChAd, $2x10^{8}$ pfu MVA	D0: ChAd, D56: MVA
VAC46	Kenya	ChAd63-ME-TRAP, MVA-ME-TRAP	adults	Group 1 (n=15 all time points, 60 at D63)	$5x10^{10}$vp ChAd, $2x10^{8}$ pfu MVA	D0: ChAd, D56: MVA
VAC50	Burkina Faso	ChAd63-ME-TRAP, MVA-ME-TRAP	5-17 months	Group A (Phase I, n=30)	$5x10^{10}$vp ChAd, $1x10^{8}$ pfu MVA	D0: ChAd, D56: MVA
VAC60	Burkina Faso	R21/MM	adults	Groups 1 & 3 (n=12)	10µg R21, 50µg MM or saline control	R21/MM at D0, D28 and D56
EBL01	UK	ChAd3-EBO-Z, MVA-BN Filo	adults	Groups 1-3 (n=60), post-boost groups b & c (n=30)	1, 2.5 or $5x10^{10}$vp ChAd, 1.5 or $3x10^{8}$ pfu MVA	D0: ChAd, D21-D70: MVA

Trial code	Country	Vaccines	Age Group	Group/s included in these studies	Doses	Regimen
EBL04	UK	ChAd3-EBO-Z, MVA-EBO-Z	adults	Group 2 (n=16)	$3.6x10^{10}$vp ChAd, $1x10^{8}$ pfu MVA	D0: ChAd, D7: MVA
EBL06	Senegal	ChAd3-EBO-Z, MVA-EBO-Z	adults	Groups 1 & 2 (n=40)	$3.6x10^{10}$vp ChAd, $1x10^{8}$ pfu MVA	D0: ChAd, D7: MVA

4.3. Results

4.3.1. Relationship between antibody against *P. falciparum* and Ebola GP

Median Ebola GP IgG titres were low at baseline in the UK (median: 1, IQR: 1-15) and Senegal (median: 9, IQR: 1-20). There was one individual in the UK cohort (with no travel history to an affected country) and two individuals in the Senegalese cohort that had responses above the seropositive cut-off value (166 EUs, determined by mean + 3 SD of the UK "Ebola naïve" cohort), suggesting that there may be a certain amount of background or cross-reactivity observed with the assay. A high level of malaria exposure has previously been associated with high assay background in ELISAs but is not often taken into account [449]. Therefore, samples were tested from Burkina Faso, which has higher malaria transmission than Senegal [450] but also no history of Ebola.

Samples from 100 Burkinabe adults and children aged 10-45 years were taken as part of a study to determine the seroprevalence of anti-ChAd antibodies in West Africa [254]. Samples from the UK, Senegal and Burkina Faso were tested for anti-schizont IgG as a surrogate for malaria exposure (Figure 4.1A). There was no evidence of anti-schizont antibody in the UK cohort, whilst the Senegalese cohort had a low level of anti-schizont IgG (48% were positive) and all of the Burkinabe cohort were positive. Of the Burkinabe samples 11% (11/100) were also positive for Ebola GP IgG and the titres were significantly higher than those in the UK and Senegal (Figure 4.1B, $P<0.0001$). Whilst there was no association between anti-schizont IgG titres (as a surrogate

for malaria exposure) and anti-Ebola GP IgG titres in the Senegalese cohort (Figure 4.1C, r:-0.038, P=0.81), there was a positive association in the Burkina Faso cohort (r:0.44, P<0.0001). However, the majority of samples were below the Ebola GP ELISA seropositive cut-off value.

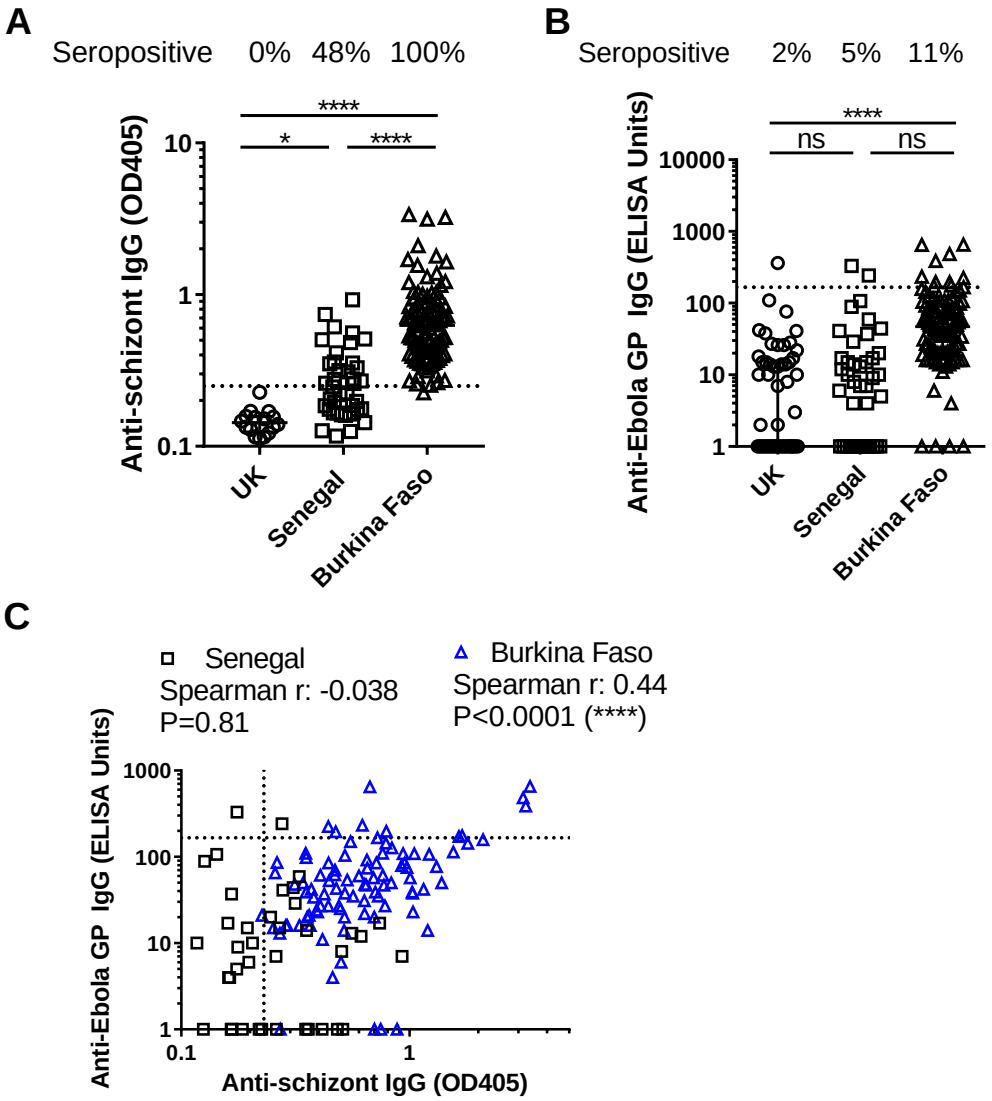

Figure 4.1. Relationship between malaria exposure and presence of anti-Ebola GP antibody

A) Anti-schizont IgG in malaria-naïve UK adults (EBL04, G2), Senegalese adults (EBL06) and Burkinabe adults (anti-ChAd vector antibody seroprevalence study). Kruskal-Wallis P<0.0001. **B**) Anti-Ebola GP IgG. Kruskal-Wallis with Dunn's post-test comparisons P<0.0001. **C**) Relationship between anti-schizont antibody and baseline anti-Ebola GP IgG in Senegal (low malaria exposure) and Burkina Faso (high malaria exposure). Dotted lines indicate positive cut-off for anti-schizont (OD405=0.250), and anti-Ebola GP IgG (166 EUs) ELISAs. * P<0.05, **** P<0.0001, ns: not significant. OD405: optical density at 405nm.

4.3.2. High plate background in malaria-exposed individuals – (AIAD)

Burkinabe samples demonstrated a high level of binding even when the ELISA plate was not coated with antigen (but still blocked with blocking buffer). A cut-off value of 0.200 OD405 (1.5x the level observed in UK volunteers) was used as an arbitrary a cut-off value for positive plate binding. The level of plate binding observed was significantly higher than in the UK and Senegalese samples (Figure 4.2A, Kruskal-Wallis P<0.0001, median OD405 values, UK: 0.128, Senegal anti-schizont IgG negative: 0.123, Senegal anti-schizont IgG positive: 0.123, Burkina Faso: 0.154). The level of plate binding, or antigen-independent antibody deposition (AIAD) observed in the Burkinabe cohort was associated with both anti-schizont IgG (Figure 4.2B, Spearman r:0.41, P<0.0001) and Ebola GP IgG titres (Figure 4.2C, Spearman r:0.29, P=0.0037) in this cohort.

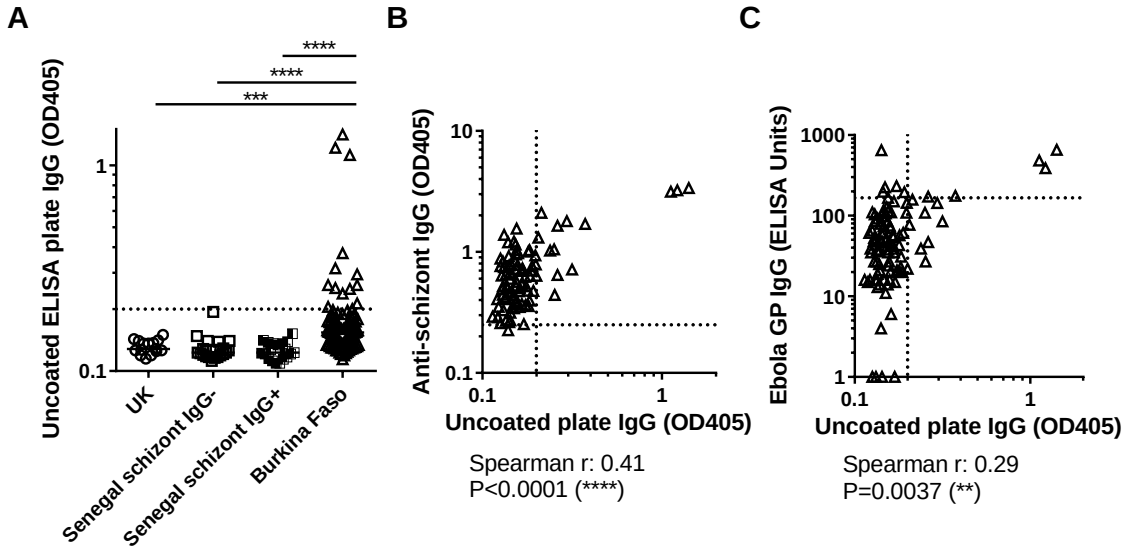

Figure 4.2. Antigen-independent antibody deposition in highly malaria-exposed individuals

A) IgG bound to blocked, uncoated ELISA plates. Kruskal-Wallis comparison with UK samples P<0.0001. Relationship between IgG bound to uncoated ELISA plates and: **B**) anti-schizont IgG, **C**) anti-Ebola GP IgG in the Burkina Faso data set. Dotted lines indicate positive cut-off for plate-binding IgG (OD405=0.200) and anti-schizont (OD405=0.250) ELISAs. ** P<0.01, *** P<0.001, **** P<0.0001. OD405: optical density at 405nm.

EUs calculated for each sample from the OD values in uncoated or Ebola GP-coated wells were compared (Figure 4.3). Samples were split into a number of different categories: 1. “High malaria exposure” (Burkina Faso samples with very high anti-schizont IgG, n=3, OD>1.000), 2: “Cross-reactive/ borderline positive” (Burkina Faso samples with titres close to or above the Ebola GP ELISA seropositive threshold but without very high anti-schizont IgG titres, n=8), 3: Post-Ebola vaccination (samples from UK adults in EBL04 (G2, 28 days after MVA boost, n=16), 4: Naïve UK (UK adults pre-vaccination, EBL04 G2, n=9). The Burkinabe individuals with high anti-schizont results also had high titres of Ebola GP-specific IgG (291, 437 and 470 EUs). However the titres calculated from the OD values in the uncoated wells were even higher for these samples (575, 584 and 729 EUs). Samples in the cross-reactive/ borderline positive group had significantly lower OD values in the uncoated wells (P=0.016) and all were below the positive cut-off threshold, although some background binding was still observed. Naïve UK samples were negative in both the coated and uncoated wells and only one volunteer had a baseline Ebola GP IgG response >1 EU. None of the UK post-vaccination samples bound to the uncoated plate and all were positive for Ebola GP IgG in the coated wells. Ebola GP IgG EUs calculated from the coated wells were significantly higher than the uncoated wells for these individuals (P<0.0001).

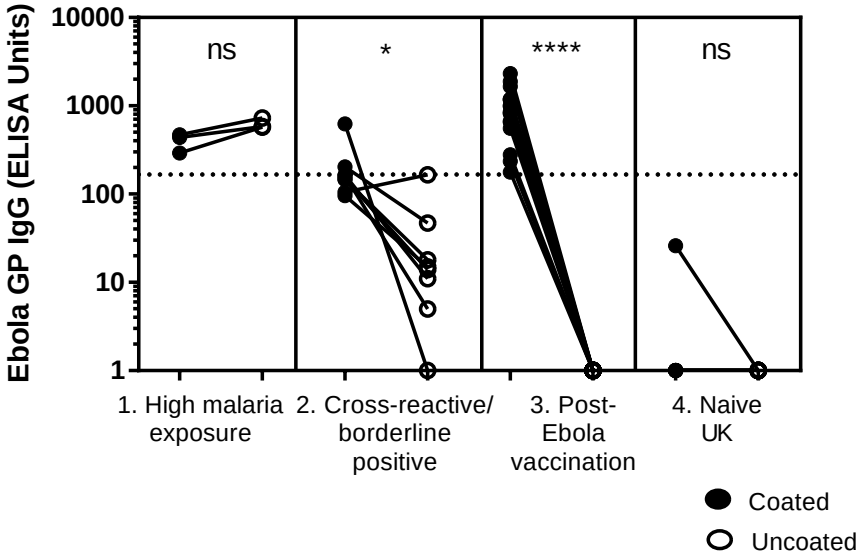

Figure 4.3. Impact of antigen-independent antibody deposition on Ebola GP IgG results
Ebola GP IgG EUs calculated for samples in GP-coated (closed circles) or uncoated (open circles) wells assayed simultaneously. 1: Burkina Faso adult samples with high anti-schizont IgG responses ("high malaria exposure", n=3), 2: Samples that are borderline/ low positive for Ebola GP IgG (Burkina Faso adults from ChAd seroprevalence study, n=8), 3: UK adults post ChAd3-MVA-EBO-Z vaccination (n=16, EBL04), 4: Ebola GP IgG negative UK adults (n=9, EBL04 baseline). Dotted line indicates seropositive cut-off (166 EUs).Wilcoxon matched-pairs analyses. *** P<0.001, **** P<0.0001, ns: not significant. Ebola GP-coated wells: closed circles, uncoated wells: open circles.

A further set of experiments was conducted to characterise the nature of the AIAD observed in the Burkinabe samples. Total IgG, IgA and IgM binding to uncoated plates developed for 20 minutes or 1 hour was tested (Figure 4.4). These development times were chosen to cover the range of development times that could be used for these assays. Assay background, measured by OD values in blank wells (with blocking buffer and secondary antibody but no serum) was comparable for anti-IgG, anti-IgM and anti-IgA assays. After 20 minutes of development, there was no evidence of plate-binding IgG, IgA or IgM in UK samples, which were comparable to the assay blanks. However, 13% of Burkinabe samples (11/86 tested) were positive for plate-binding IgG and the OD values were significantly higher than the blanks and the UK samples (Kruskal-Wallis P<0.0001). Plate-binding IgM was also evident in 9% (8/86) of Burkinabe samples, whilst plate-binding IgA was only observed in one individual. After one hour of development, plate-

binding IgG OD significantly increased in the Burkinabe samples (P<0.0001) and 97% were positive. In contrast, although there was a significant increase in the OD of the UK samples (P=0.031), none were positive. Plate-binding IgA remained low at one hour of development and although there were significant increases in the OD (UK P=0.031, Burkina Faso P<0.0001), there were no positive UK samples and only three positive Burkinabe samples. Samples from both cohorts also showed significant increases in plate-binding IgM after one hour (UK P=0.031, Burkina Faso P<0.0001) and 30% of both the UK (2/6) and Burkinabe (26/86) samples were positive.

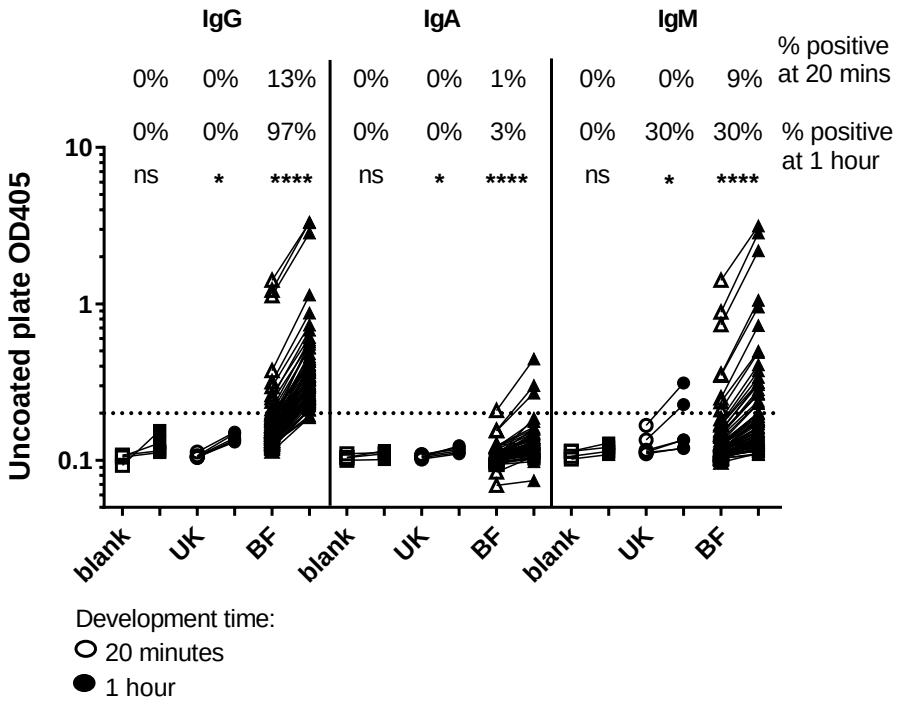

Figure 4.4. Characterising antigen-independent antibody deposition
OD405 (optical density at 405nm) values for blanks (casein blocking buffer), UK and Burkina Faso (BF) samples in an ELISA using an uncoated plate at 20 minutes and 1 hour of development. Secondary antibodies against IgG, IgA or IgM. Dotted line indicates assay positive cut-off (OD405=0.200). Percentages shown indicate the percentage of samples that were above this threshold. Wilcoxon paired tests. * P<0.05, ** P<0.01, *** P<0.001, **** P<0.0001, ns: not significant.

4.3.3. Testing ELISA conditions to reduce AIAD

A series of experiments was conducted to find conditions for the assay that reduced or blocked AIAD. Initially, heat-inactivation of the serum samples was tested as a potential method for reducing plate background. An aliquot of each of the Burkinabe samples used in this experiment was heat-inactivated (30 minutes at 56°C). The level of plate-binding IgG, IgM and IgA was compared between heat-inactivated (HI) and non-heat-inactivated (non-HI) samples after 20 minutes of development (Figure 4.5). There were no significant differences in IgG, IgA or IgM AIAD between HI and non-HI samples.

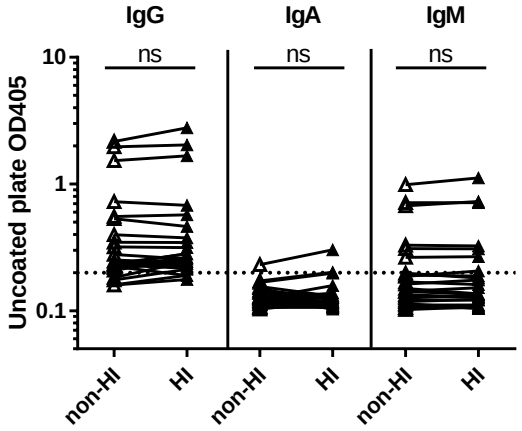

Figure 4.5. Serum heat inactivation
Comparison of binding to an uncoated plate by serum that is heat-inactivated (HI) or not (non-HI), 20 minutes development. Mann-Whitney analysis. ns: not significant. OD405: optical density at 405nm. Dotted line shows assay positive cut-off (OD405=0.200).

A number of different blocking reagents were tested during the development of the Ebola GP IgG ELISA. Of those tested (casein blocking buffer, 1% milk powder and 1% BSA in PBS/T), casein was optimal for blocking non-specific signal (i.e. gave the lowest OD values in the assay blanks and naïve serum). In order to reduce the non-specific signal caused by AIAD, a range of additional blocking conditions were tested. A selection of samples was tested including the three Burkinabe samples with the highest plate binding and anti-schizont results ("high malaria exposure"), the "cross-reactive/ borderline positive samples" and a selection of UK post-

vaccination samples. Each of these samples was tested in Ebola GP-coated and uncoated wells on plates blocked with: casein + 1% Tween20, casein + 10% FCS or casein + 10% naïve human sera (Figure 4.6). In all of these conditions, as with casein alone, the three Burkinabe samples with high anti-schizont IgG results demonstrated a comparable level of binding to uncoated and coated wells. For each condition the "cross-reactive/ borderline positive" and UK post-vaccination samples had significantly lower EUs in uncoated wells (Figure 4.6A-C). Casein + 10% naïve human serum reduced the binding of cross-reactive/ borderline positive samples in uncoated plates, with only one individual still demonstrating a response >1EU. However, there was no reduction in the plate-binding background in the "high malaria exposure" samples. Additionally, the ratio of the signal in coated to uncoated plates was significantly reduced in the UK post-vaccination samples when the plate was blocked with casein + 10% FCS or naïve human serum, suggesting that these conditions may reduce the antigen-specific signal (Figure 4.6D).

A selection of these samples was run on two different types of ELISA plates. All other ELISAs in this thesis were run using MAXIsorp plates (ThermoFisher 442404). MAXIsorp plates are highly hydrophilic and optimised for enhanced binding of coating proteins. However this may also increase background due to antibody and other serum proteins binding to the plate. Therefore AIAD was compared on MAXIsorp plates and an alternative – MEDIsorp plates (ThermoFisher 467320). These plates have reduced hydrophilicity and are designed to reduce non-specific adsorption of serum-containing samples. Samples were run on MAXIsorp and MEDIsorp plates to determine if this could reduce the effect of AIAD (Figure 4.7). Ebola GP IgG EUs for samples in coated or uncoated wells were comparable between plates: MEDIsorp plates did not reduce the level of AIAD observed.

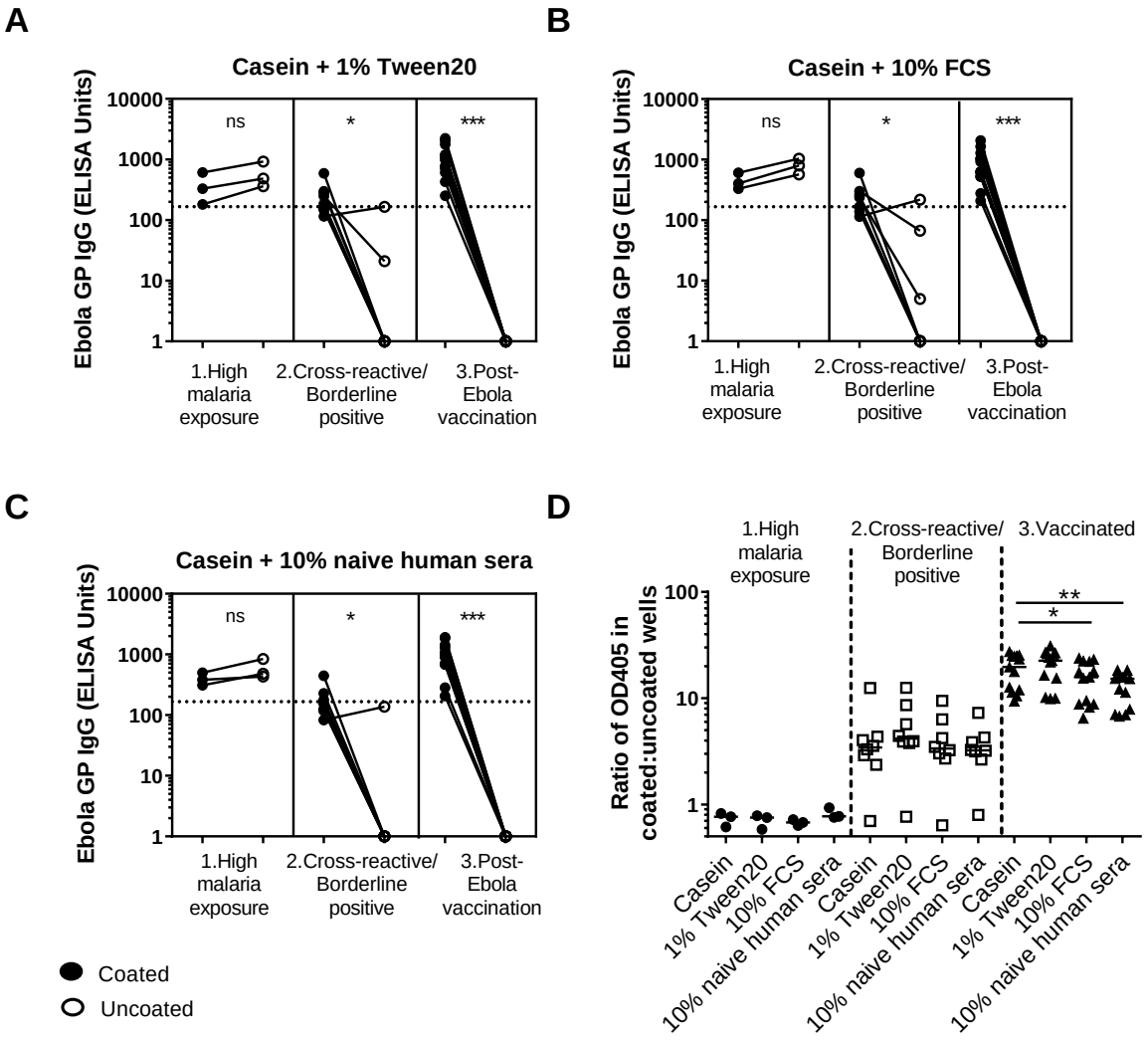

Figure 4.6. Testing of different blocking conditions for the reduction of antigen-independent antibody deposition

Comparison of ELISA Units in Ebola GP-coated (closed circles) or uncoated (open circles) wells assayed with different blocking conditions: **A**) casein + 1% Tween20, **B**) casein + 10% foetal calf serum (FCS), **C**) casein + 10% naïve human sera. Wilcoxon matched-pairs analyses. **D**) Ratio of the OD values in coated and uncoated wells tested with each of the different blocking conditions. Kruskal-Wallis with Dunn's post-test comparison to the casein blocking condition. 1: "High malaria exposure" (n=3), 2: "Cross-reactive/borderline positive", (n=8), 3: UK adults post-ChAd3-MVA-EBO-Z vaccination (EBL04, n=13 samples with a range of titres). Dotted line indicates seropositive cut-off (166 EUs). * P<0.05, ** P<0.01, *** P<0.001, **** P<0.0001, ns: not significant. OD405: optical density at 405nm. Ebola GP-coated wells: closed circles, uncoated wells: open circles.

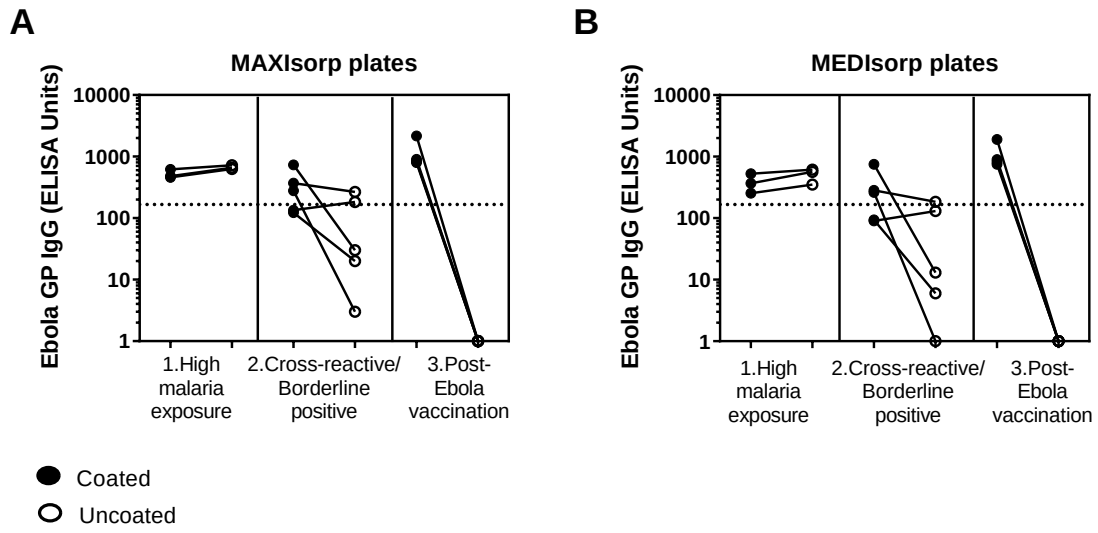

Figure 4.7. Testing of different ELISA plates for the reduction of antigen-independent antibody deposition

Comparison of EUs in Ebola GP-coated (closed circles) and uncoated (open circles) wells when assay was run on: **A**) MAXIsorp plates or **B**) MEDIsorp plates. 1: Burkina Faso adult samples with high anti-schizont IgG responses (n=3), 2: Samples that are borderline/ low positive for Ebola GP IgG (Burkina Faso samples from ChAd seroprevalence study, n=5), 3: UK adults at peak post ChAd3-MVA-EBO-Z vaccination (n=4, EBL04, range of titres). Both plates were blocked with casein. Dotted line indicates seropositive cut-off (166 EUs). No significant differences by Wilcoxon paired analyses. Ebola GP-coated wells: closed circles, uncoated wells: open circles.

4.3.4. ChonBlock™ effectively reduces AIAD

The phenomenon of AIAD has been described in autoimmune subjects and appears to be associated with increased levels of circulating IgG and inflammatory mediators in these individuals compared with healthy controls [451,452]. A proprietary blocking buffer – ChonBlock™ (Chondrex) has previously been shown to reduce the AIAD in autoimmune individuals [453]. This blocking buffer was tested to determine if it could reduce AIAD in the Burkinabe samples. (Figure 4.8A). The same subset of samples were compared on a plate blocked with casein and a plate blocked with ChonBlock™ (Figure 4.8B, 4.8C). ChonBlock™ reduced AIAD in all samples, reducing the uncoated well result to 1 EU for all individuals. Reduction of AIAD in the "high malaria exposure" samples also resulted in a reduction in the Ebola GP IgG EUs calculated in the coated wells. None of the "high malaria exposure" samples were positive for Ebola GP IgG once AIAD was removed by the use of ChonBlock™ in the assay. GP-specific IgG signals were also reduced for the "cross-reactive/ borderline positive" samples,

although 3/5 were still positive on the Ebola GP coated wells despite complete removal of background for these samples in uncoated wells. From the samples run in this small test, the specific signal in UK post-vaccination samples did not appear to be affected by the use of ChonBlock™.

A

		"High malaria exposure"			"Potentially cross-reactive"					UK post-vaccination			
	sample #:	1	2	3	1	2	3	4	5	1	2	3	4
uncoated	A	2.002	2.128	2.382	0.484	0.237	1.072	0.24	0.244	0.115	0.124	0.114	0.111
	B	1.857	1.97	2.397	0.378	0.177	0.837	0.214	0.234	0.117	0.117	0.11	0.115
	C	1.979	1.91	2.195	0.431	0.176	0.9545	0.181	0.209	0.113	0.109	0.108	0.121
Ebola GP coated	D	1.567	1.397	1.821	0.9	1.655	0.551	0.652	0.607	2.981	2.778	2.838	1.235
	E	1.579	1.519	1.815	0.996	1.61	0.531	0.659	0.593	2.876	3.039	2.625	1.153
	F	1.301	1.251	1.701	0.998	1.588	0.503	0.554	0.572	2.725	2.795	2.67	1.165

Plate 1: Casein

		1	2	3	4	5	6	7	8	9	10	11	12
uncoated	A	0.297	0.182	0.235	0.223	0.175	0.194	0.191	0.177	0.116	0.124	0.135	0.111
	B	0.23	0.168	0.161	0.185	0.183	0.181	0.166	0.162	0.11	0.114	0.117	0.111
	C	0.207	0.168	0.168	0.184	0.169	0.175	0.175	0.163	0.125	0.11	0.113	0.106
Ebola GP coated	D	0.3	0.216	0.391	0.928	1.046	0.24	0.494	0.846	2.416	2.194	2.268	0.985
	E	0.281	0.238	0.419	0.984	1.093	0.257	0.514	0.806	2.468	2.16	2.316	1.003
	F	0.28	0.231	0.377	0.911	1.031	0.233	0.472	0.767	2.386	2.144	2.229	1.026

Plate 2: ChonBlock™

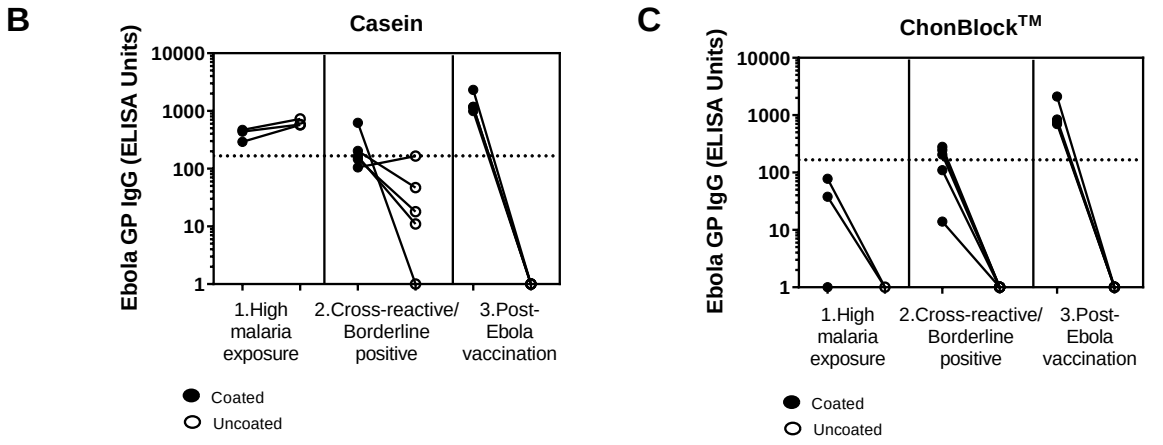

Figure 4.8. ChonBlock™ effectively reduces antigen-independent antibody deposition
A) ELISA plate optical density at 405nm (OD405) values for samples run simultaneously in Ebola GP-coated wells (rows A-C on each plate) and uncoated wells (rows D-F on each plate) on a plate blocked with casein (top) and a plate blocked with ChonBlock™ (bottom). Several samples in each category (high malaria exposure, cross-reactive/ borderline positive and post-vaccination) were run. Each plate also had a standard curve in Ebola GP-coated wells (rows G and H, not shown in image). **B**) Ebola GP IgG EUs calculated from the OD values for each sample on the plate blocked with Casein and **C**) on the plate blocked with ChonBlock™. Ebola GP-coated wells: closed circles, uncoated wells: open circles. Dotted line indicates seropositive cut-off (166 EUs). No significant differences by Wilcoxon paired analyses.

A larger set of samples were run on uncoated plates blocked with casein or ChonBlock™ (Figure 4.9A). ChonBlock™ significantly reduced AIAD for samples that were positive (OD>0.200) in uncoated wells blocked with casein (Figure 4.9A, P=0.0023). However for samples that were negative in uncoated wells blocked with casein, there was actually a significant increase in the non-specific background when the plate was blocked with ChonBlock™ (P<0.0001). Ebola GP IgG titres in UK post-vaccination samples were comparable when the plate was blocked with casein or ChonBlock™, whilst titres in individuals with evidence of AIAD were reduced to below the positive cut-off when the plates were blocked with ChonBlock™ (Figure 4.9B). Ebola GP-specific IgG titres in UK post-vaccination samples measured after blocking with casein were highly correlated with titres measured after blocking with ChonBlock™ (Figure 4.9C, r:0.80, P=0.0003).

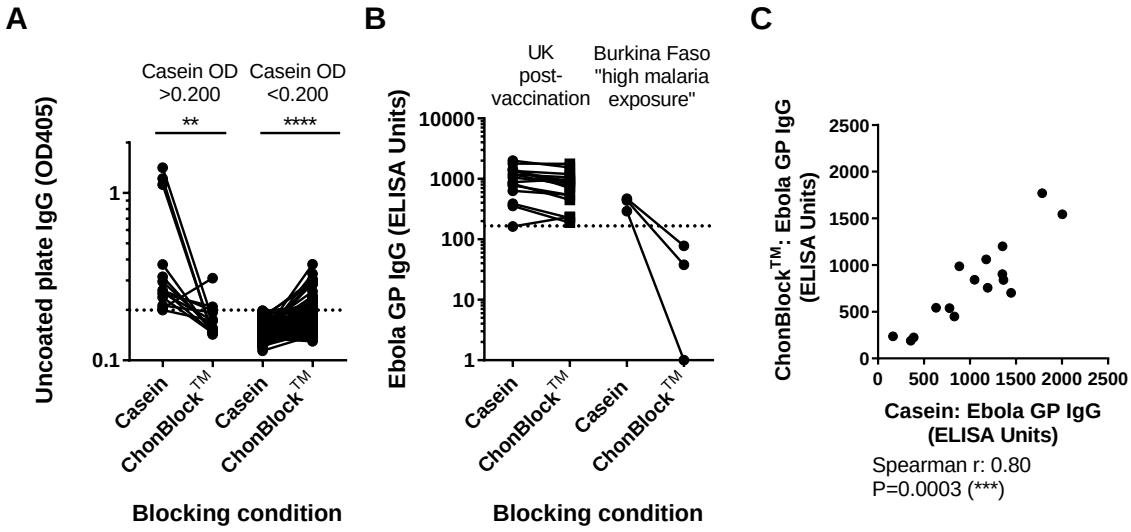

Figure 4.9. Effect of ChonBlock™ on samples positive and negative for AIAD
A) Comparison of antibody binding to the plate after blocking with casein or with ChonBlock™. Samples split by those with OD405 of plate-binding IgG >0.200 or <0.200 when blocked with casein. Wilcoxon paired tests. **B**) Ebola GP IgG in an assay blocked with casein or ChonBlock™. UK post-vaccination and the three Burkina Faso samples with the highest plate-binding and anti-schizont IgG results. **C**) Relationship between Ebola GP IgG titres in the assay with casein block and ChonBlock™ (UK post-vaccination samples). Dotted lines indicates seropositive threshold for the Ebola GP (166 EUs) and uncoated plate (OD405=0.200) ELISAs. ** P<0.01, *** P<0.001, *** P<0.0001. OD405: optical density at 405nm.

4.3.5. Malaria exposure and AIAD across clinical trial cohorts

In light of the discovery of ELISA background signal caused by AIAD, where possible (i.e. access to samples and enough serum remaining), samples from malaria-exposed individuals were tested with anti-schizont or AMA-1 ELISAs and on uncoated plates to check for AIAD (Figure 4.10). These controls were conducted for Gambian adults in VAC41, Gambian children and infants in VAC42, Senegalese adults in EBL06, Burkinabe children and infants in VAC50 and Burkinabe adults in VAC60. Unfortunately, these tests could not be conducted for Kenyan adults in VAC40 or VAC46, therefore it is unknown if AIAD occurred in these cohorts. However, malaria exposure in these populations, around the coast of Kenya, is likely to be comparable to the low level of malaria exposure in Dakar, Senegal [450], in which no AIAD was observed.

None of the samples used in the following analyses tested positive for AIAD. However, uncoated control wells should be run to check for AIAD in each new cohort of malaria-exposed individuals. For samples in which AIAD is an issue, ChonBlock™ can be used to block the non-specific signal or the OD value from the uncoated wells subtracted from the OD of the coated wells for each sample. Samples from Senegal (EB06), the Gambia (VAC41) and Burkina Faso (VAC60 and the ChAd63 seroprevalence study) had anti-schizont antibody levels significantly above the UK malaria-naïve population (Figure 4.10A, $P<0.0001$). Samples from Burkinabe children and infants aged 5-17 months (VAC50) also had significantly higher anti-schizont IgG levels than the malaria-naïve UK cohort. However, Gambian children and infants aged 10 weeks, 5-12 months and 2-6 years (VAC41 and VAC42) did not have anti-schizont IgG levels higher than the UK cohort. Additionally, there was no evidence of anti-schizont IgG in UK volunteers 35 days after CHMI, indicating the antibodies were not detected after a single primary infection. Samples were tested from a broad range of clinical trials in adults, children and infants to check for AIAD in different cohorts (Figure 4.10B). The majority of samples did not display AIAD greater than twice the assay background. AIAD above this cut-off was only evident in samples from Burkinabe and

Gambian adults. The Gambian 2-6 year olds, 5-12 month olds and 10 week olds had median values significantly greater than the assay blanks (P=0.0025, 0.025, 0.047 respectively), but there were no samples with AIAD above the assay cut-off. Data are summarised in Table 4.2.

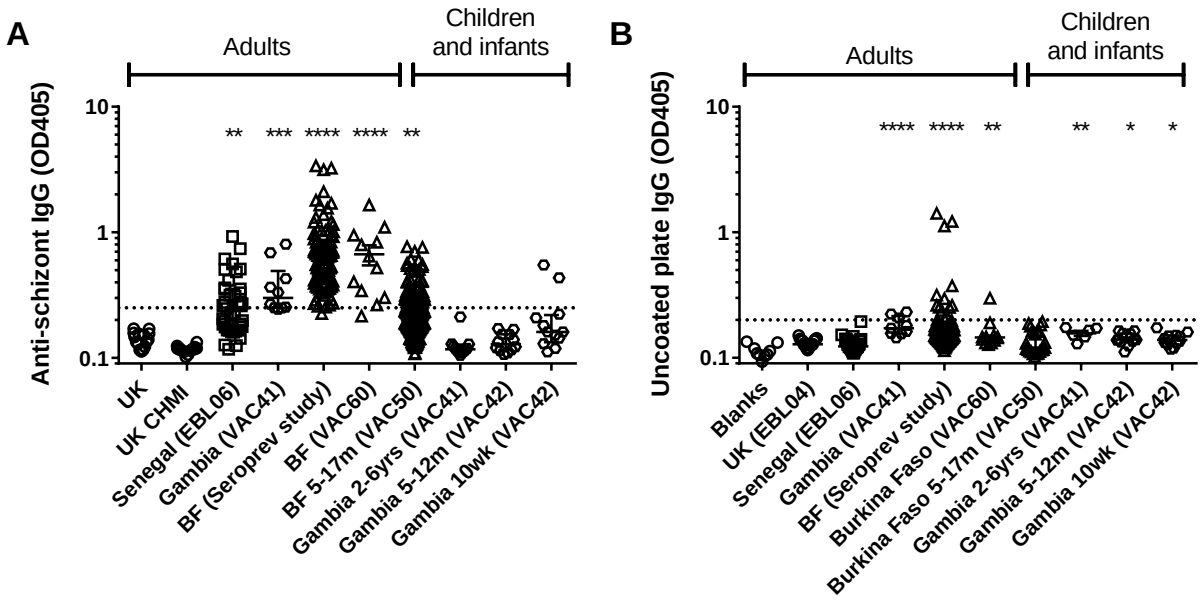

Figure 4.10. Anti-schizont IgG and AIAD across populations in clinical trials
A) Anti-schizont IgG in clinical trial cohorts. Kruskal-Wallis with Dunn's post-test comparisons to UK P<0.001. **B**) Antigen-independent antibody deposition (AIAD, IgG binding on uncoated plates) in malaria-exposed clinical trial cohorts compared with UK samples and assay blanks (casein blocking buffer only). Kruskal-Wallis with Dunn's post-test comparing each data set to blanks, P=<0.0001 "BF": Burkina Faso, "2-6yrs": children aged 2-6 years at vaccination, "5-17m": infant/children aged 5-17 months at vaccination, "5-12m": infants aged 5-12 months at vaccination, "10 wks": infants aged 10 weeks at vaccination. Dotted lines indicate assay cut-off (OD405=0.200) * P<0.05, ** P<0.01, *** P<0.001, **** P<0.0001. OD405: optical density at 405nm.

Table 4.2. Summary anti-schizont IgG and AIAD results across clinical trial cohorts
Anti-schizont IgG and antigen-independent antibody deposition (AIAD) results across malaria-exposed clinical trial cohorts. "BF": Burkina Faso, "CHMI": controlled human malaria infection – UK individuals at 35 days after CHMI (C+35). All 100 samples from the BF seroprevalence study were run on the uncoated plate. Only 92 of these were also run on the anti-schizont assay due to limitations in the batch of schizont lysate. Not all paediatric samples were available to test on uncoated plates. NT: not tested.

	Anti-schizont IgG			AIAD (uncoated plate IgG)		
	Number of samples tested	Median (OD405)	% seropositive	Number of samples tested	Median (OD405)	% seropositive
UK	15	0.140	0	15	0.128	0
UK CHMI	14	0.117	0	NT	NT	NT
Senegal (EBL06)	40	0.236	48	40	0.123	0
Gambia (VAC41)	10	0.300	70	9	0.172	33
BF (Seroprevalence study)	92	0.628	99	100	0.154	13
BF (VAC60)	12	0.582	8	12	0.145	8
BF 5-17m (VAC50)	190	0.211	35	25	0.120	0
Gambia 2-6yrs (VAC41)	12	0.117	0	6	0.159	0
Gambia 5-12m (VAC42)	12	0.128	0	12	0.139	0
Gambia 10wk (VAC42)	12	0.161	17	12	0.138	0

4.4. Discussion

4.4.1. AIAD in malaria-exposed populations

Antibody responses, most often measured by ELISA are an essential measure of immunogenicity for vaccines which induce antibody-mediated efficacy. For some vaccines, the antibody response is a defined correlate of protection [454]. Therefore, it is essential to be able to measure these responses accurately, particularly within the target populations. Excessive ELISA background in the absence of capture antigen was reported in a malaria-endemic population almost three decades ago [449]. However, there are very few studies in which samples have been tested on uncoated plates to check for this background effect, which may lead to the reporting of false positives. In the cohorts I tested, there were several results that led me to believe that there might be increased assay background in some cohorts. Individuals from Burkina Faso, which has never reported any Ebola cases, were positive for Ebola GP IgG measured by the standardised ELISA. As the level of anti-schizont IgG (as a proxy for malaria exposure) was associated with the level of Ebola GP IgG in these volunteers, I considered whether this might be caused by high assay background as previously reported in individuals from high malaria transmission settings [449].

Background signal in the ELISA assay can be caused by: 1) non-specific binding of the secondary antibody to the plate or coating antigen, 2) hydrophobic binding of Ig in the sample to the plate, 3) ionic or protein-protein interactions between Ig in the sample and the coating antigen and 4) binding of natural antibodies in the sample to the blocking agent [455]. All of these interactions give non-specific signal which is not caused by specific antibody-antigen interactions and may cause a false-positive result. For this reason, an optimised blocking step is included in most protocols after the plate has been coated with antigen. Blocking buffers usually contain an irrelevant protein or mixture of proteins that adsorb to the remaining binding surfaces on the plate and prevent non-specific binding by antigen or antibody. Blocking buffers such as bovine

serum albumin (BSA), casein or milk powder dissolved in PBS are most commonly used and the optimal buffer is usually chosen as part of the assay development process. However, this is often based on the reduction of OD in blank wells (in which no serum is added) and therefore the ability to block non-specific signal caused by serum components is not assessed.

During the setup of the Ebola GP standardised ELISA, I determined that casein provided the optimal blocking in blank wells. As I was measuring pre-vaccination samples from a naïve population (which should display very low or no binding to Ebola GP-coated ELISA plates), I was also able to determine that this blocking buffer successfully blocked non-specific signal from serum in the UK cohort. However, further testing revealed that samples from the Burkina Faso cohort bound to the uncoated ELISA plate giving an intense false positive result. Antibody binding to uncoated plates in this manner, or antigen-independent antibody deposition (AIAD) has been observed to be a particular issue in the field of autoimmunity, where it has been reported to be increased in individuals with diseases such as rheumatoid arthritis compared with healthy controls [451-453]. Güven *et al* described AIAD in patients with autoimmune disease and demonstrated that it was associated with increased concentrations of Ig and other inflammatory mediators such as CRP and complement component C3 [452]. One feature of many autoimmune diseases is hypergammaglobulinaemia and in the Güven study the concentration of IgG was associated with the level of AIAD observed. However, dilution of the sera to a total IgG concentration within the normal range did not completely remove the non-specific signal suggesting that other serum components or assay conditions likely play a role. Complement components can cause non-specific signal if they become activated by binding to the polystyrene plate surface, revealing neoisotopes that are targeted by antibodies in the sample [456]. Additionally, immune complexes have previously been associated with increased background [457]. In addition to autoimmune patients, AIAD was observed in sera from over 40% of individuals with ongoing or recent bacterial infections and it was suggested that non-specific IgG deposition could be a general trait of inflammation or infection [452]. In this study,

AIAD could be induced in normal human serum (NHS) that did not previously bind to uncoated plates by heat treatment at 60°C for 10 minutes or 40°C overnight. It was suggested that elevated temperatures such as those that might be found in the body during a severe fever might lead to a conformational change that may cause an increase in binding to uncoated plates. However, I did not see a difference in AIAD between heat-inactivated and non-heat-inactivated samples in our studies, although I did not test heat treatment overnight at 40°C.

It is likely that multiple factors contribute to the occurrence of AIAD in the Burkinabe samples. These may include higher sample transport and processing temperatures, longer sample processing times and more frequent or recent infection of volunteers, including with malaria. The initial association observed between AIAD and anti-schizont IgG may have been caused by false positives caused by AIAD in the anti-schizont ELISA. However, this association remained when the anti-schizont ELISA was conducted using ChonBlock™ (which successfully eliminated AIAD), suggesting that the association between malaria exposure and AIAD was real.

AIAD is unique to each individual sample and therefore either needs to removed completely through the use of an effective blocking buffer, or accounted for and removed from each individual sample. Testing samples in parallel in coated and uncoated wells would allow a measurement of AIAD for each sample, which could be subtracted from the value in the coated well to reveal the real result. However, this increases the amount of reagents required and may not be a cost-effective solution for clinical trials on a large scale. Therefore, I sought to find a blocking solution that could reduce or eliminate AIAD. Previous studies have determined multiple different methods that have this effect, and the optimal solution varies for each assay. The addition of normal rabbit serum (NRS) or FCS to the blocking solution can have a blocking effect due to competitive binding of rabbit or calf IgG on the plastic surface, which then can not be bound by the anti-human secondary antibody [451]. The mechanism of blocking by naïve human serum (NHS, which does not display AIAD) is less clear but could be due to competitive

binding of other serum components to the plate, preventing Ig binding once a sample is added. Other tested methods included adding casein into the coating buffer, using detergent (e.g. Tween20) in the blocking buffer or treating the samples with heat, centrifugation or sterile filtration [449]. In the standardised Ebola GP ELISA, neither sample heat inactivation or adding detergent (1% Tween20) to the blocking step had an effect on background binding. Addition of 10% NHS or FCS to the blocking buffer reduced AIAD in some samples but did not reduce binding in the samples with the highest AIAD and reduced the specific signal from vaccinated individuals.

A novel proprietary blocking buffer, ChonBlock™ has been developed specifically to reduce the intense background signal caused by AIAD, particularly in autoimmune patients [453,455,458]. I found that ChonBlock™ eliminated AIAD-associated background signal in samples from malaria-exposed individuals without reducing specific signal in positive samples. Given the findings here, it is important that samples are tested in parallel in uncoated wells where possible to check for the presence of AIAD. This may be particularly important for samples from malaria-exposed populations or trials sites where sample processing times might be extended and occur at high ambient temperature. When AIAD is a problem in a sample set, background OD on uncoated wells could be removed for each sample or the commercially available blocking buffer ChonBlock™ could be used to successfully eliminate non-specific signals.

4.4.2. Ebola GP IgG seroprevalence

The use of ChonBlock™ successfully removes background signal caused by AIAD. However, there were a few samples from Burkina Faso that were still positive after AIAD was successfully eliminated. This could be high background caused by another unknown phenomenon that is not eliminated by ChonBlock™ or cross-reactivity as there was also one positive sample at baseline in the UK cohort and two in the Senegalese cohort. However, if this is Ebola GP-specific IgG in the Burkina Faso samples, this would be particularly interesting. Burkina Faso has never reported any Ebola cases, and before the 2014-2016 outbreak, there had not been any reported

cases of Ebola in West Africa at all, except for a single non-fatal case of *Taï Forest ebolavirus* in Côte d'Ivoire in 1994 [459]. There is a growing body of evidence suggesting that seroprevalence of Ebola-specific antibody is higher than expected in West Africa and that antibodies exist in populations that have never reported Ebola cases. There have been over 50 seroprevalence studies (reviewed in [460]) since the first outbreak in Zaire (now Democratic Republic of Congo, DRC) that have identified Ebola-specific antibodies in individuals that were either asymptomatic case contacts, individuals from the local community with no reported contact or individuals from countries that have never reported a case. It should be noted that earlier studies used immunofluorescence assays that reportedly had high rates of false positives and even among recent studies, in which ELISAs with high cut-off thresholds are used, AIAD is seldom measured or taken into account when interpreting the results [461]. However, aside from false positive results possibly caused by high assay background, there at least three possible explanations for the unexpected results: 1) asymptomatic infection with *Zaire ebolavirus*, 2) cross-reactive antibodies against another, less virulent species of Filovirus and 3) cross-reactive antibodies against something other than a Filovirus.

Asymptomatic *Zaire ebolavirus* is thought to occur, although estimates for this range from 1-46% of cases [462-469]. A robustly investigated example of this is a study in which Ebola virus antibody was present in up to 20% of individuals in Gabon in regions that had never documented an Ebola case [462]. The specificity of anti-EBOV IgG in this study was confirmed by Western blot and EBOV-specific T cell responses were also observed in some positive individuals. Additionally, there is some evidence that asymptomatic infection may have occurred during the 2014-2016 outbreak in Sierra Leone, although this was estimated to be low [464]. Of household contacts with high level exposure that were not diagnosed with EVD, only 2.6% of individuals with no symptoms were seropositive, while 12% that reported symptoms were positive.

Ebola viruses may be circulating in countries that have not reported cases previously. For example, until recently it was not thought that EBOV was present in Sierra Leone prior to the 2014 epidemic. However, evidence is now emerging that EBOV may have been circulating since at least 2006. Sierra Leone is in the Lassa fever belt and experiences multiple cases annually [470]. The Lassa Diagnostic Laboratory in Kenema Government Hospital receives approximately 500-700 suspected cases annually, of which only 30-40% are diagnosed as Lassa virus infection [471] A study of samples from patients with suspected Lassa fever from 2007-2014 identified only 50% of the samples as positive for antibodies against Lassa virus [472]. Of these samples 5% were positive for antibodies against EBOV and 11% were positive for antibodies against Marburg virus. This suggests a significant burden of undiagnosed acute febrile disease and evidence of circulating undiagnosed Filovirus infections prior to the 2014 EBOV epidemic.

Alternatively, cross-reactive antibodies against other *Ebolavirus* species may be responsible for the unexpected seropositive results. Zaire Ebola GP, which is the most commonly investigated antibody target in these seroprevalence studies, has relatively little sequence identity even with glycoproteins from other *Ebolavirus* species (*Bundibugyo ebolavirus*: 66%, *Taï Forest ebolavirus*: 63%, *Reston ebolavirus*: 59%, *Sudan ebolavirus*: 56%) [473]. Zaire Ebola nucleoprotein (NP), which is an alternative antibody target used in some studies has a slightly higher level of sequence identity between species (*Bundibugyo ebolavirus*: 75%, *Taï Forest ebolavirus*: 75%, *Reston ebolavirus*: 68%, *Sudan ebolavirus*: 68%) [473]. However, survivors of EVD caused by *Zaire ebolavirus* have been shown to produce antibodies that are cross-reactive against multiple *Ebolavirus* species [474,475]. Strong cross-reactive antibody responses against heterologous Ebola viruses were observed in convalescent serum from individuals infected with EBOV, SUDV, BDBV and RESTV [476]. Additionally some of these studies have demonstrated antibodies against multiple Ebola proteins [463,469], further supporting the view that the antibody is specific for a species of *Ebolavirus*.

There may be further species of *Ebolavirus* circulating that could cause asymptomatic or mild infection in humans and induce cross-reactive antibodies against *Zaire ebolavirus* GP. In fact, a sixth species of *Ebolavirus, Bombali ebolavirus,* was very recently identified in bats in Sierra Leone [279]. It is not known if this species has caused human infections or could induce cross-reactive antibody but demonstrates that there are Ebola viruses circulating without our knowledge that may cause mild or asymptomatic infections and induce cross-reactive antibody.

Antibody is thought to be important for survival of EVD in humans as poor humoral responses have been associated with fatal outcomes [320,477]. Therefore, it is possible that cross-reactive antibody could provide some level of protection against EVD. During the epidemic, 1,050 confirmed cases of EVD were reported in the Bombali district where the new *Ebolavirus* species was recently discovered. In a seroprevalence study conducted in this district after the 2014-2016 *Zaire ebolavirus* epidemic a relatively high percentage (6-20%) of asymptomatic community contacts (individuals from communities placed under quarantine but not diagnosed with EVD) were seropositive for antibodies against the Zaire Ebola NP [478]. The highest seroprevalences observed in this study occurred in the villages with the lowest incidence of EVD cases, which may mean that *Zaire ebolavirus* was able to circulate in these populations without causing disease. An alternative explanation could be that pre-existing antibodies against a less virulent species (such as *Bombali ebolavirus*) that had previously circulated in the area were able to provide some level of cross-protection in these populations.

4.5. Conclusions

Samples from highly malaria exposed individuals may demonstrate AIAD. This phenomenon can cause intense false positive results in ELISAs and should be considered, particularly when measuring humoral responses in malaria-exposed cohorts. AIAD can be measured by assaying samples in uncoated wells in parallel to antigen-coated wells. The OD value from the uncoated well could then be subtracted from the antigen-coated result for each individual. Alternatively,

an appropriate blocking buffer, such as ChonBlock™ which successfully removes AIAD-associated background, could be used for all samples in cohorts where AIAD occurs. However, the optimal solution to reduce assay background and ensure accurate comparisons across trial cohorts should be determined. The removal of AIAD is important to reveal the true seroprevalence within a population, particularly within malaria-exposed populations, for which this effect has previously been documented [449]. Having done this, we have discovered samples from Burkina Faso that may contain IgG against *Zaire ebolavirus* GP. Although the explanation for this is currently unclear, it fits with a growing body of evidence that the occurrence of Ebola-specific antibody is more widespread than previously appreciated.

5

Vaccine responses in malaria-exposed populations

5.1. Introduction

Many of the vaccines currently being developed target populations within lower income or lower-middle income countries which bear the largest burden of infectious disease [479-481]. For many of these diseases there is no effective vaccine available (e.g. malaria, HIV, diarrhoeal illnesses, helminth diseases). Phase I clinical trials for most vaccines occur in developed countries, most often with very different climates to those in which the target population are living. These trials generate the initial safety and immunogenicity data that allow further development and testing in Phase Ib trials in the target populations. However, immunogenicity is often reduced in the target population [482-485]. This is likely to be multifactorial and contributing factors may include pathogen exposure, genetic differences, microflora composition and nutritional status [486-489]. It is clearly essential that these vaccines are immunogenic and efficacious within the target populations and not just the population in which the vaccine is first tested.

Many of these populations are living in malaria-endemic regions and therefore have high levels of malaria exposure from a young age. Concurrent or recent malaria infection has been particularly noted for reducing vaccine responses [158-160]. Severe malaria infections predominantly occur in children under 5 years [490], the same age group that are receiving their childhood vaccination within the Expanded Program on Immunization (EPI) schedule. Therefore,

malaria infection may interfere with responses to vaccines, including malaria vaccines, in these populations [491]. However, it is not clear if lifelong repeated malaria infections (and often asymptomatic parasitaemia) have longer term impacts on the immune system and could also impact vaccine immunogenicity in adults in these populations. This would be important for the development of malaria vaccines, since although infants are the ultimate target population, candidate vaccines are first tested in age-de-escalation studies and may only proceed through the vaccine development pipeline if they first show reasonable immunogenicity in adults [492]. Aside from this, vaccine immunogenicity in adults within these populations is also important for routine vaccinations given to pregnant women [493] and for outbreak pathogens [494].

The vaccines that are the focus of this thesis (ChAd63-ME-TRAP, MVA-ME-TRAP, RTS,S and R21 for malaria and ChAd3-EBO-Z and MVA-EBO-Z for Ebola) predominantly target populations with high levels of malaria exposure and therefore it is critical to assess how these vaccines function in malaria-exposed populations. We have run a number of Phase Ib clinical vaccine trials in populations across sub-Saharan Africa to evaluate these vaccines in the target populations (summarised in Table 5.1). The aim of this study was to compare vaccine immunogenicity in malaria-naïve and malaria-exposed cohorts and to determine if any reduction in immunogenicity was associated with malaria exposure. I compared the immunogenicity of several malaria vaccine candidates and an Ebola vaccine candidate between malaria-naïve UK and malaria-exposed African cohorts and determined if there was an association between immunogenicity and malaria exposure. The comparison of Ebola vaccine immunogenicity was particularly useful as it allowed for a cleaner study of the effect of malaria exposure on vaccine responses without a background of pre-existing immunity.

5.2. Study-specific methods

5.2.1. Samples and study details

Study details for the samples used in this chapter are summarised in Table 5.1. Full sample and study details, as well as ethics statements for the samples used in this chapter can be found in Chapter 2.2.3.

Table 5.1. Summary of clinical trials used to compare immunogenicity in malaria-exposed and malaria-naïve populations
ChAd63: Chimpanzee adenovirus serotype 63, ME: multi-epitope string, TRAP: Thrombospondin related adhesion protein, MVA: modified vaccinia virus Ankara, D0: day 0, D28: day 28, D56: day 56, MM: Matrix-M vp: viral particles, pfu: plaque forming units. n=total number of volunteers enrolled in each group.

Trial code	Country	Vaccines	Age Group	Group/s included in these studies	Doses	Regimen
VAC40	Kenya	ChAd63-ME-TRAP, MVA-ME-TRAP	adults	Group 2 (n=20)	$5x10^{10}$vp ChAd, $2x10^{8}$ pfu MVA	D0: ChAd, D56: MVA
VAC41	The Gambia	ChAd63-ME-TRAP, MVA-ME-TRAP	adults	Group 1B (n=10)	$5x10^{10}$vp ChAd, $2x10^{8}$ pfu MVA	D0: ChAd, D56: MVA
			2-6 years	Group 3B (n=6)	$5x10^{10}$vp ChAd, $1x10^{8}$ pfu MVA	D0: ChAd, D56: MVA
VAC42	The Gambia	ChAd63-ME-TRAP, MVA-ME-TRAP	5-12 months	Group 1B (n=12)	$5x10^{10}$vp ChAd, $1x10^{8}$ pfu MVA	D0: ChAd, D56: MVA
			10 weeks	Group 2B (n=12)	$5x10^{10}$vp ChAd, $1x10^{8}$ pfu MVA	D0: ChAd, D56: MVA
VAC45	UK	ChAd63-ME-TRAP, MVA-ME-TRAP	adults	Group 2 (n=15)	$5x10^{10}$vp ChAd, $2x10^{8}$ pfu MVA	D0: ChAd, D56: MVA
VAC46	Kenya	ChAd63-ME-TRAP, MVA-ME-TRAP	adults	Group 1 (n=15 all time points, 60 at D63)	$5x10^{10}$vp ChAd, $2x10^{8}$ pfu MVA	D0: ChAd, D56: MVA
VAC50	Burkina Faso	ChAd63-ME-TRAP, MVA-ME-TRAP	5-17 months	Group A (Phase I, n=30)	$5x10^{10}$vp ChAd, $1x10^{8}$ pfu MVA	D0: ChAd, D56: MVA
VAC53	UK	R21/MM	adults	Group 1 (n=10)	10µg R21, 50µg MM	D0, D28, D56
VAC60	Burkina Faso	R21/MM	adults	Groups 1 & 3 (n=12)	10µg R21, 50µg MM or saline control	D0, D28, D56
EBL04	UK	ChAd3-EBO-Z, MVA-EBO-Z	adults	Group 2 (n=16)	$3.6x10^{10}$vp ChAd, $1x10^{8}$ pfu MVA	D0: ChAd, D7: MVA
EBL06	Senegal	ChAd3-EBO-Z, MVA-EBO-Z	adults	Groups 1 & 2 (n=40)	$3.6x10^{10}$vp ChAd, $1x10^{8}$ pfu MVA	D0: ChAd, D7: MVA

5.3. Results

5.3.1. Responses to malaria vaccines in malaria-exposed adults

5.3.1.1. ChAd63-MVA-ME-TRAP

The ChAd63-MVA-ME-TRAP vaccine regimen has been tested in adults in the UK and a number of African countries including Kenya and The Gambia. Those trials with directly comparable dosing and schedules are compared here (summarised in Table 5.1). ChAd63-ME-TRAP was given intramuscularly into the deltoid region of the arm at a dose of $5x10^{10}$ vp in each of the study groups compared here. The MVA-ME-TRAP boost vaccination was given eight weeks later using the same route and a dose of $2x10^{8}$ pfu in adults and $1x10^{8}$ pfu in children and infants. TRAP-specific T cell responses measured by IFNγ ELISpot were compared at baseline and peak post-boost between the UK and African cohorts (Figure 5.1). Although there were no significant differences in the level of TRAP-specific T cell responses at baseline (summed ME + TRAP pools) between UK, Kenyan and Gambian adults at baseline (Figure 5.1A, P=0.053, median SFC/10^{6} PBMC UK: 62 IQR[28-140], Kenya VAC46: 118[44-335], Kenya VAC40: 35[28-116], Gambia: 36[28-92]), Kenyan adults had higher baseline T cell responses and a higher responder frequency. There was a significant increase in TRAP-specific T cells after ChAd63-ME-TRAP prime in all cohorts except Kenya VAC46, (Figure 5.1B, UK P=0.0002, Kenya VAC46 P=0.90, Kenya VAC40 P<0.0001, Gambia P=0.047). There was a significant increase in TRAP-specific T cell responses post-boost in all cohorts (UK: P=0.0012, Kenya VAC46 P=0.0098, Kenya VAC40 P<0.0001, Gambia P=0.016). There were no significant differences in the TRAP-specific T cell responses between the cohorts post-prime (Figure 5.1C, P=0.088, median SFC/10^{6} PBMC UK: 546 IQR[278-1352], Kenya VAC46: 236[79-522], Kenya VAC40: 234[140-560], Gambia: 138[62-566]) or post-boost (Figure 5.1D, P=0.41, median SFC/10^{6} PBMC UK: 2028 IQR[1160-2650], Kenya VAC46: 1778[1170-2540], Kenya VAC40: 1536[793-2382], Gambia: 1558[333-2443]).

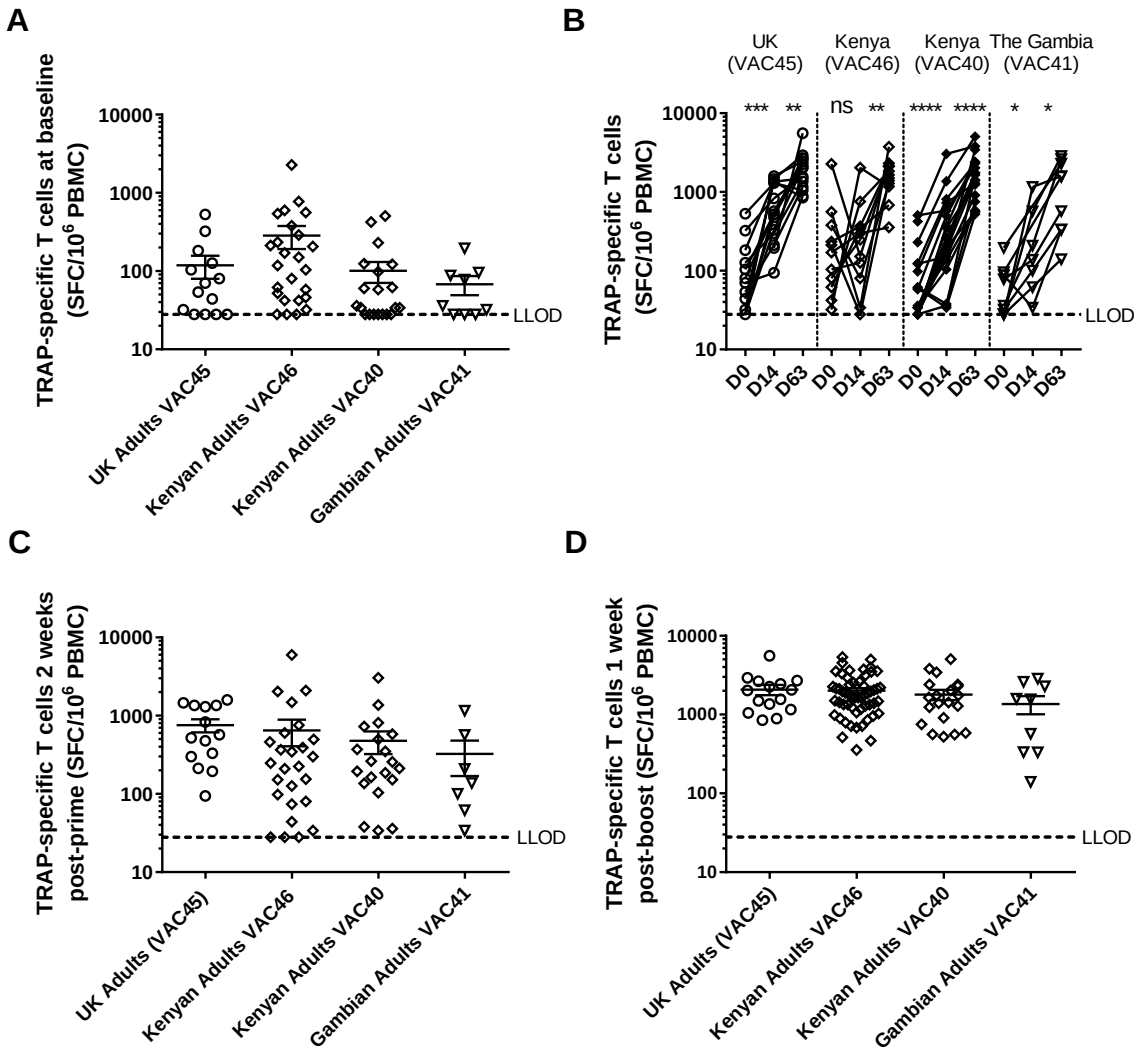

Figure 5.1. TRAP-specific T cell responses to ChAd63-MVA-ME-TRAP in UK and African cohorts

A) TRAP-specific T cell responses (summed IFNγ ELISpot ME+TRAP peptide pools) at baseline (day 0, D0), Kruskal-Wallis analysis. **B**) Change in TRAP-specific T cell levels in each cohort from baseline to post-prime and from post-prime to post-boost, Wilcoxon paired tests. Data from VAC46 vaccinees with samples at all time points. **C**) TRAP-specific T cell responses post-prime (D14, two weeks after ChAd63-ME-TRAP) and **D**) post-boost (D63, one week after MVA-ME-TRAP boost vaccination). Data from all VAC46 vaccinees. Kruskal-Wallis analyses with Dunn's post-test comparisons to the UK cohort. Data points for some individuals are missing if ELISpot QC failed. * P<0.05, ** P<0.01, **** P<0.0001, ns: not significant. SFC/10^6 PBMC: spot-forming cells per million peripheral blood mononucleocytes, dashed lines show LLOD: lower limit of detection – 28 SFC/10^6 PBMC.

Antibody responses against the vaccine insert (TRAP) were measured by ELISA at baseline, one or two weeks post-prime (D14/D28) and one week post-boost in all cohorts (D63) (Figure 5.2). All but one UK adult (VAC45) had undetectable TRAP-specific IgG titres at baseline (Figure 5.2A). Baseline TRAP IgG was significantly higher in Kenyan and Gambian adults (Medians [IQRs], Kenyan VAC46: 67 [47-110], Kenyan VAC40: 75 [51-145], Gambian VAC41: 46 [30-82], Kruskal-Wallis P<0.0001). The UK individual with TRAP IgG at baseline had 156 EUs, a level higher than the seropositive cut-off (65 EUs, determined by the mean + 3SD of TRAP IgG levels in 148 malaria-naïve UK adults) and higher than the median baseline responses in Kenyan adults. However, this individual did not have anti-schizont IgG or a history of travel to malaria-endemic countries, therefore it is unlikely that this response is specific for *P. falciparum* TRAP. If this is a cross-reactive response, it is unclear what the cross-reactive antigen would be. At baseline 52% and 65% of Kenyans (VAC46 and VAC40 respectively) had responses above the seropositive cut-off value, compared with just 33% of Gambians.

In UK adults, ChAd63-ME-TRAP vaccination induced a significant TRAP-specific antibody response (Figure 5.2B, P=0.0010, median at D28: 136 EUs IQR [1-258]). However, as more than half of the Kenyans and a third of the Gambians had low levels of pre-existing TRAP antibody, ChAd63-ME-TRAP was not acting as a priming vaccination in these populations. There was no D28 blood draw in these trials therefore a direct comparison to the UK cohort is not possible and responses may have increased from D14 to D28. However, at D14 there were significant increases from baseline in the Gambian and Kenyan VAC46 cohorts (P=0.027 median: 103 EUs [77-394], P=0.0012 median: 104 EUs [68-493], respectively) but not in the Kenyan VAC40 cohort (P=0.055, median: 116 EUs [67-288]), in which some volunteers had an increase, whilst others did not. TRAP IgG responses were significantly boosted by MVA-ME-TRAP vaccination in the UK and Kenyan VAC40 cohorts (P=0.0017, median: 703 EUs [85-1619], P=0.0009, median: 321 EUs [181-469]). There were no significant increases in the Kenyan VAC46 or Gambian cohorts (P=0.12, median: 240 EUs [127-562], P=0.20, median: 145 EUs [120-348]). In the UK cohort, a

significant increase in TRAP antibody is evident after both priming and boost. In contrast, in each of the African cohorts there was only a significant increase in TRAP antibody after either ChAd63-ME-TRAP or MVA-ME-TRAP but not after each. TRAP-specific IgG levels after ChAd63-ME-TRAP vaccination were comparable across the cohorts (Figure 5.2C, P=0.97). TRAP IgG levels one week post-MVA boost were around three logs higher than baseline in the UK cohort (Figure 5.2D) and 4-5-fold higher than baseline in the African cohorts. Titres at this time point were comparable across the UK and Kenyan cohorts but significantly lower in the Gambian cohort (P=0.042). All Kenyan and Gambian vaccinees had TRAP-specific IgG responses above the seropositive cut-off at this time point but there were three UK vaccinees that did not have detectable TRAP IgG at this time point. All Kenyan (VAC46) vaccinees had a D63 serum sample but only a selection had blood taken for immunology at other time points. Figure 5.2B only includes data from individuals that had samples at all time points. Figure 5.2D includes data from all individuals.

Time courses of TRAP-specific IgG responses reveal that the time points used in the African trials may have missed the peak antibody response (Figure 5.3A). TRAP-specific antibody responses are highest in the UK cohort at D76 (three weeks after MVA-ME-TRAP). TRAP IgG titres at D112 (eight weeks after MVA-ME-TRAP) in the UK cohort were significantly higher than those at D90 (five weeks after MVA-ME-TRAP) in the Kenyan and Gambian cohorts (Figure 5.3B, P=0.0004). However, it should be noted that this time point in the UK cohort is 35 days after CHMI and although TRAP IgG levels are not boosted by malaria challenge, this could have altered the kinetics, for example by slowing the decay in antibody levels.

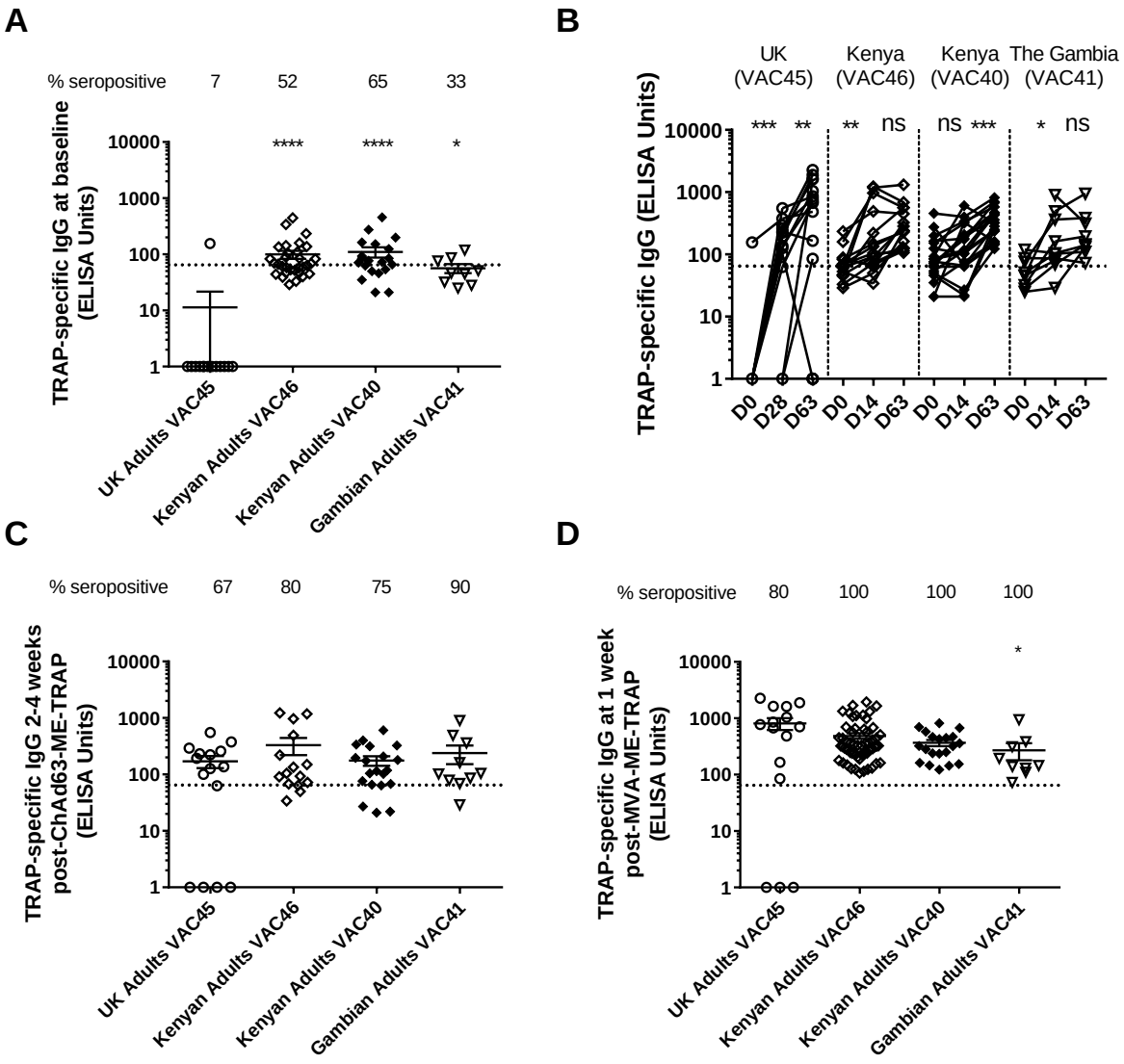

Figure 5.2. TRAP-specific IgG responses to ChAd63-MVA-ME-TRAP in UK and African adults

A) TRAP-specific IgG responses at baseline (day 0, D0), Kruskal-Wallis analysis. **B**) Change in TRAP-specific IgG levels in each cohort from baseline to post-prime and from post-prime to post-boost, Wilcoxon paired tests. Data from VAC46 vaccinees with samples at all time points. **C**) TRAP-specific IgG responses post-prime (D14 or D28) and **D**) post-boost (D63, one week after MVA-ME-TRAP boost vaccination). Data from all VAC46 vaccinees. Kruskal-Wallis analyses with Dunn's post-test comparisons to the UK cohort. One Gambian vaccine did not have a D63 sample. * P<0.05, ** P<0.01, *** P<0.001, **** P<0.0001. Dotted lines show seropositive cut-off for TRAP ELISA (65 EUs).

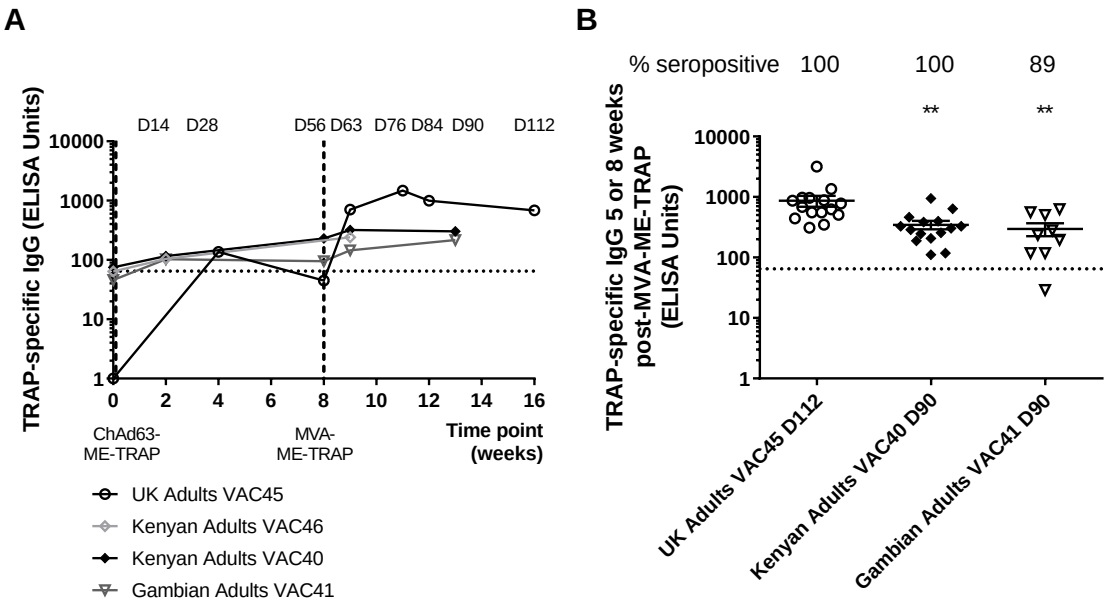

Figure 5.3. TRAP-specific IgG responses to ChAd63-MVA-ME-TRAP in UK and African cohorts

A) Median TRAP-specific IgG time course for each cohort. Vaccination time points are indicated by dashed lines. **B**) TRAP-specific IgG titres at D112 (C+35) in the UK and D90 in the Kenyan and Gambian trials that included this time point. Only 15/20 Kenyan and 9/10 Gambian vaccinees had a sample taken at D90. Dotted lines indicate seropositive cut-off value for the TRAP ELISA (65 EUs). Kruskal-Wallis analysis. **** P<0.0001.

5.3.1.2. R21

In contrast to the viral vectored vaccines described in the previous section, the VLP vaccine R21 is specifically designed to induce an antibody response[242]. Comparable regimens have been tested in the UK (VAC53 G1, n=10) and Burkina Faso (VAC60, vaccinees n=8, controls n=4). Volunteers were vaccinated with 10µg R21 adjuvanted with 50µg Matrix-M (MM) at D0, D28 and D56. The primary immunological read-out for these trials was IgG against the NANP repeat region of CSP, measured by ELISA (described in methods Chapter 2.4.14.2). CSP-specific T cell responses to R21 and RTS,S as measured by IFNγ ELISpot are generally very low ([401], VAC53/VAC60 – manuscript in preparation). Therefore, this assay was not conducted in the Burkinabe trial; to reduce bleed volumes and trial costs, only serum for ELISA was collected.

Burkinabe adults had pre-existing CSP-specific IgG significantly higher than malaria-naïve UK adults (Figure 5.4A, 5.4B, P<0.0001], UK: no detectable responses >1 EU, Burkina Faso median:

25 [20-70]). After the first dose of R21, responses were comparable between the UK and Burkinabe volunteers (P=0.76, medians: UK 71 [57-352], Burkina Faso 117 [72-150]). Responses were also comparable at D56, after two doses (P=0.12, medians: UK 854 [601-2020], Burkina Faso 362 [241-2793]). However, the third R21 dose failed to boost Burkinabe vaccinees, which had significantly lower anti-CSP IgG levels than UK vaccinees at D84 (P=0.021, medians: UK 1335 [654-2978], Burkina Faso 361 [241-986]). Additionally, a control group vaccinated with saline was included in the Burkina Faso trial to check that levels of CSP-specific IgG were not increasing with exposure to natural infection over the course of the trial. CSP-specific IgG tires remained stable in this group (medians D0: 35, D28: 23, D56: 40, D84: 8).

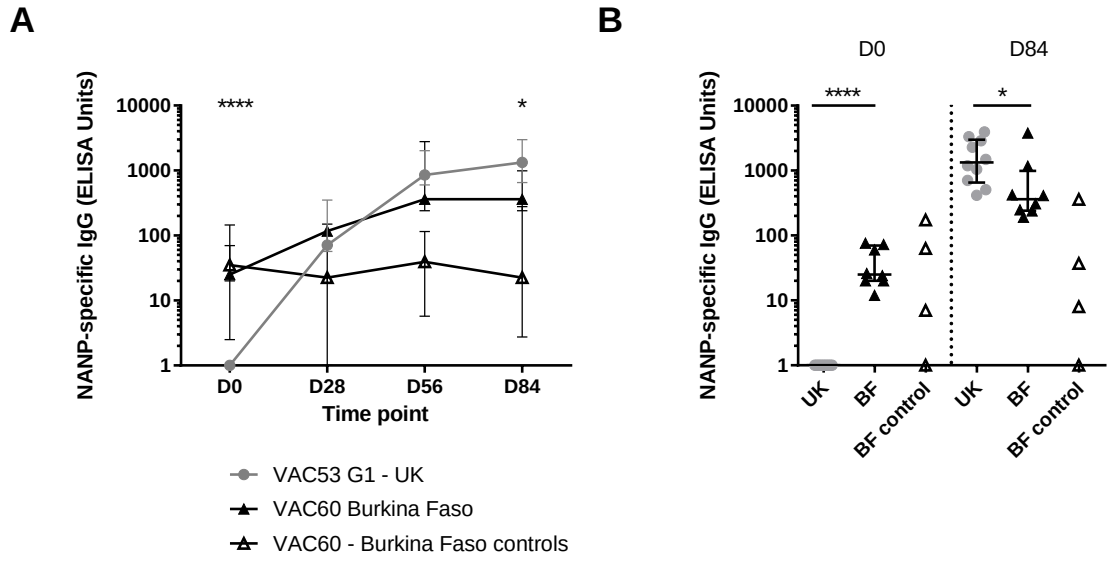

Figure 5.4. NANP-specific IgG responses to R21 in the UK and Burkina Faso
NANP-specific IgG responses in UK (VAC53 G1) and Burkinabe adults (VAC60) vaccinated with R21 at Day 0 (D0), D28 and D56: **A**) Median time courses (error bars show interquartile ranges). Control volunteers were vaccinated with saline. **B**) Individual responses at D0 and D84. One Burkinabe control volunteer did not have a sample taken at D84. Mann-Whitney analyses comparing UK and Burkinabe vaccinees at each time point: D0 P<0.0001, D84 P=0.021. * P<0.05, **** P<0.0001.

5.3.1.3. Relationship between malaria exposure and responses to malaria vaccines in adults

As there was some evidence that malaria-exposed populations may respond less well to these candidate malaria vaccines (failure to boost pre-existing antibody responses or failure of subsequent vaccine doses to further boost responses), the level of malaria exposure and the relationship with vaccine responses was examined. Antibodies against *P. falciparum* schizont lysate were used as a surrogate for malaria exposure as they have previously been shown to be highly associated [495,496]. Samples were available for these analyses from the Gambian (VAC41) and Burkinabe (VAC60) cohorts. There was no association between baseline anti-schizont IgG and TRAP-specific T cells at baseline or post-boost (Figure 5.5A D0 TRAP T cells r:-0.25 P=0.51, D63 TRAP T cells r:0.42 P=0.27). There was no significant association between baseline anti-schizont IgG and TRAP-specific IgG at baseline (Figure 5.5B, r: 0.67, P=0.059) or at D90 (r:-0.025, P=0.96). There was also no association between baseline anti-schizont IgG and NANP-specific IgG at baseline (Figure 5.5C r: 0.61, P=0.12) or at D84 (r:0.095, P=0.84) in Burkina Faso (VAC60).

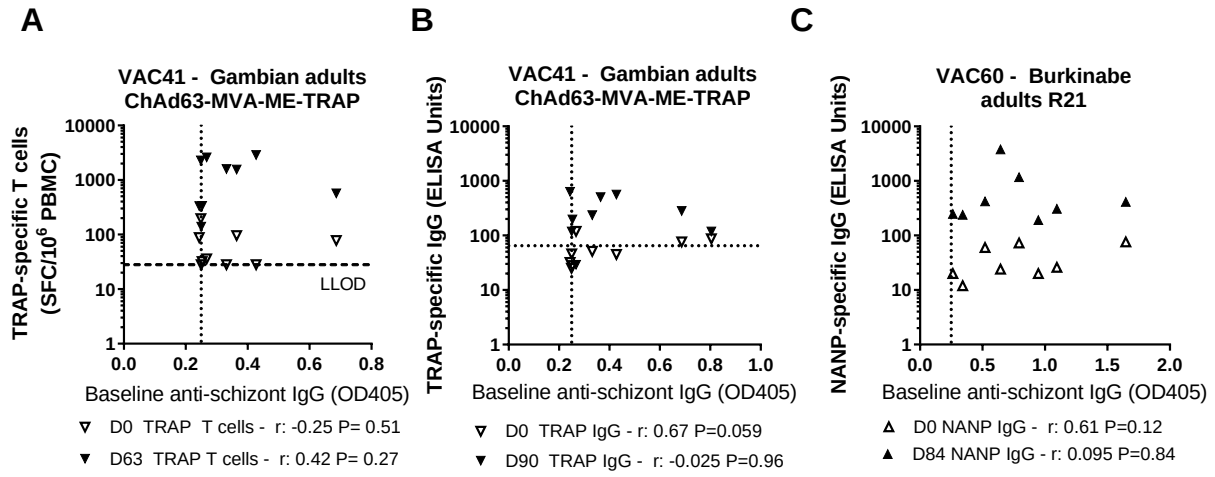

Figure 5.5. Relationship between anti-schizont IgG and malaria vaccine responses in adults

Relationship between anti-schizont IgG at baseline and: **A**) TRAP-specific T cell responses by IFNγ ELISpot at baseline (D0) or peak post-boost (one week post-boost, D63) and **B**) TRAP-specific IgG at baseline (D0) or post-boost (D90), both in Gambian adults vaccinated with ChAd63-ME-TRAP and boosted with MVA-ME-TRAP (VAC41, G1B). **C**) Relationship between anti-schizont IgG at baseline and NANP-specific IgG at D0 and D84 in Burkinabe adults vaccinated with R21 (VAC60). Spearman's rank analyses. SFC/10^6 PBMC: spot-forming cells per million peripheral blood mononucelocytes. OD405: optical density at 405nm. Dashed line indicates ELISpot LLOD: lower limit of detection (28 SFC/10^6PBMC), dotted lines indicate seropositive cut-off for the anti-schizont (OD405=0.250), TRAP (65 EUs).

5.3.2. Responses to malaria vaccines in malaria-exposed children and infants

ChAd63-ME-TRAP and MVA-ME-TRAP have also been tested in children aged 2-6 years (The Gambia, VAC41 group 3B n=6), and in infants aged 5-12 months (The Gambia, VAC42 group 1B n=12), 5-17 months (Burkina Faso, VAC50 group A [phase I lead-in study] n=30) and infants aged 10 weeks (VAC42, The Gambia group 2B n=12). Vaccine responses were compared across age groups and the relationship with malaria exposure assessed. All children and infants compared here received $5x10^{10}$ vp of ChAd63-ME-TRAP at D0 followed by a boost with $1x10^8$ pfu MVA-ME-TRAP eight weeks later. Children aged 2-6 years received vaccinations intramuscularly into the deltoid region of the arm. All other paediatric cohorts received vaccinations intramuscularly in the anterolateral thigh.

Baseline TRAP-specific T cells were significantly lower in Gambian infants aged 5-12 months or 10 weeks at vaccination compared with UK adults (Figure 5.6A, 5-12 months P=0.022, 10 weeks P=0.0084) and African adults (5-12 months P=0.032, 10 weeks P=0.011). The median baseline TRAP-specific T cells were not above the LLOD in any of the paediatric cohorts. Paediatric TRAP-specific T cell responses post-boost were comparable to African and UK adult responses, except Burkinabe 5-17 month olds, which had significantly lower responses than either African (P<0.0001) or UK adults (P<0.0001)(Figure 5.6B UK adults median SFC/10^6 PBMC: 2028 IQR[1160-2650], African adults: 1558[577-2353], Gambian 2-6 years: 763[507-1285], Burkinabe 5-17 months: 396[227-652], Gambian 5-12 months: 734[608-1048], Gambian 10 weeks: 2077[903-2530]).

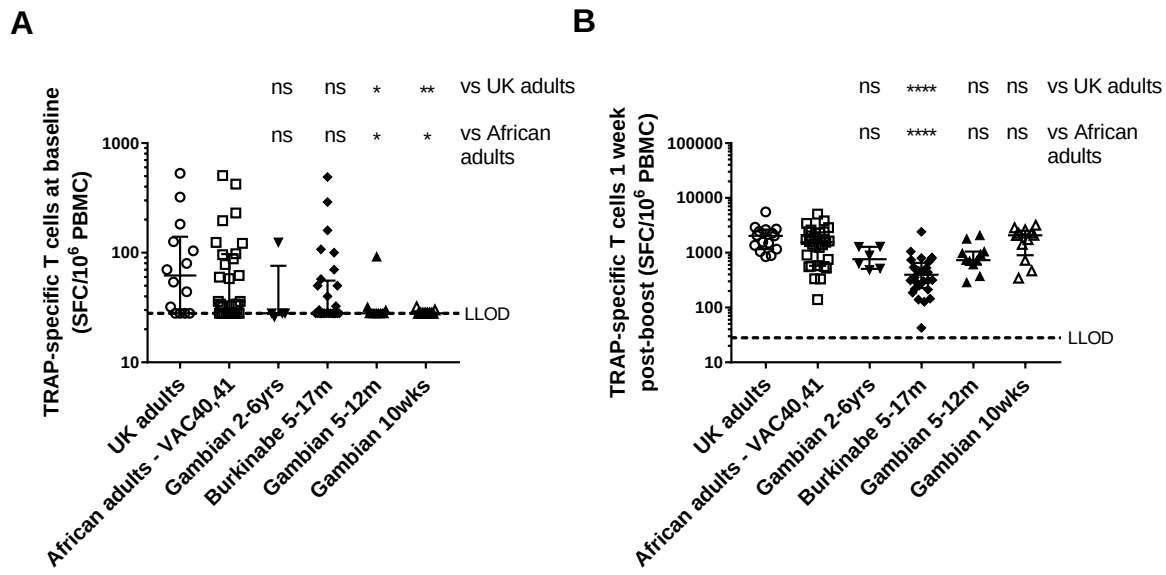

Figure 5.6. T cell responses in malaria-exposed children and infants
TRAP-specific T cell responses (IFNγ ELISpot summed ME+TRAP pools) at: **A**) baseline and **B**) one week after MVA-ME-TRAP (day 63, D63). Kruskal-Wallis analyses with Dunn's multiple comparisons to African or UK adults.* P<0.05, **** P<0.0001, ns: not significant, yrs: years, m: months, wks: weeks. SFC/10^6 PBMC: spot-forming cells per million peripheral blood mononucelocytes. LLOD: lower limit of detection - 28 SFC/10^6 PBMC.

TRAP-specific IgG titres at baseline and post-ChAd63-MVA-ME-TRAP vaccinations in children and infants were compared with titres in African adults. Gambian children aged 2-6 years had a level of TRAP-specific IgG comparable to Gambian and Kenyan adults (Figure 5.7A). Younger children and infants had significantly lower baseline TRAP IgG than African adults and most individuals under two years did not have TRAP IgG above the seropositive cut-off of 65 EUs (P<0.0001 median EUs UK adults: 1, African adults: 71 IQR[46-106], Gambian 2-6 years: 105 [66-258], Burkinabe 5-17 months: 33 [17-50], Gambian 5-12 months: 17 [12-20], Gambian 10 weeks: 3 [1-8]). After vaccination, Gambian children aged 2-6 years had titres comparable to UK and African adults while all other paediatric cohorts had significantly higher TRAP-specific responses than UK or African adults (Figure 5.7B, Kruskal-Wallis P <0.0001 for UK and African adult comparisons, median EUs UK adults: 703 [85-1619], African adults: 283 [146-458], Gambian 2-6 years: 1033 [619-2441], Burkinabe 5-17 months: 4953 [4127-6519], Gambian 5-12 months: 4604 [2399-7340], Gambian 10 weeks: 5956 [2665-9216]). Although, as discussed in a previous section (Chapter 5.3.1.1) D63 is likely not the peak of the antibody response, this time point was used for these comparisons as it was shared across all of these trials.

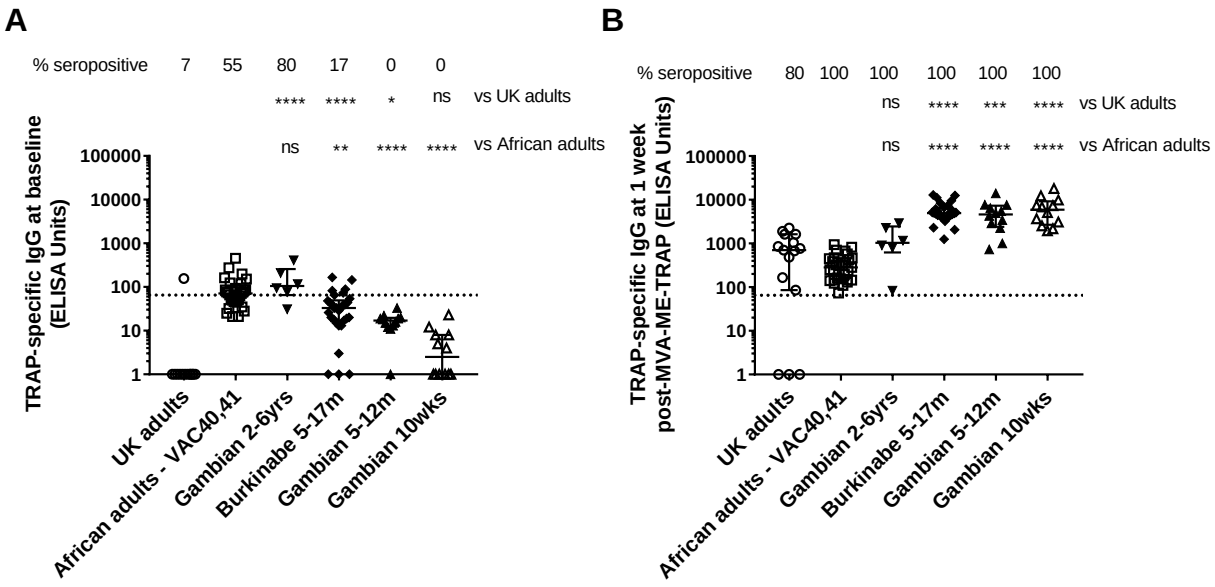

Figure 5.7. Antibody responses in malaria-exposed children and infants
TRAP-specific IgG at: **A**) baseline and **B**) one week after MVA-ME-TRAP (day 63, D63). Dotted lines indicate seropositive cut-off (65 EUs). Kruskal-Wallis analyses with Dunn's multiple comparisons to the African or UK adult responses.* P<0.05, ** P<0.01, *** P<0.001, **** P<0.0001, ns: not significant, yrs: years, m: months, wks: weeks.

As there was some evidence of pre-existing TRAP-specific antibody in African paediatric cohorts, baseline anti-schizont IgG was also measured in these cohorts. The level of anti-schizont IgG in Gambian children and infants was not significantly different to malaria-naïve UK adults and only two individuals, both in the 10 week old group, had anti-schizont IgG above the cut-off value (Figure 5.8A). Burkinabe infants aged 5-17 months had significantly higher anti-schizont IgG than UK malaria naïve adults (P=0.0008) and 61% had responses above the seropositive cut-off. Anti-schizont IgG was not associated with baseline TRAP-specific IgG (Figure 5.8B, r:-0.016 P=0.94) but was negatively associated with TRAP-specific IgG levels at one week post-boost (r:-0.45 P=0.023). There was no association between baseline anti-schizont IgG and TRAP-specific T cells at baseline (Figure 5.8C, r:-0.19, P=0.35) or post-boost (r:-0.092, P=0.66). Age at vaccination was not associated with the level of anti-schizont IgG (Figure 5.8D, r:0.24 P=0.22), TRAP-specific IgG (Figure 5.8E, r:-0.27 P=0.16) or TRAP-specific T cell responses (Figure 5.8F, r:-0.048, P=0.81).

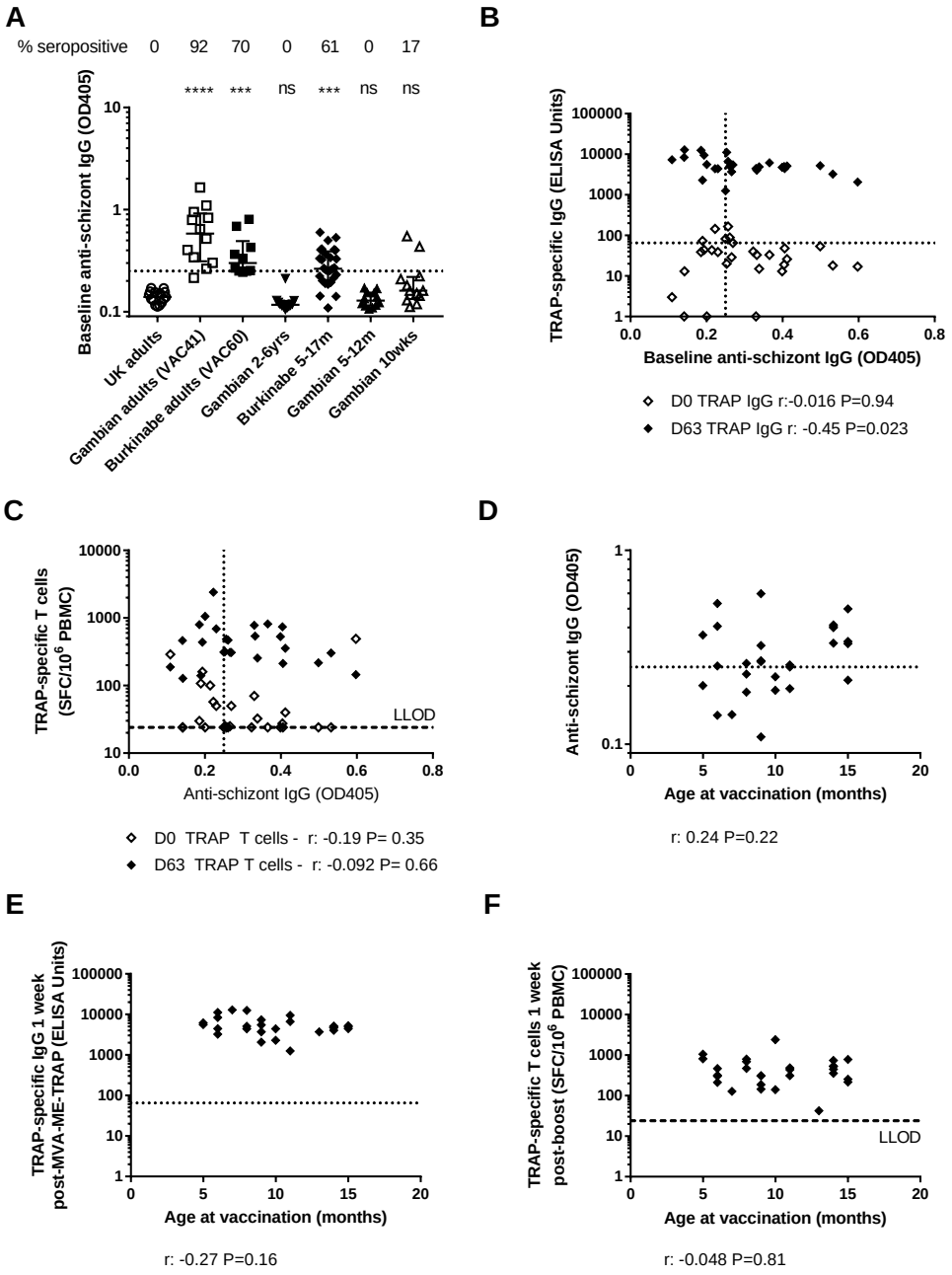

Figure 5.8. Relationship between anti-schizont IgG and vaccine responses in children and infants

A) Anti-schizont IgG at baseline. Kruskal-Wallis analysis with Dunn's post-test comparing paediatric cohorts to UK malaria-naïve adults. **B**) Relationship between baseline anti-schizont IgG and TRAP IgG at baseline (day 0, D0) and post-boost (D63) in Burkinabe infants (VAC50 Group A). **C**) Relationship between baseline anti-schizont IgG and TRAP-specific T cells at D0 and D63. Relationship between age at vaccination and: **D**) Baseline anti-schizont IgG, **E**) post-boost TRAP IgG. **F**) post-boost TRAP-specific T cells. Spearman's rank analyses. Dotted lines indicate seropositive cut-off values for the TRAP (65 EUs) and anti-schizont (OD405=0.250) ELISAs. Dashed lines indicate ELISpot lower limit of detection (LLOD, 28 SFC/10^6PBMC). *** P<0.001, **** P<0.0001, ns: not significant. OD405: optical density at 405nm. SFC/10^6PBMC: spot-forming cells per million peripheral blood mononucleocytes.

5.3.3. Responses to Ebola vaccines in malaria-exposed adults

The candidate Ebola virus vaccines ChAd3-EBO-Z and MVA-EBO-Z were tested in Phase 1 clinical trials in healthy adults in the UK (EBL04 G2, n=16) and Senegal (EBL06, n=40). Volunteers were vaccinated with $3.6x10^{10}$ vp of ChAd3-EBO-Z at day 0 (D0) and boosted with $1x10^{8}$ pfu of MVA-EBO-Z one week later. Antibody responses were measured using a standardised indirect ELISA against recombinant trimeric Ebola GP (as described in methods Chapter 2.4.14.3). ELISAs were conducted at baseline, seven days after ChAd3-EBO-Z vaccination (D7), seven days after MVA-EBO-Z (M+7), D28(Senegal)/M+28(UK), D90 (Senegal)/ M+84 (UK) and D180 (Senegal)/M+168 (UK). T cell responses in each cohort were measured by IFNγ ELISpot using a pool of peptides from the Zaire Ebola GP. ELISpots were conducted for both cohorts at baseline and M+7. In the UK cohort additional ELISpots were conducted seven days after ChAd3-EBO-Z vaccination (D7) and at 28, 84 and 168 days after MVA-EBO-Z (M+28, M+84, M+168).

Antibody responses were significantly lower in the Senegalese cohort than the UK cohort at M+7 (Figures 5.9A, 5.9B, P=0.020, median EUs [IQRs] UK: 907 [267-1748], Senegal: 394 [172-691]), M+84/D90 (P=0.0025, median EUs UK: 469 [390-740], Senegal: 265 [145-408]) and M+168/D180 (P=0.0082, UK: 311 [181-467], Senegal: 158 [109-265]). In contrast, there was no significant difference in the M+7 ELISpot responses between the cohorts (Figure 5.9C, P=0.64 UK median SFC/10^{6} PBMC: 1586 IQR [1203-2745], Senegal: 2017 [1016-4798]).

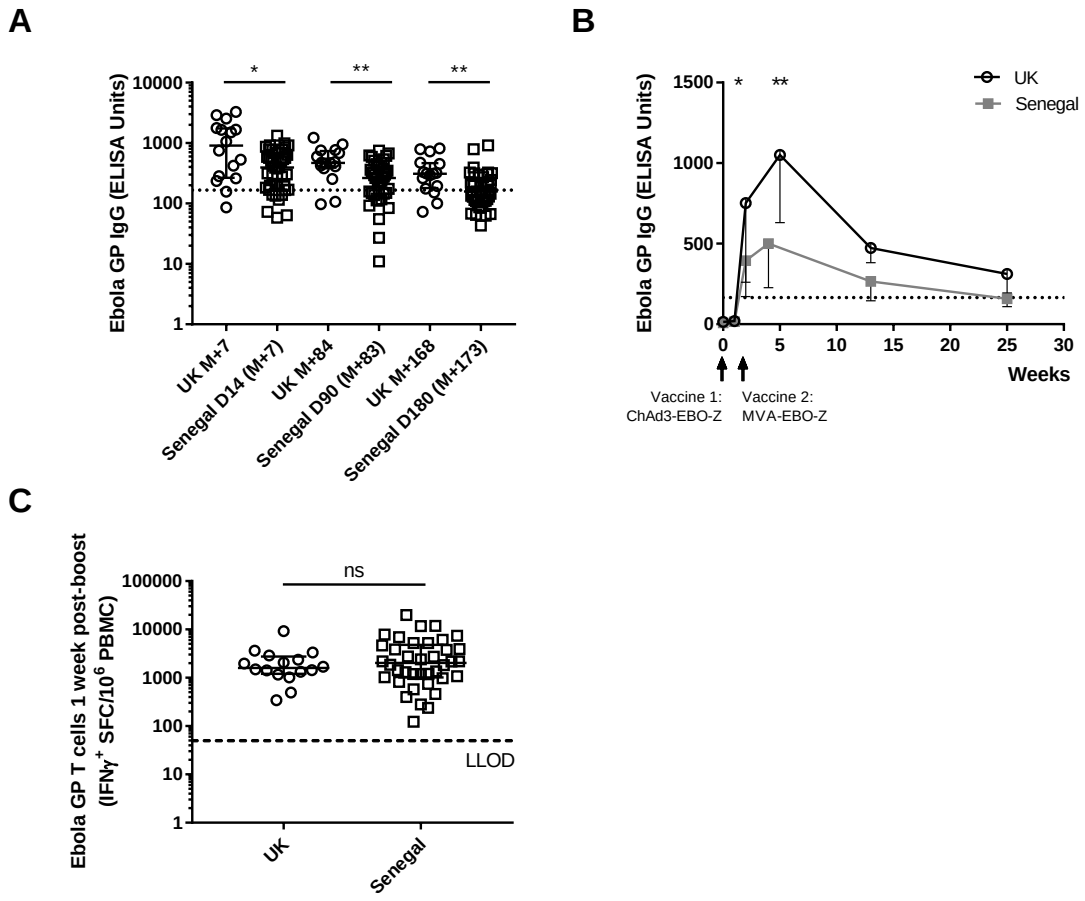

Figure 5.9. Reduced antibody but not T cell responses to ChAd3-MVA-EBO-Z in Senegal
A) Ebola GP-specific IgG at D14 (seven days after MVA-EBO-Z/M+7), at D91 (M+84) and at six months (D175/M+168 in UK and D180/M+173 in Senegal). Dotted line indicates seropositive cut-off (166 EUs). **B**) Ebola GP-specific IgG time courses (median and interquartile ranges). **C**) Ebola GP-specific T cell responses measured by IFNγ ELISpot seven days after MVA-EBO-Z. Mann-Whitney analyses. Dashed line indicates lower limit of detection (LLOD) – 50 SFC/10^6 PBMC. * P<0.05, ** P<0.01, ns: not significant. SFC/10^6 PBMC: spot-forming cells per million peripheral blood mononucleocytes.

Of the Senegalese cohort, 48% (19/40) were positive for anti-schizont IgG and titres were significantly higher than the UK cohort (Figure 5.10A, P<0.0001, median OD405 UK: 0.143 IQR[0.124 – 0.157], Senegal: 0.236 [0.169 – 0.353]). One individual in the UK cohort had grown up in Kenya and was borderline positive for anti-schizont IgG (OD405 0.227, seropositive cut-off OD405: 0.250). This individual is highlighted red in subsequent figures that include data for this volunteer. All individuals were also tested for AMA-1- and MSP-1-specific IgG at baseline (Figure 5.10B). AMA-1 and MSP-1 ELISAs were conducted as described in methods Chapter 2.4.14.4.

Schizont IgG+ Senegalese vaccinees had significantly higher AMA-1 and MSP-1 IgG compared with the UK cohort (Kruskal-Wallis P<0.0001 for both AMA-1 and MSP-1). However schizont IgG- Senegalese vaccinees also had significantly higher AMA-1 (P=0.047) and MSP-1 (P=0.0069) IgG than UK vaccinees. Median time courses of the antibody responses in the UK and Senegalese cohorts split by anti-schizont IgG status indicate that vaccine-specific antibody responses were lowest in schizont IgG+ individuals, highest in the UK and that the schizont IgG- Senegalese group had intermediate responses (Figure 5.10C). However, there were no significant differences between the UK and schizont IgG- Senegalese antibody responses at peak (Figure 5.10D, D28/M+28) or at six months (D180/M+168), whilst schizont IgG+ individuals had significantly lower responses than both the UK and Senegalese schizont IgG- individuals at each of these time points (D28/M+28 P=0.0010 vs UK and P=0.010 vs schizont IgG-, D180/M+168 P=0.0011 vs UK and P=0.025 vs schizont IgG-). The percentage of individuals with responses above the seropositive cut-off value (166 EUs) was also lower in schizont IgG- individuals at M+7 (UK: 94%, Senegalese schizont IgG-: 90%, Senegalese schizont IgG+: 79%) and was particularly low at D180/M+168 (UK: 81%, Senegalese schizont IgG-: 62%, Senegalese schizont IgG+: 26%).

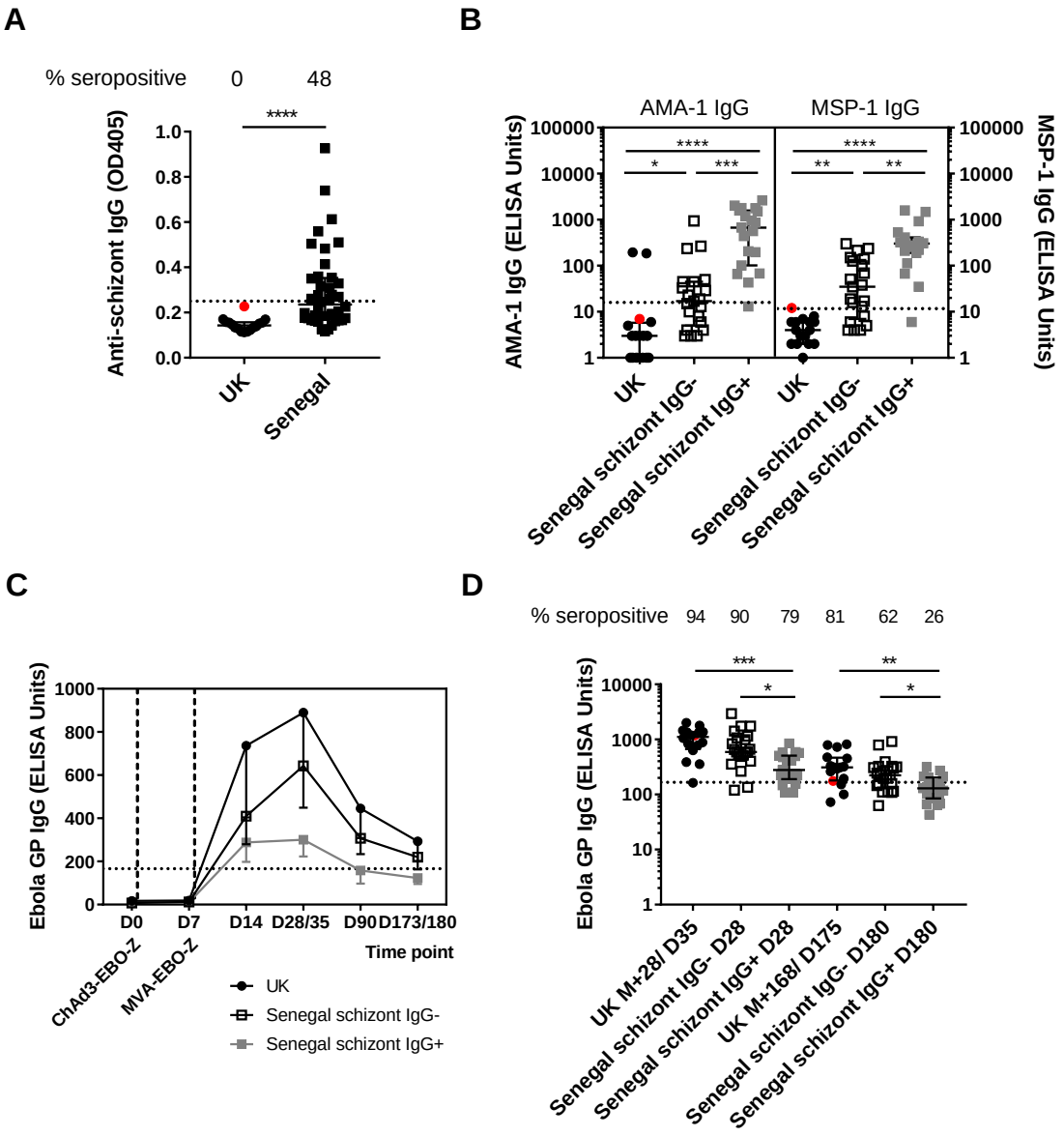

Figure 5.10. Reduced antibody responses to ChAd3-MVA-EBO-Z in malaria-exposed individuals

A) Anti-schizont IgG at day 0 (D0). Mann-Whitney analysis. **B**) Baseline anti-AMA-1 IgG and anti-MSP-1 IgG in the UK compared with Senegalese volunteers split by anti-schizont IgG status. Kruskal-Wallis analysis. **C**) Median Ebola GP IgG time courses. Bars show inter-quartile ranges. Dashed lines indicate vaccination time points. **D**) Ebola GP IgG responses at peak (M+28/D35 in the UK and D28 in Senegal) and six months (M+168/D175 in the UK and D180 in Senegal). Kruskal-Wallis analyses. Volunteer highlighted in red was Kenyan and borderline positive for anti-schizont IgG. Dotted lines indicate the seropositive cut-off values for the anti-schizont (OD405=0.250), AMA-1 (14 EUs), MSP-1 (11 EUs) and Ebola GP (166 EUs) ELISAs. * P<0.05, **P<0.01, *** P<0.001, **** P<0.0001, ns: not significant, OD405: optical density at 405nm.

Antibodies against *P. falciparum* schizont lysate, AMA-1 and MSP-1 were negatively associated with peak Ebola GP-specific antibody responses in the Senegalese cohort (Figures 5.11A: anti-schizont IgG r:-0.37 P=0.020, 5.11B: MSP-1 r:-0.44 P=0.0042, 5.11C: AMA-1 r:-0.40, P=0.011).

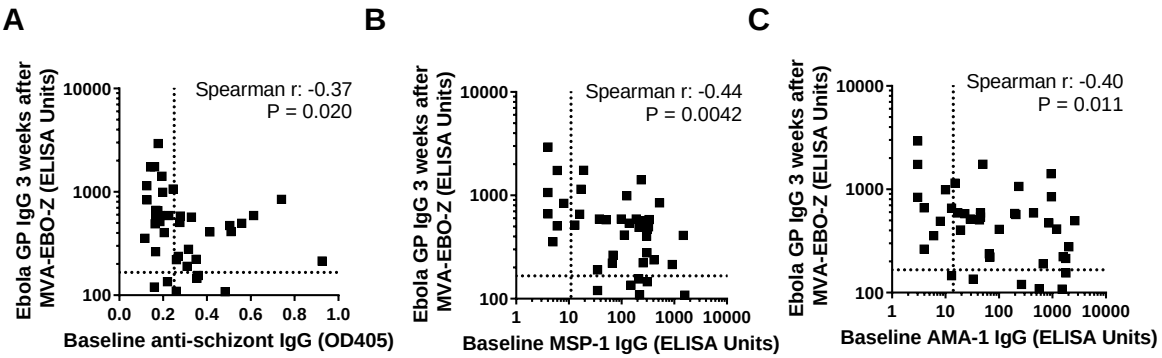

Figure 5.11. Association between malaria exposure and reduced antibody responses to ChAd3-MVA-EBO-Z

A) Relationship between anti-schizont IgG at baseline (day 0, D0) and Ebola GP IgG three weeks after MVA-EBO-Z boost (D28) in the Senegalese cohort. **B**) Relationship between anti-MSP-1 IgG at D0 and Ebola GP IgG at D28. **C**) Relationship between anti-AMA-1 IgG at D0 and Ebola GP IgG at D28. Volunteer highlighted in red was Kenyan and borderline positive for anti-schizont IgG. Dotted lines indicate the seropositive cut-off for Ebola GP (166 ELISA Units), anti-schizont (OD405=0.250), MSP-1 (11 EUs) and AMA-1 (14 EUs) ELISAs. OD405: optical density at 405nm.

When ELISpot responses were stratified by anti-schizont IgG status, there were no significant differences between any of the groups (Figure 5.12A, median SFC/10^6 PBMC UK: 1586 IQR[1203-2745] Senegalese schizont IgG-: 2762 [1330-5252], Senegalese schizont IgG+: 1194 [717-2189]). In addition to IFNγ ELISpot, T cell responses were measured at M+7 by intracellular cytokine staining (ICS) in both cohorts. The frequency of GP-specific IFNγ$^+$ CD4$^+$ T cells was significantly lower (Figure 5.12B, P=0.025) in schizont IgG+ compared with schizont IgG- individuals but there was no significant difference in the frequency of IFNγ$^+$ CD8$^+$ T cells (P=0.43). The level of anti-schizont IgG at baseline was negatively associated with the frequency of GP-specific IFNγ$^+$ CD4$^+$ T cells in the Senegalese cohort (Figure 5.12C r:-0.58, P=0.0096).

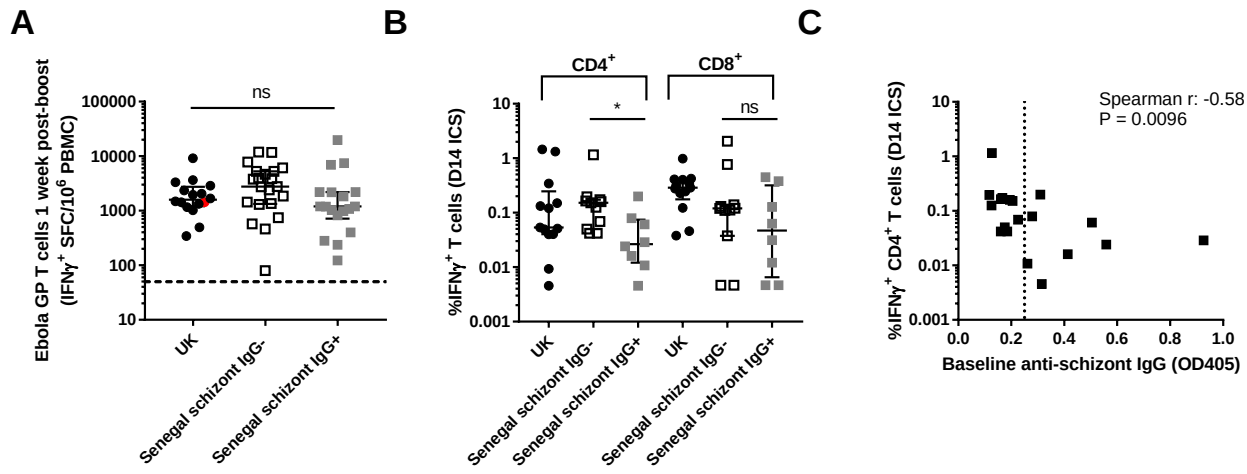

Figure 5.12. Association between malaria exposure and reduced CD4⁺ T cell responses to ChAd3-MVA-EBO-Z

A) Ebola GP-specific T cell responses by ELISpot at D14 (M+7). Kruskal-Wallis analysis. **B**) Percentage of IFNγ⁺ GP-specific CD4⁺ and CD8⁺ T cells measured by ICS at D14 (M+7). Mann-Whitney analyses comparing Senegalese schizont IgG- and schizont IgG+. **C**) Relationship between baseline anti-schizont IgG and percentage of IFNγ⁺ GP-specific CD4⁺ T cells at D14. Volunteer highlighted in red was Kenyan and borderline positive for anti-schizont IgG. No ICS data available for this volunteer. Dotted line indicates the seropositive cut-off values for the Ebola GP ELISA (166 EUs) Dashed line is the ELISpot LLOD (50 SFC/10^6 PBMC). SFC/10^6 PBMC: spot forming cells per million peripheral blood mononucleocytes, * P<0.05, ns: not significant, OD405: optical density at 405nm.

Phenotypes of B cells and circulating T follicular helper cells (cTfh) were compared between the two cohorts and the relationship with malaria exposure and/or reduced vaccine responses was assessed. B cells and cTfh were phenotyped by flow cytometry as described in methods Chapter 2.4.9. There were no significant differences in the frequency of B cells ($CD19^+$) within lymphocytes between the UK and Senegalese cohorts or between Senegalese schizont IgG- and schizont IgG+ groups (Figure 5.13A). The frequencies of different phenotypes within the total B cell population was compared between the UK and Senegalese cohorts (Figure 5.13B). Cells were defined as naïve ($CD21^+CD27^-$), classical memory B cell (cMBC, $CD21^+CD27^+$), atypical MBC ($CD21^-CD27^-$) or activated MBC ($CD21^-CD27^+$). The frequency of atypical MBC was significantly higher in the Senegalese cohort than the UK cohort (P=0.0004, UK median: 3.3% IQR[2.5-4.0], Senegalese: 8.2% [5.4-16.5]). There were no significant differences in the frequencies of any of the other B cell subsets. The frequency of atypical MBCs was significantly higher in both anti-

schizont IgG- and anti-schizont IgG+ Senegalese individuals compared with the UK (Figure 5.13C, P=0.0052 and P=0.0005 respectively). However, there was no significant difference between the schizont IgG- and schizont IgG+ individuals (P>0.99).

The expression of the transcription factor T-bet was examined in each of the B cell subsets within a sample of the UK and Senegalese individuals with sufficient cells remaining for this additional analysis. Frequencies of T-bet expression in each B cell subset were comparable between the UK and Senegal (Figure 5.13D). In both cohorts atypical MBCs contained the highest frequency of T-bet^{+} cells (UK median: 34% IQRs[11-55], Senegalese: 28% [17-43]). A relatively high frequency of activated B cells also expressed T-bet (UK: 12% [6-17], Senegalese: 12% [8-18]). In contrast, the frequency of T-bet expression was low in both classical MBCs (UK: 1% [1-2], Senegalese: 2% [1-7]) and naïve B cells (UK: 1% [1-3], Senegalese: 1% [1-3]).

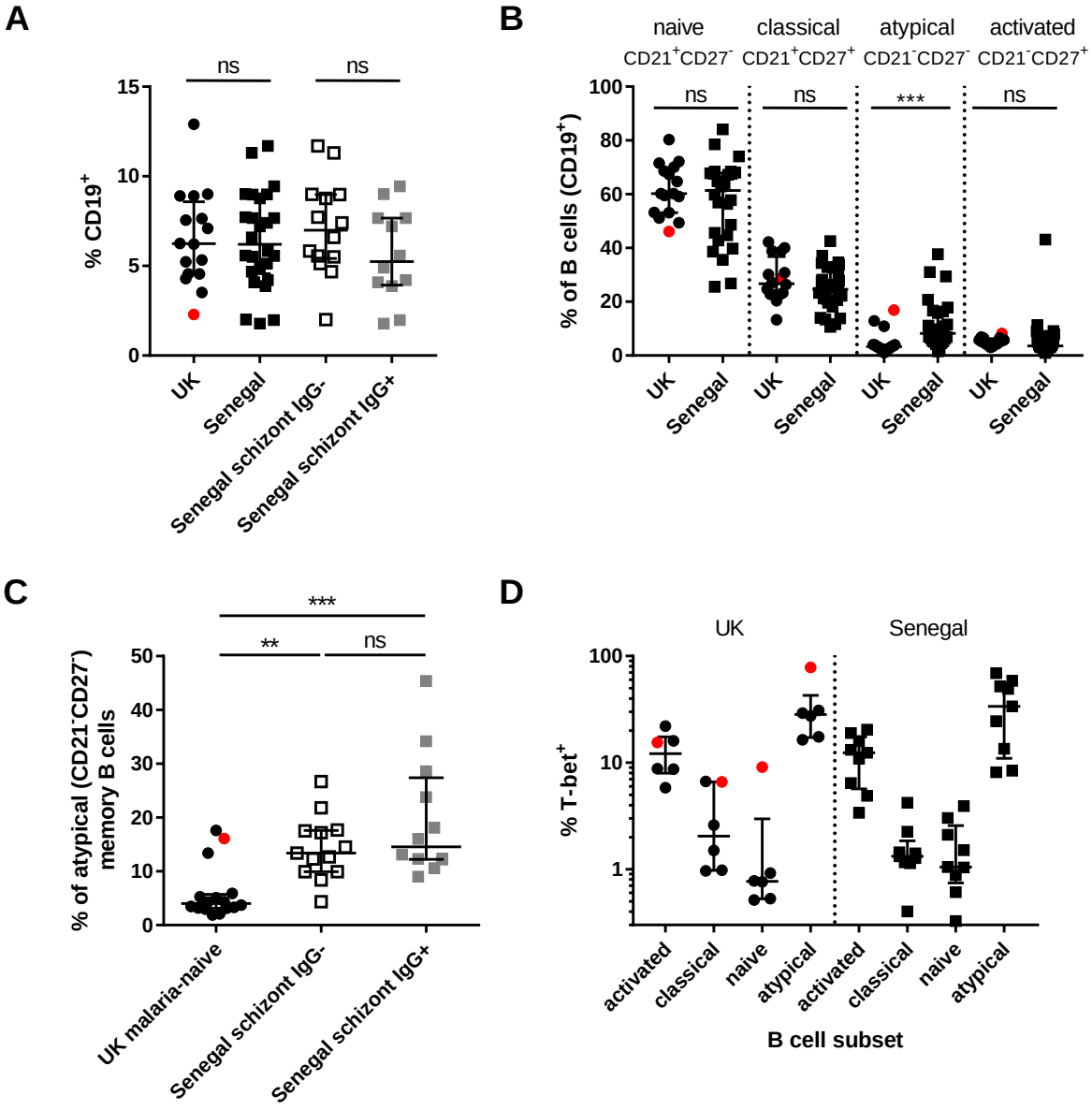

Figure 5.13. Differences in B cell phenotypes in Senegal

A) % of B cells (CD19⁺) within lymphocytes at baseline. Mann-Whitney analyses between Senegal and UK and between schizont IgG- and schizont IgG+. **B**) Phenotypes within B cells at baseline. Mann-Whitney analyses between Senegal and UK. **C**) % of atypical memory B cells in UK, Senegal schizont IgG- and schizont IgG+ groups at baseline. Kruskal-Wallis analysis. **D**) % of each B cell phenotype expressing T-bet in a sample of UK and Senegalese individuals at baseline. Volunteer highlighted in red was Kenyan and borderline positive for anti-schizont IgG.

Similarly, circulating T follicular helper cells (cTfh) phenotypes in the Senegalese and UK cohorts were compared. Circulating Tfh were defined as $PD1^{+}CXCR5^{+}CD45RA^{-}CD4^{+}$ T cells and subsets within cTfh were defined using the chemokine receptors CXCR3 and CCR6: Tfh1 $CXCR3^{+}CCR6^{-}$, Tfh2 $CXCR3^{-}CCR6^{-}$, Tfh17 $CXCR3^{-}CCR6^{+}$, double positive (dp) $CXCR3^{+}CCR6^{+}$. The antibodies and gating strategy used are the same as those used in Chapter 3.3.5 and are described in detail in methods Chapter 2.4.9. There was no significant difference in the frequency of $CD4^{+}$ T cells within lymphocytes between the UK and Senegalese cohorts, or between the schizont IgG- and schizont IgG+ individuals (Figure 5.14A). The frequency of cTfh ($PD1^{+}CXCR5^{+}$) within $CD45RA^{-}$ $CD4^{+}$ T cells was significantly higher in the Senegalese cohort compared with the UK cohort (Figure 5.14B, P=0.036, UK median: 1.1% IQRs[0.2-1.8], Senegalese: 1.6% [0.8-3.6]). However, there was no significant difference between the schizont IgG- and schizont IgG+ groups (P=0.67). Frequencies of subsets within cTfh were comparable between the UK and Senegalese cohorts (Figure 5.14C). There was also no difference in the total frequency of $CXCR3^{+}$ cTfh (Tfh1 + dp) between the UK and Senegalese cohorts (Figure 5.14D, P=0.36). However, schizont IgG+ individuals had significantly higher $CXCR3^{+}$ cTfh frequencies compared with schizont IgG- individuals (P=0.046, schizont IgG- median: 25% IQRs[17-33], schizont IgG+: 33% [27-44]).

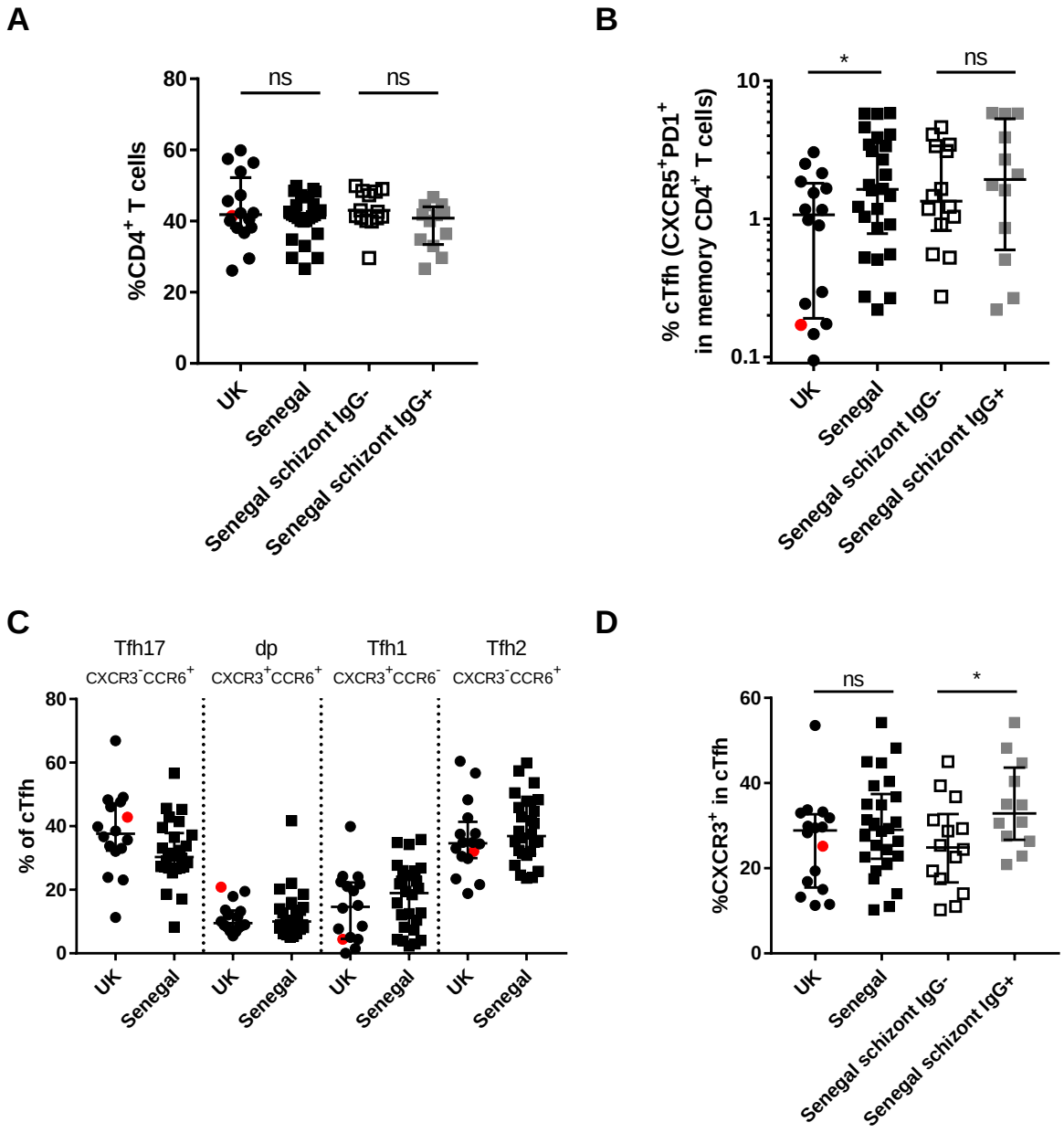

Figure 5.14. Differences in circulating Tfh phenotypes in Senegalese and UK cohorts
A) % of $CD4^+$ T cells within lymphocytes. **B**) % of circulating T follicular helper cells (cTfh, $\%PD1^+CXCR5^+$ in $CD45RA^-CD4^+$ T cells). **C**) Frequencies of phenotypes within cTfh. **D**) Frequency of $CXCR3^+$ (dp + Tfh1) in cTfh. Mann-Whitney analyses between UK and Senegalese cohorts, and schizont IgG+ and schizont IgG- individuals. * $P<0.05$, ns: not significant, dp: double positive. Volunteer highlighted in red was Kenyan and borderline positive for anti-schizont IgG.

For those parameters that differed between the UK and Senegalese cohorts (atypical MBC, total cTfh and CXCR3$^+$ cTfh), the relationship between the frequency of the cell subset and malaria exposure measured by anti-schizont IgG was assessed. There were no significant associations between anti-schizont IgG and the frequency of atypical MBC (Figure 5.15A, r:0.33 P=0.10), cTfh (Figure 5.15B, r:0.17 P=0.40) or CXCR3$^+$ cTfh (Figure 5.15C, r:0.16 P=0.45).

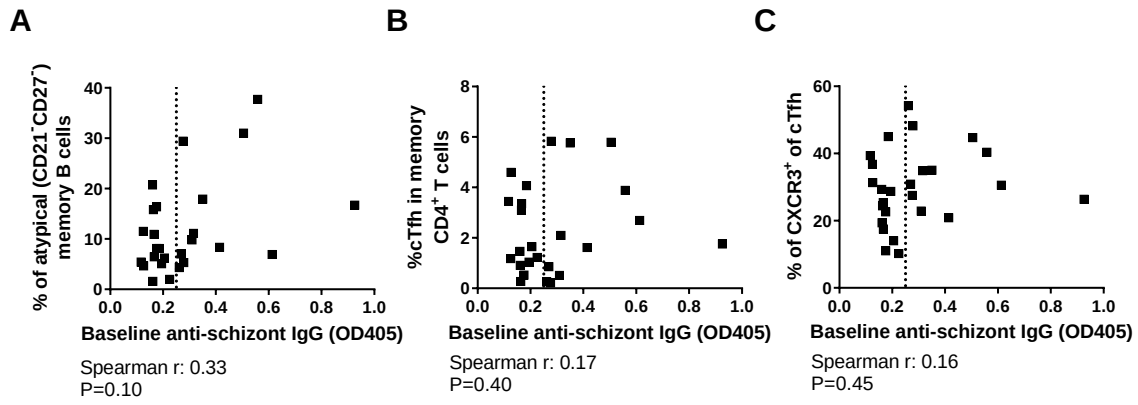

Figure 5.15. Associations between cTfh and B cell phenotypes and malaria
Relationship between baseline anti-schizont IgG in Senegalese cohort and: **A**) % of atypical memory B cells (CD21$^-$CD27$^-$) within B cells, **B**) % of cTfh within memory CD4$^+$ T cells and **C**) % CXCR3$^+$ within cTfh. Spearman's rank analyses. Dotted lines indicate seropositive cut-off for anti-schizont ELISA (OD405=0.250). OD405: optical density at 405nm.

The relationship between these parameters and vaccine responses was also assessed. The frequency of atypical MBCs significantly increased from baseline to M+7 in both cohorts (Figure 5.16A UK: P=0.025, Senegal: P=0.030). At M+7 atypical MBCs were 4% [3-6] of the total B cell population in UK vaccinees and 16% [11-24] in Senegalese participants. Neither the frequency of atypical MBC at baseline (Figure 5.16B) or at M+7 (data not shown) was associated with vaccine responses (D28 Ebola GP IgG, D14 ELISpot response or D14 frequency of GP-specific IFNγ$^+$CD4$^+$ T cells) in the Senegalese cohort. The frequency of cTfh at baseline had a weak positive association with D14 ELISpot responses (Figure 5.16C, r:0.43, P=0.035), but was not associated with Ebola GP IgG or ICS responses. There was no association between the baseline frequency of CXCR3$^+$ cTfh and vaccine responses in the Senegalese cohort (Figure 5.16D).

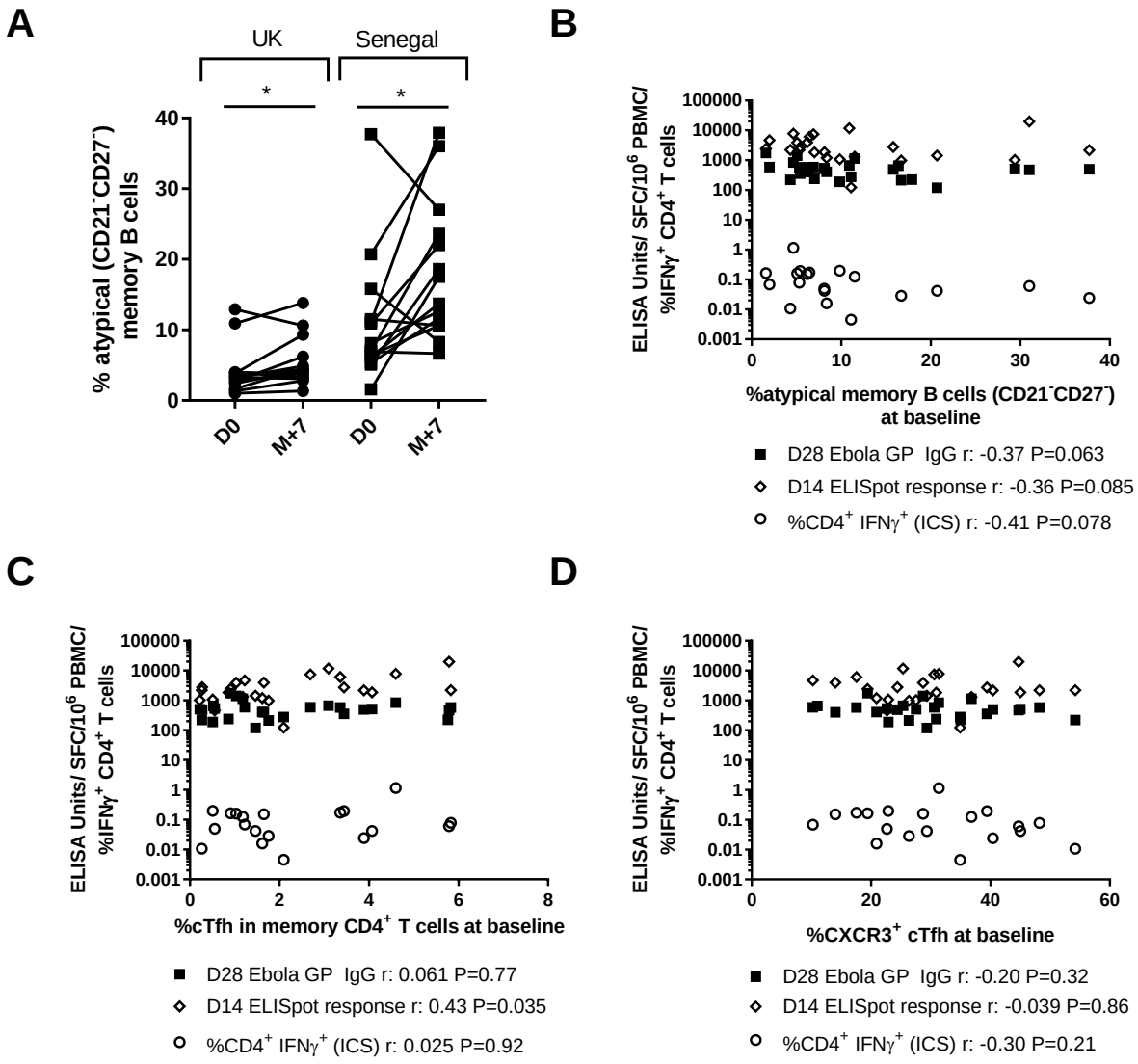

Figure 5.16. Associations between B cell and cTfh phenotypes and reduced vaccine responses

A) % of atypical memory B cells ($CD21^-CD27^-$) within B cells at day 0 (D0) and seven days after MVA-EBO-Z (D14, M+7). Wilcoxon signed rank tests. Relationship between: **B**) frequency of atypical memory B cells at D0, **C**) frequency of cTfh and **D**) frequency of $CXCR3^+$ cTfh and vaccine responses: D28 Ebola GP IgG, D14 ELISpot response and frequency of GP-specific $IFN\gamma^+$ $CD4^+$ T cells at D14 in the Senegalese cohort. Spearman's rank analyses. SFC/10^6 PBMC: spot-forming cells per million peripheral blood mononucelocytes.

An additional immunophenotypic difference between the cohorts detected during the Tfh phenotyping, was a significant expansion of $CD45RA^-$ memory $CD4^+$ T cells in the Senegalese cohort relative to the UK cohort (Figure 5.17A P<0.0001 UK median: 35% [28-46], Senegal: 53% [44-62]). The frequency of $CD45RA^-$ $CD4^+$ T cells was comparable between the schizont IgG- and schizont IgG+ groups (P=0.28). The frequency of $CD45RA^-$ $CD4^+$ T cells was negatively associated with Ebola GP IgG titres six months after MVA-EBO-Z in both the UK (Figure 5.17B, r:-0.57, P=0.024) and Senegalese (r:-0.62, P=0.0008) cohorts. There was no association between the frequency of $CD45RA^-CD4^+$ T cells and Ebola-specific ELISpot responses in the UK (Figure 5.17C, r:-0.13 P=0.63) but there was a negative association in the Senegalese cohort (r:-0.54, P=0.006). In contrast, there was a weakly positive association with $IFN\gamma^+$ GP-specific $CD4^+$ T cells in the UK cohort (Figure 5.17D, r:0.60, P=0.034), but no association in the Senegalese cohort (r:-0.14, P=0.57).

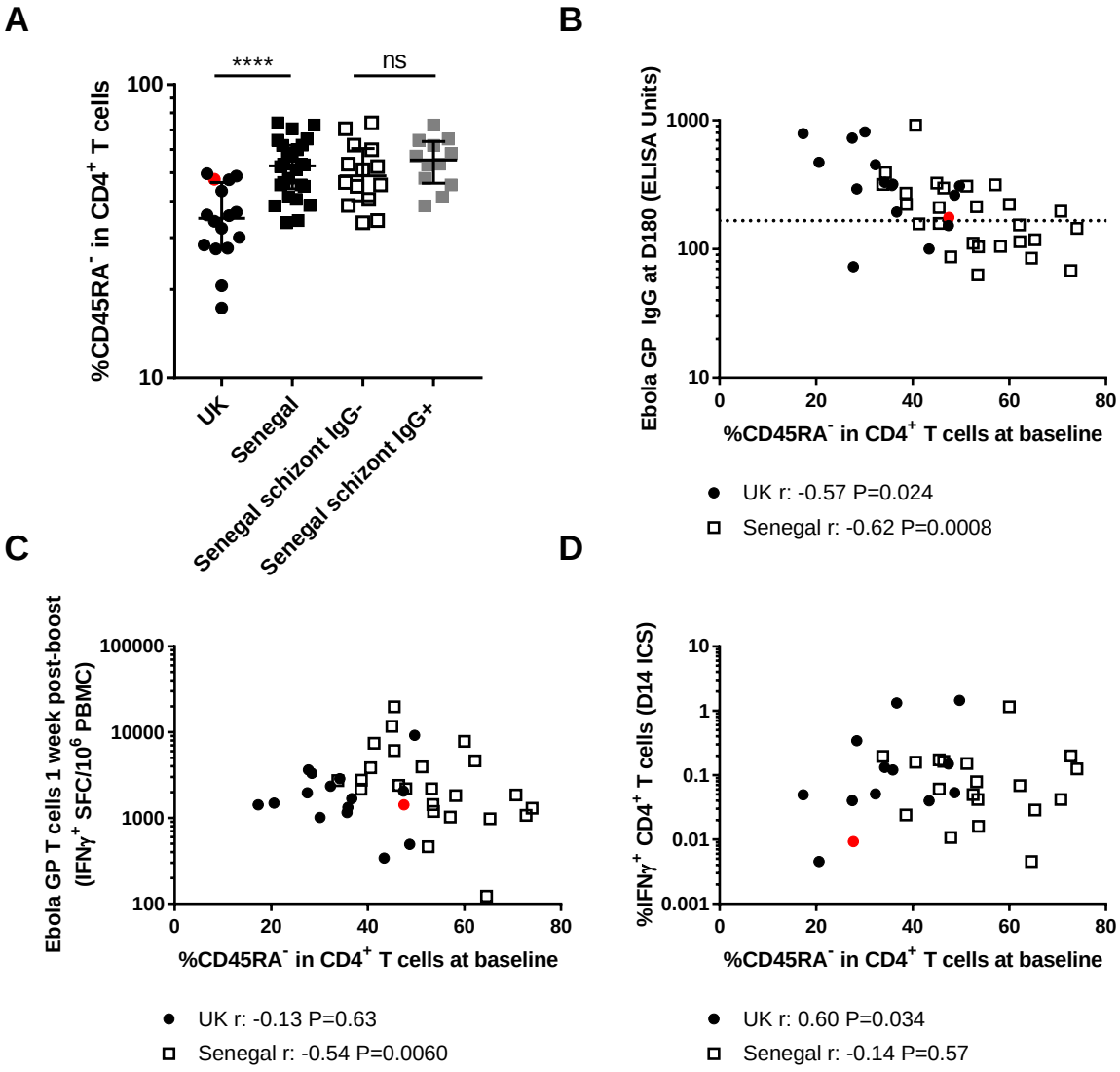

Figure 5.17. Expansion of memory CD4⁺ T cells at baseline in Senegal

A) % CD45RA⁻ cells within CD4⁺ T cells. Mann-Whitney analyses between UK and Senegal and between schizont IgG- and schizont IgG+. Relationship between baseline %CD45RA⁻ in CD4⁺ T cells and: **B**) D28 Ebola GP IgG responses, **C**) Ebola GP-specific T cell responses seven days after boost and **D**) frequency of GP-specific IFNγ⁺ CD4⁺ T cells at D14 in the UK and Senegalese cohorts. Spearman's rank analyses. SFC/10^6 PBMC: spot-forming cells per million peripheral blood mononucleocytes. Volunteer highlighted in red was Kenyan and borderline positive for anti-schizont IgG. Dotted line indicates Ebola GP ELISA seropositive cut-off (166 EUs).

5.4. Discussion

Despite having lifelong malaria exposure, adults in Burkina Faso, Kenya and The Gambia had detectable but low levels of antibody against vaccine candidate antigens CSP and TRAP. TRAP-specific T cell responses, although above the LLOD, were low and were comparable to the baseline responses in the UK. A relatively high level of natural immunity develops against blood-stage antigens such as AMA-1 and MSP-1 and has been associated with protection from clinical disease [496-498]. In contrast, antigens expressed on the sporozoite or infected hepatocytes during the pre-erythrocytic stages are exposed to the immune system for a much shorter period of time and natural immunity against these antigens is much lower [499]. Sporozoites only spend a few hours in the skin and circulation before entry into the liver and once there, continue development within hepatocytes, where they are no longer visible to many aspects of the immune system [103]. Parasite antigens are expressed on the surface of infected hepatocytes but it is estimated that only around one in 100 million hepatocytes is infected [500], therefore even with a high number of circulating antigen-specific T cells, detection of all infected hepatocytes may be unlikely. Additionally the liver-stage of infection only lasts around seven days and therefore there is a limited window of development for liver-stage immunity. For these reasons, it is expected that pre-existing immunity against pre-erythrocytic antigens is low even in populations with lifelong malaria exposure.

However, even this low level of pre-existing immunity may impact the vaccine responses in these populations compared with malaria-naïve populations. One question was whether these responses could be boosted by a single vaccination with ChAd63-ME-TRAP or R21. After a single vaccination, responses were generally comparable to the post-prime responses in malaria-naïve cohorts and there was no significant boosting of the pre-existing liver-stage immunity in malaria-exposed cohorts. Additionally, in several of these cohorts there was a failure to boost after subsequent vaccinations (MVA-ME-TRAP or a 3rd dose of R21) leading to peak responses

significantly lower than those induced in malaria-naïve populations. This may suggest that malaria exposure could suppress responses to malaria vaccines. Vaccine responses are rarely directly compared between malaria-exposed and -naïve populations but where they have been, responses are often lower in the malaria-exposed cohort [257,501,502].

Concurrent or recent malaria exposure at the time of vaccination has been shown in several studies to suppress vaccine responses [158-160]. Recent studies have demonstrated that blood-stage malaria infection may directly suppress the development of immunity to malaria [161-163]. In these studies, the inflammatory environment (particularly IFNγ and TNF) induced during severe malaria infection directly impaired germinal centre responses, disrupted lymph node architecture and inhibited or altered Tfh and MBC development. These changes caused by the inflammatory response to blood-stage infection inhibited the development of both blood- and liver-stage immunity. These studies demonstrate how the inflammatory microenvironment caused by concurrent malaria infections might suppress immune responses not only to malaria but also to heterologous antigens. However, the effect of prior malaria exposure, particularly with lifelong repeated infections and period of asymptomatic parasitaemia is less clear and may be underappreciated [491]. It is possible that repeated exposure to blood-stage malaria over many years may have a more lasting impact on the inflammatory environment and immunophenotypes that could alter immune responses to multiple antigens in malaria-exposed populations.

In our studies, antibody responses to two different pre-erythrocytic malaria antigens (TRAP and CSP) induced by two different vaccine platforms (VLP R21 and viral-vectored vaccines ChAd63- and MVA-ME-TRAP) were reduced in malaria-exposed cohorts (from Burkina Faso, Kenya and The Gambia) compared with malaria-naïve cohorts (UK). There was no association between the level of anti-schizont antibody in the Gambian or Burkinabe cohorts (anti-schizont IgG was not measured in the Kenyan cohorts) and vaccine responses. However, this may be because malaria

exposure was uniformly high and anti-schizont IgG may not be an accurate measure of exposure level in these cohorts. Although the presence of anti-schizont IgG may be a useful binary measure of malaria exposure, the level of anti-schizont antibodies may not necessarily correlate with malaria exposure. A recent study demonstrated that the half-life of antibodies differs for different *P. falciparum* antigens, as does the pattern of acquisition [503]. It was suggested that the use of a single antigen or a combination of antigens may allow better estimation of recent compared with past exposure. The results of this study suggest that AMA-1 may be a good candidate antigen for measuring antibody responses as a proxy for historic malaria exposure as AMA-1-specific antibodies are acquired rapidly and decline slowly. In contrast, pre-erythrocytic antigens such as CSP or TRAP might be give a better indication of more recent malaria exposure as half-lives of these antibodies were observed to be very short, even in adults. Additionally, the schizont lysate used in this assay is derived from a single *P. falciparum* strain (3D7) and therefore differences in titres between different populations may be due to differences in the strains circulating in each region. Multiple other studies have also investigated the use of different *P. falciparum* antigens for determining transmission intensity [504-506] and the antigen or antigens used for measuring malaria exposure is something which we will optimise for future clinical studies.

In a Burkinabe paediatric cohort, antibody responses to ChAd63-MVA-ME-TRAP were significantly higher than African or UK adults. This may be partly due to a higher vaccine dose per kilogram (paediatric cohorts were given the same dose of ChAd63-ME-TRAP, $5x10^{10}$ vp, and a half dose of MVA-ME-TRAP, $1x10^{8}$ pfu). However, there was a significant negative association between vaccine-induced antibody responses and development of anti-schizont antibody, while no association with age was observed. This suggests that increasing malaria exposure may be associated with reduced antibody responses to vaccination.

Maternal antibody may play a role in the vaccine responses observed in the youngest infants (10 week olds, VAC42, The Gambia). Two infants in this group had high baseline levels of anti-schizont IgG which was most likely of maternal origin given their age, the low malaria incidence and the limited time for malaria exposure and development of antibody responses. Several reports have indicated that maternal antibodies may interfere with vaccine responses in infants [507-509]. However, the sample size of infants this age was too small to analyse this effect and both of the infants with baseline anti-schizont IgG had vaccine-specific antibody responses comparable to the rest of the group. It was previously shown that maternal antibodies against malaria have generally waned by around 20 weeks of age [510] and therefore most of the anti-schizont IgG in the infants aged 5-17 months is likely to be non-maternal and therefore indicate the infant's exposure to malaria.

Of note, antibody but not T cell responses were reduced in malaria-exposed cohorts and only antibody responses were negatively associated with anti-schizont IgG levels in the Burkinabe infant cohort. Most licensed vaccines work by inducing protective antibody responses [454]. However, in order to induce protective responses against pre-erythrocytic malaria, it may be necessary to induce T cells targeting infected hepatocytes [444,500]. Viral vectored vaccines ChAd63- and MVA-ME-TRAP are designed to induce $CD8^+$ T cell responses [511]. We have found TRAP-specific $CD8^+$ T cells induced by these vaccines to be associated with protection against liver-stage infection in a human challenge model [252]. However, there is evidence that antibodies could also contribute [260] and the precise mechanism of protection provided by these vaccines is far from clear. In malaria-exposed populations, antibodies against TRAP have been associated with reduced parasitaemia [512], protection from cerebral malaria [513] and protection from infection [514]. For these reasons it was important to assess both the antibody and T cell responses induced by these vaccinations. Additionally, even if antibodies do not play a role in any protective immunity induced by these vaccines in particular, it is an important finding that antibody responses induced by some vaccines may be reduced in malaria-exposed

populations. The fact that CSP antibody responses induced by the VLP vaccine R21 (which is designed to induce antibody responses against CSP, [242]) were also reduced provides further evidence that there may be a more generalised suppression of antibody responses in malaria-exposed populations. This may be particularly important as both viral vectored and VLP-based vaccines have broad potential for use as vaccine platforms against multiple pathogens.

In addition to reduced responses to malaria vaccine candidates in malaria-exposed populations, we also observed reduced antibody responses to heterologous antigens in malaria-exposed populations. The Ebola vaccine cohorts in the UK and Senegal provided a clearer way of assessing the impact of malaria exposure on vaccine responses as individuals were Ebola-naïve and did not have pre-existing antibody or T cell responses against the vaccine antigen, therefore the impact of pre-existing immunity to the vaccine antigen was not a confounding factor. Malaria transmission in Dakar is relatively low [515]. For this reason, it was expected that malaria immunity in this cohort would be low.

Half of the participants in the Senegalese cohort did not have evidence of significant malaria exposure as measured by anti-schizont IgG. However, it was clear that these individuals were not completely naïve and some antibody was detected against single blood-stage antigens, AMA-1 and MSP-1. As malaria exposure was not uniformly high within this cohort, this provided an opportunity to assess the impact of exposure on immune responses to vaccination. As in the previously investigated cohorts, there was a significant reduction in antibody, but not T cell responses in the African cohort compared with the UK. However, Senegalese individuals that were schizont IgG- had responses comparable to the UK, whilst schizont IgG+ Senegalese vaccinees had significantly lower responses, supporting the hypothesis that malaria exposure was associated with the observed reduction in vaccine responses. This was strengthened by the negative association between all measures of malaria exposure/ immunity that were used (anti-

schizont IgG, anti-AMA-1 IgG and anti-MSP IgG) and vaccine-induced antibody responses in this cohort.

In each of the vaccine regimens investigated, there was a reduction in antibody but not T cell (measured by IFNγ ELISpot) responses in malaria-exposed cohort compared with the matched malaria-naïve cohort. In the Ebola vaccine trials in the UK and Senegal, vaccine responses were also measured by ICS. This revealed that there was a significant reduction in the IFNγ responses by $CD4^+$ but not $CD8^+$ T cells in anti-schizont IgG+ individuals. It is not entirely clear why malaria-mediated immune suppression would solely affect the $CD4^+$ T cell and antibody responses and not the $CD8^+$ T cell responses. However, previous studies have shown that malaria infection has an impact on Tfh [197] and MBC phenotypes [83,86] as well as germinal centre architecture [162,163], all of which might impact $CD4^+$ T cell and antibody responses more than $CD8^+$ T cell responses. Additionally there is growing evidence that *P. falciparum* may evade the immune system through dysregulation of B cell responses [516-518]. For this reason, I also examined the baseline B cell and cTfh phenotypes in the UK and Senegal and investigated associations with malaria exposure and vaccine responses.

An expansion of "atypical" memory B cells ($CD21^-CD27^-$) associated with malaria exposure has been suggested to contribute to the slow acquisition of humoral immunity to malaria [83,85,171]. These cells resemble exhausted B cells induced in chronic infections such as HIV and Hepatitis C [81,82] and are largely absent in the blood of healthy individuals. The role of these cells in malaria immunity is unclear as one study demonstrated that VH and VL genes cloned from atypical MBCs from malaria-exposed adults encoded broadly neutralizing antibodies against *P. falciparum* antigens [193]. However, atypical MBCs have also been shown to have markedly reduced signalling through the BCR and a reduced ability to differentiate into ASCs [86]. Additionally, these cells express high levels of the transcription factor T-bet, which was negatively associated with BCR signalling [196].

In the Senegalese cohort there was also an expansion of atypical MBC (13%) compared with individuals from the UK (4%), which is comparable to previous reports (12% in Malian children compared with 2.5% in US adults [196]). However, this expansion was present even in anti-schizont IgG- individuals and was not associated with any measure of malaria exposure (anti-schizont IgG, AMA-1 IgG, MSP-1 IgG) or reduced vaccine responses. Additionally atypical MBC were >10% of the B cell population in two malaria-naïve UK adults and a Kenyan adult was borderline positive for anti-schizont IgG. Interestingly, atypical MBC also increased after vaccination in both cohorts. It has been demonstrated that exposure to malaria-induced Th1 cytokines might drive the expansion of T-bet$^+$ atypical MBC [196]. If this is the case, exposure to other strongly Th1-skewed cytokine responses (including those induced by viral-vectored vaccines [406]) might cause an expansion in this B cell phenotype.

Similarly within cTfh, Th1-like (CXCR3$^+$) cells were preferentially activated during acute malaria episodes in Malian children [197]. This cTfh subset were inferior to CXCR3$^-$ cTfh for providing help to MBC *in vitro* and it was suggested that this Th1-skewed cTfh expansion may also contribute to the slow and inefficient acquisition of humoral immunity to malaria. Similarly, it has been shown in mice that malaria-induced Th1 cytokine responses drives Th1-skewed Tfh expansions with increased expression of CXCR3 and T-bet [162]. These cells were negatively associated with the development of humoral immunity to malaria. However the long-term impact of repeated or chronic infections on cTfh phenotypes in these populations has not been assessed. In the Senegalese cohort I observed an expansion of total cTfh compared with the UK cohort. Within cTfh, the frequency of CXCR3$^+$ cells was significantly increased in anti-schizont IgG+ individuals, suggesting that malaria exposure could also be associated with expansion of Th1-like CXCR3$^+$ cTfh in adults. However, it is unclear if this is a long-term impact of malaria exposure or the result of more recent infection in the schizont IgG+ compared with schizont IgG- individuals. Larger studies are required to answer this question.

There was no association between the frequency of $CXCR3^+$ cTfh and vaccine responses in this cohort. The lack of association here may be to do with the timing of vaccination. $CXCR3^+$ cTfh responses have been both negatively and positively associated with antibody responses to infection or vaccination [65,68,441,446] and associations may be dependent on the context of the immune response. The results in Chapter 3.3.5 demonstrated a negative association between $CXCR3^+$ cTfh and antibody responses to RTS,S in a co-administration vaccine when viral vectored vaccines were given two weeks after RTS,S (Chapter 3.3.5, [406]). However, there was no association between $CXCR3^+$ cTfh and antibody responses in the groups given RTS,S alone. A possible explanation for this association is that MVA-ME-TRAP vaccination given during the ongoing antibody response to the RTS,S vaccination given two weeks earlier caused a Th1-skewed Tfh response and drew these Tfh out of the lymph node, preventing continued B cell help and further expansion of the CSP-specific humoral response. However, in Senegal, the CXCR3-skewed phenotype existed prior to vaccination and were not associated with the observed reduction in antibody responses in this cohort. Tfh responses post-vaccination may not have been phenotypically different in this cohort compared with the UK (this was not assesse) and what occurs in the periphery may also not be representative of the Tfh response in the DLN after vaccination.

Finally, a dramatic expansion of $CD45RA^-$ memory $CD4^+$ T cells was observed in the Senegalese cohort (53% of $CD4^+$ T cells) compared with the UK cohort (35% of $CD4^+$ T cells) at baseline. This expansion was not associated with malaria exposure. Equally, some individuals in the UK cohort also had frequencies of $CD45RA^-$ $CD4^+$ T cells greater than 40% of their $CD4^+$ T cells and these were negatively associated with vaccine responses in both cohorts, particularly with the durability of antibody responses.

5.5. Conclusions

This work clearly demonstrates reduced vaccine responses (and reduced humoral responses in particular) in malaria-exposed cohorts compared with malaria-naïve cohorts. This is the case not just for malaria antigens but also for heterologous antigens and the effect may be particularly clear in cohorts from low transmission areas or cohorts in which people have different levels of exposure. There is a reasonable amount of evidence that vaccination in the context of an inflammatory microenvironment caused by recent or concurrent malaria infections is likely to results in reduced humoral responses. However, repeated exposure over a lifetime may have a lasting impact on immune phenotype and an associated reduction in vaccine responses. Other infections that induce strong Th1 cytokine responses may also have a similar impact. It is clear that the "immune history" of a population targeted for vaccination needs to be taken into consideration during rational design in order to achieve optimal immunogenicity and efficacy.

6

Activation-induced markers (AIM) assay

6.1. Introduction

Almost all currently licensed vaccines mediate protection by inducing antibody responses [519]. Immunogenicity of these vaccines is most often measured by ELISAs that measure total antigen-specific antibody titres or assays that measure antibody function. These well-established vaccination programs often have gold-standard assays with a threshold value known to provide clinical protection [454]. Many vaccines currently being developed target pathogens for which neutralising antibodies are difficult to produce (e.g. HIV) [520,521], that have multiple serotypes (staphylococci and streptococci) [522] or are intracellular (TB, liver-stage malaria) [215,523]. Additionally, many new vaccines are being developed to target non-communicable diseases such as autoimmunity and cancer [524,525]. It may be necessary for vaccines against many of these targets to induce potent T cell responses, instead of, or in addition to humoral responses, in order to elicit protection [511]. This new generation of vaccines requires a set of assays that effectively capture antigen-specific T cell responses.

A number of assays are conventionally used to measure the quantity and quality of antigen-specific T cells in humans [526]. The assays most frequently used for this purpose in clinical vaccine trials are the ELISpot and ICS assays [527-529]. The ELISpot assay involves stimulating PBMC with antigen in 96-well plates with membranes coated in anti-cytokine capture antibody. Cytokine produced by antigen-specific T cells binds the capture antibody and is detected using an enzyme-conjugated secondary antibody and a chromogenic development substrate. This method is highly sensitive (cells producing fewer than 100 cytokine molecules can be detected

[530]) and the LLOD can be under 10 cytokine-producing cells per million [531].ELISpots are currently one of the most frequently used and highly validated assays for detection of antigen-specific T cell responses in clinical trials [531-533]. The major disadvantages of using this assay to investigate vaccine responses are a limit in the number of parameters than can be investigated, lack of phenotypic information and preferential detection of effector cells. This likely results in an underestimation of the total antigen-specific T cell response. An alternative type of assay that is frequently used to provide further information on the quantity and quality of vaccine-induced T cells is ICS. Antigen-stimulated PBMC are stained with fluorescently labelled anti-cytokine antibodies and analysed by flow cytometry. This allows detailed phenotypic and functional analysis of antigen-specific T cell populations.

However, ICS assays are also limited in the number of parameters that can be assessed and these must be pre-determined, therefore these assays can be biased towards detection of a particular type of T cells. Standard panels in clinical trials often use IFNγ, IL-2 and TNFα and therefore detect Th1-biased responses [534-536]. T cell responses to vaccination and infection can be highly heterogeneous and therefore detection based on expression of one or more cytokines may significantly underestimate the frequency of antigen-specific cells [537,538]. Multiple groups have overcome these limitations by developing T cell assays that define antigen-specificity on the basis of upregulation of TCR-stimulated surface markers – termed activation-induced markers (AIM). These include an assay based on detection of OX40 and CD25 co-expression on $CD4^+$ T cells in whole blood [539] or PBMC [403,404], and assays detecting CD40L [442,540], or co-expression of CD40L and CD69 [541]. Similarly, activation-induced markers such as CD107a and CD137 (4-1BB) have been used to identify antigen-specific $CD8^+$ T cells [542,543]. Additional markers of activation such as OX40 and CD25 are expressed on activated $CD8^+$ T cells and could be used in a similar way [544]. The advantages of these assays over conventional methods are that they do not rely on prior knowledge of the epitope or HLA type and they are not limited by pre-determination of the cytokine/s to be analysed.

AIM assays can provide a broader picture of the overall antigen-specific T cell response. Increasing knowledge about the total quantity and quality of these responses could significantly aid clinical development, regulatory approval and licensure applications for vaccine candidates [511]. AIM assays have been used to detect vaccine-specific T cell responses in humans [403,545] and we routinely use CD107a as a marker of antigen-specific degranulation in our clinical trials [248,401,546]. However, AIM assays have not been fully evaluated and compared with cytokine-based methods for their use within the clinical trial setting.

In this study, I investigated the use of AIM assays to detect antigen-specific $CD4^+$ and $CD8^+$ T cell responses to vaccination. I then compared the sensitivity and specificity to assays we currently use to investigate vaccine immunogenicity – an IFNγ ELISpot and ICS assay measuring frequencies of $CD4^+$ and $CD8^+$ T cells producing IFNγ, IL-2, TNFα or expressing CD107a. A detailed method for the AIM assay can be found in Chapter 2.4.10.

6.2. Study-specific methods

6.2.1. Samples and study details

PBMC and plasma from a Phase I clinical trial of Ebola vaccine candidates ChAd3-EBO-Z and MVA-EBO-Z (EBL04) were used in this study. Further details of the trial and ethics statements can be found in Table 2.2 (Chapter 2.2.1) and Table 2.3 (Chapter 2.2.3). Further details of the vaccines used are provided in 2.1.3.5 and 2.1.3.6.

6.3. Results

6.3.1. Detection of vaccine-specific T cells using AIMs

Vaccine-specific T cell responses were measured using AIMs OX40, CD25 and PDL1 in $CD4^+$ T cells and OX40, CD25 and CD107a in $CD8^+$ T cells. PBMC from the peak post-boost time point (one week after MVA-EBO-Z, M+7) were stimulated overnight (20h) with a pool of overlapping peptides spanning the length of Ebola Glycoprotein (GP). The expression of combinations of

activation-induced markers on $CD4^+$ and $CD8^+$ T cells was assessed by flow cytometry using the gating strategy defined in Figure A7. Very little CD107a expression was detected in $CD4^+$ T cells and PDL1 expression on $CD8^+$ T cells was also low, therefore these markers were not included in the analysis of antigen-specific $CD4^+$ and $CD8^+$ T cell responses, respectively. Vaccine-specific T cell responses could clearly be detected in the $CD4^+$ T cell subset as $OX40^+CD25^+$ or $OX40^+PDL1^+$ and in the $CD8^+$ T cell subset as $OX40^+CD25^+$ or $CD25^+CD107a^+$. For each sample, an unstimulated control was run to determine background AIM expression and an SEB-stimulated positive control was included. Representative FACS plots of AIM^+ populations in each condition are shown in Figure 6.1A. Frequencies of AIM expression in GP-stimulated PBMC were significantly higher than the corresponding background for all four of the AIM populations measured (Figure 6.1B, 6.1C, $P<0.0001$ for all populations).

Within the $CD4^+$ T cell subset, background levels of AIM expression in unstimulated cells were generally low and were comparable between the $OX40^+CD25^+$ and $OX40^+PDL1^+$ populations (Figure 6.1B, median $OX40^+CD25^+$: 0.110% IQR[0.069 – 0.172] and $OX40^+PDL1^+$: 0.102% [0.044 – 0.131], P=0.47). The background was also low in the $CD8^+$ subset and comparable between the two AIM populations (Figure 6.1C, $OX40^+CD25^+$: 0.021% [0.010 – 0.033] and $CD25^+CD107a^+$: 0.020% [0.012 – 0.036], P=0.93). Frequencies of GP-specific $CD4^+$ T cells measured using $OX40^+CD25^+$ or $OX40^+PDL1^+$ were comparable (Figure 6.1B, $OX40^+CD25^+$: 0.870% [0.493 – 1.088] and $OX40^+PDL1^+$: 0.736% [0.389 – 1.088], P=0.77). Similar frequencies of GP-specific $CD8^+$ T cells were detected and were also comparable for the two different AIM populations in this subset (Figure 6.1C, $OX40^+CD25^+$: 0.633% [0.319 – 0.837] and $CD25^+CD107a^+$: 0.882% [0.406 – 1.258], P=0.22). Due to the lower background in the $CD8^+$ subset, the fold-change in the frequency of AIM^+ cells (GP-stimulated / unstimulated) was higher for the $CD8^+$ subset than the $CD4^+$ subset (Figure 6.1D, $OX40^+CD25^+$ $CD4^+$: 9 [4 – 14], $OX40^+PDL1^+$ $CD4^+$: 9 [4 – 26], $OX40^+CD25^+$ $CD8^+$: 31 [12 – 73], $CD25^+CD107a^+$ $CD8^+$: 47 [17 – 68]). However, there was no difference between the marker combinations in either of the subsets ($CD4^+$: P=0.66, $CD8^+$ P=0.62).

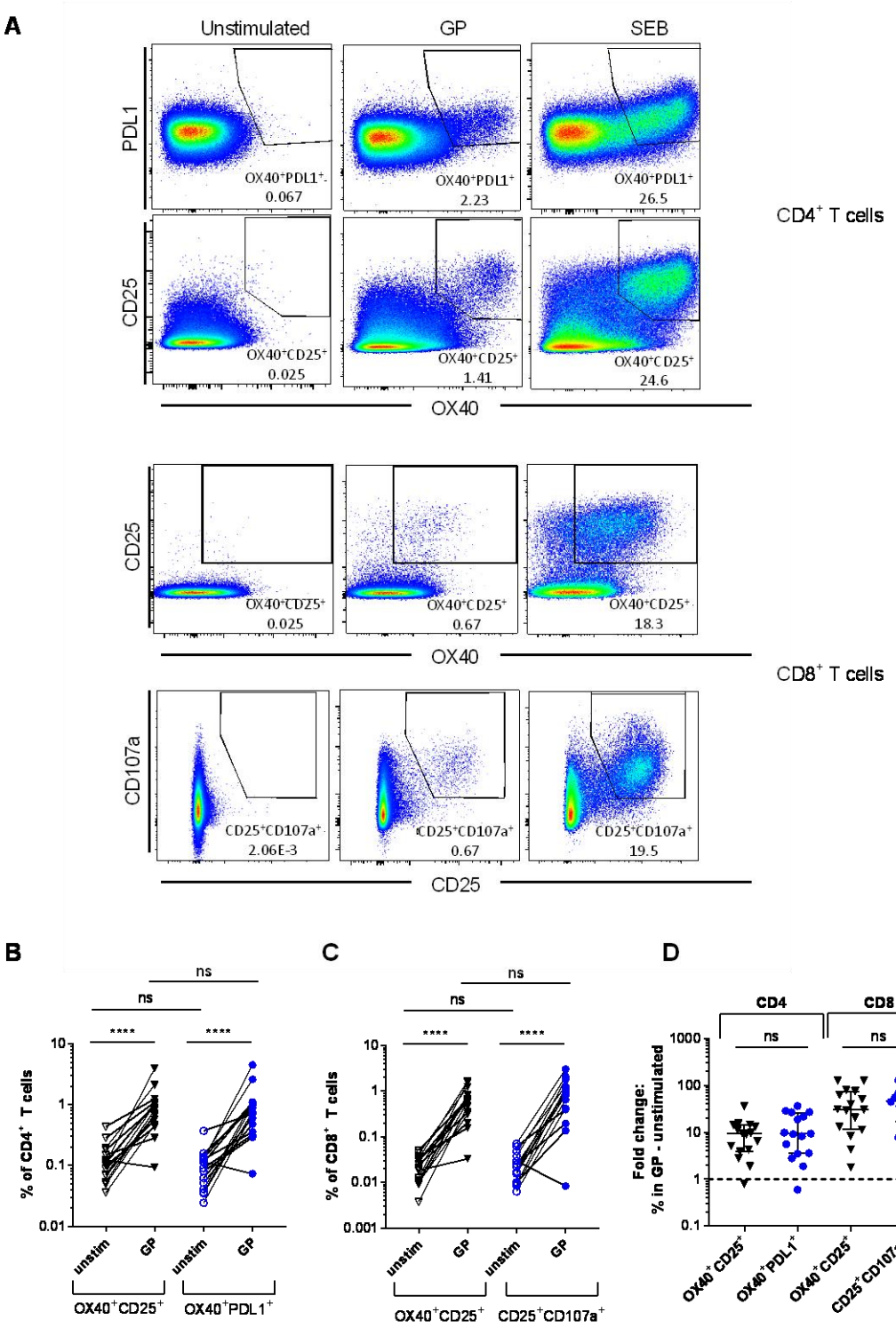

Figure 6.1. Detection of vaccine-specific T cells using an AIM assay

A) Representative flow cytometry plots detailing AIM$^+$ populations in unstimulated, GP-stimulated and SEB-stimulated CD4$^+$ and CD8$^+$ T cells. **B**) AIM$^+$ responses in CD4$^+$ T cells. **C**) AIM$^+$ responses in CD8$^+$ T cells. Mann-Whitney analyses between stimulation conditions within each population and between the same stimulation conditions in different populations. Medians and IQR shown. **D**) Fold change in frequency of AIM$^+$ cells (GP-stimulated/ unstimulated conditions). Individuals below the dashed line did not have responses greater than the background. **** P<0.0001, ns: not significant (P>0.05).

6.3.2. Comparison of different activation-induced markers

The frequency of GP-specific T cell responses was compared between the different AIM^+ subsets after subtracting the corresponding background for each sample (AIM^+ frequency in the unstimulated condition, Figure 6.2). Frequencies of $OX40^+CD25^+$ and $OX40^+PDL1^+$ in $CD4^+$ T cells were comparable (Figure 6.2A, 0.753% [0.445 – 0.924] and 0.700% [0.259 – 0.961], respectively, P=0.88). All but one individual (15/16) had responses above the LLOD (0.003%) in both AIM populations. The frequencies of AIM^+ cells detected by either of the marker combinations in the $CD8^+$ subset were also comparable (Figure 6.2B, $OX40^+CD25^+$: 0.601% [0.304 – 0.826] and $CD25^+CD107a^+$: 0.861% [0.359 – 1.219], P=0.20). Almost all vaccinees had detectable levels of AIM^+ $CD8^+$ T cells measured by both marker combinations. One individual did not have a $CD25^+CD107a^+$ response above the LLOD (0.005%), although they did have a detectable $OX40^+CD25^+CD8^+$ population. Frequencies of GP-specific T cells measured by each of the combinations of AIM markers was highly correlated in both $CD4^+$ (Figure 6.2C, Spearman r:0.83, P=0.0001) and $CD8^+$ T cells (Figure 6.2D, Spearman r:0.91, P<0.0001).

Boolean gates were used to determine the frequency of $CD4^+$ and $CD8^+$ T cells expressing each combination of the three activation-induced markers used in each T cell subset (Figure 6.3). In $CD4^+$ T cells, 38.8% of the AIM^+ (expressing two or more activation-induced markers) cells were triple positive, indicating an overlap between the $OX40^+CD25^+$ and $OX40^+PDL1^+$ populations. However, distinct populations of $CD25^+OX40^+PDL1^-$, $CD25^+OX40^-PDL1^+$ and $CD25^-OX40^+PDL1^+$ were observed. In $CD8^+$ T cells, there was less of an overlap between the AIM populations analysed ($OX40^+CD25^+$ and $OX40^+CD107a^+$), with only 17% of the AIM^+ cells expressing all three markers. Distinct populations of $CD25^+CD107a^+OX40^-$, $CD25^+CD107a^-OX40^+$ and $CD25^-CD107a^+OX40^+$ were observed. It should be noted that this analysis was conducted for GP-stimulated cells without background subtraction. Background levels of CD107a expression were

relatively high (4.1%) compared with other markers (CD25: 0.27%, OX40: 0.20% of $CD8^+$ T cells) and therefore background subtraction is likely to effect different results for subsets differently.

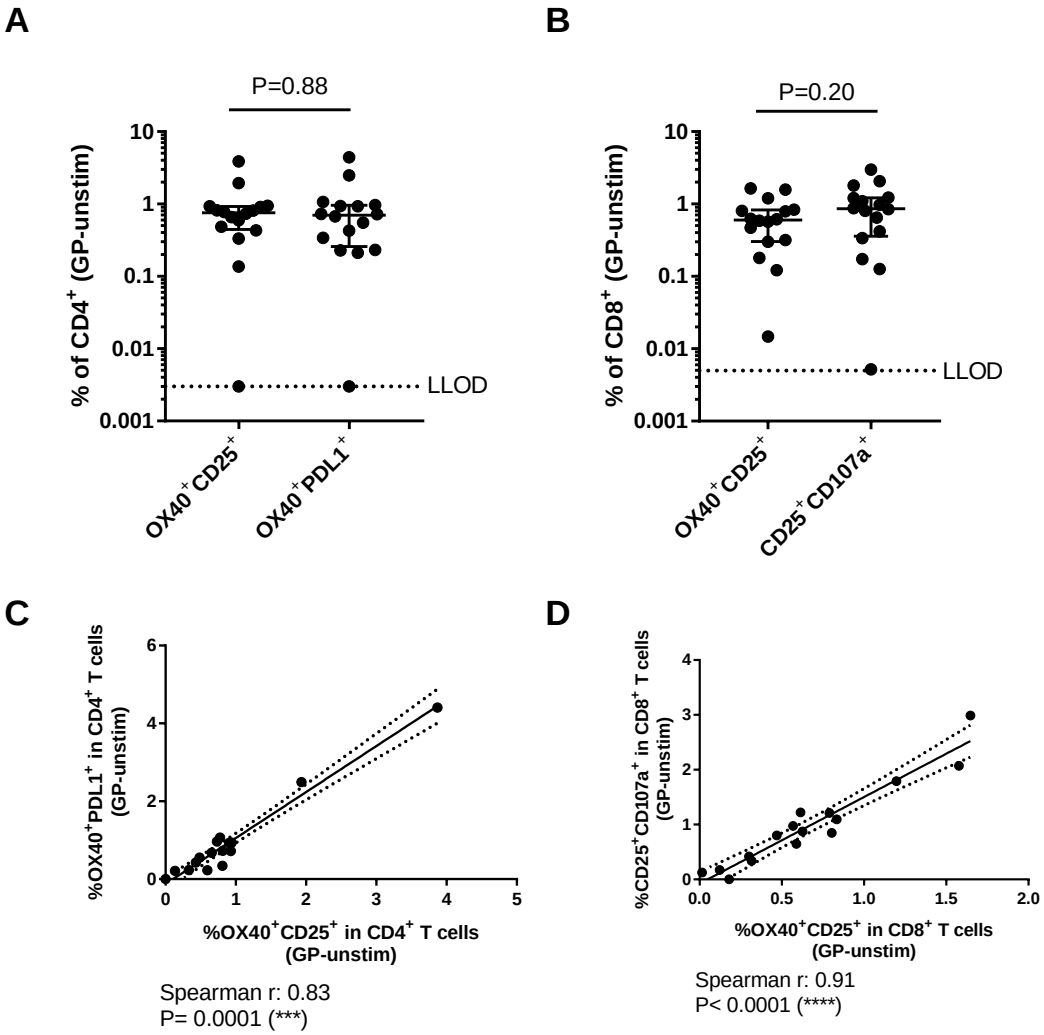

Figure 6.2. Comparison of activation-induced markers for detection of Ebola GP-specific T cells

Proportion of AIM^+ cells in GP-stimulated: **A**) $CD4^+$ T cells and **B**) $CD8^+$ T cells subsets after removal of background (frequency in unstimulated condition). Dotted lines indicate AIM assay lower limit of detection (LLOD). Mann-Whitney analyses used for comparisons between markers. **C**) Relationship between the frequency of GP-specific $CD4^+$ T cells measured by $OX40^+CD25^+$ and $OX40^+PDL1^+$. **D**) Relationship between the frequency of GP-specific $CD8^+$ T cells measured by $OX40^+CD25^+$ and $CD25^+CD107a^+$.

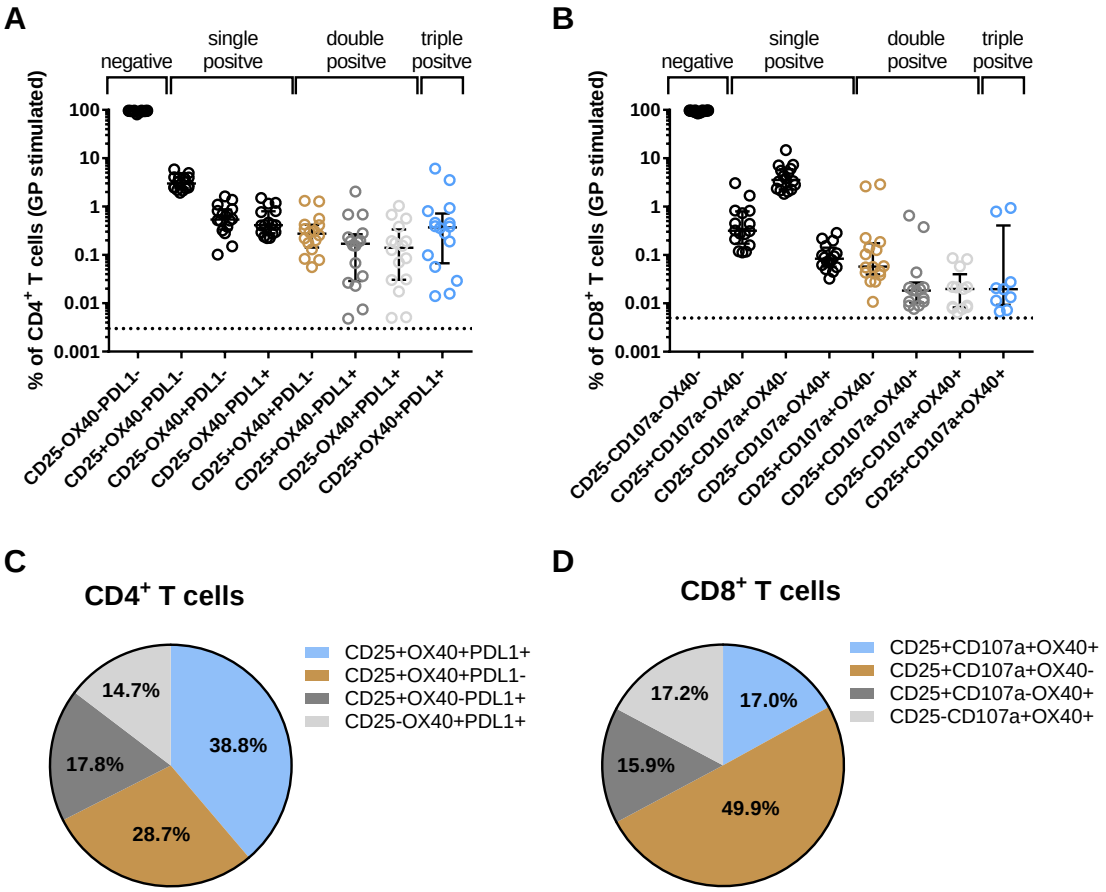

Figure 6.3. Overlap in expression of activation-induced markers

A) Frequency of GP-stimulated CD4$^+$ T cells expressing combinations of CD25, OX40 and PDL1. **B**) Frequency of GP-stimulated CD8$^+$ T cells expressing combinations of CD25, OX40 and CD107a. Dotted lines indicate AIM assay lower limit of detection (LLOD). Samples below the LLOD were removed for this analysis. **C**) Proportions of subsets within AIM$^+$ CD4$^+$ T cells (expressing at least two AIM markers). **D**) Proportions of subsets within AIM$^+$ CD8$^+$ T cells (expressing at least two AIM markers).

6.3.3. Relationship between AIM and other measures of antigen-specific T cells

The relationships between the frequency of GP-specific T cells detected by the AIM assay and other methods used in the clinical vaccine trial were then assessed. At the peak time point (seven days after MVA boost, M+7) GP-specific T cell responses were measured using IFNγ ELISpot. Responses were further dissected using ICS to analyse the frequency of $CD4^+$ and $CD8^+$ T cells producing IFNγ, IL-2, TNFα, or expressing CD107a. Frequencies of AIM^+ $CD8^+$ T cells measured using either combination of markers were correlated with all other methods used to detect GP-specific $CD8^+$ T cell responses at this time point (Figure 6.4). In contrast, the frequency of GP-specific $OX40^+CD25^+$ $CD4^+$ T cells did not correlate with any of the other measures of GP-specific $CD4^+$ responses and there were only weak associations between GP-specific $OX40^+PDL1^+$ and $IFNγ^+$ (Spearman r:0.57, P=0.047) or $TNFα^+$ (Spearman r:0.59, P=0.039) $CD4^+$ T cells measured by ICS (Figure 6.5).

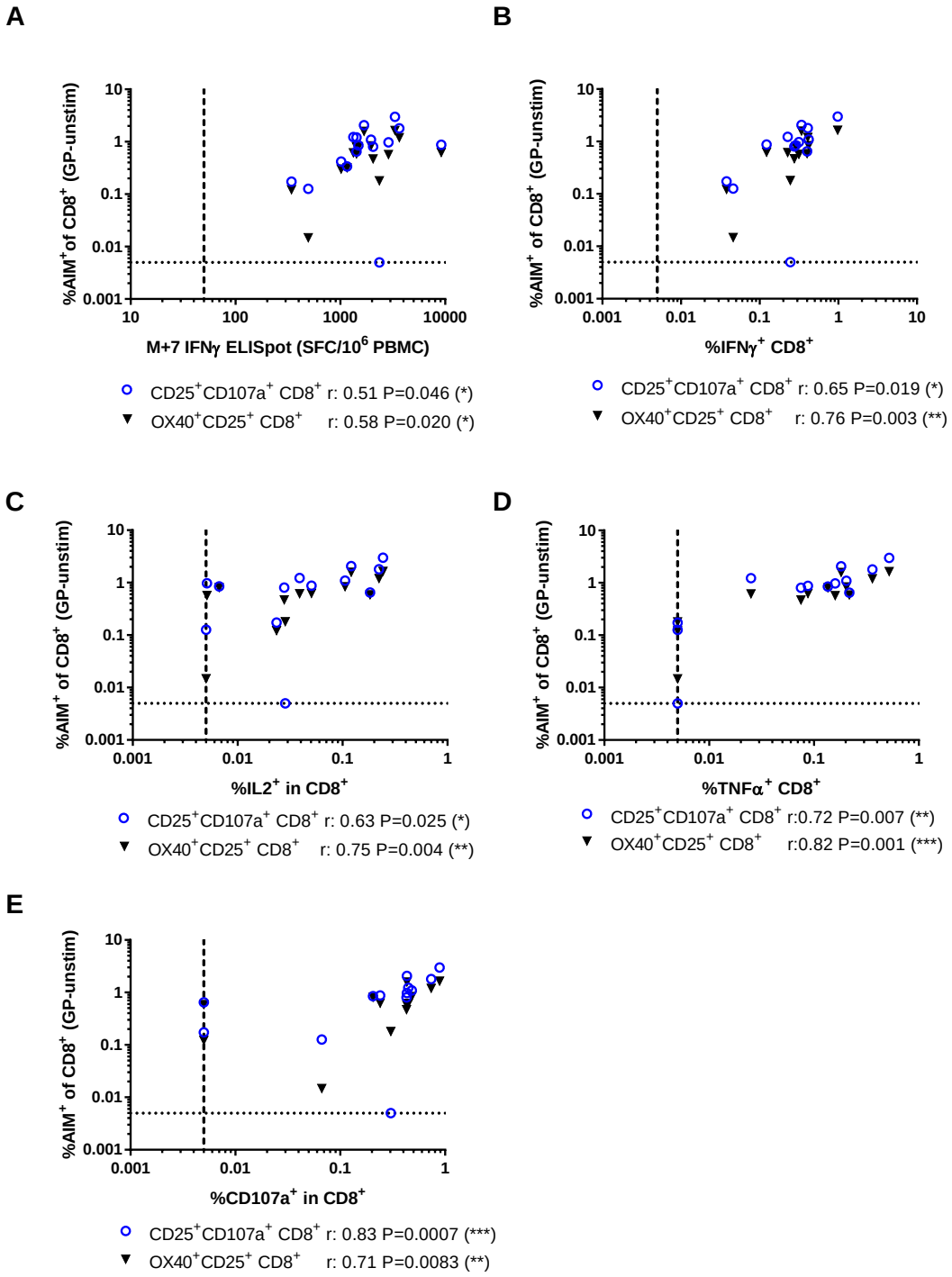

Figure 6.4. Relationships between activation-induced markers on CD8⁺ T cells and other measures of vaccine-specific CD8⁺ T cells

Relationship between AIM on CD8⁺ T cells and: **A**) IFNγ ELISpot, **B**) frequency of IFNγ⁺ CD8⁺ T cells measured by ICS, **C**) frequency of IL-2⁺ CD8⁺ T cells measured by ICS, **D**) frequency of TNFα⁺ CD8⁺ T cells measured by ICS, **E**) frequency of CD107a⁺ CD8⁺ T cells measured by ICS. SFC/10^6 PBMC: spot-forming cells per million peripheral blood mononucleocytes. Spearman's rank analyses. Dashed lines indicate ELISpot and ICS lower limit of detection (LLOD). Dotted lines indicate AIM assay LLOD.

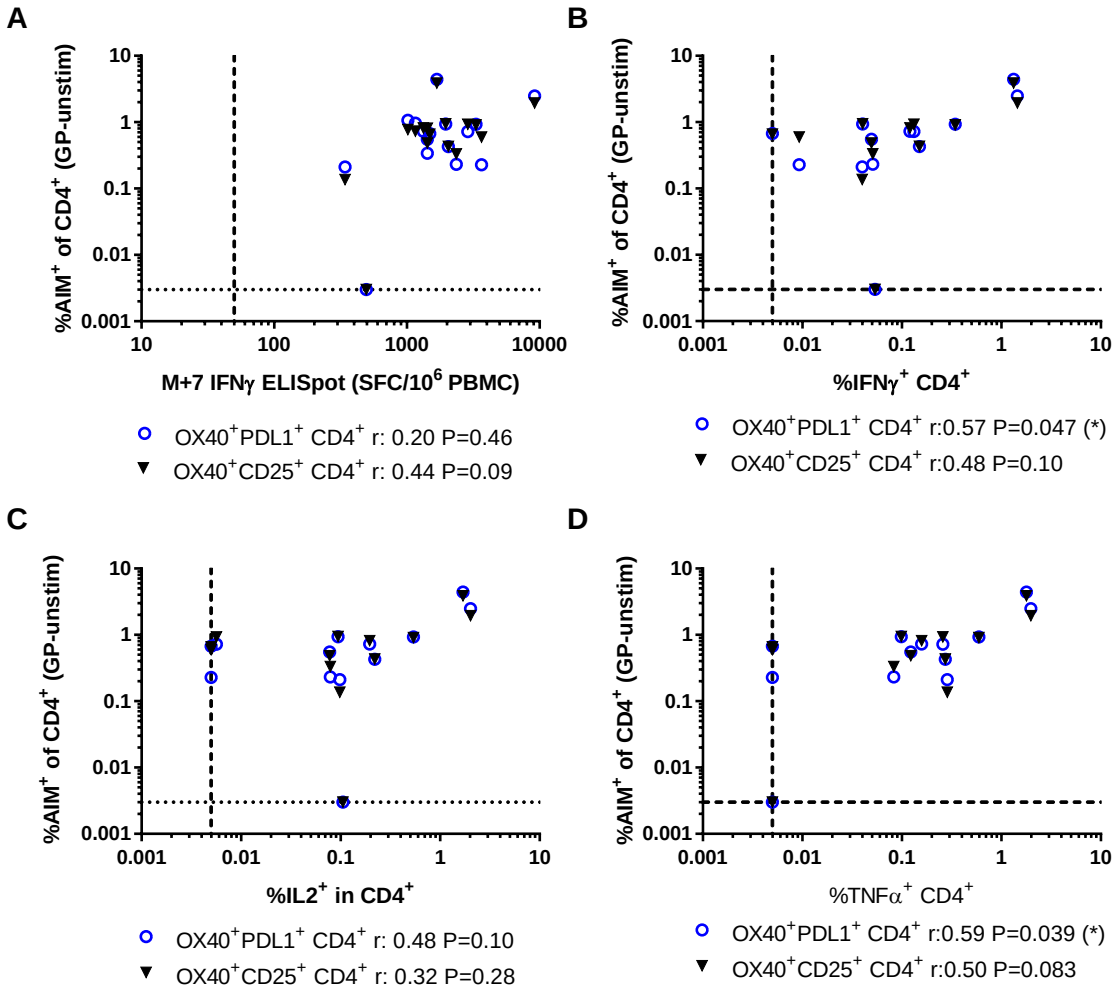

Figure 6.5. Relationships between activation-induced markers on CD4⁺ T cells and other measures of vaccine-specific CD4⁺ T cells

Relationship between AIM on CD4⁺ T cells and: **A**) IFNγ ELISpot, **B**) frequency of IFNγ⁺ CD4⁺ T cells measured by ICS, **C**) frequency of IL-2⁺ CD4⁺ T cells measured by ICS, **D**) frequency of TNFα⁺ CD4⁺ T cells measured by ICS. SFC/10^6 PBMC: spot-forming cells per million peripheral blood mononucleocytes. Spearman's rank analyses. Dashed lines indicate ELISpot and ICS lower limit of detection values (LLOD). Dotted lines indicate AIM assay LLOD.

The specificity of the AIM assay for detecting GP-specific T cells was compared with the ICS assay (Figure 6.6A, 6.5B). The frequency of AIM expression in unstimulated $CD4^+$ T cells was not significantly different to the frequency of cytokine production by unstimulated cells in the ICS assay (Figure 6.6A, $OX40^+CD25^+$: 0.110 [0.069 – 0.172], $OX40^+PDL1^+$: 0.102 [0.044 – 0.131], ICS "any of three": 0.064 [0.045 – 0.096], Kruskal-Wallis P=0.092). The frequency of AIM expression in unstimulated $CD8^+$ T cells was lower than the frequency of cytokine production in unstimulated $CD8^+$ T cells in the ICS assay (Figure 6.6B, $OX40^+CD25^+$: 0.021 [0.010 – 0.033], $CD25^+CD107a^+$: 0.020 [0.012 – 0.036], ICS "any of three": 0.033 [0.020 – 0.048], ICS "any of four": 0.067 [0.053 – 0.15], Kruskal-Wallis P=0.0001).

The sensitivity of the AIM assay for detecting GP-specific T cells was compared with the ICS assay (Figure 6.6C, 6.6D). Within $CD4^+$ T cells, this was defined as the frequency producing any of the three cytokines tested: IFNγ, IL-2 or TNFα, "any of three". Within $CD8^+$ T cells, this was defined as either "any of three" or as the frequency producing any of the three cytokines or expressing CD107a, "any of four". For each of these assays GP-specific T cell frequency was calculated by subtracting the frequency in the unstimulated condition from that in the GP-stimulated condition. Within the $CD4^+$ subset, the LLOD for the AIM assay was lower (0.003%) than for the ICS assay (0.005%) and the frequency of GP-specific $CD4^+$ T cells detected was higher ($OX40^+CD25^+$: 0.753% [0.445 – 0.924], $OX40^+PDL1^+$: 0.700% [0.259 – 0.961]) than detected by ICS "any of three" (0.265% [0.069 – 0.527]). There were three individuals whose responses were below the LLOD in the ICS assay, whilst there was only one individual whose response was below the LLOD in the AIM assay. In the $CD8^+$ subset, the LLOD was the same for both assays (0.005%). Again, the frequency of GP-specific T cells detected by the AIM assay was higher than by the ICS assay ($OX40^+CD25^+$: 0.601% [0.304 – 0.826], $CD25^+CD107a^+$: 0.861% [0.359 – 1.219], ICS "any of three": 0.298% [0.210 – 0.456], ICS "any of four": 0.492% [0.341 – 0.676]). The AIM assay using CD25 and CD107a markers detected a significantly higher

frequency of GP-specific $CD8^+$ T cells than the ICS "any of three", but there were no other significant differences across the four measures (Kruskal-Wallis P=0.027).

AIM^+ populations within $CD4^+$ and $CD8^+$ T cells were combined (frequency AIM^+CD4^+ + AIM^+ $CD8^+$ in $CD3^+$) to compare the specificity and sensitivity of AIM and ELISpot assays for detecting the frequency of antigen-specific total T cells (Figure 6.7). The frequency of AIM^+CD3^+ cells was calculated using each of the combinations of CD4 and CD8 AIM markers and an average taken across the combinations of markers. The frequency of AIM^+CD3^+ within PBMC was also calculated for a more direct comparison with the ELISpot assay, for which the input is PBMC and therefore the result is the frequency of $IFN\gamma^+$ PBMC. The LLOD for AIM^+ cells within total T cells was 0.001%. There were no significant differences in the level of background AIM^+ T cells between the different marker combinations (Figure 6.7A, $OX40^+CD25^+CD4^+$ and $OX40^+CD25^+CD8^+$: 0.073 [0.047–0.116], $OX40^+CD25^+CD4^+$ and $CD25^+CD107a^+CD8^+$: 0.072 [0.046–0.122], $OX40^+PDL1^+CD4^+$ and $OX40^+CD25^+CD8^+$: 0.061 [0.030–0.091], $OX40^+PDL1^+CD4^+$ and $CD25^+CD107a^+CD8^+$: 0.063 [0.034–0.095], Kruskal-Wallis P=0.68). The average AIM^+ frequency from these populations was compared with the background in the ELISpot (Figure 6.7B). The ELISpot results were converted from SFC/10^6 PBMC to percentages for these analyses. The background level of AIM^+ T cells was significantly higher than the background in the ELISpot assay, in which no individuals had responses above the LLOD of 50 SFC/10^6 PBMC or 0.005% (%AIM^+ in T cells: 0.067 [0.040-0.104], %AIM^+ T cells in PBMC: 0.026 [0.016-0.039], ELISpot: 0.005, Kruskal-Wallis P<0.0001). The frequency of antigen-specific total T cells (frequency in GP-stimulated after background subtraction) was compared for each of these marker combinations and there were no significant differences (Figure 6.7C $OX40^+CD25^+CD4^+$ and $OX40^+CD25^+CD8^+$: 0.593 [0.399–0.804], $OX40^+CD25^+CD4^+$ and $CD25^+CD107a^+CD8^+$: 0.641 [0.477–0.866], $OX40^+PDL1^+CD4^+$ and $OX40^+CD25^+CD8^+$: 0.590 [0.343–0.803], $OX40^+PDL1^+CD4^+$ and $CD25^+CD107a^+CD8^+$: 0.661 [0.434– 0.850], Kruskal-Wallis P=0.90). The frequency of antigen-specific cells within total T cells detected by the AIM assay was significantly greater than the

antigen-specific response detected by the ELISpot. However, the frequency of antigen-specific PBMC detected by each assay was not significantly different (Figure 6.7D, %AIM$^+$ in T cells: 0.633 [0.443-0.820], %AIM$^+$ T cells in PBMC: 0.227 [0.111-0.364], %IFNγ$^+$ PBMC measured by ELISpot: 0.159 [0.120-0.275], P=0.0009). Comparisons of the AIM and cytokine-based assays are summarised in Table 6.3.

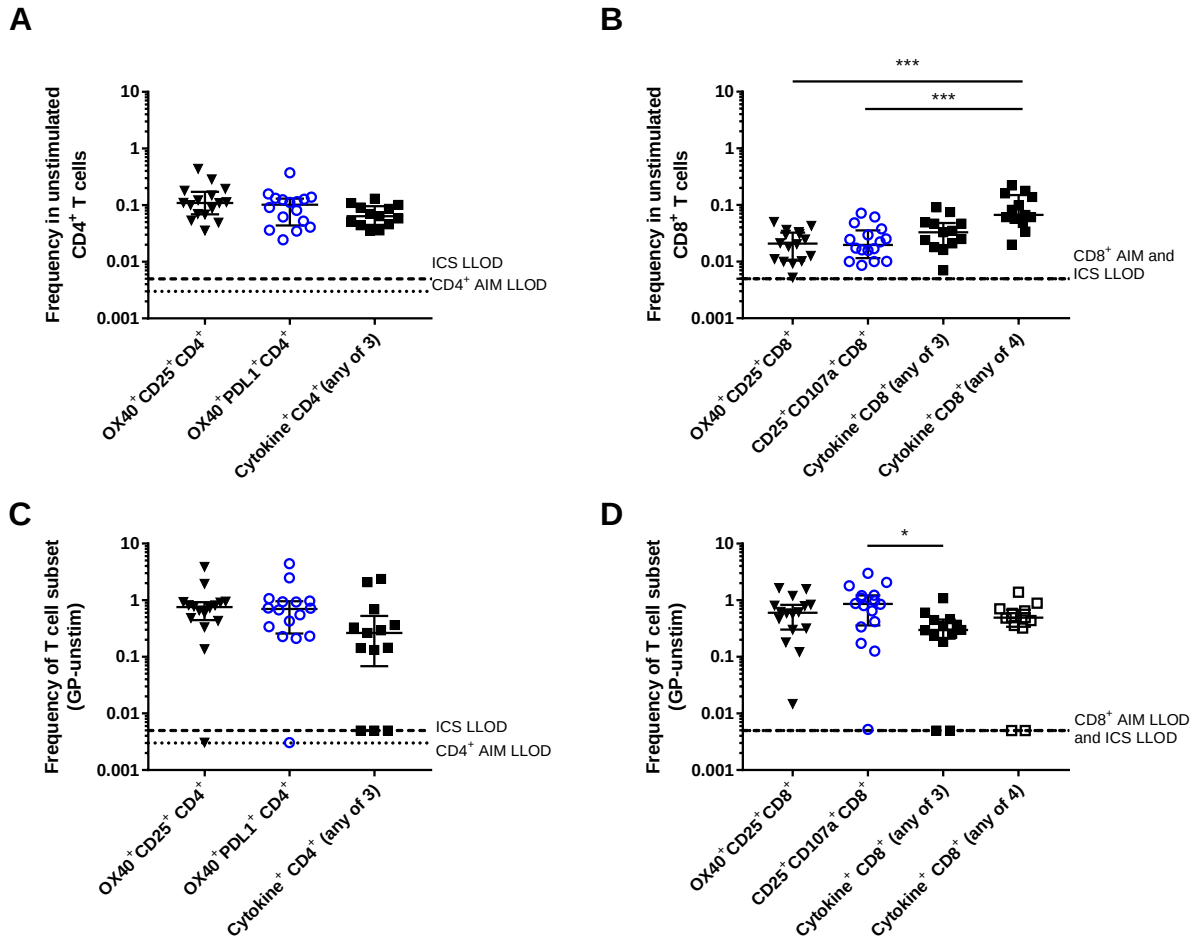

Figure 6.6. Specificity and sensitivity of AIM assay compared with trials ICS protocol
A) Frequency of AIM$^+$ cells or cells producing at least one of the three cytokines measured (IL-2, TNFα or IFNγ) by ICS in unstimulated CD4$^+$ T cells. Kruskal-Wallis P=0.092. **B**) Frequency of AIM$^+$ cells, cells producing at least one of the three cytokines measured (IL-2, TNFα or IFNγ), or producing/expressing any of four (IL-2, TNFα, IFNγ or CD107a) in unstimulated CD8$^+$ T cells. Kruskal-Wallis P=0.0001. **C**) Frequency of GP-specific AIM$^+$ cells in the CD4$^+$ T cell subset or producing at least one of the three cytokines measured (IL-2, TNFα or IFNγ). Kruskal-Wallis P=0.058. **D**) Frequency of AIM$^+$ cells in the CD8$^+$ T cell subset, producing at least one of the three cytokines measured (IL-2, TNFα or IFNγ), or producing/expressing any of four (IL-2, TNFα, IFNγ or CD107a). Kruskal-Wallis P=0.027. Dotted lines show LLOD for CD4 AIM assay Dashed lines show LLOD for ICS assays (0.005 for both CD4$^+$ and CD8$^+$ T cells), * P<0.05, *** P<0.001. Dotted lines show LLOD for CD4 or CD8 AIM assay as labelled.

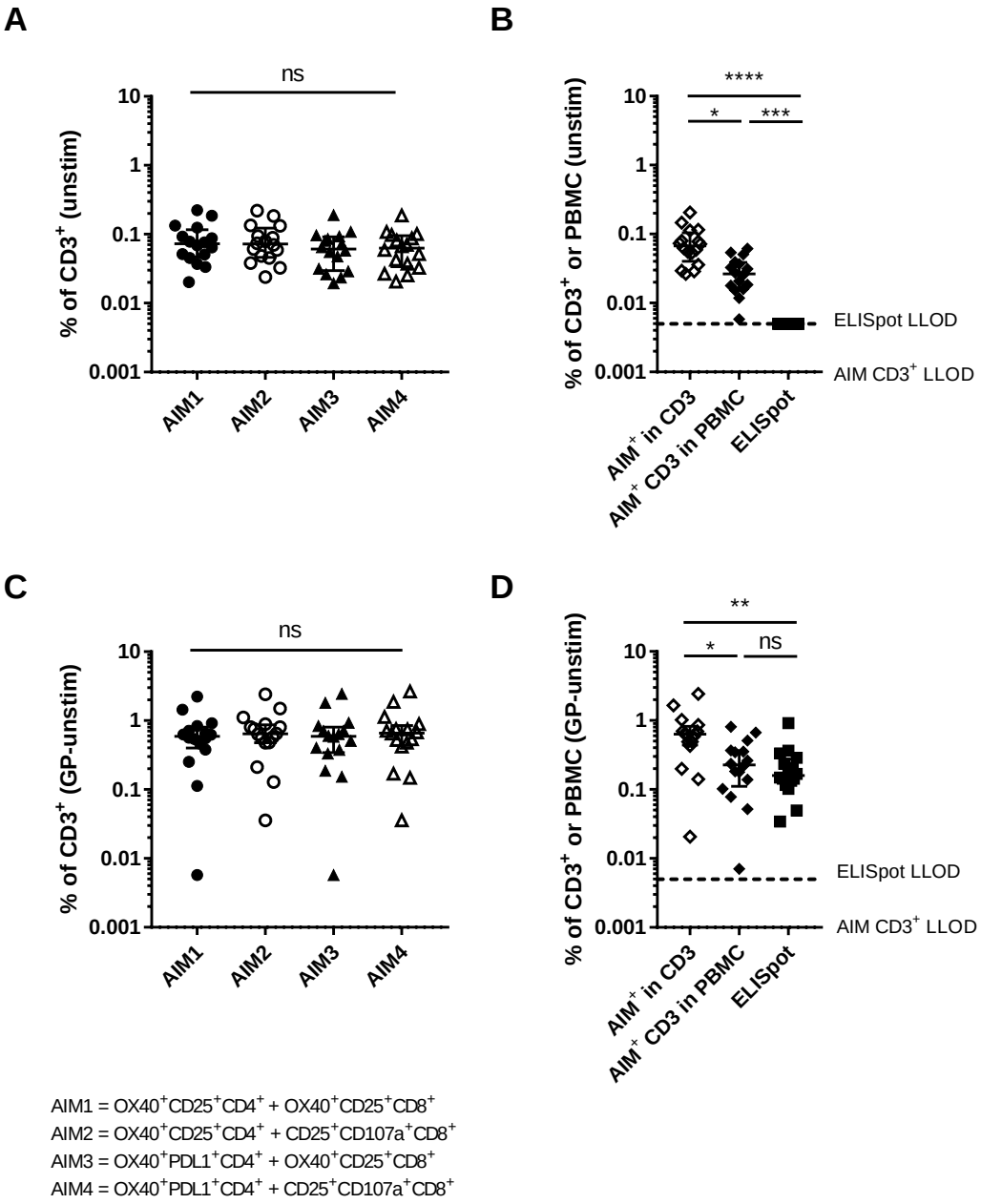

Figure 6.7. Specificity and sensitivity of AIM assay compared with ELISpot

Specificity and sensitivity of AIM assay compared with ELISpot using cells at M+7: **A**) Frequency of AIM$^+$ cells within total T cells using each combination of AIM markers in CD4$^+$ and CD8$^+$ T cells (Kruskal-Wallis P=0.68). **B**) Average of the four AIM combinations as a frequency of CD3$^+$ T cells and as a frequency of PBMC compared with background in the ELISpot assay (%IFNγ$^+$ PBMC) (Mann-Whitney P<0.0001). **C**) Frequency of antigen-specific T cells (AIM$^+$ in GP-stimulated cells after background subtraction) detected using each of the marker combinations (Kruskal-Wallis P=0.90). **D**) Average of these combinations as a frequency of CD3$^+$ T cells and as a frequency of PBMC compared with the ELISpot (%IFNγ$^+$ PBMC) results (Kruskal-Wallis P=0.0018). Dashed lines show LLOD for ELISpot (0.005), dotted lines show LLOD for AIM in total T cells (0.001). ns: no significance, * P<0.05, ** P<0.01, *** P<0.001, **** P<0.0001.

Table 6.3. Comparison of sensitivity and specificity of AIM and cytokine-based assays
Medians (inter-quartile ranges), NA- not applicable – assay not conducted at this time point

Assay/ markers	Lower limit of detection (% of subset)	Frequency in unstimulated (% of subset)	Antigen-specific signal at M+7 (GP-unstim, % of subset)	Antigen-specific signal at M+84 (GP-unstim, % of subset)
ELISpot	0.005	0.005	0.159 (0.120-0.275)	0.015 (0.010-0.032)
ICS: $CD4^+$ "any of three"	0.005	0.064 (0.045-0.096)	0.265 (0.069-0.527)	NA
ICS: $CD8^+$ "any of three"	0.005	0.033 (0.020-0.048)	0.298 (0.210-0.456)	NA
ICS: $CD8^+$ "any of four"	0.005	0.067 (0.053-0.150)	0.492 (0.341-0.676)	NA
AIM: $CD4^+$ $OX40^+CD25^+$	0.003	0.110 (0.069-0.172)	0.753 (0.445-0.924)	0.153 (0.064-0.231)
AIM: $CD4^+$ $OX40^+PDL1^+$	0.003	0.102 (0.044-0.131)	0.700 (0.259-0.961)	0.230 (0.020-0.443)
AIM: $CD8^+$ $OX40^+CD25^+$	0.005	0.021 (0.010-0.033)	0.601 (0.304-0.826)	0.056 (0.026-0.101)
AIM: $CD8^+$ $CD25^+CD107a^+$	0.005	0.020 (0.012-0.036)	0.861 (0.359-1.219)	0.048 (0.024-0.112)
AIM: $CD3^+$ (average of marker combinations)	0.001	0.067 (0.040-0.104)	0.633 (0.443-0.820)	0.150 (0.039-0.236)
AIM^+CD3^+ (average of marker combinations) in PBMC	0.001	0.026 (0.016-0.039)	0.227 (0.111-0.364)	0.058 (0.012-0.095)

6.3.4. The AIM assay effectively measures durable vaccine responses

The durability of vaccine responses in this clinical trial were measured by IFNγ ELISpot three months after MVA-EBO-Z vaccination (M+84). The frequency of GP-specific T cell responses detected by the ELISpot and AIM assays at this time point was compared. GP-specific T cell responses measured by all methods were significantly reduced from peak to three months post-boost (Figure 6.8A, 6.8B). However, almost all individuals still had detectable AIM responses. GP-specific $CD8^+$ responses were detectable for 14/16 individuals, whilst GP-specific $CD4^+$ responses were detectable for 13/16 individuals by OX40 and PDL1 markers or 14/16 by OX40

and CD25 markers. At M+84 there was a higher frequency of GP-specific $CD4^+$ T cells than $CD8^+$ T cells measured by the AIM assay (Figure 6.8A, $OX40^+CD25^+CD4^+$: 0.153% [0.064–0.231], $OX40^+PDL1^+CD4^+$: 0.230% [0.020–0.443], $OX40^+CD25^+CD8^+$: 0.056% [0.026–0.101], $CD25^+CD107a^+CD8^+$: 0.048% [0.024–0.112]). IFNγ ELISpot results at this time point, which include both $CD4^+$ and $CD8^+$ responses, were 10-fold lower than peak (Figure 6.8B, 0.0155% [0.010-0.032] compared with peak responses of 0.159% [0.120-0.275]). Additionally, 2/16 volunteers did not have detectable ELISpot responses at this time point. In comparison AIM^+ cells as a frequency of total T cells were only four-fold lower than peak (M+84: 0.150% [0.039-0.236], M+7: 0.633% [0.443-0.820]) and AIM^+ T cells as a frequency of PBMC were also four-fold lower than peak (M+84: 0.058% [0.012-0.095], M+7: 0.227% [0.111-0.364]). There was no correlation between the AIM assay and ELISpot at this late time point (Figures 6.7C, 6.7D, 6.7E. frequency of AIM^+ cells in $CD4^+$, $CD8^+$ or $CD3^+$, or frequency of AIM^+CD3^+ cells in PBMC).

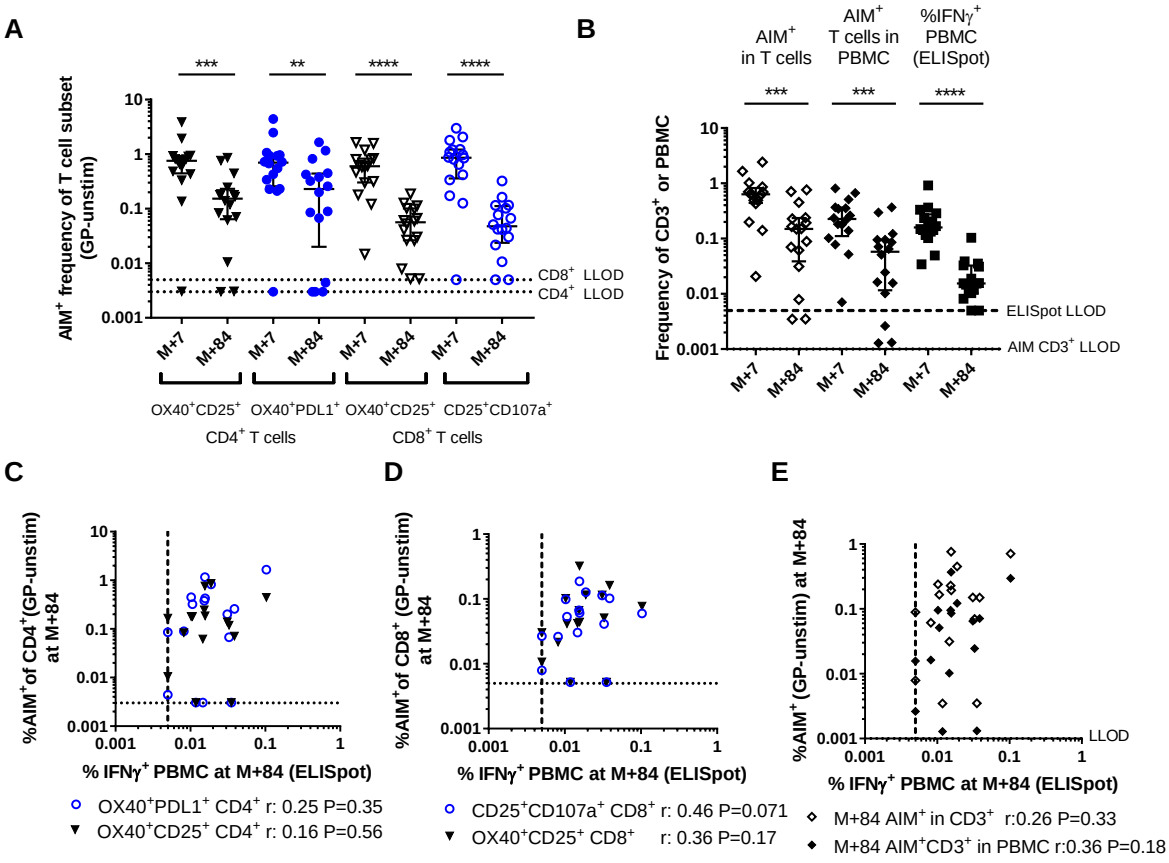

Figure 6.8. Detection of AIM⁺ T cells at late time points

A) Frequency of AIM⁺ cells within the CD4⁺ and CD8⁺ T cell subsets three months after MVA-EBO-Z vaccination (M+84) compared with peak responses seven days after vaccination (M+7). **B**) GP-specific T cells measured by ELISpot (%IFNγ⁺ PBMC) or AIM⁺ cells in total T cells or PBMC at M+7 and M+84. Wilcoxon matched-pairs analyses for comparisons across time points. Relationship between the proportion of GP-specific T cells at M+84 measured by IFNγ ELISpot and: **C**) frequency of AIM⁺ CD4⁺ T cells at M+84, **D**) frequency of AIM⁺ CD8⁺ T cells at M+84, **E**) frequency of AIM⁺ cells within T cells or AIM⁺ T cells within PBMC at M+84. Spearman rank analyses. Dashed lines indicate ELISpot and ICS lower limit of detection (LLOD). Dotted lines indicate AIM assay LLOD. ** P<0.01, *** P<0.001, **** P<0.0001.

6.4. Discussion

Antigen-specific T cell responses in clinical trials have classically been determined using cytokine-based approached such as ELISpot and ICS assays [527-529]. These assays allow for sensitive and specific detection of antigen-responsive T cells. However, these methods require pre-determination of the cytokines to be analysed. This can cause a bias in the type of T cells detected, and could also lead to an underestimation of the size of the antigen-specific response. For example, memory cells that are produced in response to both infection and vaccination consist of multiple populations with different gene expression profiles and functional capacity [547,548]. Crucially, these cells differ in their ability to secrete cytokines [549]. In particular, in several studies it has been observed that the majority of antigen-specific central memory $CD4^+$ T cells were not secreting TNFα or IFNγ and therefore weren't detected by assays based on cytokine secretion [550,551]. Especially at late time points after infection and vaccination when the ratio of central to effector memory T cells is likely to be higher, the majority of the antigen-specific T cells may be undetectable by cytokine-based assays [552]. ICS is often not performed at these time points in clinical trials as the ability to detect IFNγ secreting cells is relatively low and very few responses are detected [537]. The ELISpot assay is sensitive enough to detect antigen-specific IFNγ-secreting cells in almost all volunteers at least three months after the peak response. However, the AIM assay results at this late time point indicate that antigen-specific $CD4^+$ T cells may be particularly well maintained, an observation that could not be made from the ELISpot assay. The ICS and ELISpot assays routinely used in clinical trials are highly effective at identifying antigen-specific effector cells at the peak time point. The AIM assays capture a comparable level of vaccine-specific T cells in the $CD8^+$ subset at the peak time point. However, there was much less agreement between the assays in the $CD4^+$ subset. The data suggest that we may be missing a substantial portion of the $CD4^+$ T cell response to vaccination when using traditional ICS and IFNγ ELISpot assays, particularly at late time points. Detection of $CD4^+$ T cells

and central memory cells not producing cytokine may be an important part of the durability of vaccine responses that may be being underestimated.

The markers tested here each have different mechanisms of induction, signalling pathways and downstream effector functions. Therefore, each of these can reveal something different about the vaccine-induced T cell response. OX40 expression on activated $CD4^+$ and $CD8^+$ T cells is induced by TCR stimulation and augmented by other co-stimulatory signals such as CD28-B7.1/7.2 interaction [553]. Although OX40 stimulation can regulate cytokine production, its dominant activity is providing signals that augment clonal expansion and maintain late proliferation of effector and memory T cells [554]. This means that OX40 may be a useful marker for antigen-responsive cells that are not producing cytokines (particularly memory T cells), and could also be a useful marker of the durability of the T cell response. CD25 (IL-2Rα) expression is regulated by both TCR stimulation and IL-2 signalling [555]. CD25 forms the high affinity receptor for IL-2 in combination with the IL-2Rβ and IL-2Rγ chains, which are constitutively expressed on quiescent T cells [556]. Expression of CD25 increases IL-2R affinity for IL-2 by around 100-fold, allowing responses to low concentrations of IL-2. The IL2 receptor signals through Jak1 and Jak3 to induce Stat5-dependent regulation of genes, including genes for cell cycle progression [555]. However, IL2R expression is more transient than OX40 and requires a sustained IL-2 signal (except in Tregs, in which it is apparently constitutive) [555]. For this reason, CD25 may be a useful marker for antigen-stimulated T cells in ongoing immune responses, in addition to identifying Tregs (in combination with other makers, such as FOXP3). CD107a is expressed on lysosomal membranes within $CD8^+$ T cells and NK cells. CD107a is expressed on the cell surface after fusion of the lysosomal membrane with the cell membrane and is therefore an effective marker of cytotoxic activity [557]. Release of cytokines from NK and T cells is also dependent on secretory pathways but these are likely independent from exocytosis of secretory lysosomes [558], suggesting that this marker also provides novel information not provided by cytokine analysis. PDL1 expressed on APCs interacts with PD1 on T cells and induces an inhibitory signal

that reduces proliferation of antigen-specific T cells and can also induce Treg differentiation. This process is involved in ligand-induced TCR down-modulation to regulate TCR signalling and is essential for the maintenance of peripheral tolerance [559]. PDL1 expression in response to antigen stimulation has also been shown on Tfh despite high expression of PD1 on these cells [404]. The combination of PDL1 with OX40 and CD25 can be used to discriminate antigen-responsive Tregs [402,404].

Although these markers all detect antigen-activated T cells, the expression patterns of these markers likely indicate different contexts of cell activation and differing cell fates. For this reason, the use of these markers (perhaps in combination with alternative measures such as cytokine production and proliferation) can provide novel information about the antigen-responsive T cell population that may not be gained through analysis of cytokine production alone.

An alternative method of detecting antigen-specific T cells that does not rely on a functional property would be to use MHC-peptide complexes [560]. However, this requires MHC matching, meaning that multiple MHC-peptide complexes would be required to measure the responses in all individuals. Although this may be possible small UK cohorts, it would not generally be feasible for use in clinical trials, which often involve large numbers of individuals and include people with diverse MHC haplotypes. Additionally, a recent study showed that the frequency of antigen-specific $CD4^+$ T cells detected by cytokine secretion was significantly reduced (between three and five-fold) after cryopreservation; ICS or ELISpot using thawed cells showed lower and more CD8-biased responses than those using PBMC *ex vivo* [561]. The ability to perform T cell assays using cryopreserved cells is crucial in many clinical trials – particularly those involving multiple centres. Equally, conducting assays using cryopreserved cells allows samples from multiple time points to be batched, increasing efficiency and reducing experimental variation. Although I have not directly assessed AIM expression on fresh and frozen PBMC, the results shown here indicate

that AIM assays conducted using cryopreserved cells give comparable or higher antigen-specific signals than ICS and ELISpot using PBMC *ex vivo*.

One possible issue with the AIM assay is background caused by bystander activation. This has been investigated in a study that found the level of bystander activation to be relatively low [402]. I found that the AIM assay provided a high level of specificity with background levels comparable or lower than those in the ICS assay and typically with frequencies lower than 0.15% of the $CD4^+$ or $CD8^+$ T cell subset. This is lower than, or comparable to the level of background observed for these and other combinations of AIMs previously investigated [402,403,542]. An issue with the use of OX40 and CD25 markers is the inclusion of antigen-responsive Tregs. This was addressed in a previous study by the addition of PDL1 to discriminate between antigen-responsive Tregs and non-Tregs [402]. In this study by Reiss *et al*, several marker combinations were directly compared in T cells stimulated with tetanus peptides. In each of these populations, only a minority of the cells were Tregs (based on FOXP3 expression): 1.6% of $OX40^+PDL1^+$ $CD4^+$ T cells, 6.8% of $CD69^+CD40L^+$ $CD4^+$ T cells and 16% in the $OX40^+CD25^+$ $CD4^+$ T cells. These data suggest that OX40/CD25 are useful markers for identifying the maximal antigen-specific population, whilst OX40/PDL1 or CD69/CD40L can be used to discriminate antigen-specific non-Tregs. In the study presented here, AIM frequencies in GP-stimulated $CD4^+$ T cells detected using either of the marker combinations tested were comparable and the two populations were highly correlated. However, this may not be the case for all vaccine antigens, at all time points or in all populations. Therefore, an assay including OX40, CD25 and PDL1 could be of use in clinical trials in order to measure both the maximal antigen-specific response and to discriminate non-Tregs. This may be particularly useful in some circumstances where antigen-specific Tregs may be increased or play a role in disease pathology, such as in malaria-exposed populations [164,201,562] or in CMV [563].

All of the AIM marker combinations used in this study sensitively detected antigen-specific T cells. The lower limit of detection for the AIM assay in this study was either comparable to ($CD8^+$ AIM 0.005%) or lower than ($CD4^+$ AIM 0.003%) the ICS assay (0.005% for $CD4^+$ and $CD8^+$ T cells). Antigen-specific T cells detected using the AIM assay were 2.6-2.8-fold higher than ICS for $CD4^+$ T cells and 1.2-1.8-fold higher than ICS for $CD8^+$ T cells at the peak time point. Although ELISpot assays are highly specific, the AIM assay tested here was much more sensitive and had a higher signal-to-noise ratio. However it should be noted that the LLOD for the AIM and ICS assays are calculated by the reciprocal of the lowest number of events collected in the appropriate gate ($CD4^+$, $CD8^+$ or $CD3^+$) and will therefore vary depending on the number of cells used in each assay and their viability. In this study $2x10^6$ PBMC were used for the ICS, which was conducted as a primary immunological assay in the clinical trial according to an established standard operating procedure. For the AIM assay $1\text{-}2x10^6$ PBMC were used depending on the number of cryopreserved cells remaining.

In this study, I directly compared the use of AIM and cytokine-based assays for the identification of vaccine-specific T cell responses in clinical trials. For many of the vaccines currently in development, there are no clear immunological correlates of protection in humans. Therefore, determination of protective correlates is an important part of the vaccine development process [454,564-566]. The AIM assay is a tool, which in combination with functional measures, could aid the search for immunological correlates of protection because of its unbiased approach. In fact, antigen-specific T cells defined by CD40L expression that were also producing TNFα or IL-2 induced by RTS,S/AS vaccination were higher in individuals protected from malaria [186]. However, the markers used in this study have not yet been used to detect antigen-specific T cells in a Phase II vaccine study. It would be useful to include this assay in Phase II clinical studies in order to determine the clinical relevance of these subsets. There has been substantial work towards standardising T cell assays for use in human trials and further studies are required to develop and validate AIM assays to a similar level [567-569]. These would include studies to

optimise the concentration of stimulating antigen and markers to use, compare responses *ex vivo* and on frozen PBMC and assess inter-operator variability. Additionally it will be important to characterise the functionality of these cells and determine their clinical relevance.

6.5. Conclusions

This study demonstrates that AIM assays can be used to detect antigen-specific T cells with a sensitivity and specificity comparable to or higher than the cytokine-based assays conventionally used in clinical vaccine trials. Additionally, AIM assays may provide novel information about non-cytokine-secreting cells and the durability of the response, particularly in the $CD4^+$ subset. AIM assays may provide a more comprehensive account of the total antigen-specific response and, in combination with additional phenotypic and functional markers, could be a valuable tool for more detailed assessments of vaccine-specific responses. A combination of AIM assays with traditional cytokine analysis could provide a more complete assessment of the antigen-specific response to vaccination, particularly within $CD4^+$ T cells and when assessing durability. Further validation of these assays would be required for use as primary immunogenicity measure within clinical trials. However, this could significantly enhance knowledge about vaccine-specific T cell responses to aid vaccine development.

7

CMV-associated reduction in vaccine responses

7.1. Introduction

In Chapter 5 I discussed the possible impact of malaria exposure on the response to ChAd3-MVA-EBO-Z vaccination in the Senegalese cohort. Individuals with evidence of significant malaria exposure (determined by the presence of anti-schizont IgG) had significantly lower anti-Ebola GP antibody responses than those who were anti-schizont IgG negative. However these individuals had an intermediate level of anti-Ebola GP IgG that was lower (although not significantly) than the responses in the UK cohort. Clearly there are many factors other than malaria exposure that differentiate the UK and Senegalese cohorts and may have had an impact on the responses to vaccination. These include genetics (including HLA type), nutritional status, microbiome differences and exposure to other pathogens [486-489]. These are small studies that are not powered to investigate all of these factors. However, one striking phenotypic difference that stood out during the analysis of the cTfh data was the expansion of $CD45RA^-$ memory $CD4^+$ T cells in the Senegalese cohort: 50% (33.8 – 74) of the total $CD4^+$ T cell subset were $CD45RA^-$ in the Senegalese cohort compared with 35% (range: 17.3 – 49.7) in the UK cohort. Almost all of the Senegalese volunteers had an expansion of this population relative to the UK median. However, around 30% of the UK individuals had frequencies of memory $CD4^+$ T cells comparable with the Senegalese cohort. A literature search for factors (particularly pathogens) that may cause memory inflation and occur in around 30% of young adults in developed countries and all,

or almost all, young adults in developing countries, highlighted CMV as a potential influencing factor.

As discussed in Chapter 1 in more detail, CMV is a highly prevalent betaherpesvirus that establishes life-long latent infections. Around 30-50% of young adults in developed countries are infected, with seroprevalence increasing to >90% in elderly adults [329]. Prevalence in populations within developing countries can be particularly high, where seroconversion occurs in the first few years of life and almost all young adults are infected [570]. CMV has previously been associated with reduced responses to vaccination in elderly cohorts [377,378,381] but its impact in young adults is less clear [382,384].

Primary infection, which is most often asymptomatic, induces a broad immune response involving both T cells and antibodies specific for CMV [362]. After resolution of acute infection, CMV establishes latency and persists for life with occasional, usually subclinical reactivation events. Congenital CMV and reactivation of infection in seriously immunocompromised individuals can be life-threatening but infection is most often considered benign in immunologically mature, immunocompetent individuals [571,572]. However, even in healthy adults CMV has a significant impact on the immune system, leaving a clear imprint of infection: Greater than 30% of the $CD4^+$ and $CD8^+$ T cells in a healthy middle-aged adult may be specific for CMV and this can rise to 70% in some elderly individuals [360,361]. There is also increasing evidence that CMV may play a significant role in the aging of the immune system, or immunosenescence. One characteristic of this process is an accumulation of late-differentiated effector memory T cells [362]. These cells may lose expression of co-stimulatory receptors CD27 and CD28, gain expression of the inhibitory receptor killer cell lectin-like receptor G1 (KLRG1) and terminal differentiation marker CD57 and exhibit decreased proliferative capacity, increased activation of senescence signalling pathways and a greater susceptibility to apoptosis *in vitro* [573]. In longitudinal studies of elderly populations CMV seropositivity was identified as one

parameter in an “immune risk phenotype”, which also included lower proportions of naïve T cells, accumulation of late-differentiated T cells and an inverted CD4:CD8 ratio (<1), and was associated with increased mortality [373-375].

In elderly populations, CMV-driven changes in the immune system have been associated with reduced responses to vaccination [377,378,381,574]. Marked changes in immune phenotype and significant proportions of CMV-specific T cells are also observed in seropositive young adults and even in children [382,575,576]. However, the impact of CMV carriage and the associated immune phenotype changes on responses to vaccination or infection in young adults and children is less clear. One study reported early signs of immunosenescence in CMV+ young adults and a negative association with responses to influenza vaccination [382]. However, other studies have shown either a neutral or even beneficial impact of CMV [384-386,577,578], and all such studies have been in populations within developed countries. If CMV carriage can negatively impact on vaccine responses in children and young adults under certain circumstances, the reduction in vaccine immunogenicity in developing countries might at least partially be explained by the substantially increased seroprevalence of CMV compared with the same age groups in developed countries.

The concurrent trials of ChAd3-MVA-EBO-Z in the UK and Senegal (EBL04 and EBL06) provided the opportunity to investigate the impact of CMV seropositivity on immune phenotype and responses to vaccination in young adults. I initially assessed the CMV serostatus of each individual in these two cohorts. I then phenotyped baseline T cells in all individuals to determine whether CMV seropositivity was associated with phenotypic differences in total T cells and whether these were associated with vaccine responses. In a collaboration with Tim Waterboer’s group at the German Cancer Research Center, Heidelberg (Infection and Cancer Program), we used multiplex serology to determine the serostatus of individuals in each of these cohorts for a number of chronic infections, including CMV. We then assessed whether these

phenotypes were a unique characteristic of CMV infection or whether they were also associated with other chronic infections. In order to detect antigen-specific T cells independently of their functional capacity, I used the AIM assay described in Chapter 6 to compare the phenotype of vaccine-specific T cells in CMV- and CMV+ UK adults. I also investigated functional properties of these cells to determine if they were directly involved in the reduction of vaccine responses (i.e. reduced cytokine production).

7.2. Study-specific methods

7.2.1. Samples and study details

PBMC and plasma from two Phase I clinical trials were used in this study. The UK cohort consisted of all 16 volunteers in group 2 of EBL04 and the Senegalese cohort consisted of all 40 volunteers in EBL06. All volunteers were healthy adults aged 18-50 years and received $3.6x10^{10}$ viral particles (vp) of ChAd3-MVA-EBO-Z followed by $1.0x10^{8}$ plaque forming units (pfu) of MVA-EBO-Z seven days later. Trial information and ethics statements are detailed in Table 2.2 (Chapter 2.2.1) and Table 2.3 (Chapter 2.2.3). Further details of the vaccines used are provided in 2.1.3.5 and 2.1.3.6.

7.3. Results

7.3.1. CMV seropositivity is associated with reduced responses to vaccination with ChAd3-MVA-EBO-Z

CMV serostatus was determined by ELISA at baseline for all individuals in the UK and Senegalese cohorts (Figure 7.1A). Demographics of both cohorts are shown in Table 7.1. One of the volunteers in the UK cohort, although recruited in the UK, grew up in Kenya and had only been resident in the UK for three years (highlighted in grey in Figure 7.1A). This volunteer had evidence of malaria exposure (malaria-specific IgG measured by ELISA against *P. falciparum* schizont lysate) and was excluded from further analyses comparing the UK and Senegalese

cohorts. Therefore, in the final data set for the UK cohort 47% (7/15) were positive for CMV IgG compared with 100% of the Senegalese cohort. Titres of CMV IgG were comparable in UK CMV+ and Senegalese individuals. Volunteer ages in the UK CMV-, UK CMV+ and Senegalese cohorts were comparable and did not correlate with CMV IgG titre (Figure 7.1B, Table 7.1. average ages 33, 33 and 28 years respectively).

Table 7.1. Cohort demographics

*Race was self-reported. %The body-mass index is the weight in kilograms divided by the square of the height in meters. Height was not recorded for one Senegalese volunteer.

Cohort		UK CMV-	UK CMV+	Senegal
Number of volunteers, *n*		8	8	40
		Number of individuals (percentage)		
Gender, *n* (%)	Female	6 (75)	4 (50)	11 (27.5)
	Male	2 (25)	4 (50)	29 (72.5)
Age, years	18-20	0	0	9 (22.5)
	21-30	5 (62.5)	4 (50)	17 (42.5)
	31-40	1 (12.5)	2 (25)	12 (30)
	41-50	2 (25)	2 (25)	2 (5)
	Mean	33	33	28
Ethnicity*	White	7 (87.5)	6 (75)	0
	Black	0	1 (12.5)	40 (100)
	Asian	1 (12.5)	0	0
	Mixed	0	1 (12.5)	0
	Other	0	0	0
Body-mass index%	< 18.5	0	0	1 (2.5)
	18.5-24.9	3 (37.5)	3 (37.5)	27 (67.5)
	25-29.9	2 (25)	3 (37.5)	7 (17.5)
	≥ 30	3 (37.5)	2 (25)	4 (10)
	Mean	28	27	23.7

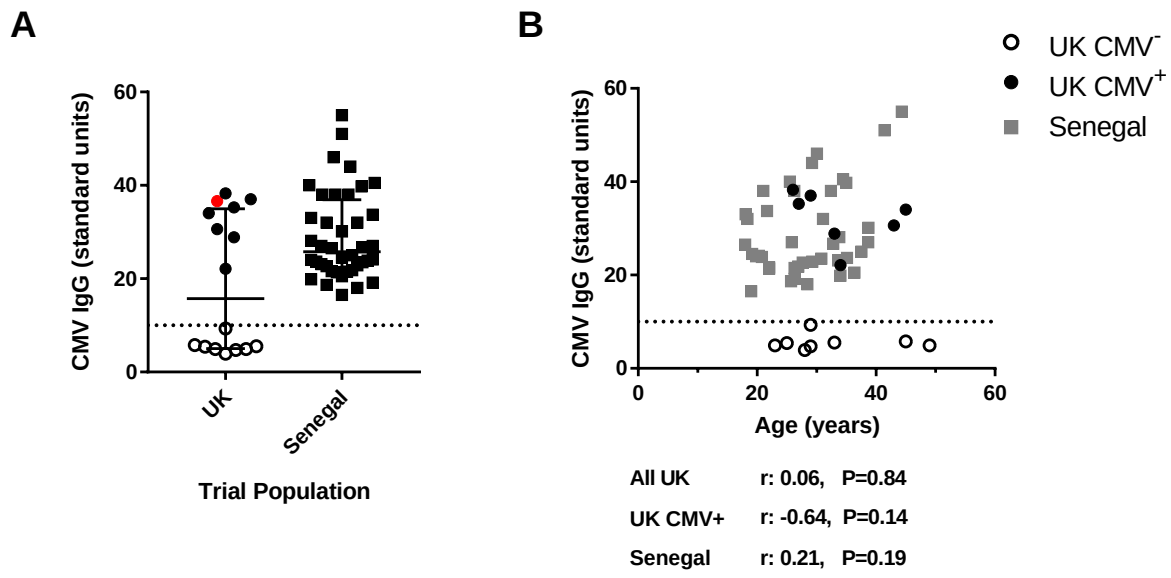

Figure 7.1. CMV serostatus
A) CMV IgG titres in UK and Senegalese cohorts. UK volunteer that grew up in Kenya is highlighted in red and was excluded from further analyses comparing the two cohorts. **B**) Relationship between CMV IgG titre and age in each population (Spearman's rank analysis, all UK volunteers r:0.06, P=0.84, UK CMV+ r:-0.64, P=0.14, Senegal r:0.21, P=0.19). Dashed lines indicate the seropositive threshold (10 standard units as defined by the ELISA kit manufacturer's instructions.

T cell responses to vaccination were measured by IFNγ ELISpot using a pool of peptides from the Zaire Ebola GP (Figures 7.2A, 7.2B). Responses were measured in Senegal and the UK at baseline and peak (seven days after MVA-EBO-Z, M+7). In the UK cohort additional assays were conducted seven days after ChAd3-EBO-Z vaccination (D7) and at 28, 84 and 168 days after MVA-EBO-Z (M+28, M+84, M+168). There were no differences in peak ELISpot responses between the UK and Senegalese cohorts (Chapter 5.3.4, Figure 5.9B) but within the UK cohort CMV+ individuals had significantly lower vaccine-specific T cell responses than CMV- individuals (Figure 7.2B P=0.0093). However, Senegalese individuals had a wide range of responses (123 – 19780 SFC/10^6 PBMC) and there were no significant differences across the three groups (P=0.10). Antibody responses were measured by indirect ELISA against recombinant Ebola GP at baseline, D7, M+7, M+28, M+84 and M+168 in both the UK and Senegalese cohorts (Figures 7.2C, 7.2D). Antibody responses to Ebola vaccination were significantly lower in CMV+ UK

individuals compared with CMV- individuals (P=0.029). Overall, antibody responses were significantly lower in the Senegalese cohort (P=0.020 at M+7, P=0.0025 at M+84/D90, Chapter 5.3.4, Figure 5.9A). However, when stratified by CMV serostatus, Senegalese individuals had responses that were comparable to UK CMV+ individuals (P=0.91) but significantly lower than UK CMV- individuals (P=0.0037).

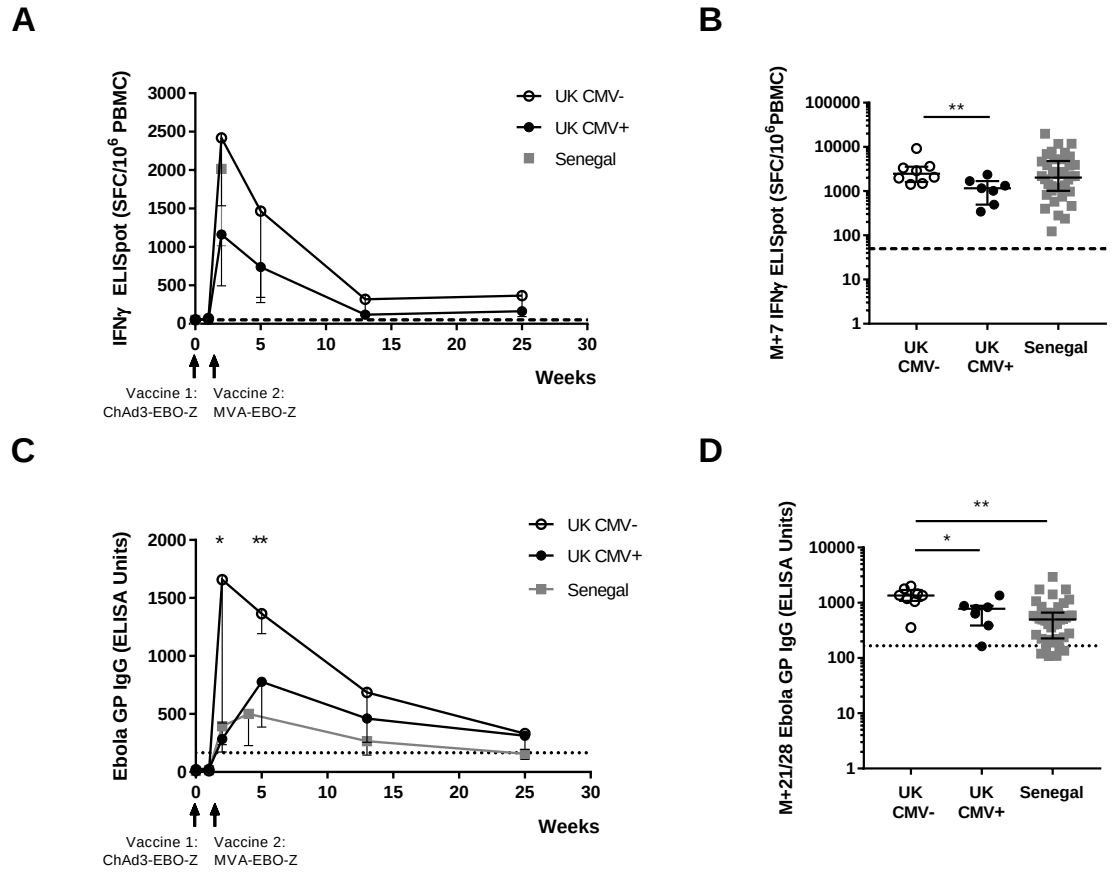

Figure 7.2. Reduced vaccine responses in CMV+ individuals

A) Time courses of T cell responses to vaccination measured by IFNγ ELISpot. Median and inter-quartile range (IQR) of responses against summed Ebola GP peptide pools. Only baseline (D0) and peak (D14, M+7) were measured in the Senegalese cohort. **B**) IFNγ ELISpot responses at M+7. Comparison of responses in UK CMV- and CMV+ individuals, Mann-Whitney P=0.0093. No significant differences by Kruskal-Wallis comparison across all three groups (P=0.10). **C**) Time courses of antibody responses against Ebola GP. Medians and IQRs shown. **D**) Peak antibody responses (four weeks after MVA vaccination, M+28). Comparison of UK CMV- and CMV+ individuals, Mann-Whitney P=0.029. Kruskal-Wallis analysis across all three groups P=0.0037, significantly lower responses in Senegal compared with UK CMV- individuals. Medians and IQRs shown for column graphs. Dashed lines indicate ELISpot LLOD (50 SFC/10^6 PBMC), dotted lines indicate ELISA seropositive cut-off (166 EUs). SFC/10^6 PBMC = spot-forming cells per million PBMC, * P<0.05, ** P<0.01.

GP-specific cytokine production was measured by ICS at the peak post-boost time point (M+7 in each cohort. Comparisons between the UK and Senegalese cohorts were difficult as the background in the unstimulated condition was higher in the Senegalese samples than the UK samples and therefore many of the Senegalese responses (which are calculated as the frequency in the GP stimulation after subtraction of the frequency in the unstimulated control) were below the LLOD. Therefore the ICS responses are only compared between CMV- and CMV+ UK individuals. ICS data were available for 8/8 of the CMV- individuals and 5/8 CMV+ individuals (three data points were excluded from the dataset as they did not meet the QC criteria). There were no significant differences in the frequency of GP-specific IFNγ, IL-2 or TNFα production by $CD4^+$ T cells in CMV- and CMV+ individuals (Figure 7.3A). There was also no significant difference in the frequency of GP-specific $CD8^+$ T cells producing IL-2 or expressing CD107a in CMV- and CMV+ individuals (Figure 7.3B). However, the frequencies of GP-specific $CD8^+$ T cells producing IFNγ or TNFα were significantly lower in CMV+ individuals (P=0.023 and P=0.019, respectively).

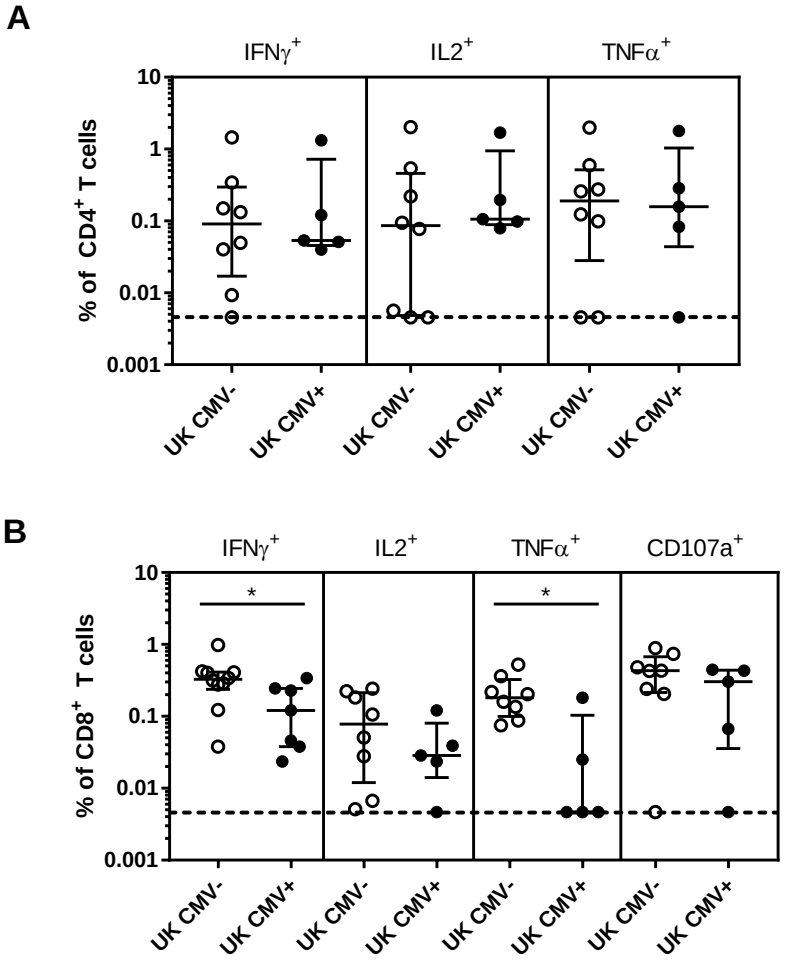

Figure 7.3. Reduced cytokine responses in CMV+ individuals
GP-specific cytokine responses measured by ICS at M+7 in the UK cohort. **A**) Frequency of $CD4^+$ T cells producing IFNγ, IL-2 or TNFα. **B**) Frequency of $CD8^+$ T cells producing IFNγ, IL-2 or TNFα, or expressing CD107a. Medians and IQRs shown. Mann-Whitney tests between CMV- and CMV+ individuals: $IFN\gamma^+$ $CD8^+$ P=0.023, $TNFa^+$ $CD8^+$ P=0.019. * P<0.05. Dashed lines indicate LLOD for intracellular cytokine staining assay.

7.3.2. CMV+ individuals have altered $CD4^+$ and $CD8^+$ T cell populations

7.3.2.1. CMV+ individuals have different proportions of memory T cell subsets

T cell phenotypes were measured in each of these groups by flow cytometry. Memory populations within $CD4^+$ and $CD8^+$ T cells were defined as: $CD45RA^+CCR7^+$ naïve (N), $CD45RA^-CCR7^+$ central memory (T_{CM}), $CD45RA^-CCR7^-$ effector memory (T_{EM}) and $CD45RA^+CCR7^-$ terminal effector memory re-expressing CD45RA (T_{EMRA}) [579]. Additionally, expression of costimulatory

receptors CD27 and CD28, inhibitory receptor KLRG1 and terminal differentiation marker CD57 were included in the analysis to further characterise the T cell subsets [580-583] (gating strategy: Figure A5). The frequency of $CD4^+$ within $CD3^+$ T cells was reduced (although not significantly lower, P=0.19) from a median of around 70% in CMV- UK individuals to 60% in CMV+ individuals and was significantly lower in Senegalese individuals (58%) compared with UK CMV- individuals (Figure 7.4A, P=0.029). There were no significant differences in the frequencies of $CD8^+$ T cells across groups (Figure 7.4B, P=0.14). The CD4:CD8 ratio was not significantly different across the three groups (Figure 7.4C, P=0.11) although there was one UK CMV+ individual with an inverted CD4:CD8 ratio (a male aged 34 years) and a number of Senegalese volunteers with ratios of less than 1.5 (5 males, 1 female, aged 21-34 years). Proportions of memory populations within both $CD4^+$ and $CD8^+$ T cells did not significantly differ between UK CMV+ and Senegalese individuals but there were multiple significant differences compared with UK CMV- individuals (Figure 7.4D). The proportion of EM within $CD4^+$ T cells was higher in UK CMV+ individuals and was significantly increased in Senegalese individuals (Figure 7.4E, P=0.094 and P=0.0016, respectively). The proportion of T_{EMRA} in $CD4^+$ T cells was increased in the UK CMV+ but not the Senegalese cohort (P=0.022 and P=0.11), whilst the proportion of naïve $CD4^+$ T cells was only significantly lower in the Senegalese cohort (P=0.27 for UK CMV+ and P=0.050 for Senegalese compared with UK CMV- individuals) and there were no differences in the proportions of T_{CM} $CD4^+$ T cells. Within the $CD8^+$ T cell subset the proportion of T_{EMRA} was significantly increased in both the UK CMV+ and Senegalese groups compared with UK CMV- (P=0.020 and P=0.0020 respectively).

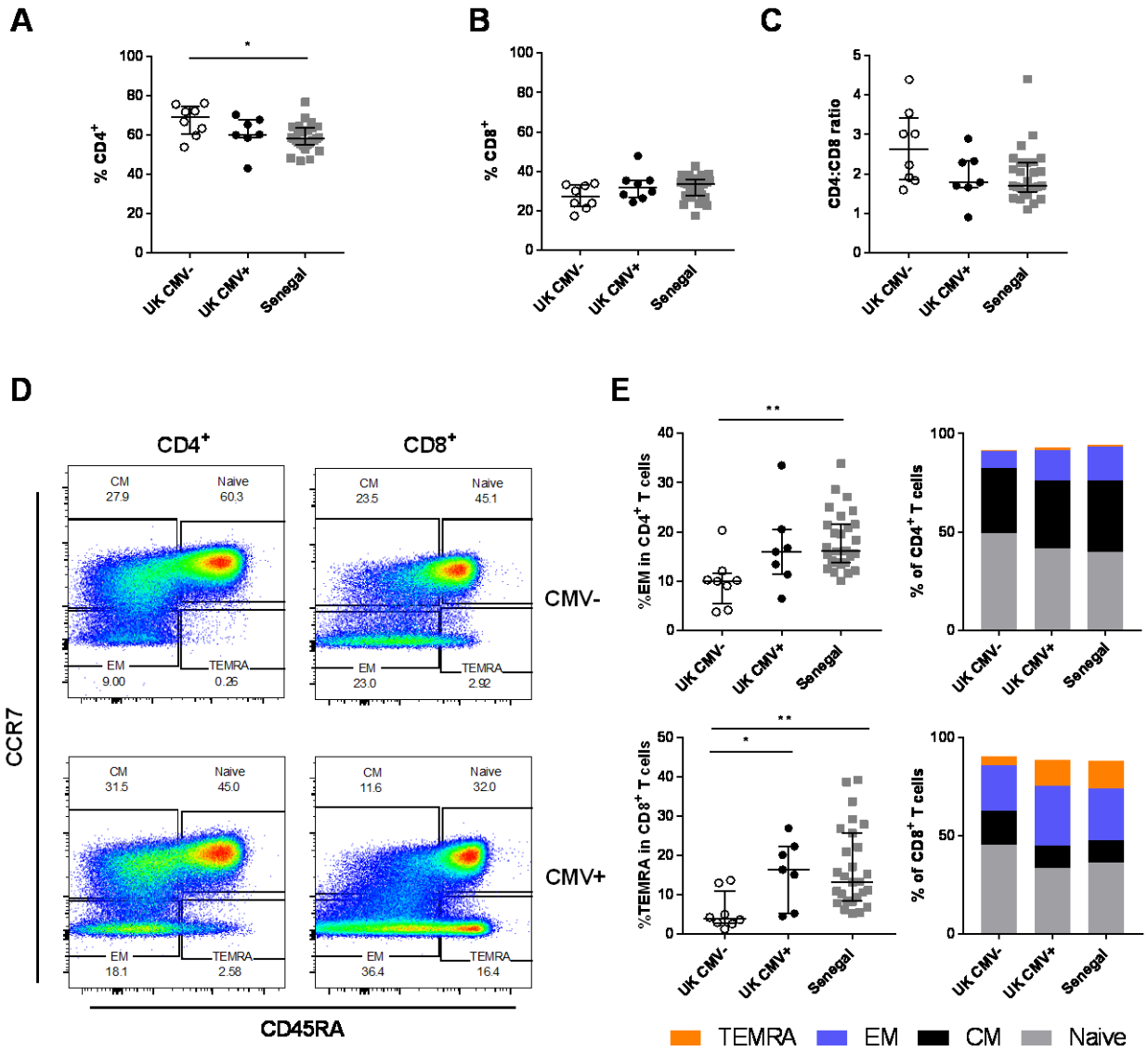

Figure 7.4. Altered memory T cell populations in CMV+ individuals

A) Frequency of $CD4^+$ T cells in the UK in CMV seronegative and seropositive individuals and in Senegal (all Senegalese individuals were CMV seropositive). **B**). Frequency of $CD8^+$ T cells **C**) Ratio of CD4:CD8 T cells. **D**) Representative flow cytometry plots of subsets within $CD4^+$ and $CD8^+$ T cells in CMV- and CMV+ individuals; naïve: $CD45RA^+CCR7^+$, central memory (T_{CM}) $CD45RA^-CCR7^+$, effector memory (T_{EM}): $CD45RA^-CCR7^-$, terminally differentiated effector memory $CD45RA^+$ T cells (T_{EMRA}): $CD45RA^+CCR7^-$ **E**) Subsets within $CD4^+$ and $CD8^+$ T cells as defined by the gating strategy above. Clockwise from top-left: Proportion of T_{EM} in $CD4^+$ T cells, geomeans of subset frequencies within $CD4^+$ T cells, geomeans of subset frequencies within $CD8^+$ T cells, Proportion of T_{EMRA} in $CD8^+$ T cells. Kruskal-Wallis analysis with Dunn's post-test comparisons of groups. Medians and IQRs shown. * P<0.05, ** P<0.01.

7.3.2.2. CMV+ individuals have increased proportions of $CD27^-CD28^-$ and $CD57^+KLRG1^+$ T cells

The proportion of T cells that were $CD27^-CD28^-$ within both the $CD4^+$ and $CD8^+$ subsets was 10-fold higher in UK CMV+ and Senegalese adults compared with UK CMV- adults (Figures 7.5A-C). In all CMV- individuals less than 0.2% of total $CD4^+$ T cells were $CD27^-CD28^-$. In contrast, the median frequency of $CD27^-CD28^-$ in $CD4^+$ T cells in CMV+ UK adults was 2.4%, whilst some individuals had frequencies as high as 10%. In $CD8^+$ T cells the median $CD27^-CD28^-$ frequency was 2.5% in CMV- individuals, whilst CMV+ UK and Senegalese adults had median frequencies of 26.4% and 18.5% respectively. In some individuals more than 50% of $CD8^+$ T cells did not express CD27 or CD28. There was a similar pattern within individual memory populations as well. Within both T_{EM} ($CD45RA^-CCR7^-$) $CD4^+$ and $CD8^+$ T cells the ratio of $CD27^+CD28^+$ to $CD27^-CD28^-$cells was significantly reduced in UK CMV+ and Senegalese adults compared with UK CMV- adults (Figures 7.5D, 7.5E, Kruskal-Wallis $P<0.0001$ and $P=0.0070$, respectively).

Both $CD4^+$ and $CD8^+$ T cells also contained significantly increased proportions of $CD57^+KLRG1^+$ cells in the UK CMV+ and Senegalese cohorts (Figures 7.6A, 7.6B, Kruskal-Wallis $P=0.0002$ and $P=0.0021$, respectively). In $CD4^+$ T cells the majority of cells are $CD57^-KLRG1^-$ but both $CD57^-KLRG1^+$ and $CD57^+KLRG1^+$ were expanded in UK CMV+ and in Senegalese adults (Figure 7.6C). Similarly, these populations were also expanded within $CD8^+$ T cells in the CMV+ and Senegalese cohorts. $CD57^+KLRG1^+$ T cells were around 2.6% of $CD8^+$ T cells in CMV- individuals, compared with 14% in UK CMV^+ and 10.9% in Senegal. Additionally, $CD57^+KLRG1^-$ cells, which represented only a very small proportion of total $CD8^+$ T cells (0.3%) in CMV- subjects, were over two-fold higher in CMV+ individuals and represented almost 2% of $CD8^+$ T cells within Senegalese individuals. Differences were also observed within $CD27^-CD28^-$ $CD4^+$ and $CD8^+$ T cells. Within $CD27^-CD28^-$ $CD4^+$ T cells in CMV- individuals 12.8% were $CD57^+KLRG1^+$ and 16.4% were $CD57^-KLRG1^+$ while over 70% were $CD57^-KLRG1^-$ (Figure 7.6D). In contrast, within this subset in CMV+ individuals, only 3.9% of cells were $CD57^-KLRG1^-$ whilst 41.8% were $CD57^-KLRG1^+$ and 53.3%

were $CD57^{+}KLRG1^{+}$. In the Senegalese cohort, $CD57^{-}KLRG1^{+}$ cells were not as greatly increased (26.3%), $CD57^{-}KLRG1^{-}$ cells were not as reduced (12.7%) and an expanded proportion of $CD57^{+}KLRG1^{-}$ cells was observed (6.2% compared with 1% in UK CMV+ and 0.2% in CMV- individuals). In $CD27^{-}CD28^{-}CD8^{+}$ T cells $CD57^{+}KLRG1^{+}$ and $CD57^{-}KLRG1^{+}$ cells predominated (48.4% and 41.4% respectively in CMV- individuals). In CMV+ UK and Senegalese individuals $CD57^{+}KLRG1^{+}$ cells were expanded (67.3% in CMV+ UK individuals and 63.9% in Senegalese individuals) while $CD57^{-}KLRG1^{+}$ cells were reduced (29.8% in CMV+ UK and 24.1% in Senegalese individuals). An additional difference seen in the Senegalese cohort was an expansion of $CD57^{+}KLRG1^{-}$ (3.1% in UK CMV-, 1.3% in UK CMV+, and 6.8% in Senegalese individuals).

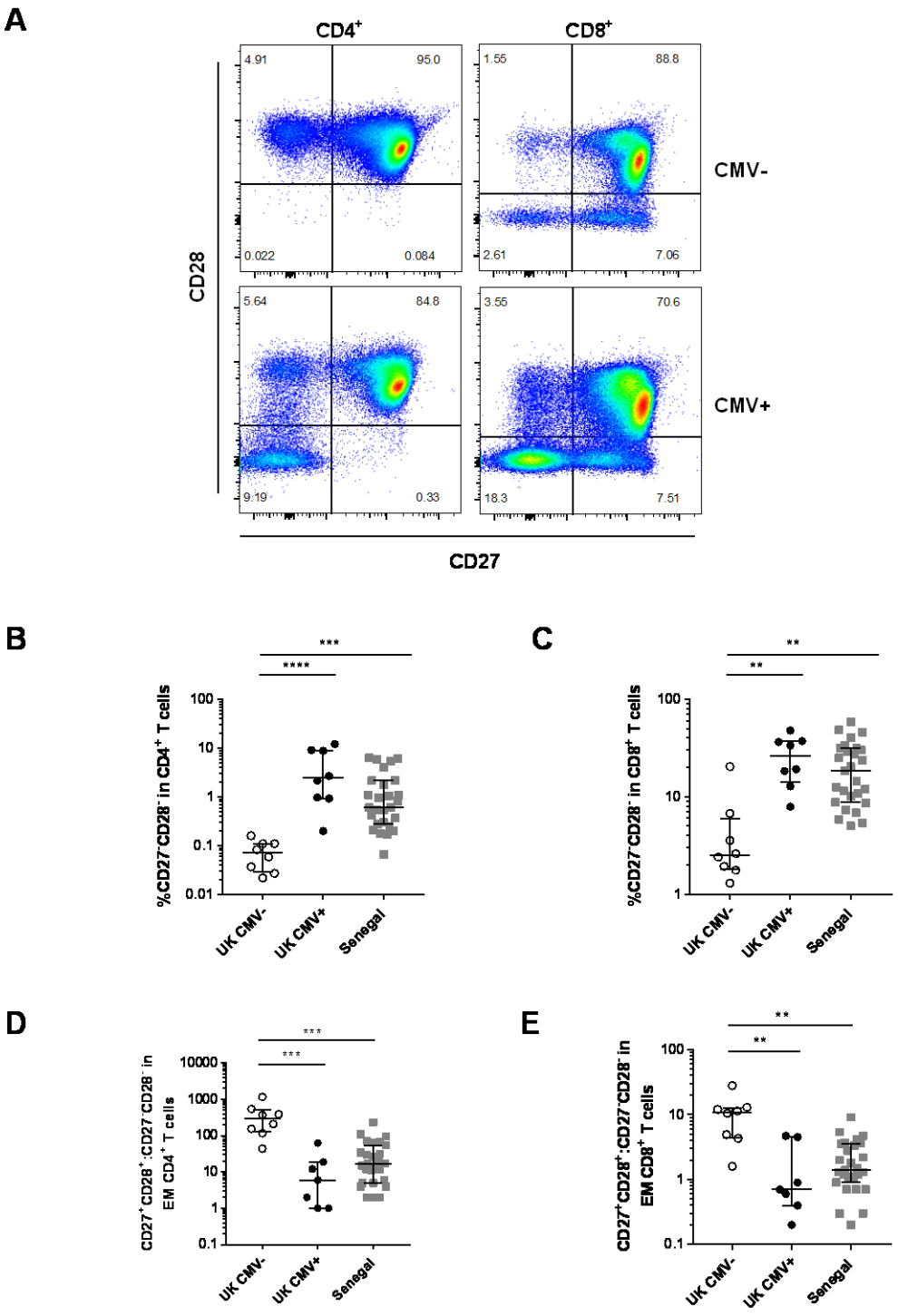

Figure 7.5 Reduced CD27 and CD28 expression on T cells in CMV$^+$ individuals

A) Representative flow plots showing CD27 and CD28 expression on CD4$^+$ (left) and CD8$^+$ (right) T cells in CMV seronegative (top row) and CMV seropositive (bottom row) individuals. **B**) Frequency of CD4$^+$ T cells that are CD27$^-$CD28$^-$. **C**) Frequency of CD8$^+$ T cells that are CD27$^-$CD28$^-$. **D**) Ratio of CD27$^+$CD28$^+$ to CD27$^-$CD28$^-$ within effector memory (CD45RA$^-$CCR7$^-$) CD4$^+$ and **E**) effector memory CD8$^+$ T cells. * P<0.05, ** P<0.01, ***P<0.001, ****P<0.0001.

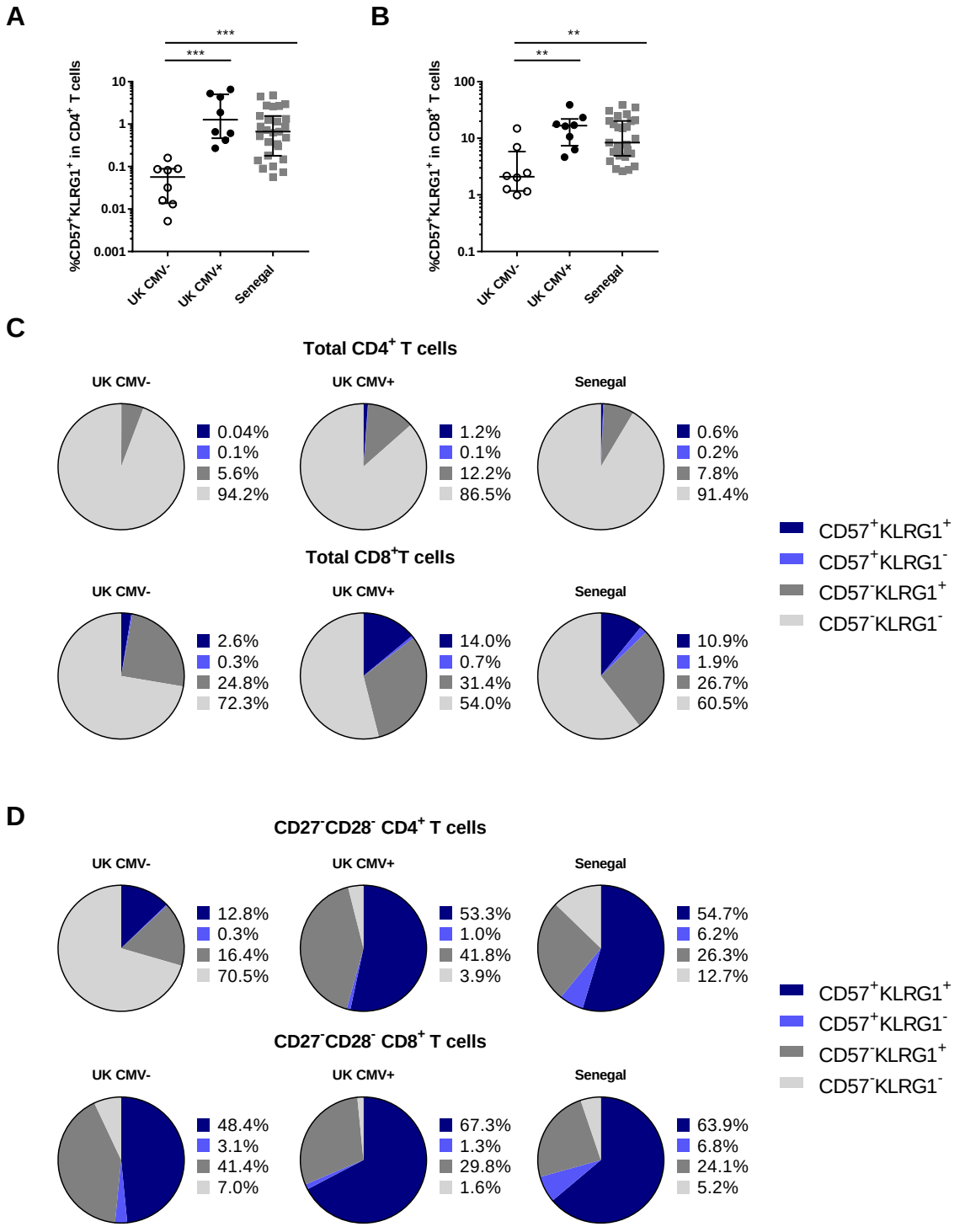

Figure 7.6. Increased CD57⁺KLRG1⁺ T cells in CMV+ individuals

Representative frequencies of CD57⁺KLRG1⁺ double-positive cells within **A**) total CD4⁺ T cells and **B**) total CD8⁺ T cells. Kruskal-Wallis analyses with Dunn's post-comparison tests. ** P<0.01, *** P<0.001. Medians and IQRs shown. **C**) Subsets based on the expression of CD57 and KLRG1 in total CD4⁺ (top row) or CD8⁺ (bottom row) T cells in each group. **D**) Subsets based on the expression of CD57 and KLRG1 on CD27⁻CD28⁻CD4⁺ (top row) or CD27⁻CD28⁻CD8⁺ (bottom row) T cells in each group.

7.3.3. Negative correlation between CMV-associated T cell phenotypes and vaccine responses

The proportion of $CD4^+$ T cells expressing both CD57 and KLRG1 was negatively associated with the T cell responses (peak IFNγ ELISpot) to vaccination in the UK cohort but not in in the Senegalese cohort (Figure 7.7A, Spearman r:-0.66, P=0.0085 in the UK cohort and r:-0.01, P=0.96 in the Senegalese cohort). The frequency of $CD57^+KLRG1^+$ $CD4^+$ T cells was also negatively associated with antibody responses to vaccination (Ebola GP-specific IgG measured by ELISA at M+28) in both the UK and Senegalese cohorts (Figure 7.7B, r:0.65, P=0.011 for UK and r:-0.39, P=0.044 for Senegal, r:-0.50 P=0.0008 overall). CMV IgG titre was positively associated with the frequency of $CD57^+KLRG1^+$ $CD4^+$ T cells (Figure 7.7C) in the UK (r:0.69, P=0.0054) and Senegalese cohorts (r:0.46, P=0.018) as well as the whole data set (r:0.63 P<0.0001). CMV IgG titres were also positively associated with the expansion of $CD27^-CD28^-$ cells within the $CD4^+$ subset (Figure 7.8A). However, the association between this subset and vaccine responses was much weaker. There was a negative association between this subset and peak vaccine-specific T cells in the UK cohort (Figure 7.8B, r:-0.59 P=0.023) and peak antibody responses in the whole data set (Figure 7.8C, r:-0.31 P=0.045) but no other associations. Within the $CD8^+$ T cell subset, the frequency of $CD57^+KLRG1^+$ T cells was only weakly associated with CMV IgG titres in the total data set (Figure 7.8D, r:0.37 P=0.019) and there were no associations with vaccine responses (Figure 7.8E, 7.8F). Equally, the frequency of $CD27^-CD28^-$ $CD8^+$ T cells was only weakly associated with CMV IgG titre (Figure 7.8G, UK: r:0.56 P=0.032, all data: r:0.38 P=0.015) and there were no associations with vaccine responses (Figure 7.8H, 7.8I).

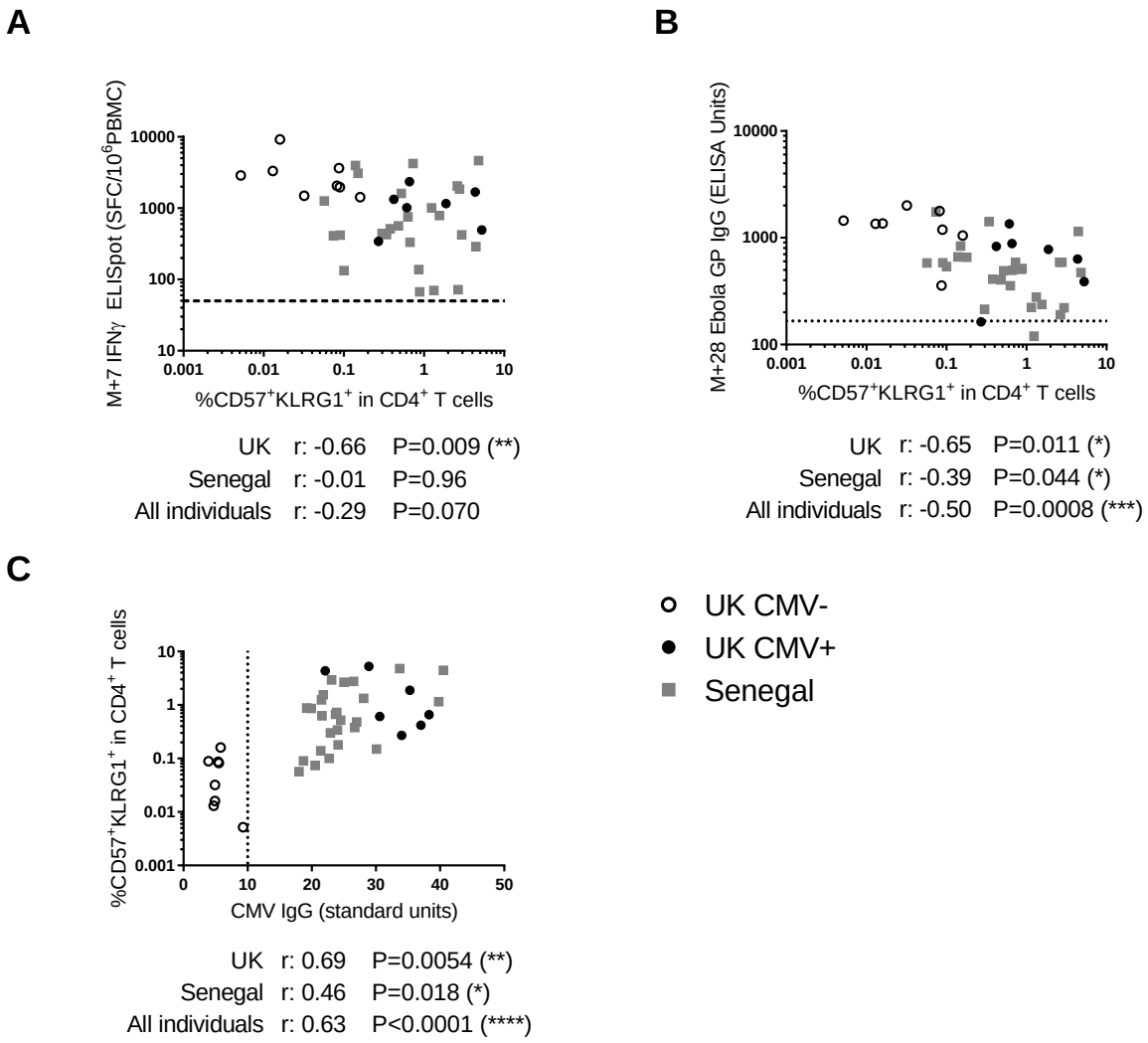

Figure 7.7. Association between CD57⁺KLRG1⁺ frequencies within CD4⁺ T cells and reduced vaccine responses

Relationship between the proportion of CD57⁺KLRG1⁺ CD4⁺ T cells and: **A**) Peak IFNγ ELISpot responses; **B**) Peak antibody responses; **C**) CMV IgG titre. Dashed lines indicate ELISpot lower limit of detection (50 SFC/10^6 PBMC), dotted lines indicate seropositive cut-off for Ebola GP (166 EUs) or CMV (10 standard units) ELISAs.

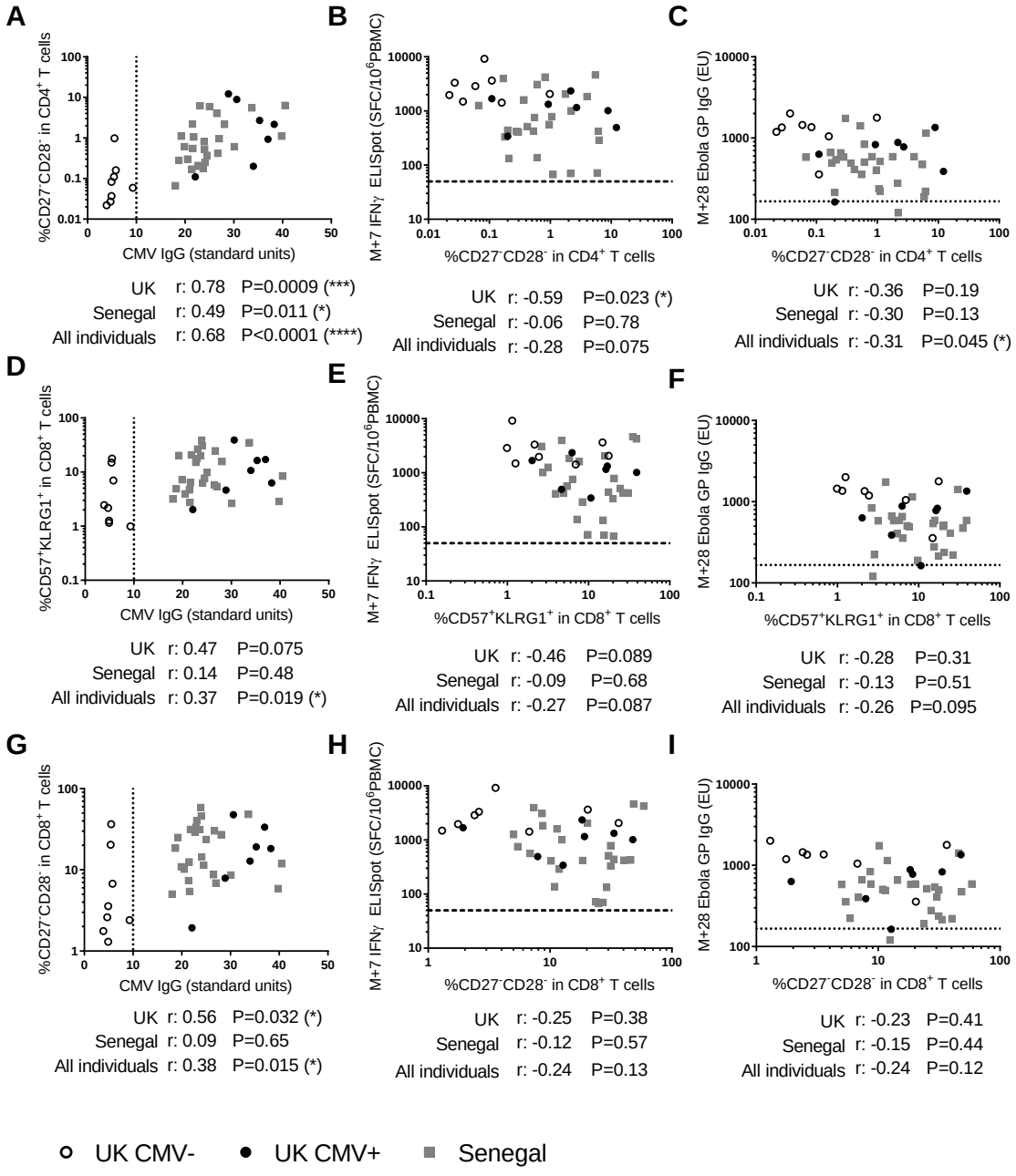

Figure 7.8. Associations between other T cell frequencies and vaccine responses
Relationship between the proportion of $CD27^-CD28^-$ $CD4^+$ T cells and: **A**) CMV IgG titre; **B**) Peak IFNγ ELISpot; **C**) Peak antibody responses. Relationship between the proportion of $CD57^+KLRG1^+$ $CD8^+$ T cells and: **D**) CMV IgG titre; **E**) Peak IFNγ ELISpot; **F**) Peak antibody responses. Relationship between the proportion of $CD27^-CD28^-$ $CD8^+$ T cells and: **G**) CMV IgG titre; **H**) Peak IFNγ ELISpot; **I**) Peak antibody responses. Dashed lines indicate ELISpot LLOD (50 SFC/10^6 PBMC), dotted lines indicate seropositive cut-off for Ebola GP (166 EUs) or CMV (10 standard units) ELISAs.

7.3.4. Exposure to other potentially chronic pathogens

A number of other pathogens that can cause chronic or latent infections have previously been shown to impact frequencies of different immune cell subsets and may play a role in reduced responses to vaccination [584]. Serostatus for a range of pathogens that can cause chronic infections and may have influenced vaccine responses in both of these populations was assessed. This data was used to further investigate the potential involvement of CMV in the observed changes to T cell phenotype and reduction in vaccine responses. The proportion of individuals in each of the cohorts that were seropositive for 17 different pathogens was determined using a multiplex assay (antigens tested are detailed in Table 2.9. Details of how seropositivity was determined for pathogens where multiple antigens were tested are included in Chapter 2.4.20. CMV seropositivity was determined by ELISA and confirmed by the multiplex results (Figure 7.9). Anti-schizont ELISAs were used to measure antibodies to *P. falciparum* as discussed in Chapter 5.3.4. Median titres and frequencies of individuals seropositive for each of the antigens are summarised in Table 7.2. EBV, HHV-7 and BKV were particularly prevalent in the UK cohort, with only one seronegative individual for each. The pattern of seroprevalence was very different in Senegal. Seroprevalence of EBV and BKV was comparably high, however most or all volunteers were also positive for HSV-1, *H. pylori* and MCV. In addition to *P. falciparum* (UK: 0% positive, Senegal: 48%, discussed in Chapter 5.3.4) and CMV (UK: 47% Senegal: 100%), HSV-1 (UK: 27%, Senegal: 95%), *H. pylori* (UK: 13%, Senegal: 95%), HBV (UK: 0%, Senegal: 63%) and HHV-7 (UK: 93%, Senegal: 56%) were the pathogens with the most striking differences in seroprevalence between the two cohorts.

Antibody titres against antigens for each of these pathogens are shown in Figure 7.10. Vaccine responses (peak Ebola GP IgG measured by ELISA at M+21/M+28 and Ebola GP-specific T cell responses measured by IFNγ ELISpot at M+7) were stratified by exposure to each of the

pathogens that showed significant differences between populations and compared with responses stratified by *P. falciparum* and CMV serostatus (Figure 7.11). Only *P. falciparum* and CMV seropositivity were clearly associated with reduced antibody or T cell responses in either of the cohorts.

Although high, this HBV seroprevalence is in line with what has previously been reported in Senegal [487]. HBV seropositivity was determined by positive responses against both the HBV core antigen (HBcAg) and HBV antigen e (HBeAg). Presence of antibodies against these antigens indicates previous exposure to HBV. However, all volunteers screened negative for HBV surface antigen (HBsAg) prior to enrolment and therefore did not have active hepatitis B infections. There were also significant differences in titres between the two cohorts for some other antigens including some from KSHV, *T. gondii*, *C. trachomatis* and HTLV-1. However, despite the difference in titres, most individuals in each population did not have titres above the positive cut-off value, indicating that the difference may be caused by increased background or cross-reactivity in the Senegalese population. The same is true for HIV: Although the anti-gag and anti-env titres were significantly higher in the Senegalese cohort than the UK cohort, none of these individuals were seropositive for HIV and were screened negative for HIV at enrolment. Three antigens from CMV (pp28, pp52 and pp150N) were also included in the multiplex assay and the results correlated well with the ELISA results (Figure 7.12).

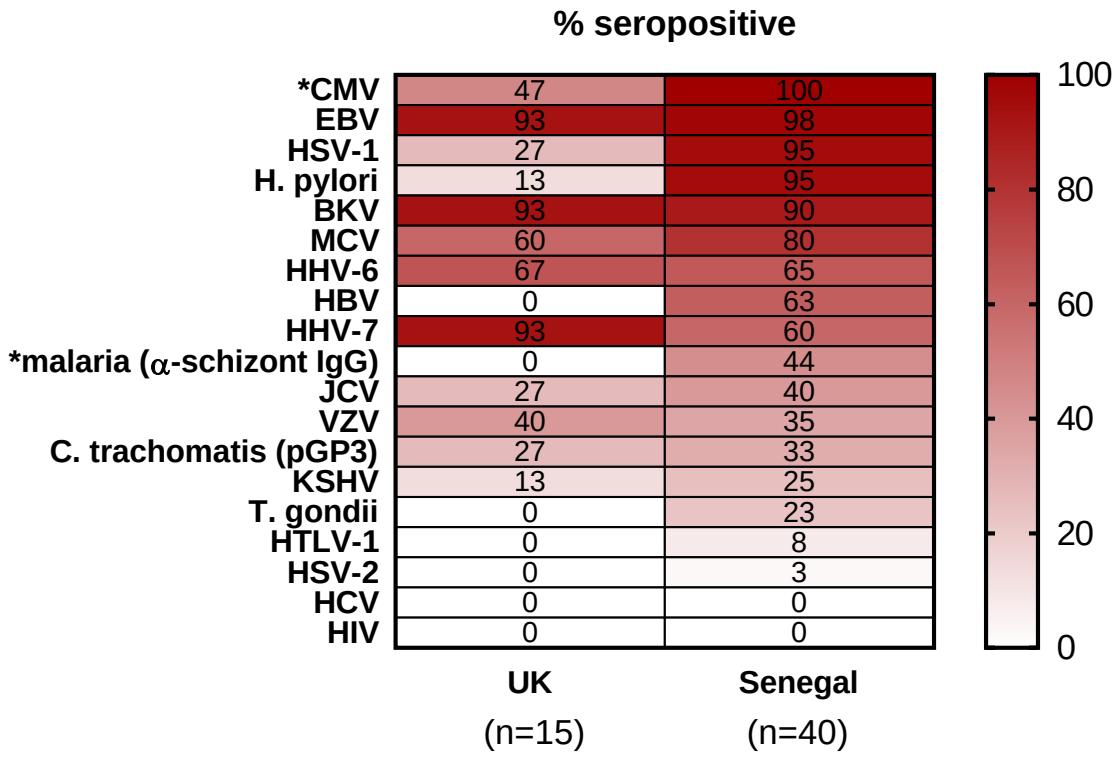

Figure 7.9. Seropositivity rates in the UK and Senegalese cohorts
Percentage of individuals in each cohort seropositive for each of the pathogens as measured by the multiplex serology or ELISA (*).

Table 7.2. Summary of multiplex serology data

Multiplex serology results for all 40 Senegalese volunteers and 15 UK volunteers (malaria-exposed Kenyan from UK cohort was excluded for these analyses). IQR: interquartile range.

Pathogen	Antigen	Seropositive, *n* (%)		Titres				Seropositive cut-off	UK vs Senegalese Mann-Witney P-value
				UK		Senegalese			
		UK (n=15)	Senegalese (n=40)	Median	IQR	Median	IQR		
HSV-1	**1gG**	4 (27%)	38 (95%)	8	5-1887	3573	2656-4681	150	**<0.0001**
HSV-2	**2mgG**	0 (0%)	1 (3%)	1	1-6	3	1-6.75	150	0.55
VZV	**gEgI**	6 (40%)	14 (35%)	32	26-97	51.5	21.75-95	60	0.94
EBV	**VCAp18**	15 (100%)	40 (100%)	9205	4732-10280	4634	3081-9942	250	0.22
	EBNA1	14 (93%)	35 (88%)	1783	1434-4935	3680	837.3-6201	200	0.49
	ZEBRA	9 (60%)	11 (28%)	433	116-979	82.5	21.75-228.5	200	**0.026**
	EAD	7 (47%)	14 (35%)	190	26-831	113	21.75-311.8	200	0.41
CMV	**pp150N**	7 (47%)	35 (88%)	18	4-715	1194	366.5-3553	200	**0.0003**
	pp52	8 (53%)	38 (95%)	327	12-5473	3263	1087-4661	200	0.075
	pp28	7 (47%)	35 (88%)	25	7-822	679.5	311-1387	200	**0.041**
HHV-7	**U14**	14 (93%)	24 (60%)	368	181-704	129	72.25-241	100	**0.0006**
KSHV	**LANA**	2 (13%)	9 (23%)	1	1-9	15	25-44.75	150	**0.0004**
	K81	0 (0%)	7 (18%)	59	54-114	93	51.25-189.3	250	0.43
HHV-6	**IE1B**	8 (53%)	19 (48%)	131	88-320	98	55.25-257.8	100	0.39
	IE1A	4 (27%)	16 (40%)	76	30-101	76	41.5-142.3	100	0.37
	p101k	3 (20%)	6 (15%)	14	4-27	6.5	1-35	50	0.39
HBV	**HBc**	0 (0%)	25 (63%)	1	1-3	673	6-3707	100	**<0.0001**
	HBe	0 (0%)	25 (63%)	5	2-7	474	12-2625	100	**<0.0001**
HCV	**Core**	1 (7%)	1 (3%)	1	1-4	1	1-1	100	0.61
	NS3	0 (0%)	0 (0%)	1	1-2	2.5	1-7.75	50	0.088
T. gondii	**p22**	0 (0%)	6 (15%)	1	1-1	3.5	1-24.5	50	**0.0012**
	sag1	0 (0%)	8 (20%)	6	3-11	17.5	11.25-39.5	50	**<0.0001**
HTLV-1	**gag**	0 (0%)	3 (8%)	1	1-5	15	1-49.5	100	**0.0023**
	env	0 (0%)	0 (0%)	6	1-8	9	5.25-14.75	50	**0.011**
HIV	**gag**	0 (0%)	3 (8%)	2	1-9	12.5	7-31.5	200	**0.001**
	env	0 (0%)	0 (0%)	7	2-9	15	6.25-25	100	**0.0086**
BKV	**VP1**	14 (93%)	36 (90%)	2321	873-5905	3135	1140-5863	250	0.90
JCV	**VP1**	4 (27%)	16 (40%)	112	33-287	189.5	88.25-479	250	0.092
MCV	**VP1**	9 (60%)	32 (80%)	729	63-4659	4212	390.3-6193	250	0.096
C. trachomatis	**mompD**	0 (0%)	5 (13%)	7	1-21	20.5	11-54.75	100	**0.006**
	mompA	0 (0%)	6 (15%)	8	4-9	13	5.25-51.25	100	**0.036**
	tarpDF2	2 (13%)	5 (13%)	1	1-35	10	1-46.25	100	0.16
	tarpDF1	0 (0%)	18 (45%)	2	1-39	158	4.75-536	200	**0.001**
	PorB	0 (0%)	2 (5%)	13	9-20	23	12.5-38	60	**0.022**
	pGP3	4 (27%)	13 (33%)	1	1-20	5.5	1-371	200	0.27
H. pylori	**CagA**	3 (20%)	34 (85%)	6	1-40	8330	1220-11740	300	**<0.0001**
	VacA	3 (20%)	31 (78%)	10	4-34	309	117.8-1076	100	**<0.0001**
	OMP	1 (7%)	35 (88%)	10	2-48	1279	534.3-5086	150	**<0.0001**
	GroEL	2 (13%)	31 (78%)	1	1-3	2241	134-3890	80	**<0.0001**
	Catalase	2 (13%)	10 (25%)	14	1-19	29.5	13.5-212	120	**0.003**
	Urea	0 (0%)	9 (23%)	4	1-15	1.5	1-57.5	100	0.98

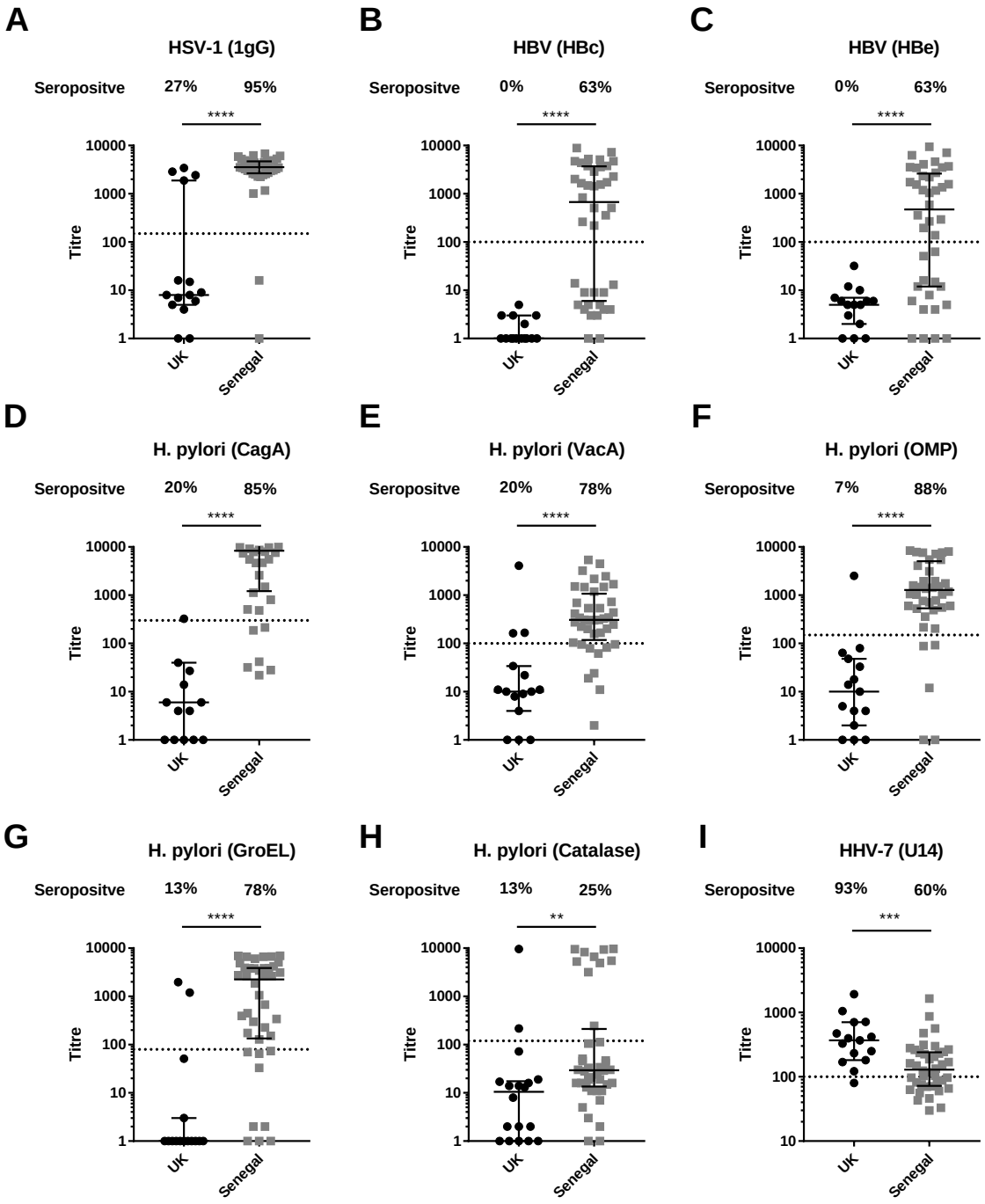

Figure 7.10. Antibody titres against pathogens that differ in seroprevalence between the UK and Senegalese cohorts

Antibody titres measured in the multiplex serology assay for UK (n=15) and Senegalese (n=40) cohorts. Differences in titres between the two cohorts are shown for antigens that were significantly different between the two cohorts and had a seroprevalence of >50% in one or both of the populations. Dotted lines indicate seropositive cut-off values for each of the antigens. Mann-Witney analyses. * P<0.05, ** P<0.01, *** P<0.001, **** P<0.0001. Exact P-values are given in Table 7.2.

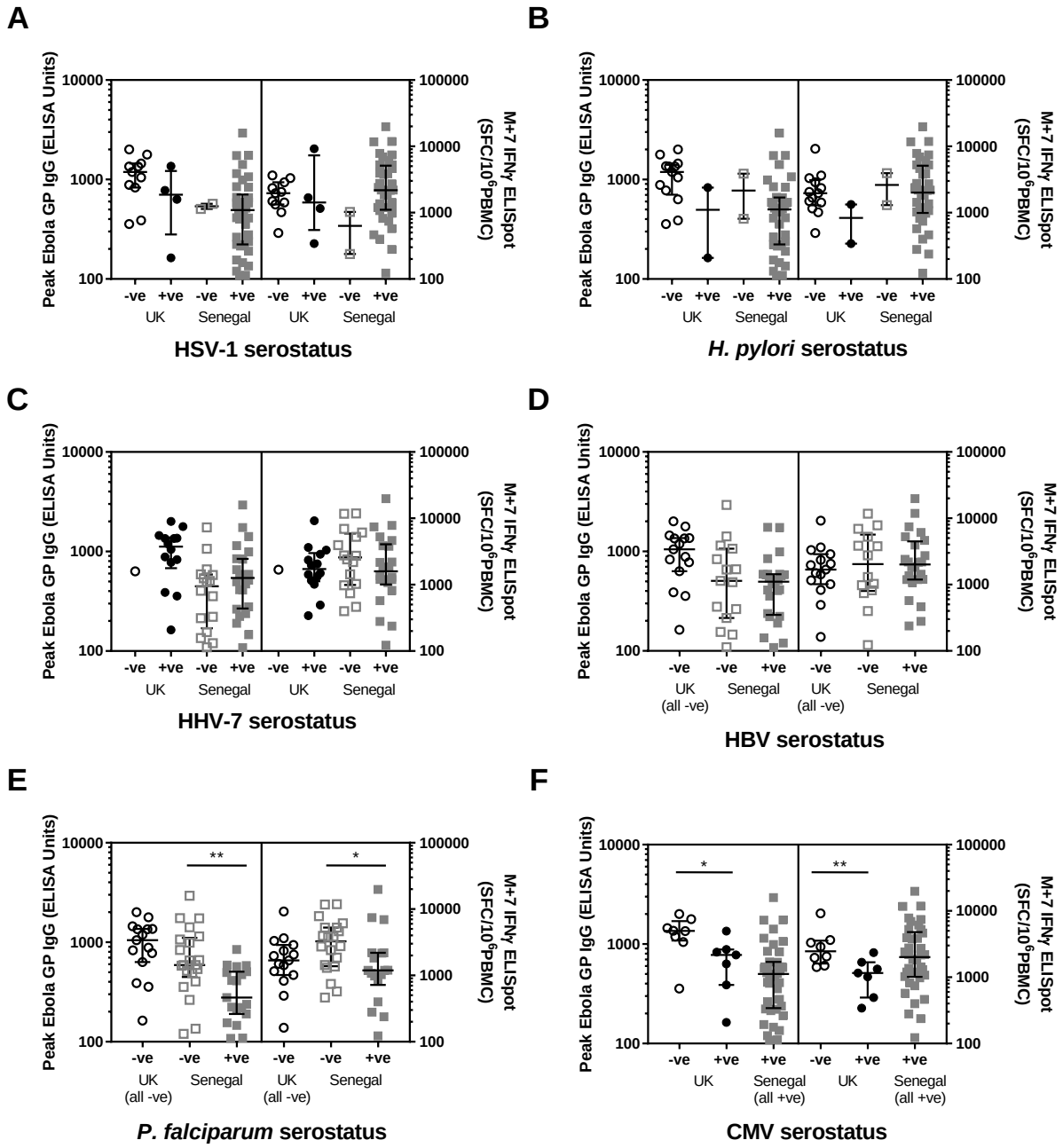

Figure 7.11. Stratification of vaccine responses by pathogen exposure

Peak Ebola GP IgG responses (M+21/M+28, left Y-axes) and M+7 Ebola IFNγ ELISpot responses (right Y-axes) in each cohort stratified by serostatus for: **A**) HSV-1; **B**) H. pylori; **C**) HHV-7; **D**) HBV; **E**) *P. falciparum*; **F**) CMV. Mann-Witney analyses between negative and positive volunteers within each cohort. * P<0.05, ** P<0.01.

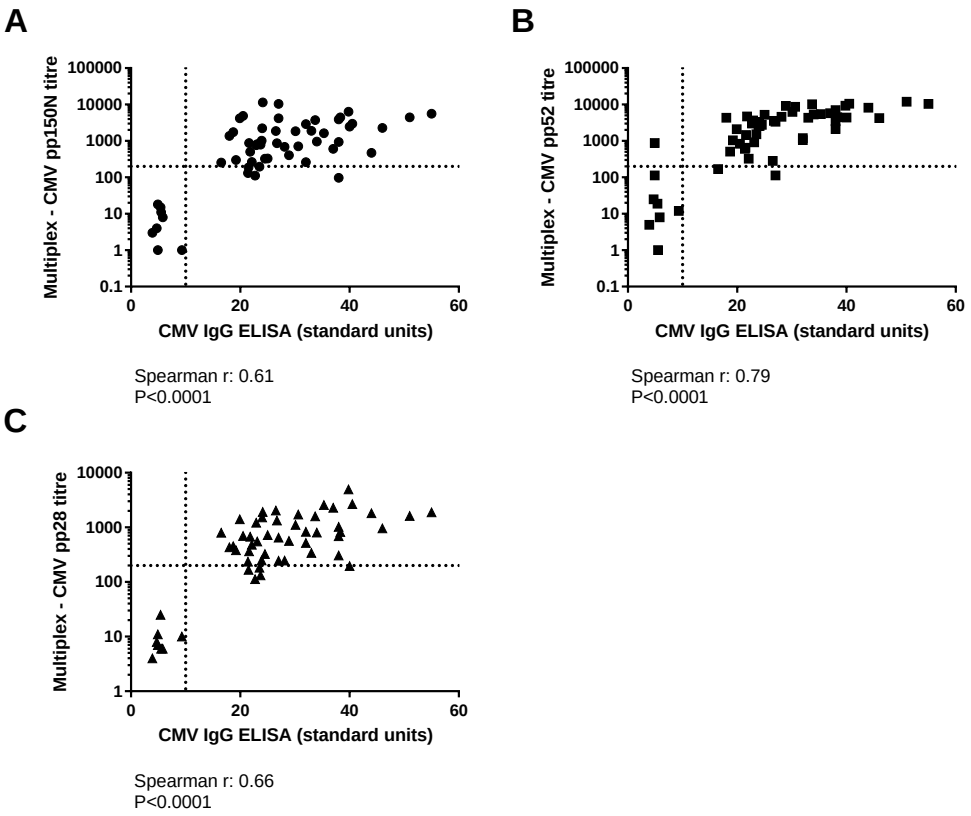

Figure 7.12. Relationship between CMV titres measured by ELISA and multiplex assay
Relationship between CMV-specific IgG measured by ELISA and: **A**) Anti-CMV pp150N antibody; **B**) anti-CMV pp52 antibody; **C**) Anti-CMV pp28 antibody. Data include both UK and Senegalese cohorts. Spearman rank analyses. Dotted lines show seropositive cut-off values.

As anti-schizont serostatus was associated with reduced vaccine responses in analyses conducted in Chapter 5, a multiple linear regression analysis was used to determine the relative contributions of CMV serostatus, anti-schizont serostatus and cohort to the peak ELISpot and antibody responses after ChAd3-MVA-EBO-Z vaccination. The independent variables were CMV serostatus, anti-schizont serostatus and cohort (UK vs Senegal). The dependent variable was peak ELISpot response (summed GP-specific SFC/106 PBMC at M+7) for the first analysis and peak antibody response (Ebola GP-specific IgG at M+21/M+28) for the second analysis. The T cell analysis was conducted for all 16 UK volunteers and 38/40 Senegalese volunteers as two individuals did not have ELISpot data at this time point. The antibody analysis was conducted for all UK and Senegalese volunteers. None of these factors independently predicted peak T cell responses (Table 7.3). However, both CMV serostatus and anti-schizont serostatus predicted peak antibody responses (Table 7.4). The immune markers examined here were also added to

the model (proportion of $CD57^+KLRG1^+$ or $CD27^-CD28^-$ $CD4^+$ and $CD8^+$ T cells). However, these markers were not independently associated with the T cell and antibody responses to vaccination and both anti-schizont and CMV serostatus were still the only predictors of vaccine responses in these models (Tables 7.5 and 7.6).

Table 7.3. Multiple linear regression for effects on peak T cell response
Dependent variable: M+7 GP ELISpot responses (summed pools, SFC/10^6 PBMC)

Variable	B	SE	|t|	P value
Intercept	3245	1258	2.579	**0.0129**
Senegal vs UK	2768	1489	1.859	0.0689
CMV serostatus	-2019	1780	1.134	0.262
Anti-schizont serostatus	-1158	1156	1.001	0.3215

Table 7.4. Multiple linear regression for effects on peak antibody response
Dependent variable: M+21/28 GP-specific IgG (ELISA Units)

Variable	B	SE	|t|	P value
Intercept	1319	172.6	7.638	**<0.0001**
Senegal vs UK	71.37	202.9	0.3518	0.7264
CMV serostatus	-543.4	244.1	2.226	**0.0304**
Anti-schizont serostatus	-490.4	154.6	3.172	**0.0025**

Table 7.5. Multiple linear regression for effects on peak T cell response – immune markers added
Dependent variable: M+7 GP ELISpot responses (summed pools, SFC/10^6 PBMC)

Variable	B	SE	|t|	P value
Intercept	3341	1478	2.261	0.0305
Senegal vs UK	4157	1836	2.264	0.0303
CMV serostatus	-3556	2471	1.439	0.1595
Anti-schizont serostatus	-1424	1748	0.8147	0.4211
$CD57^+KLRG1^+$ CD4	426.1	422.4	1.009	0.3205
$CD27^-CD28^-$ CD4	-23.57	33.43	0.7051	0.4857
$CD57^+KLRG1^+$ CD8	157.6	212.8	0.7408	0.464
$CD27^-CD28^-$ CD8	-46.86	157.2	0.298	0.7676

Table 7.6. Multiple linear regression for effects on peak antibody response – immune markers added

Dependent variable: M+21/28 GP-specific IgG (ELISA Units)

Variable	**B**	**SE**	|t|	P value
Intercept	1366	153.2	8.918	<0.0001
Senegal vs UK	48.28	187.8	0.2571	0.7986
CMV serostatus	-668.4	255	2.621	0.0129
Anti-schizont serostatus	-441.9	168.2	2.627	0.0127
$CD57^+KLRG1^+$ CD4	17.84	43.71	0.4082	0.6856
$CD27^-CD28^-$ CD4	-2.989	3.372	0.8865	0.3814
$CD57^+KLRG1^+$ CD8	-19.73	21.78	0.906	0.3712
$CD27^-CD28^-$ CD8	18.7	16.04	1.166	0.2516

To examine the potential associations between the pathogens tested for and the expansion of $CD57^+KLRG1^+$ and/or $CD27^-CD28^-$ T cells, the seroconversion profile for each individual was compared (Figure 7.13). All CMV+ individuals in the UK had frequencies of $CD27^-CD28^-$ and/or $CD57^+KLRG1^+$ $CD4^+$ T cells greater than 0.2% and all CMV- individuals had frequencies less than 0.2%. The serostatus of other pathogens was assessed in relation to this. No other pathogen was exclusive to either group within this cohort, although two Senegalese individuals did not exhibit an expansion of $CD27^-CD28^-$ or $CD57^+KLRG1^+$ $CD4^+$ T cells despite being CMV+.

A previous study showed that carriage of HHV-6 may also be associated with the expansion of $CD27^-CD28^-$ T cells [585]. For this reason, the association between HHV-6 seropositivity vaccine responses, the expansion of $CD27^-CD28^-$, and the expansion of $CD57^+KLRG1^+$ CD4 and CD8 T cells was also assessed (Figure 7.14). HHV-6 was not associated with a reduction in vaccine-specific antibody or T cell responses in either cohort. Equally, there was no association between HHV-6 status and expansion of $CD27^-CD28^-$ or $CD57^+KLRG1^+$ T cells in either cohort.

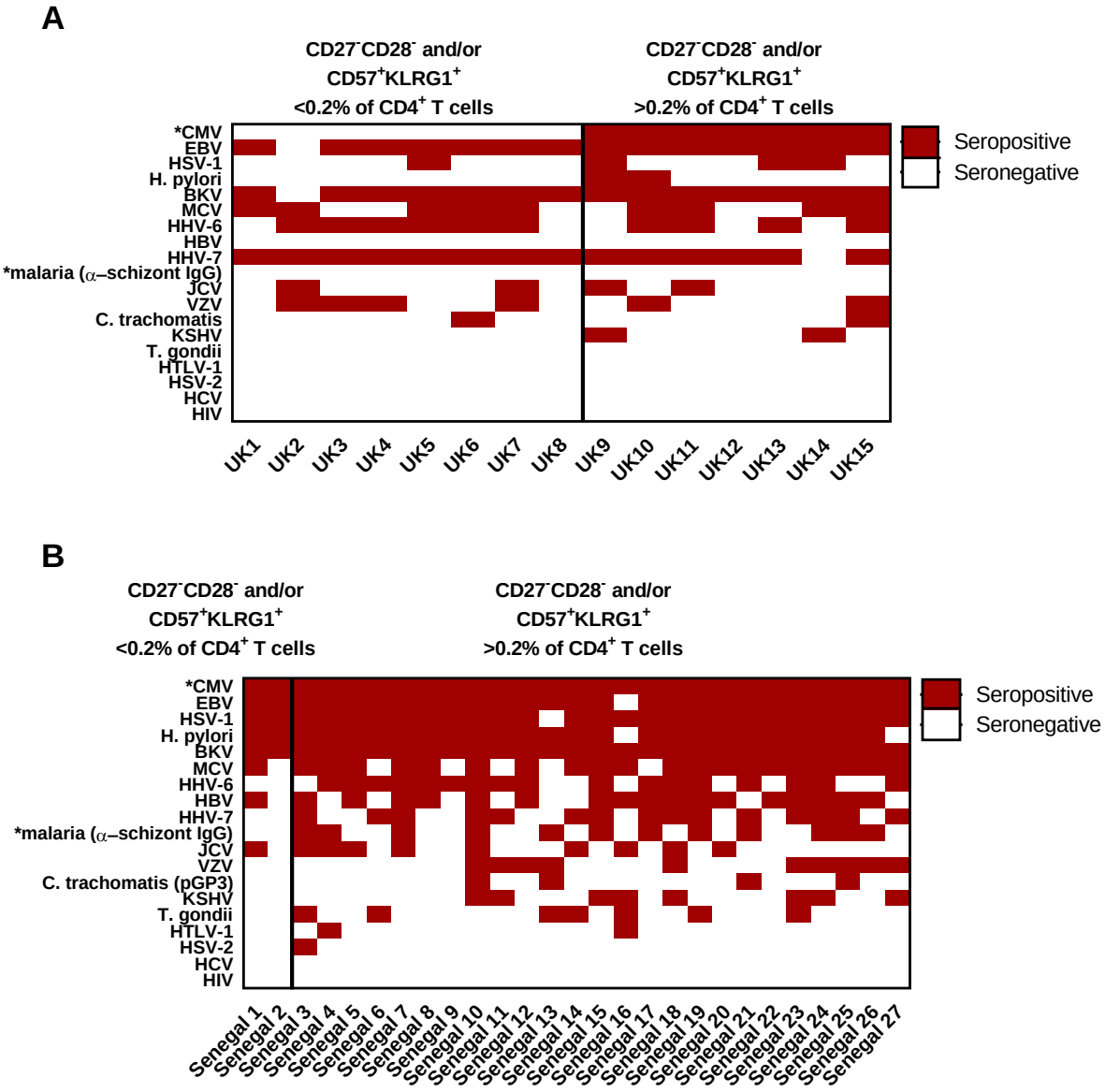

Figure 7.13. Pathogen exposure and expansion of $CD27^{-}CD28^{-}$ or $CD57^{+}KLRG1^{+}$ T cells
Serostatus of individuals with T cell data (UK n=15, Senegal n=27) in each cohort. **A**) Individuals in the UK cohort were split by CMV serostatus and expansion of T cell populations associated with CMV seropositivity. Serostatus for all other pathogens tested was then marked for each individual to assess association with the expanded T cell subsets. **B**) Serostatuses illustrated for the Senegalese cohort in the same way as the UK cohort.

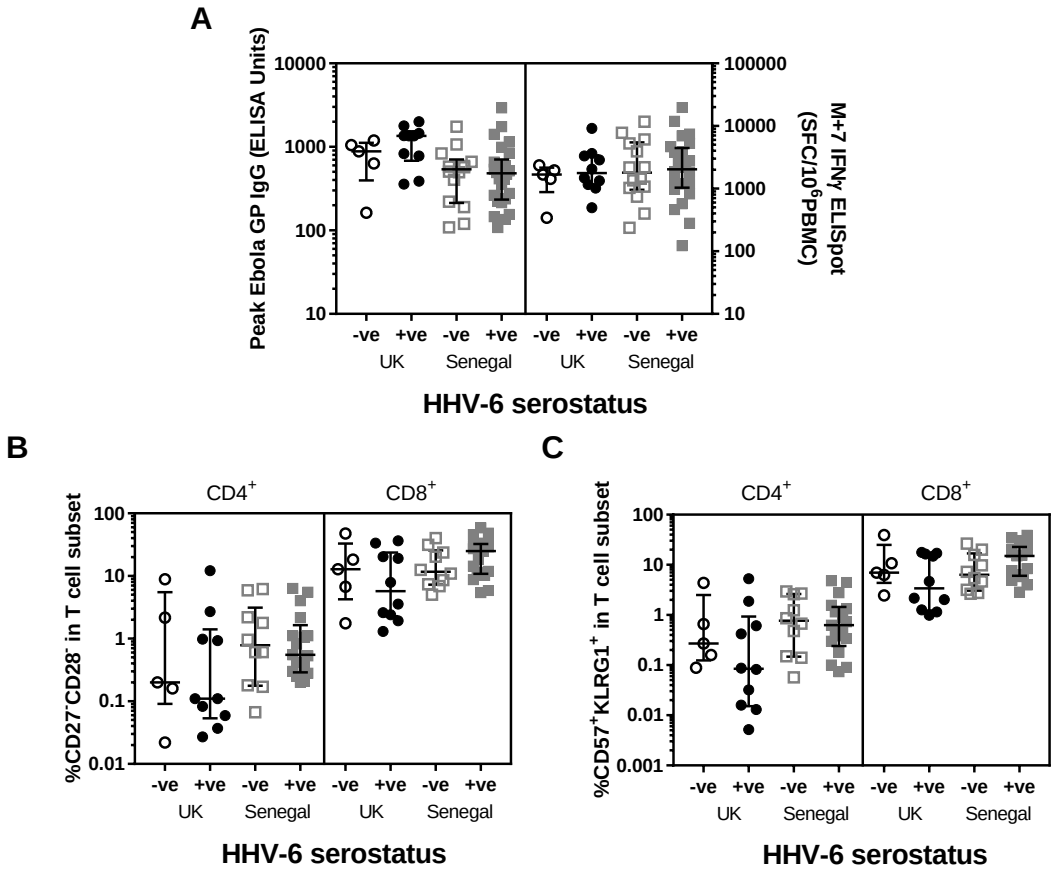

Figure 7.14. Human-herpes virus 6 (HHV-6)
A) Peak Ebola GP IgG responses (M+21/M+28, left Y-axes) and M+7 Ebola IFNγ ELISpot responses (right Y-axes) in each cohort stratified by serostatus for HHV-6. **B**) Frequency of $CD27^-CD28^-$ T cells within $CD4^+$ and $CD8^+$ subsets in HHV-6 seronegative and seropositive individuals in each cohort. **C**) Frequency of $CD57^+KLRG1^+$ T cells within $CD4^+$ and $CD8^+$ subsets in HHV-6 seronegative and seropositive individuals in each cohort. No significant differences between HHV-6 negative and positive individuals in each cohort by Mann-Witney tests for any of the analyses.

7.3.5. HLA types

HLA-typing was only conducted in the UK cohort as consent was not sought for genetic testing in the Senegalese cohort. The presence of different alleles within the HLA-A, -B, -C, -DR and –DQ loci was determined for volunteers that either had expanded $CD57^+KLRG1^+$ or $CD27^-CD28^-$ $CD4^+$ T cells (CMV+) or did not (CMV-) to assess HLA-type as a potential confounding factor (Figure 7.15). No individual HLA alleles were over-represented in either group, suggesting that HLA-types were not a major factor confounding the result that individuals in the CMV+ group had

reduced responses to vaccination. As the Senegalese cohort were not HLA-typed, it is not known if particular HLA types were associated with reduced vaccine responses in that cohort.

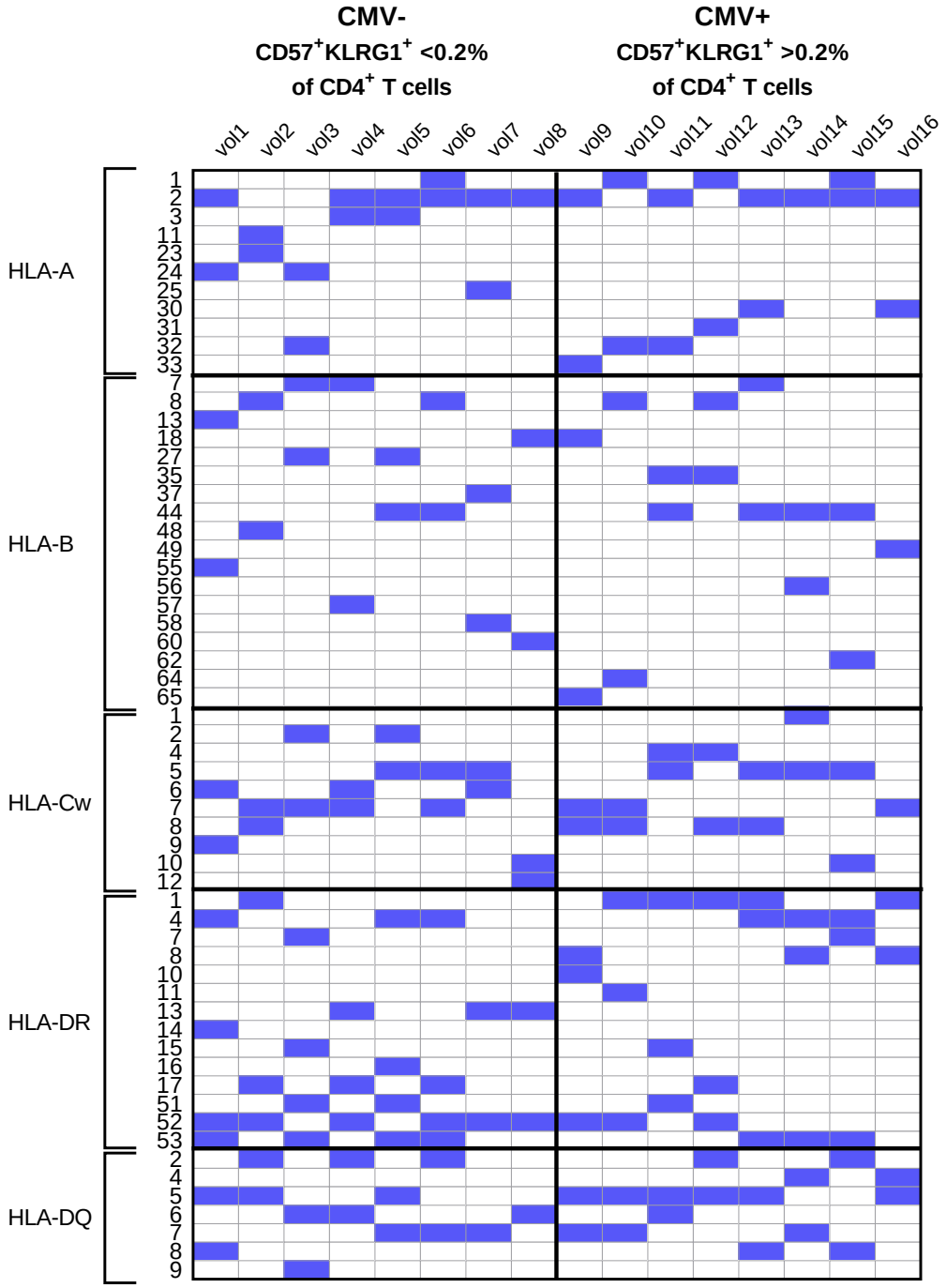

Figure 7.15. HLA types in UK adults
HLA types in all 16 of the UK cohort split by presence or absence of the expanded population of $CD27^{-}CD28^{-}$ or $CD57^{+}KLRG1^{+}$ $CD4^{+}$ T cells as in Figure 6.12. Numbers on the left hand side are different alleles. Presence of a particular allele is indicated for each individual by a blue rectangle.

7.3.6. Antigen-specific T cells are phenotypically different in CMV- and CMV+ individuals

The primary assays used for detecting antigen-specific T cells in these clinical trials were IFNγ ELISpot and ICS analysing the frequencies of $CD4^+$ and $CD8^+$ T cells producing IFNγ, IL-2, TNFα or expressing CD107a after stimulation with Ebola GP. As shown earlier in this chapter, cytokine-secreting T cell responses were lower in CMV+ individuals. It was important to investigate whether this was a reduction in the total frequency of vaccine-specific T cell responses, a functional impairment, or an induction of different phenotypes that were not secreting IFNγ, TNFα or IL-2 and therefore were not detected by the ELISpot or ICS assays used. To obtain a broader picture of the total antigen-responsive T cell population irrespective of cytokine secretion, the AIM assay (development of which is described in Chapter 6) was used to detect and phenotype antigen-specific T cell responses against CMV (pp65) and Ebola GP in the UK cohort.

As shown in Figure 6.2, there were no differences in the frequencies of GP-specific $CD4^+$ T cells detected using OX40/CD25 compared with OX40/PDL1 or in the frequencies of GP-specific $CD8^+$ T cells detecting using OX40/CD25 compared with CD25/CD107a. Additionally the expression of each of these marker combinations was highly correlated. For the main analysis of antigen-specific T cell phenotypes the OX40/CD25 marker combination was used in $CD4^+$ T cells in order to include all antigen-responsive T cells (including Tregs) and therefore analyse phenotypic differences in the total antigen-responsive T cell populations between CMV- and CMV+ individuals. The main analysis for the $CD8^+$ subset was also conducted using this marker combination for consistency and because the OX40/CD25 population was more distinctive than the CD25/CD107a population in this subset therefore this population was easier to gate and analyse accurately.

Representative populations detected in CMV- and CMV+ individuals are shown in Figure 7.16A. The proportions of $CD4^+$ and $CD8^+$ T cells expressing OX40 and CD25 in response to stimulation with vaccine antigen (Ebola GP) or CMV (pp65) were assessed (Figure 7.16B, 7.16C). Background levels of expression in unstimulated cells were low (median 0.123% IQR[0.069 – 0.313] for $CD4^+$ and 0.031% IQR[0.017 – 0.044] for $CD8^+$ T cells). Significant CMV-specific T cell responses were detected in CMV+ individuals compared with CMV- individuals ($CD4^+$: P=0.0002, $CD8^+$: and P=0.0002), in which the proportion of AIM^+ cells was comparable to background. The frequency of GP-specific $CD4^+$ and $CD8^+$ T cells seven days after MVA boost was not significantly different between CMV- and CMV+ individuals, although some CMV+ individuals had lower GP-specific $CD8^+$ T cell responses ($CD4^+$: median 0.853% for CMV- and 0.870% for CMV+ , $CD8^+$: median 0.731% for CMV- and 0.329% for CMV+). There were no significant differences in the GP-specific T cell frequencies in CMV- compared with CMV+ individuals in either $CD4^+$ (Figure 7.17A) or CD8+ (Figure 7.17B) T cell subsets at peak (M+7) or late (M+84) time points.

Antigen-specific T cells were further characterised by expression of CD57 and KLRG1. CMV-specific $CD8^+$ but not $CD4^+$ T cells were enriched for $CD57^+KLRG1^+$ cells compared with the total T cell subsets (Figure 7.18A, 7.18B P=0.46 for $CD4^+$ and P=0.015 for $CD8^+$ T cells). This subset constituted around 40% of the CMV-specific $CD8^+$ T cell population. Both the GP-specific $CD4^+$ and $CD8^+$ T cells contained significantly higher proportions of $CD57^+KLRG1^+$ cells in CMV+ individuals than in CMV- individuals. This was only a small proportion (~1%) of the GP-specific $CD4^+$ T cells but there was a pronounced difference in the $CD8^+$ subsets at M+7, 19% of which were $CD57^+KLRG1^+$ in CMV+ individuals compared with only 5% in CMV- individuals (Figure 7.18C, 7.18D, P=0.015 for $CD4^+$ and P=0.0002 for $CD8^+$ T cells). As shown in Figure 7.17, one individual did not have detectable GP-specific $CD4^+$ T cells at M+7 and two individuals did not have detectable GP-specific $CD8^+$ T cells at M+84, therefore phenotypic analysis does not include data from these subjects. In both the $CD4^+$ and $CD8^+$ GP-specific T cells, the frequency of $CD57^+KLRG1^+$ cells in CMV+ individuals was highest at M+7 and reduced at later time points

(Figure 7.19). In contrast, the phenotypic compositions of the total T cell populations were more consistent, except that the proportion of $CD57^+KLRG1^+$ in total $CD8^+$ T cells was slightly reduced in CMV+ individuals at M+84 compared with M+7 and M+28. The frequency of $CD57^+KLRG1^+$ cells within GP-specific $CD4^+$ T cells was not significantly associated with either peak ELISpot responses (Figure 7.20A, r:-0.50, P=0.060) or peak antibody responses (Figure 7.20B, r:-0.30, P=0.28). The frequency of $CD57^+KLRG1^+$ cells within GP-specific $CD8^+$ T cells was negatively associated with both peak ELISpot responses (Figure 7.20C, r:-0.74, P=0.002) and peak antibody responses (Figure 7.20D, r:-0.58, P=0.038).

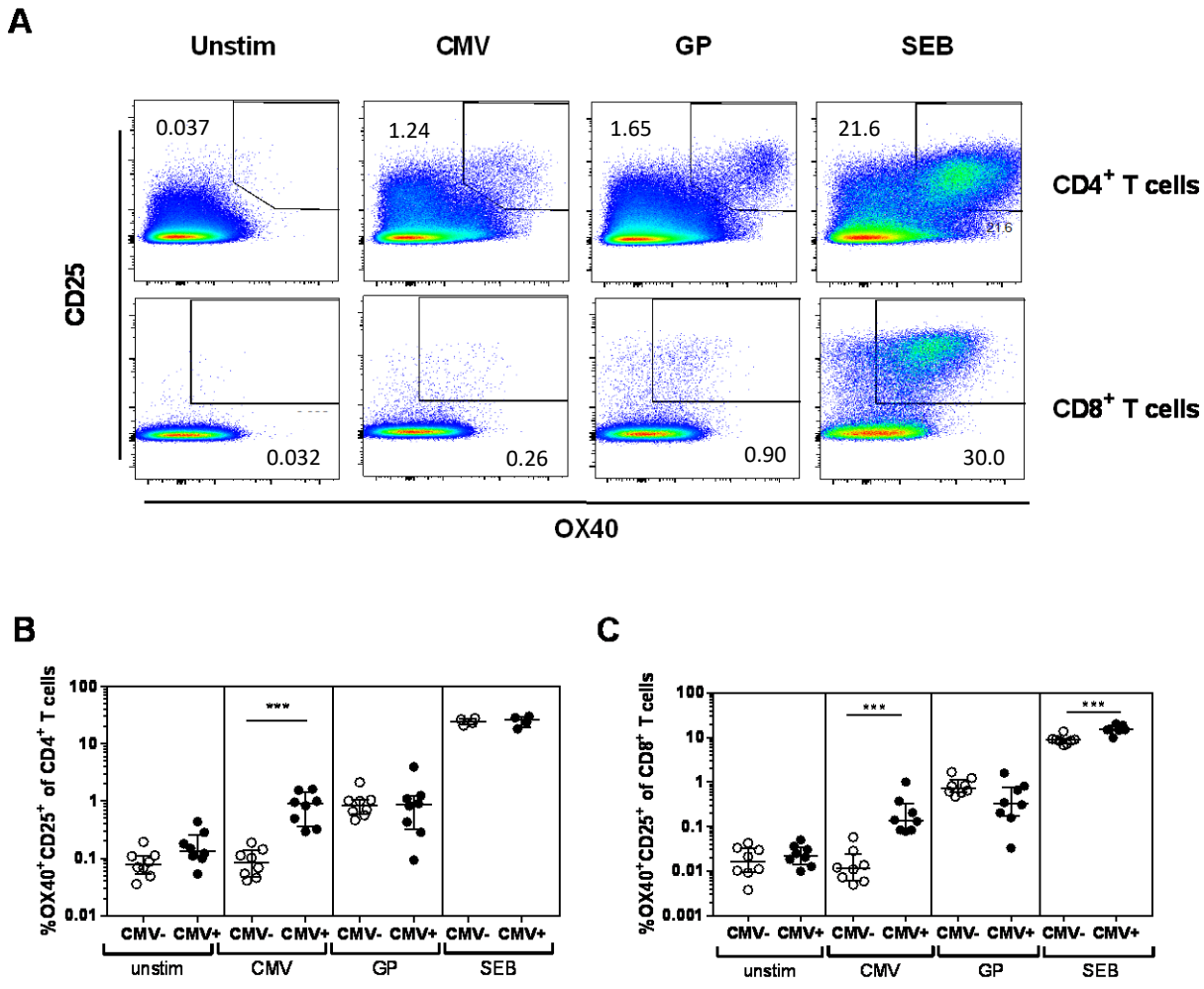

Figure 7.16. Detection of vaccine-specific T cells in CMV- and CMV+ individuals
A) Expression of activation-induced markers OX40 and CD25 on $CD4^+$ and $CD8^+$ T cells in PBMC that were unstimulated (unstim) or stimulated with CMV pp65, Ebola GP or SEB. Frequency of $OX40^+CD25^+$ cells in **B**) $CD4^+$ T cells and **C**) $CD8^+$ T cells in CMV- and CMV+ individuals. Mann-Whitney analyses. *** P<0.001.

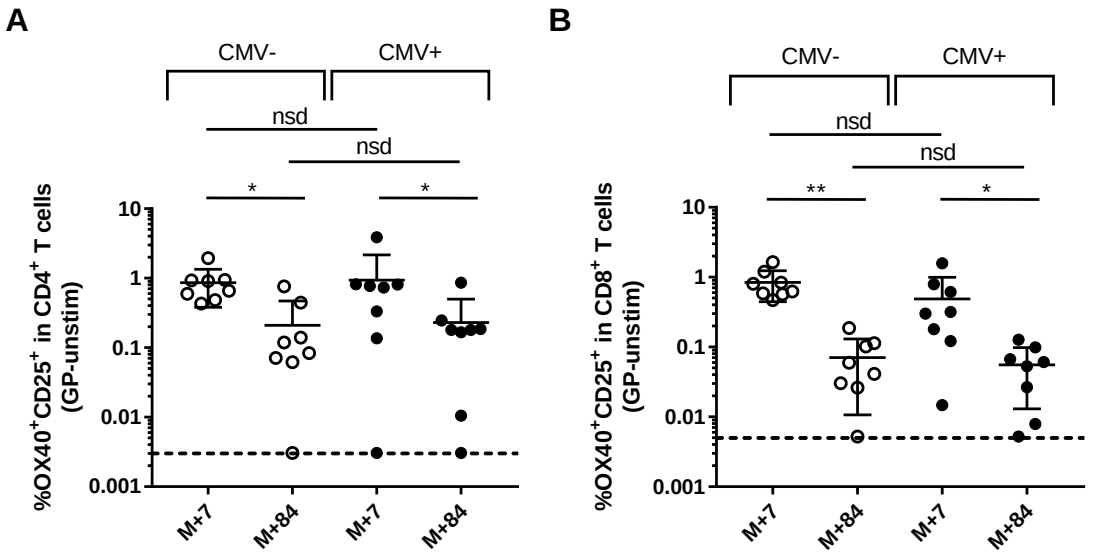

Figure 7.17. Peak and durable GP-specific T cell frequencies in CMV- and CMV+ individuals

Frequency of GP-specific cells in CMV- and CMV+ individuals (GP stimulated, %OX40$^+$CD25$^+$ after subtraction of frequency in unstimulated condition): **A**) Frequency in CD4$^+$ T cells. Wilcoxon matched-pairs analyses between time points for CMV- (P=0.016) and CMV+ individuals (P=0.023), Mann-Whitney analyses for comparison of CMV- and CMV+ individuals at M+7 (P=0.44) and M+84 (P=0.46). **B**) Frequency in CD8$^+$ T cells. Dashed line indicates the LLOD. Wilcoxon matched-pairs analyses between time points for CMV- (P=0.008) and CMV+ individuals (P=0.016), Mann-Whitney analyses for comparison of CMV- and CMV+ individuals at M+7 (P=0.065) and M+84 (P=0.82), nsd: no significant difference, * P<0.05, ** P<0.01.

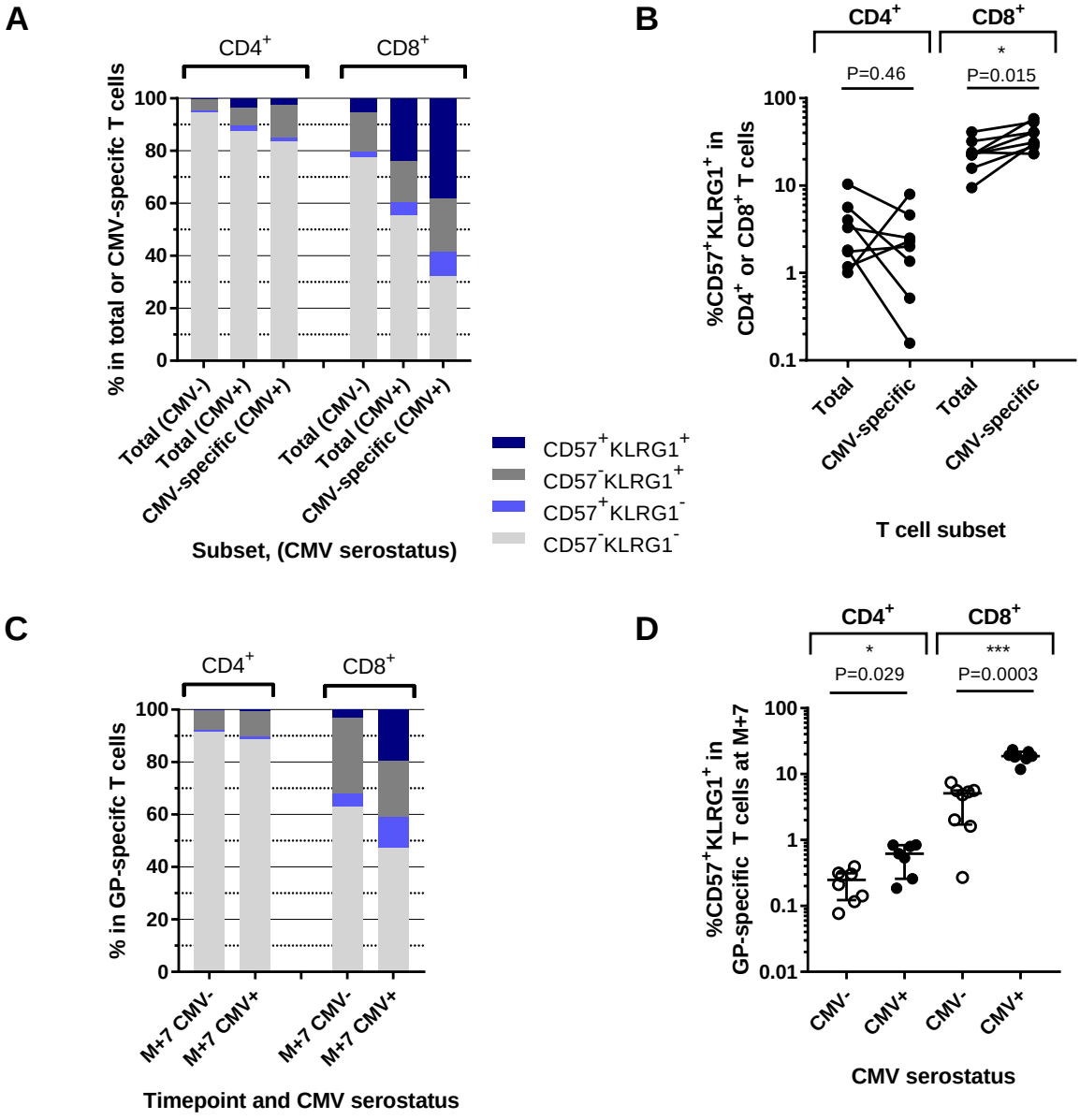

Figure 7.18. Phenotype of antigen-specific T cells

A) Geomean frequencies of subsets within total CD4$^+$ and CD8$^+$ T cells in CMV- and CMV+ individuals and CMV-specific (pp65 stimulated, OX40$^+$CD25$^+$) T cells in CMV+ individuals at M+7. **B**) Frequency of CD57$^+$KLRG1$^+$ cells within the total and CMV-specific CD4$^+$ and CD8$^+$ T cells in CMV+ individuals at M+7. **C**) Geomean frequencies of subsets within GP-specific (GP-stimulated, OX40$^+$CD25$^+$) CD4$^+$ and CD8$^+$ T cells in CMV- and CMV+ individuals at M+7. **D**) Frequency of CD57$^+$KLRG1$^+$ cells within GP-specific CD4$^+$ and CD8$^+$ T cells in CMV- and CMV+ individuals at M+7. One individual did not have detectable GP-specific CD4$^+$ T cells at M+7 and two individuals did not have detectable GP-specific CD8$^+$ T cells at M+84, therefore phenotypic analysis does not include data from these subjects.

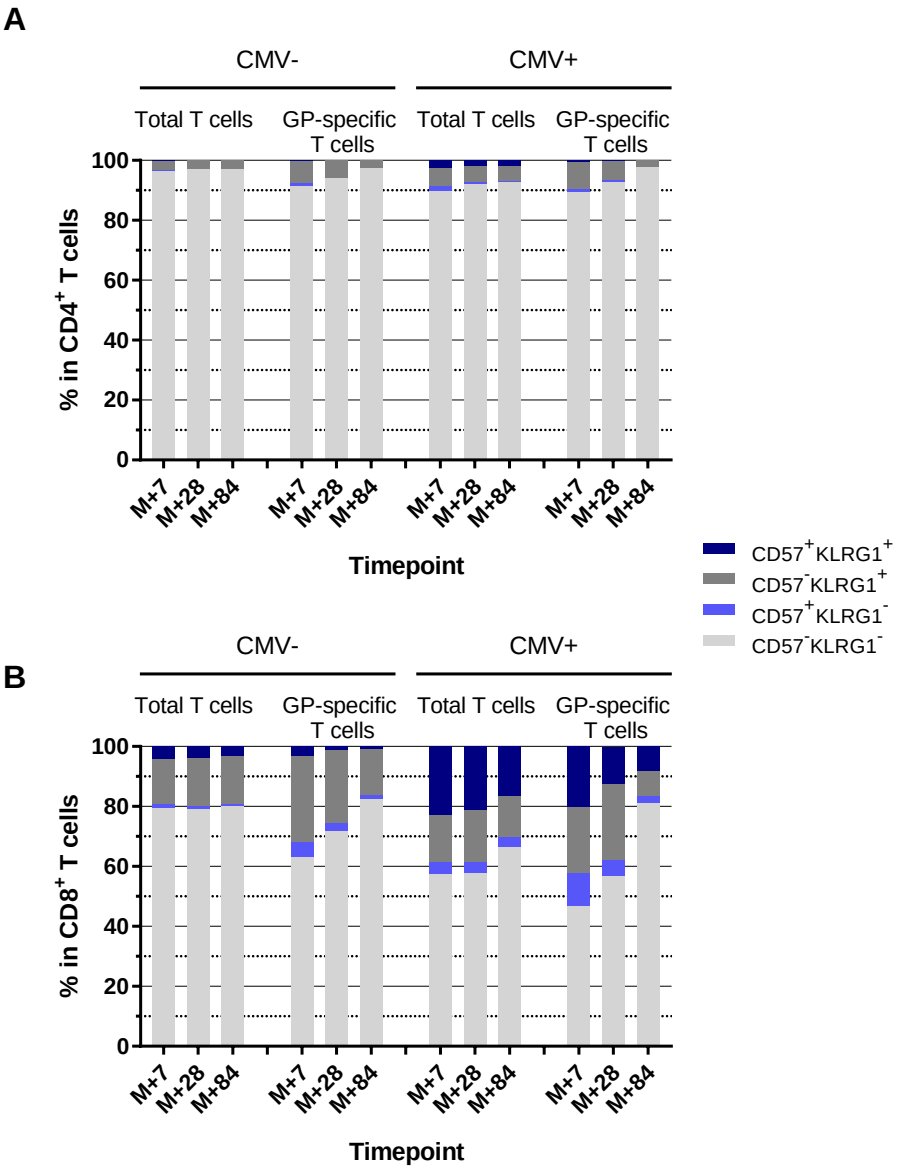

Figure 7.19. Phenotype of antigen-specific T cells over time

Geomean frequencies of subsets within total and GP-specific (GP-stimulated, $OX40^+CD25^+$): **A**) $CD4^+$ T cells and **B**) $CD8^+$ T cells in CMV- and CMV+ individuals at M+7, M+28 and M+84. Geomean subsets were calculated using only those volunteers with detectable GP-specific $CD4^+$ or $CD8^+$ T cell responses at each time point.

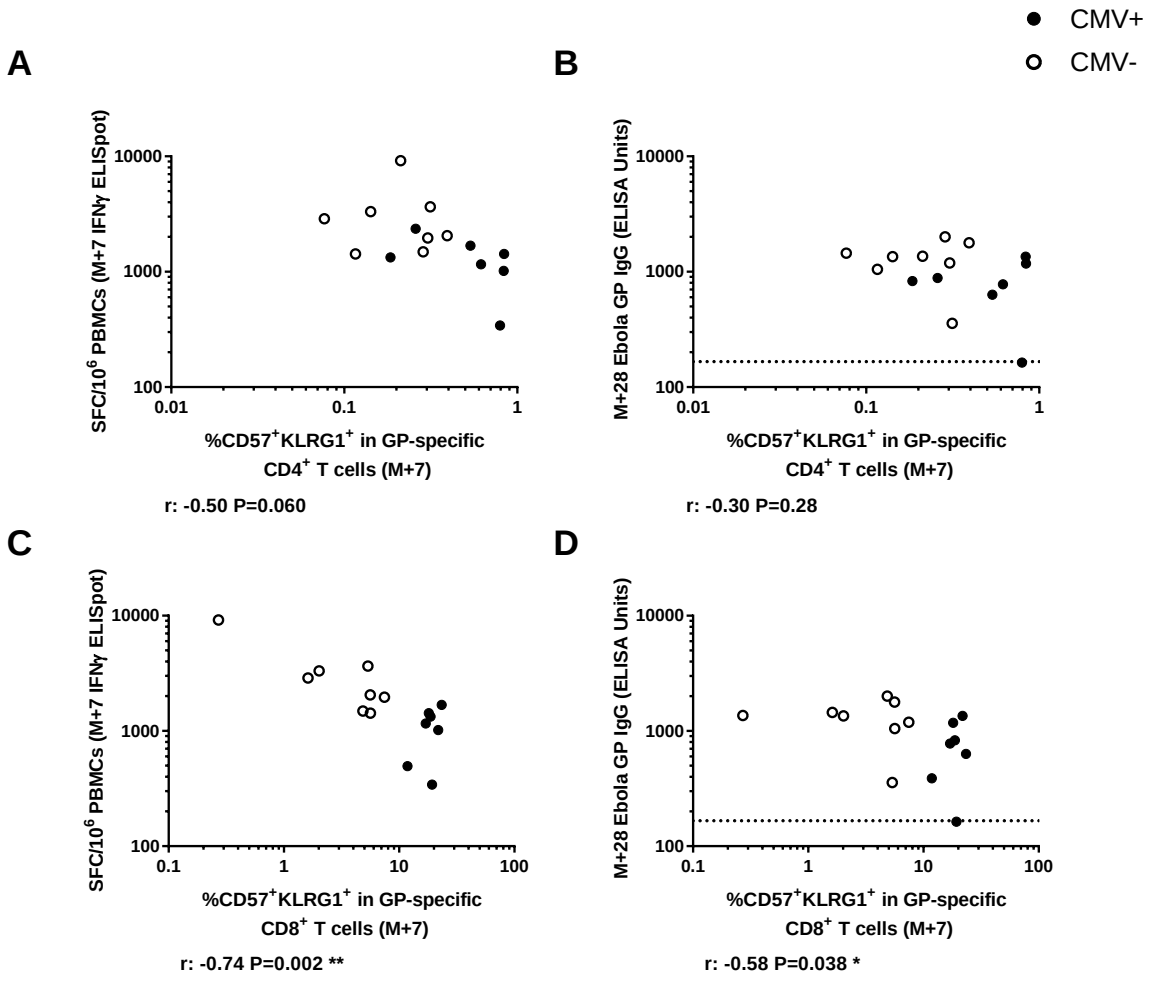

Figure 7.20. Relationship between CD57$^+$KLRG1$^+$ antigen-specific T cells and vaccine responses.

Relationship between frequency of CD57$^+$KLRG1$^+$ cells in CD4$^+$ (GP-stimulated, AIM+) T cells at M+7 and: **A**) peak (M+7) IFNγ ELISpot; **B**) peak (M+28) anti-GP IgG responses. Relationship between frequency of CD57$^+$KLRG1$^+$ cells in CD8$^+$ (GP-stimulated, AIM$^+$) T cells at M+7 and: **C**) peak (M+7) IFNγ ELISpot; **D**) peak (M+28) anti-GP IgG responses. Spearman rank analyses, * P<0.05. One individual did not have detectable GP-specific CD4$^+$ T cells at M+7, therefore there is no phenotypic data for this individual and they are not included in the analyses shown here. Dotted lines indicate seropositive cut-off for Ebola GP (166 ELISA Units). SFC/10^6 PBMC: spot-forming cells per million peripheral blood mononucleocytes.

7.4. Discussion

The design of these two concurrently run Ebola vaccine trials in healthy young adults in the UK and Senegal provided an opportunity to directly compare vaccine immunogenicity in developed and developing countries with very different levels of pathogen exposure. Vaccine-induced antibody responses were significantly lower in the Senegalese cohort, although T cell responses were comparable. After observing expanded populations of memory T cells within the Senegalese cohort, I decided to investigate CMV seroprevalence in these cohorts. CMV infection is known to cause expansion of late-differentiated memory T cells in a process termed "memory inflation"[362] and although highly prevalent globally, is more prevalent amongst young adults in developing countries than it is in developed countries [570]. CMV has also been associated with reduced vaccine responses in elderly [377,378,381] and possibly young adults [382], therefore I hypothesised that CMV seropositivity, in addition to malaria exposure as discussed in Chapter 5, might be associated with the observed reduction in vaccine immunogenicity in Senegal.

7.4.1. Association between CMV and reduced responses to ChAd3-MVA-EBO-Z

In this study CMV seroprevalence was 47% in the UK and 100% in Senegal, in line with what has previously been reported in European and West African populations [329,586]. Although CMV acquisition increases with age in developed countries, in our study there were no significant differences in age between the UK CMV-, CMV+ and Senegalese populations and CMV IgG titres were not associated with age in either the UK or Senegal. CMV seropositivity was associated with a significant reduction in the T cell response to vaccination in the UK (measured by IFNγ ELISpot after stimulation with peptides from Ebola glycoprotein), and with reduced antibody responses in both the UK and Senegalese cohorts. Previous studies that have observed negative associations between CMV seropositivity and vaccine responses have shown a reduction in humoral immune responses but have not measured T cell responses to vaccination, which are

usually of less interest as almost all licensed vaccines exhibit antibody-mediated mechanisms of protection [272,377,378,381,382,454]. Both antibody and T cell responses are likely relevant for durable protection against Ebola and therefore evaluating responses in both arms of the immune system was of importance in these vaccine trials [303].

7.4.2. CMV-associated changes in the global T cell phenotype

In this study I observed marked differences in the global T cell repertoires of CMV- and CMV+ individuals. In elderly individuals, a reduction in CD4:CD8 ratio is characteristic of immunosenescence and reversal of this ratio (to <1) is part of the "immune risk phenotype" associated with increased mortality in longitudinal studies of elderly populations [374,375]. In elderly individuals this appears to be predominantly driven by expansion of $CD8^+$ T cells specific for CMV [587]. In our cohorts, CMV seropositivity was associated with reduced proportions of $CD4^+$ T cells, whilst there was no significant increase in $CD8^+$ T cells. Although this did not have a significant impact on the overall CD4:CD8 ratios in these cohorts, some individuals had ratios lower than the 1.5-2.5:1 expected in healthy young adults [588], with one CMV^+ UK individual exhibiting an inverted ratio. In non-HIV infected young adults, CMV has been reported as a significant driver of the reduction in CD4:CD8 ratio [382]. In addition to expansion of $CD8^+$ T cells, of which there was no evidence here, an inverted ratio could also be caused by reduction of circulating $CD4^+$ T cells due to recruitment to peripheral sites of infection. CMV-specific $CD4^+$ T cells are thought to play an important role in containing CMV infection and in mouse models $CD4^+$ T cells were abundant in infected peripheral tissues [589,590]. It may be that in young CMV+ adults, there is a reduction of peripheral $CD4^+$ T cells as they are recruited to sites of CMV infection to exert effector functions and contain the virus. As infected individuals age, multiple reactivation events over many decades result in a gradual expansion of CMV-specific $CD8^+$ T cells and this becomes the predominant driving force in reducing the CD4:CD8 ratio [587].

The increase in the proportion of late-differentiated $CD4^+$ and $CD8^+$ T cells (EM $CD45RA^-CCR7^-$ and T_{EMRA} $CD45RA^+CCR7^+$) observed in CMV+ individuals in this study is consistent with previous studies in both young and older adults associating CMV with the expansion of these subsets [574,591-594]. Many of these studies included CD27 and CD28, with $CD27^-CD28^-$ cells identified as being further differentiated [364,595,596]. At birth essentially all human T cells express CD28, while in young adults 20-30% of $CD8^+$ T cells are $CD28^-$, increasing to 50-60% by aged 80 [597]. Common persistent viral infections and particularly CMV, are implicated in the expansion of this population with age [598]. T cells that have lost expression of CD27 and CD28 have many functional and phenotypic characteristics of senescence including reduced telomere length, lower telomerase activity, reduced capacity to proliferate and increased expression of cytolytic molecules such as perforin [599-601]. However, $CD27^-CD28^-$ $CD4^+$ and $CD8^+$ T cells appear to be heterogeneous populations and it has been suggested that the use of CD57 and KLRG1 might further refine characterisation of T cell subsets [583,602]. The inhibitory receptor KLRG1 is expressed on T cells that have previously undergone a large number of divisions, are capable of secreting cytokines but in some circumstances fail to proliferate after stimulation and are unable to undergo further clonal expansion [603-605]. KLRG1 expression is observed on 40-73% of cells specific for influenza, an infection which is resolved, but much higher (>92%) on cells specific for persistent infections such as CMV and EBV [602]. Therefore KLRG1 can be used as a marker to identify cells that have undergone a greater number of rounds of cell division due to increased numbers of antigen encounters. The terminal differentiation marker CD57 is also associated with a history of a greater number of cell divisions, shorter telomeres and markers of cellular senescence [606]. A combination of these two markers may be used to give a more precise delineation of the phenotypic profiles of $CD4^+$ and $CD8^+$ T cells within CMV- and CMV+ individuals. In a previous study $KLRG1^+$ lymphocytes could produce IFNγ on stimulation with CMV, EBV or influenza peptides and $CD57^-$ $KLRG1^+$ cells retained some capacity to proliferate, however $CD57^+KLRG1^+$ $CD8^+$ T cells were a terminally differentiated effector population which

lacked proliferative capacity and did not produce IFNγ after antigen stimulation [602]. In the study presented here $CD57^+KLRG1^+$ cells were increased in CMV+ UK and Senegalese individuals in total $CD4^+$ and $CD8^+$ T cells and within $CD27^-CD28^-$ $CD4^+$ and $CD8^+$ T cells suggesting further differentiation and functional inhibition. The frequency of $CD57^+KLRG1^+$ cells within total $CD4^+$ T cells was negatively associated with both T cell and antibody responses to vaccination in the UK and with antibody responses in Senegal.

In a recent study $CD57^+KLRG1^+CD4^+$ T cells were found to be increased in patients with active TB compared with healthy controls [607]. Although these cells produced more IFNγ, IL-2 and TNFα after antigen-specific stimulation than their $KLRG1^-$ counterparts, they had increased rates of apoptosis and blocking KLRG1 increased the overall IFNγ and IL-2 production in response to antigen-specific stimulation. Previous work in mice and humans has indicated that antigen-driven expression of KLRG1 in $CD4^+$ T cells might be detrimental for the anti-TB responses [608-611]. Equally, loss of BCG protection has been associated with an expansion of KLRG1-expressing T cells (in mice) [612]. These studies suggest that KLRG1 can act as a marker for $CD4^+$ T cells driven to a less protective terminally differentiated state, which may be partly responsible for the inadequate T cell responses in chronic *M.tuberculosis* infection [608,613].

Previous reports of CMV-related reduction in vaccine responses in the elderly have also demonstrated negative associations between expansions of late-differentiated memory $CD4^+$ and $CD8^+$ T cells (often marked by loss of CD28 alone or in addition to CD27) and vaccine responses [378,574,614,615]. There are several reasons that may explain these associations. The size and constituents of the peripheral T cell pool are regulated by thymic output and homeostatic mechanisms [616]. Marked clonal expansions of late-differentiated CMV-specific memory T cells may compromise *de novo* responses to antigens by decreasing the diversity of the remaining naïve T cells or out-competing naïve T cells for resources [617]. It is likely that most of these $CD28^-CD4^+$ and $CD8^+$ T cells are CMV-specific [618], but it is also possible that CD27

and CD28 loss may be induced on non CMV-specific T cells through cytokine-mediated effects, thereby impacting on T cell responses to heterologous antigens [619]. There are also reports (from mouse models) that $CD28^{-}CD8^{+}$ T cells might directly exert suppressive effects on immune function by preventing upregulation of costimulatory molecules on APCs and subsequent reduction of $CD4^{+}$ T cell responses, although the exact mechanism is unclear [620]. Equally, it has been suggested that $CD27^{-}CD28^{-}CD4^{+}$ T cells may act as regulatory T cells inhibiting proliferation and contributing to the downregulation of both CMV-specific and nonspecific immune responses in CMV+ individuals [563,621]. Additionally, an increased proinflammatory background (higher levels of IL-6 or CRP) in CMV-infected individuals could reduce responses to new antigens [622,623].

7.4.3. Impact of other chronic pathogens

It is also possible that an increased overall burden of exposure to infection, which was observed in the Senegalese cohort, might restrict the expansion of terminally-differentiated CMV-specific T cells, reducing the impact of CMV compared with that seen in developed populations. This may be one reason why there was a significant reduction in T cell responses to vaccination in CMV+ UK individuals but not in Senegal, despite universal CMV seropositivity. However, antibody responses were still affected in this population. In addition to CMV, almost all Senegalese individuals were seropositive for HSV-1 and *H. pylori* and around half had evidence of significant exposure to *P. falciparum*. These and other pathogens such as helminths have been associated with reduced vaccine responses or immune suppression and could play a role in the reduced immunogenicity observed in this population [160,624-626]. Equally, many of these pathogens impact the course of infection and the development of immune responses against other pathogens, including causing the reactivation of latent viruses such as CMV [584,627,628].

Of the 18 pathogens tested, CMV and malaria were the only two that showed significant associations with vaccine responses. Although CMV seropositive status was associated with

reduced T cell and antibody responses in the UK cohort, these were not associated with the CMV-specific IgG titre. In both cohorts CMV IgG titres were associated with an expansion of $CD57^{+}KLRG1^{+}$ $CD4^{+}$ T cells that were associated with reduced vaccine responses. However, it is difficult to dissect the individual effects of CMV and malaria exposure on vaccine responses using these cohorts as there were no individuals that were positive for *P. falciparum*-specific IgG but negative for CMV. Clearly there is a limitation on the number of different factors that can be assessed, particularly in studies of this size. Ideally, a large enough sample number would be tested to allow for multivariate analysis to assess whether serostatus for each of these pathogens were independently associated with reduced vaccine responses However there are clear associations between both malaria and CMV seropositivity and a reduction in responses to ChAd3-MVA-EBO-Z in young adults. If CMV carriage does play a role in reducing responses to some vaccines in young adults this could have a particularly marked impact on responses to these vaccines in developing countries, in which CMV infection is almost universal in this age group.

Ideally in order to dissect the impact of CMV and malaria exposure a large cohort consisting of CMV-schizont+, CMV+schizont+, CMV+schizont- and CMV-schizont- individuals would be assessed. However, it is unlikely that a large enough cohort of such people exists, given that CMV conversion is almost universal in the first few years of life in many malaria-endemic countries [629-631] and therefore likely occurs before significant malaria exposure.

7.4.4. Phenotypic differences in antigen-specific T cell responses in CMV- and CMV+ individuals

I initially used the AIM assay to investigate if the expansion of $CD57^{+}KLRG1^{+}$ T cells in CMV+ individuals was due to the presence of CMV-specific T cells with this phenotype. CMV-specific (CMV pp65 stimulated, $OX40^{+}CD25^{+}$) $CD4^{+}$ and $CD8^{+}$ T cells were detected in CMV seropositive individuals but not in CMV seronegative individuals. However, only a very small proportion of

the CMV-specific $CD4^+$ responses were $CD57^+KLRG1^+$, but 40% of the CMV-specific $CD8^+$ T cell population was $CD57^+KLRG1^+$. A previous study reported that over 90% of the CMV-specific $CD8^+$ T cells expressed KLRG1 and very few expressed CD57 [602]. However, this study used MHC class 1 peptide-tetramers carrying a single epitope from CMV pp65. It is possible that the percentage of CMV-specific $CD8^+$ T cells expressing KLRG1 (60%) was lower and CD57 expression was more frequent (45%) in my study due to including a broader range of responses (by using a pool of overlapping peptides covering the length of pp65 and not restricting the analysis to individuals with HLA-A2).

Even so, the use of just one peptide to investigate CMV-specific T cells is a limitation of this study. Clearly, with limited cells it is impossible to measure responses against the entire CMV proteome. Although CMV lysate has been used to stimulate cells with a more representative combination of CMV proteins [365], $CD8^+$ T cell responses to whole CMV are poorly detected [632]. The phenotype of T cells specific for other CMV proteins may well be different. In particular T cells against lytic and latent stage proteins may differ [633]. However, if the expansion of $CD57^+KLRG1^+$ T cells in CMV+ individuals is not due to the phenotype of the CMV-specific T cells themselves, then this may indicate that CMV carriage can cause phenotypic differences in non-CMV-specific T cells.

The frequencies of GP-specific $CD4^+$ and $CD8^+$ T cells were comparable between CMV- and CMV+ individuals suggesting that the quality rather than quantity of the antigen-specific responses may be the reason for the reduced ELISpot, ICS and antibody responses in CMV+ individuals. Therefore, I investigated whether there was a higher frequency of $CD57^+KLRG1^+$ T cells within the antigen-specific population in CMV+ compared with CMV- individuals. The $CD57^+KLRG1^+$ subset was only a very small minority (<1%) of the vaccine-specific $CD4^+$ T cell response in CMV+ individuals but comprised almost 20% of the vaccine-specific $CD8^+$ T cell response and in both subsets the proportion was significantly higher than in CMV- individuals. The frequency of

$CD57^+KLRG1^+$ in antigen-specific T cells in CMV+ individuals was highest at the peak of the response and decreased at later time points, while total T cell subsets had a more consistent phenotypic composition.

One possible reason for the association between $CD57^+KLRG1^+$ T cells and reduced vaccine responses (particularly ELISpot and ICS), could be that these cells produce less or different cytokines and are therefore not measured by these assays. For $CD8^+$ T cells this is possible, since around 20% of the GP-specific cells in this subset were $CD57^+KLRG1^+$, compared with just 5% in CMV- individuals. However, this may not be a likely explanation for the association between $CD57^+KLRG1^+$ $CD4^+$ T cells and vaccine responses, since less than 1% of the GP-specific $CD4^+$ T cells expressed these markers. Additionally, the frequency of $CD57^+KLRG1^+$ cells within the antigen-specific $CD4^+$ T cell populations was not associated with vaccine responses, while the frequency of $CD57^+KLRG1^+$ cells within antigen-specific $CD8^+$ T cells was negatively associated with vaccine responses. These data may suggest that the $CD57^+KLRG1^+$ $CD8^+$ T cells are negatively associated with reduced vaccine responses in an antigen-specific manner (e.g. production of less cytokine), whilst $CD57^+KLRG1^+$ $CD4^+$ T cells could be negatively associated with vaccine responses in an antigen-independent manner (e.g. Treg function). I conducted further experiments to attempt to clarify which was the case or if both mechanisms were involved in the observed reduction of vaccine responses in CMV+ individuals.

7.5. Conclusions

CMV+ individuals had phenotypically different responses to vaccination, with increased frequencies of Ebola GP-specific T cells expressing CD57 and KLRG1, which were associated with reduced vaccine responses. Although changes in the global T cell repertoire have previously been associated with CMV, the identification of phenotypic differences in vaccine-specific T cell responses in CMV+ and CMV- individuals is novel. The observations in this study suggest that high CMV seroprevalence may have a role in driving the reduced vaccine immunogenicity observed in some developing countries. This has important implications for future vaccine studies, particularly when comparing trial outcomes between populations with different CMV seropositivity rates. Development of a vaccine against CMV could prevent acquisition of CMV and inflation of these subsets with reduced functionality, preventing the negative impacts on vaccine responses and potentially delaying or reducing the process of immunosenescence. There are several promising candidate CMV vaccines, however current efforts have been focused on prevention of primary infections in pregnant women as the highest visible morbidity and mortality stems from congenital infections [634]. This study adds to a growing body of evidence suggesting that CMV infection might have a much broader impact on public health and an effective vaccine could have farther-reaching benefits than previously appreciated.

8

Conclusions and Future directions

8.1. Overview

After decades of research a licensed malaria vaccine may finally be on the horizon. RTS,S, the only malaria vaccine candidate to have been tested in Phase III studies, has demonstrated short-term protective efficacy in infants in malaria-endemic countries [238,411-413]. However, efficacy in the target infant population was low and waned to almost nothing by four years [238]. The WHO have recommended further evaluation of a four-dose RTS,S schedule in a series of Phase III pilot implementation studies alongside vector control and seasonal chemoprophylaxis [635]. However, in order to eliminate malaria, particularly in high transmission settings, a more efficacious vaccine will be needed. Towards this goal, there are vaccines being developed for each of the lifecycle stages [216] and a combination approach may be required to achieve optimal efficacy.

One issue with combination regimens is the need to find the optimal delivery strategy and schedule for each of the vaccines. Vaccines may be co-administered at the same or different sites (e.g. opposite arms), mixed or given at staggered time points. The optimal regimen will depend on both efficacy and the feasibility of implementing the regimen in resource-poor settings. It is hoped that by combining vaccines that target *Plasmodium* through multiple different mechanisms, an additive or even synergistic effect of efficacy could be achieved [636] but combination regimens of malaria vaccines in both mice and humans have had mixed results [401,637,638]. Although vaccines are often co-administered (e.g. the measles, mumps and rubella

[MMR] vaccine, the diphtheria, pertussis and tetanus [DPT] vaccine and others in the EPI schedule), development of these combination vaccines and co-administration schedules can be challenging [639]. Interactions between components in the different vaccines may cause immune interference through antigen competition [640] or induction of interferon by live viral vaccines, which may inhibit replication of other live viral vaccines [641]. Induction of both potent antibody and T cell responses without immune interference will likely require careful optimisation of the vaccines, delivery routes, administration sites and regimen.

Effectively vaccinating individuals in the context of ongoing malaria transmission may provide an additional challenge. There is evidence that blood-stage malaria infection directly inhibits the development of effective memory responses against PE stage malaria [161-163]. Recent and concurrent malaria infections have been shown to inhibit heterologous vaccine responses in children and infants [158-160]. The potential long term impacts of repeated infections and chronic asymptomatic parasitaemia are also beginning to be understood [209-212]. These exposures may have profound impacts on the immune system, skewing Tfh [197] and memory B cells [83,85,171] towards phenotypes less able to support robust antibody responses [86,196].

The key target population for malaria vaccines is infants aged 5-17 months. For some of the vaccines that have been studied in this age group, robust responses to vaccination are restored if the vaccine is given after clearance of parasitaemia, however a month after clearance, responses to meningococcal vaccines were still impaired [160]. The long-term effects of malaria exposure on vaccine responses in older children and adults have not been widely studied. Vaccine responses are rarely compared head-to-head in malaria-naïve and malaria-exposed populations. Of course, many factors aside from malaria exposure may play a role in this phenomenon including other pathogen exposure, genetic differences, microflora composition and nutritional status [486-489,642]. Although the key target population for malaria vaccines is 5-17 month olds, vaccinating adults may be important to reduce transmission, particularly in

high transmission settings where semi-immune adults may carry high burdens of asymptomatic parasitaemia [204].

The 2014-2016 Ebola outbreak in West Africa highlighted the threat of emerging infectious diseases and the need to develop effective vaccines against outbreak pathogens [310,494,643]. Outbreak pathogens for which vaccines are currently being developed as a priority include Ebola, Zika, Chikungunya, Lassa and Marburg viruses [310,643]. Many of these pathogens have geographical distributions that overlap with areas of malaria transmission and therefore being able to effectively vaccinate malaria-exposed adults is a key requirement for these vaccines.

Amongst other factors that could affect vaccine responses in Africa is CMV infection, which is almost universally prevalent [329]. Although also highly prevalent in developed countries, in children and young adults seroprevalence is much lower in these countries – around 30-50% [329]. CMV infection has a profound impact on the immune system characterised by the expansion of terminally differentiated memory T cells, dominance of CMV-specific cells within the T cell pool and expansion of particular NK cell subsets [345,358-362,593]. There is growing evidence that CMV may be associated with the aging of the immune system or immunosenescence and is part of an immune risk profile for all-cause mortality in elderly individuals [373-375,587]. Latent CMV carriage has been associated with reduced responses to vaccination in elderly individuals in some cases [377,574] but not others [379,380]. However the impact on children and young adults is even less clear [381-385]. If CMV impacts immune responses to certain vaccinations in young adults and children, this could also have a profound impact on vaccine immunogenicity and efficacy in Africa compared with initial results from trials in the UK and USA where CMV seroprevalence is lower.

This thesis addresses some of these issues, characterising the immunogenicity of combination malaria vaccine regimens, measuring immune responses to vaccination in malaria-exposed

populations and exploring the impact of malaria and CMV on the immune responses to vaccination.

8.2. Summary of findings, implications and future directions

8.2.1. Combination malaria vaccines

Initial work in this thesis aimed to evaluate the immunogenicity and efficacy in combination regimens of RTS,S/AS01B and viral-vectored vaccines. The immunogenicity of RTS,S/AS01B was significantly reduced when doses were co-administered with a prime-boost regimen of ChAd63-ME-TRAP and MVA-ME-TRAP. Both the quality and quantity of the antibody response to RTS,S were reduced with lower NANP-specific antibody titres and reduced ability to block sporozoite invasion in an *in vitro* assay. Co-administration also resulted in a significant reduction in efficacy – 60% compared with 75% when RTS,S/AS01B was administered alone (standard dose regimens). This effect was not seen if the vaccines were given at two week intervals (82% efficacy) and there was no effect on the T cell response induced by viral vectored vaccines in either the staggered or co-administration regimens compared with single administration of viral vectored vaccines.

Analysis of the underlying cellular differences revealed a potential role for the strong Th1 cytokine responses induced by viral vectors in skewing Tfh towards a $CXCR3^+$ phenotype that may be less efficient at helping B cells produce antibody [68,197]. Interestingly, this may recapitulate to some extent what occurs in acute malaria infections, with a preferential activation and expansion of $CXCR3^+$ Tfh and a resultant inhibition in the generation of effective antibody responses [197].

This was the first time we have used the ISI in a clinical trial to enable us to gain an insight into potential mechanisms of vaccine-induced protection in our studies. Inhibition of sporozoite

invasion was significantly higher in protected individuals, whilst there was no association between NANP-specific IgG titre and protection. Use of this and similar functional studies in future Phase II studies will be important in gaining an insight into how these vaccines work and potentially finding an immunological correlate of protection.

This study additionally tested a fractional third dose of RTS,S/AS01B, which may provide a higher level of protection than three standard doses [416,420]. However, the trial was not designed to answer that question and the different spacing of doses (0, 1, 7 months instead of 0, 1, 2 months) may have also been a cause for the difference in efficacy. In our trial, we did not have power to detect a significant difference in efficacy between the standard and fractional third dose regimens, however we did observe a significantly high blocking ability by antibody from the reduced third dose groups. Differences in the antibody responses induced by standard and reduced third dose regimens have been previously identified [644]. However, this is the first demonstration of a functional difference that was associated with protection and may explain how this regimen could have better efficacy.

The implications of this work are that further Phase I and II trials of combination vaccine regimens must be carefully designed in order to determine the optimal administration protocol and schedule for immunogenicity and efficacy. This may be especially challenging for combinations of malaria vaccines that aim to induce both potent T cell and antibody responses. For infant vaccines the challenge is even greater to include these vaccines within the EPI schedule. Viral vectored TRAP vaccines and RTS,S have already been tested alongside EPI vaccines and did not cause a reduction in responses to those vaccines or any safety concerns [645,646]. However, any new combination would also need to be tested in this way.

8.2.2. Measuring immunogenicity in malaria-endemic populations

A further aim of this thesis was to develop assays to accurately measure humoral immunogenicity in malaria-exposed populations. ELISAs completed using samples from Burkina

Faso, led to the discovery of significant levels of antigen-independent antibody deposition (AIAD) on ELISA plates in samples from areas of high malaria transmission. This caused intense background signal and potentially false positive results. Although significant background signal in malaria-exposed populations several decades ago [449], very few studies in these populations adjust for or even test for this. In order to accurately measure humoral immunogenicity in malaria-exposed populations, background signal caused by AIAD should be tested for and appropriate steps taken to remove this background. I found that a commercially available blocking buffer, ChonBlock™ specifically designed to remove AIAD background signal in autoimmune subjects with high levels of circulating IgG [453,455,458], was also able to block AIAD in samples from malaria-exposed subjects. The use of such a blocking buffer or the subtraction of AIAD signal from the antigen-specific response should be used to ensure accurate measurement of humoral immunogenicity in populations where AIAD is an issue.

8.2.3. Impact of malaria exposure on vaccine responses

Both RTS,S and viral vectored malaria vaccines have been tested in numerous trials in the UK/USA and malaria-endemic African countries [240,252,257,258,262,410,411,419-422,428,502,646]. However due to differences in trial design and immunological readouts used, it is often difficult to draw comparisons between the immunogenicity in malaria-naïve and malaria-exposed populations. We have run a number of malaria vaccine trials in which the same vaccine doses, regimen and assays have been used enabling head-to-head comparisons in different cohorts. In addition to malaria vaccines, we have also run directly comparable trials of the viral vectored vaccines ChAd3-EBO-Z and MVA-EBO-Z in the UK and Senegal. The aim of this research was to compare the immunogenicity of viral vectored vaccines and R21 in malaria-exposed and malaria-naïve cohorts and to determine if malaria exposure might be associated with differences in vaccine immunogenicity.

TRAP-specific IgG responses induced by ChAd63-MVA-ME-TRAP and Ebola GP-specific IgG responses induced by ChAd3-MVA-EBO-Z were significantly reduced in malaria-exposed cohorts (in Kenya, The Gambia and Senegal) compared with malaria-naïve UK cohorts. In the Senegalese cohort, Ebola GP-specific IgG responses were negatively associated with malaria exposure measured by antibody against AMA-1, MSP-1 or Pf-infected RBC lysate. Additionally, the increased frequency of $CXCR3^+$ cTfh and atypical memory B cells in this cohort compared with the UK cohort was interesting given that these phenotypes have previously been associated with malaria and may be less functional [85,86,196,197]. However, these cell subsets showed a limited association with vaccine responses, suggesting that if malaria is involved in reducing responses to these vaccines, there is an alternative underlying mechanism. Interestingly, there was no impact on $CD8^+$ T cell responses and both T cell and antibody responses in malaria-exposed infants were comparable to or higher than malaria-naïve adults. Further work is needed to determine why humoral immunogenicity is primarily affected and why responses did not appear to be reduced in infants (although there is no malaria-naïve infant group for direct comparison).

Immunogenicity and efficacy of vaccines should be optimised for the target populations. It is therefore important that future trials are designed to enable comparisons to be drawn between cohorts as much as possible. This will enable any reduction of responses in particular cohorts to be easily detected. The thorough investigation of underlying associations with reduced vaccine immunogenicity would allow further optimisation of these vaccines to provide the optimal level of best protection in the populations that need it most.

8.2.4. Impact of CMV on vaccine responses

Further analysis of the reduced humoral immunogenicity of ChAd3-MVA-EBO-Z in Senegal compared with the UK revealed an association with CMV seroprevalence. The results from this research showed that vaccine responses in UK CMV+ individuals were significantly lower than UK CMV- individuals and comparable to those in the Senegalese cohort (in which all individuals

were CMV+). These individuals demonstrated expansions of terminally differentiated memory T cells that have previously been associated with CMV [358-362,380] and were negatively associated with vaccine responses in this study. The association between CMV and reduced responses to vaccination could have important implications for vaccination in many countries in Africa, in which CMV seroprevalence in children and young adults is extremely high. Future studies should be designed to address why responses to these vaccines in particular were lower in CMV+ individuals and what might be done in order to enhance responses in this context.

I adapted and tested an activation-induced markers assay to measure antigen-specific T cell responses in these cohorts independently of functional output (e.g. cytokine production) [647]. This enables us to measure antigen-specific T cell responses in an unbiased way (no pre-determination of the types of cytokines produced) and to compare the total antigen-responsive T cell populations. This assay will be a useful tool in future trials and it is already planned for use in the next Phase IIa malaria vaccine trial being conducted at the Jenner Institute. Further optimisation of the assay to include functional measures would be useful to integrate our current cytokine panel and the total antigen-specific T cell data provided by the AIM assay.

Initial work I have conducted using these assays suggests that the frequency of antigen-responsive T cells is similar in CMV- and CMV+ individuals but may be phenotypically different. Antigen-responsive cells in CMV+ individuals contained an increased frequency of terminally differentiated $CD57^{+}KLRG1^{+}$ T cells. Initial work suggests that IFNγ production by these expanded $CD57^{+}KLRG1^{+}$ T cells may be reduced compared with $CD57^{-}KLRG1^{-}$ T cells and may explain the reduction in T cell responses measured by IFNγ ELISpot in these individuals. However, further studies will be needed to fully characterise the functional differences in the cell subsets and determine the clinical relevance of their expansion. Work has already begun within the group to try to answer some of these outstanding questions. This work includes analysing cytokine production by $CD57^{+}KLRG1^{+}$ compared with $CD57^{-}KLRG1^{-}$ cells when stimulated with the vaccine

antigen or SEB and further phenotyping to determine the frequency of Tregs within these populations in CMV+ and CMV- individuals. $CD57^{+}KLRG1^{+}$ T cells have been shown to be poor cytokine producers [602]. Therefore, the increased proportion of this phenotype within the vaccine-specific T cells in CMV+ individuals could explain the reduced IFNγ ELISpot responses. Although bystander activation was shown to have a minimal impact in these assays in a previous study [402], it would be useful to use use peptide-MHC staining to confirm whether $CD57^{+}KLRG1^{+}$ AIM^{+} cells in CMV+ individuals were definitely specific for the vaccine antigen. If these cells are not actually specific for Ebola GP, then this would mean that CMV+ individuals had a lower frequency of antigen-specific T cells than CMV- individuals. This could provide an alternative explanation for the reduced IFNγ ELISpot responses in CMV+ individuals. Additional ongoing work includes phenotyping of NK cells and analysis of NK cell responses to vaccination within CMV- and CMV+ individuals.

It is particularly interesting that $CD8^{+}$ T cell responses in malaria-exposed, CMV+ adults are comparable to malaria-naïve CMV- adults (and higher than malaria-naïve CMV+ individuals), whilst antibody responses are reduced. As chronic malaria exposure appears to induce an immunoregulatory environment, it is unlikely that these enhanced $CD8^{+}$ IFNγ responses are associated with malaria exposure. Speculatively, $CD8^{+}$ T cell activation and IFNγ production in could be increased by exposure to another pathogen. Around a third of the global population is estimated to carry latent TB infection (LTBI) and prevalence is thought to range from 30-55% in sub-Saharan Africa [648]. LTBI has been associated with increased levels of circulating IFNγ [649] and T cell activation [650] This increased Th1-skewed immune activation may further suppress humoral responses whilst enhancing cellular immunity. The direct effects of IFNγ on T cells can be suppressive [651]. However, IFNγ can enhance $CD8^{+}$ T cells indirectly through upregulation of the immunoproteasome and MHC class I antigens, increasing antigen presentation. Therefore, increased circulating IFNγ in these individuals could result in increased presentation and recognition of vaccine antigens increasing vaccine-specific $CD8^{+}$ T cell responses. It would be

useful in larger studies in the future to include a test for LTBI amongst the other pathogens in the multiplex serology presented in this thesis.

The impact of CMV on the immune system and response to vaccination is a growing field with varying associations reported. Further studies clarifying the impact of CMV on vaccine responses and the mechanisms underlying these will be a significant addition to the field. Development of a vaccine against CMV could prevent acquisition of CMV and inflation of these subsets with reduced functionality, preventing the negative impacts on vaccine responses and potentially delaying or reducing the process of immunosenescence. There are several promising candidate CMV vaccines, however current efforts have been focused on prevention of primary infections in pregnant women as the highest visible morbidity and mortality stems from congenital infections [634]. This study and a growing body of evidence suggest that CMV infection might have a much broader impact on public health and an effective vaccine could have farther-reaching benefits.

8.3. Final remarks

I believe that the work presented here adds an important body of knowledge to the vaccine field. In order to optimise vaccines for malaria and outbreak pathogens, we need a deeper understanding of how these vaccines work and what determines protection. More studies like this that evaluate the functional antibody responses and underlying cellular mechanisms are needed to accelerate vaccine development. Vaccines are often initially tested in populations within developed countries in which climate, pathogen exposure, nutritional status and genetic background can be vastly different to those in the target population. It is important that we are able to optimise vaccines to work in the populations that need them most. The work presented here emphasises the need for head-to-head comparisons of vaccine immunogenicity in these populations and exploration of the factors underlying reduced immunogenicity in the target population.

References

1. Plotkin, S.A.; Plotkin, S.L. The development of vaccines: how the past led to the future. *Nat Rev Microbiol* **2011**, *9*, 889-893, doi:10.1038/nrmicro2668.
2. Medzhitov, R.; Janeway, C. Innate immune recognition: mechanisms and pathways. *Immunol Rev* **2000**, *173*, 89-97.
3. Takeda, K.; Kaisho, T.; Akira, S. Toll-like receptors. *Annu Rev Immunol* **2003**, *21*, 335-376, doi:10.1146/annurev.immunol.21.120601.141126.
4. Kawasaki, T.; Kawai, T. Toll-like receptor signaling pathways. *Front Immunol* **2014**, *5*, 461, doi:10.3389/fimmu.2014.00461.
5. Ghosh, D.; Stumhofer, J.S. Do you see what I see: Recognition of protozoan parasites by Toll-like receptors. *Curr Immunol Rev* **2013**, *9*, 129-140, doi:10.2174/15733955096661312032259 29.
6. von Bernuth, H.; Picard, C.; Jin, Z.; Pankla, R.; Xiao, H.; Ku, C.L.; Chrabieh, M.; Mustapha, I.B.; Ghandil, P.; Camcioglu, Y., et al. Pyogenic bacterial infections in humans with MyD88 deficiency. *Science* **2008**, *321*, 691-696, doi:10.1126/science.1158298.
7. Khor, C.C.; Chapman, S.J.; Vannberg, F.O.; Dunne, A.; Murphy, C.; Ling, E.Y.; Frodsham, A.J.; Walley, A.J.; Kyrieleis, O.; Khan, A., et al. A Mal functional variant is associated with protection against invasive pneumococcal disease, bacteremia, malaria and tuberculosis. *Nat Genet* **2007**, *39*, 523-528, doi:10.1038/ng1976.
8. Matzinger, P. Tolerance, danger, and the extended family. *Annu Rev Immunol* **1994**, *12*, 991-1045, doi:10.1146/annurev.iy.12.040194.005015.
9. Seong, S.Y.; Matzinger, P. Hydrophobicity: an ancient damage-associated molecular pattern that initiates innate immune responses. *Nat Rev Immunol* **2004**, *4*, 469-478, doi:10.1038/nri1372.
10. Bianchi, M.E. DAMPs, PAMPs and alarmins: all we need to know about danger. *J Leukoc Biol* **2007**, *81*, 1-5, doi:10.1189/jlb.0306164.
11. Lotze, M.T.; Deisseroth, A.; Rubartelli, A. Damage associated molecular pattern molecules. *Clin Immunol* **2007**, *124*, 1-4, doi:10.1016/j.clim.2007.02.006.
12. Chen, G.Y.; Tang, J.; Zheng, P.; Liu, Y. CD24 and Siglec-10 selectively repress tissue damage-induced immune responses. *Science* **2009**, *323*, 1722-1725, doi:10.1126/science.1168988.
13. Zhang, N.; Bevan, M.J. CD8(+) T cells: foot soldiers of the immune system. *Immunity* **2011**, *35*, 161-168, doi:10.1016/j.immuni.2011.07.010.
14. Petersen, J.L.; Morris, C.R.; Solheim, J.C. Virus evasion of MHC class I molecule presentation. *J Immunol* **2003**, *171*, 4473-4478.
15. Ljunggren, H.G.; Kärre, K. In search of the 'missing self': MHC molecules and NK cell recognition. *Immunol Today* **1990**, *11*, 237-244.
16. Bix, M.; Liao, N.S.; Zijlstra, M.; Loring, J.; Jaenisch, R.; Raulet, D. Rejection of class I MHC-deficient haemopoietic cells by irradiated MHC-matched mice. *Nature* **1991**, *349*, 329-331, doi:10.1038/349329a0.
17. Moretta, A.; Tambussi, G.; Bottino, C.; Tripodi, G.; Merli, A.; Ciccone, E.; Pantaleo, G.; Moretta, L. A novel surface antigen expressed by a subset of human CD3- CD16+ natural killer cells. Role in cell activation and regulation of cytolytic function. *J Exp Med* **1990**, *171*, 695-714.
18. Moretta, A.; Bottino, C.; Vitale, M.; Pende, D.; Biassoni, R.; Mingari, M.C.; Moretta, L. Receptors for HLA class-I molecules in human natural killer cells. *Annu Rev Immunol* **1996**, *14*, 619-648, doi:10.1146/annurev.immunol.14.1.619.

19. Colonna, M.; Samaridis, J. Cloning of immunoglobulin-superfamily members associated with HLA-C and HLA-B recognition by human natural killer cells. *Science* **1995**, *268*, 405-408.
20. Wagtmann, N.; Rajagopalan, S.; Winter, C.C.; Peruzzi, M.; Long, E.O. Killer cell inhibitory receptors specific for HLA-C and HLA-B identified by direct binding and by functional transfer. *Immunity* **1995**, *3*, 801-809.
21. Braud, V.M.; Allan, D.S.; O'Callaghan, C.A.; Söderström, K.; D'Andrea, A.; Ogg, G.S.; Lazetic, S.; Young, N.T.; Bell, J.I.; Phillips, J.H., et al. HLA-E binds to natural killer cell receptors CD94/NKG2A, B and C. *Nature* **1998**, *391*, 795-799, doi:10.1038/35869.
22. Vance, R.E.; Kraft, J.R.; Altman, J.D.; Jensen, P.E.; Raulet, D.H. Mouse CD94/NKG2A is a natural killer cell receptor for the nonclassical major histocompatibility complex (MHC) class I molecule Qa-1(b). *J Exp Med* **1998**, *188*, 1841-1848.
23. Long, E.O.; Kim, H.S.; Liu, D.; Peterson, M.E.; Rajagopalan, S. Controlling natural killer cell responses: integration of signals for activation and inhibition. *Annu Rev Immunol* **2013**, *31*, 227-258, doi:10.1146/annurev-immunol-020711-075005.
24. Sarma, J.V.; Ward, P.A. The complement system. *Cell Tissue Res* **2011**, *343*, 227-235, doi:10.1007/s00441-010-1034-0.
25. Iles, K.E.; Forman, H.J. Macrophage signaling and respiratory burst. *Immunol Res* **2002**, *26*, 95-105, doi:10.1385/IR:26:1-3:095.
26. Holmes, B.; Page, A.R.; Good, R.A. Studies of the metabolic activity of leukocytes from patients with a genetic abnormality of phagocytic function. *J Clin Invest* **1967**, *46*, 1422-1432, doi:10.1172/JCI105634.
27. Brandstadter, J.D.; Yang, Y. Natural killer cell responses to viral infection. *J Innate Immun* **2011**, *3*, 274-279, doi:10.1159/000324176.
28. Zamai, L.; Ponti, C.; Mirandola, P.; Gobbi, G.; Papa, S.; Galeotti, L.; Cocco, L.; Vitale, M. NK cells and cancer. *J Immunol* **2007**, *178*, 4011-4016.
29. Lee, R.K.; Spielman, J.; Zhao, D.Y.; Olsen, K.J.; Podack, E.R. Perforin, Fas ligand, and tumor necrosis factor are the major cytotoxic molecules used by lymphokine-activated killer cells. *J Immunol* **1996**, *157*, 1919-1925.
30. Montel, A.H.; Bochan, M.R.; Hobbs, J.A.; Lynch, D.H.; Brahmi, Z. Fas involvement in cytotoxicity mediated by human NK cells. *Cell Immunol* **1995**, *166*, 236-246, doi:10.1006/cimm.1995.9974.
31. Bonnema, J.D.; Rivlin, K.A.; Ting, A.T.; Schoon, R.A.; Abraham, R.T.; Leibson, P.J. Cytokine-enhanced NK cell-mediated cytotoxicity. Positive modulatory effects of IL-2 and IL-12 on stimulus-dependent granule exocytosis. *J Immunol* **1994**, *152*, 2098-2104.
32. Perussia, B. The Cytokine Profile of Resting and Activated NK Cells. *Methods* **1996**, *9*, 370-378.
33. Orange, J.S. Unraveling human natural killer cell deficiency. *J Clin Invest* **2012**, *122*, 798-801, doi:10.1172/JCI62620.
34. Banchereau, J.; Steinman, R.M. Dendritic cells and the control of immunity. *Nature* **1998**, *392*, 245-252, doi:10.1038/32588.
35. Guermonprez, P.; Valladeau, J.; Zitvogel, L.; Théry, C.; Amigorena, S. Antigen presentation and T cell stimulation by dendritic cells. *Annu Rev Immunol* **2002**, *20*, 621-667, doi:10.1146/annurev.immunol.20.100301.064828.
36. Sallusto, F.; Lanzavecchia, A. The instructive role of dendritic cells on T-cell responses. *Arthritis Res* **2002**, *4 Suppl 3*, S127-132, doi:10.1186/ar567.
37. Collin, M.; McGovern, N.; Haniffa, M. Human dendritic cell subsets. *Immunology* **2013**, *140*, 22-30, doi:10.1111/imm.12117.
38. Blum, J.S.; Wearsch, P.A.; Cresswell, P. Pathways of antigen processing. *Annu Rev Immunol* **2013**, *31*, 443-473, doi:10.1146/annurev-immunol-032712-095910.

39. Mantegazza, A.R.; Magalhaes, J.G.; Amigorena, S.; Marks, M.S. Presentation of phagocytosed antigens by MHC class I and II. *Traffic* **2013**, *14*, 135-152, doi:10.1111/tra.12026.
40. Alcover, A.; Alarcón, B.; Di Bartolo, V. Cell Biology of T Cell Receptor Expression and Regulation. *Annu Rev Immunol* **2018**, *36*, 103-125, doi:10.1146/annurev-immunol-042617-053429.
41. Butz, E.A.; Bevan, M.J. Massive expansion of antigen-specific CD8+ T cells during an acute virus infection. *Immunity* **1998**, *8*, 167-175.
42. Callan, M.F.; Steven, N.; Krausa, P.; Wilson, J.D.; Moss, P.A.; Gillespie, G.M.; Bell, J.I.; Rickinson, A.B.; McMichael, A.J. Large clonal expansions of CD8+ T cells in acute infectious mononucleosis. *Nat Med* **1996**, *2*, 906-911.
43. Mescher, M.F.; Curtsinger, J.M.; Agarwal, P.; Casey, K.A.; Gerner, M.; Hammerbeck, C.D.; Popescu, F.; Xiao, Z. Signals required for programming effector and memory development by CD8+ T cells. *Immunol Rev* **2006**, *211*, 81-92, doi:10.1111/j.0105-2896.2006.00382.x.
44. Parish, I.A.; Kaech, S.M. Diversity in CD8(+) T cell differentiation. *Curr Opin Immunol* **2009**, *21*, 291-297, doi:10.1016/j.coi.2009.05.008.
45. Mitchell, D.M.; Ravkov, E.V.; Williams, M.A. Distinct roles for IL-2 and IL-15 in the differentiation and survival of CD8+ effector and memory T cells. *J Immunol* **2010**, *184*, 6719-6730, doi:10.4049/jimmunol.0904089.
46. Hickman, H.D.; Reynoso, G.V.; Ngudiankama, B.F.; Cush, S.S.; Gibbs, J.; Bennink, J.R.; Yewdell, J.W. CXCR3 chemokine receptor enables local CD8(+) T cell migration for the destruction of virus-infected cells. *Immunity* **2015**, *42*, 524-537, doi:10.1016/j.immuni.2015.02.009.
47. Andersen, M.H.; Schrama, D.; Thor Straten, P.; Becker, J.C. Cytotoxic T cells. *J Invest Dermatol* **2006**, *126*, 32-41, doi:10.1038/sj.jid.5700001.
48. Schroder, K.; Hertzog, P.J.; Ravasi, T.; Hume, D.A. Interferon-gamma: an overview of signals, mechanisms and functions. *J Leukoc Biol* **2004**, *75*, 163-189, doi:10.1189/jlb.0603252.
49. Sallusto, F.; Lenig, D.; Förster, R.; Lipp, M.; Lanzavecchia, A. Two subsets of memory T lymphocytes with distinct homing potentials and effector functions. *Nature* **1999**, *401*, 708-712, doi:10.1038/44385.
50. Gebhardt, T.; Wakim, L.M.; Eidsmo, L.; Reading, P.C.; Heath, W.R.; Carbone, F.R. Memory T cells in nonlymphoid tissue that provide enhanced local immunity during infection with herpes simplex virus. *Nat Immunol* **2009**, *10*, 524-530, doi:10.1038/ni.1718.
51. Sathaliyawala, T.; Kubota, M.; Yudanin, N.; Turner, D.; Camp, P.; Thome, J.J.; Bickham, K.L.; Lerner, H.; Goldstein, M.; Sykes, M., et al. Distribution and compartmentalization of human circulating and tissue-resident memory T cell subsets. *Immunity* **2013**, *38*, 187-197, doi:10.1016/j.immuni.2012.09.020.
52. Lanzavecchia, A.; Sallusto, F. Dynamics of T lymphocyte responses: intermediates, effectors, and memory cells. *Science* **2000**, *290*, 92-97.
53. Brack, C.; Hirama, M.; Lenhard-Schuller, R.; Tonegawa, S. A complete immunoglobulin gene is created by somatic recombination. *Cell* **1978**, *15*, 1-14.
54. Parham, P. *The Immune System*, 2nd ed.; Garland Science: 2005.
55. Crotty, S. A brief history of T cell help to B cells. *Nat Rev Immunol* **2015**, *15*, 185-189, doi:10.1038/nri3803.
56. Cooper, A.M.; Dalton, D.K.; Stewart, T.A.; Griffin, J.P.; Russell, D.G.; Orme, I.M. Disseminated tuberculosis in interferon gamma gene-disrupted mice. *J Exp Med* **1993**, *178*, 2243-2247.

57. Korn, T.; Bettelli, E.; Oukka, M.; Kuchroo, V.K. IL-17 and Th17 Cells. *Annu Rev Immunol* **2009**, *27*, 485-517, doi:10.1146/annurev.immunol.021908.132710.
58. Sakaguchi, S. Naturally arising Foxp3-expressing CD25+CD4+ regulatory T cells in immunological tolerance to self and non-self. *Nat Immunol* **2005**, *6*, 345-352, doi:10.1038/ni1178.
59. Schmitt, E.; Klein, M.; Bopp, T. Th9 cells, new players in adaptive immunity. *Trends Immunol* **2014**, *35*, 61-68, doi:10.1016/j.it.2013.10.004.
60. Jia, L.; Wu, C. The biology and functions of Th22 cells. *Adv Exp Med Biol* **2014**, *841*, 209-230, doi:10.1007/978-94-017-9487-9_8.
61. Stevens, T.L.; Bossie, A.; Sanders, V.M.; Fernandez-Botran, R.; Coffman, R.L.; Mosmann, T.R.; Vitetta, E.S. Regulation of antibody isotype secretion by subsets of antigen-specific helper T cells. *Nature* **1988**, *334*, 255-258, doi:10.1038/334255a0.
62. Crotty, S. T follicular helper cell differentiation, function, and roles in disease. *Immunity* **2014**, *41*, 529-542, doi:10.1016/j.immuni.2014.10.004.
63. Chevalier, N.; Jarrossay, D.; Ho, E.; Avery, D.T.; Ma, C.S.; Yu, D.; Sallusto, F.; Tangye, S.G.; Mackay, C.R. CXCR5 expressing human central memory CD4 T cells and their relevance for humoral immune responses. *J Immunol* **2011**, *186*, 5556-5568, doi:10.4049/jimmunol.1002828.
64. Hale, J.S.; Youngblood, B.; Latner, D.R.; Mohammed, A.U.; Ye, L.; Akondy, R.S.; Wu, T.; Iyer, S.S.; Ahmed, R. Distinct memory CD4+ T cells with commitment to T follicular helper- and T helper 1-cell lineages are generated after acute viral infection. *Immunity* **2013**, *38*, 805-817, doi:10.1016/j.immuni.2013.02.020.
65. Morita, R.; Schmitt, N.; Bentebibel, S.E.; Ranganathan, R.; Bourdery, L.; Zurawski, G.; Foucat, E.; Dullaers, M.; Oh, S.; Sabzghabaei, N., et al. Human blood CXCR5(+)CD4(+) T cells are counterparts of T follicular cells and contain specific subsets that differentially support antibody secretion. *Immunity* **2011**, *34*, 108-121, doi:10.1016/j.immuni.2010.12.012.
66. Vinuesa, C.G.; Cook, M.C. Blood relatives of follicular helper T cells. *Immunity* **2011**, *34*, 10-12, doi:10.1016/j.immuni.2011.01.006.
67. Schmitt, N.; Bentebibel, S.-E.; Ueno, H. Phenotype and Functions of Memory Tfh cells in Human Blood. *Trends in immunology* **2014**, *35*, 436-442, doi:10.1016/j.it.2014.06.002.
68. Locci, M.; Havenar-Daughton, C.; Landais, E.; Wu, J.; Kroenke, M.A.; Arlehamn, C.L.; Su, L.F.; Cubas, R.; Davis, M.M.; Sette, A., et al. Human circulating PD-1+CXCR3-CXCR5+ memory Tfh cells are highly functional and correlate with broadly neutralizing HIV antibody responses. *Immunity* **2013**, *39*, 758-769, doi:10.1016/j.immuni.2013.08.031.
69. Farooq, F.; Beck, K.; Paolino, K.M.; Phillips, R.; Waters, N.C.; Regules, J.A.; Bergmann-Leitner, E.S. Circulating follicular T helper cells and cytokine profile in humans following vaccination with the rVSV-ZEBOV Ebola vaccine. *Sci Rep* **2016**, *6*, 27944, doi:10.1038/srep27944.
70. Amanna, I.J.; Carlson, N.E.; Slifka, M.K. Duration of humoral immunity to common viral and vaccine antigens. *N Engl J Med* **2007**, *357*, 1903-1915, doi:10.1056/NEJMoa066092.
71. Radbruch, A.; Muehlinghaus, G.; Luger, E.O.; Inamine, A.; Smith, K.G.; Dörner, T.; Hiepe, F. Competence and competition: the challenge of becoming a long-lived plasma cell. *Nat Rev Immunol* **2006**, *6*, 741-750, doi:10.1038/nri1886.
72. Baumjohann, D.; Preite, S.; Reboldi, A.; Ronchi, F.; Ansel, K.M.; Lanzavecchia, A.; Sallusto, F. Persistent antigen and germinal center B cells sustain T follicular helper cell responses and phenotype. *Immunity* **2013**, *38*, 596-605, doi:10.1016/j.immuni.2012.11.020.
73. Manz, R.A.; Löhning, M.; Cassese, G.; Thiel, A.; Radbruch, A. Survival of long-lived plasma cells is independent of antigen. *Int Immunol* **1998**, *10*, 1703-1711.

74. Slifka, M.K.; Antia, R.; Whitmire, J.K.; Ahmed, R. Humoral immunity due to long-lived plasma cells. *Immunity* **1998**, *8*, 363-372.
75. McHeyzer-Williams, L.J.; McHeyzer-Williams, M.G. Antigen-specific memory B cell development. *Annu Rev Immunol* **2005**, *23*, 487-513, doi:10.1146/annurev.immunol.23.021704.115732.
76. Inoue, T.; Moran, I.; Shinnakasu, R.; Phan, T.G.; Kurosaki, T. Generation of memory B cells and their reactivation. *Immunol Rev* **2018**, *283*, 138-149, doi:10.1111/imr.12640.
77. Crotty, S.; Felgner, P.; Davies, H.; Glidewell, J.; Villarreal, L.; Ahmed, R. Cutting edge: long-term B cell memory in humans after smallpox vaccination. *J Immunol* **2003**, *171*, 4969-4973.
78. Pape, K.A.; Taylor, J.J.; Maul, R.W.; Gearhart, P.J.; Jenkins, M.K. Different B cell populations mediate early and late memory during an endogenous immune response. *Science* **2011**, *331*, 1203-1207, doi:10.1126/science.1201730.
79. Wang, N.S.; McHeyzer-Williams, L.J.; Okitsu, S.L.; Burris, T.P.; Reiner, S.L.; McHeyzer-Williams, M.G. Divergent transcriptional programming of class-specific B cell memory by T-bet and RORα. *Nat Immunol* **2012**, *13*, 604-611, doi:10.1038/ni.2294.
80. Pauli, N.T.; Henry Dunand, C.J.; Wilson, P.C. Exploiting human memory B cell heterogeneity for improved vaccine efficacy. *Front Immunol* **2011**, *2*, 77, doi:10.3389/fimmu.2011.00077.
81. Moir, S.; Ho, J.; Malaspina, A.; Wang, W.; DiPoto, A.C.; O'Shea, M.A.; Roby, G.; Kottilil, S.; Arthos, J.; Proschan, M.A., et al. Evidence for HIV-associated B cell exhaustion in a dysfunctional memory B cell compartment in HIV-infected viremic individuals. *J Exp Med* **2008**, *205*, 1797-1805, doi:10.1084/jem.20072683.
82. Charles, E.D.; Brunetti, C.; Marukian, S.; Ritola, K.D.; Talal, A.H.; Marks, K.; Jacobson, I.M.; Rice, C.M.; Dustin, L.B. Clonal B cells in patients with hepatitis C virus-associated mixed cryoglobulinemia contain an expanded anergic CD21low B-cell subset. *Blood* **2011**, *117*, 5425-5437, doi:10.1182/blood-2010-10-312942.
83. Weiss, G.E.; Crompton, P.D.; Li, S.; Walsh, L.A.; Moir, S.; Traore, B.; Kayentao, K.; Ongoiba, A.; Doumbo, O.K.; Pierce, S.K. Atypical memory B cells are greatly expanded in individuals living in a malaria-endemic area. *J Immunol* **2009**, *183*, 2176-2182, doi:10.4049/jimmunol.0901297.
84. Weiss, G.E.; Traore, B.; Kayentao, K.; Ongoiba, A.; Doumbo, S.; Doumtabe, D.; Kone, Y.; Dia, S.; Guindo, A.; Traore, A., et al. The Plasmodium falciparum-specific human memory B cell compartment expands gradually with repeated malaria infections. *PLoS Pathog* **2010**, *6*, e1000912, doi:10.1371/journal.ppat.1000912.
85. Weiss, G.E.; Clark, E.H.; Li, S.; Traore, B.; Kayentao, K.; Ongoiba, A.; Hernandez, J.N.; Doumbo, O.K.; Pierce, S.K.; Branch, O.H., et al. A positive correlation between atypical memory B cells and Plasmodium falciparum transmission intensity in cross-sectional studies in Peru and Mali. *PLoS One* **2011**, *6*, e15983, doi:10.1371/journal.pone.0015983.
86. Portugal, S.; Tipton, C.M.; Sohn, H.; Kone, Y.; Wang, J.; Li, S.; Skinner, J.; Virtaneva, K.; Sturdevant, D.E.; Porcella, S.F., et al. Malaria-associated atypical memory B cells exhibit markedly reduced B cell receptor signaling and effector function. *Elife* **2015**, *4*, doi:10.7554/eLife.07218.
87. WHO. World Malaria Report 2017: Summary. *Geneva*: *World Health Organization*; *2017*. *Licence*: *CC* BY-*NC-SA 3.0 IGO*. http://www.who.int/malaria/publications/world-malaria-report-2017/en/, 2017.
88. Gallup, J.L.; Sachs, J.D. The economic burden of malaria. *Am J Trop Med Hyg* **2001**, *64*, 85-96.
89. Gunalan, K.; Niangaly, A.; Thera, M.A.; Doumbo, O.K.; Miller, L.H. Plasmodium vivax Infections of Duffy-Negative Erythrocytes: Historically Undetected or a Recent Adaptation? *Trends Parasitol* **2018**, *34*, 420-429, doi:10.1016/j.pt.2018.02.006.

90. Cibulskis, R.E.; Alonso, P.; Aponte, J.; Aregawi, M.; Barrette, A.; Bergeron, L.; Fergus, C.A.; Knox, T.; Lynch, M.; Patouillard, E., et al. Malaria: Global progress 2000 - 2015 and future challenges. *Infect Dis Poverty* **2016**, *5*, 61, doi:10.1186/s40249-016-0151-8.
91. Bhatt, S.; Weiss, D.J.; Cameron, E.; Bisanzio, D.; Mappin, B.; Dalrymple, U.; Battle, K.; Moyes, C.L.; Henry, A.; Eckhoff, P.A., et al. The effect of malaria control on Plasmodium falciparum in Africa between 2000 and 2015. *Nature* **2015**, *526*, 207-211, doi:10.1038/nature15535.
92. WHO. Global Health Observatory data repository - Malaria incidence data by country. Availabe online: http://apps.who.int/gho/data/node.main.MALARIAINCIDENCE?lang=en (accessed on 15/09/18).
93. Imwong, M.; Suwannasin, K.; Kunasol, C.; Sutawong, K.; Mayxay, M.; Rekol, H.; Smithuis, F.M.; Hlaing, T.M.; Tun, K.M.; van der Pluijm, R.W., et al. The spread of artemisinin-resistant Plasmodium falciparum in the Greater Mekong subregion: a molecular epidemiology observational study. *Lancet Infect Dis* **2017**, *17*, 491-497, doi:10.1016/S1473-3099(17)30048-8.
94. Caminade, C.; Kovats, S.; Rocklov, J.; Tompkins, A.M.; Morse, A.P.; Colón-González, F.J.; Stenlund, H.; Martens, P.; Lloyd, S.J. Impact of climate change on global malaria distribution. *Proc Natl Acad Sci U S A* **2014**, *111*, 3286-3291, doi:10.1073/pnas.1302089111.
95. Vaccines, m.C.G.o. A research agenda for malaria eradication: vaccines. *PLoS Med* **2011**, *8*, e1000398, doi:10.1371/journal.pmed.1000398.
96. Lee, A.H.; Symington, L.S.; Fidock, D.A. DNA repair mechanisms and their biological roles in the malaria parasite Plasmodium falciparum. *Microbiol Mol Biol Rev* **2014**, *78*, 469-486, doi:10.1128/MMBR.00059-13.
97. Beier, J.C.; Koros, J.K. Anatomical dissemination of circumsporozoite protein in wild Afrotropical Anopheles affects malaria sporozoite rate determination by ELISA. *Med Vet Entomol* **1991**, *5*, 81-85.
98. Vanderberg, J.P. Plasmodium berghei: quantitation of sporozoites injected by mosquitoes feeding on a rodent host. *Exp Parasitol* **1977**, *42*, 169-181.
99. Vanderberg, J.P.; Frevert, U. Intravital microscopy demonstrating antibody-mediated immobilisation of Plasmodium berghei sporozoites injected into skin by mosquitoes. *Int J Parasitol* **2004**, *34*, 991-996, doi:10.1016/j.ijpara.2004.05.005.
100. Kebaier, C.; Voza, T.; Vanderberg, J. Kinetics of mosquito-injected Plasmodium sporozoites in mice: fewer sporozoites are injected into sporozoite-immunized mice. *PLoS Pathog* **2009**, *5*, e1000399, doi:10.1371/journal.ppat.1000399.
101. Jin, Y.; Kebaier, C.; Vanderberg, J. Direct microscopic quantification of dynamics of Plasmodium berghei sporozoite transmission from mosquitoes to mice. *Infect Immun* **2007**, *75*, 5532-5539, doi:10.1128/IAI.00600-07.
102. Amino, R.; Thiberge, S.; Martin, B.; Celli, S.; Shorte, S.; Frischknecht, F.; Ménard, R. Quantitative imaging of Plasmodium transmission from mosquito to mammal. *Nat Med* **2006**, *12*, 220-224, doi:10.1038/nm1350.
103. Yamauchi, L.M.; Coppi, A.; Snounou, G.; Sinnis, P. Plasmodium sporozoites trickle out of the injection site. *Cell Microbiol* **2007**, *9*, 1215-1222, doi:10.1111/j.1462-5822.2006.00861.x.
104. Chakravarty, S.; Cockburn, I.A.; Kuk, S.; Overstreet, M.G.; Sacci, J.B.; Zavala, F. CD8+ T lymphocytes protective against malaria liver stages are primed in skin-draining lymph nodes. *Nat Med* **2007**, *13*, 1035-1041, doi:10.1038/nm1628.
105. Tavares, J.; Formaglio, P.; Thiberge, S.; Mordelet, E.; Van Rooijen, N.; Medvinsky, A.; Ménard, R.; Amino, R. Role of host cell traversal by the malaria sporozoite during liver infection. *J Exp Med* **2013**, *210*, 905-915, doi:10.1084/jem.20121130.

106. Mota, M.M.; Pradel, G.; Vanderberg, J.P.; Hafalla, J.C.; Frevert, U.; Nussenzweig, R.S.; Nussenzweig, V.; Rodríguez, A. Migration of Plasmodium sporozoites through cells before infection. *Science* **2001**, *291*, 141-144, doi:10.1126/science.291.5501.141.
107. Sturm, A.; Amino, R.; van de Sand, C.; Regen, T.; Retzlaff, S.; Rennenberg, A.; Krueger, A.; Pollok, J.M.; Menard, R.; Heussler, V.T. Manipulation of host hepatocytes by the malaria parasite for delivery into liver sinusoids. *Science* **2006**, *313*, 1287-1290, doi:10.1126/science.1129720.
108. Weiss, G.E.; Gilson, P.R.; Taechalertpaisarn, T.; Tham, W.H.; de Jong, N.W.; Harvey, K.L.; Fowkes, F.J.; Barlow, P.N.; Rayner, J.C.; Wright, G.J., et al. Revealing the sequence and resulting cellular morphology of receptor-ligand interactions during Plasmodium falciparum invasion of erythrocytes. *PLoS Pathog* **2015**, *11*, e1004670, doi:10.1371/journal.ppat.1004670.
109. Garg, S.; Agarwal, S.; Dabral, S.; Kumar, N.; Sehrawat, S.; Singh, S. Visualization and quantification of Plasmodium falciparum intraerythrocytic merozoites. *Syst Synth Biol* **2015**, *9*, 23-26, doi:10.1007/s11693-015-9167-9.
110. Buckling, A.; Ranford-Cartwright, L.C.; Miles, A.; Read, A.F. Chloroquine increases Plasmodium falciparum gametocytogenesis in vitro. *Parasitology* **1999**, *118 (Pt 4)*, 339-346.
111. Price, R.; Nosten, F.; Simpson, J.A.; Luxemburger, C.; Phaipun, L.; ter Kuile, F.; van Vugt, M.; Chongsuphajaisiddhi, T.; White, N.J. Risk factors for gametocyte carriage in uncomplicated falciparum malaria. *Am J Trop Med Hyg* **1999**, *60*, 1019-1023.
112. Bruce, M.C.; Alano, P.; Duthie, S.; Carter, R. Commitment of the malaria parasite Plasmodium falciparum to sexual and asexual development. *Parasitology* **1990**, *100 Pt 2*, 191-200.
113. Regev-Rudzki, N.; Wilson, D.W.; Carvalho, T.G.; Sisquella, X.; Coleman, B.M.; Rug, M.; Bursac, D.; Angrisano, F.; Gee, M.; Hill, A.F., et al. Cell-cell communication between malaria-infected red blood cells via exosome-like vesicles. *Cell* **2013**, *153*, 1120-1133, doi:10.1016/j.cell.2013.04.029.
114. Mawson, A.R. The pathogenesis of malaria: a new perspective. *Pathog Glob Health* **2013**, *107*, 122-129, doi:10.1179/2047773213Y.0000000084.
115. Moya-Alvarez, V.; Abellana, R.; Cot, M. Pregnancy-associated malaria and malaria in infants: an old problem with present consequences. *Malar J* **2014**, *13*, 271, doi:10.1186/1475-2875-13-271.
116. Franke-Fayard, B.; Fonager, J.; Braks, A.; Khan, S.M.; Janse, C.J. Sequestration and tissue accumulation of human malaria parasites: can we learn anything from rodent models of malaria? *PLoS Pathog* **2010**, *6*, e1001032, doi:10.1371/journal.ppat.1001032.
117. Artavanis-Tsakonas, K.; Tongren, J.E.; Riley, E.M. The war between the malaria parasite and the immune system: immunity, immunoregulation and immunopathology. *Clin Exp Immunol* **2003**, *133*, 145-152.
118. Grau, G.E.; Taylor, T.E.; Molyneux, M.E.; Wirima, J.J.; Vassalli, P.; Hommel, M.; Lambert, P.H. Tumor necrosis factor and disease severity in children with falciparum malaria. *N Engl J Med* **1989**, *320*, 1586-1591, doi:10.1056/NEJM198906153202404.
119. Kwiatkowski, D.; Hill, A.V.; Sambou, I.; Twumasi, P.; Castracane, J.; Manogue, K.R.; Cerami, A.; Brewster, D.R.; Greenwood, B.M. TNF concentration in fatal cerebral, non-fatal cerebral, and uncomplicated Plasmodium falciparum malaria. *Lancet* **1990**, *336*, 1201-1204.
120. Kurtzhals, J.A.; Adabayeri, V.; Goka, B.Q.; Akanmori, B.D.; Oliver-Commey, J.O.; Nkrumah, F.K.; Behr, C.; Hviid, L. Low plasma concentrations of interleukin 10 in severe malarial anaemia compared with cerebral and uncomplicated malaria. *Lancet* **1998**, *351*, 1768-1772, doi:10.1016/S0140-6736(97)09439-7.

121. Day, N.P.; Hien, T.T.; Schollaardt, T.; Loc, P.P.; Chuong, L.V.; Chau, T.T.; Mai, N.T.; Phu, N.H.; Sinh, D.X.; White, N.J., et al. The prognostic and pathophysiologic role of pro- and antiinflammatory cytokines in severe malaria. *J Infect Dis* **1999**, *180*, 1288-1297, doi:10.1086/315016.
122. Amani, V.; Vigário, A.M.; Belnoue, E.; Marussig, M.; Fonseca, L.; Mazier, D.; Rénia, L. Involvement of IFN-gamma receptor-medicated signaling in pathology and anti-malarial immunity induced by Plasmodium berghei infection. *Eur J Immunol* **2000**, *30*, 1646-1655, doi:10.1002/1521-4141(200006)30:6<1646::AID-IMMU1646>3.0.CO;2-0.
123. Riley, E.M.; Jakobsen, P.H.; Allen, S.J.; Wheeler, J.G.; Bennett, S.; Jepsen, S.; Greenwood, B.M. Immune response to soluble exoantigens of Plasmodium falciparum may contribute to both pathogenesis and protection in clinical malaria: evidence from a longitudinal, prospective study of semi-immune African children. *Eur J Immunol* **1991**, *21*, 1019-1025, doi:10.1002/eji.1830210424.
124. Mshana, R.N.; Boulandi, J.; Mshana, N.M.; Mayombo, J.; Mendome, G. Cytokines in the pathogenesis of malaria: levels of IL-I beta, IL-4, IL-6, TNF-alpha and IFN-gamma in plasma of healthy individuals and malaria patients in a holoendemic area. *J Clin Lab Immunol* **1991**, *34*, 131-139.
125. Erunkulu, O.A.; Hill, A.V.; Kwiatkowski, D.P.; Todd, J.E.; Iqbal, J.; Berzins, K.; Riley, E.M.; Greenwood, B.M. Severe malaria in Gambian children is not due to lack of previous exposure to malaria. *Clin Exp Immunol* **1992**, *89*, 296-300.
126. Riley, E.M. Is T-cell priming required for initiation of pathology in malaria infections? *Immunol Today* **1999**, *20*, 228-233.
127. Anstey, N.M.; Weinberg, J.B.; Hassanali, M.Y.; Mwaikambo, E.D.; Manyenga, D.; Misukonis, M.A.; Arnelle, D.R.; Hollis, D.; McDonald, M.I.; Granger, D.L. Nitric oxide in Tanzanian children with malaria: inverse relationship between malaria severity and nitric oxide production/nitric oxide synthase type 2 expression. *J Exp Med* **1996**, *184*, 557-567.
128. Luty, A.J.; Lell, B.; Schmidt-Ott, R.; Lehman, L.G.; Luckner, D.; Greve, B.; Matousek, P.; Herbich, K.; Schmid, D.; Migot-Nabias, F., et al. Interferon-gamma responses are associated with resistance to reinfection with Plasmodium falciparum in young African children. *J Infect Dis* **1999**, *179*, 980-988, doi:10.1086/314689.
129. Gupta, S.; Snow, R.W.; Donnelly, C.A.; Marsh, K.; Newbold, C. Immunity to non-cerebral severe malaria is acquired after one or two infections. *Nat Med* **1999**, *5*, 340-343, doi:10.1038/6560.
130. Langhorne, J.; Ndungu, F.M.; Sponaas, A.M.; Marsh, K. Immunity to malaria: more questions than answers. *Nat Immunol* **2008**, *9*, 725-732, doi:10.1038/ni.f.205.
131. Griffin, J.T.; Hollingsworth, T.D.; Reyburn, H.; Drakeley, C.J.; Riley, E.M.; Ghani, A.C. Gradual acquisition of immunity to severe malaria with increasing exposure. *Proc Biol Sci* **2015**, *282*, 20142657, doi:10.1098/rspb.2014.2657.
132. Marsh, K.; Kinyanjui, S. Immune effector mechanisms in malaria. *Parasite Immunol* **2006**, *28*, 51-60, doi:10.1111/j.1365-3024.2006.00808.x.
133. COHEN, S.; McGREGOR, I.A.; CARRINGTON, S. Gamma-globulin and acquired immunity to human malaria. *Nature* **1961**, *192*, 733-737.
134. MCGREGOR, I.A. STUDIES IN THE ACQUISITION OF IMMUNITY OF PLASMODIUM FALCIPARUM INFECTIONS IN AFRICA. *Trans R Soc Trop Med Hyg* **1964**, *58*, 80-92.
135. Sabchareon, A.; Burnouf, T.; Ouattara, D.; Attanath, P.; Bouharoun-Tayoun, H.; Chantavanich, P.; Foucault, C.; Chongsuphajaisiddhi, T.; Druilhe, P. Parasitologic and clinical human response to immunoglobulin administration in falciparum malaria. *Am J Trop Med Hyg* **1991**, *45*, 297-308.
136. Arora, G.; Hart, G.T.; Manzella-Lapeira, J.; Doritchamou, J.Y.; Narum, D.L.; Thomas, L.M.; Brzostowski, J.; Rajagopalan, S.; Doumbo, O.K.; Traore, B., et al. NK cells inhibit. *Elife* **2018**, *7*, doi:10.7554/eLife.36806.

137. Dutta, S.; Haynes, J.D.; Moch, J.K.; Barbosa, A.; Lanar, D.E. Invasion-inhibitory antibodies inhibit proteolytic processing of apical membrane antigen 1 of Plasmodium falciparum merozoites. *Proc Natl Acad Sci U S A* **2003**, *100*, 12295-12300, doi:10.1073/pnas.2032858100.
138. Boyle, M.J.; Reiling, L.; Feng, G.; Langer, C.; Osier, F.H.; Aspeling-Jones, H.; Cheng, Y.S.; Stubbs, J.; Tetteh, K.K.; Conway, D.J., et al. Human antibodies fix complement to inhibit Plasmodium falciparum invasion of erythrocytes and are associated with protection against malaria. *Immunity* **2015**, *42*, 580-590, doi:10.1016/j.immuni.2015.02.012.
139. Mustaffa, K.M.F.; Storm, J.; Whittaker, M.; Szestak, T.; Craig, A.G. In vitro inhibition and reversal of Plasmodium falciparum cytoadherence to endothelium by monoclonal antibodies to ICAM-1 and CD36. *Malar J* **2017**, *16*, 279, doi:10.1186/s12936-017-1930-9.
140. Yilmaz, B.; Portugal, S.; Tran, T.M.; Gozzelino, R.; Ramos, S.; Gomes, J.; Regalado, A.; Cowan, P.J.; d'Apice, A.J.; Chong, A.S., et al. Gut microbiota elicits a protective immune response against malaria transmission. *Cell* **2014**, *159*, 1277-1289, doi:10.1016/j.cell.2014.10.053.
141. Aguilar, R.; Ubillos, I.; Vidal, M.; Balanza, N.; Crespo, N.; Jiménez, A.; Nhabomba, A.; Jairoce, C.; Dosoo, D.; Gyan, B., et al. Antibody responses to α-Gal in African children vary with age and site and are associated with malaria protection. *Sci Rep* **2018**, *8*, 9999, doi:10.1038/s41598-018-28325-w.
142. Soares, M.P.; Yilmaz, B. Microbiota Control of Malaria Transmission. *Trends Parasitol* **2016**, *32*, 120-130, doi:10.1016/j.pt.2015.11.004.
143. Doolan, D.L.; Dobaño, C.; Baird, J.K. Acquired immunity to malaria. *Clin Microbiol Rev* **2009**, *22*, 13-36, Table of Contents, doi:10.1128/CMR.00025-08.
144. Schieck, E.; Poole, E.J.; Rippert, A.; Peshu, J.; Sasi, P.; Borrmann, S.; Bull, P.C. Plasmodium falciparum variant erythrocyte surface antigens: a pilot study of antibody acquisition in recurrent natural infections. *Malar J* **2017**, *16*, 450, doi:10.1186/s12936-017-2097-0.
145. Dzikowski, R.; Templeton, T.J.; Deitsch, K. Variant antigen gene expression in malaria. *Cell Microbiol* **2006**, *8*, 1371-1381, doi:10.1111/j.1462-5822.2006.00760.x.
146. Jensen, A.T.; Magistrado, P.; Sharp, S.; Joergensen, L.; Lavstsen, T.; Chiucchiuini, A.; Salanti, A.; Vestergaard, L.S.; Lusingu, J.P.; Hermsen, R., et al. Plasmodium falciparum associated with severe childhood malaria preferentially expresses PfEMP1 encoded by group A var genes. *J Exp Med* **2004**, *199*, 1179-1190, doi:10.1084/jem.20040274.
147. Travassos, M.A.; Niangaly, A.; Bailey, J.A.; Ouattara, A.; Coulibaly, D.; Lyke, K.E.; Laurens, M.B.; Pablo, J.; Jasinskas, A.; Nakajima, R., et al. Children with cerebral malaria or severe malarial anaemia lack immunity to distinct variant surface antigen subsets. *Sci Rep* **2018**, *8*, 6281, doi:10.1038/s41598-018-24462-4.
148. King, T.; Lamb, T. Interferon-γ: The Jekyll and Hyde of Malaria. *PLoS Pathog* **2015**, *11*, e1005118, doi:10.1371/journal.ppat.1005118.
149. Overstreet, M.G.; Cockburn, I.A.; Chen, Y.C.; Zavala, F. Protective CD8 T cells against Plasmodium liver stages: immunobiology of an 'unnatural' immune response. *Immunol Rev* **2008**, *225*, 272-283, doi:10.1111/j.1600-065X.2008.00671.x.
150. Dodoo, D.; Hollingdale, M.R.; Anum, D.; Koram, K.A.; Gyan, B.; Akanmori, B.D.; Ocran, J.; Adu-Amankwah, S.; Geneshan, H.; Abot, E., et al. Measuring naturally acquired immune responses to candidate malaria vaccine antigens in Ghanaian adults. *Malar J* **2011**, *10*, 168, doi:10.1186/1475-2875-10-168.
151. Triller, G.; Scally, S.W.; Costa, G.; Pissarev, M.; Kreschel, C.; Bosch, A.; Marois, E.; Sack, B.K.; Murugan, R.; Salman, A.M., et al. Natural Parasite Exposure Induces Protective Human Anti-Malarial Antibodies. *Immunity* **2017**, *47*, 1197-1209.e1110, doi:10.1016/j.immuni.2017.11.007.
152. Migot-Nabias, F.; Deloron, P.; Ringwald, P.; Dubois, B.; Mayombo, J.; Minh, T.N.; Fievet, N.; Millet, P.; Luty, A. Immune response to Plasmodium falciparum liver stage antigen-1:

geographical variations within Central Africa and their relationship with protection from clinical malaria. *Trans R Soc Trop Med Hyg* **2000**, *94*, 557-562.
153. Schofield, L.; Villaquiran, J.; Ferreira, A.; Schellekens, H.; Nussenzweig, R.; Nussenzweig, V. Gamma interferon, CD8+ T cells and antibodies required for immunity to malaria sporozoites. *Nature* **1987**, *330*, 664-666, doi:10.1038/330664a0.
154. Jagannathan, P.; Nankya, F.; Stoyanov, C.; Eccles-James, I.; Sikyomu, E.; Naluwu, K.; Wamala, S.; Nalubega, M.; Briggs, J.; Bowen, K., et al. IFNγ Responses to Pre-erythrocytic and Blood-stage Malaria Antigens Exhibit Differential Associations With Past Exposure and Subsequent Protection. *J Infect Dis* **2015**, *211*, 1987-1996, doi:10.1093/infdis/jiu814.
155. Hoffman, S.L.; Oster, C.N.; Plowe, C.V.; Woollett, G.R.; Beier, J.C.; Chulay, J.D.; Wirtz, R.A.; Hollingdale, M.R.; Mugambi, M. Naturally acquired antibodies to sporozoites do not prevent malaria: vaccine development implications. *Science* **1987**, *237*, 639-642.
156. Owusu-Agyei, S.; Koram, K.A.; Baird, J.K.; Utz, G.C.; Binka, F.N.; Nkrumah, F.K.; Fryauff, D.J.; Hoffman, S.L. Incidence of symptomatic and asymptomatic Plasmodium falciparum infection following curative therapy in adult residents of northern Ghana. *Am J Trop Med Hyg* **2001**, *65*, 197-203.
157. Kusi, K.A.; Bosomprah, S.; Dodoo, D.; Kyei-Baafour, E.; Dickson, E.K.; Mensah, D.; Angov, E.; Dutta, S.; Sedegah, M.; Koram, K.A. Anti-sporozoite antibodies as alternative markers for malaria transmission intensity estimation. *Malar J* **2014**, *13*, 103, doi:10.1186/1475-2875-13-103.
158. BARR, M.; McGREGOR, I.A. Diphtheria antitoxin levels in the serum of Gambian Africans. *Trans R Soc Trop Med Hyg* **1962**, *56*, 368-370.
159. Greenwood, B.M.; Bradley-Moore, A.M.; Bryceson, A.D.; Palit, A. Immunosuppression in children with malaria. *Lancet* **1972**, *1*, 169-172.
160. Williamson, W.A.; Greenwood, B.M. Impairment of the immune response to vaccination after acute malaria. *Lancet* **1978**, *1*, 1328-1329.
161. Ocaña-Morgner, C.; Mota, M.M.; Rodriguez, A. Malaria blood stage suppression of liver stage immunity by dendritic cells. *J Exp Med* **2003**, *197*, 143-151.
162. Ryg-Cornejo, V.; Ioannidis, L.J.; Ly, A.; Chiu, C.Y.; Tellier, J.; Hill, D.L.; Preston, S.P.; Pellegrini, M.; Yu, D.; Nutt, S.L., et al. Severe Malaria Infections Impair Germinal Center Responses by Inhibiting T Follicular Helper Cell Differentiation. *Cell Rep* **2016**, *14*, 68-81, doi:10.1016/j.celrep.2015.12.006.
163. Keitany, G.J.; Kim, K.S.; Krishnamurty, A.T.; Hondowicz, B.D.; Hahn, W.O.; Dambrauskas, N.; Sather, D.N.; Vaughan, A.M.; Kappe, S.H.; Pepper, M. Blood Stage Malaria Disrupts Humoral Immunity to the Pre-erythrocytic Stage Circumsporozoite Protein. *Cell Rep* **2016**, *17*, 3193-3205, doi:10.1016/j.celrep.2016.11.060.
164. Ho, M.; Webster, H.K.; Looareesuwan, S.; Supanaranond, W.; Phillips, R.E.; Chanthavanich, P.; Warrell, D.A. Antigen-specific immunosuppression in human malaria due to Plasmodium falciparum. *J Infect Dis* **1986**, *153*, 763-771.
165. Troye-Blomberg, M.; Romero, P.; Patarroyo, M.E.; Björkman, A.; Perlmann, P. Regulation of the immune response in Plasmodium falciparum malaria. III. Proliferative response to antigen in vitro and subset composition of T cells from patients with acute infection or from immune donors. *Clin Exp Immunol* **1984**, *58*, 380-387.
166. Scott, J.A.; Berkley, J.A.; Mwangi, I.; Ochola, L.; Uyoga, S.; Macharia, A.; Ndila, C.; Lowe, B.S.; Mwarumba, S.; Bauni, E., et al. Relation between falciparum malaria and bacteraemia in Kenyan children: a population-based, case-control study and a longitudinal study. *Lancet* **2011**, *378*, 1316-1323, doi:10.1016/S0140-6736(11)60888-X.
167. Kleinschmidt, I.; Schwabe, C.; Shiva, M.; Segura, J.L.; Sima, V.; Mabunda, S.J.; Coleman, M. Combining indoor residual spraying and insecticide-treated net interventions. *Am J Trop Med Hyg* **2009**, *81*, 519-524.

168. Molineaux, L. Malaria and mortality: some epidemiological considerations. *Ann Trop Med Parasitol* **1997**, *91*, 811-825.
169. Alonso, P.L.; Lindsay, S.W.; Armstrong, J.R.; Conteh, M.; Hill, A.G.; David, P.H.; Fegan, G.; de Francisco, A.; Hall, A.J.; Shenton, F.C. The effect of insecticide-treated bed nets on mortality of Gambian children. *Lancet* **1991**, *337*, 1499-1502.
170. Theander, T.G.; Bygbjerg, I.C.; Jacobsen, L.; Jepsen, S.; Larsen, P.B.; Kharazmi, A. Low parasite specific T cell response in clinically immune individuals with low grade Plasmodium falciparum parasitaemia. *Trans R Soc Trop Med Hyg* **1986**, *80*, 1000-1001.
171. Illingworth, J.; Butler, N.S.; Roetynck, S.; Mwacharo, J.; Pierce, S.K.; Bejon, P.; Crompton, P.D.; Marsh, K.; Ndungu, F.M. Chronic exposure to Plasmodium falciparum is associated with phenotypic evidence of B and T cell exhaustion. *J Immunol* **2013**, *190*, 1038-1047, doi:10.4049/jimmunol.1202438.
172. Butler, N.S.; Moebius, J.; Pewe, L.L.; Traore, B.; Doumbo, O.K.; Tygrett, L.T.; Waldschmidt, T.J.; Crompton, P.D.; Harty, J.T. Therapeutic blockade of PD-L1 and LAG-3 rapidly clears established blood-stage Plasmodium infection. *Nat Immunol* **2011**, *13*, 188-195, doi:10.1038/ni.2180.
173. Behet, M.C.; Foquet, L.; van Gemert, G.J.; Bijker, E.M.; Meuleman, P.; Leroux-Roels, G.; Hermsen, C.C.; Scholzen, A.; Sauerwein, R.W. Sporozoite immunization of human volunteers under chemoprophylaxis induces functional antibodies against pre-erythrocytic stages of Plasmodium falciparum. *Malar J* **2014**, *13*, 136, doi:10.1186/1475-2875-13-136.
174. Seder, R.A.; Chang, L.J.; Enama, M.E.; Zephir, K.L.; Sarwar, U.N.; Gordon, I.J.; Holman, L.A.; James, E.R.; Billingsley, P.F.; Gunasekera, A., et al. Protection against malaria by intravenous immunization with a nonreplicating sporozoite vaccine. *Science* **2013**, *341*, 1359-1365, doi:10.1126/science.1241800.
175. Finney, O.C.; Keitany, G.J.; Smithers, H.; Kaushansky, A.; Kappe, S.; Wang, R. Immunization with genetically attenuated P. falciparum parasites induces long-lived antibodies that efficiently block hepatocyte invasion by sporozoites. *Vaccine* **2014**, *32*, 2135-2138, doi:10.1016/j.vaccine.2014.02.055.
176. Wipasa, J.; Suphavilai, C.; Okell, L.C.; Cook, J.; Corran, P.H.; Thaikla, K.; Liewsaree, W.; Riley, E.M.; Hafalla, J.C. Long-lived antibody and B Cell memory responses to the human malaria parasites, Plasmodium falciparum and Plasmodium vivax. *PLoS Pathog* **2010**, *6*, e1000770, doi:10.1371/journal.ppat.1000770.
177. Banga, S.; Coursen, J.D.; Portugal, S.; Tran, T.M.; Hancox, L.; Ongoiba, A.; Traore, B.; Doumbo, O.K.; Huang, C.Y.; Harty, J.T., et al. Impact of acute malaria on pre-existing antibodies to viral and vaccine antigens in mice and humans. *PLoS One* **2015**, *10*, e0125090, doi:10.1371/journal.pone.0125090.
178. Ng, D.H.; Skehel, J.J.; Kassiotis, G.; Langhorne, J. Recovery of an antiviral antibody response following attrition caused by unrelated infection. *PLoS Pathog* **2014**, *10*, e1003843, doi:10.1371/journal.ppat.1003843.
179. Wykes, M.N.; Zhou, Y.H.; Liu, X.Q.; Good, M.F. Plasmodium yoelii can ablate vaccine-induced long-term protection in mice. *J Immunol* **2005**, *175*, 2510-2516.
180. Millington, O.R.; Gibson, V.B.; Rush, C.M.; Zinselmeyer, B.H.; Phillips, R.S.; Garside, P.; Brewer, J.M. Malaria impairs T cell clustering and immune priming despite normal signal 1 from dendritic cells. *PLoS Pathog* **2007**, *3*, 1380-1387, doi:10.1371/journal.ppat.0030143.
181. Urban, B.C.; Willcox, N.; Roberts, D.J. A role for CD36 in the regulation of dendritic cell function. *Proc Natl Acad Sci U S A* **2001**, *98*, 8750-8755, doi:10.1073/pnas.151028698.
182. Seixas, E.; Cross, C.; Quin, S.; Langhorne, J. Direct activation of dendritic cells by the malaria parasite, Plasmodium chabaudi chabaudi. *Eur J Immunol* **2001**, *31*, 2970-2978, doi:10.1002/1521-4141(2001010)31:10<2970::AID-IMMU2970>3.0.CO;2-S.

183. Götz, A.; Tang, M.S.; Ty, M.C.; Arama, C.; Ongoiba, A.; Doumtabe, D.; Traore, B.; Crompton, P.D.; Loke, P.; Rodriguez, A. Atypical activation of dendritic cells by. *Proc Natl Acad Sci U S A* **2017**, *114*, E10568-E10577, doi:10.1073/pnas.1708383114.
184. Sun, T.; Holowka, T.; Song, Y.; Zierow, S.; Leng, L.; Chen, Y.; Xiong, H.; Griffith, J.; Nouraie, M.; Thuma, P.E., et al. A Plasmodium-encoded cytokine suppresses T-cell immunity during malaria. *Proc Natl Acad Sci U S A* **2012**, *109*, E2117-2126, doi:10.1073/pnas.1206573109.
185. Zhang, X.; Starnbach, M.N. An Excess of the Proinflammatory Cytokines IFN-γ and IL-12 Impairs the Development of the Memory CD8+ T Cell Response to Chlamydia trachomatis. *J Immunol* **2015**, *195*, 1665-1675, doi:10.4049/jimmunol.1500457.
186. Lumsden, J.M.; Schwenk, R.J.; Rein, L.E.; Moris, P.; Janssens, M.; Ofori-Anyinam, O.; Cohen, J.; Kester, K.E.; Heppner, D.G.; Krzych, U. Protective immunity induced with the RTS,S/AS vaccine is associated with IL-2 and TNF-α producing effector and central memory CD4 T cells. *PLoS One* **2011**, *6*, e20775, doi:10.1371/journal.pone.0020775.
187. Arese, P.; Schwarzer, E. Malarial pigment (haemozoin): a very active 'inert' substance. *Ann Trop Med Parasitol* **1997**, *91*, 501-516.
188. Coban, C.; Ishii, K.J.; Horii, T.; Akira, S. Manipulation of host innate immune responses by the malaria parasite. *Trends Microbiol* **2007**, *15*, 271-278, doi:10.1016/j.tim.2007.04.003.
189. Coban, C.; Ishii, K.J.; Kawai, T.; Hemmi, H.; Sato, S.; Uematsu, S.; Yamamoto, M.; Takeuchi, O.; Itagaki, S.; Kumar, N., et al. Toll-like receptor 9 mediates innate immune activation by the malaria pigment hemozoin. *J Exp Med* **2005**, *201*, 19-25, doi:10.1084/jem.20041836.
190. Parroche, P.; Lauw, F.N.; Goutagny, N.; Latz, E.; Monks, B.G.; Visintin, A.; Halmen, K.A.; Lamphier, M.; Olivier, M.; Bartholomeu, D.C., et al. Malaria hemozoin is immunologically inert but radically enhances innate responses by presenting malaria DNA to Toll-like receptor 9. *Proc Natl Acad Sci U S A* **2007**, *104*, 1919-1924, doi:10.1073/pnas.0608745104.
191. Oliviero, B.; Mantovani, S.; Ludovisi, S.; Varchetta, S.; Mele, D.; Paolucci, S.; Baldanti, F.; Mondelli, M.U. Skewed B cells in chronic hepatitis C virus infection maintain their ability to respond to virus-induced activation. *J Viral Hepat* **2015**, *22*, 391-398, doi:10.1111/jvh.12336.
192. Joosten, S.A.; van Meijgaarden, K.E.; Del Nonno, F.; Baiocchini, A.; Petrone, L.; Vanini, V.; Smits, H.H.; Palmieri, F.; Goletti, D.; Ottenhoff, T.H. Patients with Tuberculosis Have a Dysfunctional Circulating B-Cell Compartment, Which Normalizes following Successful Treatment. *PLoS Pathog* **2016**, *12*, e1005687, doi:10.1371/journal.ppat.1005687.
193. Muellenbeck, M.F.; Ueberheide, B.; Amulic, B.; Epp, A.; Fenyo, D.; Busse, C.E.; Esen, M.; Theisen, M.; Mordmüller, B.; Wardemann, H. Atypical and classical memory B cells produce Plasmodium falciparum neutralizing antibodies. *J Exp Med* **2013**, *210*, 389-399, doi:10.1084/jem.20121970.
194. Sullivan, R.T.; Kim, C.C.; Fontana, M.F.; Feeney, M.E.; Jagannathan, P.; Boyle, M.J.; Drakeley, C.J.; Ssewanyana, I.; Nankya, F.; Mayanja-Kizza, H., et al. FCRL5 Delineates Functionally Impaired Memory B Cells Associated with Plasmodium falciparum Exposure. *PLoS Pathog* **2015**, *11*, e1004894, doi:10.1371/journal.ppat.1004894.
195. Portugal, S.; Obeng-Adjei, N.; Moir, S.; Crompton, P.D.; Pierce, S.K. Atypical memory B cells in human chronic infectious diseases: An interim report. *Cell Immunol* **2017**, *321*, 18-25, doi:10.1016/j.cellimm.2017.07.003.
196. Obeng-Adjei, N.; Portugal, S.; Holla, P.; Li, S.; Sohn, H.; Ambegaonkar, A.; Skinner, J.; Bowyer, G.; Doumbo, O.K.; Traore, B., et al. Malaria-induced interferon-γ drives the expansion of Tbethi atypical memory B cells. *PLoS Pathog* **2017**, *13*, e1006576, doi:10.1371/journal.ppat.1006576.

197. Obeng-Adjei, N.; Portugal, S.; Tran, T.M.; Yazew, T.B.; Skinner, J.; Li, S.; Jain, A.; Felgner, P.L.; Doumbo, O.K.; Kayentao, K., et al. Circulating Th1-Cell-type Tfh Cells that Exhibit Impaired B Cell Help Are Preferentially Activated during Acute Malaria in Children. *Cell Rep* **2015**, *13*, 425-439, doi:10.1016/j.celrep.2015.09.004.
198. Hansen, D.S.; Obeng-Adjei, N.; Ly, A.; Ioannidis, L.J.; Crompton, P.D. Emerging concepts in T follicular helper cell responses to malaria. *Int J Parasitol* **2017**, *47*, 105-110, doi:10.1016/j.ijpara.2016.09.004.
199. Loetscher, M.; Loetscher, P.; Brass, N.; Meese, E.; Moser, B. Lymphocyte-specific chemokine receptor CXCR3: regulation, chemokine binding and gene localization. *Eur J Immunol* **1998**, *28*, 3696-3705, doi:10.1002/(SICI)1521-4141(199811)28:11<3696::AID-IMMU3696>3.0.CO;2-W.
200. Ioannidis, L.J.; Nie, C.Q.; Ly, A.; Ryg-Cornejo, V.; Chiu, C.Y.; Hansen, D.S. Monocyte- and Neutrophil-Derived CXCL10 Impairs Efficient Control of Blood-Stage Malaria Infection and Promotes Severe Disease. *J Immunol* **2016**, *196*, 1227-1238, doi:10.4049/jimmunol.1501562.
201. Kurup, S.P.; Obeng-Adjei, N.; Anthony, S.M.; Traore, B.; Doumbo, O.K.; Butler, N.S.; Crompton, P.D.; Harty, J.T. Regulatory T cells impede acute and long-term immunity to blood-stage malaria through CTLA-4. *Nat Med* **2017**, *23*, 1220-1225, doi:10.1038/nm.4395.
202. Hisaeda, H.; Maekawa, Y.; Iwakawa, D.; Okada, H.; Himeno, K.; Kishihara, K.; Tsukumo, S.; Yasutomo, K. Escape of malaria parasites from host immunity requires CD4+ CD25+ regulatory T cells. *Nat Med* **2004**, *10*, 29-30, doi:10.1038/nm975.
203. Nie, C.Q.; Bernard, N.J.; Schofield, L.; Hansen, D.S. CD4+ CD25+ regulatory T cells suppress CD4+ T-cell function and inhibit the development of Plasmodium berghei-specific TH1 responses involved in cerebral malaria pathogenesis. *Infect Immun* **2007**, *75*, 2275-2282, doi:10.1128/IAI.01783-06.
204. Lindblade, K.A.; Steinhardt, L.; Samuels, A.; Kachur, S.P.; Slutsker, L. The silent threat: asymptomatic parasitemia and malaria transmission. *Expert Rev Anti Infect Ther* **2013**, *11*, 623-639, doi:10.1586/eri.13.45.
205. Rieckmann, K.H. Asymptomatic malaria. *Lancet* **1970**, *1*, 82-83.
206. Felger, I.; Maire, M.; Bretscher, M.T.; Falk, N.; Tiaden, A.; Sama, W.; Beck, H.P.; Owusu-Agyei, S.; Smith, T.A. The dynamics of natural Plasmodium falciparum infections. *PLoS One* **2012**, *7*, e45542, doi:10.1371/journal.pone.0045542.
207. Babiker, H.A.; Abdel-Muhsin, A.M.; Ranford-Cartwright, L.C.; Satti, G.; Walliker, D. Characteristics of Plasmodium falciparum parasites that survive the lengthy dry season in eastern Sudan where malaria transmission is markedly seasonal. *Am J Trop Med Hyg* **1998**, *59*, 582-590.
208. Lacroix, R.; Mukabana, W.R.; Gouagna, L.C.; Koella, J.C. Malaria infection increases attractiveness of humans to mosquitoes. *PLoS Biol* **2005**, *3*, e298, doi:10.1371/journal.pbio.0030298.
209. Chen, I.; Clarke, S.E.; Gosling, R.; Hamainza, B.; Killeen, G.; Magill, A.; O'Meara, W.; Price, R.N.; Riley, E.M. "Asymptomatic" Malaria: A Chronic and Debilitating Infection That Should Be Treated. *PLoS Med* **2016**, *13*, e1001942, doi:10.1371/journal.pmed.1001942.
210. Lee, M.S.J.; Maruyama, K.; Fujita, Y.; Konishi, A.; Lelliott, P.M.; Itagaki, S.; Horii, T.; Lin, J.W.; Khan, S.M.; Kuroda, E., et al. products persist in the bone marrow and promote chronic bone loss. *Sci Immunol* **2017**, *2*, doi:10.1126/sciimmunol.aam8093.
211. LaBeaud, A.D.; Nayakwadi Singer, M.; McKibben, M.; Mungai, P.; Muchiri, E.M.; McKibben, E.; Gildengorin, G.; Sutherland, L.J.; King, C.H.; King, C.L., et al. Parasitism in Children Aged Three Years and Under: Relationship between Infection and Growth in Rural Coastal Kenya. *PLoS Negl Trop Dis* **2015**, *9*, e0003721, doi:10.1371/journal.pntd.0003721.

212. Robbiani, D.F.; Deroubaix, S.; Feldhahn, N.; Oliveira, T.Y.; Callen, E.; Wang, Q.; Jankovic, M.; Silva, I.T.; Rommel, P.C.; Bosque, D., et al. Plasmodium Infection Promotes Genomic Instability and AID-Dependent B Cell Lymphoma. *Cell* **2015**, *162*, 727-737, doi:10.1016/j.cell.2015.07.019.
213. Asghar, M.; Hasselquist, D.; Hansson, B.; Zehtindjiev, P.; Westerdahl, H.; Bensch, S. Chronic infection. Hidden costs of infection: chronic malaria accelerates telomere degradation and senescence in wild birds. *Science* **2015**, *347*, 436-438, doi:10.1126/science.1261121.
214. Griffin, J.T.; Hollingsworth, T.D.; Okell, L.C.; Churcher, T.S.; White, M.; Hinsley, W.; Bousema, T.; Drakeley, C.J.; Ferguson, N.M.; Basáñez, M.G., et al. Reducing Plasmodium falciparum malaria transmission in Africa: a model-based evaluation of intervention strategies. *PLoS Med* **2010**, *7*, doi:10.1371/journal.pmed.1000324.
215. Hill, A.V. Vaccines against malaria. *Philos Trans R Soc Lond B Biol Sci* **2011**, *366*, 2806-2814, doi:10.1098/rstb.2011.0091.
216. Draper, S.J.; Sack, B.K.; King, C.R.; Nielsen, C.M.; Rayner, J.C.; Higgins, M.K.; Long, C.A.; Seder, R.A. Malaria Vaccines: Recent Advances and New Horizons. *Cell Host Microbe* **2018**, *24*, 43-56, doi:10.1016/j.chom.2018.06.008.
217. Ewer, K.J.; Sierra-Davidson, K.; Salman, A.M.; Illingworth, J.J.; Draper, S.J.; Biswas, S.; Hill, A.V. Progress with viral vectored malaria vaccines: A multi-stage approach involving "unnatural immunity". *Vaccine* **2015**, *33*, 7444-7451, doi:10.1016/j.vaccine.2015.09.094.
218. HEIDELBERGER, M.; MAYER, M. Studies in human malaria; an attempt at vaccination of volunteers against mosquito-borne infection with Pl. vivax. *J Immunol* **1946**, *53*, 113-118.
219. Clinicaltrials.gov. Clincialtrials.gov malaria vaccine trials. Availabe online: https://clinicaltrials.gov/ct2/results?cond=Malaria&term=vaccine&cntry=&state=&city=&dist= (accessed on 16/09/18).
220. Moorthy, V.S.; Newman, R.D.; Okwo-Bele, J.M. Malaria vaccine technology roadmap. *Lancet* **2013**, *382*, 1700-1701, doi:10.1016/S0140-6736(13)62238-2.
221. Clyde, D.F.; Most, H.; McCarthy, V.C.; Vanderberg, J.P. Immunization of man against sporozite-induced falciparum malaria. *Am J Med Sci* **1973**, *266*, 169-177.
222. Hoffman, S.L.; Goh, L.M.; Luke, T.C.; Schneider, I.; Le, T.P.; Doolan, D.L.; Sacci, J.; de la Vega, P.; Dowler, M.; Paul, C., et al. Protection of humans against malaria by immunization with radiation-attenuated Plasmodium falciparum sporozoites. *J Infect Dis* **2002**, *185*, 1155-1164, doi:10.1086/339409.
223. Epstein, J.E.; Tewari, K.; Lyke, K.E.; Sim, B.K.; Billingsley, P.F.; Laurens, M.B.; Gunasekera, A.; Chakravarty, S.; James, E.R.; Sedegah, M., et al. Live attenuated malaria vaccine designed to protect through hepatic $CD8^+$ T cell immunity. *Science* **2011**, *334*, 475-480, doi:10.1126/science.1211548.
224. Lyke, K.E.; Ishizuka, A.S.; Berry, A.A.; Chakravarty, S.; DeZure, A.; Enama, M.E.; James, E.R.; Billingsley, P.F.; Gunasekera, A.; Manoj, A., et al. Attenuated PfSPZ Vaccine induces strain-transcending T cells and durable protection against heterologous controlled human malaria infection. *Proc Natl Acad Sci U S A* **2017**, *114*, 2711-2716, doi:10.1073/pnas.1615324114.
225. Epstein, J.E.; Paolino, K.M.; Richie, T.L.; Sedegah, M.; Singer, A.; Ruben, A.J.; Chakravarty, S.; Stafford, A.; Ruck, R.C.; Eappen, A.G., et al. Protection against. *JCI Insight* **2017**, *2*, e89154, doi:10.1172/jci.insight.89154.
226. Sissoko, M.S.; Healy, S.A.; Katile, A.; Omaswa, F.; Zaidi, I.; Gabriel, E.E.; Kamate, B.; Samake, Y.; Guindo, M.A.; Dolo, A., et al. Safety and efficacy of PfSPZ Vaccine against Plasmodium falciparum via direct venous inoculation in healthy malaria-exposed adults in Mali: a randomised, double-blind phase 1 trial. *Lancet Infect Dis* **2017**, *17*, 498-509, doi:10.1016/S1473-3099(17)30104-4.

227. Olotu, A.; Urbano, V.; Hamad, A.; Eka, M.; Chemba, M.; Nyakarungu, E.; Raso, J.; Eburi, E.; Mandumbi, D.O.; Hergott, D., et al. Advancing Global Health through Development and Clinical Trials Partnerships: A Randomized, Placebo-Controlled, Double-Blind Assessment of Safety, Tolerability, and Immunogenicity of PfSPZ Vaccine for Malaria in Healthy Equatoguinean Men. *Am J Trop Med Hyg* **2018**, *98*, 308-318, doi:10.4269/ajtmh.17-0449.
228. Roestenberg, M.; McCall, M.; Hopman, J.; Wiersma, J.; Luty, A.J.; van Gemert, G.J.; van de Vegte-Bolmer, M.; van Schaijk, B.; Teelen, K.; Arens, T., et al. Protection against a malaria challenge by sporozoite inoculation. *N Engl J Med* **2009**, *361*, 468-477, doi:10.1056/NEJMoa0805832.
229. Roestenberg, M.; Teirlinck, A.C.; McCall, M.B.; Teelen, K.; Makamdop, K.N.; Wiersma, J.; Arens, T.; Beckers, P.; van Gemert, G.; van de Vegte-Bolmer, M., et al. Long-term protection against malaria after experimental sporozoite inoculation: an open-label follow-up study. *Lancet* **2011**, *377*, 1770-1776, doi:10.1016/S0140-6736(11)60360-7.
230. Walk, J.; Reuling, I.J.; Behet, M.C.; Meerstein-Kessel, L.; Graumans, W.; van Gemert, G.J.; Siebelink-Stoter, R.; van de Vegte-Bolmer, M.; Janssen, T.; Teelen, K., et al. Modest heterologous protection after Plasmodium falciparum sporozoite immunization: a double-blind randomized controlled clinical trial. *BMC Med* **2017**, *15*, 168, doi:10.1186/s12916-017-0923-4.
231. Mueller, A.K.; Camargo, N.; Kaiser, K.; Andorfer, C.; Frevert, U.; Matuschewski, K.; Kappe, S.H. Plasmodium liver stage developmental arrest by depletion of a protein at the parasite-host interface. *Proc Natl Acad Sci U S A* **2005**, *102*, 3022-3027, doi:10.1073/pnas.0408442102.
232. Spring, M.; Murphy, J.; Nielsen, R.; Dowler, M.; Bennett, J.W.; Zarling, S.; Williams, J.; de la Vega, P.; Ware, L.; Komisar, J., et al. First-in-human evaluation of genetically attenuated Plasmodium falciparum sporozoites administered by bite of Anopheles mosquitoes to adult volunteers. *Vaccine* **2013**, *31*, 4975-4983, doi:10.1016/j.vaccine.2013.08.007.
233. Kublin, J.G.; Mikolajczak, S.A.; Sack, B.K.; Fishbaugher, M.E.; Seilie, A.; Shelton, L.; VonGoedert, T.; Firat, M.; Magee, S.; Fritzen, E., et al. Complete attenuation of genetically engineered Plasmodium falciparum sporozoites in human subjects. *Sci Transl Med* **2017**, *9*, doi:10.1126/scitranslmed.aad9099.
234. Mishra, S.; Nussenzweig, R.S.; Nussenzweig, V. Antibodies to Plasmodium circumsporozoite protein (CSP) inhibit sporozoite's cell traversal activity. *J Immunol Methods* **2012**, *377*, 47-52, doi:10.1016/j.jim.2012.01.009.
235. Foquet, L.; Hermsen, C.C.; van Gemert, G.J.; Van Braeckel, E.; Weening, K.E.; Sauerwein, R.; Meuleman, P.; Leroux-Roels, G. Vaccine-induced monoclonal antibodies targeting circumsporozoite protein prevent Plasmodium falciparum infection. *J Clin Invest* **2014**, *124*, 140-144, doi:10.1172/JCI70349.
236. Kaslow, D.C.; Biernaux, S. RTS,S: Toward a first landmark on the Malaria Vaccine Technology Roadmap. *Vaccine* **2015**, *33*, 7425-7432, doi:10.1016/j.vaccine.2015.09.061.
237. RTS, S.C.T.P. Efficacy and safety of RTS,S/AS01 malaria vaccine with or without a booster dose in infants and children in Africa: final results of a phase 3, individually randomised, controlled trial. *Lancet* **2015**, *386*, 31-45, doi:10.1016/S0140-6736(15)60721-8.
238. Olotu, A.; Fegan, G.; Wambua, J.; Nyangweso, G.; Awuondo, K.O.; Leach, A.; Lievens, M.; Leboulleux, D.; Njuguna, P.; Peshu, N., et al. Four-year efficacy of RTS,S/AS01E and its interaction with malaria exposure. *N Engl J Med* **2013**, *368*, 1111-1120, doi:10.1056/NEJMoa1207564.
239. Greenwood, B.; Doumbo, O.K. Implementation of the malaria candidate vaccine RTS,S/AS01. *Lancet* **2016**, *387*, 318-319, doi:10.1016/S0140-6736(15)00807-7.

240. White, M.T.; Verity, R.; Griffin, J.T.; Asante, K.P.; Owusu-Agyei, S.; Greenwood, B.; Drakeley, C.; Gesase, S.; Lusingu, J.; Ansong, D., et al. Immunogenicity of the RTS,S/AS01 malaria vaccine and implications for duration of vaccine efficacy: secondary analysis of data from a phase 3 randomised controlled trial. *Lancet Infect Dis* **2015**, *15*, 1450-1458, doi:10.1016/S1473-3099(15)00239-X.
241. Kazmin, D.; Nakaya, H.I.; Lee, E.K.; Johnson, M.J.; van der Most, R.; van den Berg, R.A.; Ballou, W.R.; Jongert, E.; Wille-Reece, U.; Ockenhouse, C., et al. Systems analysis of protective immune responses to RTS,S malaria vaccination in humans. *Proc Natl Acad Sci U S A* **2017**, *114*, 2425-2430, doi:10.1073/pnas.1621489114.
242. Collins, K.A.; Snaith, R.; Cottingham, M.G.; Gilbert, S.C.; Hill, A.V.S. Enhancing protective immunity to malaria with a highly immunogenic virus-like particle vaccine. *Sci Rep* **2017**, *7*, 46621, doi:10.1038/srep46621.
243. Sedegah, M.; Hedstrom, R.; Hobart, P.; Hoffman, S.L. Protection against malaria by immunization with plasmid DNA encoding circumsporozoite protein. *Proc Natl Acad Sci U S A* **1994**, *91*, 9866-9870.
244. Wang, R.; Epstein, J.; Baraceros, F.M.; Gorak, E.J.; Charoenvit, Y.; Carucci, D.J.; Hedstrom, R.C.; Rahardjo, N.; Gay, T.; Hobart, P., et al. Induction of CD4(+) T cell-dependent CD8(+) type 1 responses in humans by a malaria DNA vaccine. *Proc Natl Acad Sci U S A* **2001**, *98*, 10817-10822, doi:10.1073/pnas.181123498.
245. Schneider, J.; Gilbert, S.C.; Blanchard, T.J.; Hanke, T.; Robson, K.J.; Hannan, C.M.; Becker, M.; Sinden, R.; Smith, G.L.; Hill, A.V. Enhanced immunogenicity for CD8+ T cell induction and complete protective efficacy of malaria DNA vaccination by boosting with modified vaccinia virus Ankara. *Nat Med* **1998**, *4*, 397-402.
246. McConkey, S.J.; Reece, W.H.; Moorthy, V.S.; Webster, D.; Dunachie, S.; Butcher, G.; Vuola, J.M.; Blanchard, T.J.; Gothard, P.; Watkins, K., et al. Enhanced T-cell immunogenicity of plasmid DNA vaccines boosted by recombinant modified vaccinia virus Ankara in humans. *Nat Med* **2003**, *9*, 729-735, doi:10.1038/nm881.
247. Dunachie, S.J.; Walther, M.; Epstein, J.E.; Keating, S.; Berthoud, T.; Andrews, L.; Andersen, R.F.; Bejon, P.; Goonetilleke, N.; Poulton, I., et al. A DNA prime-modified vaccinia virus ankara boost vaccine encoding thrombospondin-related adhesion protein but not circumsporozoite protein partially protects healthy malaria-naive adults against Plasmodium falciparum sporozoite challenge. *Infect Immun* **2006**, *74*, 5933-5942, doi:10.1128/IAI.00590-06.
248. Ewer, K.; Rampling, T.; Venkatraman, N.; Bowyer, G.; Wright, D.; Lambe, T.; Imoukhuede, E.B.; Payne, R.; Fehling, S.K.; Strecker, T., et al. A Monovalent Chimpanzee Adenovirus Ebola Vaccine Boosted with MVA. *N Engl J Med* **2016**, *374*, 1635-1646, doi:10.1056/NEJMoa1411627.
249. Swadling, L.; Capone, S.; Antrobus, R.D.; Brown, A.; Richardson, R.; Newell, E.W.; Halliday, J.; Kelly, C.; Bowen, D.; Fergusson, J., et al. A human vaccine strategy based on chimpanzee adenoviral and MVA vectors that primes, boosts, and sustains functional HCV-specific T cell memory. *Sci Transl Med* **2014**, *6*, 261ra153, doi:10.1126/scitranslmed.3009185.
250. Stylianou, E.; Griffiths, K.L.; Poyntz, H.C.; Harrington-Kandt, R.; Dicks, M.D.; Stockdale, L.; Betts, G.; McShane, H. Improvement of BCG protective efficacy with a novel chimpanzee adenovirus and a modified vaccinia Ankara virus both expressing Ag85A. *Vaccine* **2015**, *33*, 6800-6808, doi:10.1016/j.vaccine.2015.10.017.
251. Coughlan, L.; Sridhar, S.; Payne, R.; Edmans, M.; Milicic, A.; Venkatraman, N.; Lugonja, B.; Clifton, L.; Qi, C.; Folegatti, P.M., et al. Heterologous Two-Dose Vaccination with Simian Adenovirus and Poxvirus Vectors Elicits Long-Lasting Cellular Immunity to Influenza Virus A in Healthy Adults. *EBioMedicine* **2018**, *29*, 146-154, doi:10.1016/j.ebiom.2018.02.011.

252. Ewer, K.J.; O'Hara, G.A.; Duncan, C.J.; Collins, K.A.; Sheehy, S.H.; Reyes-Sandoval, A.; Goodman, A.L.; Edwards, N.J.; Elias, S.C.; Halstead, F.D., et al. Protective CD8+ T-cell immunity to human malaria induced by chimpanzee adenovirus-MVA immunisation. *Nat Commun* **2013**, *4*, 2836, doi:10.1038/ncomms3836.
253. Mast, T.C.; Kierstead, L.; Gupta, S.B.; Nikas, A.A.; Kallas, E.G.; Novitsky, V.; Mbewe, B.; Pitisuttithum, P.; Schechter, M.; Vardas, E., et al. International epidemiology of human pre-existing adenovirus (Ad) type-5, type-6, type-26 and type-36 neutralizing antibodies: correlates of high Ad5 titers and implications for potential HIV vaccine trials. *Vaccine* **2010**, *28*, 950-957, doi:10.1016/j.vaccine.2009.10.145.
254. Nébié, I.; Edwards, N.J.; Tiono, A.B.; Ewer, K.J.; Sanou, G.S.; Soulama, I.; Sanon, S.; Diarra, A.; Yaro, J.B.; Kangoye, D., et al. Assessment of chimpanzee adenovirus serotype 63 neutralizing antibodies prior to evaluation of a candidate malaria vaccine regimen based on viral vectors. *Clin Vaccine Immunol* **2014**, *21*, 901-903, doi:10.1128/CVI.00723-13.
255. Sultan, A.A.; Thathy, V.; Frevert, U.; Robson, K.J.; Crisanti, A.; Nussenzweig, V.; Nussenzweig, R.S.; Ménard, R. TRAP is necessary for gliding motility and infectivity of plasmodium sporozoites. *Cell* **1997**, *90*, 511-522.
256. Gilbert, S.C.; Plebanski, M.; Harris, S.J.; Allsopp, C.E.; Thomas, R.; Layton, G.T.; Hill, A.V. A protein particle vaccine containing multiple malaria epitopes. *Nat Biotechnol* **1997**, *15*, 1280-1284, doi:10.1038/nbt1197-1280.
257. Kimani, D.; Jagne, Y.J.; Cox, M.; Kimani, E.; Bliss, C.M.; Gitau, E.; Ogwang, C.; Afolabi, M.O.; Bowyer, G.; Collins, K.A., et al. Translating the immunogenicity of prime-boost immunization with ChAd63 and MVA ME-TRAP from malaria naive to malaria-endemic populations. *Mol Ther* **2014**, *22*, 1992-2003, doi:10.1038/mt.2014.109.
258. Ogwang, C.; Kimani, D.; Edwards, N.J.; Roberts, R.; Mwacharo, J.; Bowyer, G.; Bliss, C.; Hodgson, S.H.; Njuguna, P.; Viebig, N.K., et al. Prime-boost vaccination with chimpanzee adenovirus and modified vaccinia Ankara encoding TRAP provides partial protection against Plasmodium falciparum infection in Kenyan adults. *Sci Transl Med* **2015**, *7*, 286re285, doi:10.1126/scitranslmed.aaa2373.
259. Mensah, V.A.; Gueye, A.; Ndiaye, M.; Edwards, N.J.; Wright, D.; Anagnostou, N.A.; Syll, M.; Ndaw, A.; Abiola, A.; Bliss, C., et al. Safety, Immunogenicity and Efficacy of Prime-Boost Vaccination with ChAd63 and MVA Encoding ME-TRAP against Plasmodium falciparum Infection in Adults in Senegal. *PLoS One* **2016**, *11*, e0167951, doi:10.1371/journal.pone.0167951.
260. Hodgson, S.H.; Ewer, K.J.; Bliss, C.M.; Edwards, N.J.; Rampling, T.; Anagnostou, N.A.; de Barra, E.; Havelock, T.; Bowyer, G.; Poulton, I.D., et al. Evaluation of the efficacy of ChAd63-MVA vectored vaccines expressing circumsporozoite protein and ME-TRAP against controlled human malaria infection in malaria-naive individuals. *J Infect Dis* **2015**, *211*, 1076-1086, doi:10.1093/infdis/jiu579.
261. Bliss, C.M.; Drammeh, A.; Bowyer, G.; Sanou, G.S.; Jagne, Y.J.; Ouedraogo, O.; Edwards, N.J.; Tarama, C.; Ouedraogo, N.; Ouedraogo, M., et al. Viral Vector Malaria Vaccines Induce High-Level T Cell and Antibody Responses in West African Children and Infants. *Mol Ther* **2017**, *25*, 547-559, doi:10.1016/j.ymthe.2016.11.003.
262. Afolabi, M.O.; Tiono, A.B.; Adetifa, U.J.; Yaro, J.B.; Drammeh, A.; Nébié, I.; Bliss, C.; Hodgson, S.H.; Anagnostou, N.A.; Sanou, G.S., et al. Safety and Immunogenicity of ChAd63 and MVA ME-TRAP in West African Children and Infants. *Mol Ther* **2016**, *24*, 1470-1477, doi:10.1038/mt.2016.83.
263. Longley, R.J.; Hill, A.V.; Spencer, A.J. Malaria vaccines: identifying Plasmodium falciparum liver-stage targets. *Front Microbiol* **2015**, *6*, 965, doi:10.3389/fmicb.2015.00965.

264. Teo, A.; Feng, G.; Brown, G.V.; Beeson, J.G.; Rogerson, S.J. Functional Antibodies and Protection against Blood-stage Malaria. *Trends Parasitol* **2016**, *32*, 887-898, doi:10.1016/j.pt.2016.07.003.
265. Weiss, G.E.; Crabb, B.S.; Gilson, P.R. Overlaying Molecular and Temporal Aspects of Malaria Parasite Invasion. *Trends Parasitol* **2016**, *32*, 284-295, doi:10.1016/j.pt.2015.12.007.
266. Crosnier, C.; Bustamante, L.Y.; Bartholdson, S.J.; Bei, A.K.; Theron, M.; Uchikawa, M.; Mboup, S.; Ndir, O.; Kwiatkowski, D.P.; Duraisingh, M.T., et al. Basigin is a receptor essential for erythrocyte invasion by Plasmodium falciparum. *Nature* **2011**, *480*, 534-537, doi:10.1038/nature10606.
267. Bustamante, L.Y.; Bartholdson, S.J.; Crosnier, C.; Campos, M.G.; Wanaguru, M.; Nguon, C.; Kwiatkowski, D.P.; Wright, G.J.; Rayner, J.C. A full-length recombinant Plasmodium falciparum PfRH5 protein induces inhibitory antibodies that are effective across common PfRH5 genetic variants. *Vaccine* **2013**, *31*, 373-379, doi:10.1016/j.vaccine.2012.10.106.
268. Douglas, A.D.; Williams, A.R.; Knuepfer, E.; Illingworth, J.J.; Furze, J.M.; Crosnier, C.; Choudhary, P.; Bustamante, L.Y.; Zakutansky, S.E.; Awuah, D.K., et al. Neutralization of Plasmodium falciparum merozoites by antibodies against PfRH5. *J Immunol* **2014**, *192*, 245-258, doi:10.4049/jimmunol.1302045.
269. Douglas, A.D.; Baldeviano, G.C.; Lucas, C.M.; Lugo-Roman, L.A.; Crosnier, C.; Bartholdson, S.J.; Diouf, A.; Miura, K.; Lambert, L.E.; Ventocilla, J.A., et al. A PfRH5-based vaccine is efficacious against heterologous strain blood-stage Plasmodium falciparum infection in aotus monkeys. *Cell Host Microbe* **2015**, *17*, 130-139, doi:10.1016/j.chom.2014.11.017.
270. Payne, R.O.; Silk, S.E.; Elias, S.C.; Miura, K.; Diouf, A.; Galaway, F.; de Graaf, H.; Brendish, N.J.; Poulton, I.D.; Griffiths, O.J., et al. Human vaccination against RH5 induces neutralizing antimalarial antibodies that inhibit RH5 invasion complex interactions. *JCI Insight* **2017**, *2*, doi:10.1172/jci.insight.96381.
271. Carter, R. Transmission blocking malaria vaccines. *Vaccine* **2001**, *19*, 2309-2314.
272. Kapulu, M.C.; Da, D.F.; Miura, K.; Li, Y.; Blagborough, A.M.; Churcher, T.S.; Nikolaeva, D.; Williams, A.R.; Goodman, A.L.; Sangare, I., et al. Comparative assessment of transmission-blocking vaccine candidates against Plasmodium falciparum. *Sci Rep* **2015**, *5*, 11193, doi:10.1038/srep11193.
273. Talaat, K.R.; Ellis, R.D.; Hurd, J.; Hentrich, A.; Gabriel, E.; Hynes, N.A.; Rausch, K.M.; Zhu, D.; Muratova, O.; Herrera, R., et al. Safety and Immunogenicity of Pfs25-EPA/Alhydrogel®, a Transmission Blocking Vaccine against Plasmodium falciparum: An Open Label Study in Malaria Naïve Adults. *PLoS One* **2016**, *11*, e0163144, doi:10.1371/journal.pone.0163144.
274. Bompard, A.; Da, D.F.; Yerbanga, R.S.; Biswas, S.; Kapulu, M.; Bousema, T.; Lefèvre, T.; Cohuet, A.; Churcher, T.S. Evaluation of two lead malaria transmission blocking vaccine candidate antibodies in natural parasite-vector combinations. *Sci Rep* **2017**, *7*, 6766, doi:10.1038/s41598-017-06130-1.
275. Miura, K.; Swihart, B.J.; Deng, B.; Zhou, L.; Pham, T.P.; Diouf, A.; Burton, T.; Fay, M.P.; Long, C.A. Transmission-blocking activity is determined by transmission-reducing activity and number of control oocysts in Plasmodium falciparum standard membrane-feeding assay. *Vaccine* **2016**, *34*, 4145-4151, doi:10.1016/j.vaccine.2016.06.066.
276. Beeching, N.J.; Fenech, M.; Houlihan, C.F. Ebola virus disease. *BMJ* **2014**, *349*, g7348.
277. Miranda, M.E.; Miranda, N.L. Reston ebolavirus in humans and animals in the Philippines: a review. *J Infect Dis* **2011**, *204 Suppl 3*, S757-760, doi:10.1093/infdis/jir296.

278. Formenty, P.; Hatz, C.; Le Guenno, B.; Stoll, A.; Rogenmoser, P.; Widmer, A. Human infection due to Ebola virus, subtype Côte d'Ivoire: clinical and biologic presentation. *J Infect Dis* **1999**, *179 Suppl 1*, S48-53, doi:10.1086/514285.
279. Goldstein, T.; Anthony, S.J.; Gbakima, A.; Bird, B.H.; Bangura, J.; Tremeau-Bravard, A.; Belaganahalli, M.N.; Wells, H.L.; Dhanota, J.K.; Liang, E., et al. The discovery of Bombali virus adds further support for bats as hosts of ebolaviruses. *Nat Microbiol* **2018**, doi:10.1038/s41564-018-0227-2.
280. Kucharski, A.J.; Edmunds, W.J. Case fatality rate for Ebola virus disease in west Africa. *Lancet* **2014**, *384*, 1260, doi:10.1016/S0140-6736(14)61706-2.
281. Lefebvre, A.; Fiet, C.; Belpois-Duchamp, C.; Tiv, M.; Astruc, K.; Aho Glélé, L.S. Case fatality rates of Ebola virus diseases: a meta-analysis of World Health Organization data. *Med Mal Infect* **2014**, *44*, 412-416, doi:10.1016/j.medmal.2014.08.005.
282. Ebola haemorrhagic fever in Zaire, 1976. *Bull World Health Organ* **1978**, *56*, 271-293.
283. Ebola haemorrhagic fever in Sudan, 1976. Report of a WHO/International Study Team. *Bull World Health Organ* **1978**, *56*, 247-270.
284. Pigott, D.M.; Golding, N.; Mylne, A.; Huang, Z.; Henry, A.J.; Weiss, D.J.; Brady, O.J.; Kraemer, M.U.; Smith, D.L.; Moyes, C.L., et al. Mapping the zoonotic niche of Ebola virus disease in Africa. *Elife* **2014**, *3*, e04395, doi:10.7554/eLife.04395.
285. Leendertz, S.A.; Gogarten, J.F.; Düx, A.; Calvignac-Spencer, S.; Leendertz, F.H. Assessing the Evidence Supporting Fruit Bats as the Primary Reservoirs for Ebola Viruses. *Ecohealth* **2016**, *13*, 18-25, doi:10.1007/s10393-015-1053-0.
286. Leroy, E.M.; Telfer, P.; Kumulungui, B.; Yaba, P.; Rouquet, P.; Roques, P.; Gonzalez, J.P.; Ksiazek, T.G.; Rollin, P.E.; Nerrienet, E. A serological survey of Ebola virus infection in central African nonhuman primates. *J Infect Dis* **2004**, *190*, 1895-1899, doi:10.1086/425421.
287. Leroy, E.M.; Rouquet, P.; Formenty, P.; Souquière, S.; Kilbourne, A.; Froment, J.M.; Bermejo, M.; Smit, S.; Karesh, W.; Swanepoel, R., et al. Multiple Ebola virus transmission events and rapid decline of central African wildlife. *Science* **2004**, *303*, 387-390, doi:10.1126/science.1092528.
288. Judson, S.; Prescott, J.; Munster, V. Understanding ebola virus transmission. *Viruses* **2015**, *7*, 511-521, doi:10.3390/v7020511.
289. Coltart, C.E.; Lindsey, B.; Ghinai, I.; Johnson, A.M.; Heymann, D.L. The Ebola outbreak, 2013-2016: old lessons for new epidemics. *Philos Trans R Soc Lond B Biol Sci* **2017**, *372*, doi:10.1098/rstb.2016.0297.
290. Lo, T.Q.; Marston, B.J.; Dahl, B.A.; De Cock, K.M. Ebola: Anatomy of an Epidemic. *Annu Rev Med* **2017**, *68*, 359-370, doi:10.1146/annurev-med-052915-015604.
291. Shultz, J.M.; Espinel, Z.; Espinola, M.; Rechkemmer, A. Distinguishing epidemiological features of the 2013-2016 West Africa Ebola virus disease outbreak. *Disaster Health* **2016**, *3*, 78-88, doi:10.1080/21665044.2016.1228326.
292. Uyeki, T.M.; Mehta, A.K.; Davey, R.T.; Liddell, A.M.; Wolf, T.; Vetter, P.; Schmiedel, S.; Grünewald, T.; Jacobs, M.; Arribas, J.R., et al. Clinical Management of Ebola Virus Disease in the United States and Europe. *N Engl J Med* **2016**, *374*, 636-646, doi:10.1056/NEJMoa1504874.
293. Qiu, X.; Wong, G.; Audet, J.; Bello, A.; Fernando, L.; Alimonti, J.B.; Fausther-Bovendo, H.; Wei, H.; Aviles, J.; Hiatt, E., et al. Reversion of advanced Ebola virus disease in nonhuman primates with ZMapp. *Nature* **2014**, *514*, 47-53, doi:10.1038/nature13777.
294. Davey, R.T.; Dodd, L.; Proschan, M.A.; Neaton, J.; Neuhaus Nordwall, J.; Koopmeiners, J.S.; Beigel, J.; Tierney, J.; Lane, H.C.; Fauci, A.S., et al. A Randomized, Controlled Trial of ZMapp for Ebola Virus Infection. *N Engl J Med* **2016**, *375*, 1448-1456, doi:10.1056/NEJMoa1604330.

295. van Griensven, J.; Edwards, T.; de Lamballerie, X.; Semple, M.G.; Gallian, P.; Baize, S.; Horby, P.W.; Raoul, H.; Magassouba, N.; Antierens, A., et al. Evaluation of Convalescent Plasma for Ebola Virus Disease in Guinea. *N Engl J Med* **2016**, *374*, 33-42, doi:10.1056/NEJMoa1511812.
296. Sissoko, D.; Laouenan, C.; Folkesson, E.; M'Lebing, A.B.; Beavogui, A.H.; Baize, S.; Camara, A.M.; Maes, P.; Shepherd, S.; Danel, C., et al. Experimental Treatment with Favipiravir for Ebola Virus Disease (the JIKI Trial): A Historically Controlled, Single-Arm Proof-of-Concept Trial in Guinea. *PLoS Med* **2016**, *13*, e1001967, doi:10.1371/journal.pmed.1001967.
297. Dunning, J.; Sahr, F.; Rojek, A.; Gannon, F.; Carson, G.; Idriss, B.; Massaquoi, T.; Gandi, R.; Joseph, S.; Osman, H.K., et al. Experimental Treatment of Ebola Virus Disease with TKM-130803: A Single-Arm Phase 2 Clinical Trial. *PLoS Med* **2016**, *13*, e1001997, doi:10.1371/journal.pmed.1001997.
298. Sanchez, A.; Rollin, P.E. Complete genome sequence of an Ebola virus (Sudan species) responsible for a 2000 outbreak of human disease in Uganda. *Virus Res* **2005**, *113*, 16-25, doi:10.1016/j.virusres.2005.03.028.
299. Lee, J.E.; Saphire, E.O. Ebolavirus glycoprotein structure and mechanism of entry. *Future Virol* **2009**, *4*, 621-635, doi:10.2217/fvl.09.56.
300. Venkatraman, N.; Silman, D.; Folegatti, P.M.; Hill, A.V.S. Vaccines against Ebola virus. *Vaccine* **2018**, *36*, 5454-5459, doi:10.1016/j.vaccine.2017.07.054.
301. Martin, J.E.; Sullivan, N.J.; Enama, M.E.; Gordon, I.J.; Roederer, M.; Koup, R.A.; Bailer, R.T.; Chakrabarti, B.K.; Bailey, M.A.; Gomez, P.L., et al. A DNA vaccine for Ebola virus is safe and immunogenic in a phase I clinical trial. *Clin Vaccine Immunol* **2006**, *13*, 1267-1277, doi:10.1128/CVI.00162-06.
302. Ledgerwood, J.E.; Costner, P.; Desai, N.; Holman, L.; Enama, M.E.; Yamshchikov, G.; Mulangu, S.; Hu, Z.; Andrews, C.A.; Sheets, R.A., et al. A replication defective recombinant Ad5 vaccine expressing Ebola virus GP is safe and immunogenic in healthy adults. *Vaccine* **2010**, *29*, 304-313, doi:10.1016/j.vaccine.2010.10.037.
303. Stanley, D.A.; Honko, A.N.; Asiedu, C.; Trefry, J.C.; Lau-Kilby, A.W.; Johnson, J.C.; Hensley, L.; Ammendola, V.; Abbate, A.; Grazioli, F., et al. Chimpanzee adenovirus vaccine generates acute and durable protective immunity against ebolavirus challenge. *Nat Med* **2014**, *20*, 1126-1129, doi:10.1038/nm.3702.
304. Jones, S.M.; Feldmann, H.; Ströher, U.; Geisbert, J.B.; Fernando, L.; Grolla, A.; Klenk, H.D.; Sullivan, N.J.; Volchkov, V.E.; Fritz, E.A., et al. Live attenuated recombinant vaccine protects nonhuman primates against Ebola and Marburg viruses. *Nat Med* **2005**, *11*, 786-790, doi:10.1038/nm1258.
305. Geisbert, T.W.; Daddario-Dicaprio, K.M.; Geisbert, J.B.; Reed, D.S.; Feldmann, F.; Grolla, A.; Ströher, U.; Fritz, E.A.; Hensley, L.E.; Jones, S.M., et al. Vesicular stomatitis virus-based vaccines protect nonhuman primates against aerosol challenge with Ebola and Marburg viruses. *Vaccine* **2008**, *26*, 6894-6900, doi:10.1016/j.vaccine.2008.09.082.
306. De Santis, O.; Audran, R.; Pothin, E.; Warpelin-Decrausaz, L.; Vallotton, L.; Wuerzner, G.; Cochet, C.; Estoppey, D.; Steiner-Monard, V.; Lonchampt, S., et al. Safety and immunogenicity of a chimpanzee adenovirus-vectored Ebola vaccine in healthy adults: a randomised, double-blind, placebo-controlled, dose-finding, phase 1/2a study. *Lancet Infect Dis* **2016**, *16*, 311-320, doi:10.1016/S1473-3099(15)00486-7.
307. Ledgerwood, J.E.; DeZure, A.D.; Stanley, D.A.; Coates, E.E.; Novik, L.; Enama, M.E.; Berkowitz, N.M.; Hu, Z.; Joshi, G.; Ploquin, A., et al. Chimpanzee Adenovirus Vector Ebola Vaccine. *N Engl J Med* **2017**, *376*, 928-938, doi:10.1056/NEJMoa1410863.
308. Tapia, M.D.; Sow, S.O.; Lyke, K.E.; Haidara, F.C.; Diallo, F.; Doumbia, M.; Traore, A.; Coulibaly, F.; Kodio, M.; Onwuchekwa, U., et al. Use of ChAd3-EBO-Z Ebola virus vaccine in Malian and US adults, and boosting of Malian adults with MVA-BN-Filo: a phase 1,

single-blind, randomised trial, a phase 1b, open-label and double-blind, dose-escalation trial, and a nested, randomised, double-blind, placebo-controlled trial. *Lancet Infect Dis* **2016**, *16*, 31-42, doi:10.1016/S1473-3099(15)00362-X.

309. Milligan, I.D.; Gibani, M.M.; Sewell, R.; Clutterbuck, E.A.; Campbell, D.; Plested, E.; Nuthall, E.; Voysey, M.; Silva-Reyes, L.; McElrath, M.J., et al. Safety and Immunogenicity of Novel Adenovirus Type 26- and Modified Vaccinia Ankara-Vectored Ebola Vaccines: A Randomized Clinical Trial. *JAMA* **2016**, *315*, 1610-1623, doi:10.1001/jama.2016.4218.
310. Lambe, T.; Bowyer, G.; Ewer, K.J. A review of Phase I trials of Ebola virus vaccines: what can we learn from the race to develop novel vaccines? *Philos Trans R Soc Lond B Biol Sci* **2017**, *372*, doi:10.1098/rstb.2016.0295.
311. Henao-Restrepo, A.M.; Longini, I.M.; Egger, M.; Dean, N.E.; Edmunds, W.J.; Camacho, A.; Carroll, M.W.; Doumbia, M.; Draguez, B.; Duraffour, S., et al. Efficacy and effectiveness of an rVSV-vectored vaccine expressing Ebola surface glycoprotein: interim results from the Guinea ring vaccination cluster-randomised trial. *Lancet* **2015**, *386*, 857-866, doi:10.1016/S0140-6736(15)61117-5.
312. Henao-Restrepo, A.M.; Camacho, A.; Longini, I.M.; Watson, C.H.; Edmunds, W.J.; Egger, M.; Carroll, M.W.; Dean, N.E.; Diatta, I.; Doumbia, M., et al. Efficacy and effectiveness of an rVSV-vectored vaccine in preventing Ebola virus disease: final results from the Guinea ring vaccination, open-label, cluster-randomised trial (Ebola Ça Suffit!). *Lancet* **2017**, *389*, 505-518, doi:10.1016/S0140-6736(16)32621-6.
313. Wise, J. WHO is "cautiously optimistic" about Ebola ring vaccination programme in DRC. *BMJ* **2018**, *361*, k2388.
314. Medaglini, D.; Siegrist, C.A. Immunomonitoring of human responses to the rVSV-ZEBOV Ebola vaccine. *Curr Opin Virol* **2017**, *23*, 88-94, doi:10.1016/j.coviro.2017.03.008.
315. Agnandji, S.T.; Huttner, A.; Zinser, M.E.; Njuguna, P.; Dahlke, C.; Fernandes, J.F.; Yerly, S.; Dayer, J.A.; Kraehling, V.; Kasonta, R., et al. Phase 1 Trials of rVSV Ebola Vaccine in Africa and Europe. *N Engl J Med* **2016**, *374*, 1647-1660, doi:10.1056/NEJMoa1502924.
316. Huttner, A.; Dayer, J.A.; Yerly, S.; Combescure, C.; Auderset, F.; Desmeules, J.; Eickmann, M.; Finckh, A.; Goncalves, A.R.; Hooper, J.W., et al. The effect of dose on the safety and immunogenicity of the VSV Ebola candidate vaccine: a randomised double-blind, placebo-controlled phase 1/2 trial. *Lancet Infect Dis* **2015**, *15*, 1156-1166, doi:10.1016/S1473-3099(15)00154-1.
317. Regules, J.A.; Beigel, J.H.; Paolino, K.M.; Voell, J.; Castellano, A.R.; Hu, Z.; Muñoz, P.; Moon, J.E.; Ruck, R.C.; Bennett, J.W., et al. A Recombinant Vesicular Stomatitis Virus Ebola Vaccine. *N Engl J Med* **2017**, *376*, 330-341, doi:10.1056/NEJMoa1414216.
318. Dahlke, C.; Kasonta, R.; Lunemann, S.; Krähling, V.; Zinser, M.E.; Biedenkopf, N.; Fehling, S.K.; Ly, M.L.; Rechtien, A.; Stubbe, H.C., et al. Dose-dependent T-cell Dynamics and Cytokine Cascade Following rVSV-ZEBOV Immunization. *EBioMedicine* **2017**, *19*, 107-118, doi:10.1016/j.ebiom.2017.03.045.
319. Medaglini, D.; Santoro, F.; Siegrist, C.A. Correlates of vaccine-induced protective immunity against Ebola virus disease. *Semin Immunol* **2018**, doi:10.1016/j.smim.2018.07.003.
320. Baize, S.; Leroy, E.M.; Georges-Courbot, M.C.; Capron, M.; Lansoud-Soukate, J.; Debré, P.; Fisher-Hoch, S.P.; McCormick, J.B.; Georges, A.J. Defective humoral responses and extensive intravascular apoptosis are associated with fatal outcome in Ebola virus-infected patients. *Nat Med* **1999**, *5*, 423-426, doi:10.1038/7422.
321. McElroy, A.K.; Akondy, R.S.; Davis, C.W.; Ellebedy, A.H.; Mehta, A.K.; Kraft, C.S.; Lyon, G.M.; Ribner, B.S.; Varkey, J.; Sidney, J., et al. Human Ebola virus infection results in substantial immune activation. *Proc Natl Acad Sci U S A* **2015**, *112*, 4719-4724, doi:10.1073/pnas.1502619112.

322. Zeitlin, L.; Whaley, K.J.; Olinger, G.G.; Jacobs, M.; Gopal, R.; Qiu, X.; Kobinger, G.P. Antibody therapeutics for Ebola virus disease. *Curr Opin Virol* **2016**, *17*, 45-49, doi:10.1016/j.coviro.2016.01.006.
323. Sullivan, N.J.; Hensley, L.; Asiedu, C.; Geisbert, T.W.; Stanley, D.; Johnson, J.; Honko, A.; Olinger, G.; Bailey, M.; Geisbert, J.B., et al. CD8+ cellular immunity mediates rAd5 vaccine protection against Ebola virus infection of nonhuman primates. *Nat Med* **2011**, *17*, 1128-1131, doi:10.1038/nm.2447.
324. Liu, X.; Speranza, E.; Muñoz-Fontela, C.; Haldenby, S.; Rickett, N.Y.; Garcia-Dorival, I.; Fang, Y.; Hall, Y.; Zekeng, E.G.; Lüdtke, A., et al. Transcriptomic signatures differentiate survival from fatal outcomes in humans infected with Ebola virus. *Genome Biol* **2017**, *18*, 4, doi:10.1186/s13059-016-1137-3.
325. Sinclair, J.; Sissons, P. Latency and reactivation of human cytomegalovirus. *J Gen Virol* **2006**, *87*, 1763-1779, doi:10.1099/vir.0.81891-0.
326. Crough, T.; Khanna, R. Immunobiology of human cytomegalovirus: from bench to bedside. *Clin Microbiol Rev* **2009**, *22*, 76-98, Table of Contents, doi:10.1128/CMR.00034-08.
327. Emery, V.C. Investigation of CMV disease in immunocompromised patients. *J Clin Pathol* **2001**, *54*, 84-88.
328. Pass, R.F.; Anderson, B. Mother-to-Child Transmission of Cytomegalovirus and Prevention of Congenital Infection. *J Pediatric Infect Dis Soc* **2014**, *3 Suppl 1*, S2-6, doi:10.1093/jpids/piu069.
329. Cannon, M.J.; Schmid, D.S.; Hyde, T.B. Review of cytomegalovirus seroprevalence and demographic characteristics associated with infection. *Rev Med Virol* **2010**, *20*, 202-213, doi:10.1002/rmv.655.
330. Bates, M.; Brantsaeter, A.B. Human cytomegalovirus (CMV) in Africa: a neglected but important pathogen. *J Virus Erad* **2016**, *2*, 136-142.
331. Davison, A.J.; Dolan, A.; Akter, P.; Addison, C.; Dargan, D.J.; Alcendor, D.J.; McGeoch, D.J.; Hayward, G.S. The human cytomegalovirus genome revisited: comparison with the chimpanzee cytomegalovirus genome. *J Gen Virol* **2003**, *84*, 17-28, doi:10.1099/vir.0.18606-0.
332. Basta, S.; Bennink, J.R. A survival game of hide and seek: cytomegaloviruses and MHC class I antigen presentation pathways. *Viral Immunol* **2003**, *16*, 231-242, doi:10.1089/088282403322396064.
333. Ahn, K.; Gruhler, A.; Galocha, B.; Jones, T.R.; Wiertz, E.J.; Ploegh, H.L.; Peterson, P.A.; Yang, Y.; Früh, K. The ER-luminal domain of the HCMV glycoprotein US6 inhibits peptide translocation by TAP. *Immunity* **1997**, *6*, 613-621.
334. Furman, M.H.; Dey, N.; Tortorella, D.; Ploegh, H.L. The human cytomegalovirus US10 gene product delays trafficking of major histocompatibility complex class I molecules. *J Virol* **2002**, *76*, 11753-11756.
335. Jones, T.R.; Sun, L. Human cytomegalovirus US2 destabilizes major histocompatibility complex class I heavy chains. *J Virol* **1997**, *71*, 2970-2979.
336. Tomazin, R.; Boname, J.; Hegde, N.R.; Lewinsohn, D.M.; Altschuler, Y.; Jones, T.R.; Cresswell, P.; Nelson, J.A.; Riddell, S.R.; Johnson, D.C. Cytomegalovirus US2 destroys two components of the MHC class II pathway, preventing recognition by CD4+ T cells. *Nat Med* **1999**, *5*, 1039-1043, doi:10.1038/12478.
337. Mocarski, E.S. Immunomodulation by cytomegaloviruses: manipulative strategies beyond evasion. *Trends Microbiol* **2002**, *10*, 332-339.
338. Tomasec, P.; Braud, V.M.; Rickards, C.; Powell, M.B.; McSharry, B.P.; Gadola, S.; Cerundolo, V.; Borysiewicz, L.K.; McMichael, A.J.; Wilkinson, G.W. Surface expression of HLA-E, an inhibitor of natural killer cells, enhanced by human cytomegalovirus gpUL40. *Science* **2000**, *287*, 1031.

339. McSharry, B.P.; Avdic, S.; Slobedman, B. Human cytomegalovirus encoded homologs of cytokines, chemokines and their receptors: roles in immunomodulation. *Viruses* **2012**, *4*, 2448-2470, doi:10.3390/v4112448.
340. Minton, K. Viral immunity: How CMV bypasses immune memory. *Nat Rev Immunol* **2010**, *10*, 288, doi:10.1038/nri2768.
341. La Rosa, C.; Diamond, D.J. The immune response to human CMV. *Future Virol* **2012**, *7*, 279-293, doi:10.2217/fvl.12.8.
342. Delale, T.; Paquin, A.; Asselin-Paturel, C.; Dalod, M.; Brizard, G.; Bates, E.E.; Kastner, P.; Chan, S.; Akira, S.; Vicari, A., et al. MyD88-dependent and -independent murine cytomegalovirus sensing for IFN-alpha release and initiation of immune responses in vivo. *J Immunol* **2005**, *175*, 6723-6732.
343. Bukowski, J.F.; Warner, J.F.; Dennert, G.; Welsh, R.M. Adoptive transfer studies demonstrating the antiviral effect of natural killer cells in vivo. *J Exp Med* **1985**, *161*, 40-52.
344. Venema, H.; van den Berg, A.P.; van Zanten, C.; van Son, W.J.; van der Giessen, M.; The, T.H. Natural killer cell responses in renal transplant patients with cytomegalovirus infection. *J Med Virol* **1994**, *42*, 188-192.
345. Goodier, M.R.; Jonjić, S.; Riley, E.M.; Juranić Lisnić, V. CMV and natural killer cells: shaping the response to vaccination. *Eur J Immunol* **2018**, *48*, 50-65, doi:10.1002/eji.201646762.
346. Gumá, M.; Angulo, A.; Vilches, C.; Gómez-Lozano, N.; Malats, N.; López-Botet, M. Imprint of human cytomegalovirus infection on the NK cell receptor repertoire. *Blood* **2004**, *104*, 3664-3671, doi:10.1182/blood-2004-05-2058.
347. Monsiváis-Urenda, A.; Noyola-Cherpitel, D.; Hernández-Salinas, A.; García-Sepúlveda, C.; Romo, N.; Baranda, L.; López-Botet, M.; González-Amaro, R. Influence of human cytomegalovirus infection on the NK cell receptor repertoire in children. *Eur J Immunol* **2010**, *40*, 1418-1427, doi:10.1002/eji.200939898.
348. Lopez-Vergès, S.; Milush, J.M.; Schwartz, B.S.; Pando, M.J.; Jarjoura, J.; York, V.A.; Houchins, J.P.; Miller, S.; Kang, S.M.; Norris, P.J., et al. Expansion of a unique $CD57^{+}$NKG2Chi natural killer cell subset during acute human cytomegalovirus infection. *Proc Natl Acad Sci U S A* **2011**, *108*, 14725-14732, doi:10.1073/pnas.1110900108.
349. Foley, B.; Cooley, S.; Verneris, M.R.; Curtsinger, J.; Luo, X.; Waller, E.K.; Anasetti, C.; Weisdorf, D.; Miller, J.S. Human cytomegalovirus (CMV)-induced memory-like NKG2C(+) NK cells are transplantable and expand in vivo in response to recipient CMV antigen. *J Immunol* **2012**, *189*, 5082-5088, doi:10.4049/jimmunol.1201964.
350. Prod'homme, V.; Tomasec, P.; Cunningham, C.; Lemberg, M.K.; Stanton, R.J.; McSharry, B.P.; Wang, E.C.; Cuff, S.; Martoglio, B.; Davison, A.J., et al. Human cytomegalovirus UL40 signal peptide regulates cell surface expression of the NK cell ligands HLA-E and gpUL18. *J Immunol* **2012**, *188*, 2794-2804, doi:10.4049/jimmunol.1102068.
351. Lee, J.; Zhang, T.; Hwang, I.; Kim, A.; Nitschke, L.; Kim, M.; Scott, J.M.; Kamimura, Y.; Lanier, L.L.; Kim, S. Epigenetic modification and antibody-dependent expansion of memory-like NK cells in human cytomegalovirus-infected individuals. *Immunity* **2015**, *42*, 431-442, doi:10.1016/j.immuni.2015.02.013.
352. Darboe, A.; Danso, E.; Clarke, E.; Umesi, A.; Touray, E.; Wegmuller, R.; Moore, S.E.; Riley, E.M.; Goodier, M.R. Enhancement of cytokine-driven NK cell IFN-γ production after vaccination of HCMV infected Africans. *Eur J Immunol* **2017**, *47*, 1040-1050, doi:10.1002/eji.201746974.
353. Wirtz, N.; Schader, S.I.; Holtappels, R.; Simon, C.O.; Lemmermann, N.A.; Reddehase, M.J.; Podlech, J. Polyclonal cytomegalovirus-specific antibodies not only prevent virus dissemination from the portal of entry but also inhibit focal virus spread within target tissues. *Med Microbiol Immunol* **2008**, *197*, 151-158, doi:10.1007/s00430-008-0095-0.

354. Terrazzini, N.; Kern, F. Cell-mediated immunity to human CMV infection: a brief overview. *F1000Prime Rep* **2014**, *6*, 28, doi:10.12703/P6-28.
355. Mutter, W.; Reddehase, M.J.; Busch, F.W.; Bühring, H.J.; Koszinowski, U.H. Failure in generating hemopoietic stem cells is the primary cause of death from cytomegalovirus disease in the immunocompromised host. *J Exp Med* **1988**, *167*, 1645-1658.
356. Li, C.R.; Greenberg, P.D.; Gilbert, M.J.; Goodrich, J.M.; Riddell, S.R. Recovery of HLA-restricted cytomegalovirus (CMV)-specific T-cell responses after allogeneic bone marrow transplant: correlation with CMV disease and effect of ganciclovir prophylaxis. *Blood* **1994**, *83*, 1971-1979.
357. Reusser, P.; Cathomas, G.; Attenhofer, R.; Tamm, M.; Thiel, G. Cytomegalovirus (CMV)-specific T cell immunity after renal transplantation mediates protection from CMV disease by limiting the systemic virus load. *J Infect Dis* **1999**, *180*, 247-253, doi:10.1086/314879.
358. Crough, T.; Burrows, J.M.; Fazou, C.; Walker, S.; Davenport, M.P.; Khanna, R. Contemporaneous fluctuations in T cell responses to persistent herpes virus infections. *Eur J Immunol* **2005**, *35*, 139-149, doi:10.1002/eji.200425548.
359. Gillespie, G.M.; Wills, M.R.; Appay, V.; O'Callaghan, C.; Murphy, M.; Smith, N.; Sissons, P.; Rowland-Jones, S.; Bell, J.I.; Moss, P.A. Functional heterogeneity and high frequencies of cytomegalovirus-specific CD8(+) T lymphocytes in healthy seropositive donors. *J Virol* **2000**, *74*, 8140-8150.
360. Sylwester, A.W.; Mitchell, B.L.; Edgar, J.B.; Taormina, C.; Pelte, C.; Ruchti, F.; Sleath, P.R.; Grabstein, K.H.; Hosken, N.A.; Kern, F., et al. Broadly targeted human cytomegalovirus-specific CD4+ and CD8+ T cells dominate the memory compartments of exposed subjects. *J Exp Med* **2005**, *202*, 673-685, doi:10.1084/jem.20050882.
361. Hosie, L.; Pachnio, A.; Zuo, J.; Pearce, H.; Riddell, S.; Moss, P. Cytomegalovirus-Specific T Cells Restricted by HLA-Cw*0702 Increase Markedly with Age and Dominate the CD8+ T-Cell Repertoire in Older People. *Front Immunol* **2017**, *8*, 1776, doi:10.3389/fimmu.2017.01776.
362. Klenerman, P.; Oxenius, A. T cell responses to cytomegalovirus. *Nat Rev Immunol* **2016**, *16*, 367-377, doi:10.1038/nri.2016.38.
363. Dunn, H.S.; Haney, D.J.; Ghanekar, S.A.; Stepick-Biek, P.; Lewis, D.B.; Maecker, H.T. Dynamics of CD4 and CD8 T cell responses to cytomegalovirus in healthy human donors. *J Infect Dis* **2002**, *186*, 15-22, doi:10.1086/341079.
364. Appay, V.; Dunbar, P.R.; Callan, M.; Klenerman, P.; Gillespie, G.M.; Papagno, L.; Ogg, G.S.; King, A.; Lechner, F.; Spina, C.A., et al. Memory CD8+ T cells vary in differentiation phenotype in different persistent virus infections. *Nat Med* **2002**, *8*, 379-385, doi:10.1038/nm0402-379.
365. Pourgheysari, B.; Khan, N.; Best, D.; Bruton, R.; Nayak, L.; Moss, P.A. The cytomegalovirus-specific CD4+ T-cell response expands with age and markedly alters the CD4+ T-cell repertoire. *J Virol* **2007**, *81*, 7759-7765, doi:10.1128/JVI.01262-06.
366. Einsele, H.; Roosnek, E.; Rufer, N.; Sinzger, C.; Riegler, S.; Löffler, J.; Grigoleit, U.; Moris, A.; Rammensee, H.G.; Kanz, L., et al. Infusion of cytomegalovirus (CMV)-specific T cells for the treatment of CMV infection not responding to antiviral chemotherapy. *Blood* **2002**, *99*, 3916-3922.
367. Sester, U.; Gärtner, B.C.; Wilkens, H.; Schwaab, B.; Wössner, R.; Kindermann, I.; Girndt, M.; Meyerhans, A.; Mueller-Lantzsch, N.; Schäfers, H.J., et al. Differences in CMV-specific T-cell levels and long-term susceptibility to CMV infection after kidney, heart and lung transplantation. *Am J Transplant* **2005**, *5*, 1483-1489, doi:10.1111/j.1600-6143.2005.00871.x.

368. Sester, M.; Sester, U.; Gärtner, B.; Kubuschok, B.; Girndt, M.; Meyerhans, A.; Köhler, H. Sustained high frequencies of specific CD4 T cells restricted to a single persistent virus. *J Virol* **2002**, *76*, 3748-3755.
369. Casazza, J.P.; Betts, M.R.; Price, D.A.; Precopio, M.L.; Ruff, L.E.; Brenchley, J.M.; Hill, B.J.; Roederer, M.; Douek, D.C.; Koup, R.A. Acquisition of direct antiviral effector functions by CMV-specific CD4+ T lymphocytes with cellular maturation. *J Exp Med* **2006**, *203*, 2865-2877, doi:10.1084/jem.20052246.
370. Verma, S.; Weiskopf, D.; Gupta, A.; McDonald, B.; Peters, B.; Sette, A.; Benedict, C.A. Cytomegalovirus-Specific CD4 T Cells Are Cytolytic and Mediate Vaccine Protection. *J Virol* **2016**, *90*, 650-658, doi:10.1128/JVI.02123-15.
371. Pawelec, G.; Akbar, A.; Caruso, C.; Solana, R.; Grubeck-Loebenstein, B.; Wikby, A. Human immunosenescence: is it infectious? *Immunol Rev* **2005**, *205*, 257-268, doi:10.1111/j.0105-2896.2005.00271.x.
372. Fülöp, T.; Montgomery, R.R. Editorial overview: Immune senescence: known knowns and unknown unknowns. *Curr Opin Immunol* **2014**, *29*, vii-ix, doi:10.1016/j.coi.2014.06.005.
373. Ferguson, F.G.; Wikby, A.; Maxson, P.; Olsson, J.; Johansson, B. Immune parameters in a longitudinal study of a very old population of Swedish people: a comparison between survivors and nonsurvivors. *J Gerontol A Biol Sci Med Sci* **1995**, *50*, B378-382.
374. Wikby, A.; Johansson, B.; Ferguson, F.; Olsson, J. Age-related changes in immune parameters in a very old population of Swedish people: a longitudinal study. *Exp Gerontol* **1994**, *29*, 531-541.
375. Wikby, A.; Johansson, B.; Olsson, J.; Löfgren, S.; Nilsson, B.O.; Ferguson, F. Expansions of peripheral blood CD8 T-lymphocyte subpopulations and an association with cytomegalovirus seropositivity in the elderly: the Swedish NONA immune study. *Exp Gerontol* **2002**, *37*, 445-453.
376. Weinberger, B.; Lazuardi, L.; Weiskirchner, I.; Keller, M.; Neuner, C.; Fischer, K.H.; Neuman, B.; Würzner, R.; Grubeck-Loebenstein, B. Healthy aging and latent infection with CMV lead to distinct changes in CD8+ and CD4+ T-cell subsets in the elderly. *Hum Immunol* **2007**, *68*, 86-90, doi:10.1016/j.humimm.2006.10.019.
377. Moro-García, M.A.; Alonso-Arias, R.; López-Vázquez, A.; Suárez-García, F.M.; Solano-Jaurrieta, J.J.; Baltar, J.; López-Larrea, C. Relationship between functional ability in older people, immune system status, and intensity of response to CMV. *Age (Dordr)* **2012**, *34*, 479-495, doi:10.1007/s11357-011-9240-6.
378. Derhovanessian, E.; Theeten, H.; Hähnel, K.; Van Damme, P.; Cools, N.; Pawelec, G. Cytomegalovirus-associated accumulation of late-differentiated CD4 T-cells correlates with poor humoral response to influenza vaccination. *Vaccine* **2013**, *31*, 685-690, doi:10.1016/j.vaccine.2012.11.041.
379. O'Connor, D.; Trück, J.; Lazarus, R.; Clutterbuck, E.A.; Voysey, M.; Jeffery, K.; Pollard, A.J. The effect of chronic cytomegalovirus infection on pneumococcal vaccine responses. *J Infect Dis* **2014**, *209*, 1635-1641, doi:10.1093/infdis/jit673.
380. den Elzen, W.P.; Vossen, A.C.; Cools, H.J.; Westendorp, R.G.; Kroes, A.C.; Gussekloo, J. Cytomegalovirus infection and responsiveness to influenza vaccination in elderly residents of long-term care facilities. *Vaccine* **2011**, *29*, 4869-4874, doi:10.1016/j.vaccine.2011.03.086.
381. Trzonkowski, P.; Myśliwska, J.; Szmit, E.; Wieckiewicz, J.; Lukaszuk, K.; Brydak, L.B.; Machała, M.; Myśliwski, A. Association between cytomegalovirus infection, enhanced proinflammatory response and low level of anti-hemagglutinins during the anti-influenza vaccination--an impact of immunosenescence. *Vaccine* **2003**, *21*, 3826-3836.
382. Turner, J.E.; Campbell, J.P.; Edwards, K.M.; Howarth, L.J.; Pawelec, G.; Aldred, S.; Moss, P.; Drayson, M.T.; Burns, V.E.; Bosch, J.A. Rudimentary signs of immunosenescence in

Cytomegalovirus-seropositive healthy young adults. *Age (Dordr)* **2014**, *36*, 287-297, doi:10.1007/s11357-013-9557-4.
383. Wald, A.; Selke, S.; Magaret, A.; Boeckh, M. Impact of human cytomegalovirus (CMV) infection on immune response to pandemic 2009 H1N1 influenza vaccine in healthy adults. *J Med Virol* **2013**, *85*, 1557-1560, doi:10.1002/jmv.23642.
384. Furman, D.; Jojic, V.; Sharma, S.; Shen-Orr, S.S.; Angel, C.J.; Onengut-Gumuscu, S.; Kidd, B.A.; Maecker, H.T.; Concannon, P.; Dekker, C.L., et al. Cytomegalovirus infection enhances the immune response to influenza. *Sci Transl Med* **2015**, *7*, 281ra243, doi:10.1126/scitranslmed.aaa2293.
385. van den Berg, S.P.H.; Wong, A.; Hendriks, M.; Jacobi, R.H.J.; van Baarle, D.; van Beek, J. Negative Effect of Age, but Not of Latent Cytomegalovirus Infection on the Antibody Response to a Novel Influenza Vaccine Strain in Healthy Adults. *Front Immunol* **2018**, *9*, 82, doi:10.3389/fimmu.2018.00082.
386. Holder, B.; Miles, D.J.; Kaye, S.; Crozier, S.; Mohammed, N.I.; Duah, N.O.; Roberts, E.; Ojuola, O.; Palmero, M.S.; Touray, E.S., et al. Epstein-Barr virus but not cytomegalovirus is associated with reduced vaccine antibody responses in Gambian infants. *PLoS One* **2010**, *5*, e14013, doi:10.1371/journal.pone.0014013.
387. Lasaviciute, G.; Björkander, S.; Carvalho-Queiroz, C.; Hed Myrberg, I.; Nussbaum, B.; Nilsson, C.; Bemark, M.; Nilsson, A.; Sverremark-Ekström, E.; Saghafian-Hedengren, S. Epstein-Barr Virus, but Not Cytomegalovirus, Latency Accelerates the Decay of Childhood Measles and Rubella Vaccine Responses-A 10-Year Follow-up of a Swedish Birth Cohort. *Front Immunol* **2017**, *8*, 1865, doi:10.3389/fimmu.2017.01865.
388. Nielsen, C.M.; White, M.J.; Bottomley, C.; Lusa, C.; Rodríguez-Galán, A.; Turner, S.E.; Goodier, M.R.; Riley, E.M. Impaired NK Cell Responses to Pertussis and H1N1 Influenza Vaccine Antigens in Human Cytomegalovirus-Infected Individuals. *J Immunol* **2015**, *194*, 4657-4667, doi:10.4049/jimmunol.1403080.
389. Goodier, M.R.; Rodriguez-Galan, A.; Lusa, C.; Nielsen, C.M.; Darboe, A.; Moldoveanu, A.L.; White, M.J.; Behrens, R.; Riley, E.M. Influenza Vaccination Generates Cytokine-Induced Memory-like NK Cells: Impact of Human Cytomegalovirus Infection. *J Immunol* **2016**, *197*, 313-325, doi:10.4049/jimmunol.1502049.
390. Lopez-Vergès, S.; Milush, J.M.; Pandey, S.; York, V.A.; Arakawa-Hoyt, J.; Pircher, H.; Norris, P.J.; Nixon, D.F.; Lanier, L.L. CD57 defines a functionally distinct population of mature NK cells in the human CD56dimCD16+ NK-cell subset. *Blood* **2010**, *116*, 3865-3874, doi:10.1182/blood-2010-04-282301.
391. White, M.J.; Nielsen, C.M.; McGregor, R.H.; Riley, E.H.; Goodier, M.R. Differential activation of CD57-defined natural killer cell subsets during recall responses to vaccine antigens. *Immunology* **2014**, *142*, 140-150, doi:10.1111/imm.12239.
392. Rentenaar, R.J.; Gamadia, L.E.; van DerHoek, N.; van Diepen, F.N.; Boom, R.; Weel, J.F.; Wertheim-van Dillen, P.M.; van Lier, R.A.; ten Berge, I.J. Development of virus-specific CD4(+) T cells during primary cytomegalovirus infection. *J Clin Invest* **2000**, *105*, 541-548, doi:10.1172/JCI8229.
393. Bitmansour, A.D.; Douek, D.C.; Maino, V.C.; Picker, L.J. Direct ex vivo analysis of human CD4(+) memory T cell activation requirements at the single clonotype level. *J Immunol* **2002**, *169*, 1207-1218.
394. van Leeuwen, E.M.; Remmerswaal, E.B.; Heemskerk, M.H.; ten Berge, I.J.; van Lier, R.A. Strong selection of virus-specific cytotoxic CD4+ T-cell clones during primary human cytomegalovirus infection. *Blood* **2006**, *108*, 3121-3127, doi:10.1182/blood-2006-03-006809.
395. Lanzieri, T.M.; Dollard, S.C.; Bialek, S.R.; Grosse, S.D. Systematic review of the birth prevalence of congenital cytomegalovirus infection in developing countries. *Int J Infect Dis* **2014**, *22*, 44-48, doi:10.1016/j.ijid.2013.12.010.

396. O'Hara, G.A.; Duncan, C.J.; Ewer, K.J.; Collins, K.A.; Elias, S.C.; Halstead, F.D.; Goodman, A.L.; Edwards, N.J.; Reyes-Sandoval, A.; Bird, P., et al. Clinical assessment of a recombinant simian adenovirus ChAd63: a potent new vaccine vector. *J Infect Dis* **2012**, *205*, 772-781, doi:10.1093/infdis/jir850.
397. Ogwang, C.; Afolabi, M.; Kimani, D.; Jagne, Y.J.; Sheehy, S.H.; Bliss, C.M.; Duncan, C.J.; Collins, K.A.; Garcia Knight, M.A.; Kimani, E., et al. Safety and immunogenicity of heterologous prime-boost immunisation with Plasmodium falciparum malaria candidate vaccines, ChAd63 ME-TRAP and MVA ME-TRAP, in healthy Gambian and Kenyan adults. *PLoS One* **2013**, *8*, e57726, doi:10.1371/journal.pone.0057726.
398. Kimani, D.; Jagne, Y.J.; Cox, M.; Kimani, E.; Bliss, C.M.; Gitau, E.; Ogwang, C.; Afolabi, M.O.; Bowyer, G.; Collins, K.A., et al. Translating the Immunogenicity of Prime-boost Immunization With ChAd63 and MVA ME-TRAP From Malaria Naive to Malaria-endemic Populations. *Molecular Therapy* **2014**, *22*, 1992-2003, doi:10.1038/mt.2014.109.
399. Bliss, C.M.; Bowyer, G.; Anagnostou, N.A.; Havelock, T.; Snudden, C.M.; Davies, H.; de Cassan, S.C.; Grobbelaar, A.; Lawrie, A.M.; Venkatraman, N., et al. Assessment of novel vaccination regimens using viral vectored liver stage malaria vaccines encoding ME-TRAP. *Scientific Reports* **2018**, *8*, 3390, doi:10.1038/s41598-018-21630-4.
400. Ogwang, C.; Kimani, D.; Edwards, N.J.; Roberts, R.; Mwacharo, J.; Bowyer, G.; Bliss, C.; Hodgson, S.H.; Njuguna, P.; Viebig, N.K., et al. Prime-boost vaccination with chimpanzee adenovirus and modified vaccinia Ankara encoding TRAP provides partial protection against Plasmodium falciparum infection in Kenyan adults. *Sci Transl Med* **2015**, *7*, 286re285, doi:10.1126/scitranslmed.aaa2373.
401. Rampling, T.; Ewer, K.J.; Bowyer, G.; Bliss, C.M.; Edwards, N.J.; Wright, D.; Payne, R.O.; Venkatraman, N.; de Barra, E.; Snudden, C.M., et al. Safety and High Level Efficacy of the Combination Malaria Vaccine Regimen of RTS,S/AS01B With Chimpanzee Adenovirus 63 and Modified Vaccinia Ankara Vectored Vaccines Expressing ME-TRAP. *J Infect Dis* **2016**, *214*, 772-781, doi:10.1093/infdis/jiw244.
402. Reiss, S.; Baxter, A.E.; Cirelli, K.M.; Dan, J.M.; Morou, A.; Daigneault, A.; Brassard, N.; Silvestri, G.; Routy, J.P.; Havenar-Daughton, C., et al. Comparative analysis of activation induced marker (AIM) assays for sensitive identification of antigen-specific CD4 T cells. *PLoS One* **2017**, *12*, e0186998, doi:10.1371/journal.pone.0186998.
403. Dan, J.M.; Lindestam Arlehamn, C.S.; Weiskopf, D.; da Silva Antunes, R.; Havenar-Daughton, C.; Reiss, S.M.; Brigger, M.; Bothwell, M.; Sette, A.; Crotty, S. A Cytokine-Independent Approach To Identify Antigen-Specific Human Germinal Center T Follicular Helper Cells and Rare Antigen-Specific CD4+ T Cells in Blood. *J Immunol* **2016**, *197*, 983-993, doi:10.4049/jimmunol.1600318.
404. Havenar-Daughton, C.; Reiss, S.M.; Carnathan, D.G.; Wu, J.E.; Kendric, K.; Torrents de la Peña, A.; Kasturi, S.P.; Dan, J.M.; Bothwell, M.; Sanders, R.W., et al. Cytokine-Independent Detection of Antigen-Specific Germinal Center T Follicular Helper Cells in Immunized Nonhuman Primates Using a Live Cell Activation-Induced Marker Technique. *J Immunol* **2016**, *197*, 994-1002, doi:10.4049/jimmunol.1600320.
405. Rodríguez-Galán, A.; Salman, A.M.; Bowyer, G.; Collins, K.A.; Longley, R.J.; Brod, F.; Ulaszewska, M.; Ewer, K.J.; Janse, C.J.; Khan, S.M., et al. An in vitro assay to measure antibody-mediated inhibition of P. berghei sporozoite invasion against P. falciparum antigens. *Sci Rep* **2017**, *7*, 17011, doi:10.1038/s41598-017-17274-5.
406. Bowyer, G.; Grobbelaar, A.; Rampling, T.; Venkatraman, N.; Morelle, D.; Ballou, R.W.; Hill, A.V.S.; Ewer, K.J. CXCR3. *Front Immunol* **2018**, *9*, 1660, doi:10.3389/fimmu.2018.01660.
407. Hodgson, S.H.; Juma, E.; Salim, A.; Magiri, C.; Kimani, D.; Njenga, D.; Muia, A.; Cole, A.O.; Ogwang, C.; Awuondo, K., et al. Evaluating controlled human malaria infection in Kenyan adults with varying degrees of prior exposure to Plasmodium falciparum using

sporozoites administered by intramuscular injection. *Front Microbiol* **2014**, *5*, 686, doi:10.3389/fmicb.2014.00686.
408. Ndungu, F.M.; Bull, P.C.; Ross, A.; Lowe, B.S.; Kabiru, E.; Marsh, K. Naturally acquired immunoglobulin (Ig)G subclass antibodies to crude asexual Plasmodium falciparum lysates: evidence for association with protection for IgG1 and disease for IgG2. *Parasite Immunol* **2002**, *24*, 77-82.
409. Waterboer, T.; Sehr, P.; Michael, K.M.; Franceschi, S.; Nieland, J.D.; Joos, T.O.; Templin, M.F.; Pawlita, M. Multiplex human papillomavirus serology based on in situ-purified glutathione s-transferase fusion proteins. *Clin Chem* **2005**, *51*, 1845-1853, doi:10.1373/clinchem.2005.052381.
410. Agnandji, S.T.; Lell, B.; Soulanoudjingar, S.S.; Fernandes, J.F.; Abossolo, B.P.; Conzelmann, C.; Methogo, B.G.; Doucka, Y.; Flamen, A.; Mordmüller, B., et al. First results of phase 3 trial of RTS,S/AS01 malaria vaccine in African children. *N Engl J Med* **2011**, *365*, 1863-1875, doi:10.1056/NEJMoa1102287.
411. Agnandji, S.T.; Lell, B.; Fernandes, J.F.; Abossolo, B.P.; Methogo, B.G.; Kabwende, A.L.; Adegnika, A.A.; Mordmüller, B.; Issifou, S.; Kremsner, P.G., et al. A phase 3 trial of RTS,S/AS01 malaria vaccine in African infants. *N Engl J Med* **2012**, *367*, 2284-2295, doi:10.1056/NEJMoa1208394.
412. Olotu, A.; Fegan, G.; Wambua, J.; Nyangweso, G.; Leach, A.; Lievens, M.; Kaslow, D.C.; Njuguna, P.; Marsh, K.; Bejon, P. Seven-Year Efficacy of RTS,S/AS01 Malaria Vaccine among Young African Children. *N Engl J Med* **2016**, *374*, 2519-2529, doi:10.1056/NEJMoa1515257.
413. RTS, S.C.T.P. Efficacy and safety of the RTS,S/AS01 malaria vaccine during 18 months after vaccination: a phase 3 randomized, controlled trial in children and young infants at 11 African sites. *PLoS Med* **2014**, *11*, e1001685, doi:10.1371/journal.pmed.1001685.
414. Hodgson, S.H.; Choudhary, P.; Elias, S.C.; Milne, K.H.; Rampling, T.W.; Biswas, S.; Poulton, I.D.; Miura, K.; Douglas, A.D.; Alanine, D.G., et al. Combining viral vectored and protein-in-adjuvant vaccines against the blood-stage malaria antigen AMA1: report on a phase 1a clinical trial. *Mol Ther* **2014**, *22*, 2142-2154, doi:10.1038/mt.2014.157.
415. Moorthy, V.S.; Ballou, W.R. Immunological mechanisms underlying protection mediated by RTS,S: a review of the available data. *Malaria Journal* **2009**, *8*, 312-312, doi:10.1186/1475-2875-8-312.
416. Stoute, J.A.; Slaoui, M.; Heppner, D.G.; Momin, P.; Kester, K.E.; Desmons, P.; Wellde, B.T.; Garçon, N.; Krzych, U.; Marchand, M., et al. A Preliminary Evaluation of a Recombinant Circumsporozoite Protein Vaccine against Plasmodium falciparum Malaria. *New England Journal of Medicine* **1997**, *336*, 86-91, doi:10.1056/NEJM199701093360202.
417. White, M.T.; Bejon, P.; Olotu, A.; Griffin, J.T.; Riley, E.M.; Kester, K.E.; Ockenhouse, C.F.; Ghani, A.C. The relationship between RTS,S vaccine-induced antibodies, $CD4^+$ T cell responses and protection against Plasmodium falciparum infection. *PLoS One* **2013**, *8*, e61395, doi:10.1371/journal.pone.0061395.
418. Rampling, T.; Ewer, K.J.; Bowyer, G.; Edwards, N.J.; Wright, D.; Sridhar, S.; Payne, R.; Powlson, J.; Bliss, C.; Venkatraman, N., et al. Safety and efficacy of novel malaria vaccine regimens of RTS,S/AS01B alone, or with concomitant ChAd63-MVA-vectored vaccines expressing ME-TRAP. *NPJ Vaccines* **2018**, *3*, 49, doi:10.1038/s41541-018-0084-2.
419. Stoute, J.A.; Slaoui, M.; Heppner, D.G.; Momin, P.; Kester, K.E.; Desmons, P.; Wellde, B.T.; Garçon, N.; Krzych, U.; Marchand, M. A preliminary evaluation of a recombinant circumsporozoite protein vaccine against Plasmodium falciparum malaria. RTS,S Malaria Vaccine Evaluation Group. *N Engl J Med* **1997**, *336*, 86-91, doi:10.1056/NEJM199701093360202.

420. Regules, J.A.; Cicatelli, S.B.; Bennett, J.W.; Paolino, K.M.; Twomey, P.S.; Moon, J.E.; Kathcart, A.K.; Hauns, K.D.; Komisar, J.L.; Qabar, A.N., et al. Fractional Third and Fourth Dose of RTS,S/AS01 Malaria Candidate Vaccine: A Phase 2a Controlled Human Malaria Parasite Infection and Immunogenicity Study. *J Infect Dis* **2016**, *214*, 762-771, doi:10.1093/infdis/jiw237.
421. Olotu, A.; Moris, P.; Mwacharo, J.; Vekemans, J.; Kimani, D.; Janssens, M.; Kai, O.; Jongert, E.; Lievens, M.; Leach, A., et al. Circumsporozoite-specific T cell responses in children vaccinated with RTS,S/AS01E and protection against P falciparum clinical malaria. *PLoS One* **2011**, *6*, e25786, doi:10.1371/journal.pone.0025786.
422. Ansong, D.; Asante, K.P.; Vekemans, J.; Owusu, S.K.; Owusu, R.; Brobby, N.A.; Dosoo, D.; Osei-Akoto, A.; Osei-Kwakye, K.; Asafo-Adjei, E., et al. T cell responses to the RTS,S/AS01(E) and RTS,S/AS02(D) malaria candidate vaccines administered according to different schedules to Ghanaian children. *PLoS One* **2011**, *6*, e18891, doi:10.1371/journal.pone.0018891.
423. Agnandji, S.T.; Fendel, R.; Mestré, M.; Janssens, M.; Vekemans, J.; Held, J.; Gnansounou, F.; Haertle, S.; von Glasenapp, I.; Oyakhirome, S., et al. Induction of Plasmodium falciparum-specific CD4+ T cells and memory B cells in Gabonese children vaccinated with RTS,S/AS01(E) and RTS,S/AS02(D). *PLoS One* **2011**, *6*, e18559, doi:10.1371/journal.pone.0018559.
424. Mullarkey, C.E.; Boyd, A.; van Laarhoven, A.; Lefevre, E.A.; Veronica Carr, B.; Baratelli, M.; Molesti, E.; Temperton, N.J.; Butter, C.; Charleston, B., et al. Improved adjuvanting of seasonal influenza vaccines: preclinical studies of MVA-NP+M1 coadministration with inactivated influenza vaccine. *Eur J Immunol* **2013**, *43*, 1940-1952, doi:10.1002/eji.201242922.
425. Reyes-Sandoval, A.; Rollier, C.S.; Milicic, A.; Bauza, K.; Cottingham, M.G.; Tang, C.K.; Dicks, M.D.; Wang, D.; Longley, R.J.; Wyllie, D.H., et al. Mixed vector immunization with recombinant adenovirus and MVA can improve vaccine efficacy while decreasing antivector immunity. *Mol Ther* **2012**, *20*, 1633-1647, doi:10.1038/mt.2012.25.
426. Hutchings, C.L.; Gilbert, S.C.; Hill, A.V.; Moore, A.C. Novel protein and poxvirus-based vaccine combinations for simultaneous induction of humoral and cell-mediated immunity. *J Immunol* **2005**, *175*, 599-606.
427. Stoute, J.A.; Kester, K.E.; Krzych, U.; Wellde, B.T.; Hall, T.; White, K.; Glenn, G.; Ockenhouse, C.F.; Garcon, N.; Schwenk, R., et al. Long-term efficacy and immune responses following immunization with the RTS,S malaria vaccine. *J Infect Dis* **1998**, *178*, 1139-1144.
428. Kester, K.E.; Cummings, J.F.; Ofori-Anyinam, O.; Ockenhouse, C.F.; Krzych, U.; Moris, P.; Schwenk, R.; Nielsen, R.A.; Debebe, Z.; Pinelis, E., et al. Randomized, double-blind, phase 2a trial of falciparum malaria vaccines RTS,S/AS01B and RTS,S/AS02A in malaria-naive adults: safety, efficacy, and immunologic associates of protection. *J Infect Dis* **2009**, *200*, 337-346, doi:10.1086/600120.
429. Bliss, C.M.; Bowyer, G.; Anagnostou, N.A.; Havelock, T.; Snudden, C.M.; Davies, H.; de Cassan, S.C.; Grobbelaar, A.; Lawrie, A.M.; Venkatraman, N., et al. Assessment of novel vaccination regimens using viral vectored liver stage malaria vaccines encoding ME-TRAP. *Sci Rep* **2018**, *8*, 3390, doi:10.1038/s41598-018-21630-4.
430. EISEN, H.N.; SISKIND, G.W. VARIATIONS IN AFFINITIES OF ANTIBODIES DURING THE IMMUNE RESPONSE. *Biochemistry* **1964**, *3*, 996-1008.
431. González-Fernández, A.; Milstein, C. Low antigen dose favours selection of somatic mutants with hallmarks of antibody affinity maturation. *Immunology* **1998**, *93*, 149-153.
432. Ahman, H.; Käyhty, H.; Vuorela, A.; Leroy, O.; Eskola, J. Dose dependency of antibody response in infants and children to pneumococcal polysaccharides conjugated to tetanus toxoid. *Vaccine* **1999**, *17*, 2726-2732.

433. He, J.; Tsai, L.M.; Leong, Y.A.; Hu, X.; Ma, C.S.; Chevalier, N.; Sun, X.; Vandenberg, K.; Rockman, S.; Ding, Y., et al. Circulating precursor CCR7(lo)PD-1(hi) CXCR5^{+} CD4^{+} T cells indicate Tfh cell activity and promote antibody responses upon antigen reexposure. *Immunity* **2013**, *39*, 770-781, doi:10.1016/j.immuni.2013.09.007.
434. Heit, A.; Schmitz, F.; Gerdts, S.; Flach, B.; Moore, M.S.; Perkins, J.A.; Robins, H.S.; Aderem, A.; Spearman, P.; Tomaras, G.D., et al. Vaccination establishes clonal relatives of germinal center T cells in the blood of humans. *J Exp Med* **2017**, *214*, 2139-2152, doi:10.1084/jem.20161794.
435. Li, X.Y.; Wu, Z.B.; Ding, J.; Zheng, Z.H.; Chen, L.N.; Zhu, P. Role of the frequency of blood CD4(+) CXCR5(+) CCR6(+) T cells in autoimmunity in patients with Sjögren's syndrome. *Biochem Biophys Res Commun* **2012**, *422*, 238-244, doi:10.1016/j.bbrc.2012.04.133.
436. Romme Christensen, J.; Börnsen, L.; Ratzer, R.; Piehl, F.; Khademi, M.; Olsson, T.; Sørensen, P.S.; Sellebjerg, F. Systemic inflammation in progressive multiple sclerosis involves follicular T-helper, Th17- and activated B-cells and correlates with progression. *PLoS One* **2013**, *8*, e57820, doi:10.1371/journal.pone.0057820.
437. Gong, F.; Qian, C.; Zhu, H.; Zhu, J.; Pan, Y.; Dong, Q.; Jiang, D. Circulating follicular T-helper cell subset distribution in patients with asthma. *Allergy Asthma Proc* **2016**, *37*, 154-161.
438. Kamekura, R.; Shigehara, K.; Miyajima, S.; Jitsukawa, S.; Kawata, K.; Yamashita, K.; Nagaya, T.; Kumagai, A.; Sato, A.; Matsumiya, H., et al. Alteration of circulating type 2 follicular helper T cells and regulatory B cells underlies the comorbid association of allergic rhinitis with bronchial asthma. *Clin Immunol* **2015**, *158*, 204-211, doi:10.1016/j.clim.2015.02.016.
439. Schmitt, N.; Ueno, H. Human T follicular helper cells: development and subsets. *Adv Exp Med Biol* **2013**, *785*, 87-94, doi:10.1007/978-1-4614-6217-0_10.
440. Cunill, V.; Clemente, A.; Lanio, N.; Barceló, C.; Andreu, V.; Pons, J.; Ferrer, J.M. Follicular T Cells from smB(-) Common Variable Immunodeficiency Patients Are Skewed Toward a Th1 Phenotype. *Front Immunol* **2017**, *8*, 174, doi:10.3389/fimmu.2017.00174.
441. Bentebibel, S.E.; Lopez, S.; Obermoser, G.; Schmitt, N.; Mueller, C.; Harrod, C.; Flano, E.; Mejias, A.; Albrecht, R.A.; Blankenship, D., et al. Induction of ICOS+CXCR3+CXCR5+ TH cells correlates with antibody responses to influenza vaccination. *Sci Transl Med* **2013**, *5*, 176ra132, doi:10.1126/scitranslmed.3005191.
442. Chattopadhyay, P.K.; Yu, J.; Roederer, M. Live-cell assay to detect antigen-specific CD4+ T-cell responses by CD154 expression. *Nat Protoc* **2006**, *1*, 1-6, doi:10.1038/nprot.2006.1.
443. Ma, C.S.; Deenick, E.K.; Batten, M.; Tangye, S.G. The origins, function, and regulation of T follicular helper cells. *J Exp Med* **2012**, *209*, 1241-1253, doi:10.1084/jem.20120994.
444. Reyes-Sandoval, A.; Wyllie, D.H.; Bauza, K.; Milicic, A.; Forbes, E.K.; Rollier, C.S.; Hill, A.V. CD8+ T effector memory cells protect against liver-stage malaria. *J Immunol* **2011**, *187*, 1347-1357, doi:10.4049/jimmunol.1100302.
445. Nakajima, C.; Mukai, T.; Yamaguchi, N.; Morimoto, Y.; Park, W.R.; Iwasaki, M.; Gao, P.; Ono, S.; Fujiwara, H.; Hamaoka, T. Induction of the chemokine receptor CXCR3 on TCR-stimulated T cells: dependence on the release from persistent TCR-triggering and requirement for IFN-gamma stimulation. *Eur J Immunol* **2002**, *32*, 1792-1801, doi:10.1002/1521-4141(200206)32:6<1792::AID-IMMU1792>3.0.CO;2-0.
446. Bentebibel, S.E.; Khurana, S.; Schmitt, N.; Kurup, P.; Mueller, C.; Obermoser, G.; Palucka, A.K.; Albrecht, R.A.; Garcia-Sastre, A.; Golding, H., et al. ICOS(+)PD-1(+)CXCR3(+) T follicular helper cells contribute to the generation of high-avidity antibodies following influenza vaccination. *Sci Rep* **2016**, *6*, 26494, doi:10.1038/srep26494.
447. Groom, J.R.; Luster, A.D. CXCR3 in T cell function. *Experimental cell research* **2011**, *317*, 620-631, doi:10.1016/j.yexcr.2010.12.017.

448. Teigler, J.E.; Phogat, S.; Franchini, G.; Hirsch, V.M.; Michael, N.L.; Barouch, D.H. The Canarypox Virus Vector ALVAC Induces Distinct Cytokine Responses Compared to the Vaccinia Virus-Based Vectors MVA and NYVAC in Rhesus Monkeys. *Journal of Virology* **2014**, *88*, 1809-1814, doi:10.1128/JVI.02386-13.
449. Wirtz, R.A.; Duncan, J.F.; Njelesani, E.K.; Schneider, I.; Brown, A.E.; Oster, C.N.; Were, J.B.; Webster, H.K. ELISA method for detecting Plasmodium falciparum circumsporozoite antibody. *Bull World Health Organ* **1989**, *67*, 535-542.
450. Penny, M.A.; Maire, N.; Bever, C.A.; Pemberton-Ross, P.; Briët, O.J.; Smith, D.L.; Gething, P.W.; Smith, T.A. Distribution of malaria exposure in endemic countries in Africa considering country levels of effective treatment. *Malar J* **2015**, *14*, 384, doi:10.1186/s12936-015-0864-3.
451. Fujii, K.; Tsuji, M.; Murota, K.; Terato, K.; Shimozuru, Y.; Nagai, Y. An improved enzyme-linked immunosorbent assay of anti-collagen antibodies in human serum. *J Immunol Methods* **1989**, *124*, 63-70.
452. Güven, E.; Duus, K.; Lydolph, M.C.; Jørgensen, C.S.; Laursen, I.; Houen, G. Non-specific binding in solid phase immunoassays for autoantibodies correlates with inflammation markers. *J Immunol Methods* **2014**, *403*, 26-36, doi:10.1016/j.jim.2013.11.014.
453. Terato, K.; Do, C.T.; Cutler, D.; Waritani, T.; Shionoya, H. Preventing intense false positive and negative reactions attributed to the principle of ELISA to re-investigate antibody studies in autoimmune diseases. *J Immunol Methods* **2014**, *407*, 15-25, doi:10.1016/j.jim.2014.03.013.
454. Plotkin, S.A. Correlates of protection induced by vaccination. *Clin Vaccine Immunol* **2010**, *17*, 1055-1065, doi:10.1128/CVI.00131-10.
455. Terato, K.; Do, C.; Chang, J.; Waritani, T. Preventing further misuse of the ELISA technique and misinterpretation of serological antibody assay data. *Vaccine* **2016**, *34*, 4643-4644, doi:10.1016/j.vaccine.2016.08.007.
456. Andersson, J.; Ekdahl, K.N.; Larsson, R.; Nilsson, U.R.; Nilsson, B. C3 adsorbed to a polymer surface can form an initiating alternative pathway convertase. *J Immunol* **2002**, *168*, 5786-5791.
457. Hu, B.; Even, C.; Plagemann, P.G. Immune complexes that bind to ELISA plates not coated with antigen in mice infected with lactate dehydrogenase-elevating virus: relationship to IgG2a- and IgG2b-specific polyclonal activation of B cells. *Viral Immunol* **1992**, *5*, 27-38, doi:10.1089/vim.1992.5.27.
458. Waritani, T.; Chang, J.; McKinney, B.; Terato, K. An ELISA protocol to improve the accuracy and reliability of serological antibody assays. *MethodsX* **2017**, *4*, 153-165, doi:10.1016/j.mex.2017.03.002.
459. Le Guenno, B.; Formenty, P.; Formentry, P.; Wyers, M.; Gounon, P.; Walker, F.; Boesch, C. Isolation and partial characterisation of a new strain of Ebola virus. *Lancet* **1995**, *345*, 1271-1274.
460. Bower, H.; Glynn, J.R. A systematic review and meta-analysis of seroprevalence surveys of ebolavirus infection. *Sci Data* **2017**, *4*, 160133, doi:10.1038/sdata.2016.133.
461. Ksiazek, T.G.; West, C.P.; Rollin, P.E.; Jahrling, P.B.; Peters, C.J. ELISA for the detection of antibodies to Ebola viruses. *J Infect Dis* **1999**, *179 Suppl 1*, S192-198, doi:10.1086/514313.
462. Becquart, P.; Wauquier, N.; Mahlakõiv, T.; Nkoghe, D.; Padilla, C.; Souris, M.; Ollomo, B.; Gonzalez, J.P.; De Lamballerie, X.; Kazanji, M., et al. High prevalence of both humoral and cellular immunity to Zaire ebolavirus among rural populations in Gabon. *PLoS One* **2010**, *5*, e9126, doi:10.1371/journal.pone.0009126.
463. Leroy, E.M.; Baize, S.; Volchkov, V.E.; Fisher-Hoch, S.P.; Georges-Courbot, M.C.; Lansoud-Soukate, J.; Capron, M.; Debré, P.; McCormick, J.B.; Georges, A.J. Human asymptomatic Ebola infection and strong inflammatory response. *Lancet* **2000**, *355*, 2210-2215.

464. Glynn, J.R.; Bower, H.; Johnson, S.; Houlihan, C.F.; Montesano, C.; Scott, J.T.; Semple, M.G.; Bangura, M.S.; Kamara, A.J.; Kamara, O., et al. Asymptomatic infection and unrecognised Ebola virus disease in Ebola-affected households in Sierra Leone: a cross-sectional study using a new non-invasive assay for antibodies to Ebola virus. *Lancet Infect Dis* **2017**, *17*, 645-653, doi:10.1016/S1473-3099(17)30111-1.
465. Richardson, E.T.; Kelly, J.D.; Barrie, M.B.; Mesman, A.W.; Karku, S.; Quiwa, K.; Marsh, R.H.; Koedoyoma, S.; Daboh, F.; Barron, K.P., et al. Minimally Symptomatic Infection in an Ebola 'Hotspot': A Cross-Sectional Serosurvey. *PLoS Negl Trop Dis* **2016**, *10*, e0005087, doi:10.1371/journal.pntd.0005087.
466. Mulangu, S.; Borchert, M.; Paweska, J.; Tshomba, A.; Afounde, A.; Kulidri, A.; Swanepoel, R.; Muyembe-Tamfum, J.J.; Van der Stuyft, P. High prevalence of IgG antibodies to Ebola virus in the Efé pygmy population in the Watsa region, Democratic Republic of the Congo. *BMC Infect Dis* **2016**, *16*, 263, doi:10.1186/s12879-016-1607-y.
467. Busico, K.M.; Marshall, K.L.; Ksiazek, T.G.; Roels, T.H.; Fleerackers, Y.; Feldmann, H.; Khan, A.S.; Peters, C.J. Prevalence of IgG antibodies to Ebola virus in individuals during an Ebola outbreak, Democratic Republic of the Congo, 1995. *J Infect Dis* **1999**, *179 Suppl 1*, S102-107, doi:10.1086/514309.
468. Clark, D.V.; Kibuuka, H.; Millard, M.; Wakabi, S.; Lukwago, L.; Taylor, A.; Eller, M.A.; Eller, L.A.; Michael, N.L.; Honko, A.N., et al. Long-term sequelae after Ebola virus disease in Bundibugyo, Uganda: a retrospective cohort study. *Lancet Infect Dis* **2015**, *15*, 905-912, doi:10.1016/S1473-3099(15)70152-0.
469. Heffernan, R.T.; Pambo, B.; Hatchett, R.J.; Leman, P.A.; Swanepoel, R.; Ryder, R.W. Low seroprevalence of IgG antibodies to Ebola virus in an epidemic zone: Ogooué-Ivindo region, Northeastern Gabon, 1997. *J Infect Dis* **2005**, *191*, 964-968, doi:10.1086/427994.
470. Goba, A.; Khan, S.H.; Fonnie, M.; Fullah, M.; Moigboi, A.; Kovoma, A.; Sinnah, V.; Yoko, N.; Rogers, H.; Safai, S., et al. An Outbreak of Ebola Virus Disease in the Lassa Fever Zone. *J Infect Dis* **2016**, *214*, S110-S121, doi:10.1093/infdis/jiw239.
471. Schoepp, R.J.; Rossi, C.A.; Khan, S.H.; Goba, A.; Fair, J.N. Undiagnosed acute viral febrile illnesses, Sierra Leone. *Emerg Infect Dis* **2014**, *20*, 1176-1182, doi:10.3201/eid2007.131265.
472. O'Hearn, A.E.; Voorhees, M.A.; Fetterer, D.P.; Wauquier, N.; Coomber, M.R.; Bangura, J.; Fair, J.N.; Gonzalez, J.P.; Schoepp, R.J. Serosurveillance of viral pathogens circulating in West Africa. *Virol J* **2016**, *13*, 163, doi:10.1186/s12985-016-0621-4.
473. Pappalardo, M.; Juliá, M.; Howard, M.J.; Rossman, J.S.; Michaelis, M.; Wass, M.N. Conserved differences in protein sequence determine the human pathogenicity of Ebolaviruses. *Sci Rep* **2016**, *6*, 23743, doi:10.1038/srep23743.
474. Ayouba, A.; Touré, A.; Butel, C.; Keita, A.K.; Binetruy, F.; Sow, M.S.; Foulongne, V.; Delaporte, E.; Peeters, M. Development of a Sensitive and Specific Serological Assay Based on Luminex Technology for Detection of Antibodies to Zaire Ebola Virus. *J Clin Microbiol* **2017**, *55*, 165-176, doi:10.1128/JCM.01979-16.
475. Bramble, M.S.; Hoff, N.; Gilchuk, P.; Mukadi, P.; Lu, K.; Doshi, R.H.; Steffen, I.; Nicholson, B.P.; Lipson, A.; Vashist, N., et al. Pan-Filovirus Serum Neutralizing Antibodies in a Subset of Congolese Ebolavirus Infection Survivors. *J Infect Dis* **2018**, doi:10.1093/infdis/jiy453.
476. Macneil, A.; Reed, Z.; Rollin, P.E. Serologic cross-reactivity of human IgM and IgG antibodies to five species of Ebola virus. *PLoS Negl Trop Dis* **2011**, *5*, e1175, doi:10.1371/journal.pntd.0001175.
477. Sobarzo, A.; Groseth, A.; Dolnik, O.; Becker, S.; Lutwama, J.J.; Perelman, E.; Yavelsky, V.; Muhammad, M.; Kuehne, A.I.; Marks, R.S., et al. Profile and persistence of the virus-specific neutralizing humoral immune response in human survivors of Sudan ebolavirus (Gulu). *J Infect Dis* **2013**, *208*, 299-309, doi:10.1093/infdis/jit162.

478. Mafopa, N.G.; Russo, G.; Wadoum, R.E.G.; Iwerima, E.; Batwala, V.; Giovanetti, M.; Minutolo, A.; Turay, P.; Turay, T.B.; Kargbo, B., et al. Seroprevalence of Ebola virus infection in Bombali District, Sierra Leone. *J Public Health Afr* **2017**, *8*, 732, doi:10.4081/jphia.2017.732.
479. Lozano, R.; Naghavi, M.; Foreman, K.; Lim, S.; Shibuya, K.; Aboyans, V.; Abraham, J.; Adair, T.; Aggarwal, R.; Ahn, S.Y., et al. Global and regional mortality from 235 causes of death for 20 age groups in 1990 and 2010: a systematic analysis for the Global Burden of Disease Study 2010. *Lancet* **2012**, *380*, 2095-2128, doi:10.1016/S0140-6736(12)61728-0.
480. Bhutta, Z.A.; Sommerfeld, J.; Lassi, Z.S.; Salam, R.A.; Das, J.K. Global burden, distribution, and interventions for infectious diseases of poverty. *Infect Dis Poverty* **2014**, *3*, 21, doi:10.1186/2049-9957-3-21.
481. Bates, I.; Fenton, C.; Gruber, J.; Lalloo, D.; Medina Lara, A.; Squire, S.B.; Theobald, S.; Thomson, R.; Tolhurst, R. Vulnerability to malaria, tuberculosis, and HIV/AIDS infection and disease. Part 1: determinants operating at individual and household level. *Lancet Infect Dis* **2004**, *4*, 267-277, doi:10.1016/S1473-3099(04)01002-3.
482. Lagos, R.; Fasano, A.; Wasserman, S.S.; Prado, V.; San Martin, O.; Abrego, P.; Losonsky, G.A.; Alegria, S.; Levine, M.M. Effect of small bowel bacterial overgrowth on the immunogenicity of single-dose live oral cholera vaccine CVD 103-HgR. *J Infect Dis* **1999**, *180*, 1709-1712, doi:10.1086/315051.
483. Qadri, F.; Ahmed, T.; Ahmed, F.; Bradley Sack, R.; Sack, D.A.; Svennerholm, A.M. Safety and immunogenicity of an oral, inactivated enterotoxigenic Escherichia coli plus cholera toxin B subunit vaccine in Bangladeshi children 18-36 months of age. *Vaccine* **2003**, *21*, 2394-2403.
484. Serazin, A.C.; Shackelton, L.A.; Wilson, C.; Bhan, M.K. Improving the performance of enteric vaccines in the developing world. *Nat Immunol* **2010**, *11*, 769-773, doi:10.1038/ni0910-769.
485. Lopman, B.A.; Pitzer, V.E.; Sarkar, R.; Gladstone, B.; Patel, M.; Glasser, J.; Gambhir, M.; Atchison, C.; Grenfell, B.T.; Edmunds, W.J., et al. Understanding reduced rotavirus vaccine efficacy in low socio-economic settings. *PLoS One* **2012**, *7*, e41720, doi:10.1371/journal.pone.0041720.
486. Valdez, Y.; Brown, E.M.; Finlay, B.B. Influence of the microbiota on vaccine effectiveness. *Trends Immunol* **2014**, *35*, 526-537, doi:10.1016/j.it.2014.07.003.
487. Rey-Cuille, M.A.; Seck, A.; Njouom, R.; Chartier, L.; Sow, H.D.; Mamadou; Ka, A.S.; Njankouo, M.; Rousset, D.; Giles-Vernick, T., et al. Low immune response to hepatitis B vaccine among children in Dakar, Senegal. *PLoS One* **2012**, *7*, e38153, doi:10.1371/journal.pone.0038153.
488. Prendergast, A.J. Malnutrition and vaccination in developing countries. *Philos Trans R Soc Lond B Biol Sci* **2015**, *370*, doi:10.1098/rstb.2014.0141.
489. O'Connor, D.; Pollard, A.J. Characterizing vaccine responses using host genomic and transcriptomic analysis. *Clin Infect Dis* **2013**, *57*, 860-869, doi:10.1093/cid/cit373.
490. Roca-Feltrer, A.; Carneiro, I.; Smith, L.; Schellenberg, J.R.; Greenwood, B.; Schellenberg, D. The age patterns of severe malaria syndromes in sub-Saharan Africa across a range of transmission intensities and seasonality settings. *Malar J* **2010**, *9*, 282, doi:10.1186/1475-2875-9-282.
491. Cunnington, A.J.; Riley, E.M. Suppression of vaccine responses by malaria: insignificant or overlooked? *Expert Rev Vaccines* **2010**, *9*, 409-429, doi:10.1586/erv.10.16.
492. Han, S. Clinical vaccine development. *Clin Exp Vaccine Res* **2015**, *4*, 46-53, doi:10.7774/cevr.2015.4.1.46.
493. Beigi, R.H.; Fortner, K.B.; Munoz, F.M.; Roberts, J.; Gordon, J.L.; Han, H.H.; Glenn, G.; Dormitzer, P.R.; Gu, X.X.; Read, J.S., et al. Maternal immunization: opportunities for

scientific advancement. *Clin Infect Dis* **2014**, *59 Suppl 7*, S408-414, doi:10.1093/cid/ciu708.

494. Røttingen, J.A.; Gouglas, D.; Feinberg, M.; Plotkin, S.; Raghavan, K.V.; Witty, A.; Draghia-Akli, R.; Stoffels, P.; Piot, P. New Vaccines against Epidemic Infectious Diseases. *N Engl J Med* **2017**, *376*, 610-613, doi:10.1056/NEJMp1613577.
495. Drakeley, C.J.; Corran, P.H.; Coleman, P.G.; Tongren, J.E.; McDonald, S.L.; Carneiro, I.; Malima, R.; Lusingu, J.; Manjurano, A.; Nkya, W.M., et al. Estimating medium- and long-term trends in malaria transmission by using serological markers of malaria exposure. *Proc Natl Acad Sci U S A* **2005**, *102*, 5108-5113, doi:10.1073/pnas.0408725102.
496. Marsh, K.; Otoo, L.; Hayes, R.J.; Carson, D.C.; Greenwood, B.M. Antibodies to blood stage antigens of Plasmodium falciparum in rural Gambians and their relation to protection against infection. *Trans R Soc Trop Med Hyg* **1989**, *83*, 293-303.
497. al-Yaman, F.; Genton, B.; Kramer, K.J.; Chang, S.P.; Hui, G.S.; Baisor, M.; Alpers, M.P. Assessment of the role of naturally acquired antibody levels to Plasmodium falciparum merozoite surface protein-1 in protecting Papua New Guinean children from malaria morbidity. *Am J Trop Med Hyg* **1996**, *54*, 443-448.
498. Branch, O.H.; Udhayakumar, V.; Hightower, A.W.; Oloo, A.J.; Hawley, W.A.; Nahlen, B.L.; Bloland, P.B.; Kaslow, D.C.; Lal, A.A. A longitudinal investigation of IgG and IgM antibody responses to the merozoite surface protein-1 19-kiloDalton domain of Plasmodium falciparum in pregnant women and infants: associations with febrile illness, parasitemia, and anemia. *Am J Trop Med Hyg* **1998**, *58*, 211-219.
499. Offeddu, V.; Thathy, V.; Marsh, K.; Matuschewski, K. Naturally acquired immune responses against Plasmodium falciparum sporozoites and liver infection. *Int J Parasitol* **2012**, *42*, 535-548, doi:10.1016/j.ijpara.2012.03.011.
500. Van Braeckel-Budimir, N.; Harty, J.T. CD8 T-cell-mediated protection against liver-stage malaria: lessons from a mouse model. *Front Microbiol* **2014**, *5*, 272, doi:10.3389/fmicb.2014.00272.
501. Jiang, V.; Jiang, B.; Tate, J.; Parashar, U.D.; Patel, M.M. Performance of rotavirus vaccines in developed and developing countries. *Hum Vaccin* **2010**, *6*, 532-542.
502. Bojang, K.A.; Milligan, P.J.; Pinder, M.; Vigneron, L.; Alloueche, A.; Kester, K.E.; Ballou, W.R.; Conway, D.J.; Reece, W.H.; Gothard, P., et al. Efficacy of RTS,S/AS02 malaria vaccine against Plasmodium falciparum infection in semi-immune adult men in The Gambia: a randomised trial. *Lancet* **2001**, *358*, 1927-1934, doi:10.1016/S0140-6736(01)06957-4.
503. Ondigo, B.N.; Hodges, J.S.; Ireland, K.F.; Magak, N.G.; Lanar, D.E.; Dutta, S.; Narum, D.L.; Park, G.S.; Ofulla, A.V.; John, C.C. Estimation of recent and long-term malaria transmission in a population by antibody testing to multiple Plasmodium falciparum antigens. *J Infect Dis* **2014**, *210*, 1123-1132, doi:10.1093/infdis/jiu225.
504. Wong, J.; Hamel, M.J.; Drakeley, C.J.; Kariuki, S.; Shi, Y.P.; Lal, A.A.; Nahlen, B.L.; Bloland, P.B.; Lindblade, K.A.; Were, V., et al. Serological markers for monitoring historical changes in malaria transmission intensity in a highly endemic region of Western Kenya, 1994-2009. *Malar J* **2014**, *13*, 451, doi:10.1186/1475-2875-13-451.
505. Corran, P.; Coleman, P.; Riley, E.; Drakeley, C. Serology: a robust indicator of malaria transmission intensity? *Trends Parasitol* **2007**, *23*, 575-582, doi:10.1016/j.pt.2007.08.023.
506. Helb, D.A.; Tetteh, K.K.; Felgner, P.L.; Skinner, J.; Hubbard, A.; Arinaitwe, E.; Mayanja-Kizza, H.; Ssewanyana, I.; Kamya, M.R.; Beeson, J.G., et al. Novel serologic biomarkers provide accurate estimates of recent Plasmodium falciparum exposure for individuals and communities. *Proc Natl Acad Sci U S A* **2015**, *112*, E4438-4447, doi:10.1073/pnas.1501705112.

507. Markowitz, L.E.; Albrecht, P.; Rhodes, P.; Demonteverde, R.; Swint, E.; Maes, E.F.; Powell, C.; Patriarca, P.A. Changing levels of measles antibody titers in women and children in the United States: impact on response to vaccination. Kaiser Permanente Measles Vaccine Trial Team. *Pediatrics* **1996**, *97*, 53-58.
508. Siegrist, C.A.; Lambert, P.H. Maternal immunity and infant responses to immunization: factors influencing infant responses. *Dev Biol Stand* **1998**, *95*, 133-139.
509. Jones, C.; Pollock, L.; Barnett, S.M.; Battersby, A.; Kampmann, B. The relationship between concentration of specific antibody at birth and subsequent response to primary immunization. *Vaccine* **2014**, *32*, 996-1002, doi:10.1016/j.vaccine.2013.11.104.
510. Riley, E.M.; Wagner, G.E.; Ofori, M.F.; Wheeler, J.G.; Akanmori, B.D.; Tetteh, K.; McGuinness, D.; Bennett, S.; Nkrumah, F.K.; Anders, R.F., et al. Lack of association between maternal antibody and protection of African infants from malaria infection. *Infect Immun* **2000**, *68*, 5856-5863.
511. Gilbert, S.C. T-cell-inducing vaccines - what's the future. *Immunology* **2012**, *135*, 19-26, doi:10.1111/j.1365-2567.2011.03517.x.
512. Scarselli, E.; Tolle, R.; Koita, O.; Diallo, M.; Müller, H.M.; Früh, K.; Doumbo, O.; Crisanti, A.; Bujard, H. Analysis of the human antibody response to thrombospondin-related anonymous protein of Plasmodium falciparum. *Infect Immun* **1993**, *61*, 3490-3495.
513. Dolo, A.; Modiano, D.; Doumbo, O.; Bosman, A.; Sidibé, T.; Keita, M.M.; Naitza, S.; Robson, K.J.; Crisanti, A. Thrombospondin related adhesive protein (TRAP), a potential malaria vaccine candidate. *Parassitologia* **1999**, *41*, 425-428.
514. John, C.C.; Zickafoose, J.S.; Sumba, P.O.; King, C.L.; Kazura, J.W. Antibodies to the Plasmodium falciparum antigens circumsporozoite protein, thrombospondin-related adhesive protein, and liver-stage antigen 1 vary by ages of subjects and by season in a highland area of Kenya. *Infect Immun* **2003**, *71*, 4320-4325.
515. Pagès, F.; Texier, G.; Pradines, B.; Gadiaga, L.; Machault, V.; Jarjaval, F.; Penhoat, K.; Berger, F.; Trape, J.F.; Rogier, C., et al. Malaria transmission in Dakar: a two-year survey. *Malar J* **2008**, *7*, 178, doi:10.1186/1475-2875-7-178.
516. Hviid, L.; Barfod, L.; Fowkes, F.J. Trying to remember: immunological B cell memory to malaria. *Trends Parasitol* **2015**, *31*, 89-94, doi:10.1016/j.pt.2014.12.009.
517. Portugal, S.; Pierce, S.K.; Crompton, P.D. Young lives lost as B cells falter: what we are learning about antibody responses in malaria. *J Immunol* **2013**, *190*, 3039-3046, doi:10.4049/jimmunol.1203067.
518. Scholzen, A.; Sauerwein, R.W. How malaria modulates memory: activation and dysregulation of B cells in Plasmodium infection. *Trends Parasitol* **2013**, *29*, 252-262, doi:10.1016/j.pt.2013.03.002.
519. Plotkin, S.A. Vaccines: correlates of vaccine-induced immunity. *Clin Infect Dis* **2008**, *47*, 401-409, doi:10.1086/589862.
520. Mascola, J.R.; Haynes, B.F. HIV-1 neutralizing antibodies: understanding nature's pathways. *Immunol Rev* **2013**, *254*, 225-244, doi:10.1111/imr.12075.
521. Doria-Rose, N.A. HIV neutralizing antibodies: clinical correlates and implications for vaccines. *J Infect Dis* **2010**, *201*, 981-983, doi:10.1086/651143.
522. Schlingmann, B.; Castiglia, K.R.; Stobart, C.C.; Moore, M.L. Polyvalent vaccines: High-maintenance heroes. *PLoS Pathog* **2018**, *14*, e1006904, doi:10.1371/journal.ppat.1006904.
523. Voss, G.; Casimiro, D.; Neyrolles, O.; Williams, A.; Kaufmann, S.H.E.; McShane, H.; Hatherill, M.; Fletcher, H.A. Progress and challenges in TB vaccine development. *F1000Res* **2018**, *7*, 199, doi:10.12688/f1000research.13588.1.
524. Röhn, T.A.; Bachmann, M.F. Vaccines against non-communicable diseases. *Curr Opin Immunol* **2010**, *22*, 391-396, doi:10.1016/j.coi.2010.02.009.

525. Fishman, M. Challenges facing the development of cancer vaccines. *Methods Mol Biol* **2014**, *1139*, 543-553, doi:10.1007/978-1-4939-0345-0_39.
526. Ten Brinke, A.; Marek-Trzonkowska, N.; Mansilla, M.J.; Turksma, A.W.; Piekarska, K.; Iwaszkiewicz-Grześ, D.; Passerini, L.; Locafaro, G.; Puñet-Ortiz, J.; van Ham, S.M., et al. Monitoring T-Cell Responses in Translational Studies: Optimization of Dye-Based Proliferation Assay for Evaluation of Antigen-Specific Responses. *Front Immunol* **2017**, *8*, 1870, doi:10.3389/fimmu.2017.01870.
527. Saade, F.; Gorski, S.A.; Petrovsky, N. Pushing the frontiers of T-cell vaccines: accurate measurement of human T-cell responses. *Expert Rev Vaccines* **2012**, *11*, 1459-1470, doi:10.1586/erv.12.125.
528. Slota, M.; Lim, J.B.; Dang, Y.; Disis, M.L. ELISpot for measuring human immune responses to vaccines. *Expert Rev Vaccines* **2011**, *10*, 299-306, doi:10.1586/erv.10.169.
529. Smith, S.G.; Smits, K.; Joosten, S.A.; van Meijgaarden, K.E.; Satti, I.; Fletcher, H.A.; Caccamo, N.; Dieli, F.; Mascart, F.; McShane, H., et al. Intracellular Cytokine Staining and Flow Cytometry: Considerations for Application in Clinical Trials of Novel Tuberculosis Vaccines. *PLoS One* **2015**, *10*, e0138042, doi:10.1371/journal.pone.0138042.
530. Shirai, A.; Holmes, K.; Klinman, D. Detection and quantitation of cells secreting IL-6 under physiologic conditions in BALB/c mice. *J Immunol* **1993**, *150*, 793-799.
531. Moodie, Z.; Price, L.; Gouttefangeas, C.; Mander, A.; Janetzki, S.; Löwer, M.; Welters, M.J.; Ottensmeier, C.; van der Burg, S.H.; Britten, C.M. Response definition criteria for ELISPOT assays revisited. *Cancer Immunol Immunother* **2010**, *59*, 1489-1501, doi:10.1007/s00262-010-0875-4.
532. Britten, C.M.; Janetzki, S.; van der Burg, S.H.; Gouttefangeas, C.; Hoos, A. Toward the harmonization of immune monitoring in clinical trials: quo vadis? *Cancer Immunol Immunother* **2008**, *57*, 285-288, doi:10.1007/s00262-007-0379-z.
533. Janetzki, S.; Panageas, K.S.; Ben-Porat, L.; Boyer, J.; Britten, C.M.; Clay, T.M.; Kalos, M.; Maecker, H.T.; Romero, P.; Yuan, J., et al. Results and harmonization guidelines from two large-scale international Elispot proficiency panels conducted by the Cancer Vaccine Consortium (CVC/SVI). *Cancer Immunol Immunother* **2008**, *57*, 303-315, doi:10.1007/s00262-007-0380-6.
534. Coughlan, L.; Lambe, T. Measuring Cellular Immunity to Influenza: Methods of Detection, Applications and Challenges. *Vaccines (Basel)* **2015**, *3*, 293-319, doi:10.3390/vaccines3020293.
535. Horton, H.; Thomas, E.P.; Stucky, J.A.; Frank, I.; Moodie, Z.; Huang, Y.; Chiu, Y.L.; McElrath, M.J.; De Rosa, S.C. Optimization and validation of an 8-color intracellular cytokine staining (ICS) assay to quantify antigen-specific T cells induced by vaccination. *J Immunol Methods* **2007**, *323*, 39-54, doi:10.1016/j.jim.2007.03.002.
536. Parra, M.; Herrera, D.; Jácome, M.F.; Mesa, M.C.; Rodríguez, L.S.; Guzmán, C.; Angel, J.; Franco, M.A. Circulating rotavirus-specific T cells have a poor functional profile. *Virology* **2014**, *468-470*, 340-350, doi:10.1016/j.virol.2014.08.020.
537. De Rosa, S.C.; Lu, F.X.; Yu, J.; Perfetto, S.P.; Falloon, J.; Moser, S.; Evans, T.G.; Koup, R.; Miller, C.J.; Roederer, M. Vaccination in humans generates broad T cell cytokine responses. *J Immunol* **2004**, *173*, 5372-5380.
538. Roederer, M.; Brenchley, J.M.; Betts, M.R.; De Rosa, S.C. Flow cytometric analysis of vaccine responses: how many colors are enough? *Clin Immunol* **2004**, *110*, 199-205, doi:10.1016/j.clim.2003.11.015.
539. Seddiki, N.; Cook, L.; Hsu, D.C.; Phetsouphanh, C.; Brown, K.; Xu, Y.; Kerr, S.J.; Cooper, D.A.; Munier, C.M.; Pett, S., et al. Human antigen-specific $CD4^+$ $CD25^+$ $CD134^+$ $CD39^+$ T cells are enriched for regulatory T cells and comprise a substantial proportion of recall responses. *Eur J Immunol* **2014**, *44*, 1644-1661, doi:10.1002/eji.201344102.

540. Frentsch, M.; Arbach, O.; Kirchhoff, D.; Moewes, B.; Worm, M.; Rothe, M.; Scheffold, A.; Thiel, A. Direct access to CD4+ T cells specific for defined antigens according to CD154 expression. *Nat Med* **2005**, *11*, 1118-1124, doi:10.1038/nm1292.
541. Porichis, F.; Hart, M.G.; Zupkosky, J.; Barblu, L.; Kwon, D.S.; McMullen, A.; Brennan, T.; Ahmed, R.; Freeman, G.J.; Kavanagh, D.G., et al. Differential impact of PD-1 and/or interleukin-10 blockade on HIV-1-specific CD4 T cell and antigen-presenting cell functions. *J Virol* **2014**, *88*, 2508-2518, doi:10.1128/JVI.02034-13.
542. Betts, M.R.; Brenchley, J.M.; Price, D.A.; De Rosa, S.C.; Douek, D.C.; Roederer, M.; Koup, R.A. Sensitive and viable identification of antigen-specific CD8+ T cells by a flow cytometric assay for degranulation. *J Immunol Methods* **2003**, *281*, 65-78.
543. Wolfl, M.; Kuball, J.; Ho, W.Y.; Nguyen, H.; Manley, T.J.; Bleakley, M.; Greenberg, P.D. Activation-induced expression of CD137 permits detection, isolation, and expansion of the full repertoire of CD8+ T cells responding to antigen without requiring knowledge of epitope specificities. *Blood* **2007**, *110*, 201-210, doi:10.1182/blood-2006-11-056168.
544. Redmond, W.L.; Ruby, C.E.; Weinberg, A.D. The role of OX40-mediated co-stimulation in T-cell activation and survival. *Crit Rev Immunol* **2009**, *29*, 187-201.
545. Zaunders, J.J.; Munier, M.L.; Seddiki, N.; Pett, S.; Ip, S.; Bailey, M.; Xu, Y.; Brown, K.; Dyer, W.B.; Kim, M., et al. High levels of human antigen-specific CD4+ T cells in peripheral blood revealed by stimulated coexpression of CD25 and CD134 (OX40). *J Immunol* **2009**, *183*, 2827-2836, doi:10.4049/jimmunol.0803548.
546. Venkatraman, N.; Anagnostou, N.; Bliss, C.; Bowyer, G.; Wright, D.; Lövgren-Bengtsson, K.; Roberts, R.; Poulton, I.; Lawrie, A.; Ewer, K., et al. Safety and immunogenicity of heterologous prime-boost immunization with viral-vectored malaria vaccines adjuvanted with Matrix-M™. *Vaccine* **2017**, *35*, 6208-6217, doi:10.1016/j.vaccine.2017.09.028.
547. Abbas, A.K.; Murphy, K.M.; Sher, A. Functional diversity of helper T lymphocytes. *Nature* **1996**, *383*, 787-793, doi:10.1038/383787a0.
548. Sallusto, F.; Langenkamp, A.; Geginat, J.; Lanzavecchia, A. Functional subsets of memory T cells identified by CCR7 expression. *Curr Top Microbiol Immunol* **2000**, *251*, 167-171.
549. Seder, R.A.; Ahmed, R. Similarities and differences in CD4+ and CD8+ effector and memory T cell generation. *Nat Immunol* **2003**, *4*, 835-842, doi:10.1038/ni969.
550. Cohen, G.B.; Kaur, A.; Johnson, R.P. Isolation of viable antigen-specific CD4 T cells by CD40L surface trapping. *J Immunol Methods* **2005**, *302*, 103-115, doi:10.1016/j.jim.2005.05.002.
551. Hengel, R.L.; Thaker, V.; Pavlick, M.V.; Metcalf, J.A.; Dennis, G.; Yang, J.; Lempicki, R.A.; Sereti, I.; Lane, H.C. Cutting edge: L-selectin (CD62L) expression distinguishes small resting memory CD4+ T cells that preferentially respond to recall antigen. *J Immunol* **2003**, *170*, 28-32.
552. Macallan, D.C.; Borghans, J.A.; Asquith, B. Human T Cell Memory: A Dynamic View. *Vaccines (Basel)* **2017**, *5*, doi:10.3390/vaccines5010005.
553. Walker, L.S.; Gulbranson-Judge, A.; Flynn, S.; Brocker, T.; Raykundalia, C.; Goodall, M.; Förster, R.; Lipp, M.; Lane, P. Compromised OX40 function in CD28-deficient mice is linked with failure to develop CXC chemokine receptor 5-positive CD4 cells and germinal centers. *J Exp Med* **1999**, *190*, 1115-1122.
554. Croft, M.; So, T.; Duan, W.; Soroosh, P. The significance of OX40 and OX40L to T-cell biology and immune disease. *Immunol Rev* **2009**, *229*, 173-191, doi:10.1111/j.1600-065X.2009.00766.x.
555. Shatrova, A.N.; Mityushova, E.V.; Vassilieva, I.O.; Aksenov, N.D.; Zenin, V.V.; Nikolsky, N.N.; Marakhova, I.I. Time-Dependent Regulation of IL-2R α-Chain (CD25) Expression by TCR Signal Strength and IL-2-Induced STAT5 Signaling in Activated Human Blood T Lymphocytes. *PLoS One* **2016**, *11*, e0167215, doi:10.1371/journal.pone.0167215.

556. Wang, X.; Rickert, M.; Garcia, K.C. Structure of the quaternary complex of interleukin-2 with its alpha, beta, and gammac receptors. *Science* **2005**, *310*, 1159-1163, doi:10.1126/science.1117893.
557. Aktas, E.; Kucuksezer, U.C.; Bilgic, S.; Erten, G.; Deniz, G. Relationship between CD107a expression and cytotoxic activity. *Cell Immunol* **2009**, *254*, 149-154, doi:10.1016/j.cellimm.2008.08.007.
558. Vahlne, G.; Becker, S.; Brodin, P.; Johansson, M.H. IFN-gamma production and degranulation are differentially regulated in response to stimulation in murine natural killer cells. *Scand J Immunol* **2008**, *67*, 1-11, doi:10.1111/j.1365-3083.2007.02026.x.
559. Yokosuka, T.; Takamatsu, M.; Kobayashi-Imanishi, W.; Hashimoto-Tane, A.; Azuma, M.; Saito, T. Programmed cell death 1 forms negative costimulatory microclusters that directly inhibit T cell receptor signaling by recruiting phosphatase SHP2. *J Exp Med* **2012**, *209*, 1201-1217, doi:10.1084/jem.20112741.
560. Altman, J.D.; Moss, P.A.; Goulder, P.J.; Barouch, D.H.; McHeyzer-Williams, M.G.; Bell, J.I.; McMichael, A.J.; Davis, M.M. Phenotypic analysis of antigen-specific T lymphocytes. *Science* **1996**, *274*, 94-96.
561. Ford, T.; Wenden, C.; Mbekeani, A.; Dally, L.; Cox, J.H.; Morin, M.; Winstone, N.; Hill, A.V.S.; Gilmour, J.; Ewer, K.J. Cryopreservation-related loss of antigen-specific IFNγ producing CD4. *Vaccine* **2017**, *35*, 1898-1906, doi:10.1016/j.vaccine.2017.02.038.
562. Van Braeckel-Budimir, N.; Kurup, S.P.; Harty, J.T. Regulatory issues in immunity to liver and blood-stage malaria. *Curr Opin Immunol* **2016**, *42*, 91-97, doi:10.1016/j.coi.2016.06.008.
563. Tovar-Salazar, A.; Patterson-Bartlett, J.; Jesser, R.; Weinberg, A. Regulatory function of cytomegalovirus-specific CD4+CD27-CD28- T cells. *Virology* **2010**, *398*, 158-167, doi:10.1016/j.virol.2009.11.038.
564. Bhatt, K.; Verma, S.; Ellner, J.J.; Salgame, P. Quest for correlates of protection against tuberculosis. *Clin Vaccine Immunol* **2015**, *22*, 258-266, doi:10.1128/CVI.00721-14.
565. Valletta, J.J.; Recker, M. Identification of immune signatures predictive of clinical protection from malaria. *PLoS Comput Biol* **2017**, *13*, e1005812, doi:10.1371/journal.pcbi.1005812.
566. Franco, M.A.; Angel, J.; Greenberg, H.B. Immunity and correlates of protection for rotavirus vaccines. *Vaccine* **2006**, *24*, 2718-2731, doi:10.1016/j.vaccine.2005.12.048.
567. Janetzki, S.; Britten, C.M.; Kalos, M.; Levitsky, H.I.; Maecker, H.T.; Melief, C.J.; Old, L.J.; Romero, P.; Hoos, A.; Davis, M.M. "MIATA"-minimal information about T cell assays. *Immunity* **2009**, *31*, 527-528, doi:10.1016/j.immuni.2009.09.007.
568. Maecker, H.T.; Hassler, J.; Payne, J.K.; Summers, A.; Comatas, K.; Ghanayem, M.; Morse, M.A.; Clay, T.M.; Lyerly, H.K.; Bhatia, S., et al. Precision and linearity targets for validation of an IFNgamma ELISPOT, cytokine flow cytometry, and tetramer assay using CMV peptides. *BMC Immunol* **2008**, *9*, 9, doi:10.1186/1471-2172-9-9.
569. Nomura, L.; Maino, V.C.; Maecker, H.T. Standardization and optimization of multiparameter intracellular cytokine staining. *Cytometry A* **2008**, *73*, 984-991, doi:10.1002/cyto.a.20602.
570. Manicklal, S.; Emery, V.C.; Lazzarotto, T.; Boppana, S.B.; Gupta, R.K. The "silent" global burden of congenital cytomegalovirus. *Clin Microbiol Rev* **2013**, *26*, 86-102, doi:10.1128/CMR.00062-12.
571. Wreghitt, T.G.; Teare, E.L.; Sule, O.; Devi, R.; Rice, P. Cytomegalovirus infection in immunocompetent patients. *Clin Infect Dis* **2003**, *37*, 1603-1606, doi:10.1086/379711.
572. Arend, S.M.; Kroes, A.C. Look and ye shall find...cytomegalovirus infection in immunocompetent patients. *Clin Infect Dis* **2003**, *37*, 1607-1608, doi:10.1086/379720.

573. Henson, S.M.; Riddell, N.E.; Akbar, A.N. Properties of end-stage human T cells defined by CD45RA re-expression. *Curr Opin Immunol* **2012**, *24*, 476-481, doi:10.1016/j.coi.2012.04.001.
574. Derhovanessian, E.; Maier, A.B.; Hähnel, K.; McElhaney, J.E.; Slagboom, E.P.; Pawelec, G. Latent infection with cytomegalovirus is associated with poor memory CD4 responses to influenza A core proteins in the elderly. *J Immunol* **2014**, *193*, 3624-3631, doi:10.4049/jimmunol.1303361.
575. Brodin, P.; Jojic, V.; Gao, T.; Bhattacharya, S.; Angel, C.J.; Furman, D.; Shen-Orr, S.; Dekker, C.L.; Swan, G.E.; Butte, A.J., et al. Variation in the human immune system is largely driven by non-heritable influences. *Cell* **2015**, *160*, 37-47, doi:10.1016/j.cell.2014.12.020.
576. van den Heuvel, D.; Jansen, M.A.; Dik, W.A.; Bouallouch-Charif, H.; Zhao, D.; van Kester, K.A.; Smits-te Nijenhuis, M.A.; Kolijn-Couwenberg, M.J.; Jaddoe, V.W.; Arens, R., et al. Cytomegalovirus- and Epstein-Barr Virus-Induced T-Cell Expansions in Young Children Do Not Impair Naive T-cell Populations or Vaccination Responses: The Generation R Study. *J Infect Dis* **2016**, *213*, 233-242, doi:10.1093/infdis/jiv369.
577. Saghafian-Hedengren, S.; Sohlberg, E.; Theorell, J.; Carvalho-Queiroz, C.; Nagy, N.; Persson, J.O.; Nilsson, C.; Bryceson, Y.T.; Sverremark-Ekström, E. Epstein-Barr virus coinfection in children boosts cytomegalovirus-induced differentiation of natural killer cells. *J Virol* **2013**, *87*, 13446-13455, doi:10.1128/JVI.02382-13.
578. Sidorchuk, A.; Wickman, M.; Pershagen, G.; Lagarde, F.; Linde, A. Cytomegalovirus infection and development of allergic diseases in early childhood: interaction with EBV infection? *J Allergy Clin Immunol* **2004**, *114*, 1434-1440, doi:10.1016/j.jaci.2004.08.009.
579. Mahnke, Y.D.; Brodie, T.M.; Sallusto, F.; Roederer, M.; Lugli, E. The who's who of T-cell differentiation: human memory T-cell subsets. *Eur J Immunol* **2013**, *43*, 2797-2809, doi:10.1002/eji.201343751.
580. Appay, V.; Zaunders, J.J.; Papagno, L.; Sutton, J.; Jaramillo, A.; Waters, A.; Easterbrook, P.; Grey, P.; Smith, D.; McMichael, A.J., et al. Characterization of CD4(+) CTLs ex vivo. *J Immunol* **2002**, *168*, 5954-5958.
581. Appay, V.; van Lier, R.A.; Sallusto, F.; Roederer, M. Phenotype and function of human T lymphocyte subsets: consensus and issues. *Cytometry A* **2008**, *73*, 975-983, doi:10.1002/cyto.a.20643.
582. Larbi, A.; Fulop, T. From "truly naïve" to "exhausted senescent" T cells: when markers predict functionality. *Cytometry A* **2014**, *85*, 25-35, doi:10.1002/cyto.a.22351.
583. Koch, S.; Larbi, A.; Derhovanessian, E.; Ozcelik, D.; Naumova, E.; Pawelec, G. Multiparameter flow cytometric analysis of CD4 and CD8 T cell subsets in young and old people. *Immun Ageing* **2008**, *5*, 6, doi:10.1186/1742-4933-5-6.
584. Stelekati, E.; Wherry, E.J. Chronic bystander infections and immunity to unrelated antigens. *Cell Host Microbe* **2012**, *12*, 458-469, doi:10.1016/j.chom.2012.10.001.
585. Wang, F.; Chi, J.; Peng, G.; Zhou, F.; Wang, J.; Li, L.; Feng, D.; Xie, F.; Gu, B.; Qin, J., et al. Development of virus-specific CD4+ and CD8+ regulatory T cells induced by human herpesvirus 6 infection. *J Virol* **2014**, *88*, 1011-1024, doi:10.1128/JVI.02586-13.
586. Adland, E.; Klenerman, P.; Goulder, P.; Matthews, P.C. Ongoing burden of disease and mortality from HIV/CMV coinfection in Africa in the antiretroviral therapy era. *Front Microbiol* **2015**, *6*, 1016, doi:10.3389/fmicb.2015.01016.
587. Hadrup, S.R.; Strindhall, J.; Køllgaard, T.; Seremet, T.; Johansson, B.; Pawelec, G.; thor Straten, P.; Wikby, A. Longitudinal studies of clonally expanded CD8 T cells reveal a repertoire shrinkage predicting mortality and an increased number of dysfunctional cytomegalovirus-specific T cells in the very elderly. *J Immunol* **2006**, *176*, 2645-2653.

588. McBride, J.A.; Striker, R. Imbalance in the game of T cells: What can the CD4/CD8 T-cell ratio tell us about HIV and health? *PLoS Pathog* **2017**, *13*, e1006624, doi:10.1371/journal.ppat.1006624.
589. Reuter, J.D.; Wilson, J.H.; Idoko, K.E.; van den Pol, A.N. CD4+ T-cell reconstitution reduces cytomegalovirus in the immunocompromised brain. *J Virol* **2005**, *79*, 9527-9539, doi:10.1128/JVI.79.15.9527-9539.2005.
590. Verma, S.; Weiskopf, D.; Gupta, A.; McDonald, B.; Peters, B.; Sette, A.; Benedict, C.A. Cytomegalovirus-Specific CD4 T Cells Are Cytolytic and Mediate Vaccine Protection. *J Virol* **2015**, *90*, 650-658, doi:10.1128/JVI.02123-15.
591. van der Heiden, M.; van Zelm, M.C.; Bartol, S.J.; de Rond, L.G.; Berbers, G.A.; Boots, A.M.; Buisman, A.M. Differential effects of Cytomegalovirus carriage on the immune phenotype of middle-aged males and females. *Sci Rep* **2016**, *6*, 26892, doi:10.1038/srep26892.
592. Pangrazzi, L.; Naismith, E.; Meryk, A.; Keller, M.; Jenewein, B.; Trieb, K.; Grubeck-Loebenstein, B. Increased IL-15 Production and Accumulation of Highly Differentiated CD8+ Effector/Memory T Cells in the Bone Marrow of Persons with Cytomegalovirus. *Front Immunol* **2017**, *8*, 715, doi:10.3389/fimmu.2017.00715.
593. Almanzar, G.; Schwaiger, S.; Jenewein, B.; Keller, M.; Herndler-Brandstetter, D.; Würzner, R.; Schönitzer, D.; Grubeck-Loebenstein, B. Long-term cytomegalovirus infection leads to significant changes in the composition of the CD8+ T-cell repertoire, which may be the basis for an imbalance in the cytokine production profile in elderly persons. *J Virol* **2005**, *79*, 3675-3683, doi:10.1128/JVI.79.6.3675-3683.2005.
594. Derhovanessian, E.; Maier, A.B.; Hähnel, K.; Beck, R.; de Craen, A.J.; Slagboom, E.P.; Westendorp, R.G.; Pawelec, G. Infection with cytomegalovirus but not herpes simplex virus induces the accumulation of late-differentiated CD4+ and CD8+ T-cells in humans. *J Gen Virol* **2011**, *92*, 2746-2756, doi:10.1099/vir.0.036004-0.
595. Tomiyama, H.; Matsuda, T.; Takiguchi, M. Differentiation of human CD8(+) T cells from a memory to memory/effector phenotype. *J Immunol* **2002**, *168*, 5538-5550.
596. Okada, R.; Kondo, T.; Matsuki, F.; Takata, H.; Takiguchi, M. Phenotypic classification of human CD4+ T cell subsets and their differentiation. *Int Immunol* **2008**, *20*, 1189-1199, doi:10.1093/intimm/dxn075.
597. Fagnoni, F.F.; Vescovini, R.; Mazzola, M.; Bologna, G.; Nigro, E.; Lavagetto, G.; Franceschi, C.; Passeri, M.; Sansoni, P. Expansion of cytotoxic CD8+ CD28- T cells in healthy ageing people, including centenarians. *Immunology* **1996**, *88*, 501-507.
598. Weng, N.P.; Akbar, A.N.; Goronzy, J. CD28(-) T cells: their role in the age-associated decline of immune function. *Trends Immunol* **2009**, *30*, 306-312, doi:10.1016/j.it.2009.03.013.
599. Plunkett, F.J.; Franzese, O.; Finney, H.M.; Fletcher, J.M.; Belaramani, L.L.; Salmon, M.; Dokal, I.; Webster, D.; Lawson, A.D.; Akbar, A.N. The loss of telomerase activity in highly differentiated CD8+CD28-CD27- T cells is associated with decreased Akt (Ser473) phosphorylation. *J Immunol* **2007**, *178*, 7710-7719.
600. Le Priol, Y.; Puthier, D.; Lécureuil, C.; Combadière, C.; Debré, P.; Nguyen, C.; Combadière, B. High cytotoxic and specific migratory potencies of senescent CD8+ CD57+ cells in HIV-infected and uninfected individuals. *J Immunol* **2006**, *177*, 5145-5154.
601. Sada-Ovalle, I.; Torre-Bouscoulet, L.; Valdez-Vázquez, R.; Martínez-Cairo, S.; Zenteno, E.; Lascurain, R. Characterization of a cytotoxic CD57+ T cell subset from patients with pulmonary tuberculosis. *Clin Immunol* **2006**, *121*, 314-323, doi:10.1016/j.clim.2006.08.011.
602. Ibegbu, C.C.; Xu, Y.X.; Harris, W.; Maggio, D.; Miller, J.D.; Kourtis, A.P. Expression of killer cell lectin-like receptor G1 on antigen-specific human CD8+ T lymphocytes during active,

latent, and resolved infection and its relation with CD57. *J Immunol* **2005**, *174*, 6088-6094.
603. Beyersdorf, N.B.; Ding, X.; Karp, K.; Hanke, T. Expression of inhibitory "killer cell lectin-like receptor G1" identifies unique subpopulations of effector and memory CD8 T cells. *Eur J Immunol* **2001**, *31*, 3443-3452, doi:10.1002/1521-4141(200112)31:12<3443::AID-IMMU3443>3.0.CO;2-J.
604. Ouyang, Q.; Wagner, W.M.; Voehringer, D.; Wikby, A.; Klatt, T.; Walter, S.; Müller, C.A.; Pircher, H.; Pawelec, G. Age-associated accumulation of CMV-specific CD8+ T cells expressing the inhibitory killer cell lectin-like receptor G1 (KLRG1). *Exp Gerontol* **2003**, *38*, 911-920.
605. Voehringer, D.; Koschella, M.; Pircher, H. Lack of proliferative capacity of human effector and memory T cells expressing killer cell lectinlike receptor G1 (KLRG1). *Blood* **2002**, *100*, 3698-3702, doi:10.1182/blood-2002-02-0657.
606. Strioga, M.; Pasukoniene, V.; Characiejus, D. CD8+ CD28- and CD8+ CD57+ T cells and their role in health and disease. *Immunology* **2011**, *134*, 17-32, doi:10.1111/j.1365-2567.2011.03470.x.
607. Hu, Z.; Zhao, H.M.; Li, C.L.; Liu, X.H.; Barkan, D.; Lowrie, D.B.; Lu, S.H.; Fan, X.Y. The Role of KLRG1 in Human CD4+ T-Cell Immunity Against Tuberculosis. *J Infect Dis* **2018**, *217*, 1491-1503, doi:10.1093/infdis/jiy046.
608. Sakai, S.; Kauffman, K.D.; Schenkel, J.M.; McBerry, C.C.; Mayer-Barber, K.D.; Masopust, D.; Barber, D.L. Cutting edge: control of Mycobacterium tuberculosis infection by a subset of lung parenchyma-homing CD4 T cells. *J Immunol* **2014**, *192*, 2965-2969, doi:10.4049/jimmunol.1400019.
609. Moguche, A.O.; Shafiani, S.; Clemons, C.; Larson, R.P.; Dinh, C.; Higdon, L.E.; Cambier, C.J.; Sissons, J.R.; Gallegos, A.M.; Fink, P.J., et al. ICOS and Bcl6-dependent pathways maintain a CD4 T cell population with memory-like properties during tuberculosis. *J Exp Med* **2015**, *212*, 715-728, doi:10.1084/jem.20141518.
610. Torrado, E.; Fountain, J.J.; Liao, M.; Tighe, M.; Reiley, W.W.; Lai, R.P.; Meintjes, G.; Pearl, J.E.; Chen, X.; Zak, D.E., et al. Interleukin 27R regulates CD4+ T cell phenotype and impacts protective immunity during Mycobacterium tuberculosis infection. *J Exp Med* **2015**, *212*, 1449-1463, doi:10.1084/jem.20141520.
611. Henao-Tamayo, M.; Irwin, S.M.; Shang, S.; Ordway, D.; Orme, I.M. T lymphocyte surface expression of exhaustion markers as biomarkers of the efficacy of chemotherapy for tuberculosis. *Tuberculosis (Edinb)* **2011**, *91*, 308-313, doi:10.1016/j.tube.2011.04.001.
612. Nandakumar, S.; Kannanganat, S.; Posey, J.E.; Amara, R.R.; Sable, S.B. Attrition of T-cell functions and simultaneous upregulation of inhibitory markers correspond with the waning of BCG-induced protection against tuberculosis in mice. *PLoS One* **2014**, *9*, e113951, doi:10.1371/journal.pone.0113951.
613. Barber, D.L. Vaccination for Mycobacterium tuberculosis infection: reprogramming CD4 T-cell homing into the lung. *Mucosal Immunol* **2017**, *10*, 318-321, doi:10.1038/mi.2016.110.
614. Goronzy, J.J.; Fulbright, J.W.; Crowson, C.S.; Poland, G.A.; O'Fallon, W.M.; Weyand, C.M. Value of immunological markers in predicting responsiveness to influenza vaccination in elderly individuals. *J Virol* **2001**, *75*, 12182-12187, doi:10.1128/JVI.75.24.12182-12187.2001.
615. Saurwein-Teissl, M.; Lung, T.L.; Marx, F.; Gschösser, C.; Asch, E.; Blasko, I.; Parson, W.; Böck, G.; Schönitzer, D.; Trannoy, E., et al. Lack of antibody production following immunization in old age: association with CD8(+)CD28(-) T cell clonal expansions and an imbalance in the production of Th1 and Th2 cytokines. *J Immunol* **2002**, *168*, 5893-5899.
616. Surh, C.D.; Sprent, J. Homeostasis of naive and memory T cells. *Immunity* **2008**, *29*, 848-862, doi:10.1016/j.immuni.2008.11.002.

617. Franceschi, C.; Bonafè, M.; Valensin, S. Human immunosenescence: the prevailing of innate immunity, the failing of clonotypic immunity, and the filling of immunological space. *Vaccine* **2000**, *18*, 1717-1720.
618. van Leeuwen, E.M.; Remmerswaal, E.B.; Vossen, M.T.; Rowshani, A.T.; Wertheim-van Dillen, P.M.; van Lier, R.A.; ten Berge, I.J. Emergence of a CD4+CD28- granzyme B+, cytomegalovirus-specific T cell subset after recovery of primary cytomegalovirus infection. *J Immunol* **2004**, *173*, 1834-1841.
619. Fletcher, J.M.; Vukmanovic-Stejic, M.; Dunne, P.J.; Birch, K.E.; Cook, J.E.; Jackson, S.E.; Salmon, M.; Rustin, M.H.; Akbar, A.N. Cytomegalovirus-specific CD4+ T cells in healthy carriers are continuously driven to replicative exhaustion. *J Immunol* **2005**, *175*, 8218-8225.
620. Najafian, N.; Chitnis, T.; Salama, A.D.; Zhu, B.; Benou, C.; Yuan, X.; Clarkson, M.R.; Sayegh, M.H.; Khoury, S.J. Regulatory functions of CD8+CD28- T cells in an autoimmune disease model. *J Clin Invest* **2003**, *112*, 1037-1048, doi:10.1172/JCI17935.
621. Tovar-Salazar, A.; Weinberg, A. Cytomegalovirus infection in HIV-infected and uninfected individuals is characterized by circulating regulatory T cells of unconstrained antigenic specificity. *PLoS One* **2017**, *12*, e0180691, doi:10.1371/journal.pone.0180691.
622. Fernández-Ruiz, M.; Humar, A.; Baluch, A.; Keshwani, S.; Husain, S.; Kumar, D. Baseline serum interleukin-6 to interleukin-2 ratio is associated with the response to seasonal trivalent influenza vaccine in solid organ transplant recipients. *Vaccine* **2015**, *33*, 7176-7182, doi:10.1016/j.vaccine.2015.10.134.
623. Team, H.-C.S.P.; Consortium, H.-I. Multicohort analysis reveals baseline transcriptional predictors of influenza vaccination responses. *Sci Immunol* **2017**, *2*, doi:10.1126/sciimmunol.aal4656.
624. Cooper, P.J.; Chico, M.; Sandoval, C.; Espinel, I.; Guevara, A.; Levine, M.M.; Griffin, G.E.; Nutman, T.B. Human infection with Ascaris lumbricoides is associated with suppression of the interleukin-2 response to recombinant cholera toxin B subunit following vaccination with the live oral cholera vaccine CVD 103-HgR. *Infect Immun* **2001**, *69*, 1574-1580, doi:10.1128/IAI.69.3.1574-1580.2001.
625. Sabin, E.A.; Araujo, M.I.; Carvalho, E.M.; Pearce, E.J. Impairment of tetanus toxoid-specific Th1-like immune responses in humans infected with Schistosoma mansoni. *J Infect Dis* **1996**, *173*, 269-272.
626. Muhsen, K.; Pasetti, M.F.; Reymann, M.K.; Graham, D.Y.; Levine, M.M. Helicobacter pylori infection affects immune responses following vaccination of typhoid-naive U.S. adults with attenuated Salmonella typhi oral vaccine CVD 908-htrA. *J Infect Dis* **2014**, *209*, 1452-1458, doi:10.1093/infdis/jit625.
627. Ogunjimi, B.; Theeten, H.; Hens, N.; Beutels, P. Serology indicates cytomegalovirus infection is associated with varicella-zoster virus reactivation. *J Med Virol* **2014**, *86*, 812-819, doi:10.1002/jmv.23749.
628. Stowe, R.P.; Peek, M.K.; Cutchin, M.P.; Goodwin, J.S. Reactivation of herpes simplex virus type 1 is associated with cytomegalovirus and age. *J Med Virol* **2012**, *84*, 1797-1802, doi:10.1002/jmv.23397.
629. Gompels, U.A.; Larke, N.; Sanz-Ramos, M.; Bates, M.; Musonda, K.; Manno, D.; Siame, J.; Monze, M.; Filteau, S.; Group, C.S. Human cytomegalovirus infant infection adversely affects growth and development in maternally HIV-exposed and unexposed infants in Zambia. *Clin Infect Dis* **2012**, *54*, 434-442, doi:10.1093/cid/cir837.
630. Bello, C.; Whittle, H. Cytomegalovirus infection in Gambian mothers and their babies. *J Clin Pathol* **1991**, *44*, 366-369.
631. Williams, J.O.; Fagbami, A.H.; Omilabu, S.A. Cytomegalovirus antibodies in Nigeria. *Trans R Soc Trop Med Hyg* **1989**, *83*, 260.

632. Maecker, H.T.; Ghanekar, S.A.; Suni, M.A.; He, X.S.; Picker, L.J.; Maino, V.C. Factors affecting the efficiency of CD8+ T cell cross-priming with exogenous antigens. *J Immunol* **2001**, *166*, 7268-7275.
633. Jackson, S.E.; Mason, G.M.; Okecha, G.; Sissons, J.G.; Wills, M.R. Diverse specificities, phenotypes, and antiviral activities of cytomegalovirus-specific CD8+ T cells. *J Virol* **2014**, *88*, 10894-10908, doi:10.1128/JVI.01477-14.
634. Arvin, A.M.; Fast, P.; Myers, M.; Plotkin, S.; Rabinovich, R.; Committee, N.V.A. Vaccine development to prevent cytomegalovirus disease: report from the National Vaccine Advisory Committee. *Clin Infect Dis* **2004**, *39*, 233-239, doi:10.1086/421999.
635. Organization, W.H. Malaria vaccine: WHO position paper, January 2016 - Recommendations. *Vaccine* **2018**, *36*, 3576-3577, doi:10.1016/j.vaccine.2016.10.047.
636. White, M.T.; Smith, D.L. Synergism from combinations of infection-blocking malaria vaccines. *Malar J* **2013**, *12*, 280, doi:10.1186/1475-2875-12-280.
637. Zhang, Q.; Xue, X.; Qu, L.; Pan, W. Construction and evaluation of a multistage combination vaccine against malaria. *Vaccine* **2007**, *25*, 2112-2119, doi:10.1016/j.vaccine.2006.11.015.
638. Bauza, K.; Atcheson, E.; Malinauskas, T.; Blagborough, A.M.; Reyes-Sandoval, A. Tailoring a Combination Preerythrocytic Malaria Vaccine. *Infect Immun* **2015**, *84*, 622-634, doi:10.1128/IAI.01063-15.
639. Jatana, S.K.; Nair, M. Combination Vaccines. *Med J Armed Forces India* **2007**, *63*, 167-171, doi:10.1016/S0377-1237(07)80067-0.
640. Insel, R.A. Potential alterations in immunogenicity by combining or simultaneously administering vaccine components. *Ann N Y Acad Sci* **1995**, *754*, 35-47.
641. Berger, R.; Just, M. Interference between strains in live virus vaccines. II: Combined vaccination with varicella and measles-mumps-rubella vaccine. *J Biol Stand* **1988**, *16*, 275-279.
642. Nielsen, C.M.; Vekemans, J.; Lievens, M.; Kester, K.E.; Regules, J.A.; Ockenhouse, C.F. RTS,S malaria vaccine efficacy and immunogenicity during Plasmodium falciparum challenge is associated with HLA genotype. *Vaccine* **2018**, *36*, 1637-1642, doi:10.1016/j.vaccine.2018.01.069.
643. Gilbert, S.C.; Warimwe, G.M. Rapid development of vaccines against emerging pathogens: The replication-deficient simian adenovirus platform technology. *Vaccine* **2017**, *35*, 4461-4464, doi:10.1016/j.vaccine.2017.04.085.
644. Chaudhury, S.; Regules, J.A.; Darko, C.A.; Dutta, S.; Wallqvist, A.; Waters, N.C.; Jongert, E.; Lemiale, F.; Bergmann-Leitner, E.S. Delayed fractional dose regimen of the RTS,S/AS01 malaria vaccine candidate enhances an IgG4 response that inhibits serum opsonophagocytosis. *Sci Rep* **2017**, *7*, 7998, doi:10.1038/s41598-017-08526-5.
645. Mensah, V.A.; Roetynck, S.; Kanteh, E.K.; Bowyer, G.; Ndaw, A.; Oko, F.; Bliss, C.M.; Jagne, Y.J.; Cortese, R.; Nicosia, A., et al. Safety and Immunogenicity of Malaria Vectored Vaccines Given with Routine Expanded Program on Immunization Vaccines in Gambian Infants and Neonates: A Randomized Controlled Trial. *Front Immunol* **2017**, *8*, 1551, doi:10.3389/fimmu.2017.01551.
646. Asante, K.P.; Abdulla, S.; Agnandji, S.; Lyimo, J.; Vekemans, J.; Soulanoudjingar, S.; Owusu, R.; Shomari, M.; Leach, A.; Jongert, E., et al. Safety and efficacy of the RTS,S/AS01E candidate malaria vaccine given with expanded-programme-on-immunisation vaccines: 19 month follow-up of a randomised, open-label, phase 2 trial. *Lancet Infect Dis* **2011**, *11*, 741-749, doi:10.1016/S1473-3099(11)70100-1.
647. Bowyer, G.; Rampling, T.; Powlson, J.; Morter, R.; Wright, D.; Hill, A.V.S.; Ewer, K.J. Activation-induced Markers Detect Vaccine-Specific $CD4^+$ T Cell Responses Not Measured by Assays Conventionally Used in Clinical Trials. *Vaccines (Basel)* **2018**, *6*, doi:10.3390/vaccines6030050.

648. Basera, T.J.; Ncayiyana, J.; Engel, M.E. Prevalence and risk factors of latent tuberculosis infection in Africa: a systematic review and meta-analysis protocol. *BMJ Open* **2017**, *7*, e012636, doi:10.1136/bmjopen-2016-012636.
649. Huaman, M.A.; Deepe, G.S.; Fichtenbaum, C.J. Elevated Circulating Concentrations of Interferon-Gamma in Latent Tuberculosis Infection. *Pathog Immun* **2016**, *1*, 291-303, doi:10.20411/pai.v1i2.149.
650. Sullivan, Z.A.; Wong, E.B.; Ndung'u, T.; Kasprowicz, V.O.; Bishai, W.R. Latent and Active Tuberculosis Infection Increase Immune Activation in Individuals Co-Infected with HIV. *EBioMedicine* **2015**, *2*, 334-340, doi:10.1016/j.ebiom.2015.03.005.
651. Refaeli, Y.; Van Parijs, L.; Alexander, S.I.; Abbas, A.K. Interferon gamma is required for activation-induced death of T lymphocytes. *J Exp Med* **2002**, *196*, 999-1005.

Appendix

Table A1. CTL peptide sequences

Peptide name	Amino acid sequence	Source	Protein (region)	Length	HLA restriction
CTL1	VSDGGPNLY	Influenza A	PB1 (591-599)	9	A1
CTL2	CTELKLSDY	Influenza A	NP (44-52)	9	A1
CTL3	GLCTLVAML	EBV	BMLF1 (259-267)	9	A2
CTL4	GILGFVFTL	Influenza M	Matrix 1 (58-66)	9	A2
CTL5	NLVPMVATV	HCMV	pp65 (495-503)	9	A0201
CTL6	ILRGSVAHK	Influenza A	NP (265-273)	9	A3
CTL7	RVRAYTYSK	EBV	BRLF1 (148-156)	9	A3
CTL8	RLRAEAQVK	EBV	EBNA3A (603-611)	9	A3
CTL9	IVTDFSVIK	EBV	EBNA3B (416-424)	9	A11
CTL10	ATIGTAMYK	EBV	BRLF1 (134-143)	9	A11
CTL11	DYCNVLNKEF	EBV	BRLF1 (28-37)	10	A24
CTL12	KTGGPIYKR	Influenza A	NP (91-99)	9	A68
CTL13	RPPIFIRRL	EBV	EBNA3A (379-387)	9	B7
CTL14	TPRVTGGGAM	HCMV	pp65	10	B7
CTL15	QAKWRLQTL	EBV	EBNA3A (158-166)	9	B8
CTL16	FLRGRAYGL	EBV	EBNA3A (325-333)	9	B8
CTL17	RAKFKQLL	EBV	BZLF1 (190-197)	8	B8
CTL18	ELRSRYWAI	Influenza A	NP (380-388)	9	B8
CTL19	SRYWAIRTR	Influenza A	NP (383-391)	9	B27
CTL20	RRIYDLIEL	EBV	EBNA3C (258-266)	9	B27
CTL21	YPLHEQHGM	EBV	EBNA3A (458-466)	9	B35
CTL22	EENLLDFVRF	EBV	EBNA3C (281-290)	10	B44
CTL23	EFFWDANDIY	HCMV	pp65 (511-525)	10	B44

ME-TRAP

Assay 1						Assay 2					
R10	R10	R10	TD1	TD1	TD1	R10	R10	R10	TD1	TD1	TD1
TT1	TT1	TT1	TD2	TD2	TD2	TT1	TT1	TT1	TD2	TD2	TD2
TT2	TT2	TT2	TD3	TD3	TD3	TT2	TT2	TT2	TD3	TD3	TD3
TT3	TT3	TT3	TD4	TD4	TD4	TT3	TT3	TT3	TD4	TD4	TD4
TT4	TT4	TT4	TD5	TD5	TD5	TT4	TT4	TT4	TD5	TD5	TD5
TT5	TT5	TT5	TT MP	TT MP	TT MP	TT5	TT5	TT5	TT MP	TT MP	TT MP
TT6	TT6	TT6	TD MP	TD MP	TD MP	TT6	TT6	TT6	TD MP	TD MP	TD MP
ME	ME	ME	PHA/SEB	PHA/SEB	PHA/SEB	ME	ME	ME	PHA/SEB	PHA/SEB	PHA/SEB

CSP

Assay 1			Assay 2			Assay 3			Assay 4		
R10	R10	R10	R10	R10	R10	R10	R10	R10	R10	R10	R10
R10	R10	R10	R10	R10	R10	R10	R10	R10	R10	R10	R10
CSP 1	CSP 1	CSP 1	CSP 1	CSP 1	CSP 1	CSP 1	CSP 1	CSP 1	CSP 1	CSP 1	CSP 1
CSP 2	CSP 2	CSP 2	CSP 2	CSP 2	CSP 2	CSP 2	CSP 2	CSP 2	CSP 2	CSP 2	CSP 2
CSP 3	CSP 3	CSP 3	CSP 3	CSP 3	CSP 3	CSP 3	CSP 3	CSP 3	CSP 3	CSP 3	CSP 3
CSP MP	CSP MP	CSP MP	CSP MP	CSP MP	CSP MP	CSP MP	CSP MP	CSP MP	CSP MP	CSP MP	CSP MP
CTL	CTL	CTL	CTL	CTL	CTL	CTL	CTL	CTL	CTL	CTL	CTL
PHA/SEB	PHA/SEB	PHA/SEB	PHA/SEB	PHA/SEB	PHA/SEB	PHA/SEB	PHA/SEB	PHA/SEB	PHA/SEB	PHA/SEB	PHA/SEB

GP

Assay 1						Assay 2					
R10	R10	R10	GP1-6	GP1-6	GP1-6	R10	R10	R10	GP1-6	GP1-6	GP1-6
R10	R10	R10	GP1-7	GP1-7	GP1-7	R10	R10	R10	GP1-7	GP1-7	GP1-7
SP	SP	SP	GP2-1	GP2-1	GP2-1	SP	SP	SP	GP2-1	GP2-1	GP2-1
GP1-1	GP1-1	GP1-1	GP2-2	GP2-2	GP2-2	GP1-1	GP1-1	GP1-1	GP2-2	GP2-2	GP2-2
GP1-2	GP1-2	GP1-2	GPS MP1	GPS MP1	GPS MP1	GP1-2	GP1-2	GP1-2	GPS MP1	GPS MP1	GPS MP1
GP1-3	GP1-3	GP1-3	GPS MP2	GPS MP2	GPS MP2	GP1-3	GP1-3	GP1-3	GPS MP2	GPS MP2	GPS MP2
GP1-4	GP1-4	GP1-4	empty	empty	empty	GP1-4	GP1-4	GP1-4	empty	empty	empty
GP1-5	GP1-5	GP1-5	PHA/SEB	PHA/SEB	PHA/SEB	GP1-5	GP1-5	GP1-5	PHA/SEB	PHA/SEB	PHA/SEB

negative control | Peptide pool | Megapool (MP) | Positive

Figure A1. ELISpot plate layouts

ELISpot plate layouts for the ME-TRAP, CSP and Ebola GP assays. No TD pool 6 was included on the ME-TRAP plate as the sequences of all peptides in this pool are the same as the TT peptides. For comparing responses to the strains, the response to TT6 was added to the TD pool sum. TT: TT/96 strain TRAP, TD: 3D7 strain TRAP, SP: Ebola Zaire glycoprotein signal peptide, GPS: Sudan Ebola glycoprotein.

Table A2. TRAP peptide sequences and pool configurations

Sequences that are conserved between the T9/96 and 3D7 strains are highlighted in green. 10T and 37T do not exist because there is an insertion in the 3D7 sequence and the T9/96 sequence was shifted to aid alignment

Pool	Peptide name	Amino acid sequence	Pool	Peptide name	Amino acid sequence
TT pool 1	1T	MNHLGNVKYLVIVFLIFFDL	TD pool 1	1D	MNHLGNVKYLVIVFLIFFDL
	2T	VIVFLIFFDLFLVNGRDVQN		2D	VIVFLIFFDLFLVNGRDVQN
	3T	FLVNGRDVQNNIVDEIKYSE		3D	FLVNGRDVQNNIVDEIKYRE
	4T	NIVDEIKYSEEVCNDQVDLY		4D	NIVDEIKYREEVCNDEVDLY
	5T	EVCNDQVDLYLLMDCSGSIR		5D	EVCNDEVDLYLLMDCSGSIR
	6T	LLMDCSGSIRRHNWVNHAVP		6D	LLMDCSGSIRRHNWVNHAVP
	7T	RHNWVNHAVPLAMKLIQQLN		7D	RHNWVNHAVPLAMKLIQQLN
	8T	LAMKLIQQLNLNDNAIHLYV		8D	LAMKLIQQLNLNDNAIHLYA
	9T	LNDNAIHLYVNVFSNNAKEI		9D	LNDNAIHLYASVFSNNAREI
	10T			10D	SVFSNNAREIIRLHSDASKN
TT pool 2	11T	IRLHSDASKNKEKALIIIRS	TD pool 2	11D	IRLHSDASKNKEKALIIIKS
	12T	KEKALIIIRSLLSTNLPYGR		12D	KEKALIIIKSLLSTNLPYGK
	13T	LLSTNLPYGRTNLTDALLQV		13D	LLSTNLPYGKTNLTDALLQV
	14T	TNLTDALLQVRKHLNDRINR		14D	TNLTDALLQVRKHLNDRINR
	15T	RKHLNDRINRENANQLVVIL		15D	RKHLNDRINRENANQLVVIL
	16T	ENANQLVVILTDGIPDSIQD		16D	ENANQLVVILTDGIPDSIQD
	17T	TDGIPDSIQDSLKESRKLSD		17D	TDGIPDSIQDSLKESRKLSD
	18T	SLKESRKLSDRGVKIAVFGI		18D	SLKESRKLSDRGVKIAVFGI
	19T	RGVKIAVFGIGQGINVAFNR		19D	RGVKIAVFGIGQGINVAFNR
	20T	GQGINVAFNRFLVGCHPSDG		20D	GQGINVAFNRFLVGCHPSDG
TT pool 3	21T	FLVGCHPSDGKCNLYADSAW	TD pool 3	21D	FLVGCHPSDGKCNLYADSAW
	22T	KCNLYADSAWENVKNVIGPF		22D	KCNLYADSAWENVKNVIGPF
	23T	ENVKNVIGPFMKAVCVEVEK		23D	ENVKNVIGPFMKAVCVEVEK
	24T	MKAVCVEVEKTASCGVWDEW		24D	MKAVCVEVEKTASCGVWDEW
	25T	TASCGVWDEWSPCSVTCGKG		25D	TASCGVWDEWSPCSVTCGKG
	26T	SPCSVTCGKGTRSRKREILH		26D	SPCSVTCGKGTRSRKREILH
	27T	TRSRKREILHEGCTSEIQEQ		27D	TRSRKREILHEGCTSELQEQ
	28T	EGCTSEIQEQCEEERCPPKW		28D	EGCTSELQEQCEEERCLPKR
	29T	CEEERCPPKWEPLDVPDEPE		29D	CEEERCLPKREPLDVPDEPE
	30T	EPLDVPDEPEDDQPRPRGDN		30D	EPLDVPDEPEDDQPRPRGDN
TT pool 4	31T	DDQPRPRGDNSSVQKPEENI	TD pool 4	31D	DDQPRPRGDNFAVEKPNENI
	32T	SSVQKPEENIIDNNPQEPSP		32D	FAVEKPNENIIDNNPQEPSP
	33T	IDNNPQEPSPNPEEGKDENP		33D	IDNNPQEPSPNPEEGKGENP
	34T	NPEEGKDENPNGFDLDENPE		34D	NPEEGKGENPNGFDLDENPE
	35T	NGFDLDENPENPPNPDIPEQ		35D	NGFDLDENPENPPNPPNPPN
	36T	NPPNPDIPEQKPNIPEDSEK		36D	NPPNPPNPPNPPNPPNPPNP
	37T			37D	PPNPPNPPNPDIPEQKPNIP
	38T	DIPEQKPNIPEDSEKEVPSD		38D	DIPEQKPNIPEDSEKEVPSD
	39T	EDSEKEVPSDVPKNPEDDRE		39D	EDSEKEVPSDVPKNPEDDRE
	40T	VPKNPEDDREENFDIPKKPE		40D	VPKNPEDDREENFDIPKKPE
TT pool 5	41T	ENFDIPKKPENKHDNQNNLP	TD pool 5	41D	ENFDIPKKPENKHDNQNNLP
	42T	NKHDNQNNLPNDKSDRNIPY		42D	NKHDNQNNLPNDKSDRYIPY
	43T	NDKSDRNIPYSPLPPKVLDN		43D	NDKSDRYIPYSPLAPKVLDN
	44T	SPLPPKVLDNERKQSDPQSQ		44D	SPLAPKVLDNERKQSDPQSQ
	45T	ERKQSDPQSQDNNGNRHVPN		45D	ERKQSDPQSQDNNGNRHVPN
	46T	DNNGNRHVPNSEDRETRPHG		46D	DNNGNRHVPNSEDRETRPHG
	47T	SEDRETRPHGRNNENRSYNR		47D	SEDRETRPHGRNNENRSYNR
	48T	RNNENRSYNRKYNDTPKHPE		48D	RNNENRSYNRKHNNTPKHPE
	49T	KYNDTPKHPEREEHEKPDNN		49D	KHNNTPKHPEREEHEKPDNN
	50T	REEHEKPDNNKKKGESDNKY		50D	REEHEKPDNNKKKAGSDNKY
TT pool 6	51T	KKKGESDNKYKIAGGIAGGL	TD pool 6	51D	KKKGESDNKYKIAGGIAGGL
	52T	KIAGGIAGGLALLACAGLAY		52D	KIAGGIAGGLALLACAGLAY
	53T	ALLACAGLAYKFVVPGAATP		53D	ALLACAGLAYKFVVPGAATP
	54T	KFVVPGAATPYAGEPAPFDE		54D	KFVVPGAATPYAGEPAPFDE
	55T	YAGEPAPFDETLGEEDKDLD		55D	YAGEPAPFDETLGEEDKDLD
	56T	TLGEEDKDLDEPEQFRLPEE		56D	TLGEEDKDLDEPEQFRLPEE
	57T	EPEQFRLPEENEWN		57D	EPEQFRLPEENEWN

Table A3. ME peptide sequences

Peptide name	Amino acid sequence	Antigen source	Epitope type	HLA restriction
ls8	KPNDKSLY	LSA1	CD8	B35
cp26	KPKDELDY	CSP	CD8	B35
ls6	KPIVQYDNF	LSA1	CD8	B53
tr42/43	ASKNKEKALII	TRAP	CD8	B8
tr39	GIAGGLALL	TRAP	CD8	A0201
cp6	MNPNDPNRNV	CSP	CD8	B7
st8	MINAYLDKL	STARP	CD8	A0202
ls50	ISKYEDEI	LSA1	CD8	B17
tr26	HLGNVKYLV	TRAP	CD8	A0201
ls53	KSLYDEHI	LSA1	CD8	B58
tr29	LLMDCSGSI	TRAP	CD8	A0202
cp39	YLNKIQNSL	CSP	CD8	A0201
la72	MEKLKELEK	LSA3	CD8	B8
ex23	ATSVLAGL	Exp1	CD8	B58
csp	DPNANPNVDPNANPNV	CSP	CD4	Multiple
trapAM	DEWSPCSVTCGKGTRSRKRE	TRAP	Heparin-binding motif	Multiple
nanp	NANPNANPNANPNANP	CSP	B cell	Multiple
38H BCG	QVHFQPLPPAVVKL	BCG	CD4	Multiple
FTTp	QFIKANSKFIGITE	TT	CD4	Multiple
pb9	SYIPSAEKI	*Plasmodium bergei* CSP	CD8	Mouse H2-K^d

Table A4. CSP peptide sequences and pool configurations

Pool	Peptide name	Amino acid sequence
CSP Pool 1 NANP and conserved region	CSP1	MMAPDPNANPNANPN
	CSP2	NANPNANPNANPNAN
	CSP3	DPNANPNANPNKNNQ
	CSP4	NPNANPNKNNQGNGQ
	CSP5	NPNKNNQGNGQGHNM
	CSP6	NNQGNGQGHNMPNDP
	CSP7	NGQGHNMPNDPNRNV
	CSP8	HNMPNDPNRNVDENA
	CSP9	NDPNRNVDENANANS
	CSP10	RNVDENANANSAVKN
	CSP11	ENANANSAVKNNNNE
CSP Pool 2 TH2R region	CSP12	ANSAVKNNNNEEPSD
	CSP13	VKNNNNEEPSDKHIK
	CSP14	NNEEPSDKHIKEYLN
	CSP15	PSDKHIKEYLNKIQN
	CSP16	HIKEYLNKIQNSLST
	CSP17	YLNKIQNSLSTEWSP
	CSP18	IQNSLSTEWSPCSVT
	CSP19	LSTEWSPCSVTCGNG
CSP Pool 3 TH3R/CS.T3T region	CSP20	WSPCSVTCGNGIQVR
	CSP21	SVTCGNGIQVRIKPG
	CSP22	GNGIQVRIKPGSANK
	CSP23	QVRIKPGSANKPKDE
	CSP24	KPGSANKPKDELDYA
	CSP25	ANKPKDELDYANDIE
	CSP26	KDELDYANDIEKKIC
	CSP27	DYANDIEKKICKMEK
	CSP28	DIEKKICKMEKCSSV
	CSP29	KICKMEKCSSVFNVV
	CSP30	MEKCSSVFNVVNSSI
	CSP31	KCSSVFNVVNSSIGL

Table A5. Zaire Ebola GP peptide sequences and pool configurations

Pool	Peptide name	Sequence
SP	GP1	MGVTGILQLPRDRFK
	GP2	GILQLPRDRFKRTSF
	GP3	LPRDRFKRTSFFLWV
	GP4	RFKRTSFFLWVIILF
	GP5	TSFFLWVIILFQRTF
GP1-1	GP6	LWVIILFQRTFSIPL
	GP7	ILFQRTFSIPLGVIH
	GP8	RTFSIPLGVIHNSTL
	GP9	IPLGVIHNSTLQV
	GP10	LGVIHNSTLQVSDV
	GP11	IHNSTLQVSDVDKLV
	GP12	TLQVSDVDKLVCRDK
	GP13	SDVDKLVCRDKL
	GP14	DVDKLVCRDKLSSTNQL
	GP15	CRDKLSSTNQLRSV
	GP16	KLSSTNQLRSVGLNL
	GP17	TNQLRSVGLNLEGNGV
	GP18	SVGLNLEGNGVATDV
	GP19	NLEGNGVATDVPSA
	GP20	GNGVATDVPSATKRW
GP1-2	GP21	ATDVPSATKRWGFR
	GP22	VPSATKRWGFRSGV
	GP23	ATKRWGFRSGVPPKV
	GP24	WGFRSGVPPKVVNY
	GP25	RSGVPPKVVNYEA
	GP26	GVPPKVVNYEAGEWA
	GP27	KVVNYEAGEWAENCY
	GP28	YEAGEWAENCYNLEI
	GP29	EWAENCYNLEIKK
	GP30	AENCYNLEIKKPDGS
	GP31	YNLEIKKPDGSECL
	GP32	EIKKPDGSECLPAA
	GP33	KPDGSECLPAAPDGI
	GP34	SECLPAAPDGIRGF
	GP35	LPAAPDGIRGFPRCR
	GP36	PDGIRGFPRCRYVHK
	GP37	RGFPRCRYVHKV
	GP38	GFPRCRYVHKVSGTG
	GP39	CRYVHKVSGTGPCA
	GP40	VHKVSGTGPCAGDFA
GP1-3	GP41	SGTGPCAGDFAFHK
	GP42	GPCAGDFAFHKEGAF
	GP43	GDFAFHKEGAFFLY
	GP44	AFHKEGAFFLYDRLA
	GP45	EGAFFLYDRLASTVI
	GP46	FLYDRLASTVIYR
	GP47	YDRLASTVIYRGTTF
	GP48	ASTVIYRGTTFAEGV
	GP49	IYRGTTFAEGVVAFL
	GP50	TTFAEGVVAFLIL
	GP51	FAEGVVAFLILPQAK
	GP52	VVAFLILPQAKKDFF
	GP53	LILPQAKKDFFSSH
	GP54	PQAKKDFFSSHPLR
	GP55	KKDFFSSHPLREPV
	GP56	FFSSHPLREPVNA
	GP57	SSHPLREPVNATED
	GP58	PLREPVNATEDPSSGY
	GP59	VNATEDPSSGYY
	GP60	NATEDPSSGYYSTTI
	GP61	DPSSGYYSTTIRYQA
	GP62	GYYSTTIRYQATGF
	GP63	STTIRYQATGFGTNE
GP1-3 (continued)	GP64	RYQATGFGTNETEYL
	GP65	TGFGTNETEYLFEV
	GP66	GTNETEYLFEVDNL
	GP67	ETEYLFEVDNLTYV
	GP68	YLFEVDNLTYVQL
GP1-4	GP69	FEVDNLTYVQLESRF
	GP70	NLTYVQLESRFTPQF
	GP71	VQLESRFTPQFLLQL
	GP72	SRFTPQFLLQLNETI
	GP73	PQFLLQLNETIY
	GP74	FLLQLNETIYTSGKR
	GP75	LNETIYTSGKRSNTTGK
	GP76	TSGKRSNTTGKLIWK
	GP77	RSNTTGKLIWKV
	GP78	SNTTGKLIWKVNPEI
	GP79	GKLIWKVNPEIDTTI
	GP80	WKVNPEIDTTIGEWA
	GP81	PEIDTTIGEWAFW
	GP82	IDTTIGEWAFWETKK
	GP83	IGEWAFWETKKNLTR
GP1-5	GP84	AFWETKKNLTRKIR
	GP85	ETKKNLTRKIRSEEL
	GP86	NLTRKIRSEELSFTV
	GP87	KIRSEELSFTVV
	GP88	IRSEELSFTVVSNGA
	GP89	ELSFTVVSNGAKNI
	GP90	FTVVSNGAKNISGQSPA
	GP91	GAKNISGQSPAR
	GP92	AKNISGQSPARTSSD
	GP93	SGQSPARTSSDPGTN
	GP94	PARTSSDPGTNTTTEDH
	GP95	DPGTNTTTEDHKIMA
	GP96	NTTTEDHKIMASENSSA
	GP97	HKIMASENSSAMVQV
	GP98	ASENSSAMVQVH
	GP99	SENSSAMVQVHSQGR
	GP100	SAMVQVHSQGREAAV
	GP101	VQVHSQGREAAVSHL
	GP102	SQGREAAVSHLTTLA
	GP103	EAAVSHLTTLATI
GP1-6	GP104	AVSHLTTLATISTS
	GP105	HLTTLATISTSPQSL
	GP106	LATISTSPQSLTTK
	GP107	ISTSPQSLTTKPGPD
	GP108	PQSLTTKPGPDNSTH
	GP109	TTKPGPDNSTHNTPV
	GP110	GPDNSTHNTPVYKL
	GP111	NSTHNTPVYKLDI
	GP112	THNTPVYKLDISEA
	GP113	TPVYKLDISEATQV
	GP114	YKLDISEATQVEQHH
	GP115	ISEATQVEQHHRR
	GP116	EATQVEQHHRRTDND
	GP117	VEQHHRRTDNDSTA
	GP118	HHRRTDNDSTASDTPSA
	GP119	NDSTASDTPSATTAA
	GP120	ASDTPSATTAAGPPK
	GP121	PSATTAAGPPKA
	GP122	SATTAAGPPKAENTN
	GP123	AAGPPKAENTNTSK
	GP124	PPKAENTNTSKSTDF
	GP125	ENTNTSKSTDFLDPA
	GP126	TSKSTDFLDPATTTS
GP1-6 (continue	GP127	TDFLDPATTTSPQNH
	GP128	DPATTTSPQNHSETA
GP1-7	GP129	TTSPQNHSETAGNNNTH
	GP130	HSETAGNNNTHH
	GP131	SETAGNNNTHHQDTG
	GP132	GNNNTHHQDTGEESA
	GP133	THHQDTGEESASSGK
	GP134	DTGEESASSGKLGLI
	GP135	ESASSGKLGLITNTI
	GP136	SGKLGLITNTIAGVA
	GP137	GLITNTIAGVAGLI
	GP138	TNTIAGVAGLITGGR
	GP139	AGVAGLITGGRRTRR
	GP140	GLITGGRRTRREAIV
	GP141	GGRRTRREAIVNA
	GP142	RRTRREAIVNAQPK
	GP143	RREAIVNAQPKCNPNL
	GP144	VNAQPKCNPNLHYW
	GP145	AQPKCNPNLHYW
	GP146	PKCNPNLHYWTTQDEGA
GP2-1	GP147	LHYWTTQDEGAAIGL
	GP148	TTQDEGAAIGLAWI
	GP149	DEGAAIGLAWIPYF
	GP150	AAIGLAWIPYFGPAA
	GP151	LAWIPYFGPAAEGIY
	GP152	PYFGPAAEGIYIEGL
	GP153	PAAEGIYIEGLMH
	GP154	AEGIYIEGLMHNQDGL
	GP155	IEGLMHNQDGLICGL
	GP156	MHNQDGLICGLRQLA
	GP157	DGLICGLRQLANETTQA
	GP158	LRQLANETTQALQLF
	GP159	ANETTQALQLFLRA
	GP160	TTQALQLFLRATTEL
	GP161	LQLFLRATTELRTF
	GP162	FLRATTELRTFSIL
	GP163	ATTELRTFSILNRKA
	GP164	LRTFSILNRKAIDFL
	GP165	SILNRKAIDFLLQRW
	GP166	RKAIDFLLQRWGGTCH
GP2-2	GP167	FLLQRWGGTCHIL
	GP168	LQRWGGTCHILGPDCCI
	GP169	TCHILGPDCCIEPH
	GP170	ILGPDCCIEPHDWTK
	GP171	DCCIEPHDWTKNI
	GP172	CIEPHDWTKNITDKI
	GP173	HDWTKNITDKIDQII
	GP174	KNITDKIDQIIHDFV
	GP175	DKIDQIIHDFVDKTL
	GP176	DQIIHDFVDKTL
	GP177	IIHDFVDKTLPDQGD
	GP178	FVDKTLPDQGDNDNW
	GP179	TLPDQGDNDNWWTGW
	GP180	DQGDNDNWWTGWRQW
	GP181	NDNWWTGWRQWIPA
	GP182	WWTGWRQWIPAGIGV
	GP183	WRQWIPAGIGVTGVV
	GP184	IPAGIGVTGVVIAVI
	GP185	IGVTGVVIAVIALF
	GP186	TGVVIAVIALFCICK
	GP187	IAVIALFCICKFVF

Table A6. Sudan Ebola GP peptide sequences and pool configurations

Pool	Peptide name	Sequence	Pool	Peptide name	Sequence	Pool	Peptide name	Sequence
GPS MP1	GPS1	MGGLSLLQLPRDKFR	GPS MP1 (continued)	GPS57	FGAQHSTTLFKIDNN	GPS MP2 (continued)	GPS113	PGPTTEAPTLTTPEN
	GPS2	SLLQLPRDKFRKSSF		GPS58	HSTTLFKIDNNTFVR		GPS114	TEAPTLTTPENITTA
	GPS3	LPRDKFRKSSFFVWV		GPS59	LFKIDNNTFVRLDRP		GPS115	TLTTPENITTAVKTV
	GPS4	KFRKSSFFVWVIILF		GPS60	DNNTFVRLDRPHTPQ		GPS116	PENITTAVKTVLPQE
	GPS5	SSFFVWVIILFQKAF		GPS61	FVRLDRPHTPQFLFQ		GPS117	TTAVKTVLPQESTSN
	GPS6	VWVIILFQKAFSMPL		GPS62	DRPHTPQFLFQLNDT		GPS118	KTVLPQESTSNGLIT
	GPS7	ILFQKAFSMPLGVVT		GPS63	TPQFLFQLNDTIHLH		GPS119	PQESTSNGLITSTVT
	GPS8	KAFSMPLGVVTNSTL		GPS64	LFQLNDTIHLHQQLS		GPS120	TSNGLITSTVTGILG
	GPS9	MPLGVVTNSTLEVTE		GPS65	NDTIHLHQQLSNTTG		GPS121	LITSTVTGILGSLGL
	GPS10	VVTNSTLEVTEIDQL		GPS66	HLHQQLSNTTGRLIW		GPS122	TVTGILGSLGLRKRS
	GPS11	STLEVTEIDQLVCKD		GPS67	QLSNTTGRLIWTLDA		GPS123	ILGSLGLRKRSRRQT
	GPS12	VTEIDQLVCKDHLAS		GPS68	TTGRLIWTLDANINA		GPS124	LGLRKRSRRQTNTKA
	GPS13	DQLVCKDHLASTDQL		GPS69	LIWTLDANINADIGE		GPS125	KRSRRQTNTKATGKC
	GPS14	CKDHLASTDQLKSVG		GPS70	LDANINADIGEWAFW		GPS126	RQTNTKATGKCNPNL
	GPS15	LASTDQLKSVGLNLE		GPS71	INADIGEWAFWENKK		GPS127	TKATGKCNPNLHYWT
	GPS16	DQLKSVGLNLEGSGV		GPS72	IGEWAFWENKKNLSE		GPS128	GKCNPNLHYWTAQEQ
	GPS17	SVGLNLEGSGVSTDI		GPS73	AFWENKKNLSEQLRG		GPS129	PNLHYWTAQEQHNAA
	GPS18	NLEGSGVSTDIPSAT		GPS74	NKKNLSEQLRGEELS		GPS130	YWTAQEQHNAAGIAW
	GPS19	SGVSTDIPSATKRWG		GPS75	LSEQLRGEELSFEAL		GPS131	QEQHNAAGIAWIPYF
	GPS20	TDIPSATKRWGFRSG		GPS76	LRGEELSFEALSLNE		GPS132	NAAGIAWIPYFGPGA
	GPS21	SATKRWGFRSGVPPK		GPS77	ELSFEALSLNETEDD		GPS133	IAWIPYFGPGAEGIY
	GPS22	RWGFRSGVPPKVVSY		GPS78	EALSLNETEDDDAAS		GPS134	PYFGPGAEGIYTEGL
	GPS23	RSGVPPKVVSYEAGE		GPS79	LNETEDDDAASSRIT		GPS135	PGAEGIYTEGLMHNQ
	GPS24	PPKVVSYEAGEWAEN		GPS80	EDDDAASSRITKGRI		GPS136	GIYTEGLMHNQNALV
	GPS25	VSYEAGEWAENCYNL		GPS81	AASSRITKGRISDRA		GPS137	EGLMHNQNALVCGLR
	GPS26	AGEWAENCYNLEIKK		GPS82	RITKGRISDRATRKY		GPS138	HNQNALVCGLRQLAN
	GPS27	AENCYNLEIKKPDGS		GPS83	GRISDRATRKYSDLV		GPS139	ALVCGLRQLANETTQ
	GPS28	YNLEIKKPDGSECLP		GPS84	DRATRKYSDLVPKNS		GPS140	GLRQLANETTQALQL
	GPS29	IKKPDGSECLPPPPD	GPS MP2	GPS85	RKYSDLVPKNSPGMV		GPS141	LANETTQALQLFLRA
	GPS30	DGSECLPPPPDGVRG		GPS86	DLVPKNSPGMVPLHI		GPS142	TTQALQLFLRATTEL
	GPS31	CLPPPPDGVRGFPRC		GPS87	KNSPGMVPLHIPEGE		GPS143	LQLFLRATTELRTYT
	GPS32	PPDGVRGFPRCRYVH		GPS88	GMVPLHIPEGETTLP		GPS144	LRATTELRTYTILNR
	GPS33	VRGFPRCRYVHKAQG		GPS89	LHIPEGETTLPSQNS		GPS145	TELRTYTILNRKAID
	GPS34	PRCRYVHKAQGTGPC		GPS90	EGETTLPSQNSTEGR		GPS146	TYTILNRKAIDFLLR
	GPS35	YVHKAQGTGPCPGDY		GPS91	TLPSQNSTEGRRVGV		GPS147	LNRKAIDFLLRRWGG
	GPS36	AQGTGPCPGDYAFHK		GPS92	QNSTEGRRVGVNTQE		GPS148	AIDFLLRRWGGTCRI
	GPS37	GPCPGDYAFHKDGAF		GPS93	EGRRVGVNTQETITE		GPS149	LLRRWGGTCRILGPD
	GPS38	GDYAFHKDGAFFLYD		GPS94	VGVNTQETITETAAT		GPS150	WGGTCRILGPDCCIE
	GPS39	FHKDGAFFLYDRLAS		GPS95	TQETITETAATIIGT		GPS151	CRILGPDCCIEPHDW
	GPS40	GAFFLYDRLASTVIY		GPS96	ITETAATIIGTNGNH		GPS152	GPDCCIEPHDWTKNI
	GPS41	LYDRLASTVIYRGVN		GPS97	AATIIGTNGNHMQIS		GPS153	CIEPHDWTKNITDKI
	GPS42	LASTVIYRGVNFAEG		GPS98	IGTNGNHMQISTIGI		GPS154	HDWTKNITDKINQII
	GPS43	VIYRGVNFAEGVIAF		GPS99	GNHMQISTIGIRPSS		GPS155	KNITDKINQIIHDFI
	GPS44	GVNFAEGVIAFLILA		GPS100	QISTIGIRPSSSQIP		GPS156	DKINQIIHDFIDNPL
	GPS45	AEGVIAFLILAKPKE		GPS101	IGIRPSSSQIPSSSP		GPS157	QIIHDFIDNPLPNQD
	GPS46	IAFLILAKPKETFLQ		GPS102	PSSSQIPSSSPTTAP		GPS158	DFIDNPLPNQDNDDN
	GPS47	ILAKPKETFLQSPPI		GPS103	QIPSSSPTTAPSPEA		GPS159	NPLPNQDNDDNWWTG
	GPS48	PKETFLQSPPIREAV		GPS104	SSPTTAPSPEAQTPT		GPS160	NQDNDDNWWTGWRQW
	GPS49	FLQSPPIREAVNYTE		GPS105	TAPSPEAQTPTTHTS		GPS161	DDNWWTGWRQWIPAG
	GPS50	PPIREAVNYTENTSS		GPS106	PEAQTPTTHTSGPSV		GPS162	WTGWRQWIPAGIGIT
	GPS51	EAVNYTENTSSYYAT		GPS107	TPTTHTSGPSVMATE		GPS163	RQWIPAGIGITGIII
	GPS52	YTENTSSYYATSYLE		GPS108	HTSGPSVMATEEPTT		GPS164	PAGIGITGIIIAIIA
	GPS53	TSSYYATSYLEYEIE		GPS109	PSVMATEEPTTPPGS		GPS165	GITGIIIAIIALLCV
	GPS54	YATSYLEYEIENFGA		GPS110	ATEEPTTPPGSSPGP		GPS166	IIIAIIALLCVCKLL
	GPS55	YLEYEIENFGAQHST		GPS111	PTTPPGSSPGPTTEA		GPS167	IIALLCVCKLLC
	GPS56	EIENFGAQHSTTLFK		GPS112	PGSSPGPTTEAPTLT			

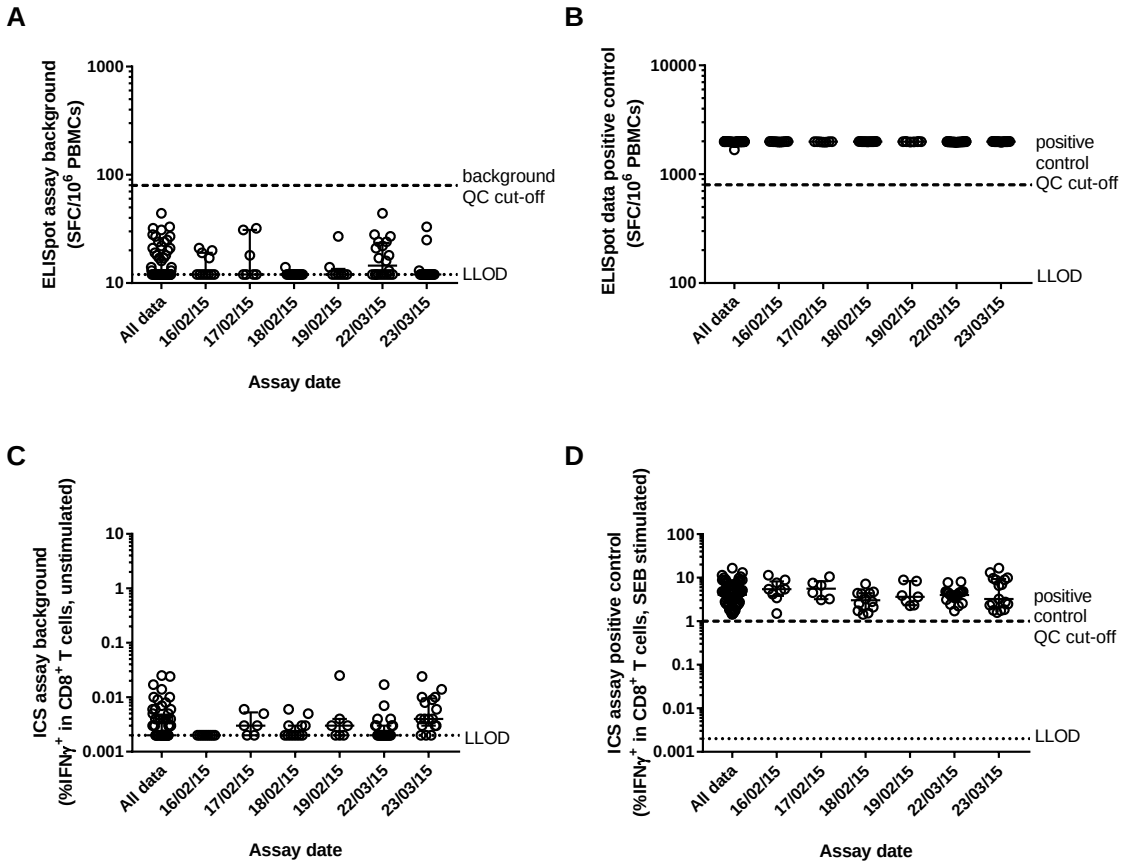

Figure A2. ELISpot and ICS QC

Unstimulated and positive controls for VAC59 ELISpot and ICS assays conducted over multiple time points. **A**) CSP ELISpot background (unstimulated cells, average of three wells per volunteer). **B**) CSP ELISpot positive control (PHA/SEB stimulated cells, average of three wells per volunteer). **C**) ICS background for IFNγ$^+$ CD8$^+$ T cells (unstimulated cells). **D**) ICS positive control for IFNγ$^+$ CD8$^+$ T cells (SEB stimulated cells). Dotted lines show lower limit of detection (LLOD), dashed lines show the QC cut-off. Assays in which the negative control value was above the QC cut-off or the positive control value was below the QC cut-off were classed as "failed" and removed from the dataset. There was no QC cut-off for ICS background. Instead, background was subtracted from the antigen-specific response for each individual. The assay was classed as "failed" if the background-subtracted response was less than twice the background response for that individual. Intra- and inter-assay variation was comparable for CD4$^+$ T cells and other cytokine responses.

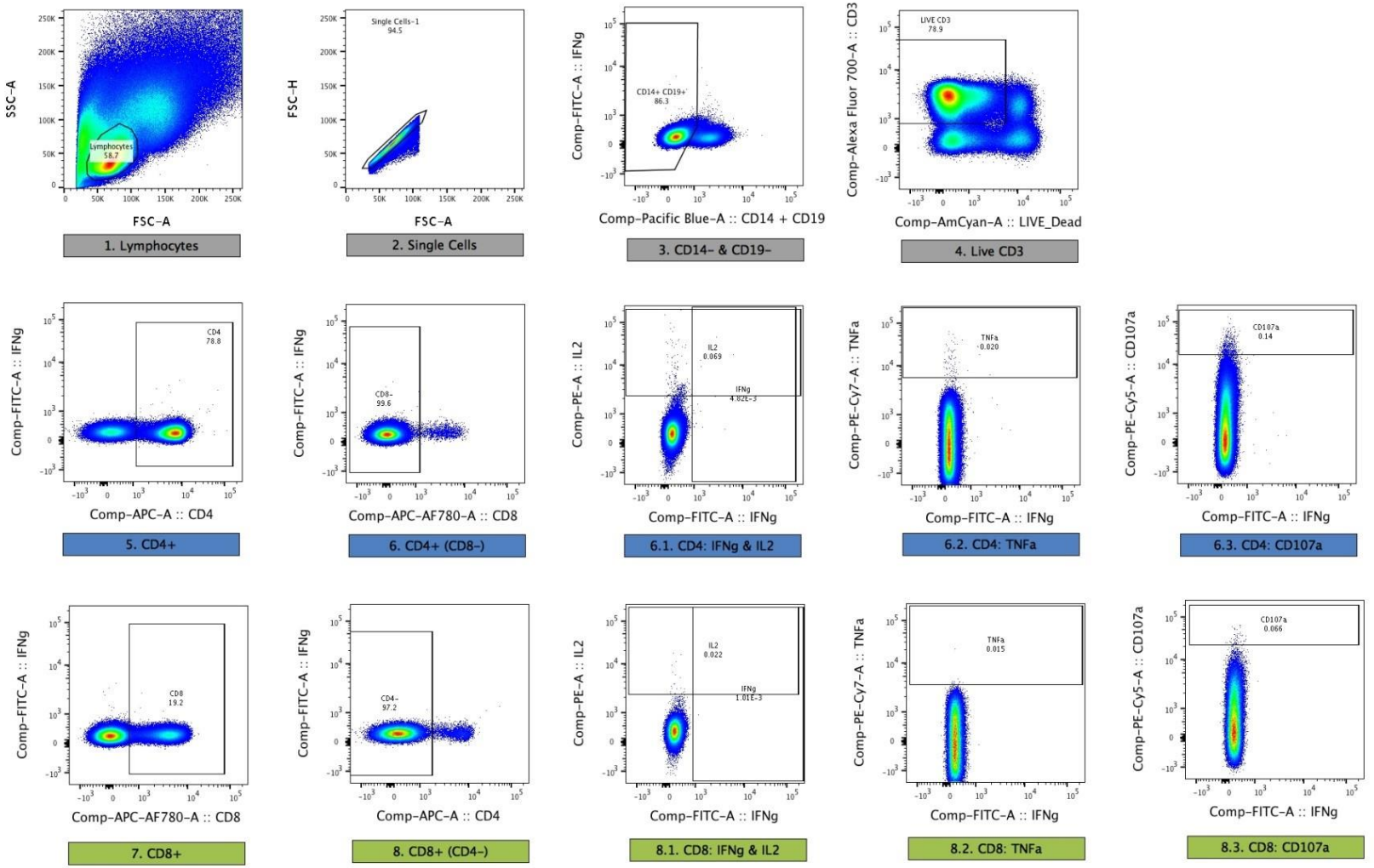

Figure A3. Gating strategy for clinical trials intracellular cytokine staining

Intracellular cytokine staining gating strategy. Cells were gated on single lymphocytes based on size. Dead cells, $CD14^+$ and $CD19^+$ cells were excluded and T cells were identified by CD3 expression. T cell subsets were gated as $CD4^+$ and $CD8^+$ populations. Cytokine expression was quantified by plotting pairs of cytokines against each other and gating positive populations.

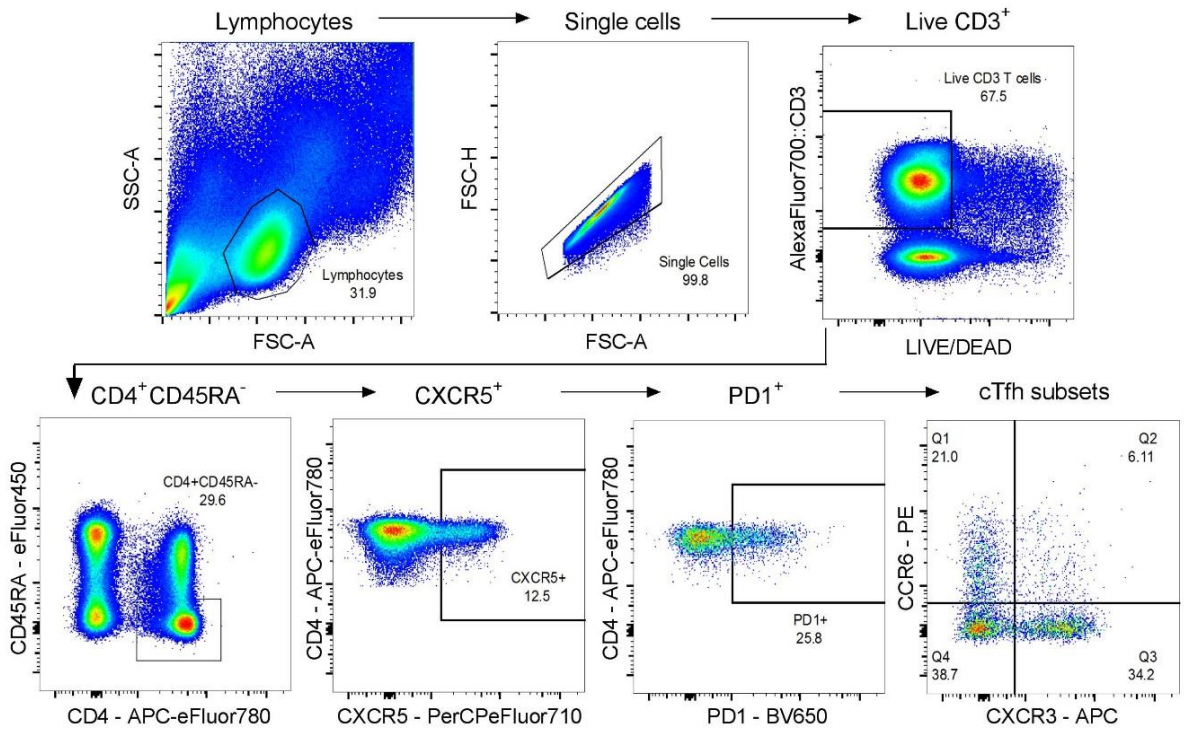

Figure A4. Gating strategy for cTfh phenotyping
Gating strategy for cTfh phenotyping using cell surface staining and flow cytometry.

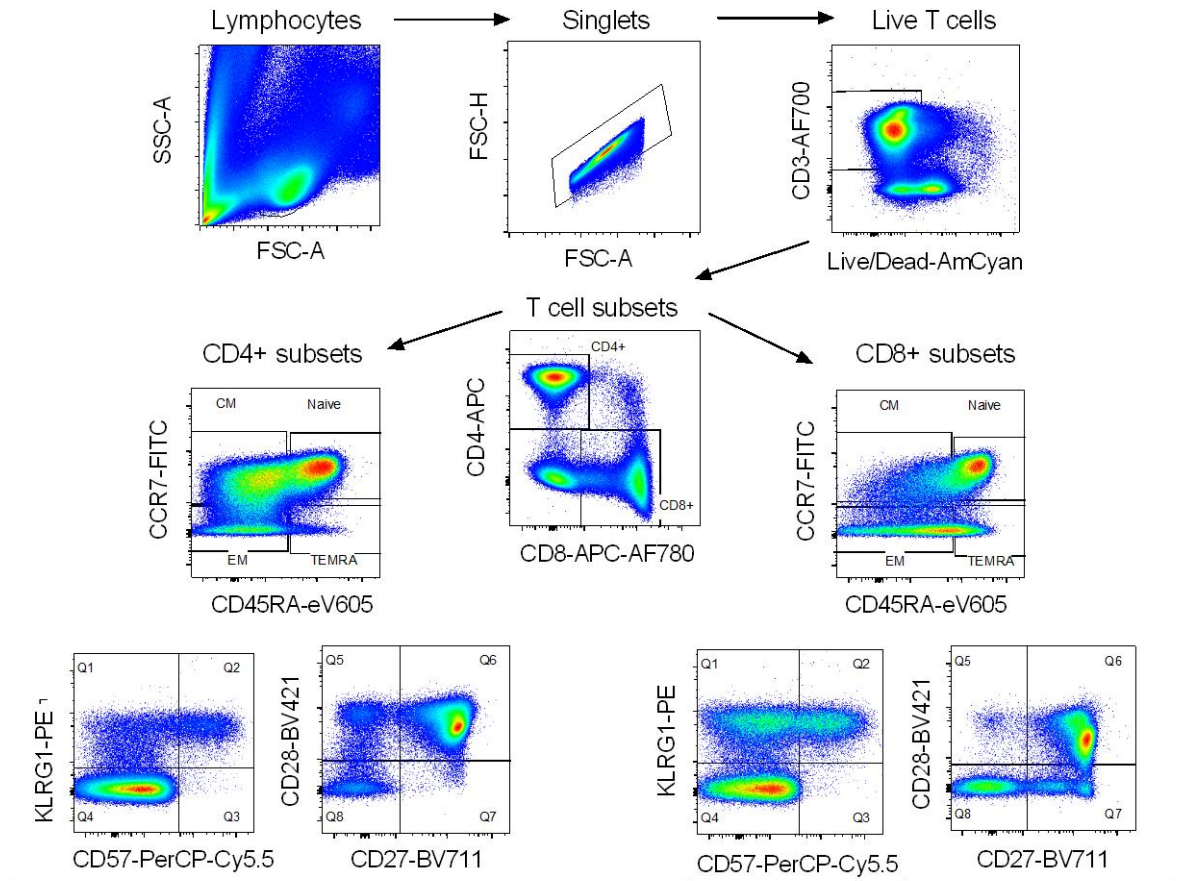

Figure A5. Gating strategy for memory T cell phenotyping
Gating strategy for memory T cell phenotyping using cell surface staining and flow cytometry.

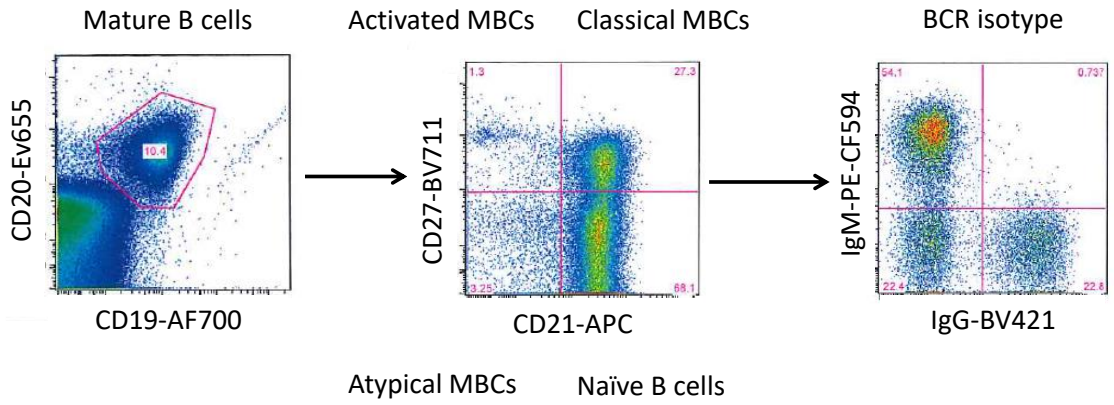

Figure A6. Gating strategy for B cell phenotyping
Gating strategy for B cell phenotyping using cell surface staining and flow cytometry. Cells were initially gated on live single lymphocytes as in Figure A5 above.

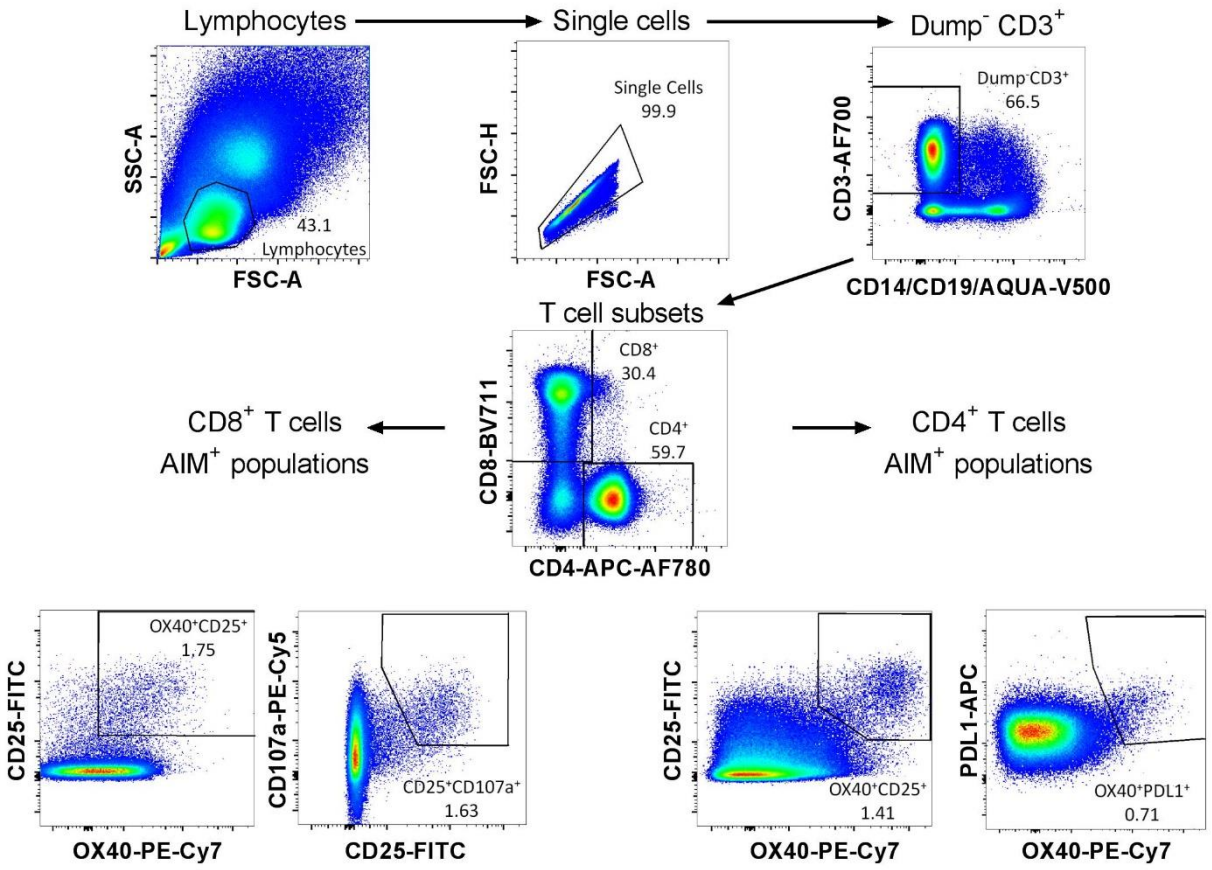

Figure A7. Gating strategy for activation-induced markers assay

Activation-induced markers gating strategy. Cells were gated on single lymphocytes based on size, then dead cells, $CD14^+$ and $CD19^+$ cells were excluded. T cell subsets were gated as $CD4^+CD8^-$ or $CD8^+CD4^-$ and then expression of AIM markers was measured within each subset. Gates displayed are representative of the top quartile of GP-specific responses in order to clearly demonstrate where these populations sit.

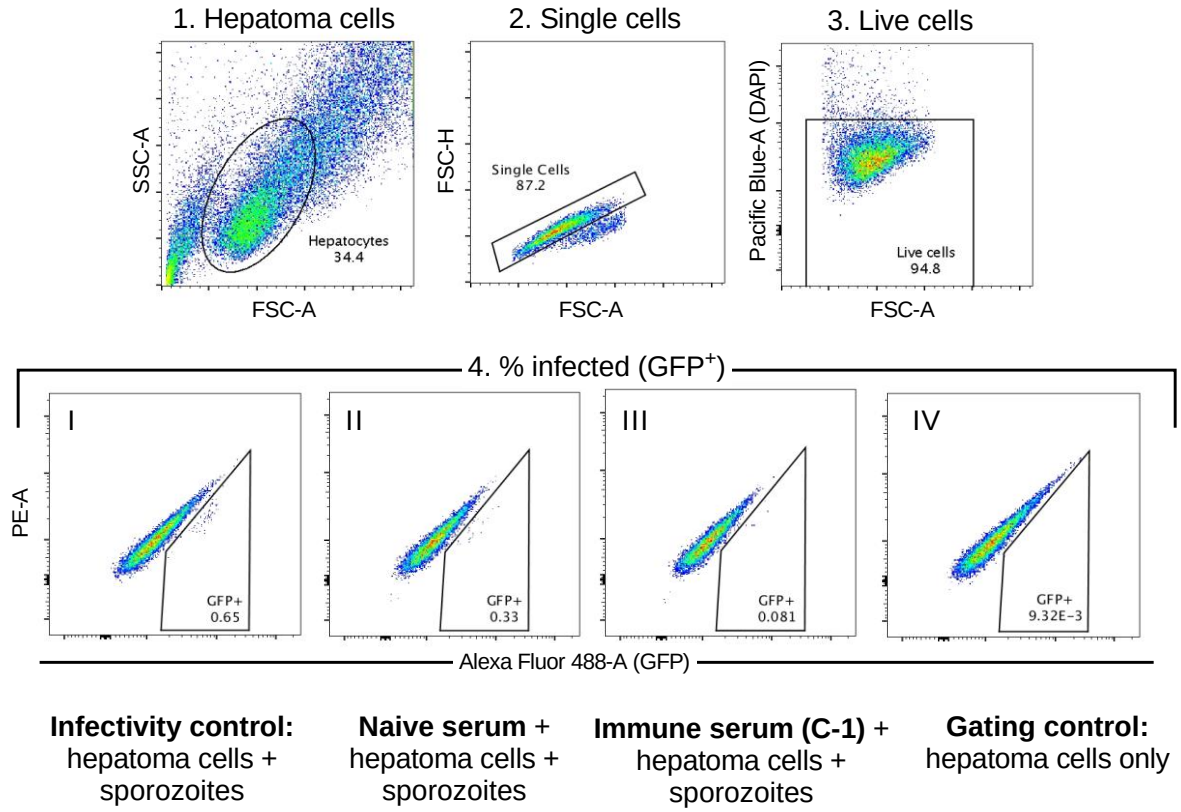

Figure A8. Gating strategy for inhibition of sporozoite invasion assay

Hierarchical gating strategy used to determine the percentage of hepatoma cells infected with GFP-expressing sporozoites. 1. Hepatoma cells are gated based on size to exclude debris and large cell clumps. 2. Singlets are gated to exclude smaller cell clumps and in doublets in particular. 3. Live cells (DAPI-negative) are gated to exclude dead cells. 4. Cells infected with the GFP-expressing sporozoites are GFP+. Cells are gated against both GFP (Alexa Fluor-AF488 channel, GFP+) and the adjacent channel (PE-) to exclude signal that is caused by autofluorescence. Representative populations in each of the conditions are shown: I. Infectivity control - sporozoite infection of hepatoma cells in the absence of any serum; II. Sporozoite infection of hepatoma cells in the presence of naïve serum (D0); III. Sporozoite infection of hepatoma cells in the presence of immune serum (C-1); IV. Gating control – hepatoma cells only, no sporozoites or serum added.